N71-25471

REPORT MDC E0298

NASA CR-103108

SPACE SHUTTLE HIGH PRESSURE AUXILIARY PROPULSION SUBSYSTEM DEFINITION STUDY

SUBTASK B REPORT

Contract Number NAS 8-26248

MCDONNELL DOUGLAS ASTRONAUTICS COMPANY - EAST

MCDONNELL DOUGLAS CORPORATION

COPY NO. 1

SPACE SHUTTLE HIGH PRESSURE AUXILIARY PROPULSION SUBSYSTEM DEFINITION STUDY

12 FEBRUARY 1971 REPORT MDC E0298

SUBTASK B REPORT

PREPARED BY:
R.D. GAINES
A.I. GOLDFORD
T.A. KAEMMING

APPROVED BY:
L.F. KOHRS, MANAGER, PROPULSION

MCDONNELL DOUGLAS ASTRONAUTICS COMPANY - EAST
Saint Louis, Missouri 63166 (314) 232-0232

MCDONNELL DOUGLAS CORPORATION

ABSTRACT

This report describes the preliminary design effort (Subtask B) of a study to define the most attractive high pressure, oxygen/hydrogen auxiliary propulsion subsystem (APS) for NASA space shuttle booster and orbiters. The study was performed for the National Aeronautics and Space Administration, Marshall Space Flight Center (MSFC), Huntsville, Alabama under Contract No. NAS8-26248.

The study program was divided into two phases. The first, Subtask A, was a conceptual subsystem definition phase to identify APS concepts best suited to each of the two baseline shuttle booster and orbiter vehicles. The second, Subtask B, (described in this report) was a preliminary design of the selected subsystem to establish a more in-depth understanding of subsystem design and operation.

The APS selected for all vehicles utilized a turbopump subassembly to provide the pressure required for subsystem operation. In this concept, hydrogen and oxygen propellants are stored as cryogenic liquids and supplied to the subsystem by turbopumps and temperature conditioned in reburn heat exchangers. Combustion products from gas generators are used in turbines to power the turbopumps. Exhaust gas from the turbines are routed to heat exchangers where additional oxygen is added and the mixture reburned to provide the energy for propellant conditioning. Resultant conditioned propellants are stored in accumulators until they are required for APS thruster usage.

The objective of Subtask B was to establish the preliminary design for the turbopump APS. This report describes the study effort; provides a definition of subsystem operating and performance characteristics, component and assembly designs, installation features, weight, and reliability estimates; and evaluates critical technology.

CONTENTS

Section		Page
	Abstract	ii
1.	Introduction	1-1
2.	Study Approach	2-1
3.	APS Requirements	3-1
4.	APS Description	4-1
5.	APS Operation and Control	5-1
6.	APS Design and Performance Summary	6-1
7.	Conclusions	7-1
8.	References	8-1

Appendix		Page
A.	APS Requirements	A-1
B.	Thermal Environment Definition	B-1
C.	APS Installation	C-1
D.	Baseline Component and Assembly Concepts	D-1
	D-1. Propellant Storage, Acquisition, and Pressurization	D-2
	D-2. Conditioner Assembly	D-38
	D-3. Turbopump Evaluation	D-67
	D-4. Heat Exchanger	D-87
	D-5. Gas Generators	D-103
	D-6. Accumulators	D-113
	D-7. Thruster Assemblies	D-122
	D-8. +X Translation Thruster Integration Study	D-154
E.	Operating Performance and Transient Analysis	E-1
F.	Subsystem Weights and Sensitivities	F-1
G.	Technology Critique	G-1
H.	Subsystem Reliability	H-1
I.	Distribution List	I-1

EFFECTIVE PAGES

TITLE

ii through iv

1-1 through 1-2

2-1 through 2-2

3-1 through 3-6

4-1 through 4-19

5-1 through 5-2

6-1 through 6-10

7-1 through 7-2

8-1 through 8-1

A-1 through A-46

B-1 through B-10

C-1 through C-21

D-1 through D-94

D-94a through D-94e

D-95 through D-108

D-108a through D-108c

D-109

D-109a through D-109c

D-110 through D-174

E-1 through E-31

F-1 through F-18

G-1 through G-12

H-1 through H-25

H-25a

H-26 through H-36

I-1 through I-8

1. INTRODUCTION

Development of the NASA space shuttle vehicle system for future manned space operations requires development of a number of subsystems which are either new or significant extensions of state-of-the-art technology. Among these is the auxiliary propulsion subsystem (APS) used for control and maneuvering of the shuttle vehicle after main engine cut-off. The magnitude of the APS control requirements far exceed those of previous space vehicles. To provide a high performance APS and, additionally, to take advantage of benefits which can be derived from propellant logistics, safety, reuse, and performance, a gaseous hydrogen/oxygen auxiliary propulsion subsystem was identified as the most desirable type of subsystem.

There are two basic means of implementing such an APS:

(1) a high pressure APS, in which propellants are stored at, or conditioned to, the most desirable thruster operating pressures

(2) a low pressure APS, in which propellants are supplied to the control thrusters from the main engine propellant tanks at normal ullage pressure.

Within these broad categories many APS options are available. Typically, storage of propellants, conditioning assembly design, integration with other propulsion subsystems, and the exact mode of APS mission usage can be implemented in various ways.

Each basic APS category and its alternate implementation scheme offers different advantages and suffers different disadvantages in terms of subsystem performance and the requisite technology developments. Thus, selection of the APS for the shuttle and definition of the advanced technology necessary for APS development required in-depth studies to select the type of APS best suited to shuttle requirements and to identify the advanced technology effort required for development of the APS.

To fulfill this need, NASA contracted for APS definition studies of both high and low pressure APS. These studies were divided into two phases. The first phase, Subtask A, was a conceptual subsystem definition to provide NASA with sufficient data for selection of the best means of APS implementation in the high and low pressure categories. The second phase, Subtask B, was a preliminary design of the particular concept(s) selected in each basic APS category. The high pressure APS study was conducted by McDonnell Douglas Astronautics Company - East under

Contract No. NAS8-26248. The Aerojet Liquid Rocket Company, under subcontract to MDAC-East, provided analyses and design support necessary to define the active components for APS evaluation. NASA technical direction for this effort was provided by the NASA Marshall Space Flight Center (MSFC) at Huntsville, Alabama, through the office of Mr. John McCarty, Deputy Chief, Propulsion and Power Branch of the Astronautics Laboratory.

The problem addressed in the high pressure APS study Subtask A was to provide sufficient comparative data on the various APS concepts to allow selection of the best high pressure approach for Subtask B preliminary design. This required consideration of a large number of high pressure APS concepts. For this phase of study, the predominant concern was the relative merit of various APS concepts, rather than their absolute performance levels. Component and assembly optimizations, within a given subsystem concept, were limited to those areas which could potentially impact subsystem selection. Thus, final data resulting from this study phase could not be considered as representative of a refined absolute performance level for any particular subsystem. That aspect of design was properly the result of the second phase of study, which provided component optimizations for the selected APS concept. Results of first phase (conceptual subsystem definition) of the high pressure APS study are summarized in Reference (a).

Subtask B was initiated using APS concepts defined in Subtask A. Vehicles considered for the Subtask B APS installation were Orbiter B, Orbiter C, and the Booster defined in Reference (b). Studies were performed to determine thruster arrangement and thrust level which would best meet maneuvering requirements and still provide the minimum weight configuration. Other criteria were accounted for, such as no heat shield penetration by thrusters during reentry, and a common thruster for orbiters and booster. In-depth component and assembly trade studies and design analyses were conducted to define the recommended baseline APS. The final baseline APS installation and preliminary design including component definition was then accomplished. Reference (c), Space Shuttle High Pressure APS Definition Study Handbook, defines in detail the preliminary design, operating performance, and weight sensitivities for the selected APS.

This report presents results of Subtask B preliminary design effort. The body of the report presents a brief overview of the various studies and their results. Included are a summary of the study approach and APS requirements, a description of the APS, a discussion of the alternatives considered for the different APS assemblies, and an APS design summary. This is followed by appendices which provide additional detail for the various studies and analyses leading to the selected design.

2. STUDY APPROACH

The overall study approach, as described previously, was conducted in two phases, defined as Subtask A and Subtask B. Reference (d) provides a detailed program plan for the complete study, and defines the objective of each task. During Subtask A, a preliminary screening of the many APS concepts was conducted. APS concepts resulting from this screening were then evaluated in more detail to establish concepts best suited to each shuttle configuration. A turbopump APS was selected as the best approach for both orbiters and the booster. The Subtask B portion of the study involved a preliminary design of the turbopump APS concept, conducted to define (in detail) component and assembly design, operation and performance, and resulting APS performance. Figure 2.1 presents a task flow chart illustrating effort during this study phase. The basic approach taken was to:

(1) update the baseline APS design points to reflect revisions in the vehicle requirements

(2) conduct component and assembly studies, using the updated APS design points and component requirements

(3) refine the APS design, and select baseline component designs best suited to the APS.

Results of these analyses and of the component studies were then used to revise and update APS schematics and baseline design point. The resulting APS design was then evaluated to define performance, operating characteristics, and the advanced technology required for subsystem development.

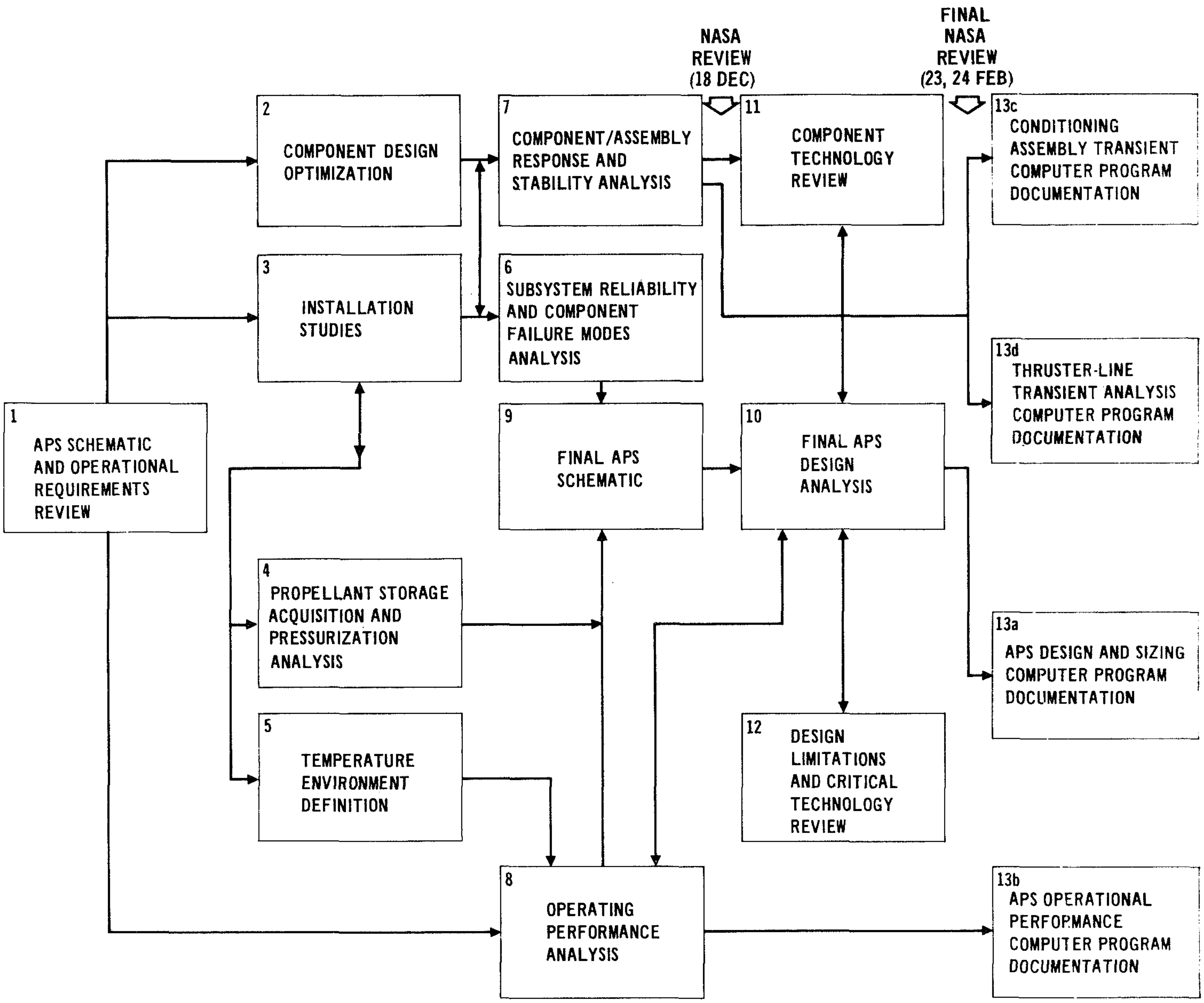

SUBTASK B – PRELIMINARY APS DESIGN

Task Description Flow Chart

FIGURE 2–1

3. APS REQUIREMENTS

The APS thrust level and total impulse were defined during Subtask A for the vehicle configurations, design characteristics, and acceleration requirements defined in the Space Shuttle Vehicle Description and Requirements Document (Reference (e)). However, subsequent to Subtask A, revisions were made to this document, Reference (b), requiring an updating of the APS requirements for Subtask B. These revisions included changes to vehicle configuration, increased acceleration requirements, and refined mission timelines. Three vehicle configurations, two orbiters and one booster, were evaluated during Subtask B. These vehicles are illustrated in Figures 3-1 through 3-3. The vehicle attitude control and translation maneuver requirements are shown in Figures 3-4 and 3-5, respectively.

A detailed evaluation of the APS thrust level, total impulse, and number of thrusters for the Subtask B study phase was made. Many options of thrust level, number of thrusters, and thruster locations are available within the constraints imposed by the vehicle acceleration requirements and vehicle configuration. The analysis described in Appendix A of this report resulted in the thruster locations shown in Figures 3-1 through 3-3, and the thrust levels and number of thrusters are summarized in Figure 3-6. As shown, a common thrust level of 1850 lb was selected for both orbiters and the booster.

In Subtask A, three levels of APS control and +X maneuvering capability were investigated for the orbiters. These were:

(1) APS designed to perform all orbiter attitude control and +X maneuvering functions after main engine shutdown

(2) APS designed to perform attitude control functions, but limited in +X maneuver capability to velocity changes of $\leq$ 50 ft/sec

(3) APS designed to perform attitude control functions, but limited in +X maneuver capability to velocity changes of $\leq$ 10 ft/sec

In the last two cases, a separate orbit maneuvering subsystem (OMS) would be required for major +X translation maneuvers with velocity changes greater than those provided by the APS. For the Subtask B, a single APS operational approach, in which the APS performs all attitude control and maneuver functions, was selected by NASA. This eliminated the requirement for a separate OMS to perform major +X translation maneuvers. Two different mission timelines for the Space Station/Base Logistics Mission were considered for Subtask B:

THRUSTER ASSEMBLY SUMMARY – ORBITER B

THRUSTER ASSEMBLY NUMBER	NUMBER OF 1850 LB_F THRUSTERS	PURPOSE
1	1	– X
2	1	– X
3	3	+ X
4	3	+ X
5	2	+ Y, + YAW
6	2	– Y, – YAW
7	1	– Z, – PITCH, – ROLL
8	1	+ Z, + PITCH, + ROLL
9	1	– Z, – PITCH, + ROLL
10	1	+ Z, + PITCH, – ROLL
11	1	– Z, + PITCH, – ROLL
12	1	+ Z, – PITCH, + ROLL
13	1	– Z, + PITCH, + ROLL
14	1	+ Z, – PITCH, – ROLL
15	2	+ Y, – YAW
16	2	– Y, + YAW

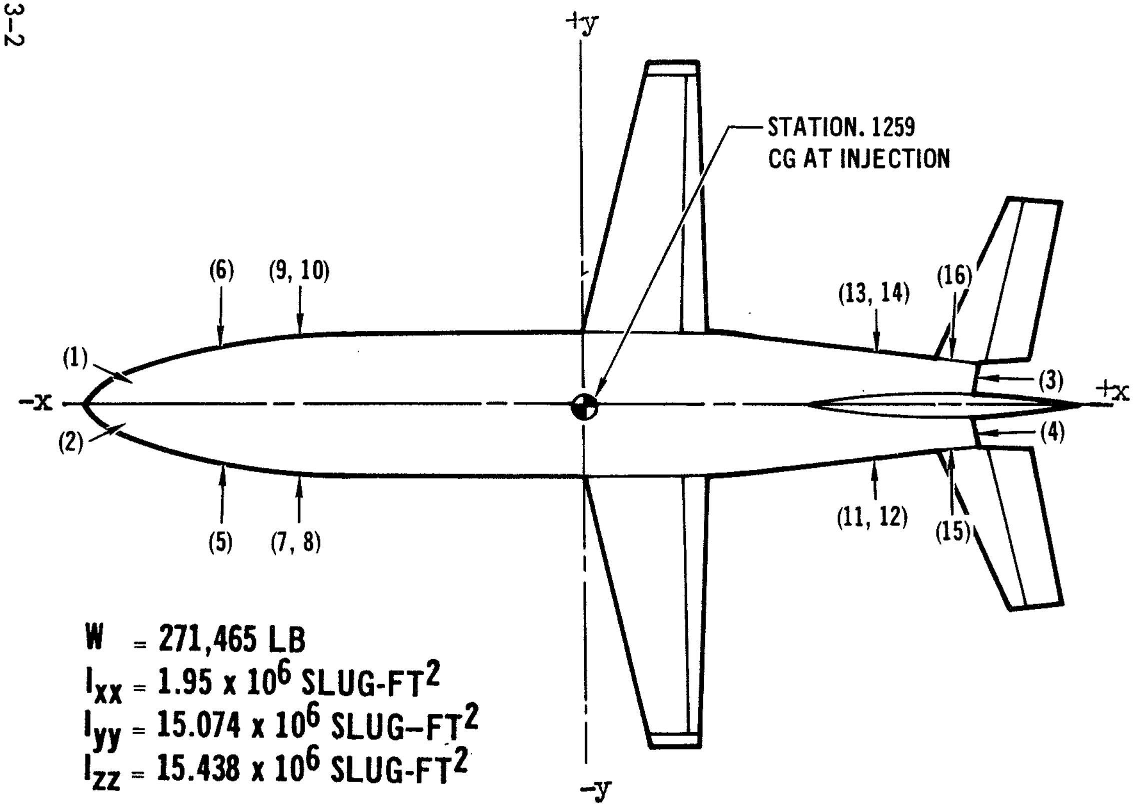

W = 271,465 LB
I_{xx} = 1.95 x 10^6 SLUG-FT^2
I_{yy} = 15.074 x 10^6 SLUG–FT^2
I_{zz} = 15.438 x 10^6 SLUG-FT^2

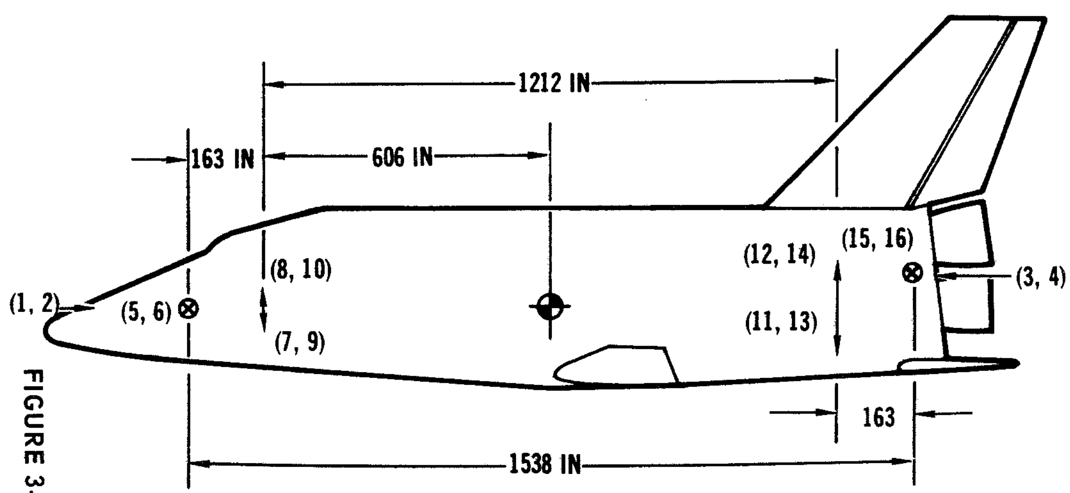

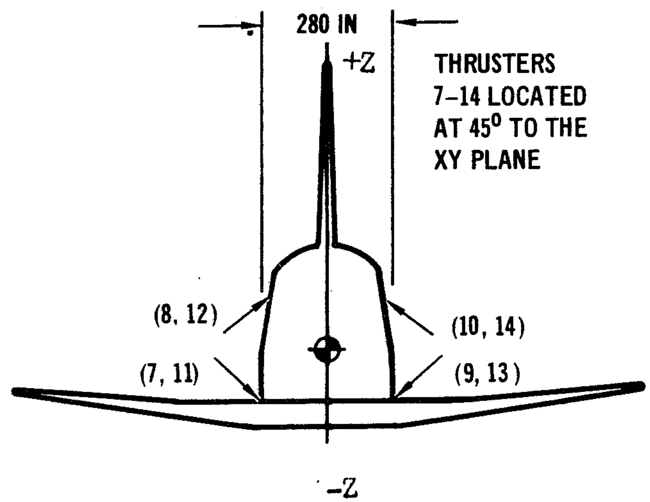

ORBITER B THRUSTER LOCATIONS

FIGURE 3–1

$W = 273{,}644$ LB
$I_{xx} = 2.059 \times 10^6$ SLUG–FT^2
$I_{yy} = 13.607 \times 10^6$ SLUG–FT^2
$I_{zz} = 14.433 \times 10^6$ SLUG–FT^2

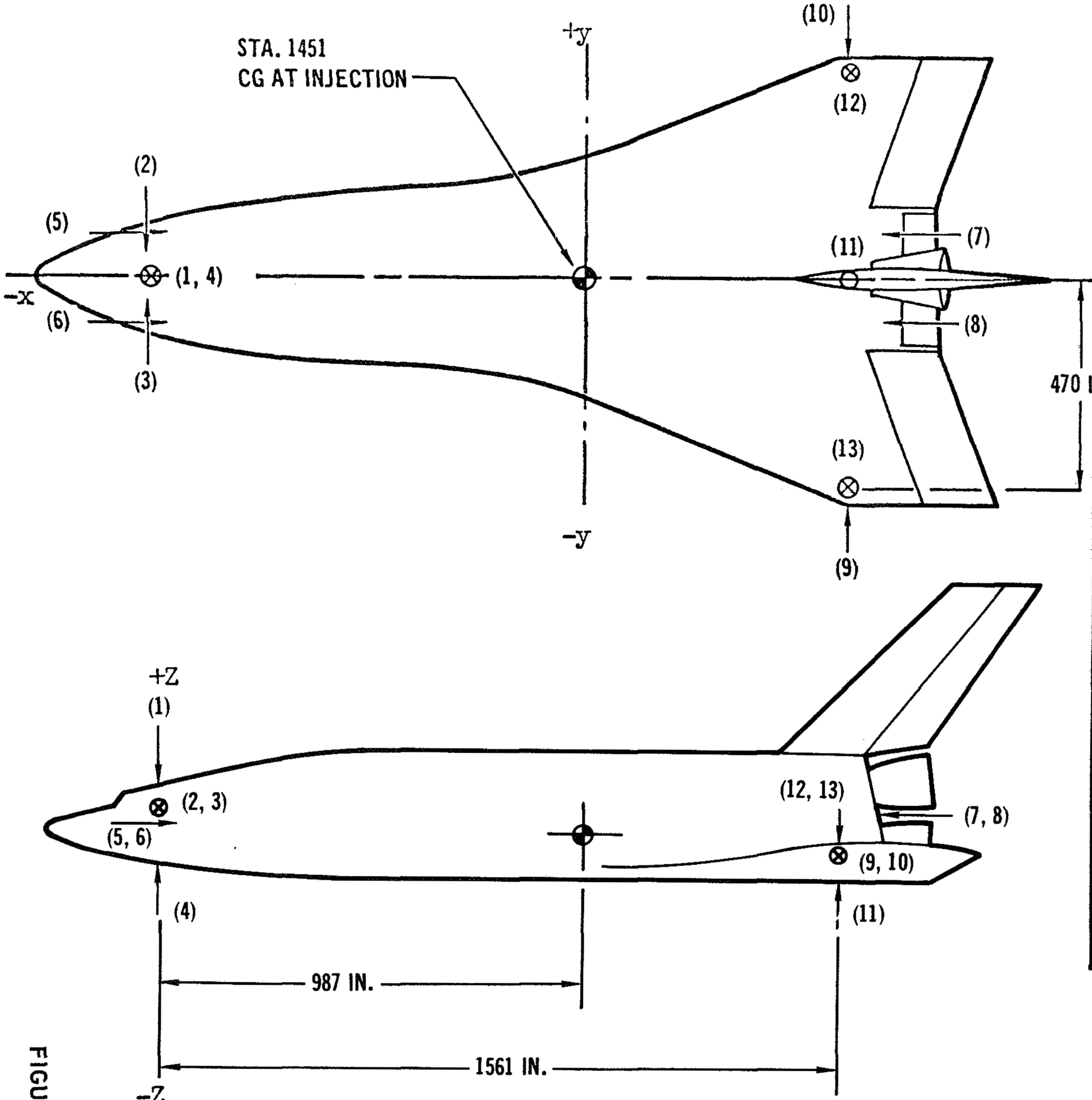

THRUSTER ASSEMBLY SUMMARY – ORBITER C

THRUSTER ASSEMBLY NUMBER	NUMBER OF 1850 LBF THRUSTERS	
1	3	–Z, – PITCH
2	2	–Y, – YAW
3	2	+Y, + YAW
4	3	+Z, + PITCH
5	1	– X
6	1	– X
7	3	+ X
8	3	+ X
9	3	+ Y, – YAW
10	3	– Y, + YAW
11	3	+ Z, ± ROLL, – PITCH
12	3	– Z, + ROLL, + PITCH
13	3	– Z, – ROLL, + PITCH

ORBITER C THRUSTER LOCATIONS

FIGURE 3–2

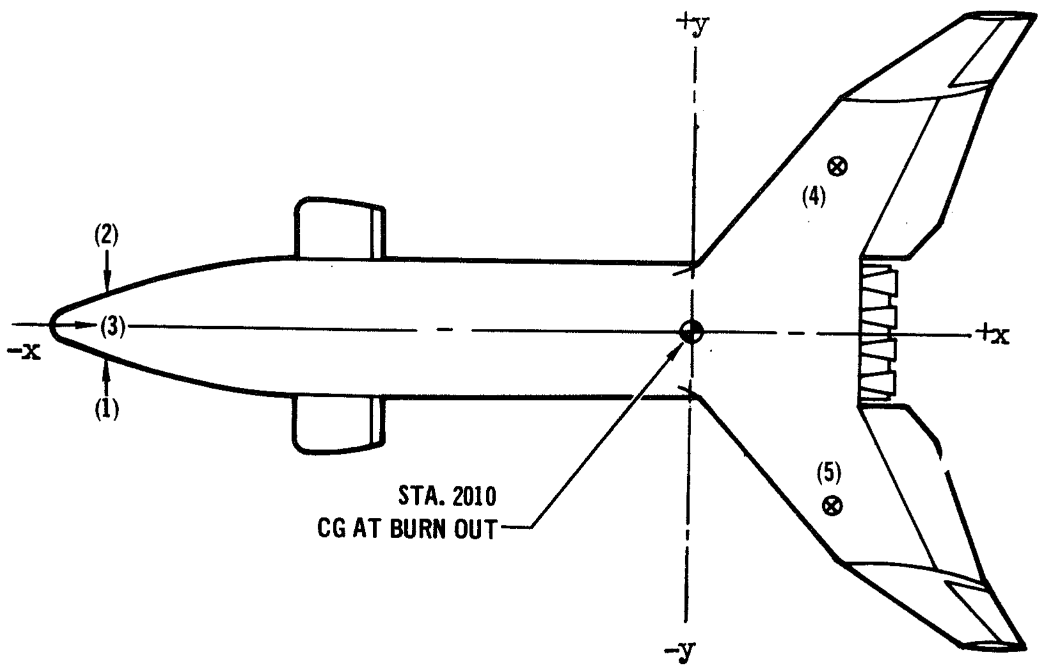

THRUSTER ASSEMBLY SUMMARY – BOOSTER

THRUSTER ASSEMBLY NUMBER	NUMBER OF 1850 LB_F THRUSTERS	PURPOSE
1	4	+ YAW
2	4	– YAW
3	4	– PITCH, ± ROLL
4	3	+ PITCH, + ROLL
5	3	+ PITCH, – ROLL

W = 474,876 LB
I_{xx} = 7.017 x 10^6 SLUG–FT^2
I_{yy} = 53.918 x 10^6 SLUG–FT^2
I_{zz} = 57.013 x 10^6 SLUG–FT^2

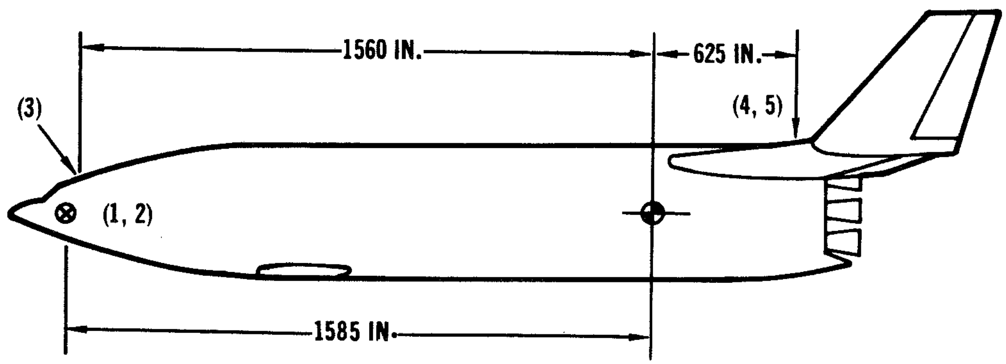

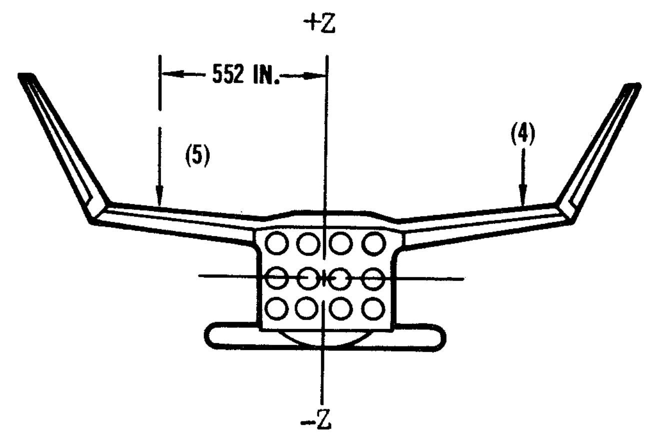

BOOSTER THRUSTER LOCATIONS

FIGURE 3–3

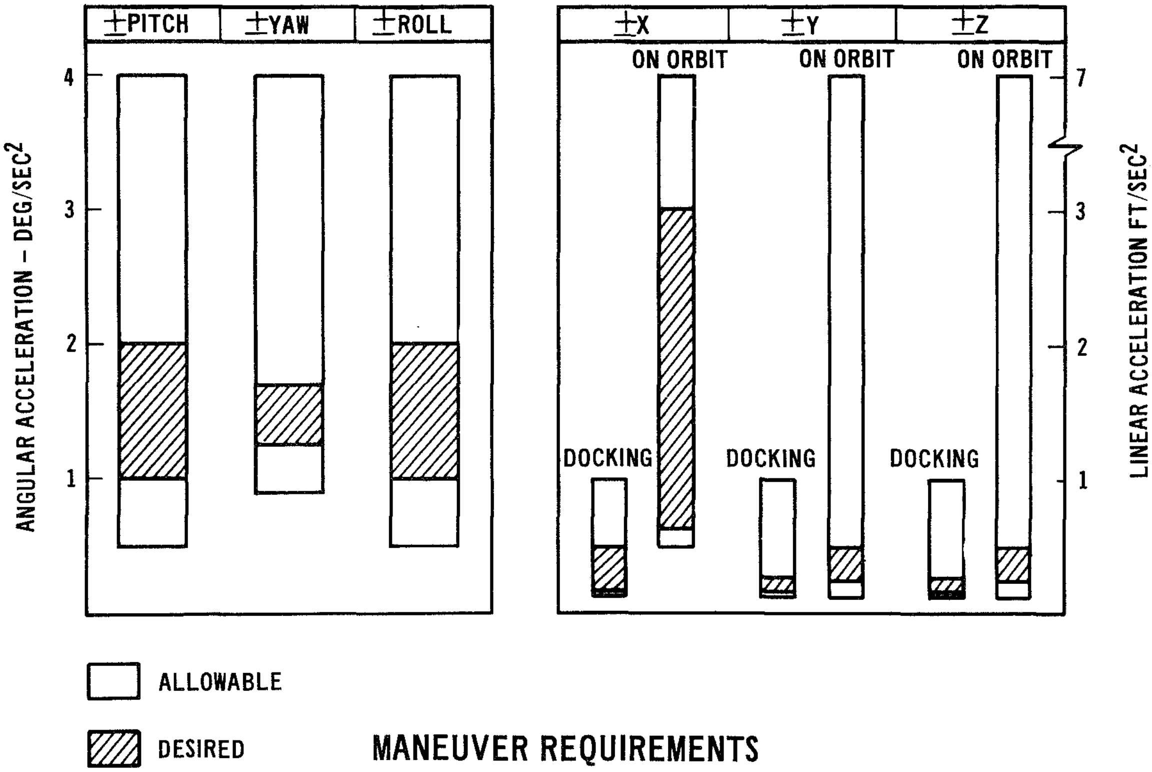

MANEUVER REQUIREMENTS
Orbiters B and C

FIGURE 3-4

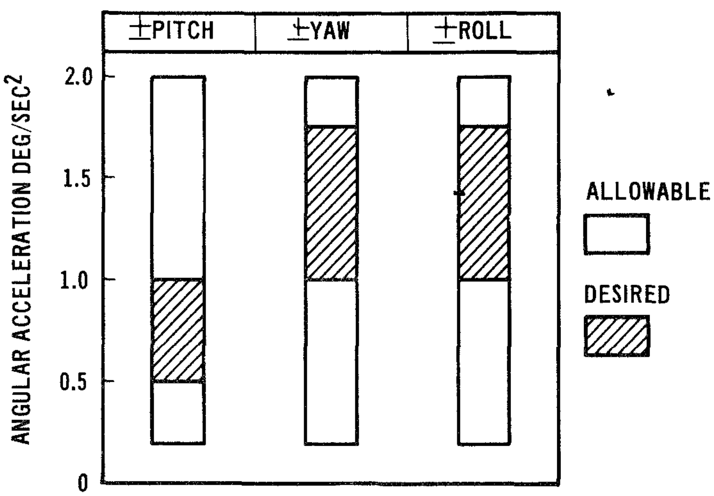

BOOSTER MANEUVER REQUIREMENTS

FIGURE 3-5

	THRUST LEVEL	NUMBER OF THRUSTERS	TOTAL IMPULSE (10^6 LB SEC)	
			BOOSTER	ORBITER
ORBITER B	1850	24		12.666*
BOOSTER	1850	18	0.860	
ORBITER C	1850	33		12.766*

* 100 LB-SEC MINIMUM IMPULSE BIT
17TH ORBIT RENDEZVOUS

REQUIREMENTS SUMMARY
Subtask B

FIGURE 3-6

(1) an early, or third, orbit rendezvous, and

(2) a late, or seventeenth, orbit rendezvous.

APS total impulse requirements for these baseline missions are shown in Figure 3-7 for both orbiters and the booster.

	MIB*	ORBITER B		ORBITER C		BOOSTER
		3RD ORBIT RENDEZVOUS	17TH ORBIT RENDEZVOUS	3RD ORBIT RENDEZVOUS	17TH ORBIT RENDEZVOUS	
ATTITUDE CONTROL	50 100 150	60,800 243,200 547,200	66,900 267,600 602,100	99,300 397,200 893,700	109,200 436,800 982,800	**
ATTITUDE MANEUVERING		843,000	861,000	702,400	720,700	864,000
TRANSLATION MANEUVERS		11,229,000	11,537,000	11,290,000	11,608,000	***
TOTAL	50 100 150	12,124,000 12,306,000 12,610,000	12,665,000 12,666,000 13,000,000	12,092,000 12,390,000 12,886,000	12,438,000 12,766,000 13,312,000	864,000

*MIB-MINIMUM IMPULSE BIT PER THRUSTER - LBF SEC/THRUSTER
**NEGLIGIBLE
***NO REQUIREMENT

IMPULSE TOTALS

FIGURE 3-7

4. APS DESCRIPTION

As noted, Subtask A results indicated the turbopump concept was the preferred ıbsystem for the booster and orbiters studied. A simplified schematic of the ydrogen side of the resulting subsystem is presented in Figure 4-1. The schematic f the oxygen side is similar. The components and assemblies making up the turbo-ımp concept were reevaluated in detail during this study phase to reflect updated equirements and to ensure that the preliminary design was best suited to the APS. ıese detailed studies and trade offs resulted in new design concepts for the APS onditioner and thruster assemblies and refined designs for other components and ssemblies. The propellant is stored as a liquid, conditioned to the required ressure and temperature by the gas generator, turbopump, and heat exchanger ssemblies and stored in an accumulator. The thruster assemblies operate from the ccumulator as stored gas bipropellant rocket engines operating at regulated inlet ressure conditions.

Figure 4-2 presents a simplified schematic of the final hydrogen side turbopump S as defined by this study. The schematic for the oxygen side is similar. The bsystem consists of four separate assemblies:

(1) thruster assemblies
(2) accumulators and feedline assembly
(3) conditioning assembly
(4) propellant storage assembly.

The accumulators decouple the thruster assemblies from the conditioning assem-lies and provide sufficient gas storage capability to limit the number of condi-ioner assembly starts to a reasonable number.

The conditioner assemblies are sized to provide a flow rate which is equivalent the flow rate of the maximum number of thruster that can operate at any given ime. These assemblies consist of a single 2000°R bipropellant gas generator, a onventional turbopump, and a reburn heat exchanger. All gas generator products e first passed through the turbopump, where the energy required to raise the iquid propellant pressure and provide flow rate required is extracted. The ıel-rich gasses are then directed to the heat exchanger where supplemental xygen is added to provide the energy required to convert the liquid propellant to

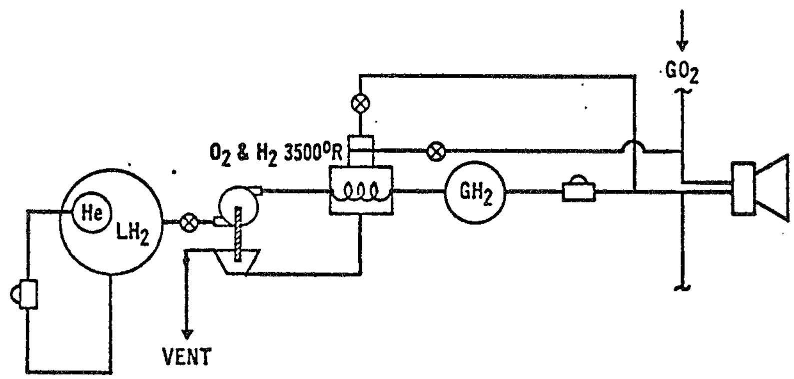

FILM COOLED THRUSTER

SUBTASK A SELECTED CONFIGURATION TURBOPUMP WITH 3500°R GAS GENERATOR/HEAT EXCHANGER

FIGURE 4–1

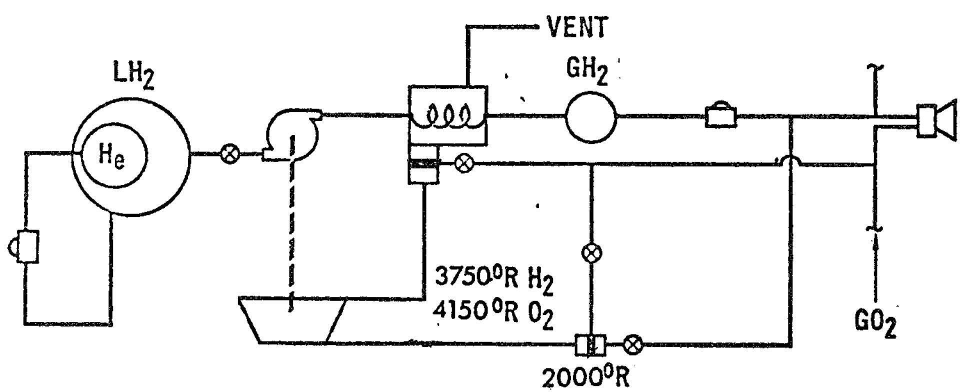

REGENERATIVE/FILM COOLED THRUSTER

FINAL APS CONFIGURATION
TURBOPUMP WITH REBURN HEAT EXCHANGER

FIGURE 4–2

gas at the desired temperature. The exhaust products are discharged from the vehicle either through opposing nozzles to eliminate disturbance forces or, if a +X axis maneuver is in process, through an aft directed convergent-divergent nozzle to provide useful +X impulse.

The propellant tankage assembly operates similarly to conventional storable propellant tankage. Pressure within the tank is maintained by mechanical regulation of the helium pressure supply. Propellants are maintained in a liquid stage by a combination of high performance insulation and propellant vaporization. Normal on-orbit heating is absorbed by a coolant loop in which propellant is extracted from the tank, and passed over the outer shell, where the heat leak is taken up by the propellant heat of vaporization. Propellants are maintained at the tank outlet by a surface tension screen device. This device provides positive propellant positioning in zero g or during low-g operation in any vehicle direction.

The following paragraphs provide a summary of the alternate design approaches considered for each APS assembly, a description of the designs selected, and the rationale for selection.

4.1 <u>APS Thruster Assemblies</u> - The APS uses gaseous hydrogen-oxygen thrusters to provide the impulse necessary for vehicle control and maneuver functions. In Subtask A a film cooled thruster assembly was used for the APS concept trade studies. During Subtask B, a detailed analysis of thruster design and performance including an evaluation of alternate cooling methods was conducted to ensure minimum weight APS design. This evaluation resulted in a selection of thruster design using regenerative cooling in conjunction with film cooling, providing an improvement in thruster specific impulse while satisfying cycle life requirements. A sketch of the selected thruster design is shown in Figure 4-3 and Appendix D-7 discusses the factors leading to design selection in more detail.

The primary components of the APS thruster are the propellant injector, combustion chamber, igniter, and propellant controls. The injector is an impinging coaxial design which is a variation of the more conventional coaxial element. In this design, hydrogen is injected normal to the axially directed oxidizer stream. Hydrogen propellant regeneratively cools the combustion chamber and the nozzle to the 11:1 area ratio, flowing forward in a single pass concept through channels toward the injector. A film cooled nozzle skirt is attached at the 11:1 area ratio. The igniter subassembly consists of a separate high-response bipropellant valve, a cooled ignition chamber, and a spark plug. Primary propellant flow to the thruster is controlled by a linked, parallel poppet valve actuated by gaseous hydrogen from

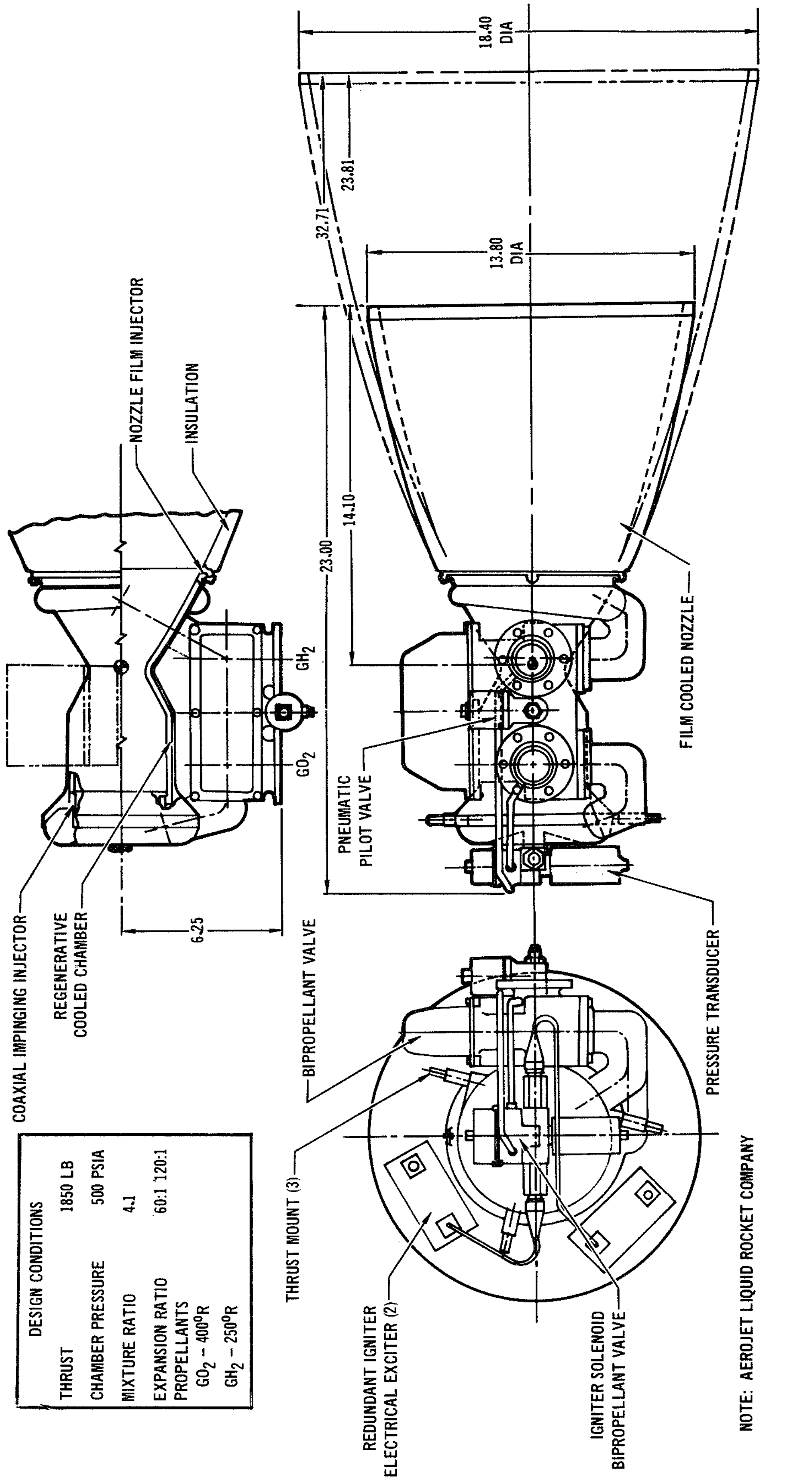

HIGH PRESSURE APS THRUSTER

FIGURE 4–3

the propellant system. Appendix D-7 provides a more detailed description of a thruster design and provides thruster performance data.

In conjunction with selection of the thruster design, a separate study was performed to explore the advantage of tailoring thruster designs to their vehicle functions (i.e., translation or attitude control). Since about 90% of the APS total impulse requirement is expended in +X translation maneuvers, it was potentially advantageous to use thrusters individually designed to provide maximum specific impulse for the +X translation functions. Investigated were:

(1) thrusters using gaseous oxygen and hydrogen, but with increased nozzle expansion ratio

(2) thrusters with increased expansion ratio, designed to operate with liquid hydrogen and gaseous oxygen

(3) thrusters with increased expansion ratio, designed to operate with liquid hydrogen and liquid oxygen.

The above options represent a continuous improvement in subsystem specific impulse at the expense of increased development effort, because each design is progressively a greater design deviation from a common attitude control thruster.

Based on comparison of APS weights and complexity using these alternates it was concluded that while the concepts using liquid hydrogen could provide weight savings, their advantage was offset by the need for development of two different thruster assemblies, i.e., both gas and liquid engines. However, the first option represented only a minimal change to the basic design as it used gaseous propellants; no changes were required in the combustion/cooling portions of the thruster assembly. The weight reduction that could be realized by this simple change in nozzle skirt size were considered to outweigh the small penalties associated with thruster commonality deviation and it was selected for incorporation in the design. Based on overall APS weight exchanges, expansion ratios of 120:1 and 60:1 were selected for the translation and attitude control thrusters, respectively. Appendix D-8 provides details on the design assumptions in this analysis, showing weight changes which result from alternate design approaches.

4.2 Accumulators and Feedline Assembly - The APS requires that conditioned propellant be available at all times for reliable and responsive thruster operation. This is accomplished by the use of accumulators, which store gaseous hydrogen and oxygen propellants, and the feedline assembly, which distributes the propellants to the thrusters.

The accumulators are the most significant weight element in this assembly.

They consist of spherical pressure vessels which operate in a blowdown pressure mode between a maximum and minimum pressure level and are recharged periodically during the mission by the conditioner assembly. Accumulators are sized to provide sufficient total impulse between the lower switch pressure level and minimum operating pressure to deliver maximum thrust over the time period required for conditioner start up. Accumulator maximum pressure limit is established by consideration of the number of recharge cycles desired in a mission. The higher the pressure, the fewer the cycles. These requirements combine to define a combination of accumulator design pressure levels and an accumulator volume which result in a minimum APS weight. Appendix D-6 provides a detailed description of the analyses used to define accumulator design, and shows that for the APS requirements and the conditioner assembly start characteristics, a minimum APS weight is provided at an overall accumulator pressure ratio of 2.26:1 (maximum to minimum), with accumulator volumes of 29 and 12 ft^3 for hydrogen and oxygen, respectively.

Feedline assembly configurations used were representative of actual installations; therefore, their weight and influence on APS design were realistically assessed. Line diameters were based on tradeoffs between weight reductions for smaller lines and weight penalties in the accumulators and conditioners with increased line pressure loss. Line lengths and routing were determined from installation layout studies described in Appendix C. Another factor of significance in feedline definition is the amount of propellant heating that occurs in the lines between accumulators and thruster assemblies. Heat transfer into the gaseous propellant will result in differences in thruster inlet propellant density with attendant thrust and mixture ratio excursions. To minimize these excursions the lines must be insulated. Two alternate means of insulation were considered:

1) vacuum jacketed lines
2) lines insulated with high performance, multi-layer mylar insulation protected by a flexible cover.

Comparison of the weight and complexity of these two approaches showed that vacuum-jacketing would result in high weight penalties and the installation would be quite complex. For this reason, the flexible jacket approach was selected for feedline insulation.

4.3 Conditioner Assembly - The conditioner concept selected during the Subtask A studies used a 3500°R gas generator to provide the energy required for turbopump operation in series with downstream propellant conditioning heat exchanger. A more detailed analysis of conditioner assembly integration and component requirements for this conditioner during Subtask B showed that the power requirements of the hydrogen pump could not be matched to the power capability of the turbine without significant increases in conditioner bypass flow and/or reductions in chamber pressure. Both these changes resulted in increased APS weight; therefore, to ensure a minimum weight APS several alternate concepts including the above changes to the Subtask A concept were evaluated. Alternate conditioner concepts were:

(1) an active propulsive vent with 2000°R gas generator

(2) two heat exchangers which allow turbine flow to be extracted at higher temperatures midpoint in the conditioning cycle,

(3) a separate 2000°R gas generator to power the turbopump and a reburn heat exchanger for propellant conditioning

(4) cold turbines which are powered by the conditioned propellant.

In this evaluation, weight increment associated with each concept relative to the Subtask A baseline was determined and the concepts were assessed to establish relative technology, simplicity and flexibility considerations. Appendix D-2 provides both a detailed discussion of the alternate conditioner concepts and the quantitative results used in making this selection. From this evaluatory process, the reburn heat exchanger was selected.

The revised conditioner concept uses a single 2000°R gas generator in each conditioner. Exhaust products from this generator are used first to drive the turbopump, then the turbine exhaust is directed to the heat exchanger, where supplemental oxygen is added to increase heat release and improve overall assembly performance.

Three approaches to the control of the heat exchanger flow and pressure during accumulator recharge were evaluated for the revised conditioner concept. The turbopump design conditions depend upon the approach used for conditioner control during recharge. Control during +X translation operation is described in paragraph 5.0.

The approaches considered were:

(1) a fixed conditioner operating point, in which conditioner flow rate and pressure were invariant during accumulator recharge

(2) a fixed conditioner flow rate, in which conditioner flow was maintained constant and turbine power was increased to provide accumulator recharge

(3) a fixed turbine power, in which turbine power was maintained constant and conditioner flow was allowed to decrease during recharge.

Since each control concept affected the conditioner design points and thus influenced APS weight, the APS was optimized for the three control concepts. Two constraints to the minimum weight operating point were:

(1) a minimum turbine discharge pressure of 30 lbf/in^2a to allow sea level testing of the heat exchanger and turbine

(2) a heat exchanger discharge temperature of 800^oR minimum to preclude H_2O condensation in the vent assembly.

These constraints were met by varying the amount of supplemental oxygen. Details of this comparison are presented in Appendix D-2. From this comparison, a control concept was selected in which the conditioner is designed to operate at constant turbine power and provides the maximum steady state thruster flow at the minimum accumulator pressure.

This control concept resulted in the best compromise between control complexity and APS weight. For the selected control concept APS weight optimized at a chamber pressure of 500 lbf/in^2a and overall conditioner mixture ratios were 2.55 and 2.69 for hydrogen and oxygen conditioning, respectively.

The baseline designs for the turbopump, gas generator and reburn heat exchanger which are required by the conditioner assembly are presented in the following paragraphs.

4.3.1 Turbopump Subassembly - In the selected conditioner design, the turbopumps are required to provide maximum flow at minimum accumulator pressure. Since turbine power is maintained constant during recharge, pump flow is reduced and speed is increased as accumulator pressure is increased. The detailed design and performance of the turbopumps are provided in Appendix D-3.

The selected turbopumps use pressure compounded, axial flow turbines, and centrifugal pumps. The LO_2 assembly uses a single-stage pump and a two-stage turbine, while the LH_2 assembly uses a two-stage pump and three-stage turbine. Pump impeller and turbine rotor are mounted on a common shaft, supported by propellent cooled/lubricated bearings. Figure 4-4 and 4-5 present sketches of the turbopump subassemblies. Turbopump design and performance were established after a detailed evaluation was performed to compare the capability of several designs. Pump and turbine steady state efficiencies were investigated in detail since these affect the APS bypass flow requirements. An efficiency of 40 percent at steady-state operating condition was selected as a design value for both pumps. This

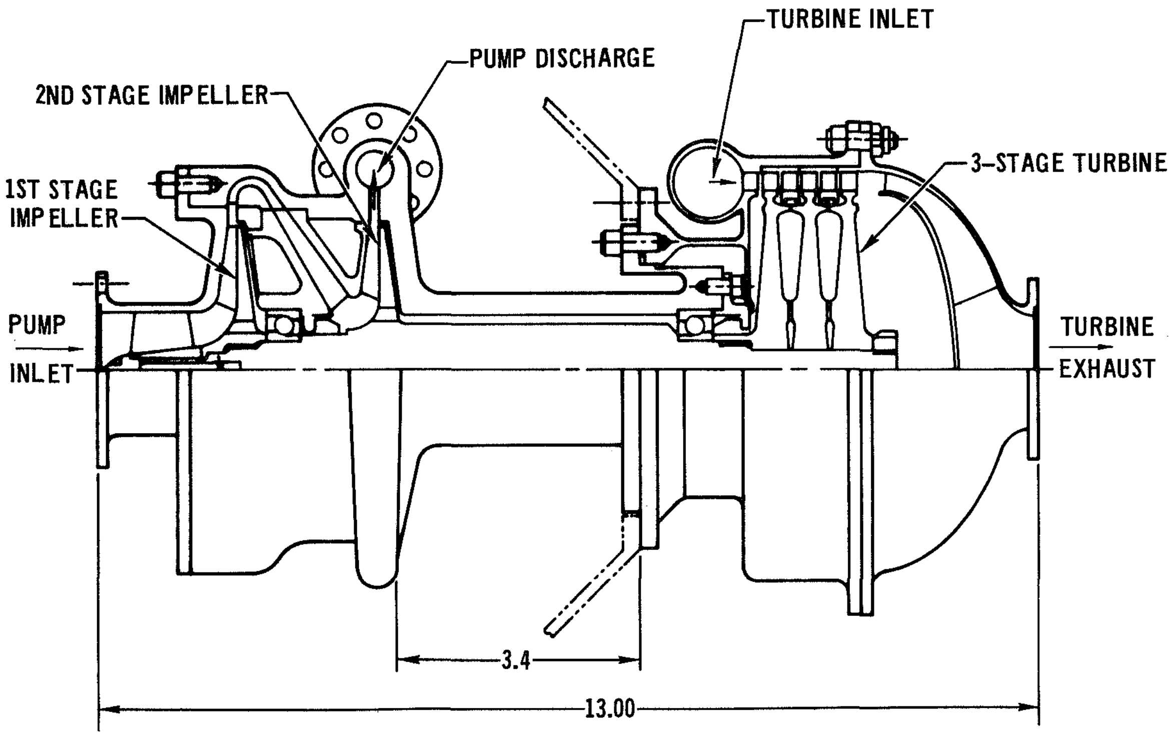

APS LH_2 TURBOPUMP

FIGURE 4-4

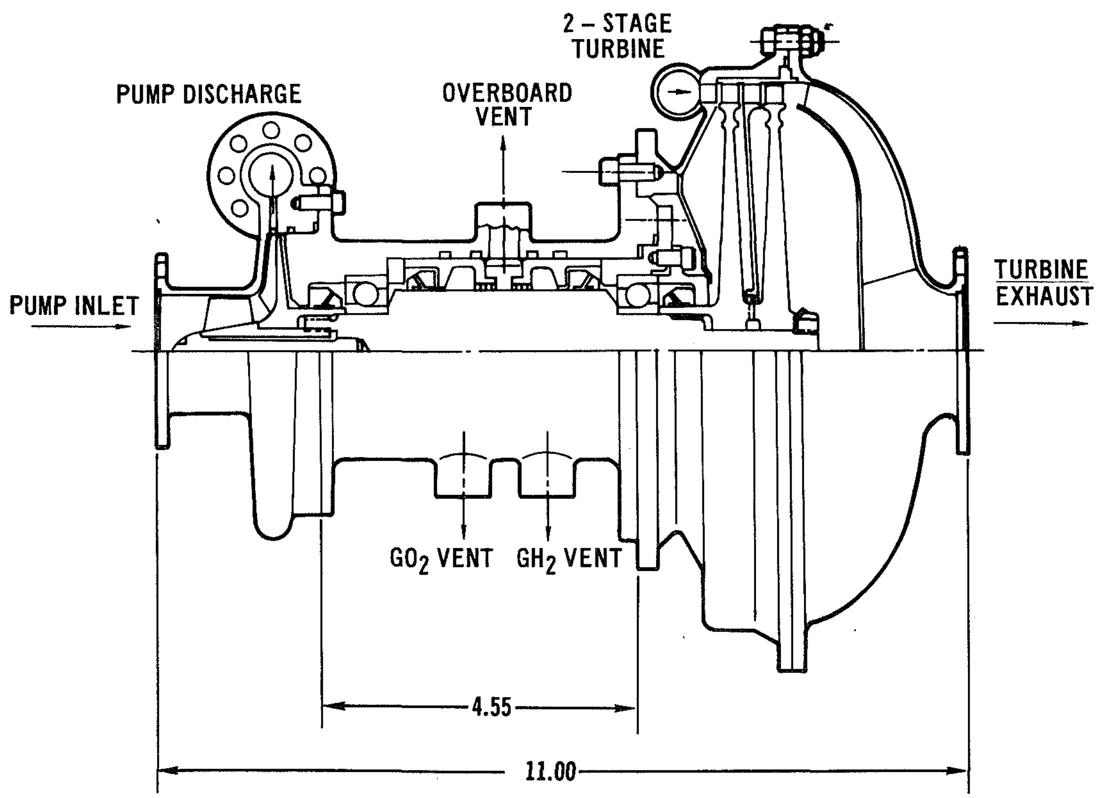

APS LO_2 TURBOPUMP

FIGURE 4-5

efficiency is less than the maximum available, but provides a design margin, and limits heat exchanger flow excursion during recharge.

The turbopump assemblies are actively cooled by hydrogen tank vent gas which is passed through a tubular heat exchanger mounted on the pump enclosure. In addition, a heat short from the turbine to the structure provides pump isolation.

4.3.2 Heat Exchanger Subassembly - The APS uses reburn heat exchanger assemblies to condition the propellant to the temperatures required. The products from a 2000°R gas generator are first used to drive the turbopump subassembly and are then directed to the APS heat exchangers where supplemental oxygen is added to the fuel rich turbine exhaust and reburned to supply the energy necessary for propellant conditioning. Three types of heat exchanger concepts were considered for this function. These varied in the number of reburn cycles used and the manner of GO_2/mixture ignition. The concepts were:

(1) multistaged oxygen injection into gas mixtures below the auto-ignition temperature

(2) multistage oxygen injection into gas mixtures above the auto-ignition temperature

(3) single point oxygen addition and ignition.

The selected design uses single point oxygen addition. This concept is based on application of injector plate fabrication technology developed for staged combustion cycles. The heat exchangers reburn the fuel-rich turbine exhaust products, for the oxygen heat exchanger at a mixture ratio of 0.85, establishing a hot side temperature of approximately 4150°R. The heat exchanger must operate in this temperature environment and have a high cycle life with large cold to hot side temperature gradients. Appendix D-4 presents a comparison of alternate approaches and provides a detailed description of the operation and performance of the selected design.

Heat exchanger design is illustrated in Figure 4-6. All propellant to be conditioned enters the heat exchanger in the base. The core consists of a series of liquid propellant platelet assemblies, each separated by a hot gas flow passage. Platelet construction techniques provide controlled heat transfer coefficients for hot gas and cold propellant sides. The exploded view of the liquid propellant platelet assembly shows that the liquid propellant enters the center of the platelet, is distributed across its width, directed up its length where the flow is split and directed back down the platelet stack. Heat exchange with the hot gas

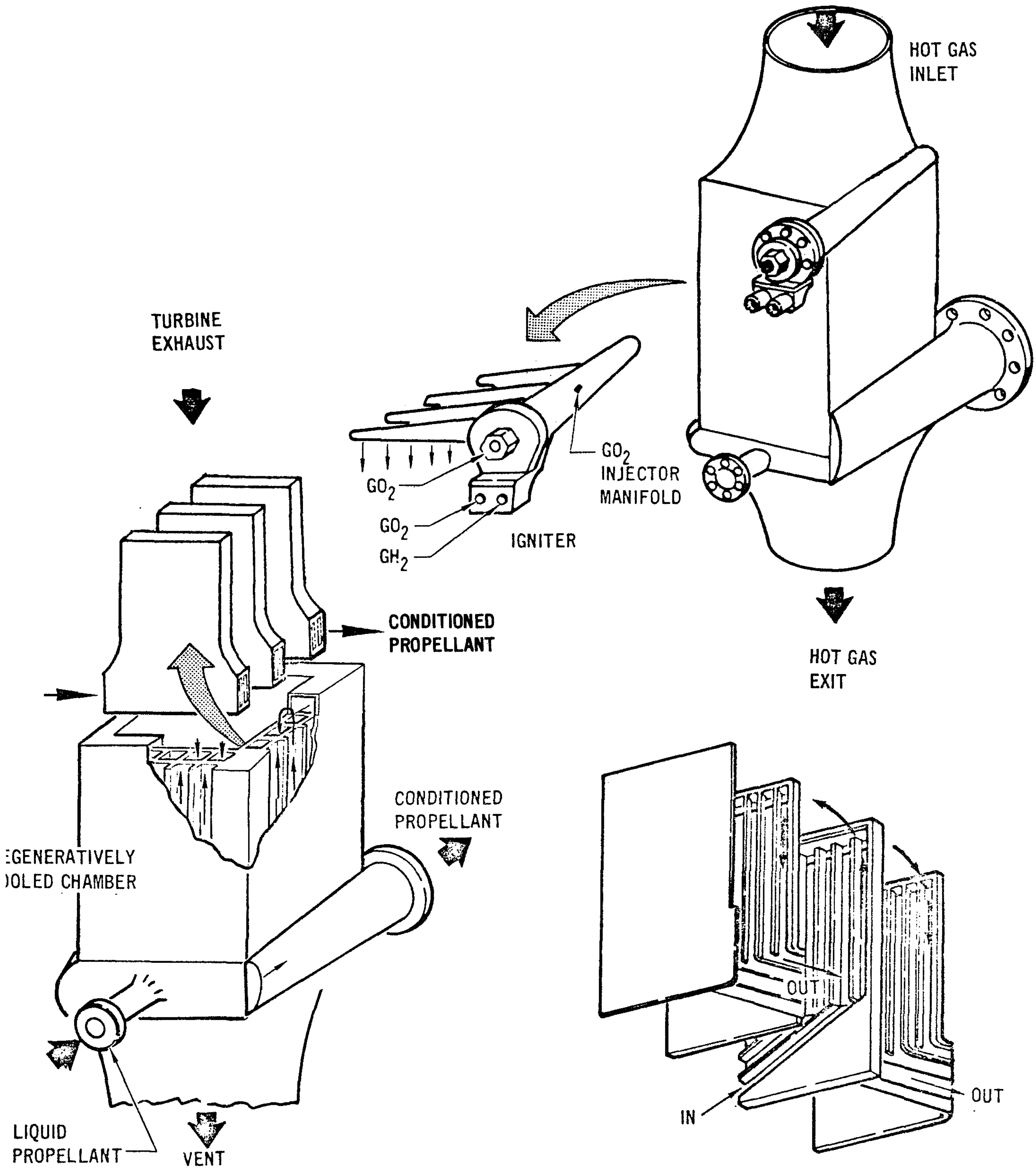

HIGH TEMPERATURE REBURN HEAT EXCHANGER

FIGURE 4–6

occurs on the downpass because the closure plate for the downpass channels is also the wall of a gas generator segment. At the bottom of the downpass, the conditioned propellant discharging from each of the platelets is gathered in a manifold assembly and directed to the accumulator.

The heat exchanger shell is regeneratively cooled and is actually one half of a main heat exchanger platelet. The liquid propellant flows up the outside passage of the shell and down the inside passage where it is conditioned. It is collected with the conditioned propellant from the main platelets.

The gas generator portion of the reburn heat exchanger is shown in Figure 4-6. The turbine exhaust gas is mixed with oxygen along the width of each gas generator panel.

A catalytic igniter in the manifold is used as the igniter source for the turbine exhaust gas/GO_2 mixture. During accumulator recharge, oxygen addition is controlled to maintain a constant propellant temperature at the heat exchanger outlet.

4.3.3 Gas Generator Subassembly - Gas generators are required to provide power for turbopump operation and energy to the reburn heat exchanger assembly. These units operate from gaseous hydrogen/oxygen propellants and provide throttling capability to limit operating temperature and to maintain accumulator pressure in the presence of varying APS flow demands. The design selected is shown in Figure 4-7. This concept employs an electrical spark igniter. The assembly operates at 2000°R combustion temperature and 500 lbf/in^2a operating pressure. Linked bipropellant valves with piloted pneumatic actuators are used. The linked valves provide fast response, added assurance of proper propellant sequencing and minimize potential mixture ratio excursions due to valve inaccuracies. Calibrated orifices, a bypass circuit and separately activated throttling valves are used to supply different power levels to the turbine upon demand. Paragraph 5.0 provides a discussion of gas generator flow control. Appendix D-5 provides more detail on gas generator design and describes performance.

4.4 Propellant Storage Assembly - The propellant storage assembly maintains the cryogenic propellants in their liquid state and positions them for delivery to the turbopumps. Three primary subassemblies are required:

(1) a propellant acquisition subassembly

(2) a thermal protection subassembly

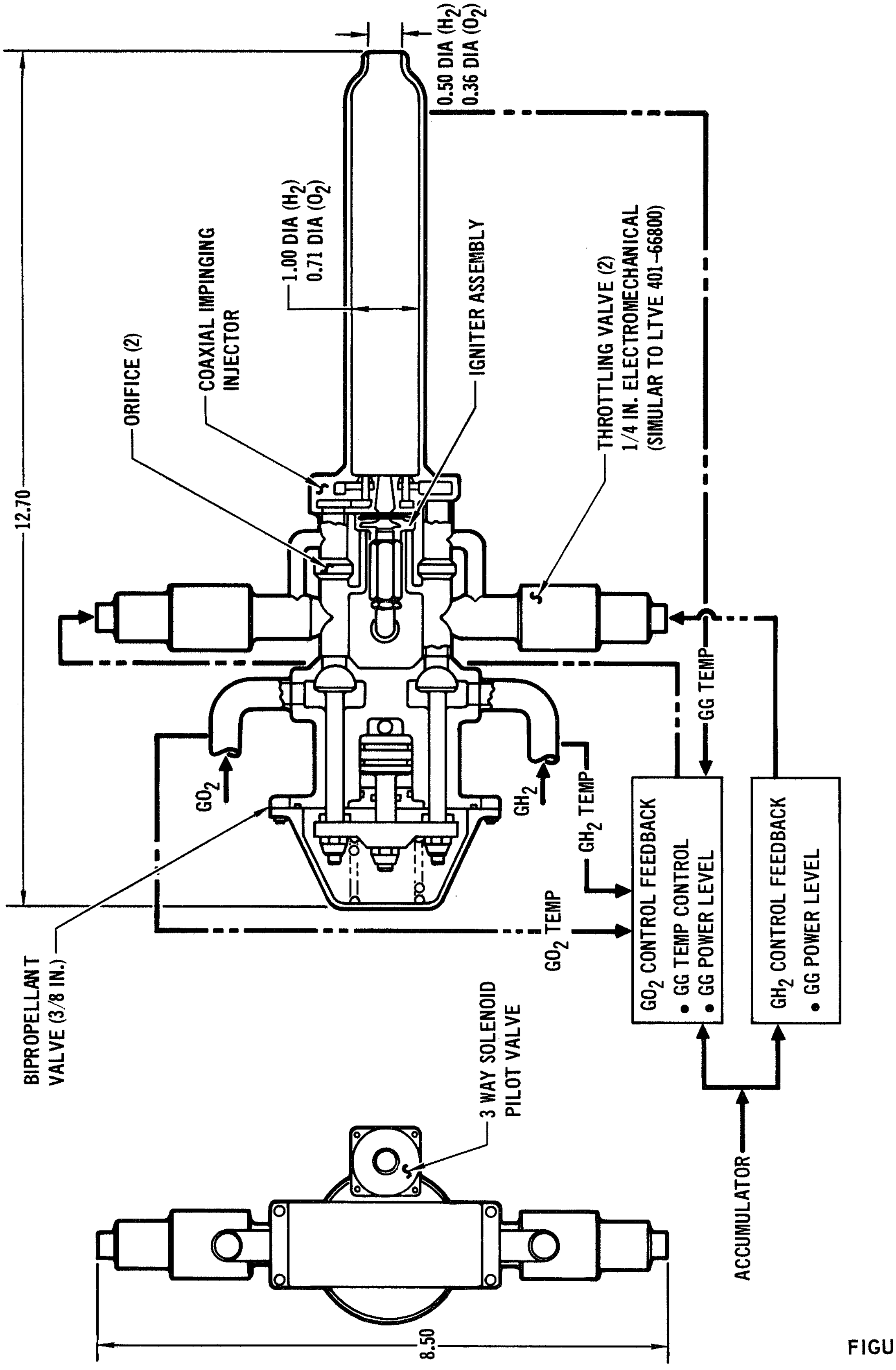

APS GAS GENERATOR

FIGURE 4-7

(3) a pressurization subassembly.

For these, several alternate approaches were available that could potentially satisfy APS requirements. Appendix D-1 provides a summary of requirements for each subassembly, compares the alternates and defines the designs selected. Appendix D-1 results are provided in the following paragraphs.

4.4.1 Propellant Acquisition Subassembly - A propellant acquisition device is required to ensure liquid outflow during low-g orbital phases of the mission. During these mission phases, vehicle acceleration will tend to randomly orient the propellant within the tank, thereby potentially uncovering the tank outlet. Some device is therefore necessary to guarantee that liquid will be retained at the outlet and to provide a flow path for communication between the liquid mass and the outlet. Of several concepts considered for this function, surface tension screen devices were the most attractive. They are passive with no moving parts, thus providing high reliability and multicycle reuse capability. Three basic screen retention concepts were evaluated:

(1) a wall orientated device

(2) a start basket

(3) a hybrid combining the above two devices.

A wall orientated device was selected.

This propellant acquisition device, shown in Figure 4-8, consists of screen channels located around the tank circumference, and a single enclosed collector manifold, which connects each channel to an outlet sump. The acquisition device will selectively pass liquid to the feed system so long as there is contact with a liquid mass. The wall oriented nature of the device ensures that contact will be made. Screen mesh and flow passage dimmensions were selected so that the pressure drop across the screen vapor/liquid interface never exceeds the screen bubble point prior to reentry. During reentry, deceleration forces will result in draining of the channels; however, these same forces will result in propellant orientation at the tank outlet.

4.4.2 Thermal Protection Subassembly - Satisfactory turbopump operation requires that the propellants be maintained as gas-free, subcooled liquids to avoid vapor ingestion and assure a net positive suction pressure at the pump inlet. To avoid excessive propellant boiloff and to prevent vaporization within the surface tension screens an efficient thermal protection subassembly must be provided. The thermal protection assembly uses high performance, multilayer, mylar insulation to reduce vaporization/boiloff loss. Also, since insulation cannot completely

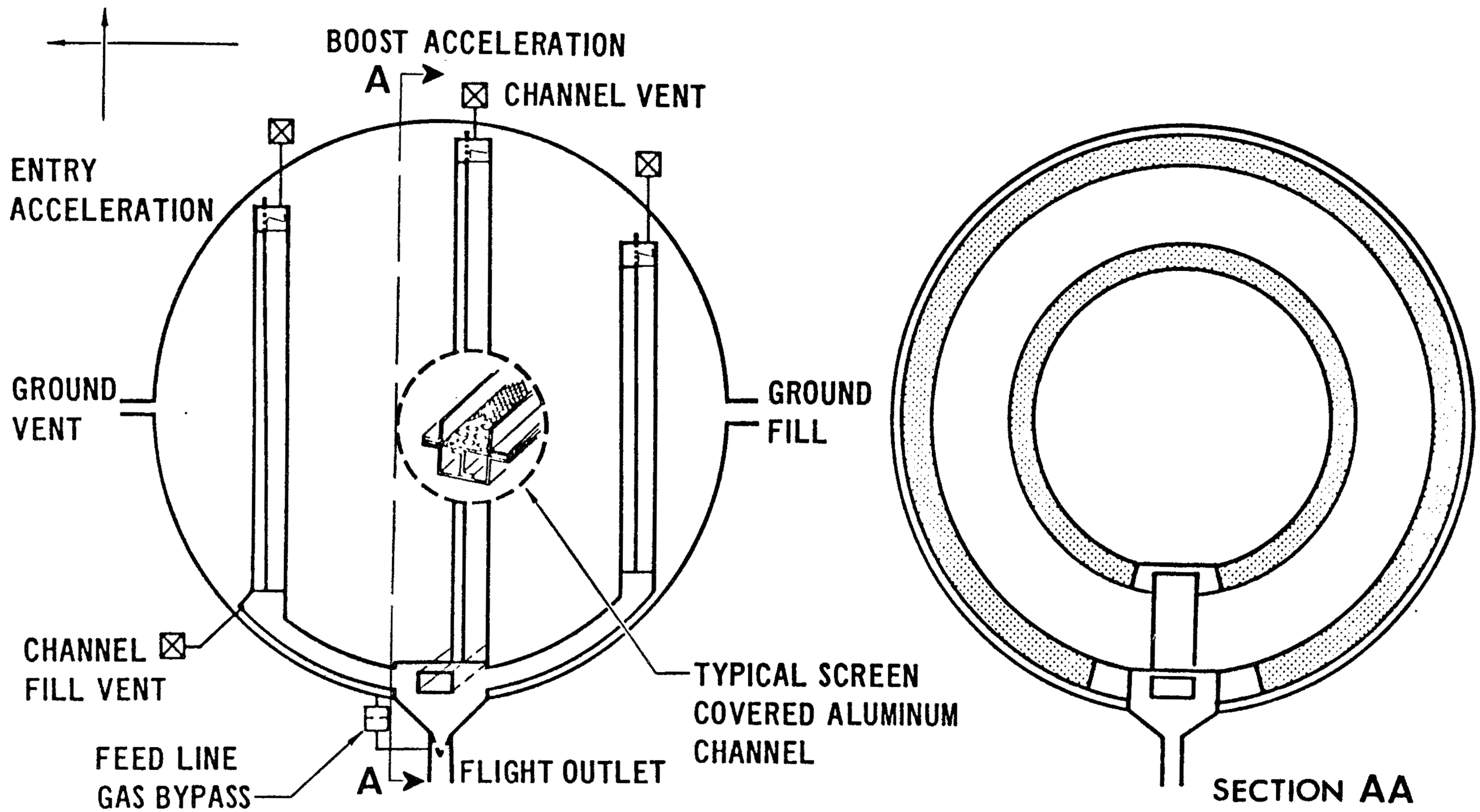

	ORBITER B	ORBITER C	BOOSTER
SCREEN SIZE	2 @ 250 x 1370 (17 μ) 1 @ 200 x 600 (40 μ)	2 @ 250 x 1370 (17 μ) 1 @ 200 x 600 (40 μ)	200 x 600 (40 μ)
CHANNEL SIZE (IN.)			
H_2	5 x 8	4 x 6	5 x 8
O_2	3 x 6	3 x 4	3 x 6

APS PROPELLANT ACQUISITION CONCEPT

FIGURE 4-8

eliminate heat leak into the tank, a heat exchanger assembly must be provided to preclude bulk liquid heating. This subassembly is shown in Figure 4-9.

Insulation protection alternates investigated were:

(1) vacuum jacketed dewars using a structural outer shell

(2) nonvacuum jacketed tanks with flexible or semirigid covers to protect the insulation.

The nonvacuum jacketed approach required noncondensable gas purging in the atmosphere to protect the insulation from water condensation damage. The dewar approach was the simplest, but the weight penalties it incurred were not considered to be justifiable and an approach requiring purge gas was selected. This approach uses a fiberglass outer shell to cover the mylar insulation. Both hydrogen and oxygen tanks use a nitrogen gas purge to prevent cryopumping during ground holds, but since nitrogen would condense at liquid hydrogen temperature, the hydrogen tank requires a layer of foam insulation to limit mylar insulation temperature. During entry, fiberglass jackets are pressurized with helium.

Three alternate heat exchangers were considered:

(1) a tubular heat exchanger mounted directly to the tank wall

(2) a tubular heat exchanger attached to a thin metal radiation shroud displaced from the tank wall.

(3) a compact heat exchanger mounted inside the tank.

The second of these options was selected. The first was considered inadequate, since it would allow temperature gradients within the tank unless circulation fans were provided. The third offered little weight advantage, and also required propellant circulation. Figure 4-10 illustrates the selected thermal protection schematic. In this approach, hydrogen is continuously circulated through cooling tubes to intercept residual heat leak through the insulation and heat short paths. Liquid hydrogen is extracted from the hydrogen tank, throttled to reduce its temperature, and then directed to the tank cooling shroud, where it absorbs heat through vaporization. The hydrogen is then used to cool the hydrogen turbopump, oxygen tank, and oxygen turbopump.

4.4.3 Pressurization Subassembly - Two candidate pressurization types were evaluated:

(1) autogenous

(2) cold helium with submerged injection.

Appendix D-1 discusses these approaches and their weight tradeoffs. The selected

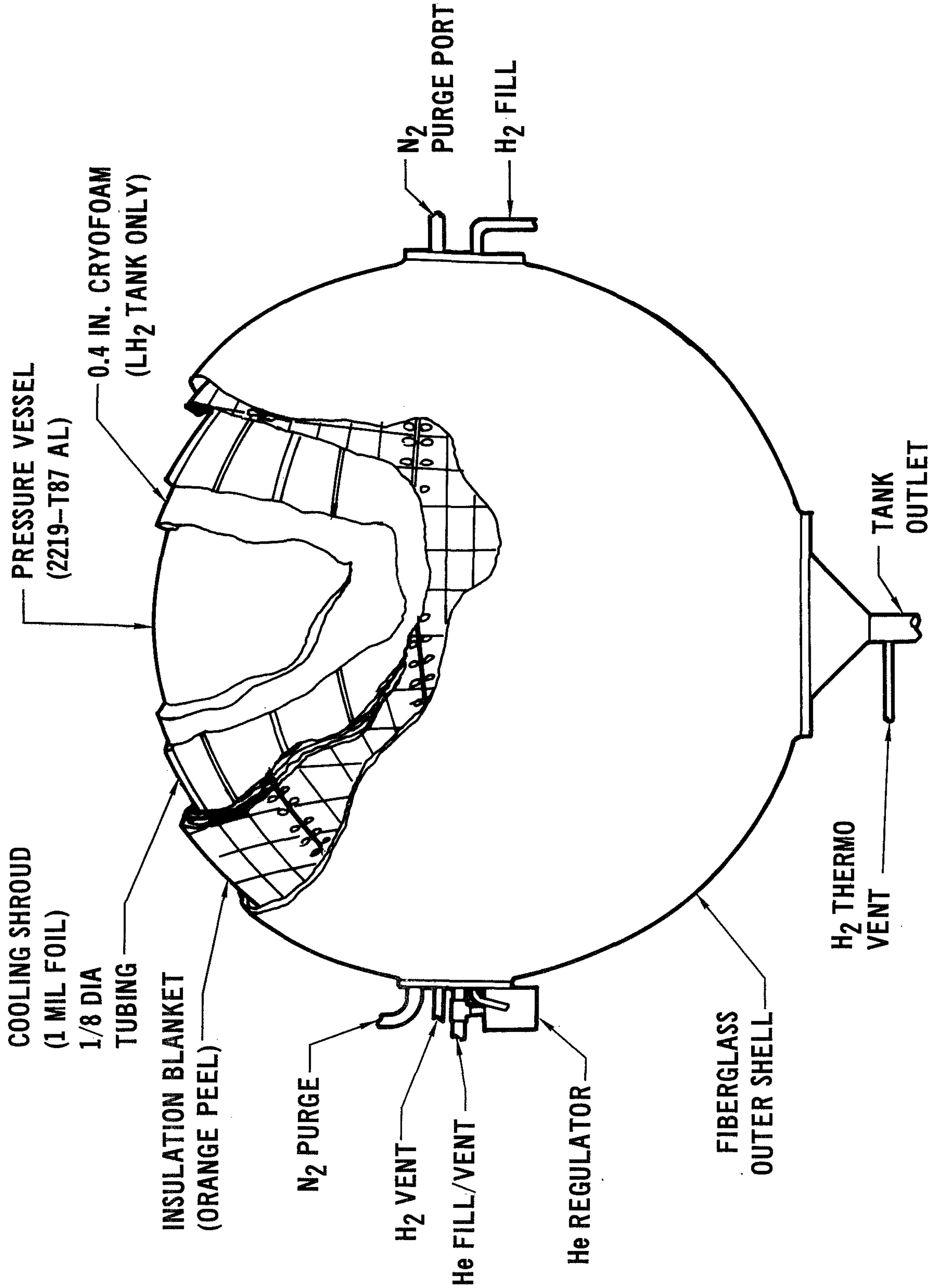

PROPELLANT TANK INSULATION/COOLING CONCEPT

FIGURE 4–9

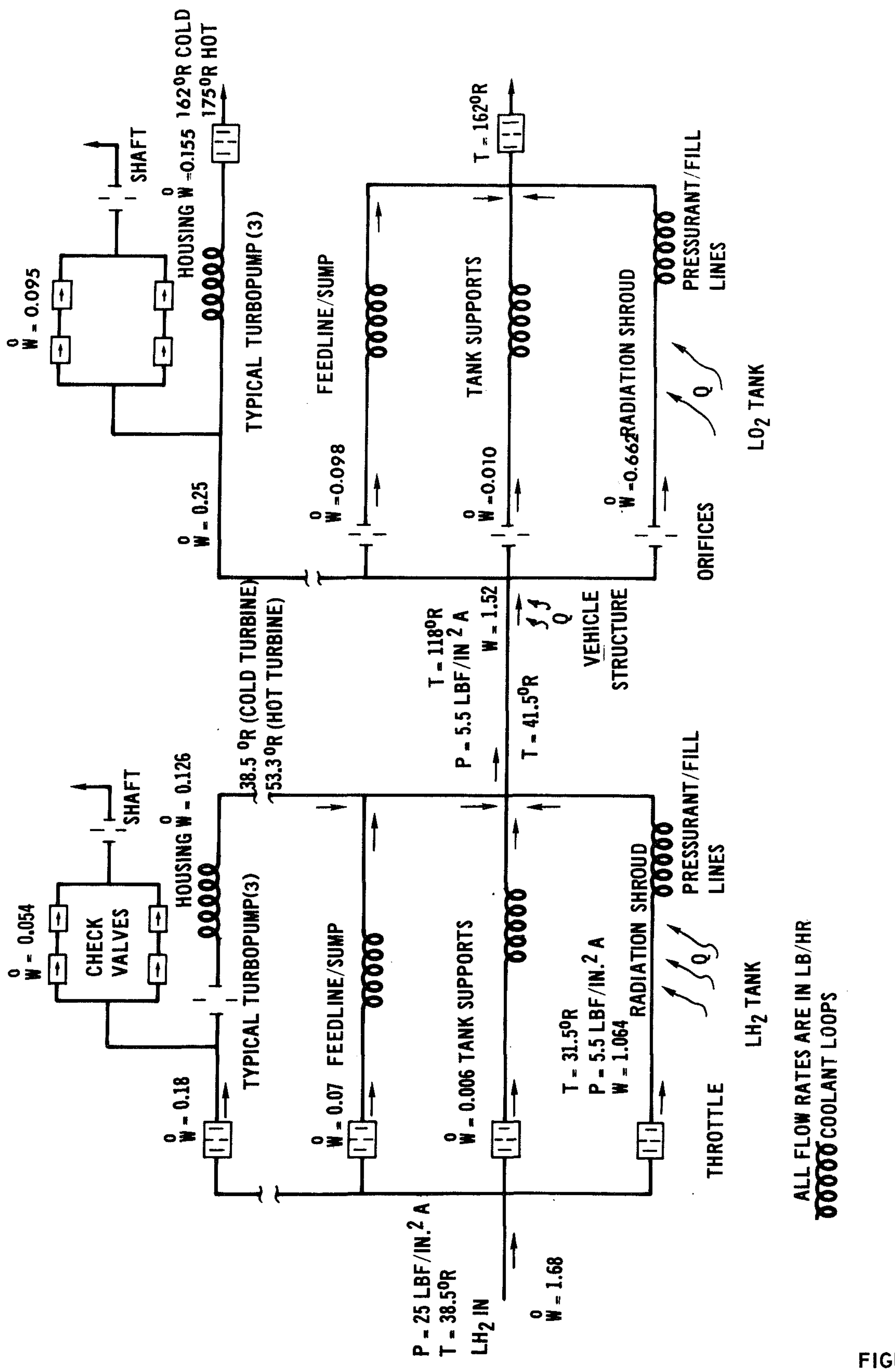

VENT SUBASSEMBLY SCHEMATIC

FIGURE 4-10

concept for the APS was cold helium using submerged helium injection, resulting in a small weight penalty which was outweighed by inherent operational simplicity and state-of-the-art technology base.

5. APS OPERATION AND CONTROL

In the selected high pressure APS, propellants are stored as liquids at low pressure, and raised to subsystem operating pressure by turbine driven pumps. Heat exchangers are employed which use hot combustion gas to condition propellants to the temperatures required for thruster operation. To avoid excessive cycling of the conditioning assembly, accumulators are provided to decouple the thrusters from the conditioners. Accumulator pressure is maintained by the conditioners, which resupply the accumulators when accumulator pressure drops below a switching pressure level. Of principal concern to this study phase is conditioner assembly control during +X translation operation.

The conditioner assembly control concept was established to satisfy three independent design criteria:

(1) rapid start transients. (The conditioner response time is a primary factor in accumulator sizing as it is directly related to accumulator volume. Slow conditioner response characteristics result in excessive accumulator weight penalties, hence high turbine power for starting was desirable.)

(2) minimum operating power. (The amount of gas generator flow required for steady state conditioner operation directly affects the effective specific impulse of the APS. Hence it was desirable to operate with minimum turbine power under normal conditions.)

(3) conditioner flow variability. (During steady state +X translation maneuvers an undefined and variable amount of propellant will be required for attitude control. Conditioners could be designed with excess flow capability but this would require additional life capability because the conditioners would cycle on-off during steady state operation. Therefore, it was desirable to control conditioner flow such that the accumulators would not recharge during +X maneuvers.)

The control concept selected to satisfy these criteria provides a maximum gas generator flow for turbopump starting and adjusts flow according to accumulator pressure during steady state operation. This is accomplished with the gas generator valves which in effect are two separate valves. One is a fast acting, pneumatically controlled on-off valve, while the other is a slower, electrically controlled, vernier throttle valve. The vernier is located downstream of the primary valve and provides up to 20 percent flow reduction according to accumulator pressure. These vernier valves also control gas generator mixture ratio by sensing combustion temperature and throttling gas generator oxygen flow to maintain proper mixture ratio (and thus turbine temperature).

APS control is illustrated in Figure 5-1. When the accumulator is fully charged, conditions are at point (A) and there is no conditioner flow at these conditions the primary gas generator valves are closed and the throttle valves are full open. With thruster usage, conditioner pressure will decay until the switching pressure is reached. The primary gas generator valves and the pump suction valves will be commanded open. Generator flow and turbine power will be a maximum (point D) and turbine spin-up is initiated. Opening the valve controlling oxygen to the heat exchanger is delayed until 50 percent of maximum turbine speed has been reached.

During the start transient, accumulator pressure will continue to decay and gas generator flow is modulated with the vernier throttle valves to control turbine power. When APS flow demands are only those corresponding to +X thruster operation, flow is controlled to provide minimum turbine power, and, thus, bypass flow at point 1. However, the conditioner must also provide the capability for attitude control thrust demands during +X thruster operation. This is accomplished by increasing generator flow (turbine power) along path 1-2 as pressure decays with increased flow demands. A resultant normal operating point (3) with attitude control demands is shown between points 1 and 2. The accumulators recharge to maximum pressure along path 1-4.

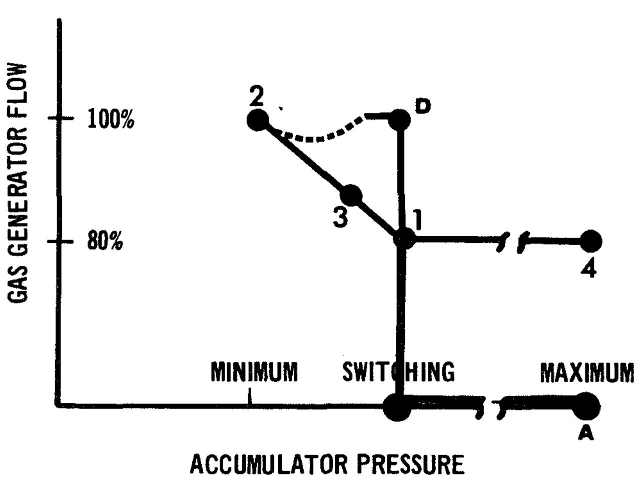

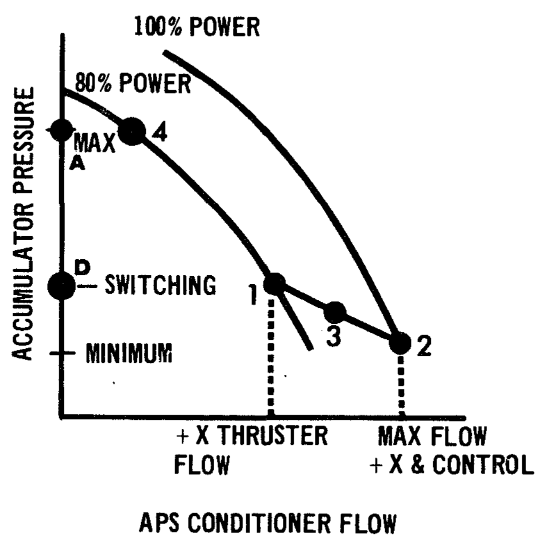

PUMP AND GAS GENERATOR VALVE OPERATION

FIGURE 5-1

6. APS DESIGN AND PERFORMANCE SUMMARY

Subtask B effort resulted in definition of design, performance and operational characteristics of the APS selected for the space shuttle high and low cross range orbiters and the booster.

APS designs were established to satisfy the vehicle control requirements of Reference (b). Figure 3-6 summarized the number of thrusters, thrust level and total impulse required for each vehicle, while Appendix A provides study results that led to these requirements. Thruster locations were illustrated in Figures 3-1, 3-2, and 3-3. These locations were established to satisfy the criteria of minimum weight, avoidance of heat shield penetration whenever possible, and use of common thrust levels between vehicles. The turbopump APS defined for the three vehicles; Orbiter B, Orbiter C and the Booster, are basically the same. The conditioning assemblies are identical for the three vehicles in configuration and operation. Minor differences result from different tank sizes and locations; line and thruster locations and vent arrangements. The following subsystem description will be addressed to Orbiter B, and except for the differences noted, also applies to Orbiter C and the Booster. The referenced report appendices provide data for all vehicles. The APS schematic for Orbiter B is shown in Figure 6-1 and defines the components required to achieve the shuttle reliability criteria. Schematic symbols are defined in Figure 6-1a. Reliability criteria and detail failure mode analyses used to establish schematics are defined in Appendix H.

Installations of the APS within the vehicles are shown in Appendix C. Component locations were defined based on the following criteria:

(1) space shuttle requirements (Reference (b))

(2) non-interference with other shuttle components

(3) accessibility for maintenance and inspection.

Subsystem design point summaries and weights are shown in Figure 6-2. These design points were developed by analyses to define APS weight sensitivity to each of the various design parameters. Appendix F summarizes the techniques applied and Figure 6-3 provides an exemplory set of weight sensitivities for Orbiter B, showing selected design points. Design points shown are for weight optimized subsystems. Component weight breakdown for these design points, and significant APS volume items, are shown in Figures 6-4. Subsystem pressure and temperature balances are also defined, along with APS pump component requirements in Figure 6-5.

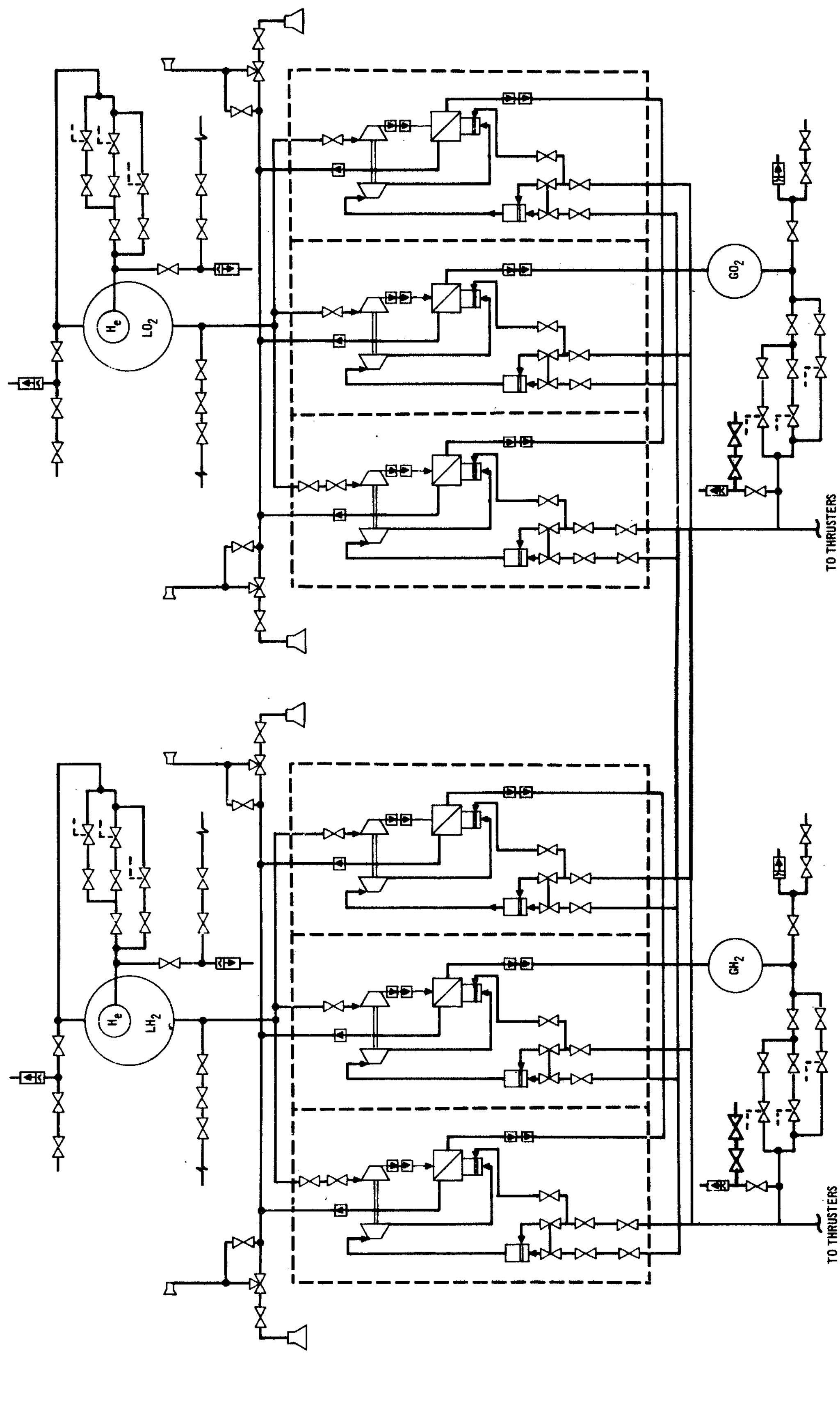

APS ORBITER B SCHEMATIC

FIGURE 6-1

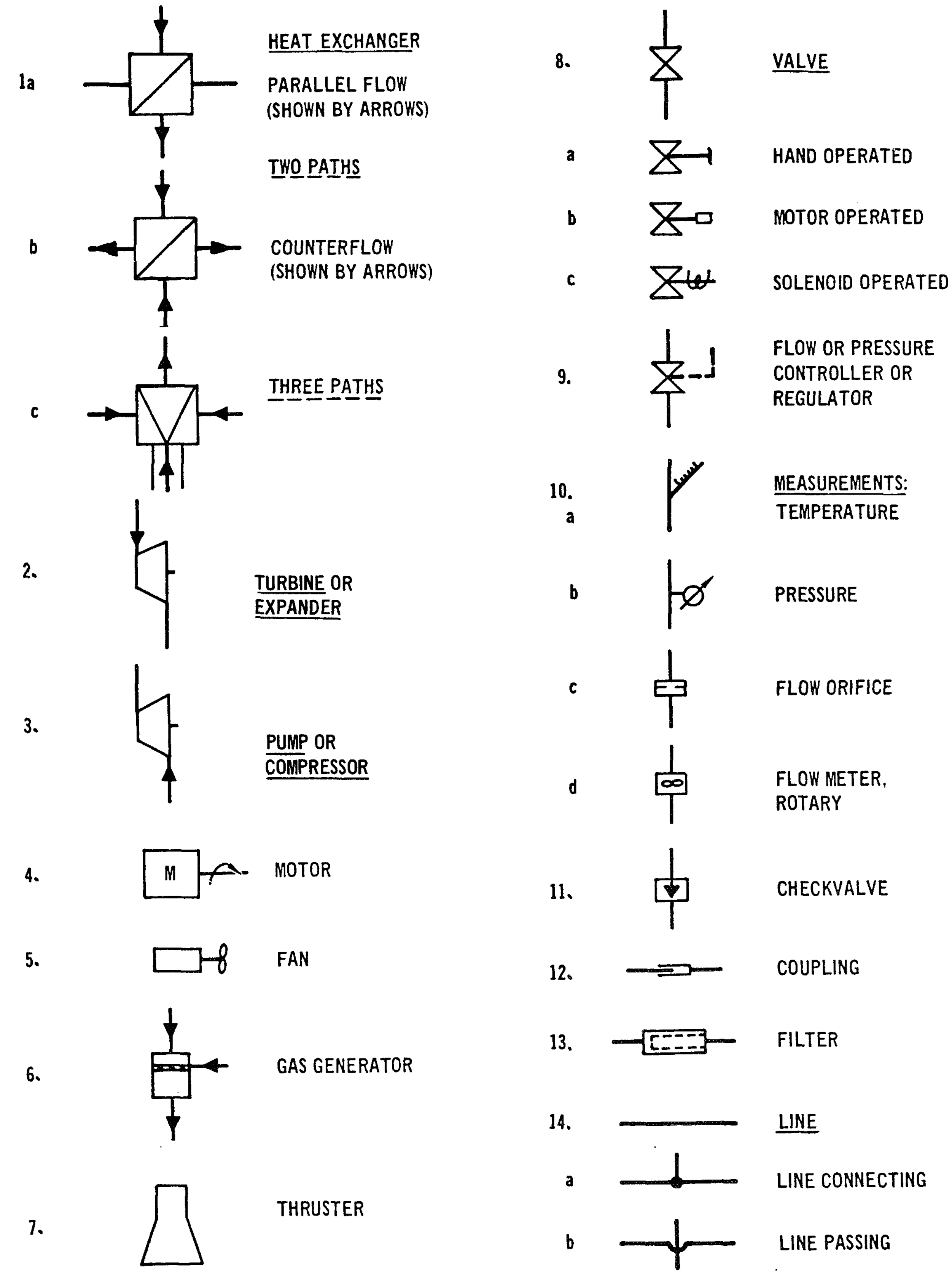

SCHEMATIC SYMBOLS

FIGURE 6-1a

DESIGN VARIABLES	ORBITER B	ORBITER C	BOOSTER
THRUSTER MIXTURE RATIO	4	4	4
EXPANSION RATIO	60/120*	60/120*	40
CHAMBER PRESSURE ($LBF/IN.^2$)	500	500	500
LINE PRESSURE DROP $LBF/IN.^2$	40	40	40
PROPELLANT TEMPERATURE (°R) – H_2	37	37	37
O_2	162	162	162
THRUSTER INLET PROPELLANT MINIMUM TEMPERATURE (°R) – H_2	200	200	200
O_2	350	350	350
ACCUMULATOR PRESSURE RATIO – MAX/SWITCH – H_2/O_2	2	2	2
SWITCH/MIN – H_2/O_2	1.135/1.13	1.13/1.125	1.24
PROPELLANT TANK PRESSURE $LBF/IN.^2A$ – H_2	25	25	25
O_2	30	30	35
THRUSTER SPECIFIC IMPULSE – SEC	446.9/455.2*	446.9/455.2*	444.9
SYSTEM SPECIFIC IMPULSE – SEC	416.0/423.7*	416.0/423.7*	410.8
SYSTEM MIXTURE RATIO	3.87	3.87	3.87
WEIGHT	35,879	37,070	5,310

*ATTITUDE CONTROL/TRANSLATION

TURBOPUMP APS DESIGN POINTS AND WEIGHTS

FIGURE 6–2

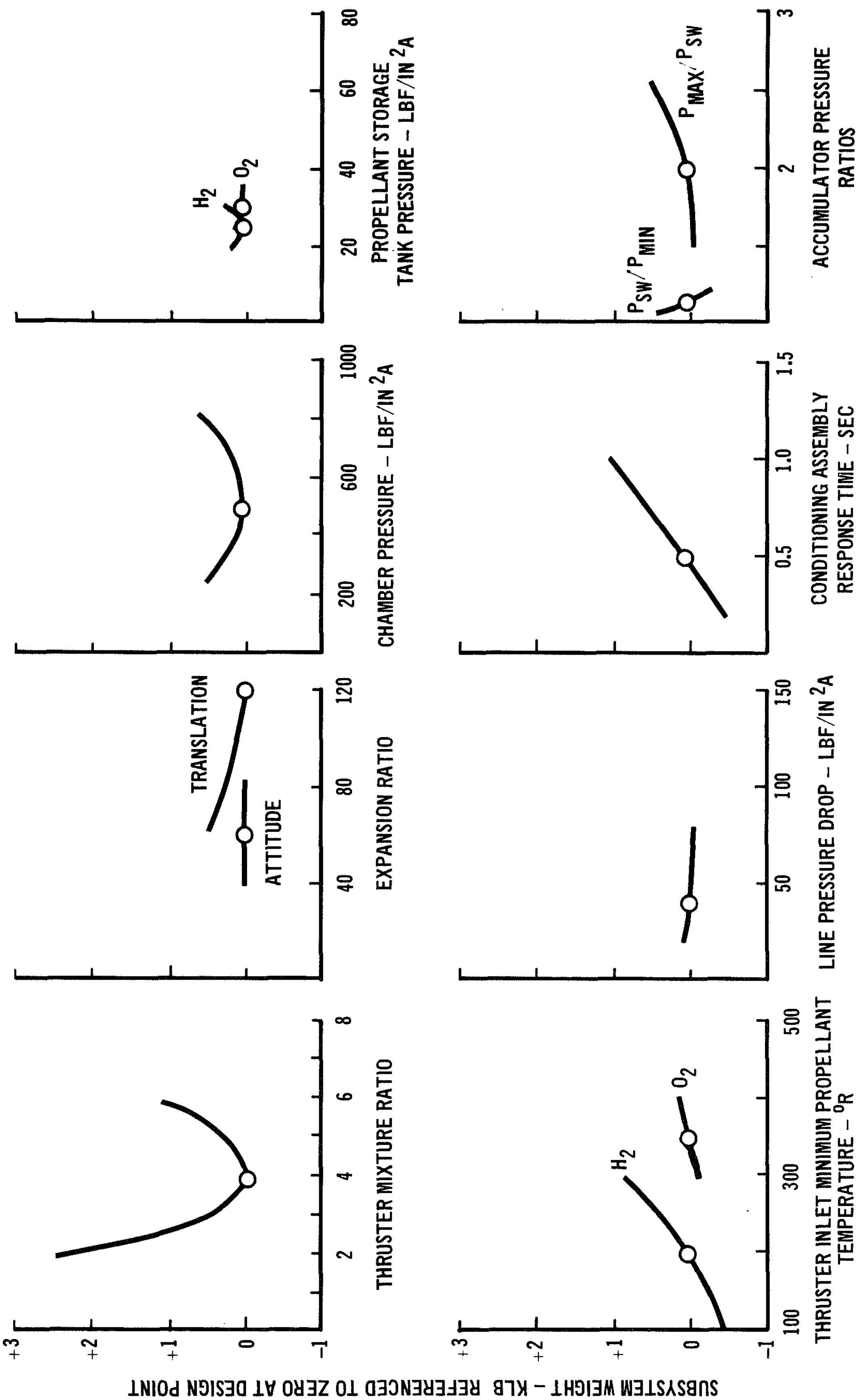

NOTE:
O DESIGN POINT

WEIGHT SENSITIVITY TO DESIGN VARIABLES

ORBITER B

FIGURE 6-3

SUBSYSTEM ELEMENTS	WEIGHT – LB		VOLUME – FT^3	
	H_2	O_2	H_2	O_2
PROPELLANT AND COMPONENTS				
TOTAL PROPELLANT	6334	23,552		
PROPELLANT TANKAGE	1036	417	1449	332
PRESSURANT AND TANKAGE	450	79		
INSULATION	248	50		
CONDITIONING ASSEMBLY				
HEAT EXCHANGERS (3)	255	297		
TURBOPUMPS (3)	76	124		
GAS GENERATORS (3)	37			
FEED ASSEMBLY				
ACCUMULATORS (1)	679	321	29	12
LINES	146	152		
REGULATORS (6)	26	29		
VALVES (THRUSTER ISOLATION (2) AND MANIFOLD)	105	90		
THRUSTER (18/6) *	917			
PROPULSIVE VENT AND LINES	275	184		
TOTAL SUBSYSTEM	35,879		1822	

* ATTITUDE/TRANSLATION

APS COMPONENT WEIGHT BREAKDOWN
Orbiter B

FIGURE 6–4

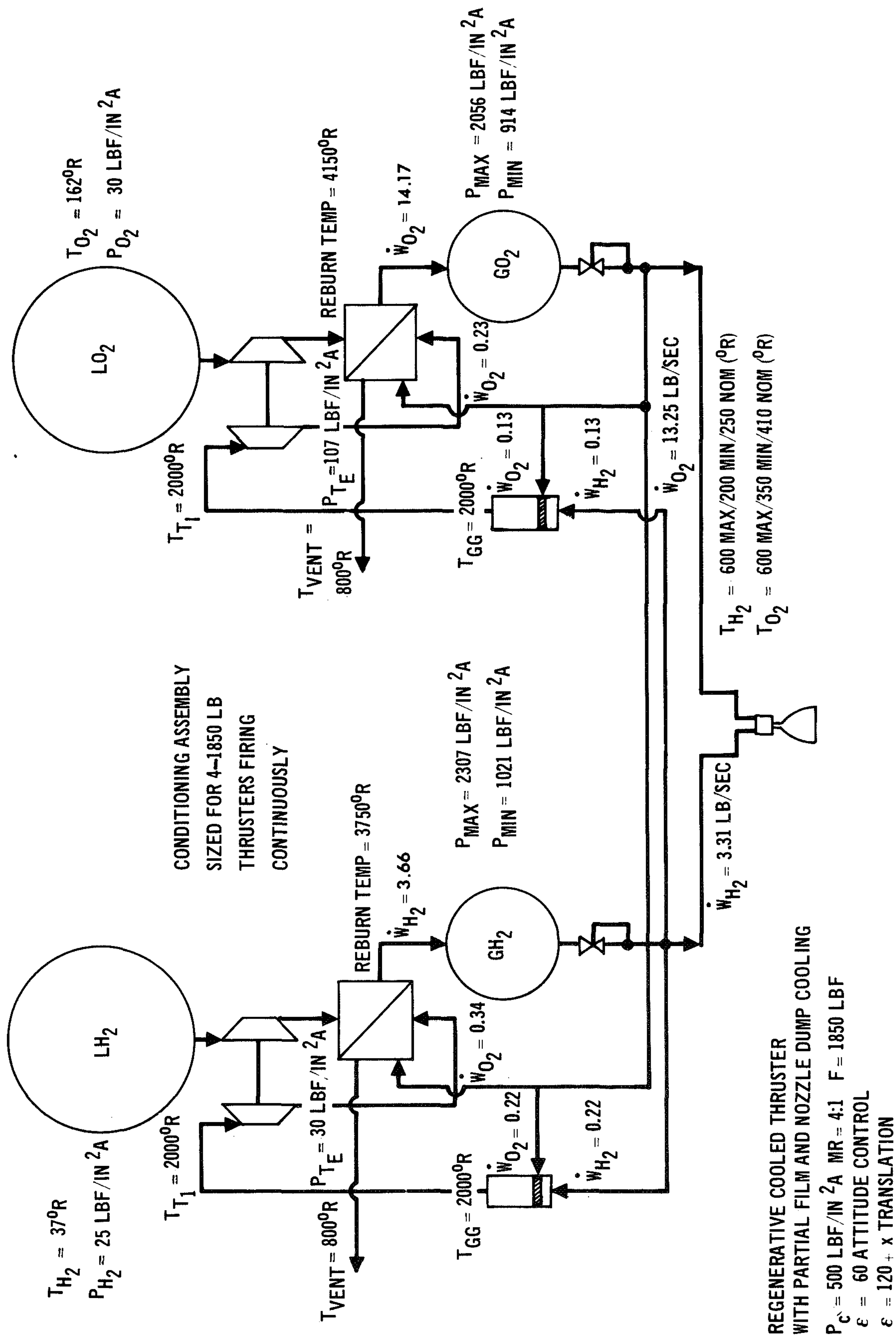

APS PRESSURES, TEMPERATURES AND FLOWS
Orbiter C

FIGURE 6–5

Parametric analyses were conducted to define the performance characteristics of the APS under simulated mission operation. These analyses included investigation of the impact of variances in propellant conditioning temperatures and pressure regulator performance. Appendix E provides a complete summary of these results and Figures 6-6 and 6-7 illustrate the operation of the subsystem during nominal mission, i.e., with all components and assemblies operating at their design values.

The results shown in Figure 6-6 and 6-7 are based on the lines being completely vented prior to separation from the station. Results presented in Appendix E show that this is necessary to avoid large mixture ratio excursions. With venting APS performance variations during the mission will be satisfactory.

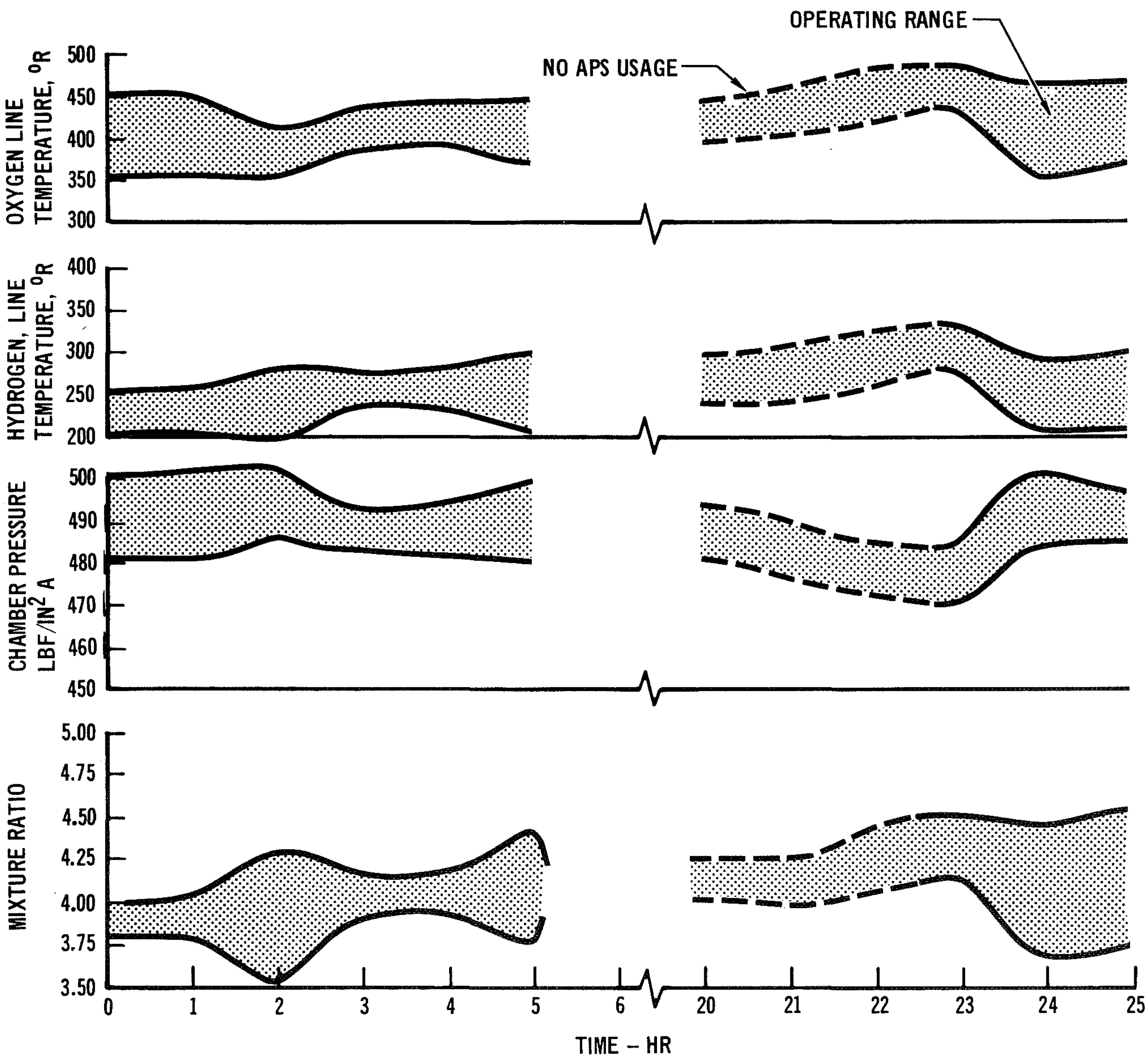

SUBSYSTEM OPERATING CHARACTERISTICS
NOMINAL DESIGN CONDITIONS
Third Orbit Rendezvous

LINES VENTED

FIGURE 6–6

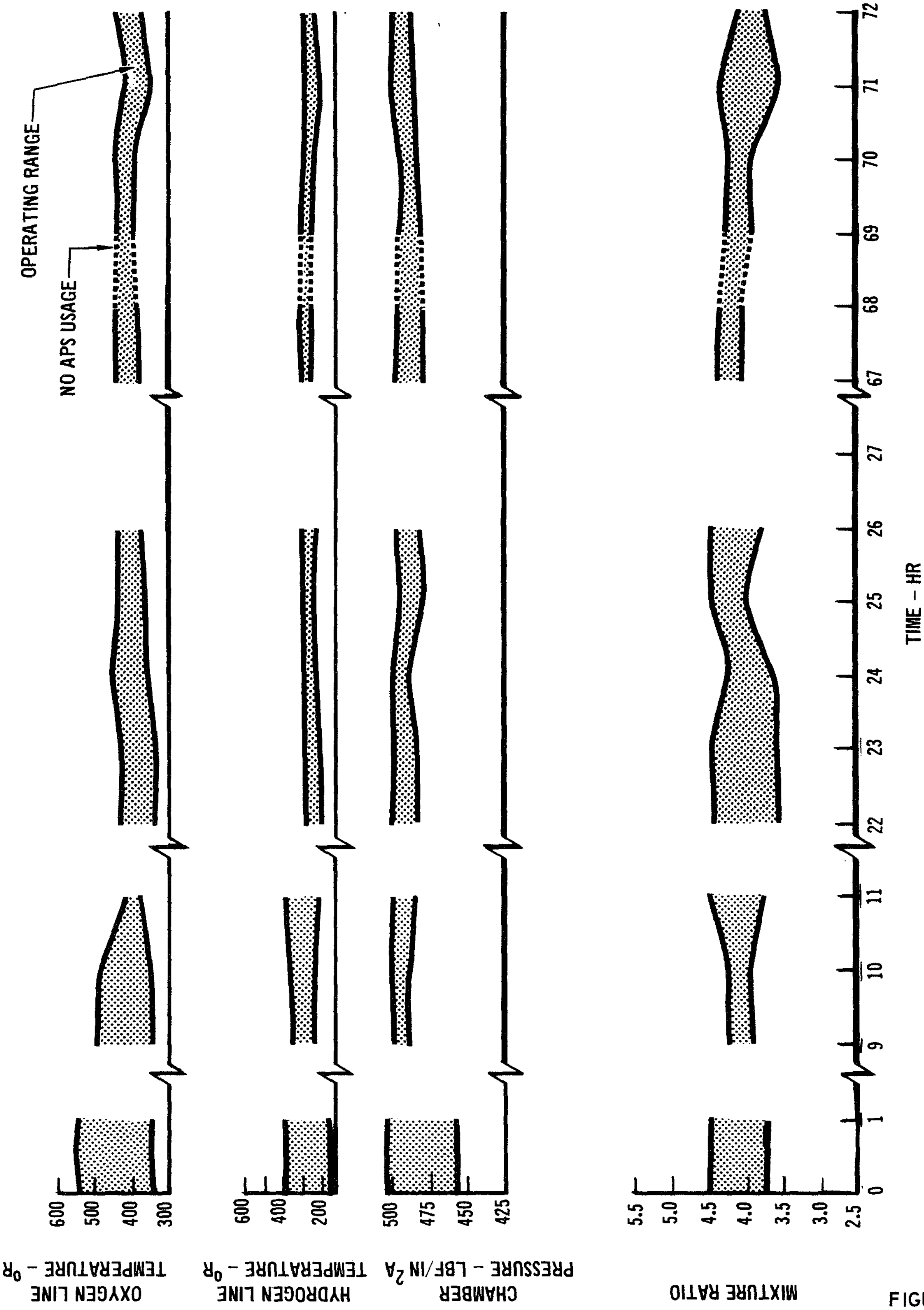

SUBSYSTEM OPERATING CHARACTERISTICS
NOMINAL DESIGN CONDITIONS
17TH ORBIT RENDEZVOUS

FIGURE 6-7

7. CONCLUSIONS

In Subtask B, a preliminary design of the turbopump APS was completed. This study provided a detailed definition of component and assembly design, operation, and performance and the resulting APS performance. The preceding sections and the appendices of this report provide the results of the study.

An assessment of assembly and component technology requirements was a primary goal of this study. In terms of thrust level for attitude control total impulse and reuse capability, shuttle requirements are far beyond those for any previous control propulsion subsystem. Therefore, no APS components capable of satisfying these requirements exist today. The preliminary turbopump APS design described in this report is a realistic configuration and can provide the performance and operational requirements. None of the components defined are currently available in their correct size, however, many of the component types are well characterized. Funded technology development programs are currently underway for thrusters, valves, ignition, and thrust chamber cooling. A detailed subassembly and component technology critique is discussed in Appendix G. A summary of that critique is shown in Figure 7-1.

TECHNOLOGY CONCERN	ALTERNATIVE APPROACH	IMPACT OF CHANGE
• TURBOPUMP COOLING/RESPONSE	• INCREASED COOLANT FLOW • REDUCED RESPONSE REQUIREMENT	• 40 LB INCREASE FOR TWICE DESIGN COOLANT FLOW • 300 LB INCREASE FOR FACTOR OF FOUR IN EQUIVALENT START TIME
• THRUSTER ASSEMBLY PERFORMANCE	• REDUCTION IN PERFORMANCE REQUIREMENTS	• INCREASED APS WEIGHT, APPROXIMATELY 100 LB PER SECOND I_{SP} REDUCTION
• THRUSTER ASSEMBLY LIFE CAPABILITY	• INCREASED COOLANT FLOW • PERIODIC REPLACEMENT	• INCREASED APS WEIGHT, APPROXIMATELY 300 LB FOR FACTOR OF 2 ERROR IN CYCLE CAPABILITY PREDICTION • INCREASED MAINTENANCE/TURN AROUND TIME
• PRESSURE VESSEL CYCLE LIFE CAPABILITY	• INCREASED DESIGN MARGIN	• INCREASED APS WEIGHT, APPROXIMATELY 500 LB FOR 50% INCREASE IN SAFETY FACTORS
• CONTROL COMPONENT LIFE CAPABILITY VALVES, IGNITERS, REGULATORS	• PERIODIC REPLACEMENT	• INCREASED MAINTENANCE/TURN AROUND TIME
• PROPELLANT ACQUISITION ASSEMBLY DESIGN AND VERIFICATION	• USE OF MULTIPLE SMALL REFILLABLE TANKS	• INCREASED WEIGHT (APPROXIMATELY 400 LB), INCREASED DESIGN AND CONTROL COMPLEXITY AND REDUCED APS FLEXIBILITY
• HIGH TEMPERATURE REBURN HEAT EXCHANGER DESIGN	• SERIES-STAGED COMBUSTION HEAT EXCHANGERS TO LIMIT MATERIAL TEMPERATURE • CONVENTIONAL–MODERATE TEMPERATURE HEAT EXCHANGERS (2000°R) • NO REBURN HEAT EXCHANGER	• INCREASED OPERATIONAL AND CONTROL COMPLEXITY WITH MULTIPLE OXYGEN INJECTION (IGNITION) • INCREASED APS WEIGHT, APPROXIMATELY 1800 LB • INCREASED APS WEIGHT, APPROXIMATELY 2200 LB
• HIGH PERFORMANCE INSULATION REUSABILITY – PROPELLANT TANKS – DISTRIBUTION LINES	 • VACUUM JACKETED DEWARS • VACUUM JACKETED LINES	 • INCREASED APS WEIGHT, APPROXIMATELY 650 LB • MAJOR INCREASES IN INSTALLATION/DESIGN COMPLEXITY, INCREASED APS WEIGHT, APPROXIMATELY 400 LB
• TURBOPUMP LIFE CAPABILITY	• REDUCE OPERATING REQUIREMENTS • PERIODIC REPLACEMENT	• INCREASED APS WEIGHT, APPROXIMATELY 700 LB FOR FACTOR OF 2 REDUCTION IN CYCLE CAPABILITY PREDICTION • INCREASED MAINTENANCE/TURN AROUND TIME

CRITIQUE OF HIGH PRESSURE APS TECHNOLOGY

FIGURE 7–1

8. REFERENCES

(a) Anglim, D. D., Baumann, T. L., and Ebbesmeyer, L. H., High Pressure Auxiliary Propulsion Subsystem Definition Study Subtask A Report: McDouglas Douglas Report No. MDC E0299, dated 12 February 1971.

(b) MSFC, "Space Shuttle Vehicle Description and Requirements Document," dated 1 October 1970.

(c) Herm, T. S. and Houte, F. W., High Pressure Auxiliary Propulsion Subsystem Definition Study Design Handbook: McDonnell Douglas Report No. MDC E0300, dated 12 February 1971.

(d) Space Shuttle High Pressure Auxiliary Propulsion Subsystem Definition, Program Plan: MDAC-East Report E0201, dated 15 July 1970.

(e) MSFC, "Space Shuttle Vehicle Description and Requirements Document," dated 15 July 1970.

APPENDIX A
APS REQUIREMENTS

Subsequent to Subtask A, the Space Shuttle Vehicle Description and Requirements Document, Reference (a), was updated to reflect revised space shuttle vehicle requirements. Vehicle design characteristics (including weight, center of gravity location, and moments of inertia) and the acceleration requirements (including reentry angular acceleration and on-orbit translation requirements) were revised. In addition, the mission timeline was updated, thereby affecting APS total impulse requirements.

Vehicles defined for Subtask B study were:

(1) Orbiter B, McDonnell Douglas design low cross range orbiter

(2) Orbiter C, McDonnell Douglas high cross range orbiter

(e) the McDonnell Douglas canard booster.

A general description of the missions and mission requirements that have been identified as being of major interest in program planning is shown in Figure A-1. The shuttle baseline missions are the Space Station/Base Logistics Missions. These mission timelines are shown in Figure A-2 for an early (3rd orbit) rendezvous and in Figure A-3 for a late (17th orbit) rendezvous. Figure A-4 presents the associated booster timeline. The mass characteristics of the orbiters and booster are shown in Figures A-5 and A-6, respectively. The maximum skin outer temperatures for the orbiters and booster are shown in Figures A-7, A-8 and A-9.

An in-depth analysis was conducted to update APS requirements for the Phase B portion of this study. In this analysis, alternate thruster locations and thrust levels for the new vehicle requirements were evaluated, and results of the analysis (in conjunction with the revised mission timelines) were used to update APS total impulse requirements. Vehicle characteristics at the time of injection were used for this analysis. Results are summarized in Figure A-10, which shows the APS thrust level and total impulse requirements for each vehicle configuration. The following sections describe the analysis and data used to arrive at the APS requirements of Figure A-10.

Orbital Characteristics \ Missions	Space Station/ Base Logistics Support	Placement and Retrieval of Satellites	Delivery of Propulsive Stages & Payload	Delivery of Propellants	Satellite Service & Maintenance	Short Duration Orb. Mission
Altitude (n. mi.)	200 - 300	100 - 800	100 - 200	200 - 300	100 - 800	100- 300
Inclination (deg)	28.5 - 90	28.5 - Sun Syn.	28.5 - 55	28.5 - 55	28.5 - Sun Syn.	28.5 - 90
On-Orbit ΔV (1000fps)	1 - 2	1 - 5	1 - 1.5	1 - 2	1 - 5	1 - 2
On-Orbit Stay Time (days)	7	7	7	7	7 - 15	7 - 30
Crew	2	2	2	2	2	2
Passengers (min)	Rotate 50 men/qtr	2	2	2	4	12
Discretionary Payload						
Weight (1000 lbs)	*70/qtr	— — — —	— — — —	— — — —	— — — —	— — — —
Volume (1000 ft^3)		5 - 10	10	10	5 - 10	4 - 6
Critical Dimen. Dia. (ft)	10 - 15	15	15	15	15	15

* Include Passengers

MISSION CHARACTERISTICS

FIGURE A-1

Event	Initiation Time (hr:min:sec)	Auxiliary Propulsion Requirements
1. Liftoff	00:00:00	No APS requirement.
2. Staging		Damp separation rates. Provide roll control for orbiter boost engine-out condition.
3. Insertion into 50 × 100 N. mi. Orbit	00:07:34	Maintain cutoff attitude. Damp boost engine cutoff transients. Deadband ± 0.5°.
4. Insertion Orbit Determination and Prethrust Targeting		Maneuver to local horizontal, heads down, + X in direction of motion. Impart orbital rate to maintain local attitude. Deadband ± 5°.
5. Prethrust Attitude Maneuver	00:39:15	Maneuver to burn attitude and maintain inertial attitude. Hold at ±0.5° deadband.
6. Phasing Burn into 249 × 100 n. mi. Orbit	00:49:15	Horizontal, in-plane, posigrade, heads-up maneuver, 350 fps ΔV.
7. Relative Tracking of Space Station and Prethrust Targeting		Maneuver to local horizontal, head up, + X in direction of motion, impart orbital rate. Deadband ± 5°.
8. Prethrust Attitude Maneuver	01:24:47	Maneuver to burn attitude and maintain inertial attitude. Hold at ± 0.5°-deadband.

SPACE STATION/BASE LOGISTICS MISSION TIMELINE
ORBITER — THIRD ORBIT RENDEZVOUS

FIGURE A-2

Event	Initiation Time (hr:min:sec)	Auxiliary Propulsion Requirements
9. Height Adjustment Burn into 260 × 249 n. mi. Orbit	01:34:47	Horizontal, in-plane, posigrade, heads-up maneuver. 279 fps ΔV.
10. Relative Tracking of Space Station and Prethrust Targeting		Maneuver to local horizontal, heads up + X in direction of motion, impart orbital rate. Deadband ± 5°.
11. Prethrust Attitude Maneuver	02:11:45	Maneuver to burn attitude and maintain inertial attitude. Hold at ± 0.5° deadband.
12. Coelliptic Burn into 260 × 260 N. mi. Orbit	02:21:45	Horizontal, inplane, posigrade, heads-up maneuver. 26 fps ΔV.
13. Relative Tracking of Space Station and Prethrust Targeting		Maneuver to line-of-sight attitude and maintain. Deadband ±5°.
14. Prethrust Attitude Maneuver	02:56:45	Maneuver to burn attitude and maintain inertial attitude Hold at ±0.5° deadband.
15. Dispersion Burn	03:06:45	Horizontal, in-plane maneuver. 0-25 fps ΔV.
16. Relative Tracking of Space Station and Prethrust Targeting		Maneuver to line-of-sight attitude and maintain. Deadband ± 5°.

SPACE STATION/BASE LOGISTICS MISSION TIMELINE
ORBITER — THIRD ORBIT RENDEZVOUS (Continued)

FIGURE A-2
CONTINUED

Event	Initiation Time (hr:min:sec)	Auxiliary Propulsion Requirements
17. Prethrust Attitude Maneuver	03:40:56	Maneuver to burn attitude and maintain inertial attitude. Hold at ± 0.5° deadband.
18. Terminal Phase Initiation (TPI)	03:50:56	In-plane, posigrade, heads up, pitched up at 27°, 22 fps ΔV.
19. Relative Tracking of Space Station and Prethrust Targeting		Maneuver to line-of-sight attitude and maintain. Deadband ± 5°.
20. Prethrust Attitude Maneuver	04:00:56	Maneuver to burn attitude and maintain inertial attitude. Hold at ± 0.5° deadband.
21. MCC-1	04:02:56	In-plane, heads up, 0-36 fps ΔV.
22. Relative Tracking of Space Station and Prethrust Targeting.		Maneuver to line-of-sight attitude and maintain. Deadband ± 5°.
23. Prethrust Attitude Maneuver	04:10:56	Maneuver to burn attitude and maintain inertial attitude. Hold at ± 0.5° deadband.
24. MCC-2	04:12:56	In-plane, heads up, 0-19 fps ΔV.

SPACE STATION/BASE LOGISTICS MISSION TIME LINE — ORBITER — THIRD ORBIT RENDEZVOUS (Continued)

FIGURE A-2 CONTINUED

Event	Initiation Time (hr:min:sec)	Auxiliary Propulsion Requirements
25. Relative Tracking of Space Station and Prethrust Targeting		Maneuver to line-of-sight attitude and maintain. Deadband ± 5°.
26. Prethrust Attitude Maneuver	04:23:06	Maneuver to burn attitude and maintain inertial attitude. Hold at ±0.5° deadband.
27. Braking Burns*	04:25:06	45 fps ΔV over series of range/range rate gates:
28. Station Keeping and Attitude Hold	04:33:11	0 - 10 fps multiaxis translation ΔV, 0 - 10 fps multiaxis attitude ΔV ± 0.5° deadband.
29. Docking	04:55:06	0 - 10 fps multiaxis translation ΔV, 0 -10 fps multiaxis attitude ΔV ± 0.5° deadband.
30. On Orbit		Passive mode.
31. Undocking	19:53:30	0.5 fps ΔV. Retrograde. ± 0.5° deadband.
32. Separation maneuver	19:53:30	10 fps ΔV retrograde. ± 0.5° deadband.
33. Attitude Hold		Deadband ± 20°
34. Preburn Targeting	22:33:30	Maneuver to local horizontal, heads down, impart orbital rate. Deadband ± 5°.

SPACE STATION/BASE LOGISTICS MISSION TIMELINE
ORBITER — THIRD ORBIT RENDEZVOUS (Continued)

FIGURE A-2
CONTINUED

Event	Initiation Time (hr:min:sec)	Auxiliary Propulsion Requirements
35. Prethrust Attitude Maneuver	22:43:30	Maneuver to burn attitude and maintain inertial attitude. Hold at ± 0.5° deadband.
36. Deorbit Burn	22:53:30	Retrograde, in-plane, heads down. 495 fps ΔV.
37. Entry Attitude Maneuver		Maneuver to + X-axis in-plane, pitched up above local horizontal. Deadband ± 0.5°.
38. (a) Entry	23:25:30	Maneuver as required. 25-60 fps ΔV. Deadband ± 2°.
(b) Entry	23:25:30	Maneuver as required. ΔV. Deadband ± .
39. (a) Completion of APS Function, High Cross-Range Orbiter		Termination attitude
(b) Completion of APS Function, Low Cross-Range Orbiter		Termination attitude

* For purposes of specific APS performance studies, the following braking burn schedule should be considered typical:

Initiation Time	ΔV, fps
04:25:06	10
04:26:46	13
04:28:01	12
04:29:31	5
04:31:11	5

SPACE STATION/BASE LOGISTICS MISSION TIMELINE
ORBITER — THIRD ORBIT RENDEZVOUS (Concluded)

FIGURE A-2
CONCLUDED

Event	Initiation Time (hr:min:sec)	Auxiliary Propulsion Requirements
1. Liftoff	00:00:00	No APS requirement.
2. Staging	00:	Damp separation rates. Provide roll control for orbiter boost engine-out condition.
3. Insertion into 50 × 100 n. mi. Orbit.	00:07:34	Maintain cutoff attitude. Damp boost engine cutoff transients. Deadband ± 0.5°.
4. Insertion Orbit Determination and Prethrust Targeting		Maneuver to local horizontal, heads down, + X in direction of motion. Impart orbital rate to maintain local attitude. Deadband ± 5°.
5. Prethrust Attitude Maneuver	00:39:14	Maneuver to burn attitude and maintain inertial attitude. Hold at ± 0.5° deadband.
6. Phasing Burn into 123 × 100 n. mi. Orbit	00:49:14	Horizontal, in-plane, posigrade, heads-up maneuver, 130 fps ΔV.
7. Random Drift		No attitude requirement defined.
8. Relative Tracking of Space Station and Prethrust Targeting	09:19:15	Maneuver to local horizontal, impart orbital rate. Deadband ± 5°.

SPACE STATION/BASE LOGISTICS MISSION TIMELINE,
ORBITER, SEVENTEENTH ORBIT RENDEZVOUS

FIGURE A-3

Event	Initiation Time (hr:min:sec)	Auxiliary Propulsion Requirements
9. Prethrust Attitude Maneuver	09:39:15	Maneuver to burn attitude and maintain inertial attitude. Hold at ± 0.5° deadband.
10. Dispersion -1	09:49:15	Horizontal, in-plane, heads-up maneuver, 0-40 fps ΔV.
11. Relative Tracking of Space Station and Prethrust Targeting		Maneuver to local horizontal, impart orbital rate. Deadband ± 5°.
12. Prethrust Attitude Maneuver	10:01:45	Maneuver to burn attitude and maintain inertial attitude. Hold at ± 0.5° deadband.
13. Dispersion -2	10:11:45	Horizontal, in-plane, heads-up maneuver. 0-25 fps ΔV.
14. Random Drift		No attitude Requirement defined.
15. Relative Tracking of Space Station and Prethrust Targeting	21:04:20	Maneuver to local horizontal, impart orbital rate. Deadband ± 5°.
16. Prethrust Attitude Maneuver	22:04:20	Maneuver to burn attitude and maintain inertial attitude. Hold at ± 0.5° deadband.
17. Height Adjustment Burn into 260 × 123 n. mi. Orbit.	22:14:20	Horizontal, in-plane, posigrade, heads-up maneuver. 282 fps ΔV.

SPACE STATION/BASE LOGISTICS MISSION TIMELINE, ORBITER, SEVENTEENTH ORBIT RENDEZVOUS (Continued)

FIGURE A-3
CONTINUED

Event	Initiation Time (hr:min:sec)	Auxiliary Propulsion Requirements
18. Relative Tracking of Space Station and Prethrust Targeting		Maneuver to local horizontal, impart orbital rate. Deadband ± 5°.
19. Prethrust Attitude Maneuver	22:50:08	Maneuver to burn attitude and maintain inertial attitude. Hold at ± 0.5° deadband.
20. Coelliptic Burn into 260 × 260 n. mi. Orbit	23:00:08	Horizontal, in-plane, posigrade, heads-up maneuver, 239 fps ΔV.
21. Attitude Hold		Deadband ± 20°.
22. Relative Tracking of Space Station and Prethrust Targeting	24:14:23	Maneuver to line-of-sight attitude to space station and maintain. Deadband ± 5°.
23. Prethrust Attitude Maneuver	24:24:23	Maneuver to burn attitude and maintain inertial attitude. Hold at ± 0.5° deadband.
24. Terminal Phase Initiation (TPI)	24:34:23	In-plane, posigrade, heads up, pitched up at 27°. 22 fps ΔV.
25. Relative Tracking of Space Station and Prethrust Targeting		Maneuver to line-of-sight attitude to space station and maintain. Deadband ± 5°.

SPACE STATION/BASE LOGISTICS MISSION TIMELINE,
ORBITER, SEVENTEENTH ORBIT RENDEZVOUS (Continued)

FIGURE A-3
CONTINUED

Event	Initiation Time (hr:min:sec)	Auxiliary Propulsion Requirements
26. Prethrust Attitude Maneuver	24:44:23	Maneuver to burn attitude and maintain inertial attitude. Hold at $\pm$ 0.5° deadband.
27. MCC-1	24:46:23	In-plane, heads-up maneuver. 0-36 fps ΔV.
28. Relative Tracking of Space Station and Prethrust Targeting		Maneuver to line-of-sight attitude to space station and maintain. Deadband $\pm$ 5°.
29. Prethrust Attitude Maneuver	24:54:23	Maneuver to burn attitude and maintain inertial attitude. Hold at $\pm$ 0.5° deadband.
30. MCC-2	24:56:23	In-plane, heads-up maneuver. 0-19 fps ΔV.
31. Relative Tracking of Space Station and Prethrust Targeting		Maneuver to line-of-sight attitude to space station and maintain. Deadband $\pm$ 5°.
32. Prethrust Attitude Maneuver	25:06:33	Maneuver to burn attitude and maintain inertial attitude. Hold at $\pm$ 0.5° deadband.
33. Braking Burns*	25:08:33	45 fps ΔV over series of range/range rate gates.
34. Stationkeeping and Attitude Hold	25:16:38	0-10 fps multiaxis translation ΔV and 0-10 fps multiaxis attitude ΔV. $\pm$ 0.5° deadband.

SPACE STATION/BASE LOGISTICS MISSION TIMELINE,
ORBITER, SEVENTEENTH ORBIT RENDEZVOUS (Continued)

FIGURE A-3
CONTINUED

Event	Initiation Time (hr:min:sec)	Auxiliary Propulsion Requirements
35. Docking	25:38:33	0-10 fps multiaxis translation ΔV and 0-10 fps multiaxis attitude ΔV. $\pm$ 0.5° deadband.
36. On Orbit		Passive
37. Undocking	67:20:03	0.5 fps ΔV. Retrograde. $\pm$ 0.5° deadband.
38. Separation Maneuver	67:20:03	10 fps ΔV. Retrograde. $\pm$ 0.5° deadband.
39. Attitude Hold		Deadband $\pm$ 20°.
40. Preburn Targeting	70:00:03	Maneuver to local horizontal, heads down, impart orbital rate. Deadband $\pm$ 5°.
41. Prethrust Attitude Maneuver	70:10:03	Maneuver to burn attitude and maintain inertial attitude. Hold at $\pm$ 0.5° deadband.
42. Deorbit Burn	70:20:03	Retrograde, in-plane, heads down. 496 fps ΔV.
43. Entry Attitude Maneuver		Maneuver to + X-axis in-plane, pitched up above local horizontal. Deadband $\pm$ 0.5°.

SPACE STATION/BASE LOGISTICS MISSION TIMELINE, ORBITER, SEVENTEENTH ORBIT RENDEZVOUS (Continued)

FIGURE A-3
CONTINUED

Event	Initiation Time (hr:min:sec)	Auxiliary Propulsion Requirements
44. (a) Entry	71:32:03	Maneuver as required. 25-60 fps ΔV. Deadband $\pm$ 2°.
(b) Entry	71:32:03	Maneuver as required. ΔV. Deadband $\pm$
45. (a) Completion of APS Function, High Cross-Range Orbiter		Termination attitude
(b) Completion of APS Function, Low Cross-Range Orbiter		Termination attitude

* For purposes of specific APS performance studies, the following braking burn schedule should be considered typical:

Initiation Time	ΔV, fps
25:08:33	10
25:10:13	13
25:11:28	12
25:12:58	5
25:14:38	5

SPACE STATION/BASE LOGISTICS MISSION TIMELINE, ORBITER, SEVENTEENTH ORBIT RENDEZVOUS

FIGURE A-3
CONCLUDED

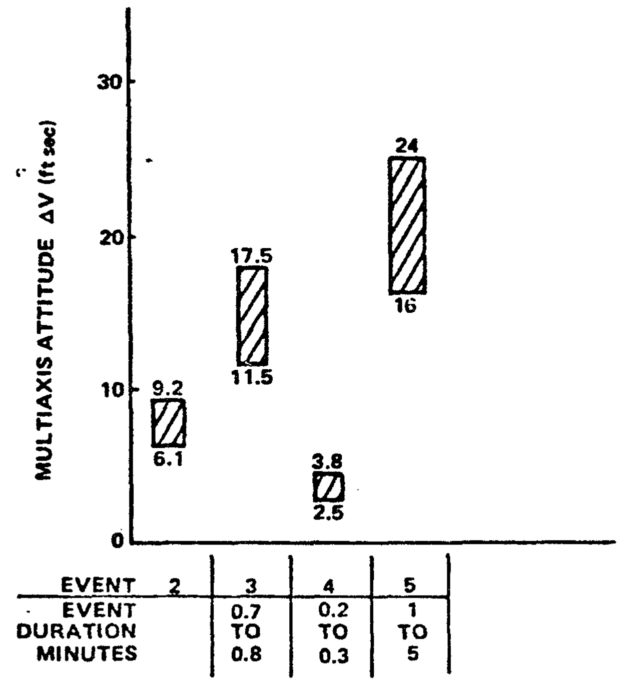

	EVENT COMPLETION TIME*	EVENT	PROPULSION REQUIREMENT DESCRIPTION
1.	0	Staging	Separation of booster and orbiter (No APS requirement)
2.	0+	Post Separation	Damping of main engine cutoff and separation transients.
3.	0.7-0.8	Orientation	Maneuver vehicle to reentry attitude.
4.	0.9-1.1	Attitude hold	±2° deadband
5.	1.9-6.1	Entry	±2° deadband

*Time is referenced to Event 1 in minutes unless otherwise stated. Both minimum and maximum cumulative times are shown.

SPACE STATION/BASE LOGISTICS MISSION
TIMELINE – BOOSTER

FIGURE A-4

Description	Nominal Weight (lb)	Center of Gravity (in.)			Moment of Inertia (slug-ft^2 × 10^6)		
		X	Y	Z	Roll	Pitch	Yaw
Launch	737,211	-945	0	262	2.052	32.123	32.385
50% Burn	504,067	-1082	0	274	2.035	23.708	23.987
Injection	271,465	-1259	0	300	1.950	15.074	15.438
Maneuver	253,613	-1275	0	299	1.933	14.177	14.559
Preretro	241,997	-1293	0	295	1.915	13.384	13.782
Reentry	234,400	-1305	0	293	1.907	12.951	13.358

MASS CHARACTERISTICS OF ORBITER B

Description	Nominal Weight (lb)	Center of Gravity (in.)			Moment of Inertia (slug-ft^2 × 10^6)		
		X	Y	Z	Roll	Pitch	Yaw
Launch	740,421	-1341	0	302	3.587	20.220	22.437
50% Burn	506,768	-1421	0	302	2.818	15.494	17.018
Injection	273,644	-1451	0	306	2.059	13.607	14.433
Maneuver	255,720	-1455	0	307	2.026	13.497	14.308
Preretro	245,236	-1457	0	309	2.015	13.433	14.240
Reentry	237,549	-1447	0	310	2.007	13.290	14.096

MASS CHARACTERISTICS OF ORBITER C

FIGURE A-5

Mass Characteristics		Staging (Booster Burnout)	Initiation of Jet Powered Flight
Weight (lb)		474,876	451,219
Center of Gravity Location (in.)	X	-2010	-2004
	Y	0	0
	Z	13	14
Moment of Inertia (slug — ft^2 $\times 10^6$)	Ixx	7.017	7.016
	Iyy	53.918	51.25
	Izz	57.013	54.354

MASS CHARACTERISTICS OF BOOSTER

FIGURE A-6

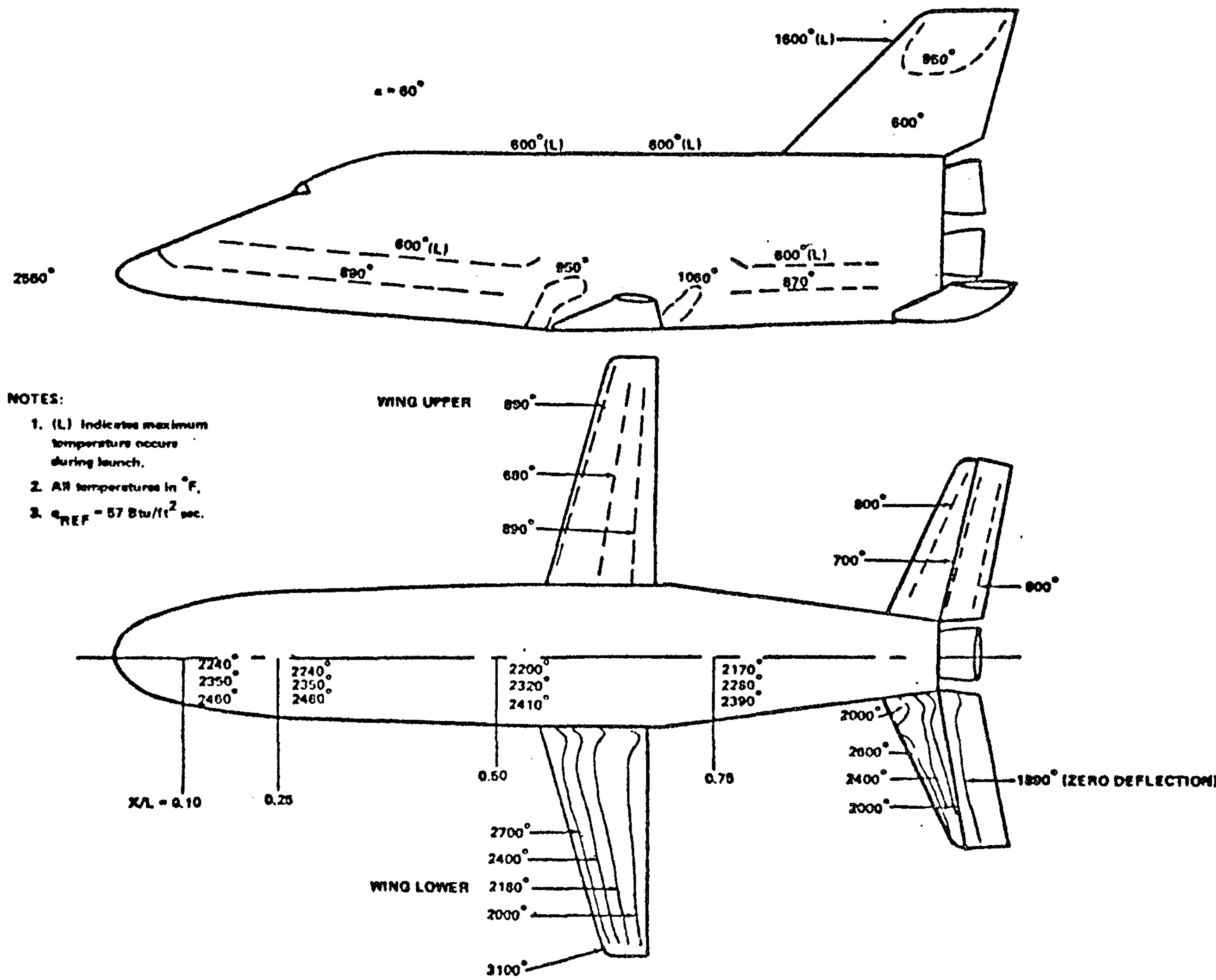

Maximum outer skin temperatures — orbiter B.

FIGURE A-7

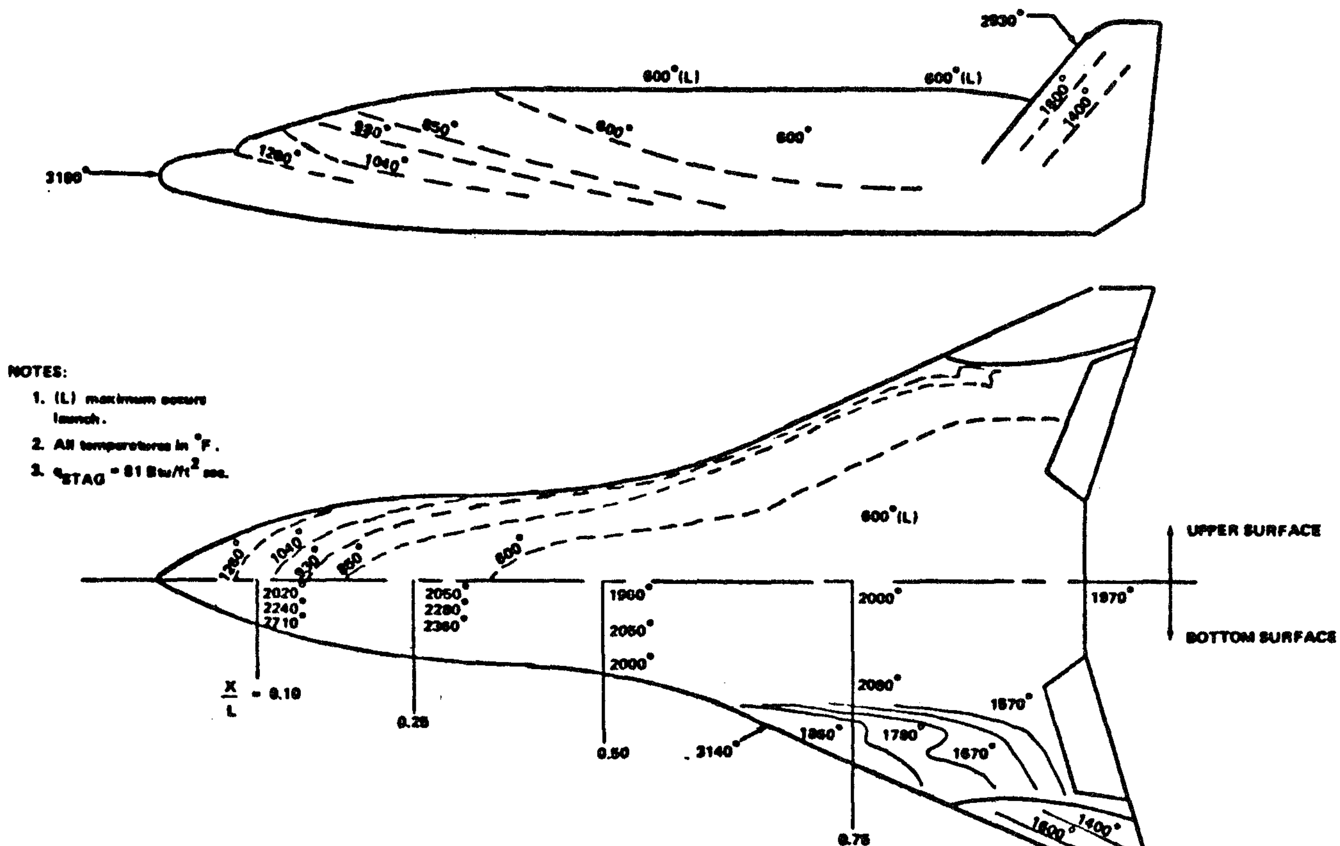

Maximum outer skin temperatures — orbiter C.

FIGURE A-8

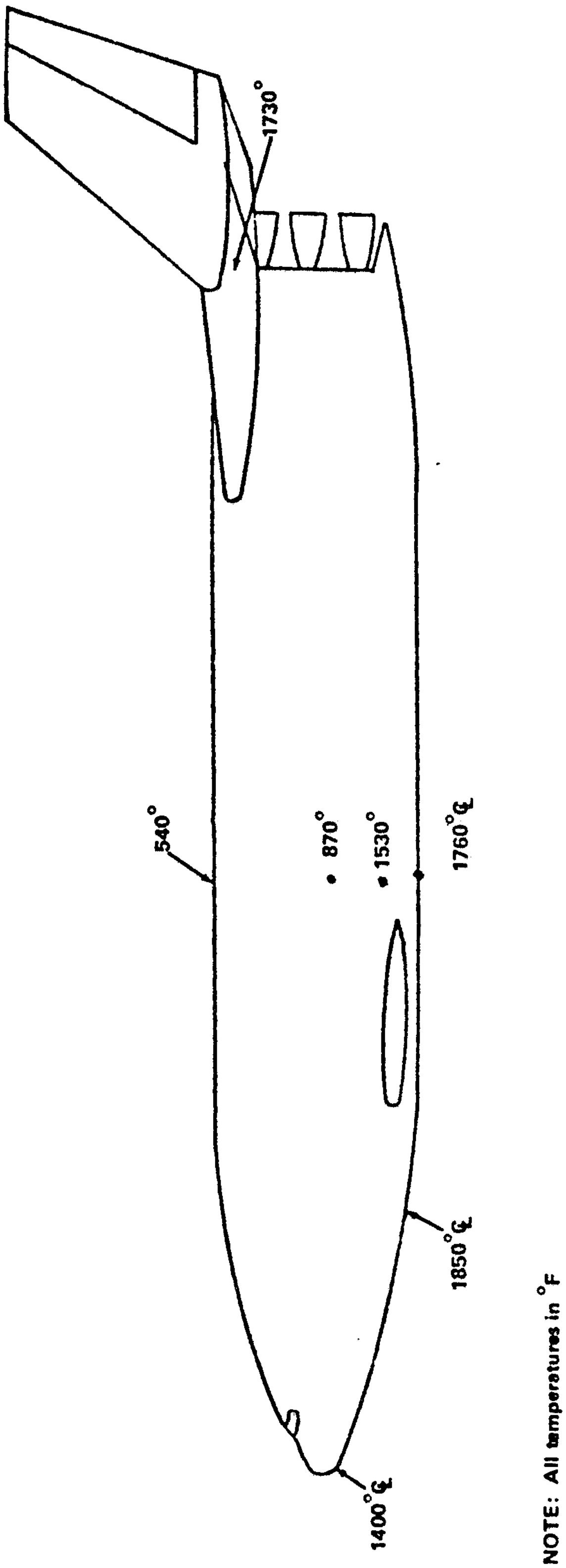

Maximum surface temperatures during entry — booster.

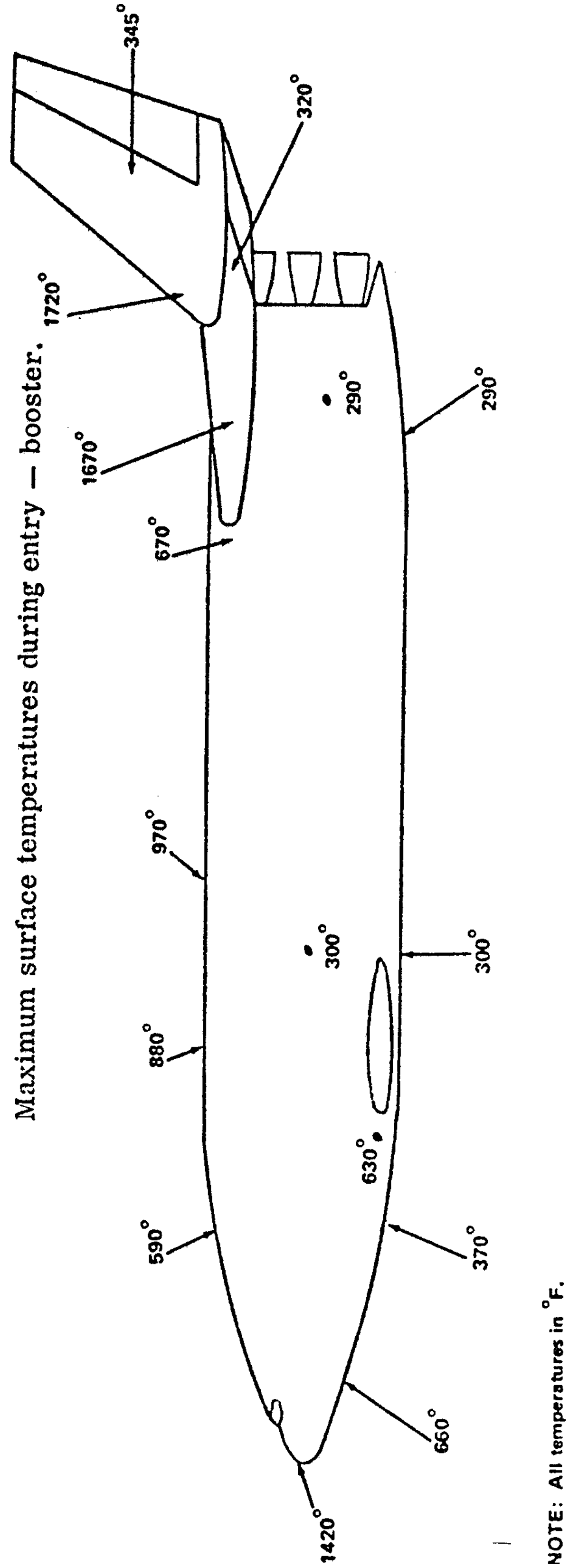

Maximum surface temperatures during ascent — booster.

FIGURE A-9

	THRUST LEVEL	NUMBER OF THRUSTERS	TOTAL IMPULSE** (10^6 LB SEC)	
			BOOSTER	ORBITER
ORBITER B	1850	24		12.666*
BOOSTER	1850	18	0.860	
ORBITER C	1850	33		12.766*

* 100 LB-SEC MINIMUM IMPULSE BIT
17TH ORBIT RENDEZVOUS
**USAGE DUE TO ERRORS IN ATTITUDE SENSORS NOT INCLUDED

REQUIREMENTS SUMMARY
Subtask B

FIGURE A-10

A-1. THRUSTER LOCATION AND THRUST LEVEL

The APS is required to provide three-axis translation and attitude control capability for the orbiters, and three-axis attitude control capability for the booster. Acceleration requirements for these functions are tabulated in Figures A-11 and A-12. All maneuvers were to be performed at an acceleration level between nominal minimum and nominal maximum, with no thruster failures. In order to provide safe return of the vehicle in the event of thruster failures, it was further required that all maneuvers be performed at an acceleration level above minimum with two thrusters inoperative.

Several factors, including thrust level, number of thrusters, thruster function, minimum cross coupling, and vehicle heat shield penetration must be considered in evaluating alternate thruster locations. These factors cannot, however, be investigated independently, since they are directly dependent upon one another (i.e., given acceleration requirements can be fulfilled by several combinations of thrust level, number of thrusters, and thruster location). However, some general ground rules were established. It is most desirable to use a common thruster design to perform all APS functions rather than to utilize thrusters of a different thrust level for each function. In this manner only a single thruster development program is required. Providing a common thrust level for all functions was accomplished by tailoring the number of thrusters and locations to meet the overall control requirements. Thrusters of a single thrust level can also be located in such a manner that they provide moments with respect to more than one axis. Thus, one group of thrusters can perform more than one function (for example, pitch and roll), resulting in fewer thrusters.

When the above guidelines are combined with the more obvious physical constraints on thruster location, it becomes apparent that choice of thruster locations becomes an iterative process. A summary of the Orbiter B thruster arrangements which were studied is presented in Figure A-13. The chosen design utilized 1850 lb thrusters with pitch and roll functions coupled. The vehicle thruster locations and functions for the chosen design are described in Figures A-14 and A-15. The various thrust level/number of thrusters combinations which were available for the chosen thruster arrangement are presented in Figure A-16 and the maneuvering requirements and capabilitites (given in terms of total thrust) are presented in

Event	3 Orbit Rendez. / 17 Orbit Rendez.	2 / 2			3-27/32-37 / 3-33/38-43			28-31 / 34-37			38 / 44		
		X	Y	Z	X	Y	Z	X	Y	Z	X	Y	Z
TRANSLATION ACCELERATION ft/sec^2	MIN	0.5	N/R†		0.5	0.1	0.1	0.07	0.07	0.07	N/R†		
	NOM MIN	0.65			0.65	0.2	0.2	0.1	0.1	0.1			
	NOM MAX	3.0			3.0	0.5	0.5	0.5	0.25	0.25			
	MAX	7.0			7.0	7.0	7.0	1.0	1.0	1.0			
		R**	P	Y	R	P	Y	R	P	Y	R	P	Y
ANGULAR ACCELERATION deg/sec^2	MIN	0.5	N/R†		0.3	0.3	0.3	0.3	0.3	0.3	0.5	0.5	0.9
	NOM MIN	0.7			0.5	0.5	0.5	0.5	0.5	0.5	1.0	1.0	1.3
	NOM MAX	2.5			2.0	2.0	2.0	2.0	2.0	2.0	2.0	2.0	1.7
	MAX	N/R†			4.0	4.0	4.0	4.0	4.0	4.0	4.0	4.0	4.0
FINE ATTITUDE LIMITS — deg		1.0	N/R†		0.5	0.5	0.5	0.5	0.5	0.5	2.0	2.0	2.0
COARSE ATTITUDE LIMITS — deg		N/R†			20	20	20	5.0	5.0	5.0	N/R†		

** Based on roll inertia
† No Requirement

SPACE STATION/BASE LOGISTICS MISSION
ORBITER MANEUVERING CAPABILITY REQUIREMENTS

FIGURE A-11

EVENT		2			3			4			5		
		X	Y	Z	X	Y	Z	X	Y	Z	X	Y	Z
TRANSLATION ACCELERATION ft/sec^2	MIN NOM MIN NOM MAX MAX	NO REQUIREMENT						NO REQUIREMENT					
		R	P	Y	R	P	Y	R	P	Y	R	P	Y
ANGULAR ACCELERATION deg/sec^2	MIN NOM MIN NOM MAX MAX	0.3 1.0 1.75 2.0	0.3 0.5 1.0 2.0	0.3 1.0 1.75 2.0	0.3 0.5 1.0 2.0	0.3 0.5 1.0 2.0	0.3 0.5 1.0 2.0	0.3 0.5 1.0 2.0	0.3 0.5 1.0 2.0	0.3 0.5 1.0 2.0	0.3 1.0 1.75 2.0	0.3 0.5 1.0 2.0	0.3 1.0 1.75 2.0
ANGULAR RATE deg/sec	MIN NOM MIN NOM MAX MAX				2	2	2						
ATTITUDE LIMITS — deg		2	2	2	2	2	2	2	2	2	2	2	2

SPACE STATION/BASE LOGISTICS MISSION — BOOSTER
MANEUVERING CAPABILITY REQUIREMENTS

FIGURE A-12

SUBSYSTEM DESCRIPTION	NO. OF THRUSTERS	THRUST LEVEL	THRUSTER WEIGHT	TOTAL SUBS. WT. COMPARISON *	RELATIVE ADVANTAGES	RELATIVE DISADVANTAGES
√ INDEPENDENT X, COUPLED Y AND YAW, COUPLED Z, PITCH, AND ROLL	24	1850	744	+ 142	SAME THRUST LEVEL AS BOOSTER	YAW, Y, AND Z TOTAL THRUST LEVELS ARE ABOVE DESIRED RANGE FOR DOCKING
INDEPENDENT X, COUPLED Y, YAW, Z, PITCH, AND ROLL	24	1225	618	+ 350	ALL ACCELERATIONS IN DESIRED RANGE	INEFFICIENT USE OF PROPELLANT FOR Y AND YAW MANEUVERS
INDEPENDENT X, COUPLED Y, YAW, COUPLED Z, PITCH, AND ROLL WITH Y AND YAW BACKUP CAPABILITY	32	1225	824	+ 352	ALL ACCELERATIONS IN DESIRED RANGE	LARGE NUMBER OF THRUSTERS
NO MULTIPLE AXIS USAGE	18 16	750 1750	1008	0 **	ALL ACCELERATIONS IN DESIRED RANGE	TWO DIFFERENT THRUSTER SIZES. LARGE NUMBER OF THRUSTERS

√ SELECTED

* TOTAL WEIGHT COMPARISON INCLUDES PROPELLANT, THRUSTERS, CONDITIONING ASSEMBLY, LINES AND VALVES

** DOES NOT INCLUDE WEIGHT OF DOORS OR WING PODS

SUMMARY OF ORBITER B THRUSTER ARRANGEMENT OPTIONS

FIGURE A-13

THRUSTER ASSEMBLY SUMMARY – ORBITER B

THRUSTER ASSEMBLY NUMBER	NUMBER OF 1850 LB_F THRUSTERS	PURPOSE
1	1	– X
2	1	– X
3	3	+ X
4	3	+ X
5	2	+ Y, + YAW
6	2	– Y, – YAW
7	1	– Z, – PITCH, – ROLL
8	1	+ Z, + PITCH, + ROLL
9	1	– Z, – PITCH, + ROLL
10	1	+ Z, + PITCH, – ROLL
11	1	– Z, ∓ PITCH, – ROLL
12	1	+ Z, – PITCH, + ROLL
13	1	– Z, + PITCH, + ROLL
14	1	+ Z, – PITCH, – ROLL
15	2	+ Y, – YAW
16	2	– Y, + YAW

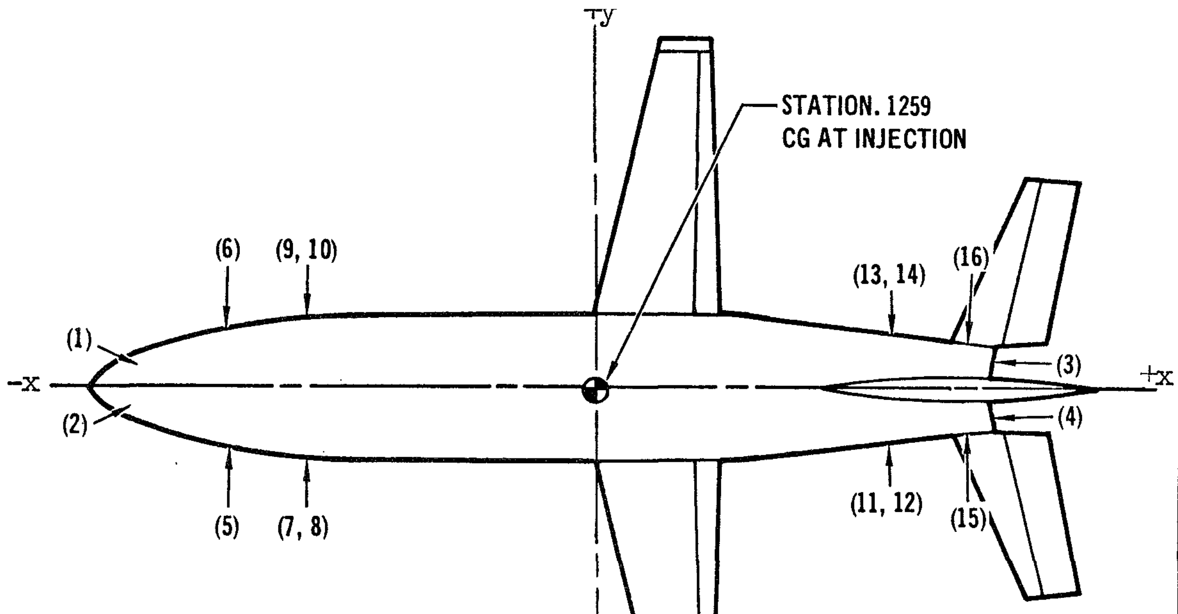

W = 271,465 LB
$I_{xx} = 1.95 \times 10^6$ SLUG-FT^2
$I_{yy} = 15.074 \times 10^6$ SLUG-FT^2
$I_{zz} = 15.438 \times 10^6$ SLUG-FT^2

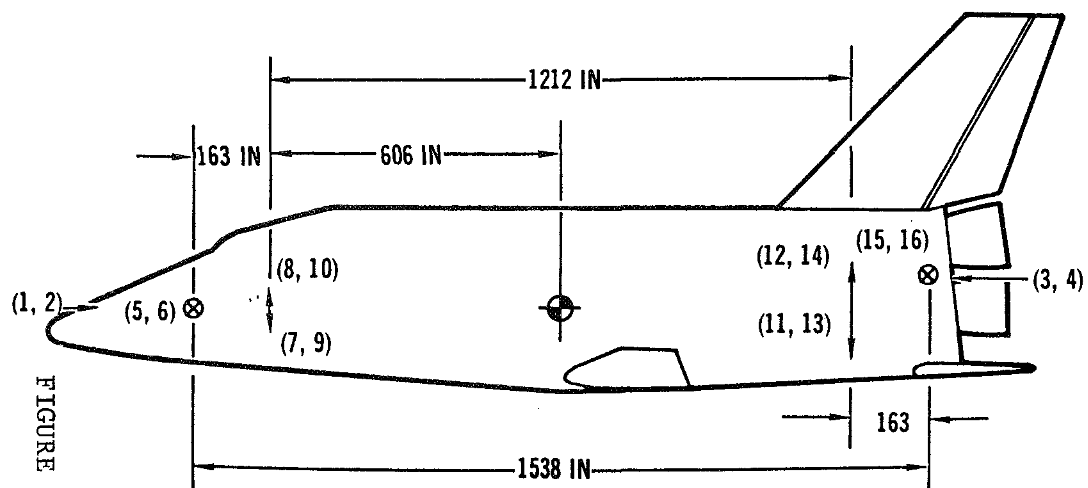

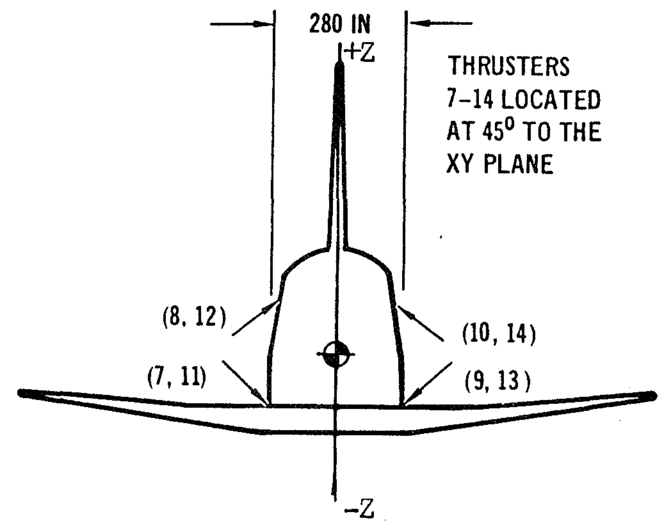

FIGURE A-14

ORBITER B THRUSTER LOCATIONS

LOCATION	MANEUVER	NO. THRUSTERS	THRUSTER COORDINATES*			DIRECTION COSINES		
			X	Y	Z	X	Y	Z
1	-X TRANS	1	-296	+45	+300	-.926	-.374	0
2	-X TRANS	1	-296	-45	+300	-.926	+.374	0
3	+X TRANS	3	-2034	+54	+362	+1.0	0	0
4	+X TRANS	3	-2034	-54	+362	+1.0	0	0
5	+YAW, +Y TRANS	2	-490	-73	+300	0	+1.0	0
6	-YAW, -Y TRANS	2	-490	+73	+300	0	-1.0	0
7	-PITCH, -ROLL, -Z TRANS	1	-653	-135	+343	0	+.707	-.707
8	+PITCH, +ROLL, +Z TRANS	1	-653	-135	+203	0	+.707	+.707
9	-PITCH, +ROLL, -Z TRANS	1	-653	+135	+343	0	-.707	-.707
10	+PITCH, -ROLL, +Z TRANS	1	-653	+135	+203	0	-.707	+.707
11	+PITCH, -ROLL, -Z TRANS	1	-1865	-110	+405	0	+.707	-.707
12	-PITCH, +ROLL, +Z TRANS	1	-1865	-110	+195	0	+.707	+.707
13	+PITCH, +ROLL, -Z TRANS	1	-1865	+110	+405	0	-.707	-.707
14	-PITCH, -ROLL, +Z TRANS	1	-1865	+110	+195	0	-.707	+.707
15	-YAW, +Y TRANS	2	-2028	-80	+360	0	+1.0	0
16	+YAW, -Y TRANS	2	-2028	+80	+360	0	-1.0	0
		24						

ORBITER B
THRUST LEVEL - 1850 LBF

THRUSTER LOCATIONS

FIGURE A-15

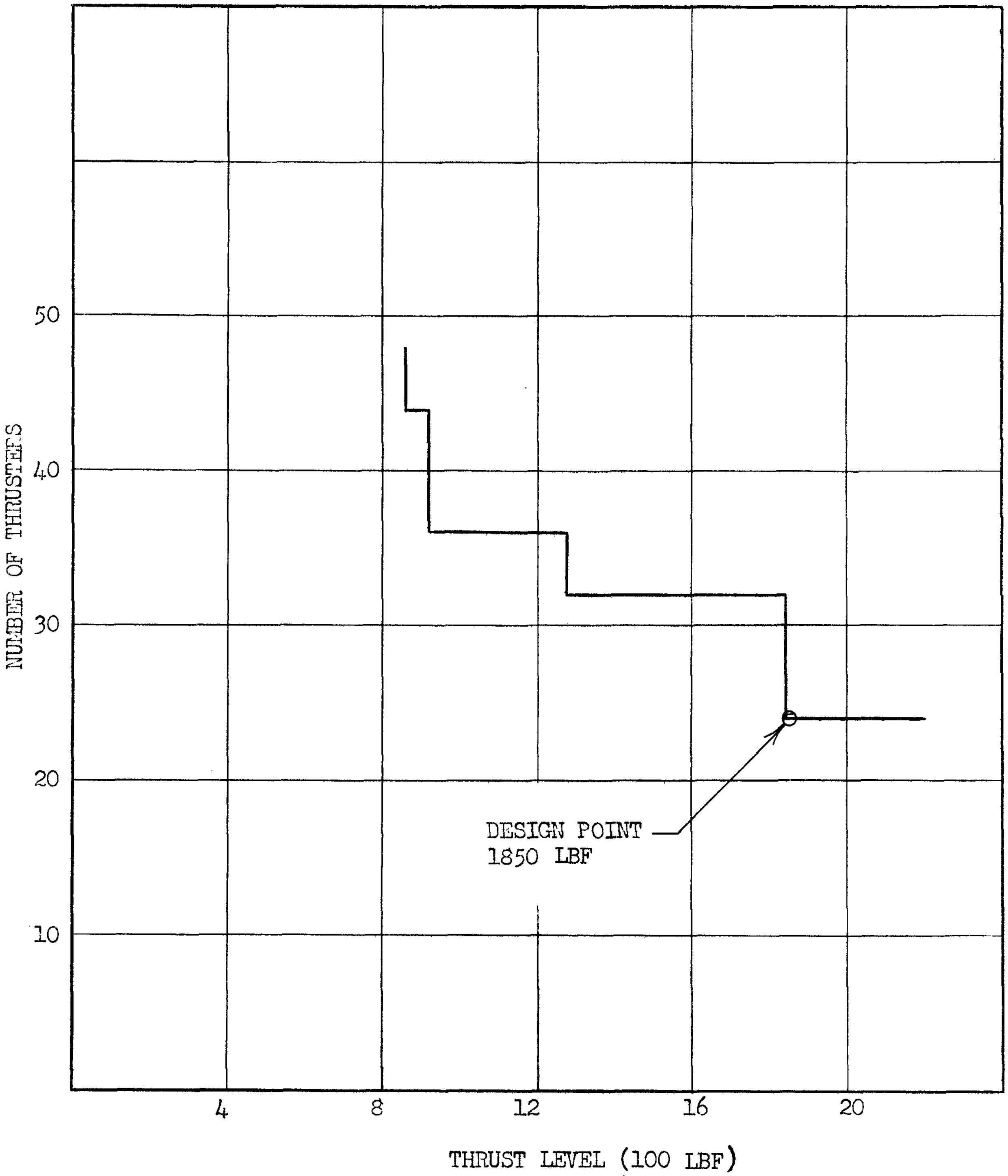

ORBITER B

THRUST REQUIREMENTS

FIGURE A-16

Figure A-17. As shown, the chosen design resulted in a thrust level in yaw and the Y and Z directions above the desired nominal maximum level. For roll, requirements can be met with less than the available number of thrusters without cross coupling. These higher than desired accelerations were offset by the advantage that this approach results in a minimum number of thrusters and has a common thrust level with the booster thruster design. Operational modes for the design are presented in Figure A-18, which shows that, for nominal operation, coupling exists only in Y translation and yaw maneuvers.

A summary of the Orbiter C thruster arrangements is presented in Figure A-19. The arrangement chosen, which provides the minimum number of thrusters and allows common thrust level with the booster thruster, was complicated by the center of gravity location. The vehicle is so shaped that for most of the length of the vehicle, the center of gravity is below the top of the heatshield; therefore, to minimize cross coupling, it would be necessary to locate the thrusters in the heat shield. Thrusters located in the heat shield cannot be used during reentry because in order to minimize heat transfer to the vehicle interior, covers must be provided. The avoidance of heat shield penetration, without excessive coupling of axes, limited the number of feasible thruster arrangements.

The vehicle thruster locations and functions for the chosen design are described in Figures A-20 and A-21. Heat shield penetration could not be avoided for thruster assemblies 4 and 11; however, during reentry, the remaining thruster assemblies satisfy the acceleration requirements but with an increase in cross coupling. Special covers are required for thruster assembly 11, but thruster assembly 4 is located in the nose landing gear well; so that the landing gear door can be used to cover these thrusters during reentry.

The thrust level/number of thruster combinations which were available for the chosen arrangement are presented in Figure A-22, and the maneuvering requirements and capabilities in terms of total thrust are presented in Figure A-23. As shown, the chosen design resulted in a thrust level, in yaw and the Y and Z directions, above the desired level. These higher than desired accelerations were offset by the advantage that this approach resulted in a minimum number of thrusters and has a common thrust level with the booster design. The operational modes for the design are presented in Figure A-24. For nominal operation, coupling is present only in yaw and in pitch during reentry.

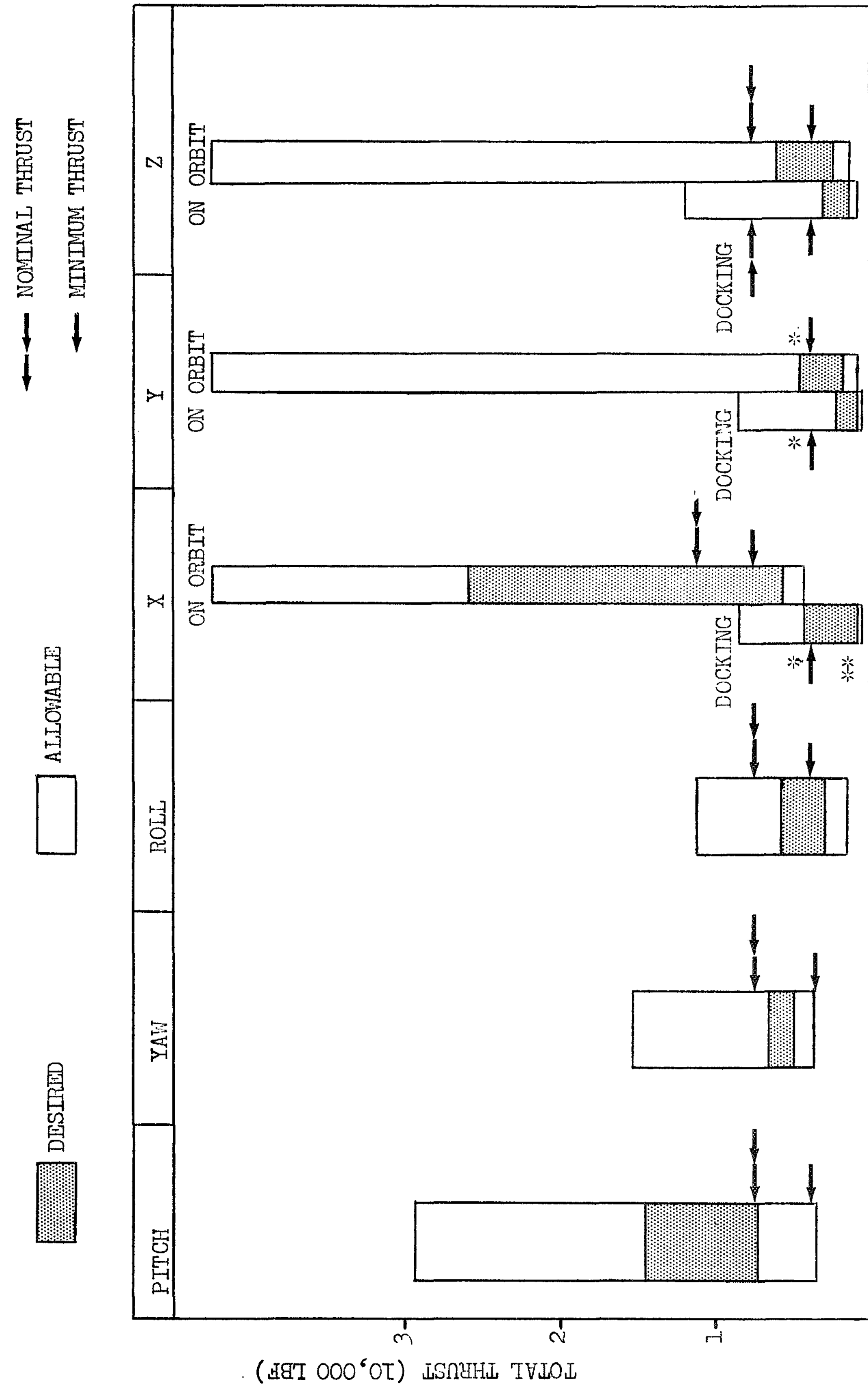

* NOMINAL AND MINIMUM
** 2 ENGINE CUT - NO -X TRANSLATION

ORBITER B

MANEUVER REQUIREMENTS AND CAPABILITY

FIGURE A-17

MANEUVER	THRUSTER ASSEMBLIES	OPERATIONAL MODE	THRUST CHAMBERS USED	ACCELERATION LEVEL (DEG/SEC²)	COUPLING EFFECTS
+ X	3 & 4	NOMINAL	3a,3b,4a,4b	.878	NONE
		ONE ENGINE OUT	3b,3c,4b,4c	.878	NONE
		TWO ENGINES OUT	3c,4a,4b,4c	.878	YAW
- X	1 & 2	NOMINAL	1,2	.439.	NONE
		ONE ENGINE OUT	2	.219	Y, YAW
		TWO ENGINES OUT	-	-	-
+ Y	5 & 15	NOMINAL	5a,15a	.439	ROLL
		ONE ENGINE OUT	5b,15a	.439	ROLL
		TWO ENGINES OUT	15a,15b	.439	ROLL
- Y	6 & 16	SAME AS + Y			
+ Z	8,10,12 & 14	NOMINAL	8,10,12,14	.621	NONE
		ONE ENGINE OUT	10,12	.312	YAW
		TWO ENGINES OUT	8,14	.312	PITCH
- Z	7,9,11 & 13	SAME AS -Z			
+ PITCH	8,10,11 & 13	NOMINAL	8,10,11,13	1.008	NONE
		ONE ENGINE OUT	10,11	.504	YAW
		TWO ENGINES OUT	11,13	.504	Z
- PITCH	7,9,12 & 14	SAME AS + PITCH			
+ YAW	5 & 16	NOMINAL	5a,5b,16a,16b	1.760	ROLL
		ONE ENGINE OUT	5b,16b	.880	ROLL
		TWO ENGINES OUT	16a,16b	.880	ROLL
- YAW	6 & 15	SAME AS + YAW			
+ ROLL	8,9,12 & 13	NOMINAL	8,9,12 & 13	2.580	NONE
		ONE ENGINE OUT	12,13	1.362	NONE
		TWO ENGINES OUT	8,9	1.220	NONE
- ROLL	7,10,11 & 14	SAME AS + ROLL			

ORBITER B

THRUSTER OPERATIONAL PROCEDURE

FIGURE A-18

SUBSYSTEM DESCRIPTION	NO OF THRUSTERS	THRUST LEVEL	TOTAL WEIGHT OF THRUSTERS	RELATIVE ADVANTAGES	RELATIVE DISADVANTAGES
INDEPENDENT X, COUPLED Y AND YAW, COUPLED Z, PITCH AND ROLL √	33	1850	1220	SAME THRUST LEVEL AS BOOSTER	YAW, Y, AND Z TOTAL THRUST LEVELS ARE ABOVE DESIRED RANGE FOR DOCKING
INDEPENDENT X, COUPLED Y AND YAW, COUPLED Z, PITCH, AND ROLL	40	960	1120	ALL THRUST LEVELS IN DESIRED RANGE	LARGE NUMBER OF THRUSTERS
INDEPENDENT X, INDEPENDENT ROLL, COUPLED Y AND YAW, COUPLED PITCH AND Z (AFT PITCH ENGINES MOUNTED IN VERTICLE STABILIZER)	42	1200	1260	ALL THRUST LEVELS IN DESIRED RANGE MINIMUM HEAT SHIELD PENETRATION	LARGE NUMBER OF THRUSTERS DIFFICULTIES EXIST FOR INSTALLATION OF AFT PITCH ENGINES

√ SELECTED

SUMMARY OF ORBITER C THRUSTER ARRANGEMENT OPTIONS

FIGURE A-19

W = 273,644 LB
I_{xx} = 2.059 x 10^6 SLUG-FT^2
I_{yy} = 13.607 x 10^6 SLUG-FT^2
I_{zz} = 14.433 x 10^6 SLUG-FT^2

THRUSTER ASSEMBLY SUMMARY
– ORBITER C

THRUSTER ASSEMBLY NUMBER	NUMBER OF 1850 LBF THRUSTERS	PURPOSE
1	3	–Z, – PITCH
2	2	–Y, – YAW
3	2	+ Y, + YAW
4	3	+ Z, + PITCH
5	1	– X
6	1	– X
7	3	+ X
8	3	+ X
9	3	+ Y, – YAW
10	3	– Y, + YAW
11	3	+ Z, ± ROLL, – PITCH
12	3	– Z, + ROLL, + PITCH
13	3	– Z, – ROLL, + PITCH

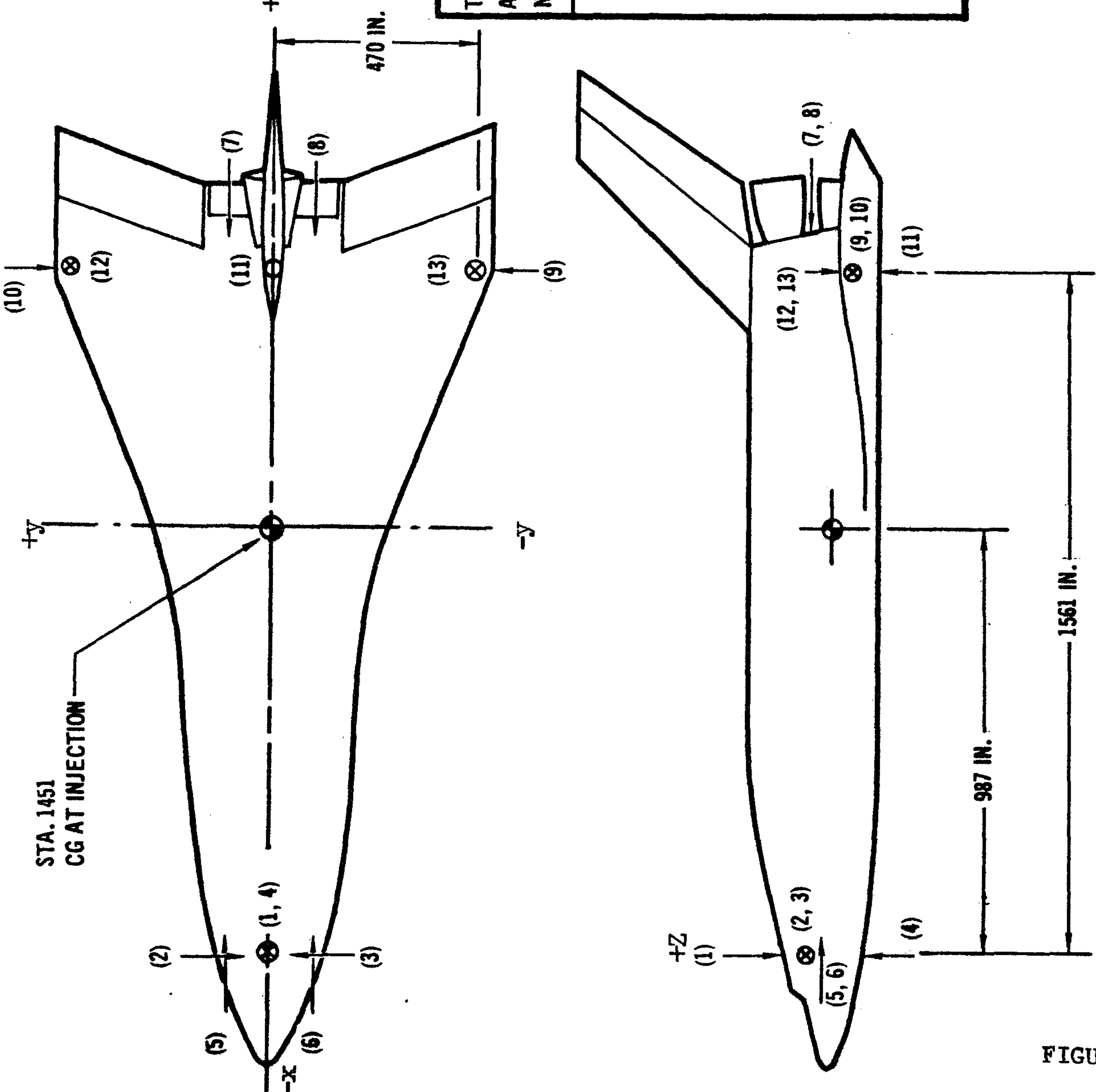

ORBITER C THRUSTER LOCATIONS

FIGURE A-20

LOCATION	MANEUVER	NO. THRUSTERS	THRUSTER COORDINATES*			DIRECTION COSINES		
			X	Y	Z	X	Y	Z
1	-PITCH, -Z TRANS	3	-464	0	+418	0	0	-1.0
2	-YAW, -Y TRANS	2	-464	+81	+364	0	-1.0	0
3	+YAW, +Y TRANS	2	-464	-81	+364	0	+1.0	0
4	+PITCH, +Z TRANS	3	-464	0	+244	0	0	+1.0
5	-X TRANS	1	-455	+54	+395	-.997	0	-.079
6	-X TRANS	1	-455	-54	+395	-.997	0	-.079
7	+X TRANS	3	-2036	+88	+307	+1.0	0	0
8	+X TRANS	3	-2086	-88	+307	+1.0	0	0
9	-YAW, +Y TRANS	3	-2025	-522	+276	0	+1.0	0
10	+YAW, -Y TRANS	3	-2025	+522	+276	0	-1.0	0
11	-PITCH, ±ROLL, +Z TRANS	3	-2000	0	+195	0	0	+1.0
12	+PITCH, +ROLL, -Z TRANS	3	-2025	+470	+290	0	0	-1.0
13	+PITCH, -ROLL, -Z TRANS	3	-2025	-470	+290	0	0	-1.0
		33						

THRUST LEVEL - 1850 LBF

ORBITER C

THRUSTER LOCATIONS

FIGURE A-21

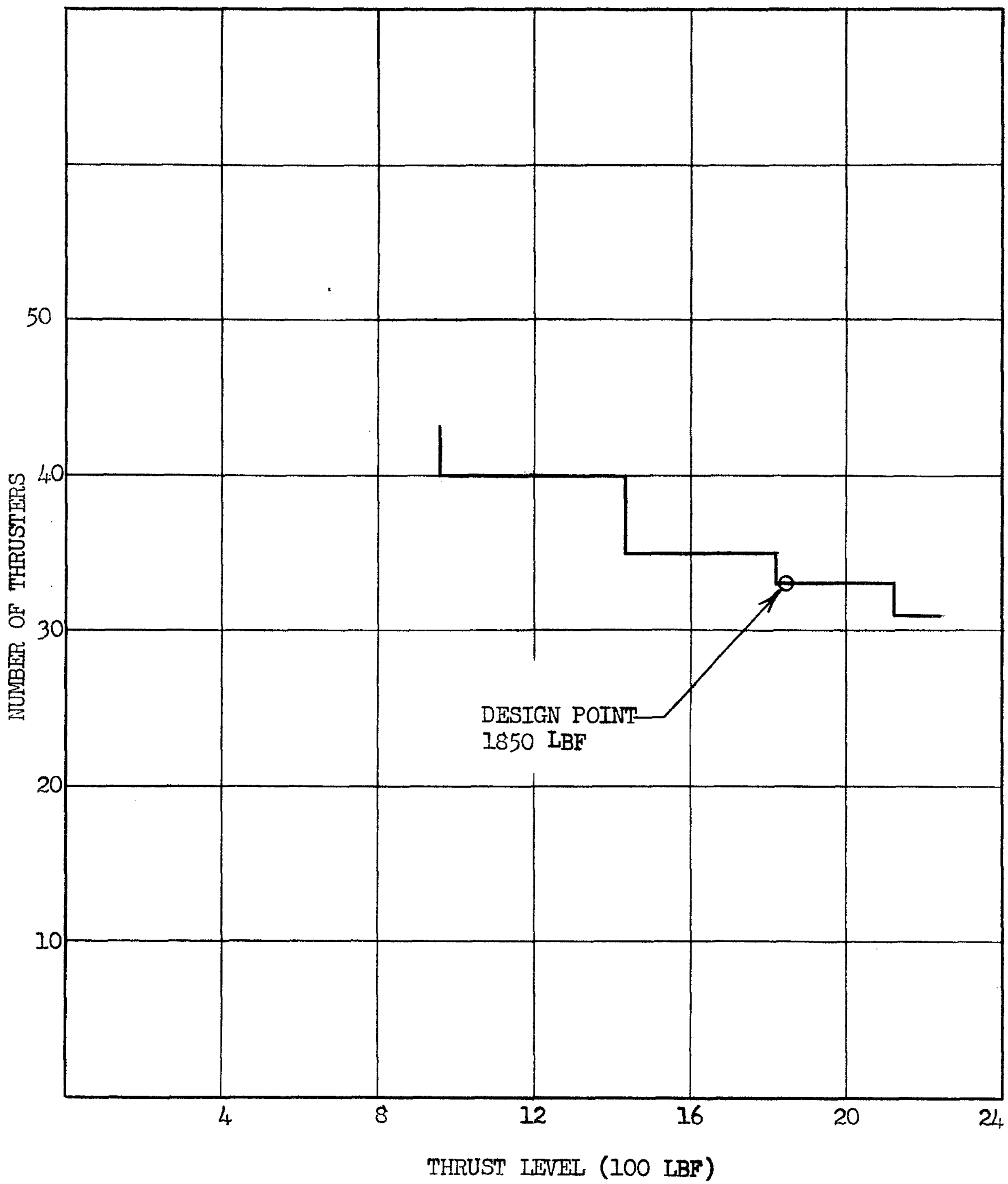

ORBITER C

THRUST REQUIREMENTS

FIGURE A-22

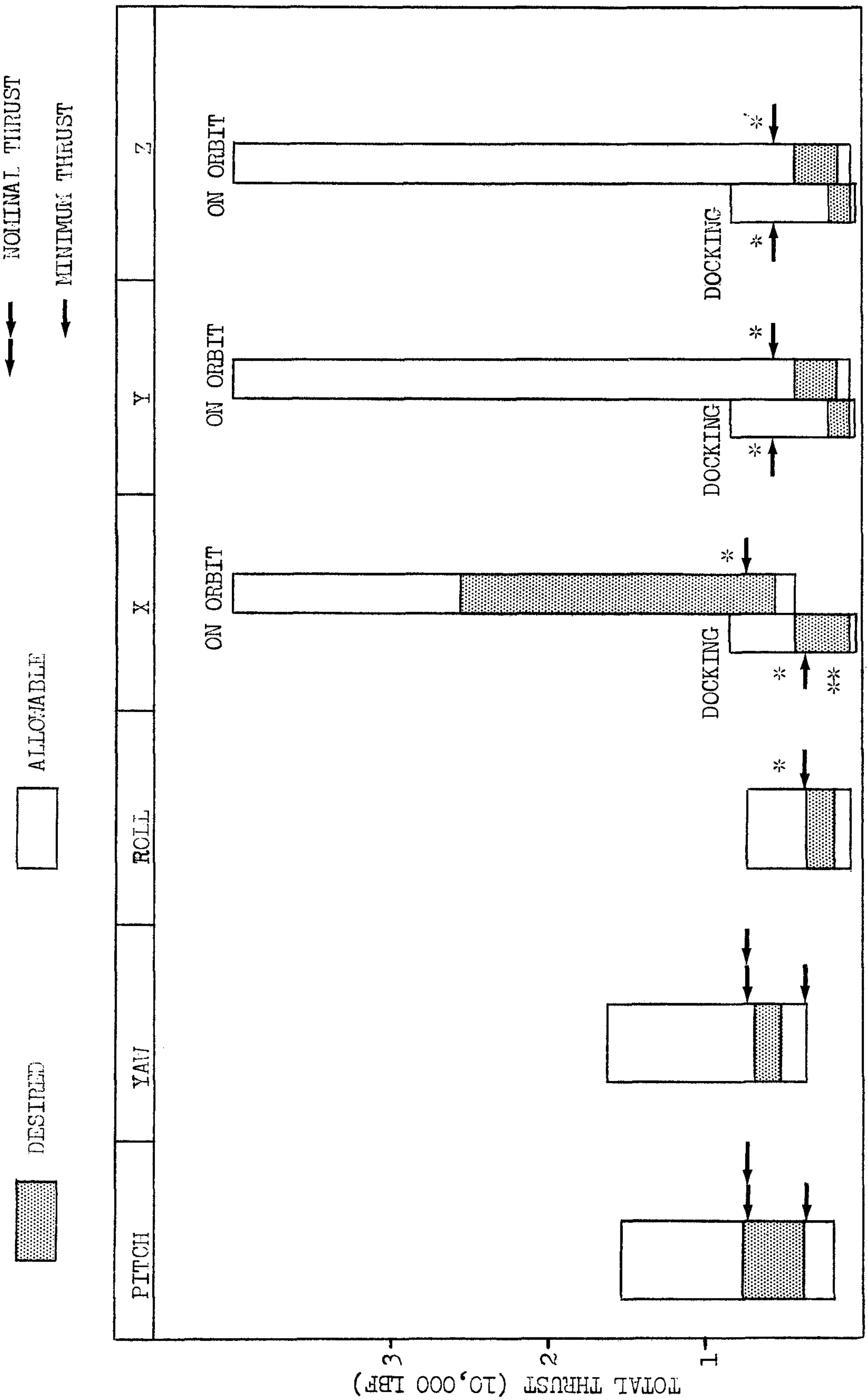

* NOMINAL AND MINIMUM
** 2 ENGINE OUT - NO -X TRANSLATION

ORBITER C

MANEUVER REQUIREMENTS AND CAPABILITY

FIGURE A-23

MANEUVER	THRUSTER ASSEMBLIES	OPERATIONAL MODE	THRUST CHAMBERS USED	ACCELERATION LEVEL (DEG/SEC^2)	COUPLING EFFECTS
+ X	7 & 8	NOMINAL	7a,7b,8a,8b	.872	NONE
		ONE ENGINE OUT	7b,7c,8a,8b	.872	NONE
		TWO ENGINES OUT	7c,8a,8b	.654	NONE
- X	5 & 6	NOMINAL	5,6	.436	NONE
		ONE ENGINE OUT	6	.218	YAW
		TWO ENGINES OUT	-	-	-
+ Y	3 & 9	NOMINAL	3a,9a,9b	.654	NONE
		ONE ENGINE OUT	3b,9a,9b	.654	NONE
		TWO ENGINES OUT	9a,9b,9c	.654	YAW
- Y	2 & 10	SAME AS + Y			
+ Z	4 & 11	NOMINAL	4a,11a,11b	.654	NONE
		ONE ENGINE OUT	4b,11a,11b	.654	NONE
		TWO ENGINES OUT	4c,11b,11c	.654	NONE
- Z	1, 12 & 13	NOMINAL	1a,12a,13a	.654	NONE
		ONE ENGINE OUT	1b,12b,13b	.654	NONE
		TWO ENGINES OUT	1c,12b,13b	.654	NONE
+ PITCH	4,12 & 13	NOMINAL	4a,4b,12a,13a	2.025	NONE
		ONE ENGINE OUT	4b,4c,12a,13a	2.025	NONE
		TWO ENGINES OUT	4c,12a,13a	1.368	Z
- PITCH	1 & 11	NOMINAL	1a,1b,11a,11b	2.025	NONE
		ONE ENGINE OUT	1b,1c,11a,11b	2.025	NONE
		TWO ENGINES OUT	1c,11a	1.012	NONE
+ PITCH DURING REENTRY	12 & 13	NOMINAL	12a,12b,13a,13b	1.430	Z
		ONE ENGINE OUT	12b,12c,13a,13b	1.430	Z
		TWO ENGINES OUT	12c,13a	.715	Z
- PITCH DURING REENTRY	1	NOMINAL	1a,1b	1.243	Z
		ONE ENGINE OUT	1b,1c	1.243	Z
		TWO ENGINES OUT	1c	.622	Z
+ YAW	3 & 10	NOMINAL	3a,3b,10a,10b	1.853	ROLL
		ONE ENGINE OUT	3b,10a	.925	ROLL
		TWO ENGINES OUT	10a,10b,10c	1.022	ROLL, Y
- YAW	2 & 9	SAME AS + YAW			
+ ROLL	11 & 12	NOMINAL	11a,12a	2.019	NONE
		ONE ENGINE OUT	11a,12b	2.019	NONE
		TWO ENGINES OUT	11a,12c	2.019	NONE
- ROLL	11 & 13	SAME AS + ROLL			

ORBITER C

THRUSTER OPERATIONAL PROCEDURE

FIGURE A-24

A summary of the booster thruster arrangements which were studied is presented in Figure A-25. The arrangement chosen uses eighteen 1850 lb thrust level thrusters. This approach provided minimum number of thrusters and subsystem weight. The vehicle thruster locations and functions for the chosen design are described in Figures A-26 and A-27. This configuration provided complete attitude control without thruster penetration of the heat shield. The various thrust level/number of thruster combinations which were available for the chosen arrangement are presented in Figure A-28, and the maneuvering requirements and capabilities in terms of total thrust are presented in Figure A-29. Thrust levels for all maneuvers are within the desired range. Operational modes for the design are presented in Figure A-30. With the exception of the double failure mode, there are no coupling effects.

SUBSYSTEM DESCRIPTION	NO. OF THRUSTERS	THRUST LEVEL	TOTAL WEIGHT OF THRUSTERS	RELATIVE ADVANTAGES	RELATIVE DISADVANTAGES
SSVDRD VEHICLE ARRANGEMENT	26	1850	953	CAPABILITY EXISTS FOR Y AND Z TRANS.	FORWARD THRUSTER LOCATION IN CONFLICT WITH VEHICLE STRUCTURE LONG LINES REQ'D TO AFT THRUSTERS (2400 INCHES)
FORWARD THRUSTERS OVER CANARD-PITCH THRUSTERS ON TAIL	26	1920	975	FORWARD THRUSTERS RIGHT AT TANK	LONG LINES REQ'D TO AFT THRUSTERS (1500 INCHES)
FORWARD THRUSTERS IN NOSE - PITCH AND ROLL THRUSTERS IN TAIL √	18	1850	667	FEWEST TOTAL NUMBER OF THRUSTERS LOWEST WEIGHT	LONG LINES TO AFT THRUSTERS (2000 INCHES) 700 INCH LINES TO FORWARD THRUSTERS
ALL THRUSTERS OVER CANARD	20	1945	760	ALL THRUSTERS CLOSE TO TANKS	

√ SELECTED

SUMMARY OF BOOSTER THRUSTER ARRANGEMENT OPTIONS

FIGURE A-25

THRUSTER ASSEMBLY SUMMARY – BOOSTER

THRUSTER ASSEMBLY NUMBER	NUMBER OF 1850 LB_F THRUSTERS	PURPOSE
1	4	+ YAW
2	4	– YAW
3	4	– PITCH, ± ROLL
4	3	+ PITCH, + ROLL
5	3	+ PITCH, – ROLL

W = 474,876 LB
I_{xx} = 7.017 x 10^6 SLUG-FT^2
I_{yy} = 53.918 x 10^6 SLUG-FT^2
I_{zz} = 57.013 x 10^6 SLUG-FT^2

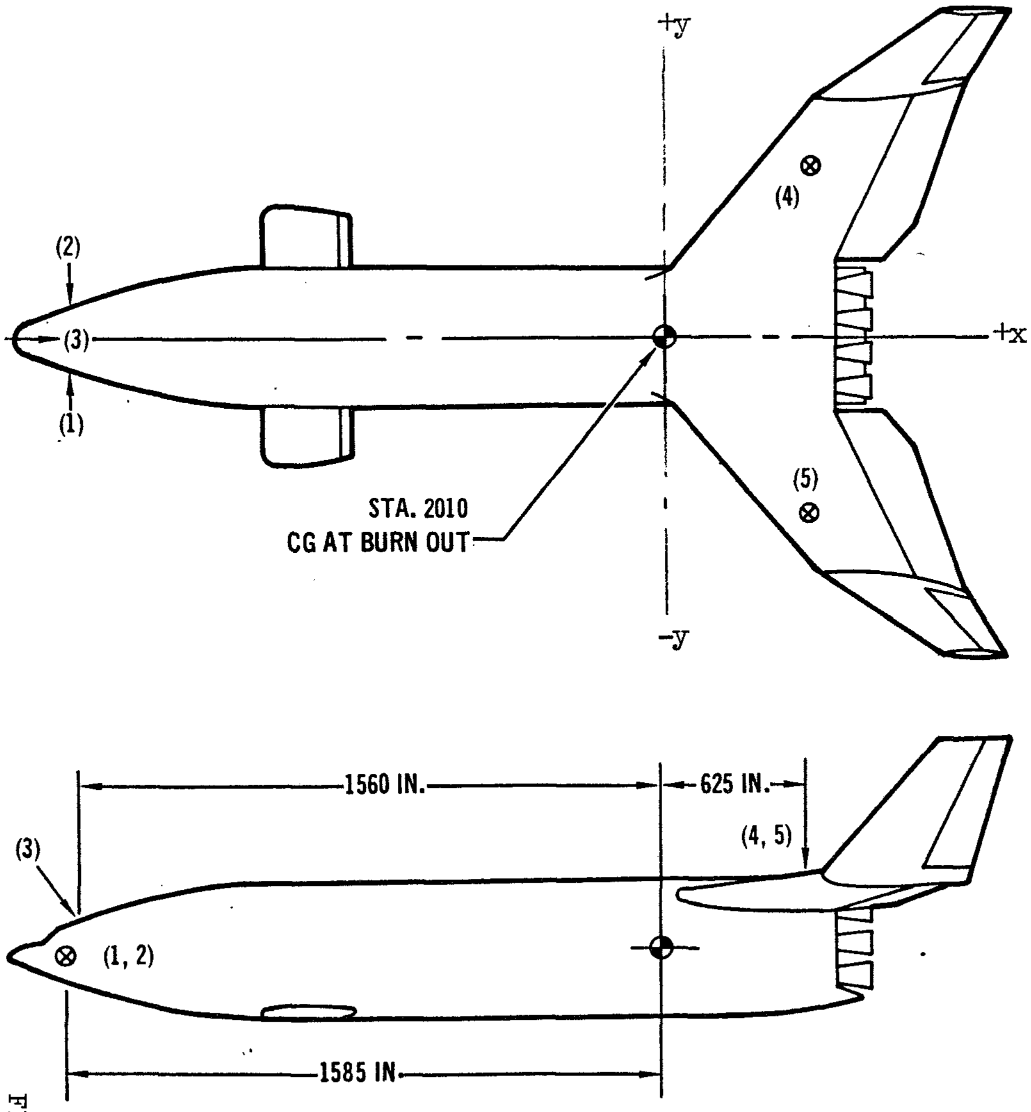

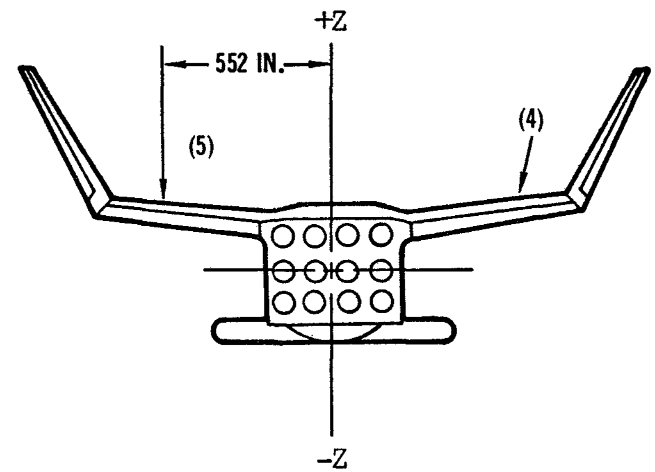

BOOSTER THRUSTER LOCATIONS

FIGURE A-26

LOCATION	MANEUVER	NO. THRUSTERS	THRUSTER COORDINATES*			DIRECTION COSINES		
			X	Y	Z	X	Y	Z
1	+ YAW	4	-425	-83	0	0	+1.0	0
2	- YAW	4	-425	+83	0	0	-1.0	0
3	- PITCH, ± ROLL	4	-450	0	+92	-.6	0	-.8
4	+ PITCH, + ROLL	3	-2635	+522	+205	0	0	-1.0
5	+ PITCH, - ROLL	3	-2635	-522	+205	0	0	-1.0
		18						

THRUST LEVEL - 1850 LBF

BOOSTER

THRUSTER LOCATIONS

FIGURE A-27

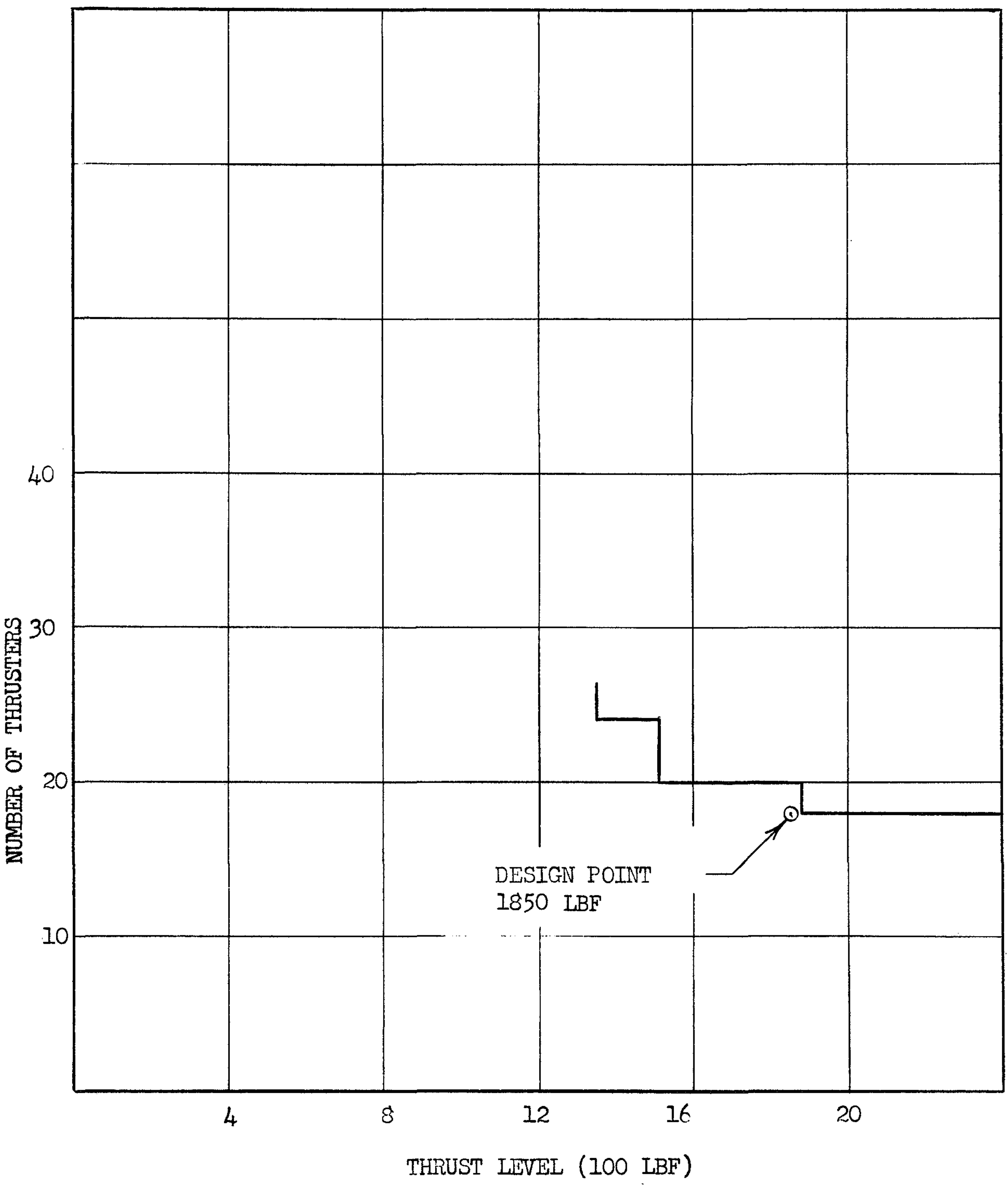

BOOSTER

THRUST REQUIREMENTS

FIGURE A-28

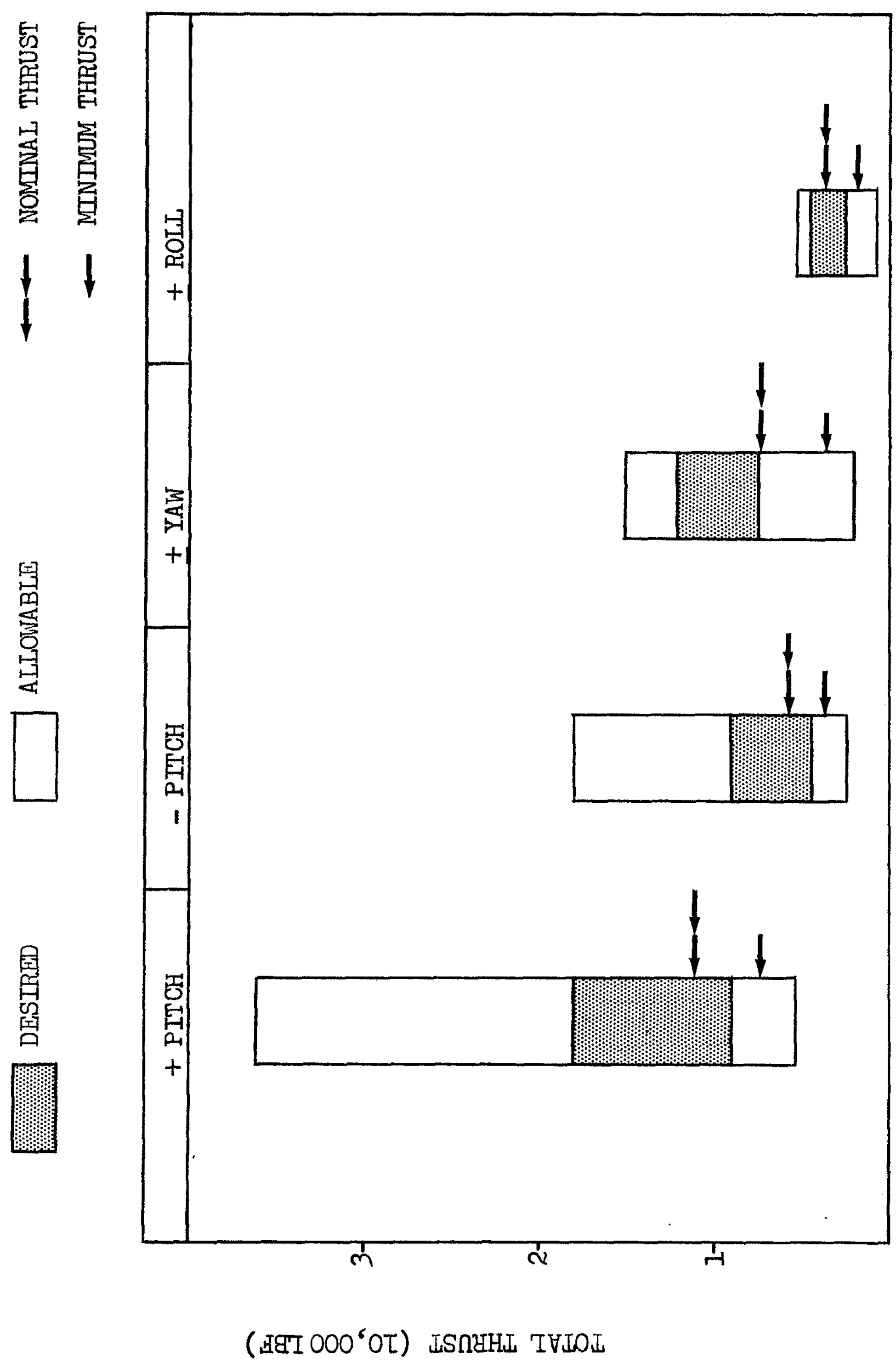

BOOSTER

MANEUVER REQUIREMENTS

FIGURE A-29

MANEUVER	THRUSTER ASSEMBLIES	OPERATIONAL MODE	THRUST CHAMBERS USED	ACCELERATION LEVEL (DEG/SEC^2)	COUPLING EFFECTS*
+ PITCH	4 & 5	NOMINAL	4a,4b,4c,5a,5b,5c	.614	NONE
		ONE ENGINE OUT	4b,4c,5b,5c	.409	NONE
		TWO ENGINES OUT	4c,5a,5b,5c	.409	ROLL
− PITCH	3	NOMINAL	3a,3b,3c,3d	.818	NONE
		ONE ENGINE OUT	3b,3c,3d	.613	NONE
		TWO ENGINES OUT	3c,3d	.409	NONE
+ YAW	1	NOMINAL	1a,1b,1c,1d	.983	NONE
		ONE ENGINE OUT	1b,1c,1d	.737	NONE
		TWO ENGINES OUT	1c,1d	.491	NONE
− YAW	2	SAME AS + YAW			
+ ROLL	4 & 3	NOMINAL	3a,4a,4b	1.391	NONE
		ONE ENGINE OUT	3a,4b,4c	1.391	NONE
		TWO ENGINES OUT	4c	.696	PITCH
− ROLL	5 & 3	SAME AS + ROLL			

* TRANSLATION EFFECTS NOT CONSIDERED

BOOSTER

THRUSTER OPERATIONAL PROCEDURE

FIGURE A-30

A-2. IMPULSE REQUIREMENTS

Revisions to the thrust level, thruster locations, vehicle characteristics and mission timeline which were made prior to Subtask B affected APS total impulse requirements. It was, therefore, necessary to update APS total impulse requirements prior to proceeding with Subtask B.

The main translation maneuver requirements are primarily a function of the +X velocity change requirements for orbit establishment, orbit transfer and deorbit. Operationally, maneuvering requirements could be fulfilled by the APS alone, or by the APS in conjunction with a separately designed orbit maneuvering subsystem (OMS). However, subsequent to Subtask A, NASA selected the operational approach wherein the APS would perform all maneuver requirements, thus eliminating the need for an orbit maneuvering subsystem. Subtask B impulse requirements were, therefore, defined only for this operational approach.

Mission impulse requirements were determined for Orbiters B and C and the Booster using the same approaches and assumptions used during Subtask A (Reference (b)). Orbiter requirements were determined for both third and seventeenth orbit rendezvous missions. In order to demonstrate the effect of minimum impulse bit (MIB), limit cycle impulse requirements were determined with MIB's of 50, 100, and 150 lb-sec. The results of this study are presented in Figure A-31.

		ORBITER B		ORBITER C		BOOSTER
	MIB*	3rd ORBIT RENDERVOUS	17th ORBIT RENDERVOUS	3rd ORBIT RENDERVOUS	17th ORBIT RENDERVOUS	
ATTITUDE CONTROL	50	60,800	66,900	99,300	109,200	**
	100	243,200	267,600	397,200	436,800	
	150	547,200	602,100	893,700	982,800	
ATTITUDE MANEUVERING		834,000	861,000	702,400	720,700	864,000
TRANSLATION MANEUVERS		11,229,000	11,537,000	11,290,000	11,608,000	***
TOTAL	50	12,124,000	12,465,000	12,092,000	12,438,000	864,000
	100	12,306,000	12,666,000	12,390,000	12,766,000	
	150	12,610,000	13,000,000	12,886,000	13,312,000	

* MIB = Minimum impulse bit per thruster - lbf-sec
** Negligible
*** No Requirement

IMPULSE TOTALS

FIGURE A-31

A-3. REFERENCES

(a) NASA-MSFC, Space Shuttle Vehicle Description and Requirements Document, dated 1 October 1970.

(b) Anglim, D. D., Baumann, T. L., Ebbesmeyer, L. H., High Pressure Auxiliary Propulsion Subsystem Definition Subtask A Report, McDonnell Douglas Report No. MDC E0297, dated 12 February 1971.

APPENDIX B
THERMAL ENVIRONMENT DEFINITION

The vehicle internal environment determines the amount of heat transferred to the APS propellant tanks and the resultant weight penalties associated with maintaining the low propellant temperatures. Heat transfer from the environment to the cold gaseous propellants in the accumulators and lines also affect the APS operational characteristics. These environmental temperatures are determined by the local vehicle external heating rate as moderated by the thermal capacity and radiative properties of elements around the region of interest. The model used to calculate typical environments is shown in Figure B-1. It consists of an external skin, a radiation gap, a layer of Micro-Quartz, another radiation gap, and a wall with a thermal thickness corresponding to that of the main engine propellant tank. Transient calculations were directed particularly toward establishing temperature histories for the inner Micro-Quartz surface and the main engine propellant tank because these surfaces provide the surrounding environment for most of the APS lines and components. Results were utilized in a conservative manner. For those APS elements where heating was deemed desirable, the temperature was assumed to correspond to the lowest surrounding temperature. The upper limit was used, however in all cases where heating was considered undesirable.

Orbiter Ascent Heating - Typical vehicle side and bottom temperature histories during ascent are shown in Figure B-2 for areas near the main engine hydrogen tank and in Figure B-3 for areas near the main engine oxygen tank. The cryogenic temperatures of the main engine propellant tanks during ascent provide component environmental temperatures below the on-orbit temperatures.

Orbiter On-Orbit Heating - During orbit the difference in heat flux associated with different vehicle locations and orbital trajectories leads to substantial variations in the vehicle internal environment. Envelopes of the orbiter environmental temperature range for components located within the vehicle are presented in Figure B-4 for high and low beta angle orbits where beta angle is defined by Figure B-5. As a simplification, the bottom of the orbiter is assumed to always face the earth. For the low beta angle case, three regions have been defined. These regions correspond to the temperature history expected for the inner surface of the Micro-Quartz at the top of the vehicle, where the orbital oscillations are most severe, at the side where the heat flux is comparatively low, and on the bottom, where the thick Micro-Quartz and the relatively constant heat flux from

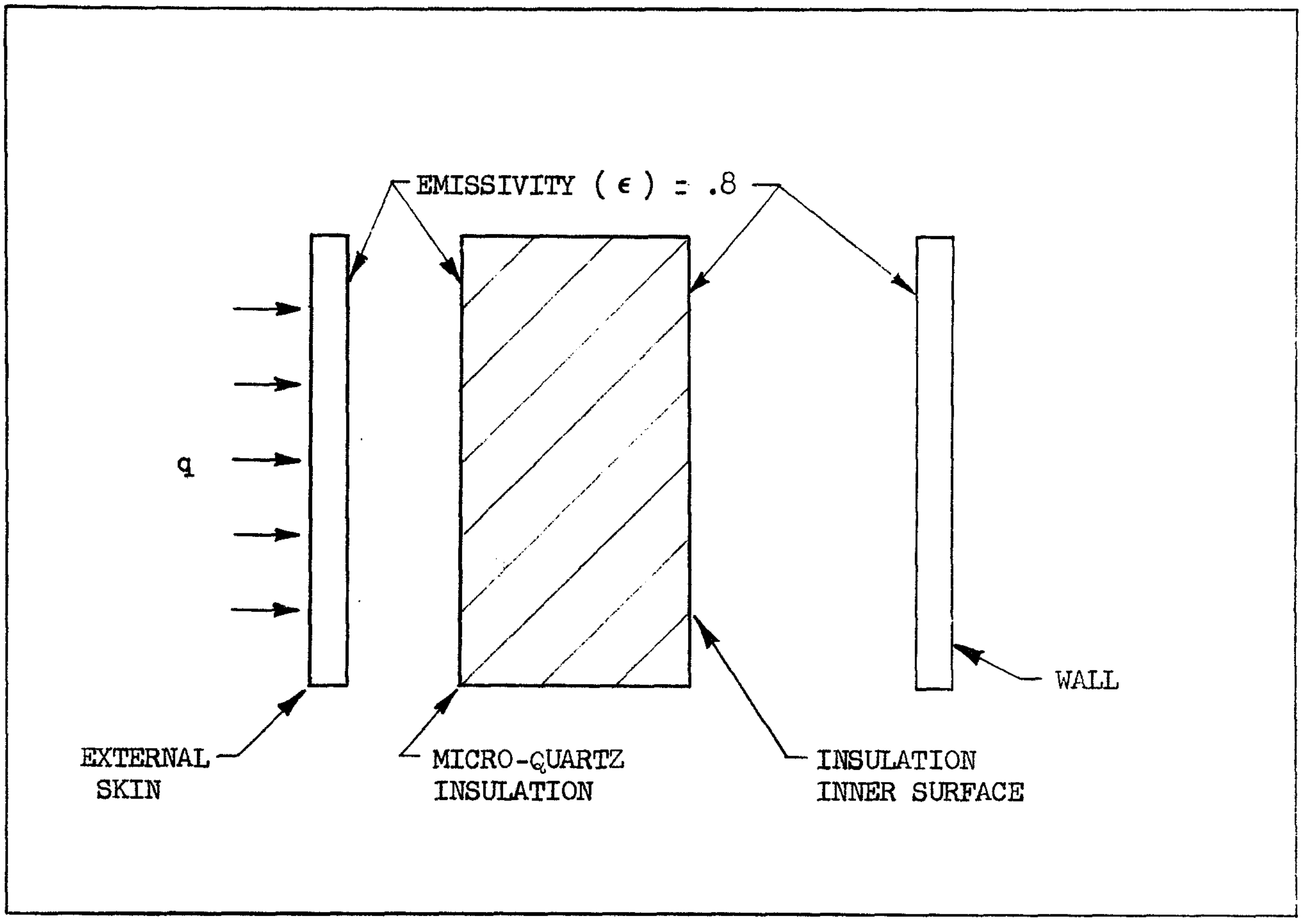

THERMAL MODEL SCHEMATIC

FIGURE B-1

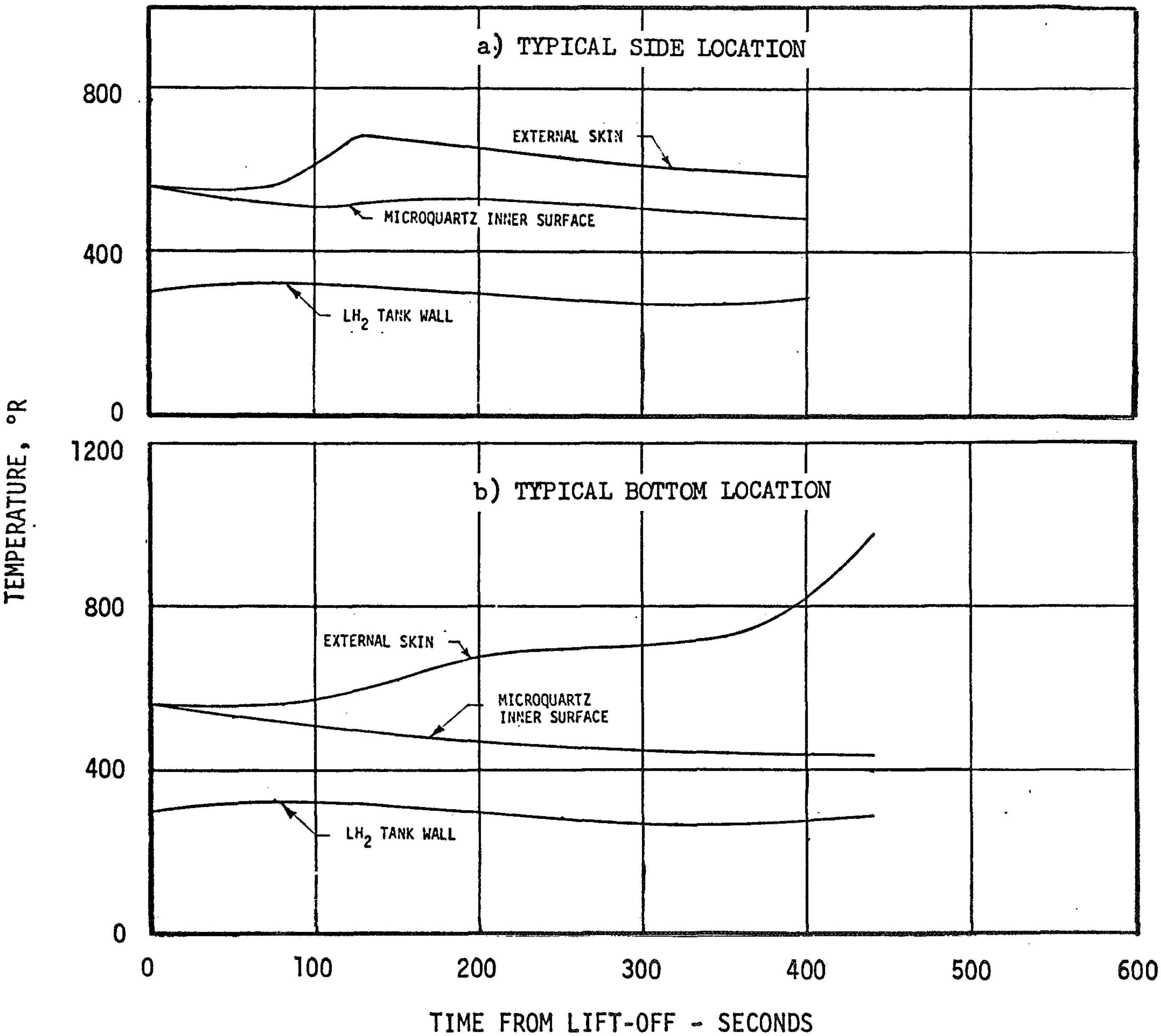

ASCENT TEMPERATURES ORBITER

: PROXIMITY TO LH_2 TANK

FIGURE B-2

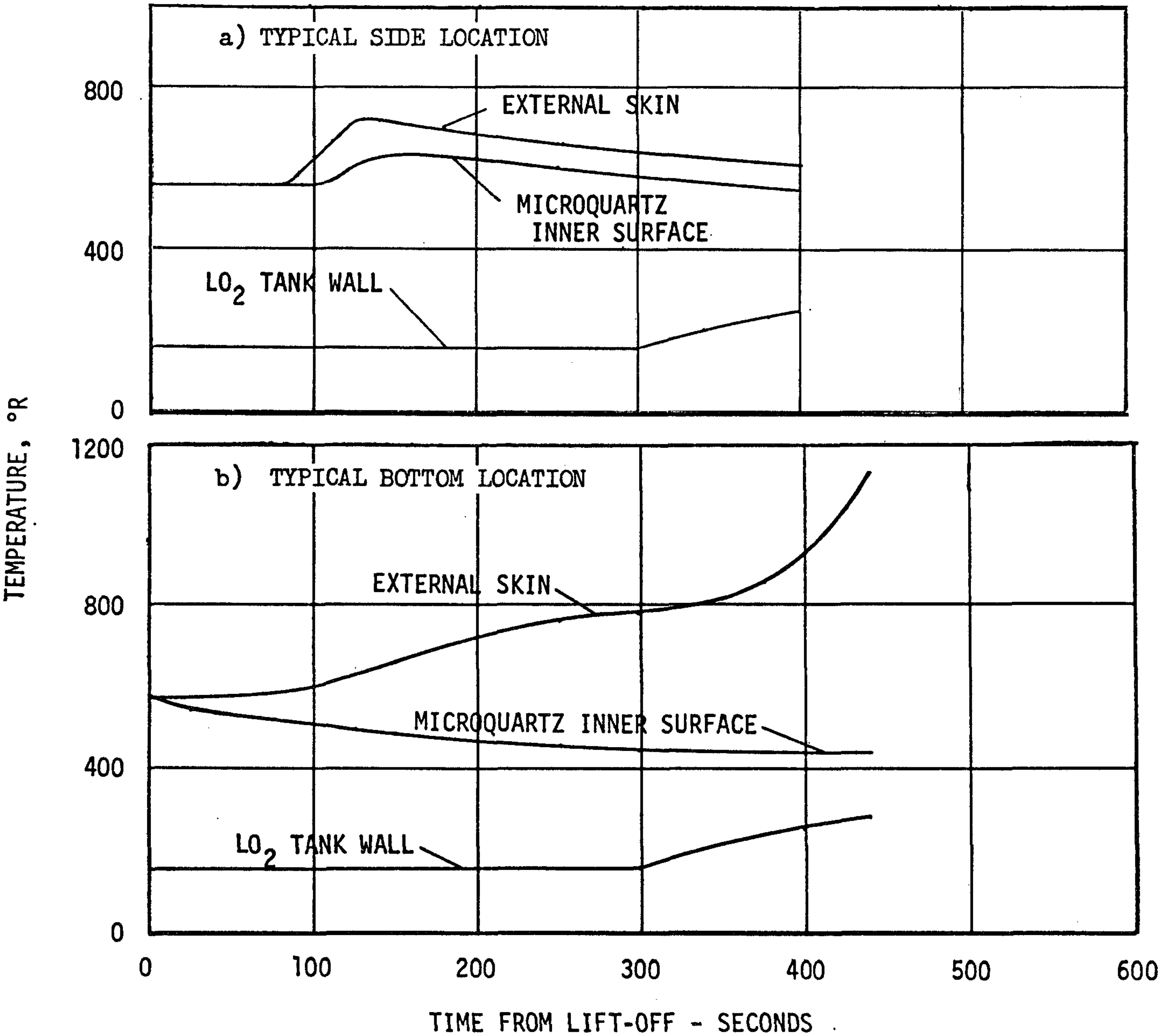

ASCENT TEMPERATURES ORBITER

: PROXIMITY TO LO_2 TANK

FIGURE B-3

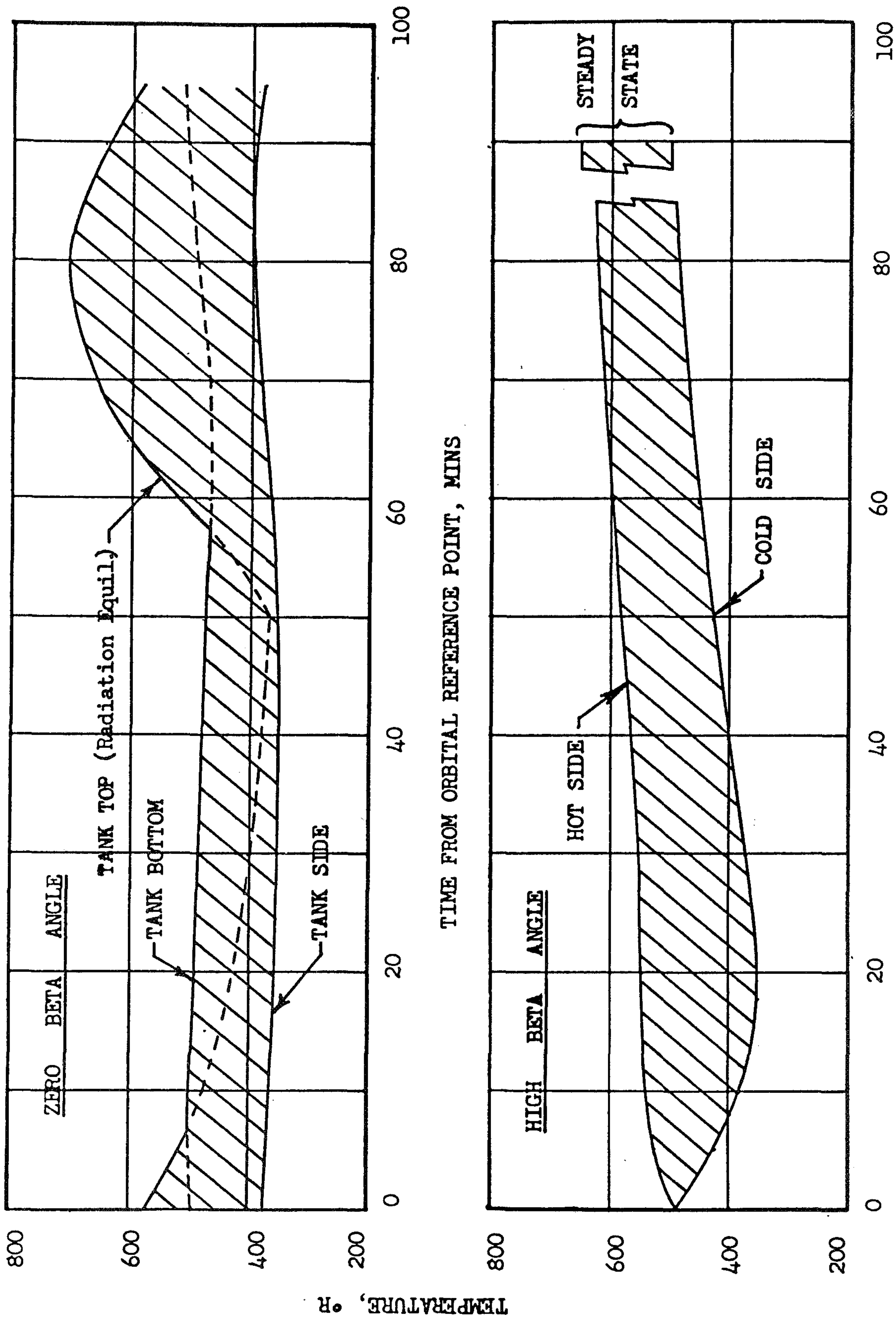

THERMAL ENVIRONMENT OF ORBITER MAIN ENGINE TANK

o ORBITAL MISSION

FIGURE B-4

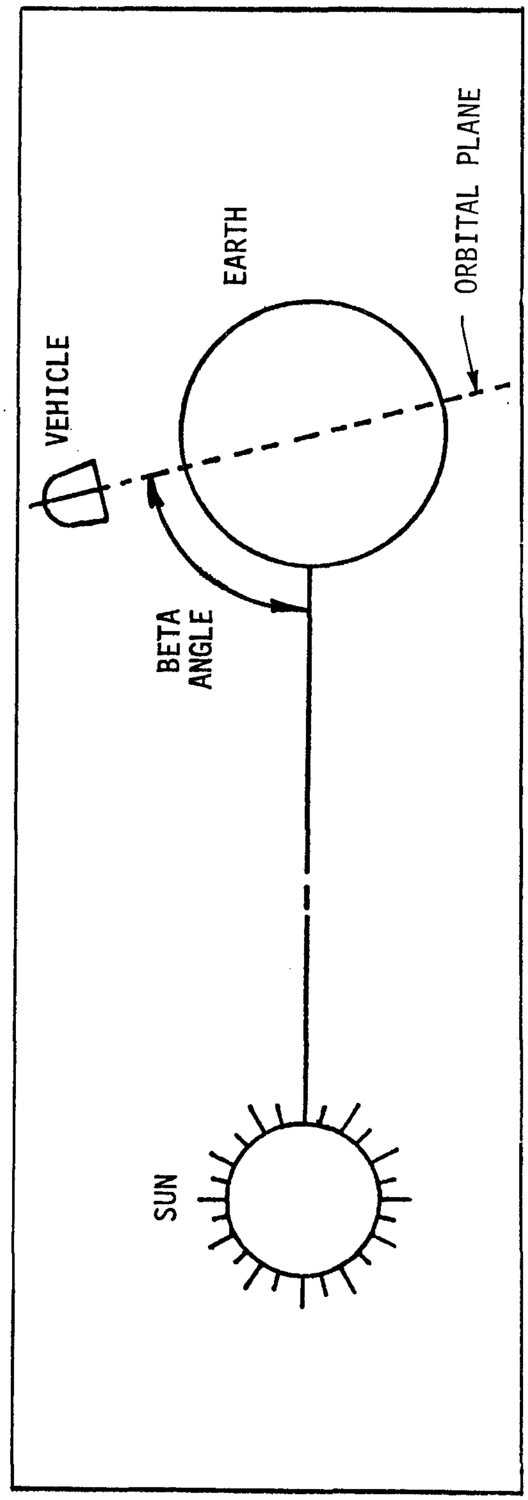

SCHEMATIC OF SUN-EARTH-VEHICLE ANGLE

FIGURE B-5

the earth maintains a nearly constant inner surface temperature. Depending upon their location, components might be required to withstand either nearly constant temperature, corresponding to a side or bottom location, or oscillations similar to those of the top. For the high beta angle case, the environment shown corresponds to that expected for the first orbit as well as an approximate steady state range.

Orbiter Reentry Heating - Orbiter reentry thermal histories are presented in Figures B-6 and B-7. The difference in the thermal histories for the various locations is caused by differences in local heating rates and variations in the insulation time constants. The reentry analysis shows an extremely slow cooling rate of the inner insulation surface even after reentry has been completed. This requires that APS components must withstand the reentry thermal environment for much longer than the actual time of reentry; however, natural convection, not included in the analysis, would provide more rapid cooling than that shown.

Booster Ascent and Reentry Heating - The thermal environment experienced by the booster is similar to that of the orbiter during ascent. The booster reentry heating is substantially less, however, than for the orbiter. The booster internal thermal environment was based on the radiative average of the tank temperature and the temperature of the surroundings. These estimates are shown in Figure B-8 for a region near the canard on the upper surface where interference heating during ascent is significant and includes the effect of a radiation shield between the skin and the APS components.

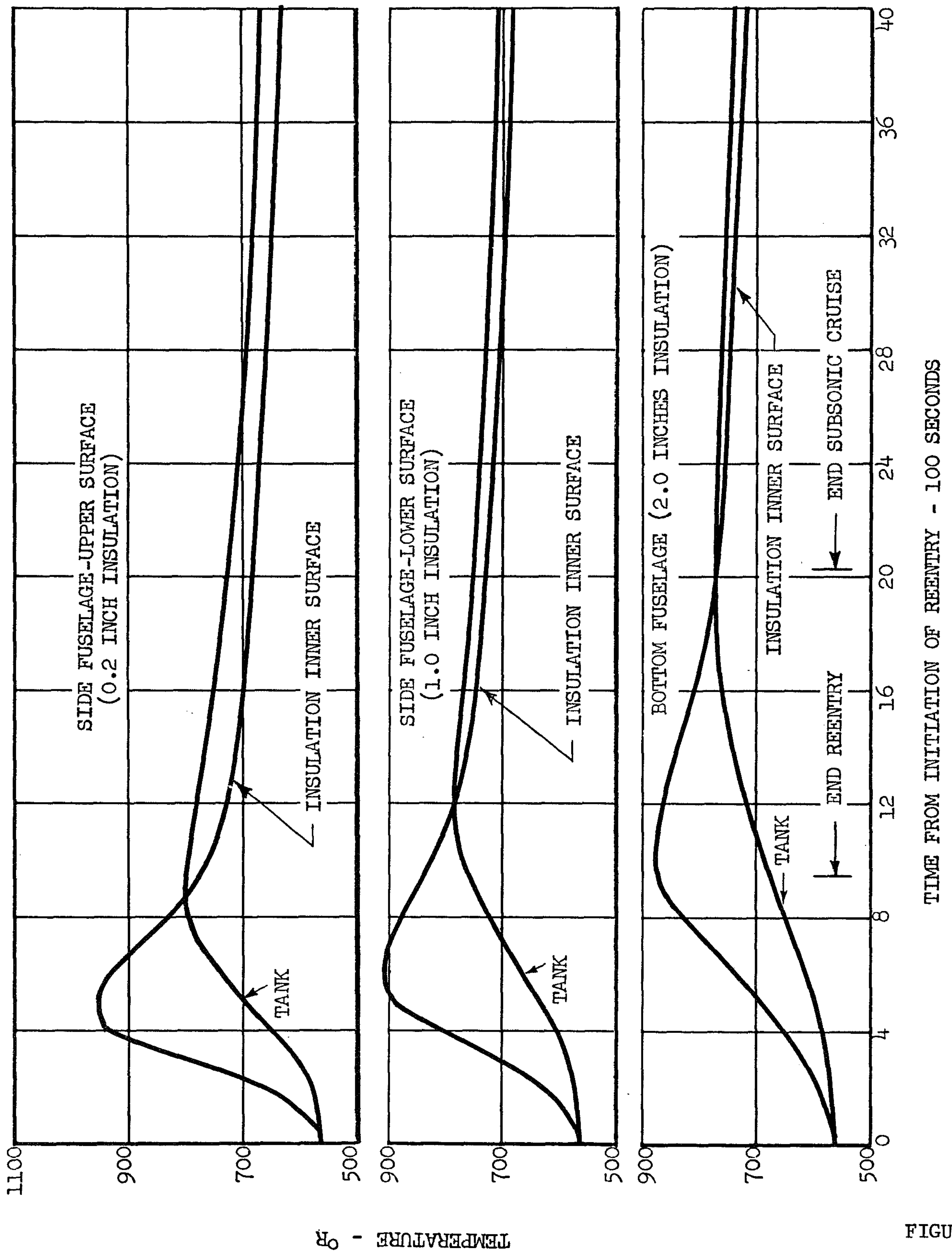

TYPICAL REENTRY TEMPERATURES

ORBITER B

FIGURE B-6

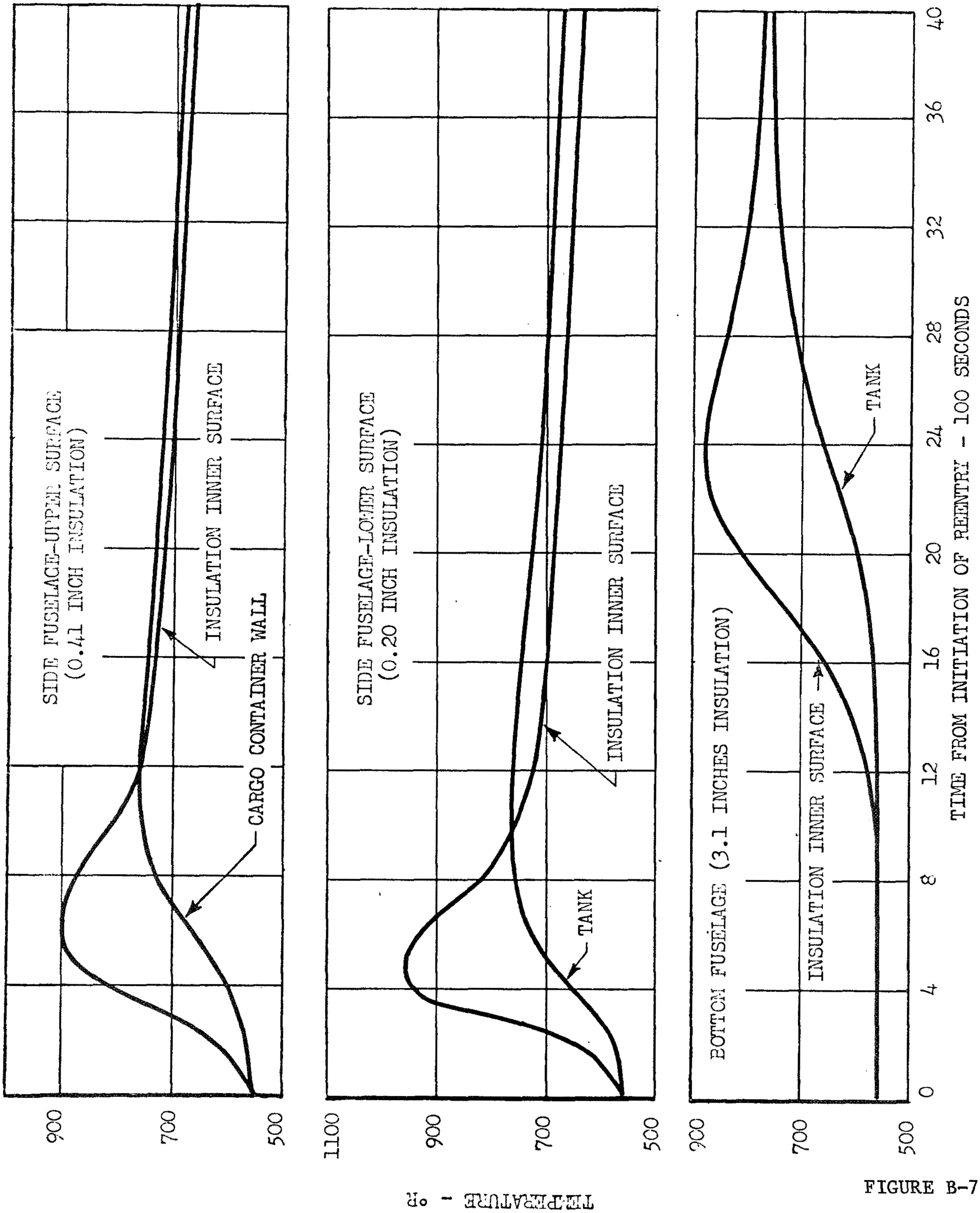

ORBITER C - TYPICAL REENTRY TEMPERATURES

FIGURE B-7

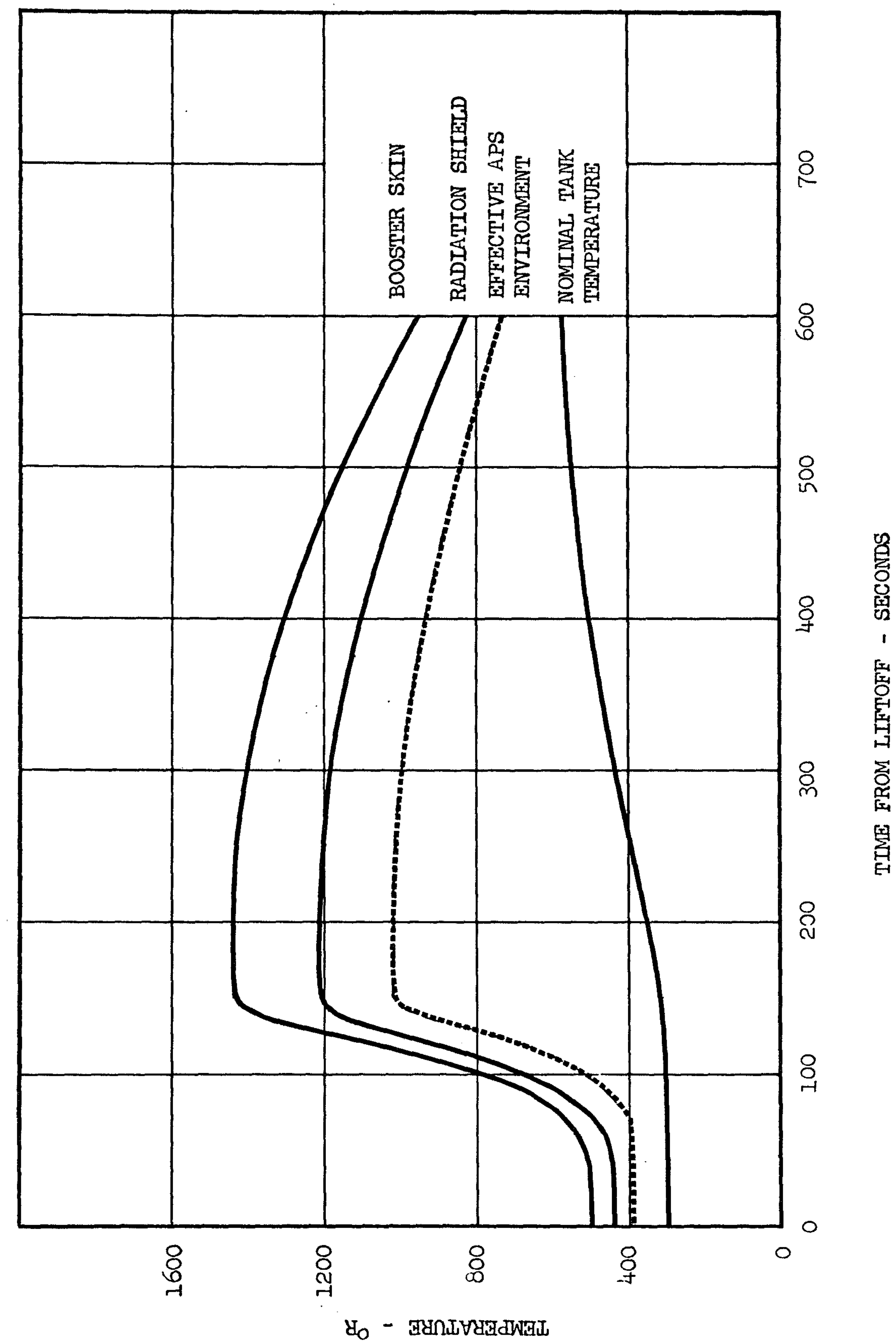

TYPICAL BOOSTER ASCENT AND REENTRY TEMPERATURE PROFILES
ON TOP OF VEHICLE NEAR CANARD

FIGURE B-8

APPENDIX C
APS INSTALLATION

A realistic installation of the APS into the space shuttle must take into consideration location of other equipment and the effect of environment on component design and operation. The location of internal shuttle equipment such as main engines, main tanks, etc. are defined in the Space Shuttle Vehicle Description and Requirements Documents, Reference (a). The internal thermal environments are defined in Appendix B. The primary thermal constraint considered for APS installation was the desire to eliminate heat shield penetration by the thrusters. In addition to component installation, a realistic supply line routing was required to allow modeling for weight definition and for development of transient operating and performance data. Where special installation considerations were required, such as heat shorts to the vehicle structure, component installation layouts were made to define the details of component design and attachment.

The APS is composed of four primary assemblies; these are:

(1) thruster assemblies including flow control valves

(2) propellant accumulators, regulators, valves, and propellant distribution lines

(3) propellant conditioning assemblies, consisting of turbopumps, gas generators, and reburn heat exchangers

(4) propellant storage assembly, consisting of tanks, insulation, propellant acquisition, and pressurization subassemblies.

Installation considerations for each of these assemblies are shown in Figures C-1, C-2, and C-3, and are discussed below.

Figures C-4, C-5, and C-6 show the selected thruster installation locations for Orbiters B and C and the Booster, respectively. No heat shield penetration was required except for Orbiter C. The Orbiter C on-orbit (+) pitch thrusters are located under the nose wheel door. These will not necessitate any additional heat shield doors as they are normally protected during entry. The aft (-) pitch thrusters or Orbiter C, which also prevent on-orbit pitch coupling during the roll maneuver, must be protected by a heat shield door that is closed during entry.

The details of thruster installation are shown in Figure C-7. The tie points to the structure are stringers which also mount the vehicle skin (shingles). These stringers are in turn attached to the main engine tank. The distance between

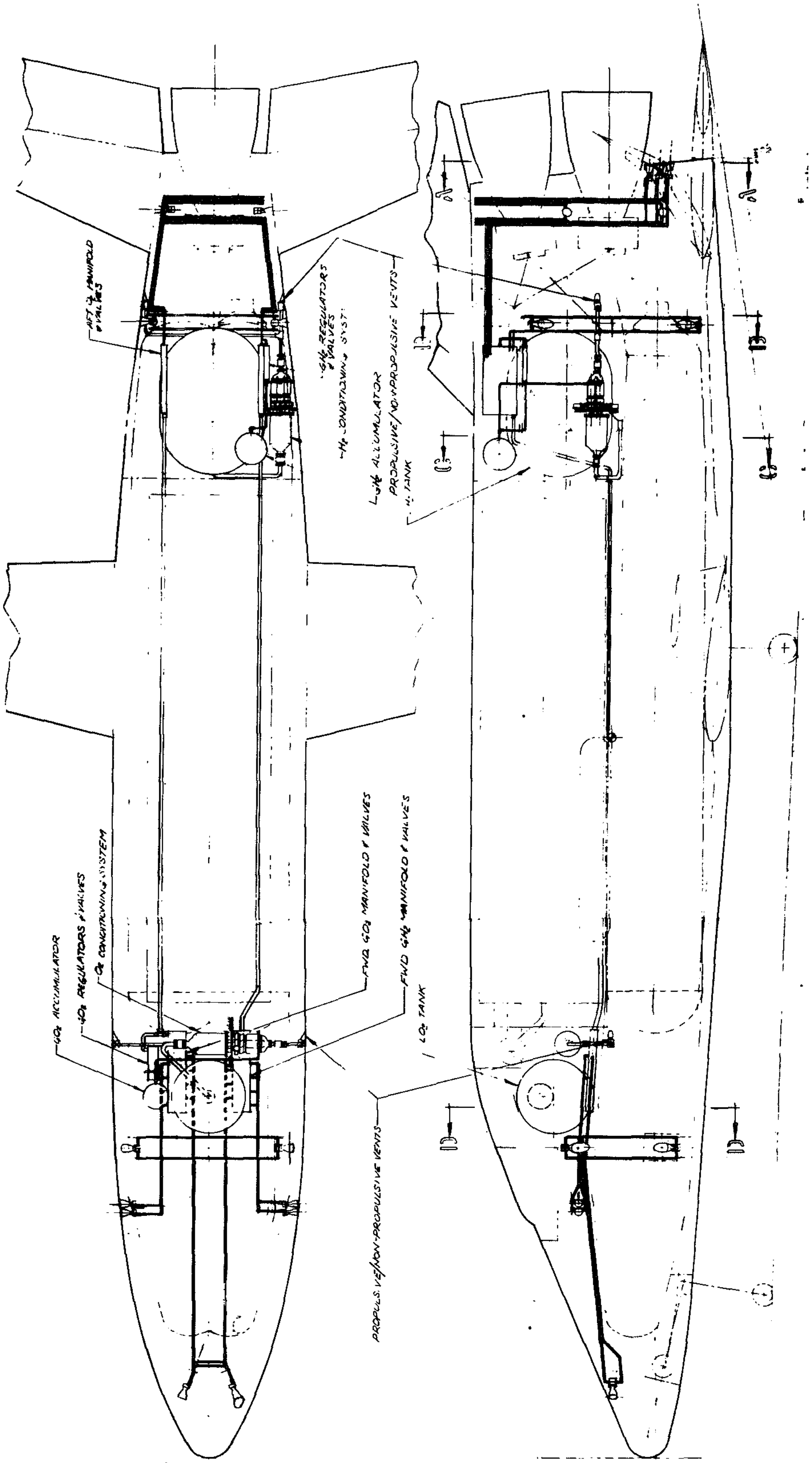

ORBITER B APS INSTALLATION

FIGURE C–1

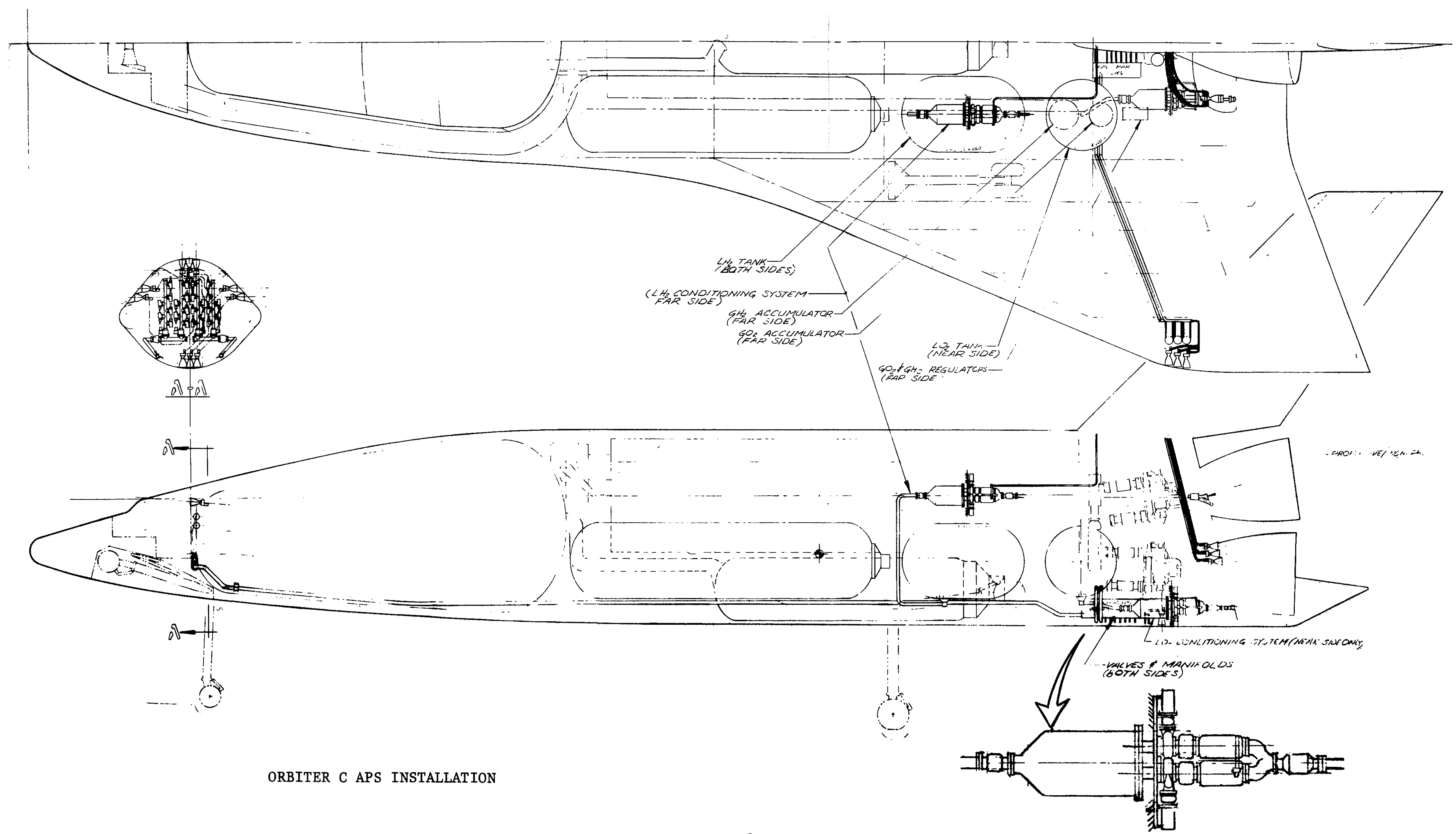

ORBITER C APS INSTALLATION

FIGURE C-2

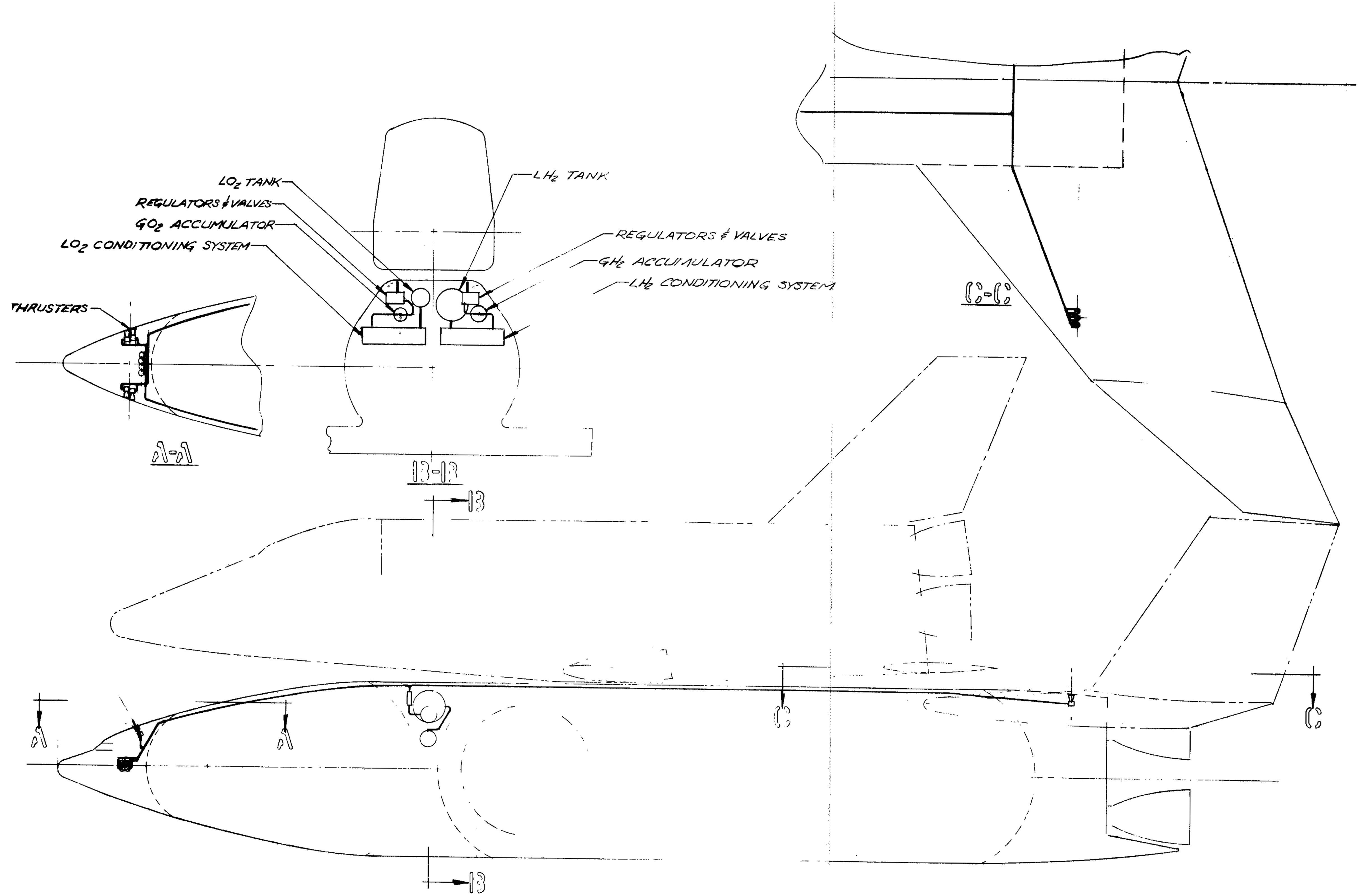

BOOSTER APS INSTALLATION

FIGURE C-3

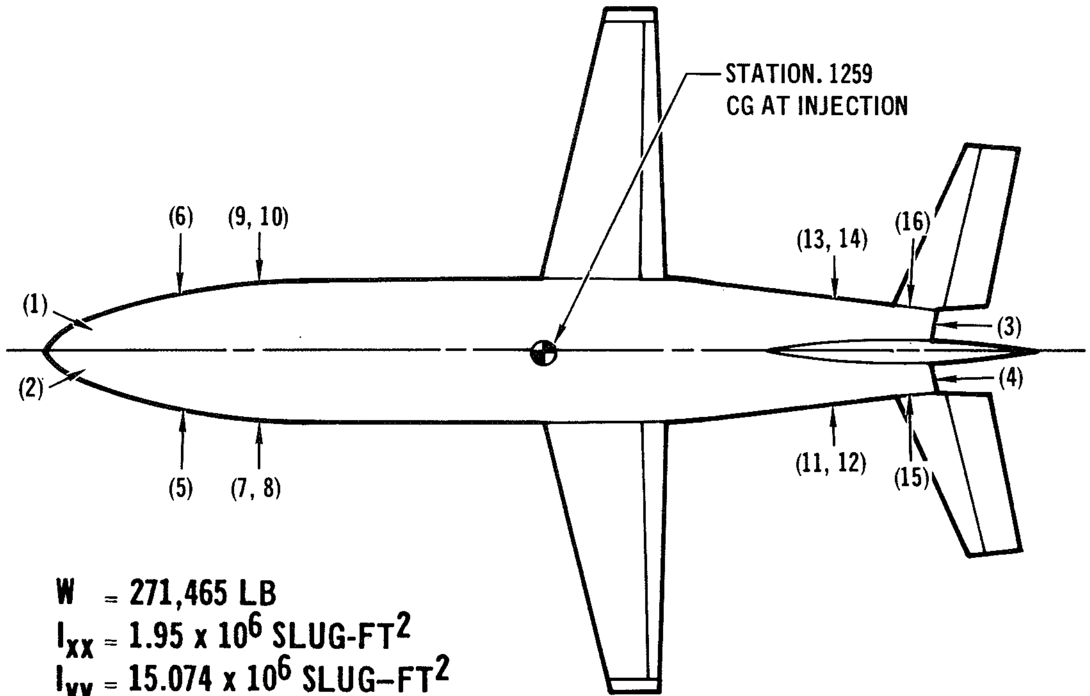

$W = 271{,}465$ LB
$I_{xx} = 1.95 \times 10^6$ SLUG-FT^2
$I_{yy} = 15.074 \times 10^6$ SLUG-FT^2
$I_{zz} = 15.438 \times 10^6$ SLUG-FT^2

THRUSTER ASSEMBLY SUMMARY ORBITER B

THRUSTER ASSEMBLY NUMBER	NUMBER OF 1850 LB_F THRUSTERS	PURPOSE
1	1	– X
2	1	– X
3	3	+ X
4	3	+ X
5	2	+ Y, + YAW
6	2	– Y, – YAW
7	1	– Z, – PITCH, – ROLL
8	1	+ Z, + PITCH, + ROLL
9	1	– Z, – PITCH, + ROLL
10	1	+ Z, + PITCH, – ROLL
11	1	– Z, + PITCH, – ROLL
12	1	+ Z, – PITCH, + ROLL
13	1	– Z, + PITCH, + ROLL
14	1	+ Z, – PITCH, – ROLL
15	2	+ Y, – YAW
16	2	– Y, + YAW

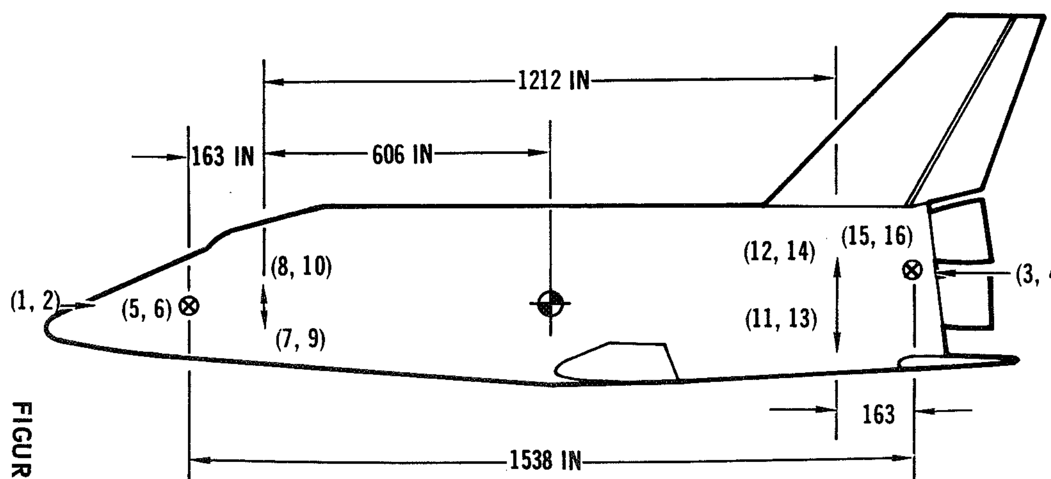

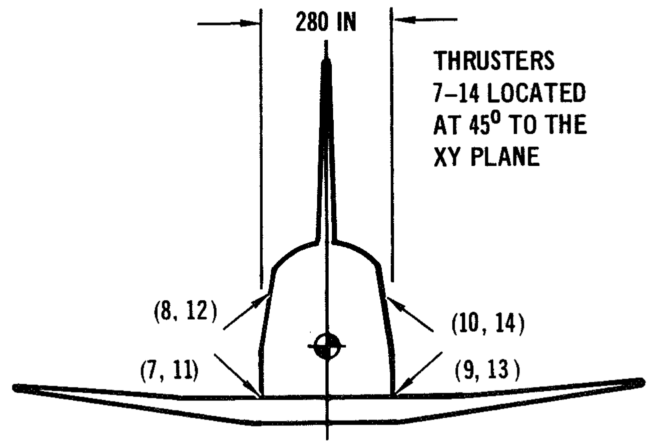

ORBITER B THRUSTER LOCATIONS

FIGURE C–4

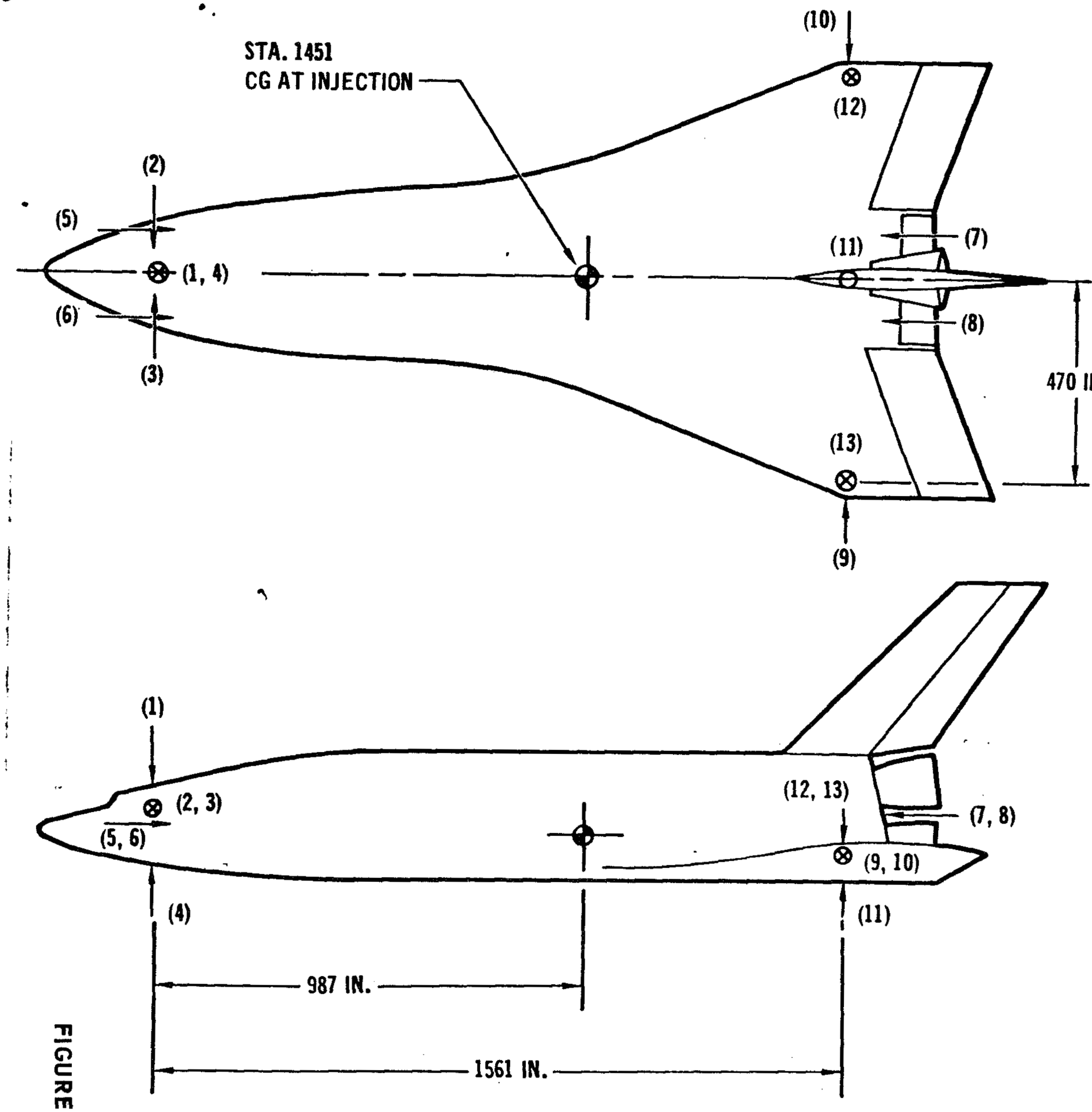

W = 273,644 LB
I_{xx} = 2.059 x 10^6 SLUG–FT^2
I_{yy} = 13.607 x 10^6 SLUG–FT^2
I_{zz} = 14.433 x 10^6 SLUG–FT^2

THRUSTER ASSEMBLY SUMMARY
– ORBITER C

THRUSTER ASSEMBLY NUMBER	NUMBER OF 1850 LBF THRUSTERS	
1	3	–Z, – PITCH
2	2	–Y, – YAW
3	2	+Y, + YAW
4	3	+Z, + PITCH
5	1	– X
6	1	– X
7	3	+ X
8	3	+ X
9	3	+ Y, – YAW
10	3	– Y, + YAW
11	3	+ Z, + ROLL, – PITCH
12	3	– Z, + ROLL, + PITCH
13	3	– Z, – ROLL, + PITCH

ORBITER C THRUSTER LOCATIONS

FIGURE C–5

THRUSTER ASSEMBLY SUMMARY – BOOSTER

THRUSTER ASSEMBLY NUMBER	NUMBER OF 1850 LB_F THRUSTERS	PURPOSE
1	4	+ YAW
2	4	– YAW
3	4	– PITCH, ± ROLL
4	3	+ PITCH, + ROLL
5	3	+ PITCH, – ROLL

$W = 474{,}876$ LB
$I_{xx} = 7.017 \times 10^6$ SLUG–FT^2
$I_{yy} = 53.918 \times 10^6$ SLUG–FT^2
$I_{zz} = 57.013 \times 10^6$ SLUG–FT^2

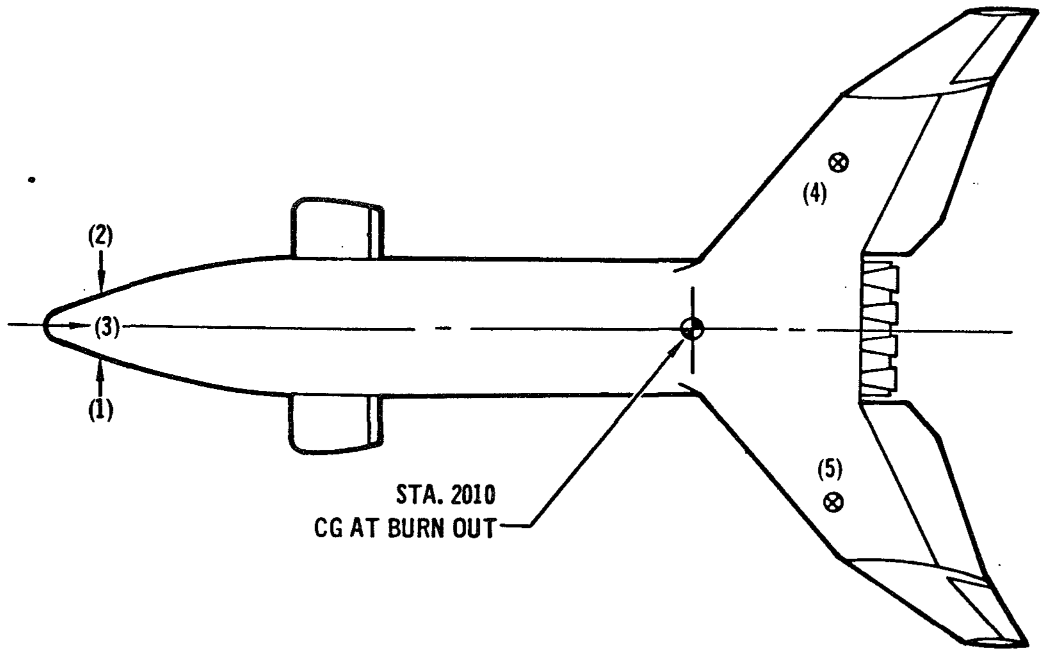

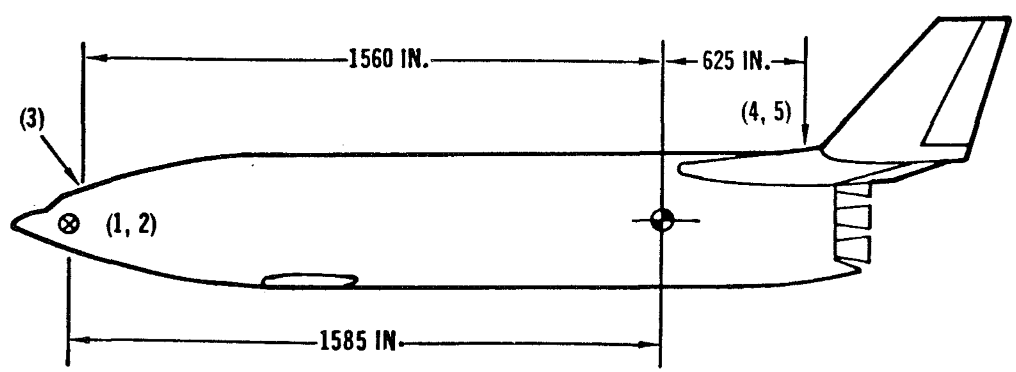

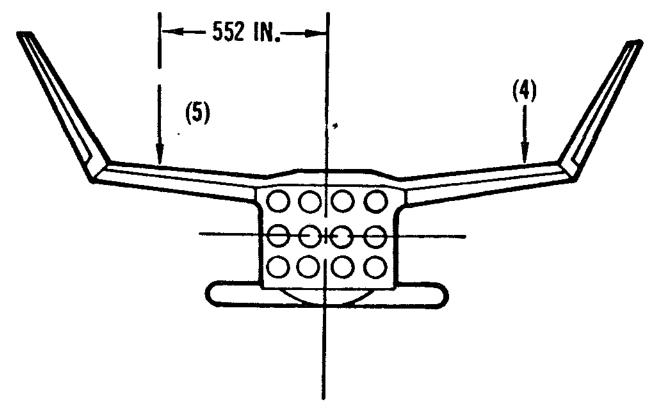

BOOSTER THRUSTER LOCATIONS

FIGURE C–6

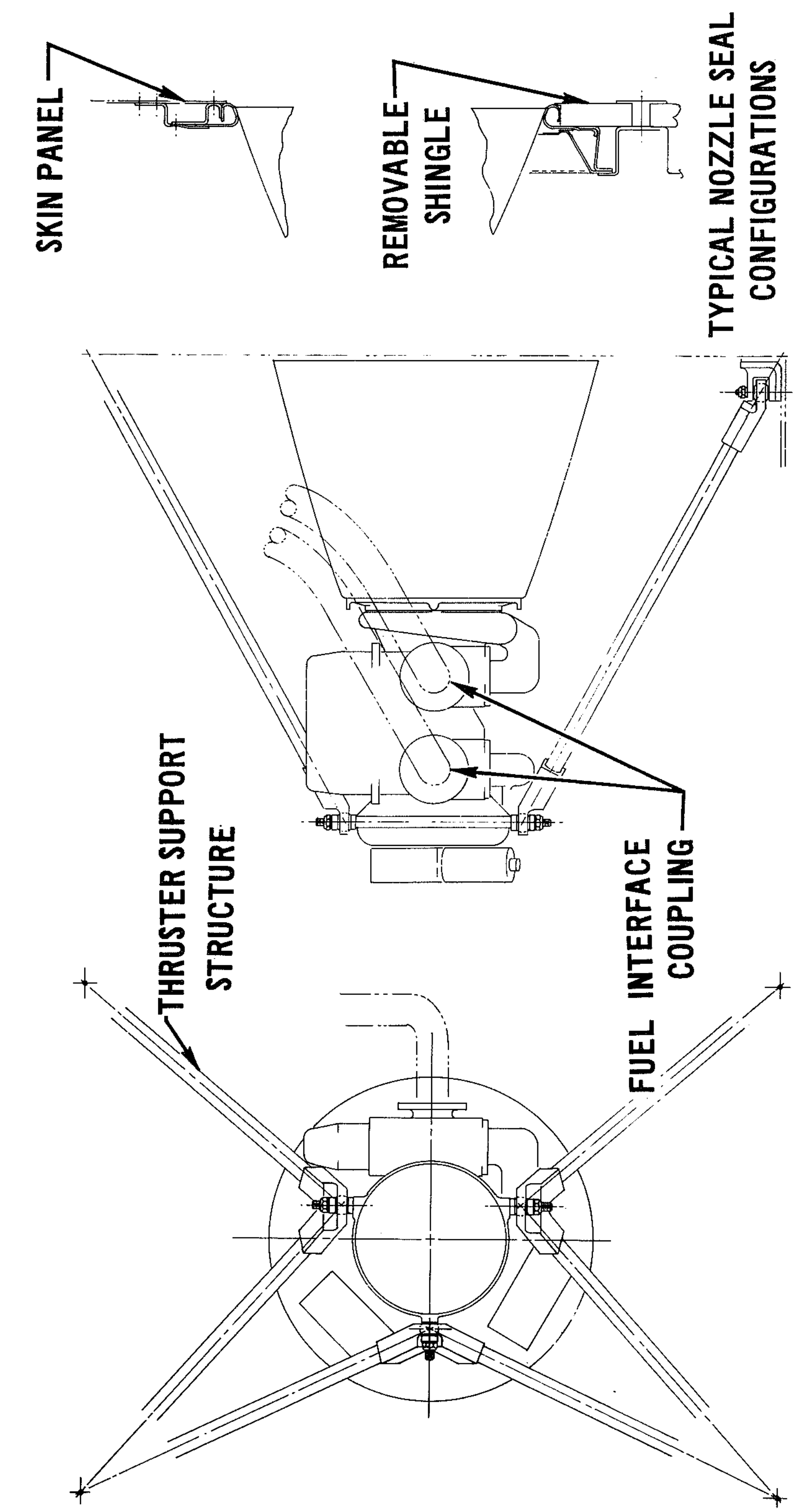

TYPICAL THRUSTER INSTALLATION

FIGURE C-7

stringers can change due to thermal expansion and the shingles are only retained, not constrained, as they will expand differently during flight. The method of mounting allows the distance between stringers to change and also allows the shingles to float around the thruster nozzle without imposing thruster stresses either at the mounting plane or at the nozzle exit. Also shown are methods of sealing the nozzle with the two types of vehicle skin through which the thrusters must fire. One configuration is for the bottom side high temperature skin penetration and one is for a lower temperature skin nearer the vehicle top. Access to the thruster mounting and to the thruster components for adjustment or replacement is by removing the skin panel surrounding the thruster nozzle. These panels are normally removable in the shuttle design to allow replacement.

C-1. ACCUMULATORS AND DISTRIBUTION LINES

Accumulators are installed in close proximity to the conditioning assembly. The criteria for line routing were minimum weight, consistent with good installation, and providing the capability for line insulation inspection and replacement if required. The main propellant lines are routed adjacent to the payload bay which provides access for inspection and maintenance. Manifolds and manifold isolation valves were located to minimize line lengths and number of isolation valves within the vehicle physical installation constraints.

The resulting line lengths and sizes for the vehicles are shown in Figures C-8, C-9 and C-10. The installation of lines between manifolds and accumulators, i.e., main distribution lines, are implemented with expansion joints, pressure balanced compensators and line supports as shown in Figure C-11 (Orbiter B). The lines to the individual thrusters from the manifold are installed such that bends and, if necessary, loops provide expansion capability. The line routings to the

Line connections are shown in Figure C-12. Connections will be bolted flanges with redundant seals in locations which are accessible to allow installation and, if necessary, removal and replacement. The other type of connectors, either swaged or welded, will be utilized in areas that are not accessible and for lines which are not thought to require any maintenance for the vehicle lifetime.

The type of line insulation to be used was defined as a result of a trade study which compared alternate methods of insulation. The alternate means of insulation considered were:

(1) vacuum jacketed lines

(2) lines insulated with high performance multilayer insulation, protected by a flexible cover.

The vacuum jacketed line would be implemented as shown in Figure C-13. The weight comparison of the alternates is shown in Figure C-14. Also shown are the various methods of implementing both the vacuum jacketing and protection of the high performance insulation. Comparison of the weight and complexity of these approaches showed that vacuum jacketing would result in high weight penalties and the installation would be quite complex. For these reasons, the flexible jacket approach was selected for feedline insulation .

The insulation thicknesses and associated temperature rise rate of the propellants within the lines is defined in Appendix E. The requirement to limit thruster mixture ratio excursions was the criteria used to define the required line insulation thickness.

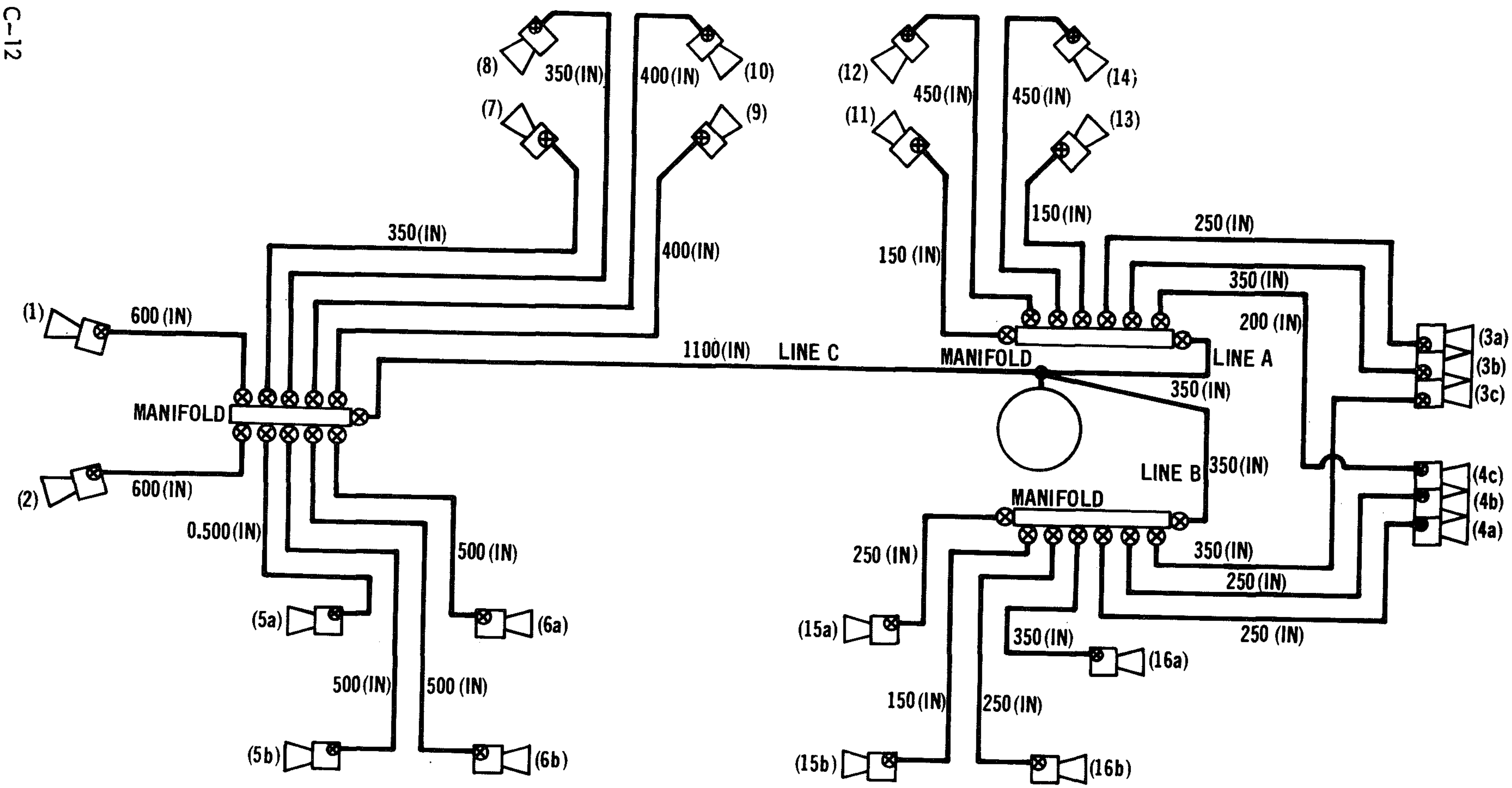

LINE TYPE	REQUIRED INNER DIAMETER	TUBE OUTER DIA USED	MIN WALL THICK REQ'D	ACTUAL WALL THICKNESS
MAIN A&B (H_2)	1.97(IN)	2.125(IN)	0.0316(IN)	0.042(IN)
MAIN A&B (O_2)	2.05(IN)	2.125(IN)	0.0316(IN)	0.042(IN)
MAIN C (H_2)	1.76(IN)	2.125(IN)	0.0316(IN)	0.042(IN)
MAIN C (O_2)	1.83(IN)	2.125(IN)	0.0316(IN)	0.042(IN)
BRANCH (H_2)	0.88(IN)	1.00(IN)	0.015(IN)	0.028(IN)
BRANCH (O_2)	0.92(IN)	1.00(IN)	0.015(IN)	0.028(IN)

ORBITER B LINE LENGTHS AND DIAMETERS

FIGURE C-8

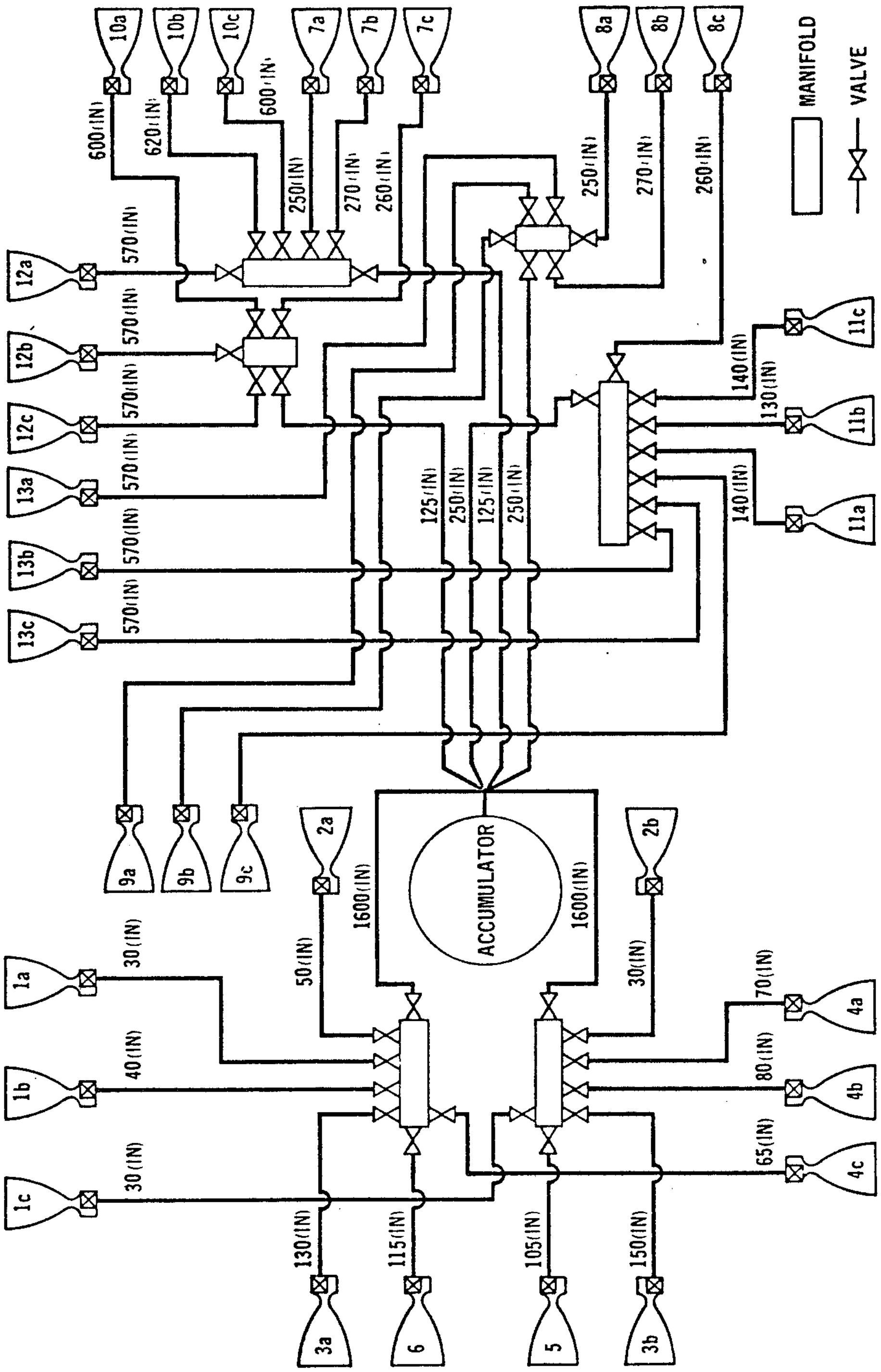

LINE TYPE	REQUIRED INNER DIAMETER	TUBE OUTER DIAMETER USED	MIN WALL THICK REQ'D	ACTUAL WALL THICKNESS
MAIN (H_2)	1.83 (IN)	2.12 (IN)	0.0316 (IN)	0.042 (IN)
MAIN (O_2)	1.90 (IN)	2.12 (IN)	0.0316 (IN)	0.042 (IN)
BRANCH (H_2)	0.92 (IN)	1.00 (IN)	0.015 (IN)	0.028 (IN)
BRANCH (O_2)	0.95 (IN)	1.00 (IN)	0.015 (IN)	0.028 (IN)

ORBITER C LINE LENGTHS AND DIAMETERS

FIGURE C-9

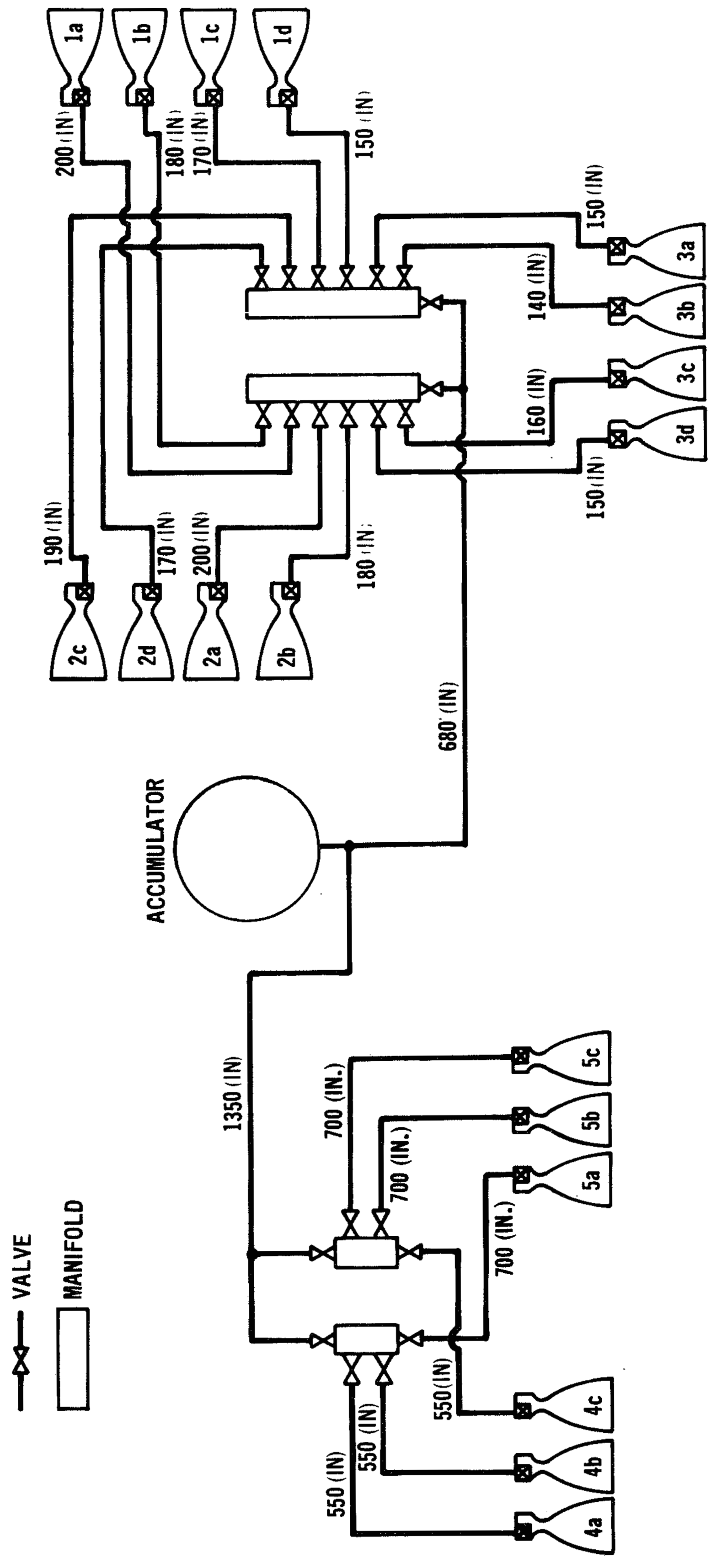

LINE TYPE	REQUIRED INNER DIA	TUBE OUTER DIA USED	MIN WALL THICK REQ'D	ACTUAL WALL THICKNESS
MAIN (H_2)	2.49 (IN)	2.75 (IN)	0.0385 (IN)	0.042 (IN)
MAIN (O_2)	2.58 (IN)	2.75 (IN)	0.0385 (IN)	0.042 (IN)
BRANCH (H_2)	1.25 (IN)	1.38 (IN)	0.0186 (IN)	0.028 (IN)
BRANCH (O_2)	1.29 (IN)	1.38 (IN)	0.0186 (IN)	0.028 (IN)

BOOSTER LINE LENGTHS AND DIAMETERS

FIGURE C-10

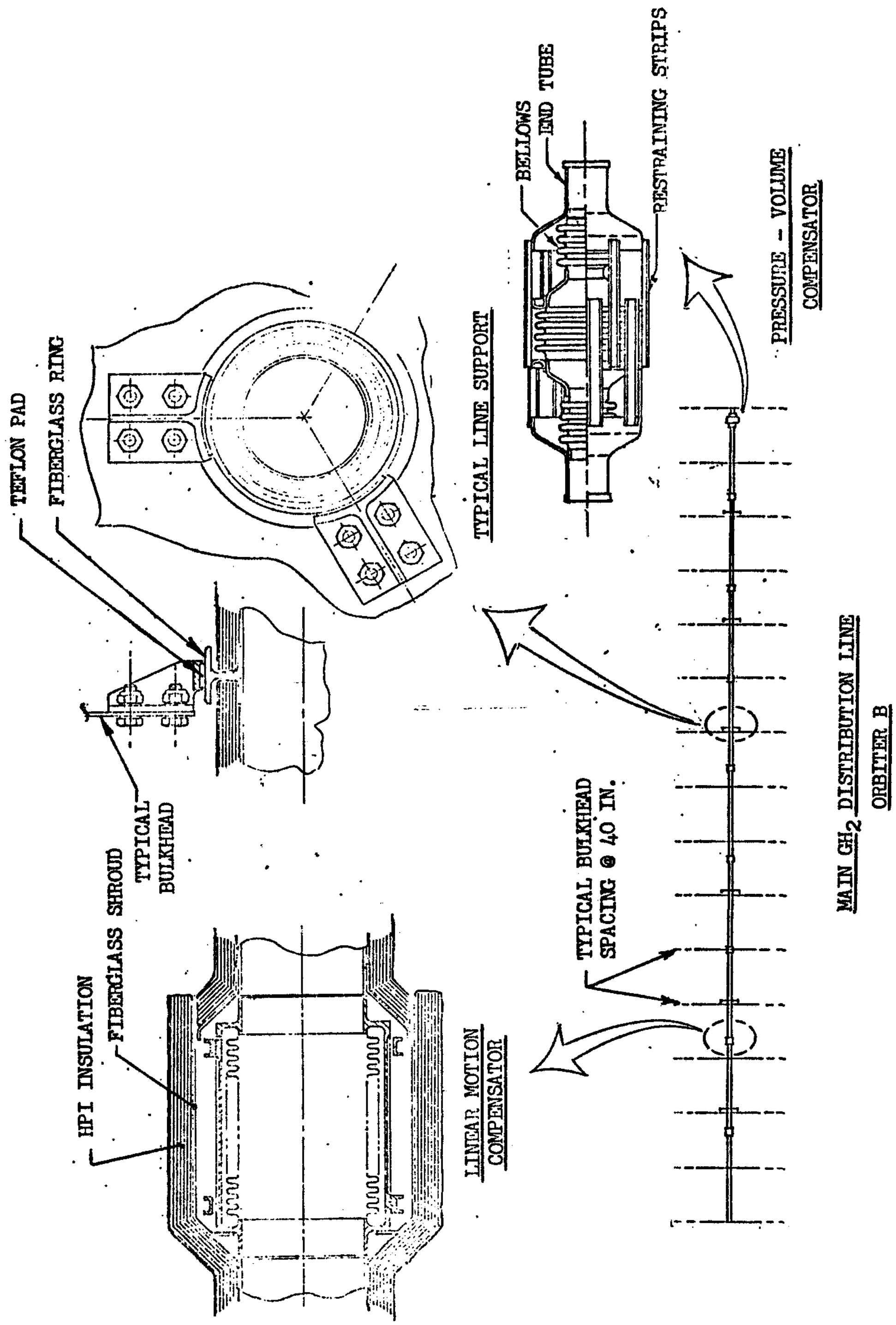

TYPICAL LINE INSTALLATION

FIGURE C-11

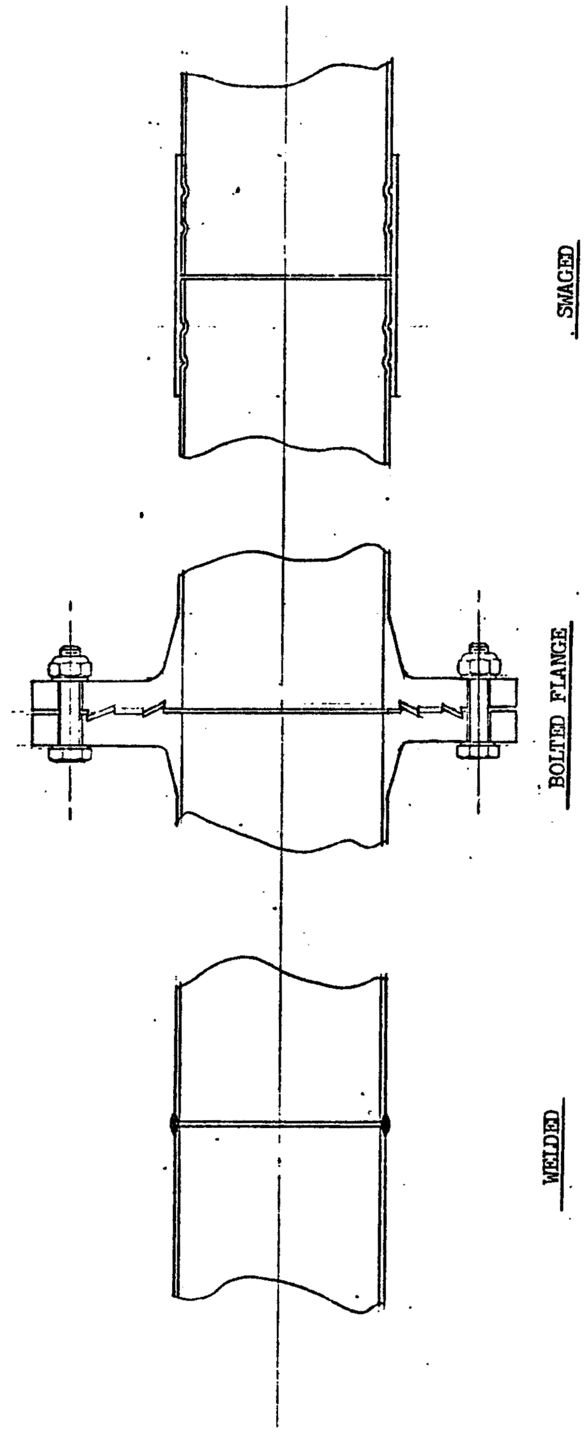

TYPICAL JOINT CONFIGURATIONS

FIGURE C-12

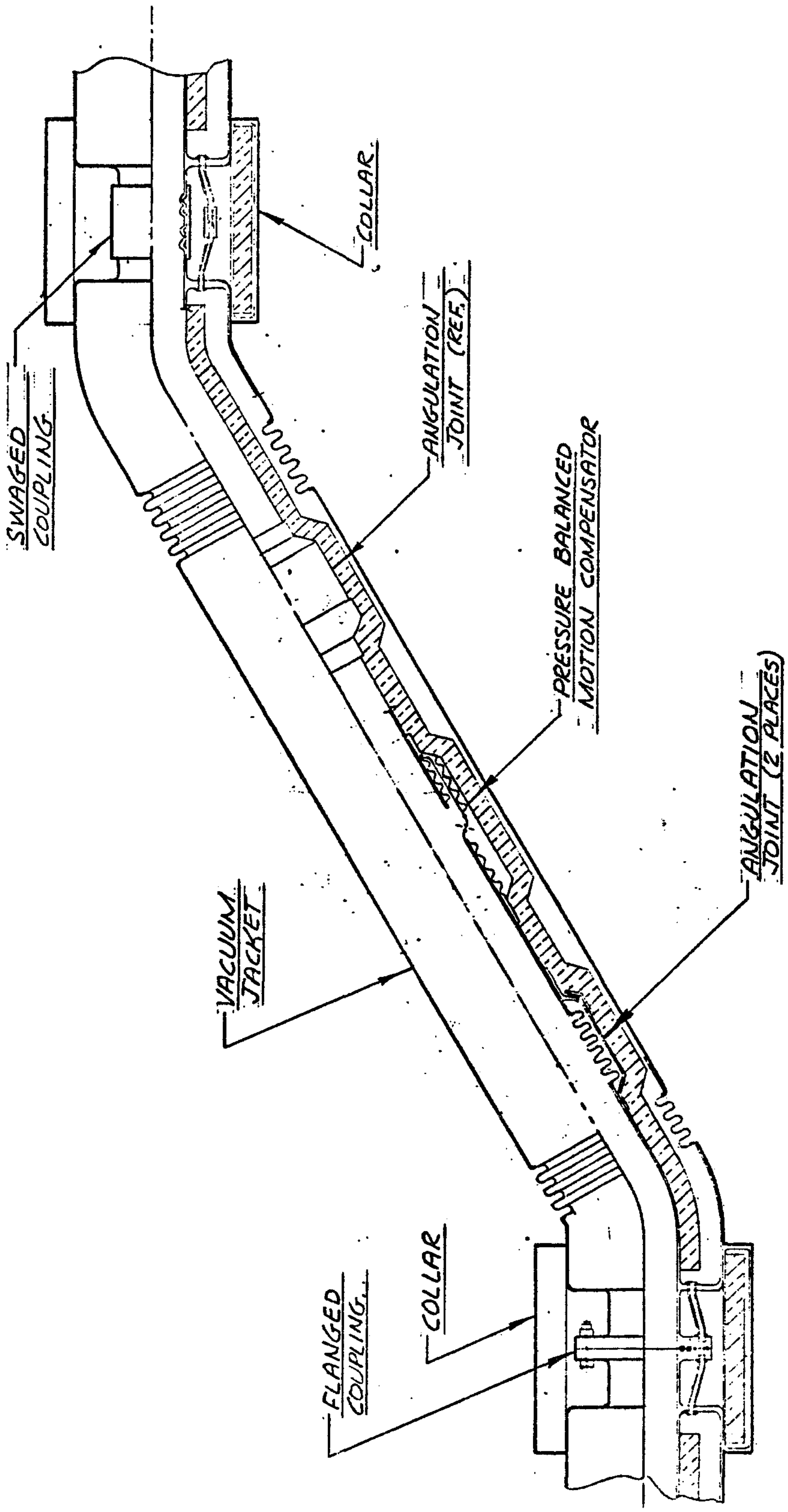

TYPICAL VACUUM JACKETED LINE

FIGURE C-13

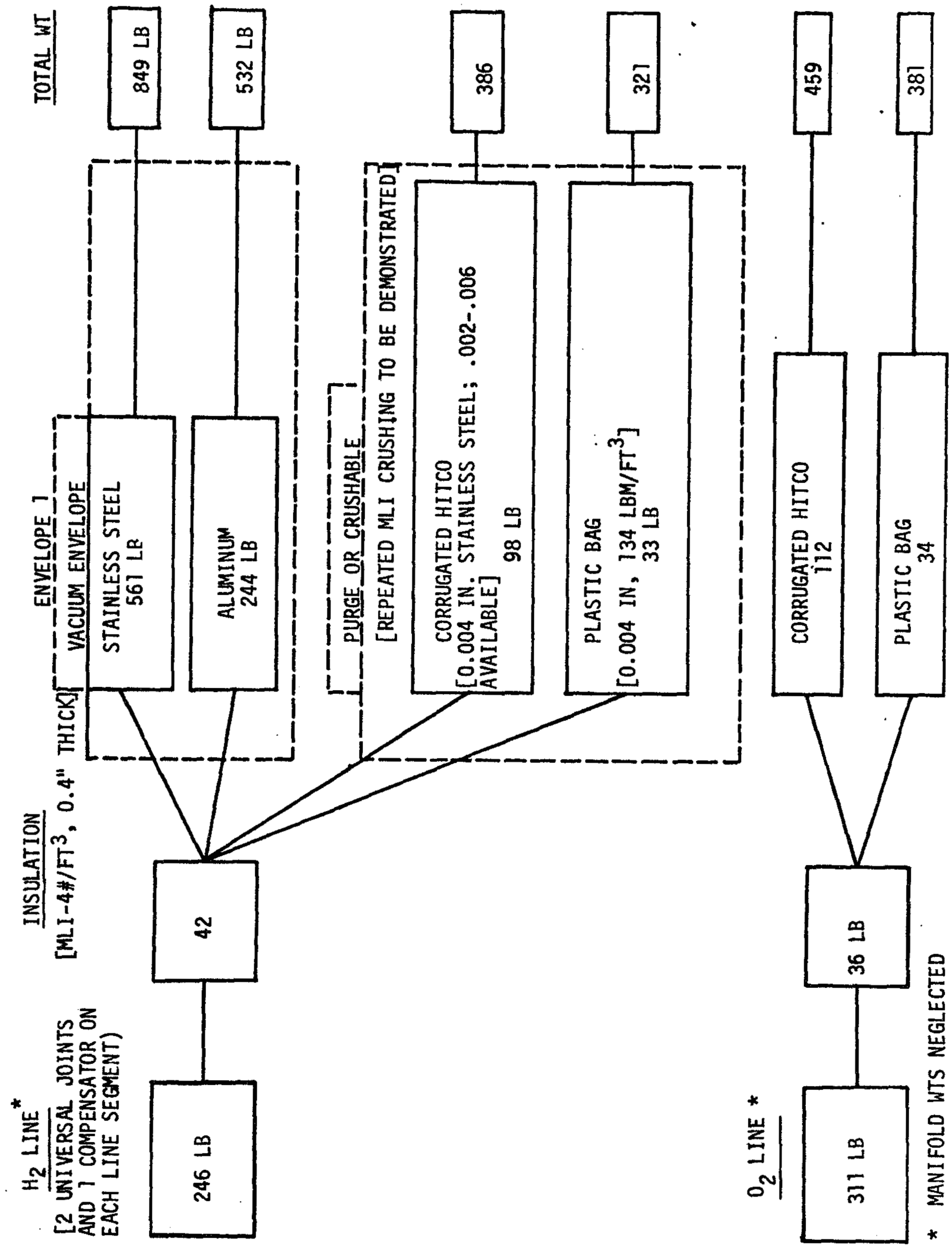

FEEDLINES AND THERMOPROTECTION WEIGHTS

FIGURE C-14

C-2. CONDITIONER ASSEMBLIES

The conditioner assemblies are mounted in as close proximity to the propellant tank outlet as allowed by physical constraints. With the oxygen tank and conditioner mounted forward of the payload bay, excessive weight penalities would be involved in ducting conditioner vent gas to the vehicle aft end; therefore, venting is accomplished on the vehicle side near the conditioner. The non-propulsive venting is at 90° to the vehicle center line and the propulsive venting is 45° aft.

C-3. PROPELLANT STORAGE ASSEMBLY

The propellant storage assembly locations were constrained to be those defined in Reference (a). For Orbiter B the oxygen tank is forward and the hydrogen tank aft of the payload bay. Orbiter C required both propellants to be aft; however, the hydrogen required two tanks because of physical installation constraints. The defined locations provide ready access for maintenance and/or installation/removal through the payload doors. The tanks are mounted by fiberglass struts in the form of 6.0 in. diameter tubes ranging in thickness from .035 to 0.10 in. Pin joints at the attachment points accommodate deflections due to loads and thermal expansions. The attachment is defined in detail in Appendix D-1.9.

C-4. REFERENCES

(a) NASA-MSFC, Space Shuttle Vehicle Description and Requirements Document, dated 1 October 1970.

(b) Anglim, D. D., Baumann, T. L., Ebbesmeyer, L. H., High Pressure Auxiliary Propulsion Subsystem Definition Subtask A Report, McDonnell Douglas Report No. MDC E0297, dated 12 February 1971.

APPENDIX D

BASELINE COMPONENT AND ASSEMBLY CONCEPTS

Component and assembly concepts of the Subtask A study were used for APS trade studies only. A detailed evaluation of component design and operational characteristics was not warranted except in specific instances where it could significantly affect the APS trade study results. During Subtask B preliminary design, all component and assembly concepts were reevaluated to the depth necessary for preliminary design of the recommended subsystem.

Trade studies of the propellant tankage assembly, conditioner assembly, and thruster concepts were conducted to determine optimum overall APS performance. These analyses resulted in selection of baseline component and assembly concepts. For these selected concepts detailed design and operating characteristics were defined. This appendix describes results of this analysis and provides data and rationale used in concept selection.

D-1. PROPELLANT STORAGE, ACQUISITION, AND PRESSURIZATION

The APS uses hydrogen and oxygen propellant stored in a subcooled state to provide the total impulse required for vehicle control. A turbopump assembly delivers these propellants from cryogenic storage tanks to the propellant conditioner assembly at the pressure and flow required for APS operation. Turbopump operation requires that the propellant temperature and pressure be such that a net positive suction pressure is available at the pump inlet. In addition, during low-g portions of flight, the propellant tank outlet must be covered with propellant so that pressurant gas is not introduced into the pump inlet. These requirements demand a tankage assembly with an efficient propellant acquisition subassembly, a propellant temperature control subassembly, and a pressurization subassembly.

During Subtask A, analyses and trade studies were conducted to identify preliminary propellant storage assembly selections. It was concluded that integrated APS and OMS tankage was the most attractive of the concepts evaluated. It was also concluded that a simple, regulated pressure, helium pressurization subassembly was most attractive for both the hydrogen and oxygen tanks. Component models used to conduct Subtask A analyses were not sophisticated, and (especially in the case of the propellant positioning and vent subassemblies) design details were not important since these had little effect on subsystem weight. During Subtask B, it was necessary to conduct the detailed analyses required to define more accurately the design and performance of propellant tankage assemblies and to confirm and/or update the propellant integration approach selected in Subtask A.

For these analyses, baseline tank sizes were established based on Subtask A requirements, alternate design approaches for different tankage assemblies were investigated, preferred approaches were selected, and design and performance characteristics were established.

Significant APS tankage requirements affecting preliminary design are shown in Figure D-1.

D-1.1 <u>Propellant Acquisition Subassembly</u> - A propellant positioning device is required in the APS tankage to ensure liquid outflow during the low-g orbital phases of the mission. During these mission phases, vehicle accelerations tend to randomly orient the bulk propellant mass within the tank, with the potential of uncovering the tank outlet and causing a loss of pressurant gas and interruption of liquid flow. Some device is required to either totally constrain the

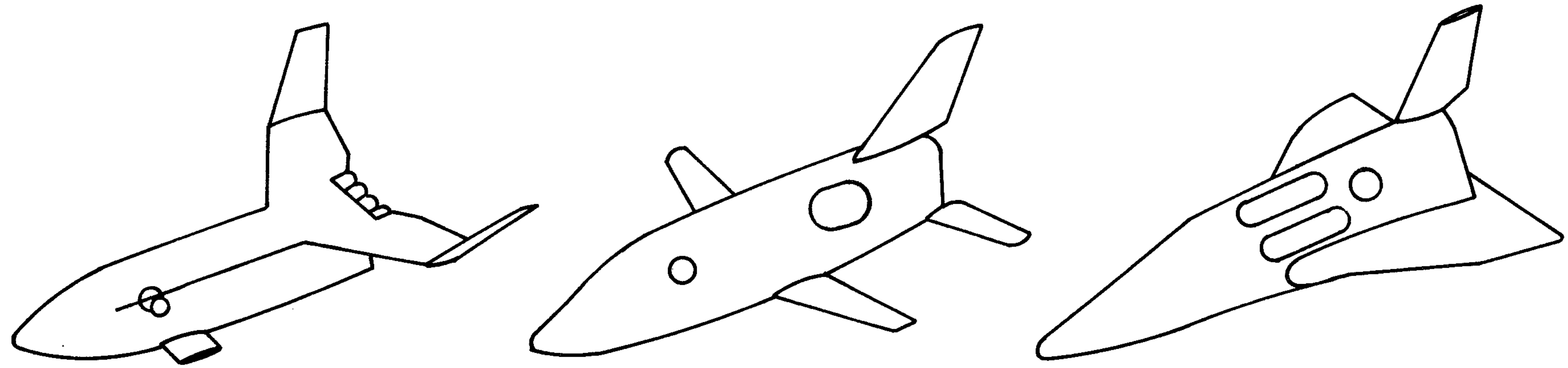

	BOOSTER	ORBITER B	ORBITER C
PROP. WT.			
H_2	469 Lb	6334 Lb	6487 Lb
O_2	1737 Lb	23552 Lb	23748 Lb
ULLAGE	5%	5%	5%
PRESSURE			
H_2	25	25	25
O_2	30	30	30
MAX ACC			
ON ORBIT	--	.87 Ft/Sec^2	.88 Ft/Sec^2
ENTRY	97 Ft/Sec^2	71.3 Ft/Sec^2	71.3 Ft/Sec^2

APS TANKAGE REQUIREMENTS

FIGURE D-1

liquid at the tank outlet or to provide a path of communication from the liquid mass to the tank outlet. Total constraint by positive expulsion was impractical because of the tank size, the number of cycles required for reuse, and the cryogenic nature of the propellant. The only reasonable approach available was to use a surface tension screen device to provide a flow path to the tank outlet.

Surface tension devices have been successfully used on several vehicles including the Agena, Apollo, X-15, and drone and target aircraft. These devices have been subject to extensive laboratory testing. They are passive in nature and have no moving parts, resulting in high reliability and multicycle reuse capability. Sufficient design information was available to establish with high confidence that a surface tension assembly could be designed for orbiter application. Basic physical processes associated with the surface tension concepts are shown in Figure D-2. Under normal operation, the screen is completely wetted on one side. If gas contacts the screen on the other side, surface tension forces prevent movement of the vapor through the screen. When liquid is in contact on the other side, liquid is free to travel from one side to the other as the surface tension effect is not present. Thus, successful acquisition of the liquids will be achieved until:

(1) there is no liquid/liquid interface
(2) acceleration forces of sufficient magnitude to exceed surface tension pressure capability are present
(3) heating below the screen causes vaporization on the liquid side and hence a gas/gas interface across the screen. In this case, the surface tension screen would preferentially flow pressurant gas.

D-1.2 Acquisition Concepts and Selection - Three basic acquisition assembly designs are available. These are illustrated schematically in Figure D-3. The first acquisition device consists of a screen configured to locate the screen surface in close proximity to the tank wall, i.e., a wall oriented screen. With this approach, liquid withdrawal is possible as long as liquid is in contact with the tank wall. This approach is, therefore, mission-independent, since the liquids are wetting and will always assume a wall contact orientation. The second device is a start basket. This approach is mission-dependent, because it must be refilled by translation accelerations periodically during the mission. It also requires two tank outlets since the large +X translation acceleration will settle propellant in the -X end of the tank (refilling the basket) while entry decelerations will settle the propellant in the -Z or bottom of the tank. The third acquisition candidate is a hybrid assembly combining the start basket with

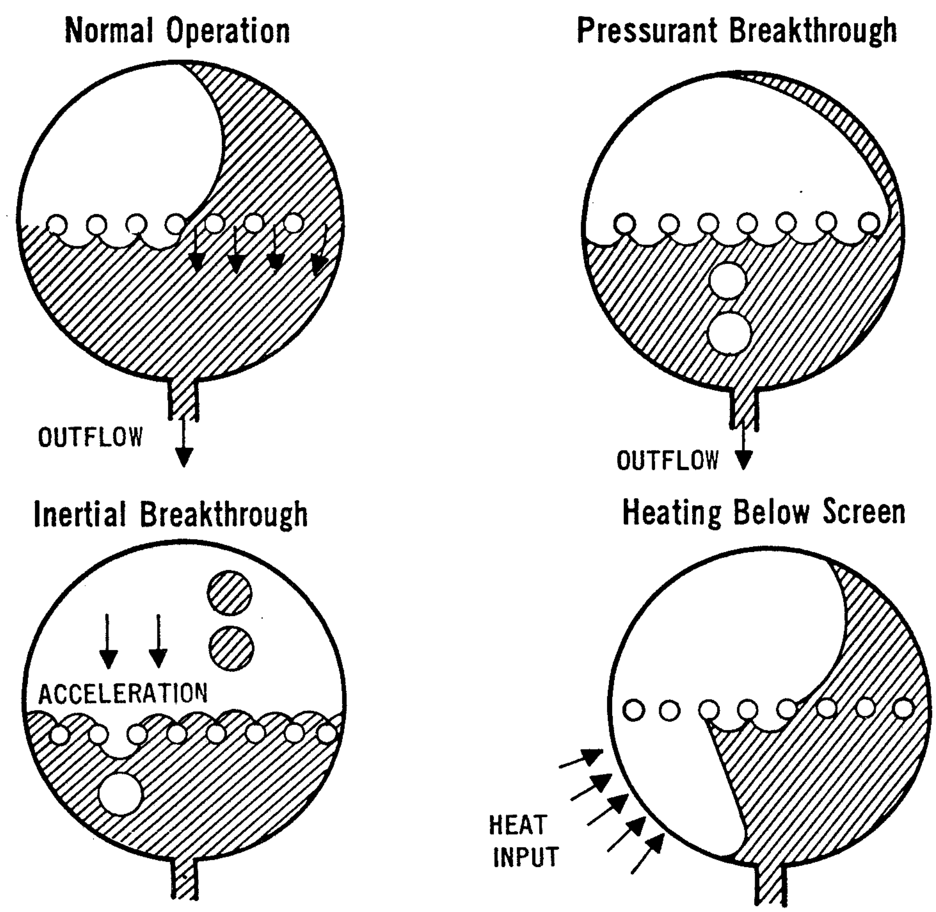

SURFACE TENSION DEVICE OPERATION

FIGURE D-2

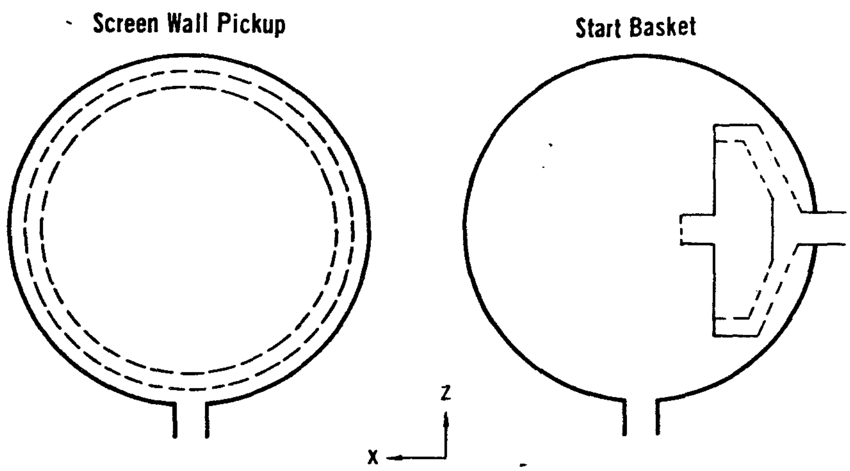

Screen Wall Pickup

1. MUST BE LAUNCHED FULL
2. MISSION-INDEPENDENT. NO SETTLING REQUIRED
3. SINGLE TANK OUTLET
4. LARGE SIZE REQUIRES FINE SCREEN MESH
5. LOW-G TRANSFER CAPABILITY

Start Basket

1. PARTIAL FULL LAUNCH POSS'BLE
2. TWO TANK OUTLETS REQUIRED
3. MISSION-DEPENDENT. SETTLING REQUIRED
4. LIQUID "FALLOUT" DURING OUT-FLOW IN LATERAL ACCELERATION

Hybrid

1. PARTIAL FULL LAUNCH POSSIBLE
2. SINGLE TANK OUT
3. BASKET SIZED TO PROVIDE LIQUID WHEN LIQUID IS IN -X END OF TANK
4. SOME SETTLING STILL REQUIRED
5. NO "FALLOUT" DURING LATERAL ACCELERATION

ACQUISITION DEVICE CANDIDATES

FIGURE D-3

a wall oriented approach. Only a single tank outlet is needed, but the device is still mission-dependent since the basket must be refilled periodically. The wall oriented device was selected because it is mission-independent, does not require two outlets, and does not require refill.

Several alternates could be conceived for a wall oriented positioning approach. The most conventional of these is a continuous tank liner made of screen. This approach has received the most attention in exploratory development testing, but was considered to be impractical for a large tank because of fabrication difficulty and boost ullage considerations.

An alternate and more practical configuration is a screen channel device, illustrated in Figures D-4 and D-5. Several aluminum channels or annular trays are located within the propellant tank in close proximity to the wall. These assure contact between the liquid and the positioning device under any random orientation conditions. The device is insensitive to boost accelerations as the trays are submerged during boost, and it is the most practical design approach from fabrication and screen size standpoints. The design provides the capability to check the screen bubble point pressure after complete tank assembly.

D-1.3 Design - The propellant acquisition device consists of three screen channels or trays, around the circumference of the propellant tank and a single, enclosed collector channel which connects each annular tray to the sump (Reference Figures D-4 and D-5). The annular trays are normal to the longitudinal (or +X) axis of the vehicle and the sump is located in the tank bottom (or the -Z) extremity of the tank. The tank outlet has a cone-shaped vapor/liquid interface screen located within the feed line below the sump. The feed line below this screen is connected to the propellant tank by a small vapor relief line to allow by-pass of any vapor developed in the line back into the tank vapor region. Screen acquisition device operation is the same for both fuel and oxidizer tanks. The solid portions of the trays are formed from 0.02 inch aluminum sheet. The center wall in the channel is present to increase the rigidity of the box cross section. It is anticipated that the channels would be fabricated in quarter sections, inspected, and then joined togehter inside the tank. Each quarter section has two points of attachment to the tank wall. At these points, thin, low conductivity fiberglass rods support the channel.

D-1.4 Operation - It is a requirement that the screen surfaces contact the bulk liquid throughout the mission and that channels remain completely full

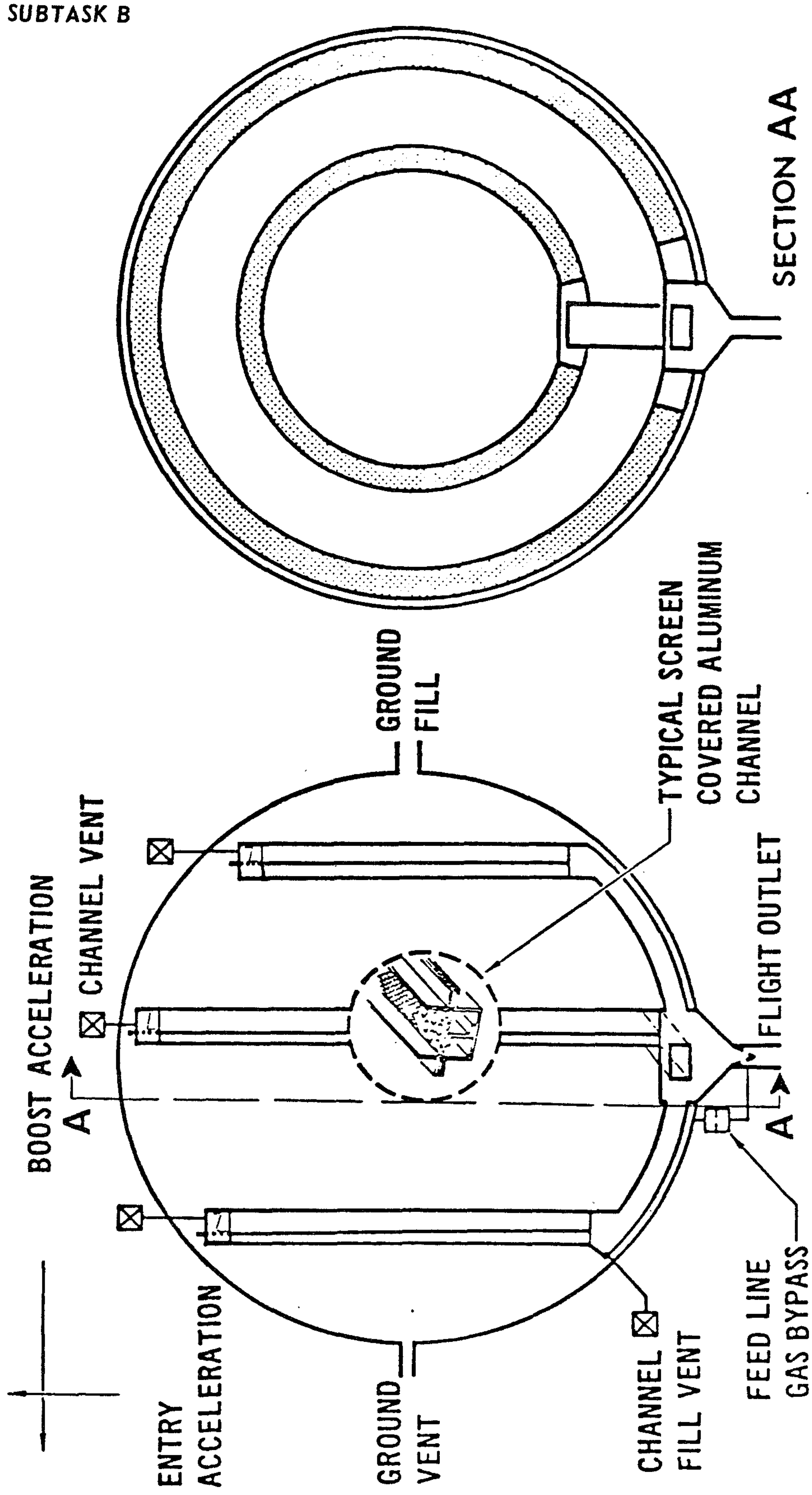

	ORBITER B	ORBITER C	BOOSTER
SCREEN SIZE	2 @ 250 x 1370 (17 μ) 1 @ 200 x 600 (40 μ)	2 @ 250 x 1370 (17 μ) 1 @ 200 x 600 (40 μ)	200 x 600 (40 μ)
CHANNEL SIZE (IN.)			
H_2	5 x 8	4 x 6	5 x 8
O_2	3 x 6	3 x 4	3 x 6

APS PROPELLANT ACQUISITION CONCEPT

FIGURE D-4

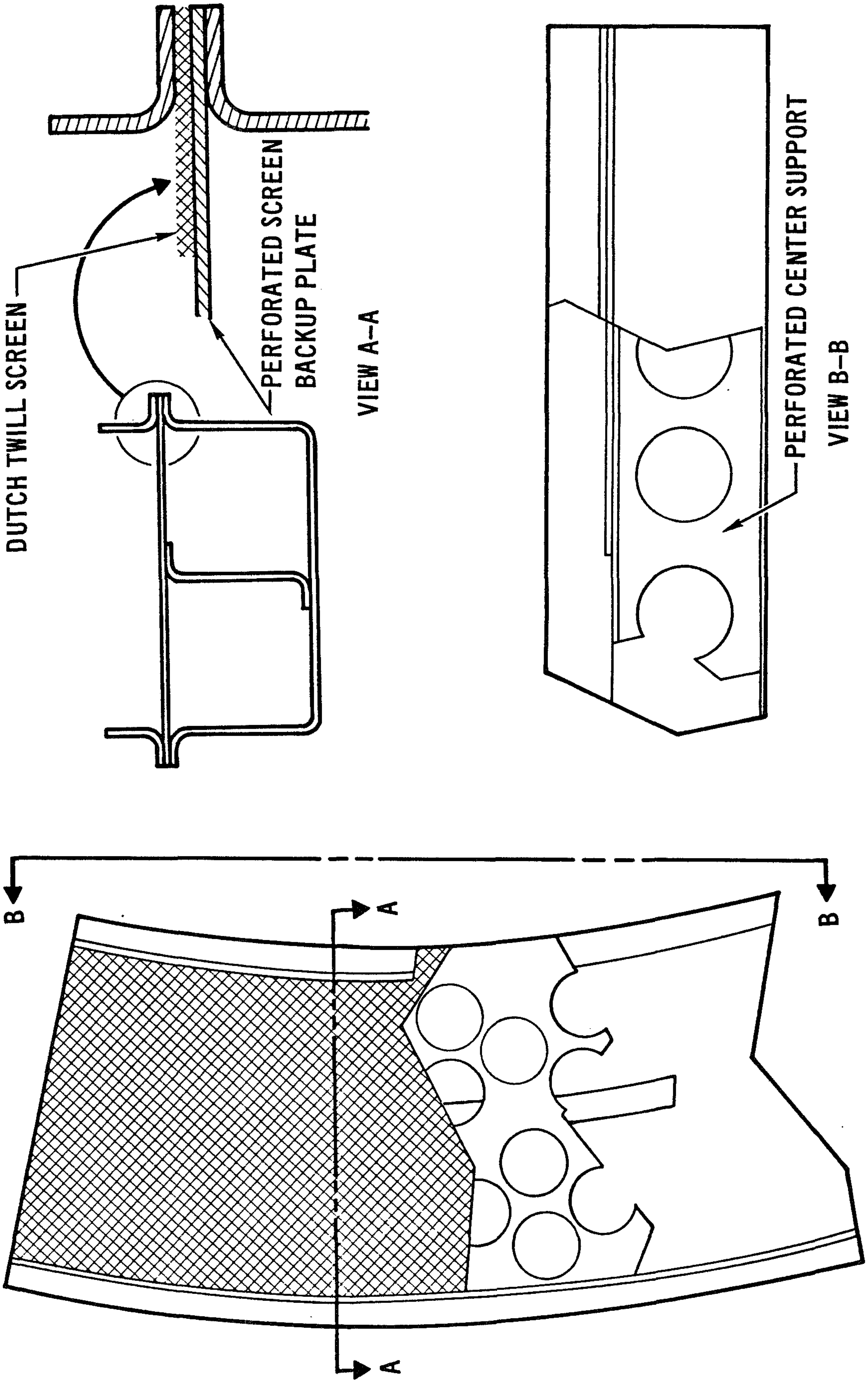

PROPELLANT ACQUISITION SCREEN CHANNEL DESIGN

FIGURE D-5

of liquid at all times. During outflow, the acquisition device will selectively pass liquid to the feed system if it is in contact with a liquid mass. The wall-oriented nature of the screen device ensures that contact will be made. Screen mesh and flow passage dimensions are selected so that the pressure drop across the screen vapor/liquid interface never exceeds the screen bubble point prior to reentry. Two different mesh sizes have been selected for use in the screen channels. A relatively coarse mesh can be used in the screen channel near the aft end of the vehicle. The other two channels require a finer mesh to withstand hydrostatic head, existing during periods of high maneuver accelerations and low propellant loading.

Screen channel ring placement within the propellant tank was based on propellant quantities prior to entry. Approximately 3 percent of the propellant will be in the APS tank prior to entry and it will be settled in the -X end of the tank during the deorbit burn. The bottom screen channel is placed just below the bulk liquid surface at this propellant loading. Subsequent to deorbit burn, propellant will be reoriented to the tank sump by entry drag forces; therefore, it will remain in contact with one or both of the remaining screen channels. High +Z acceleration levels during entry will exceed the stability limit of the acquisition device. When this occurs, pressurant enters the screen channels, the liquid levels within the channels, and the collectors will quickly drop until they match approximately the liquid level in the tank bottom (-Z).

D-1.5 Insulation - Considerable research has been, and is being, devoted to development of high performance insulation (HPI) concepts. In general, HPI concepts utilize sheets of highly reflective metallized plastic film, such as aluminized mylar, made into blankets. Separation of the sheets in the blankets is provided by embossing or flocking the basic film material or by using a separator sheet such as dacron netting or glass fabrics. Many design variations are possible and separate technology studies are currently under way to establish optimum HPI shuttle designs. For purposes of this study, however, differences in alternate HPI approaches would have little effect on overall storage weight. For this reason, a typical HPI concept was selected and used to optimize the needed amount of insulation, and to define reasonable propellant storage and vent losses.

D-1.6 Insulation Selection/Optimization - MDAC-East (under an insulation technology study with NASA, Contract No. NAS 8-21400) has investigated various HPI concepts. Based on this effort, typical insulation characteristics were selected for APS tankage analysis. The selected scheme is made up of double aluminized 0.15 mil mylar (DAM) reflectors with a dacron net separator. A density of 5 lb/ft^3 based on sheet density of 90 sheets per inch is representative of this insulation. This insulation has been experimentally evaluated through calorimeter test of blanket samples. Figure D-6 shows the basic insulation characteristics and effective conductivity degradation caused by perforations, joints, and attachments. Data of Figure D-6, together with baseline propellant requirements, were used to optimize HPI thickness for the shuttle mission. Insulation thickness was based on providing a maximum storage efficiency, (i.e., ratio of usable propellant vaporization to boil-off). This assumption accords with the thermal vent/shroud subassembly, which converts heat input into hydrogen vaporization. Resulting optimum number of insulation layers, and total weight of propellant vented (assuming no heat shorts) are shown in Figure D-7 as a function of orbit time. Optimum insulation for the Orbiter B hydrogen tank has 62 sheets, 0.68 in. thick, weighing 222 lb.

D-1.7 Reusability Characteristics - One of the major concerns in insulation design is the reusability requirement. High confidence can be placed in the prediction of basic HPI heat transfer characteristics and thermal performance; however, effects of multiple venting and pressurization cycles are not known. Data are available to show that unprotected insulation would freely vent during ascent without significant pressure gradients, but no data are available to show the effects of reentry on HPI performance. It is known, though, that any form of condensation within the mylar layers can cause severe degradation in thermal characteristics. Condensing and freezing water within the layers can remove the aluminum coating from the mylar. Thus, a means of protecting the insulation from atmospheric contamination is required. The following paragraphs describe candidate insulation concepts, their performance, and selection of the preferred concept.

Three basic insulation concepts (illustrated in Figure D-8) were evaluated for the hydrogen tank. The simplest uses an insulation purge with a noncondensable gas. This allows use of a semirigid cover, or flexible bag, to protect the HPI. Effective conductivity of the insulation approaches that of the purge gas during nonvented conditions.

The second approach is a substrate concept, in which foam insulation is used under the HPI. The foam has a lower conductivity than helium-purged HPI, and its thickness is sized so that nitrogen can be used for ascent purging rather than helium (i.e., foam provides sufficient temperature differential to prevent nitrogen condensation). For reentry, the foam will be at the temperature of the liquid

DOUBLY ALUMINIZED MYLAR (DAM) - DACRON NET SEPARATOR

15 IN LH_2 CALORIMETER TESTING - $T_H = 530°R$

BASIC INSULATION BLANKET	$K_e = 1.37 \times 10^{-5} \frac{\text{BTU-FT}}{\text{FT}^2\text{HR°R}}$
WITH 2.3% PERFORATIONS	1.69×10^{-5}
WITH 2.3% PERFORATIONS AND JOINTS	2.03×10^{-5}
WITH 2.3% PERFORATIONS, JOINTS, AND ATTACHMENTS	2.217×10^{-5}

MULTI-LAYER INSULATION

MEASURED PERFORMANCE CHARACTERISTICS

FIGURE D-6

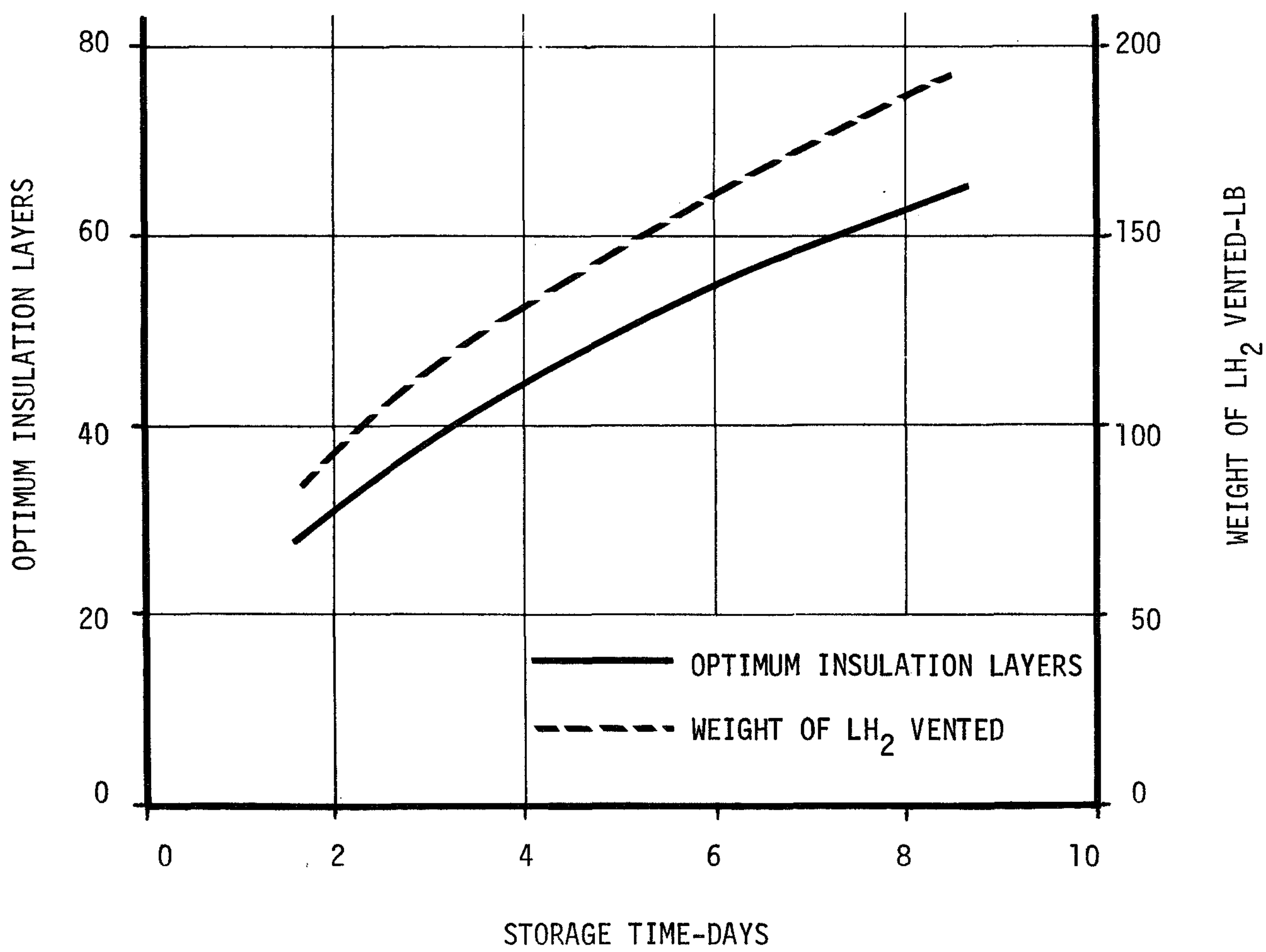

OPTIMUM LH_2 TANK INSULATION

25 LBF/IN^2 A TANK PRESSURE

FIGURE D-7

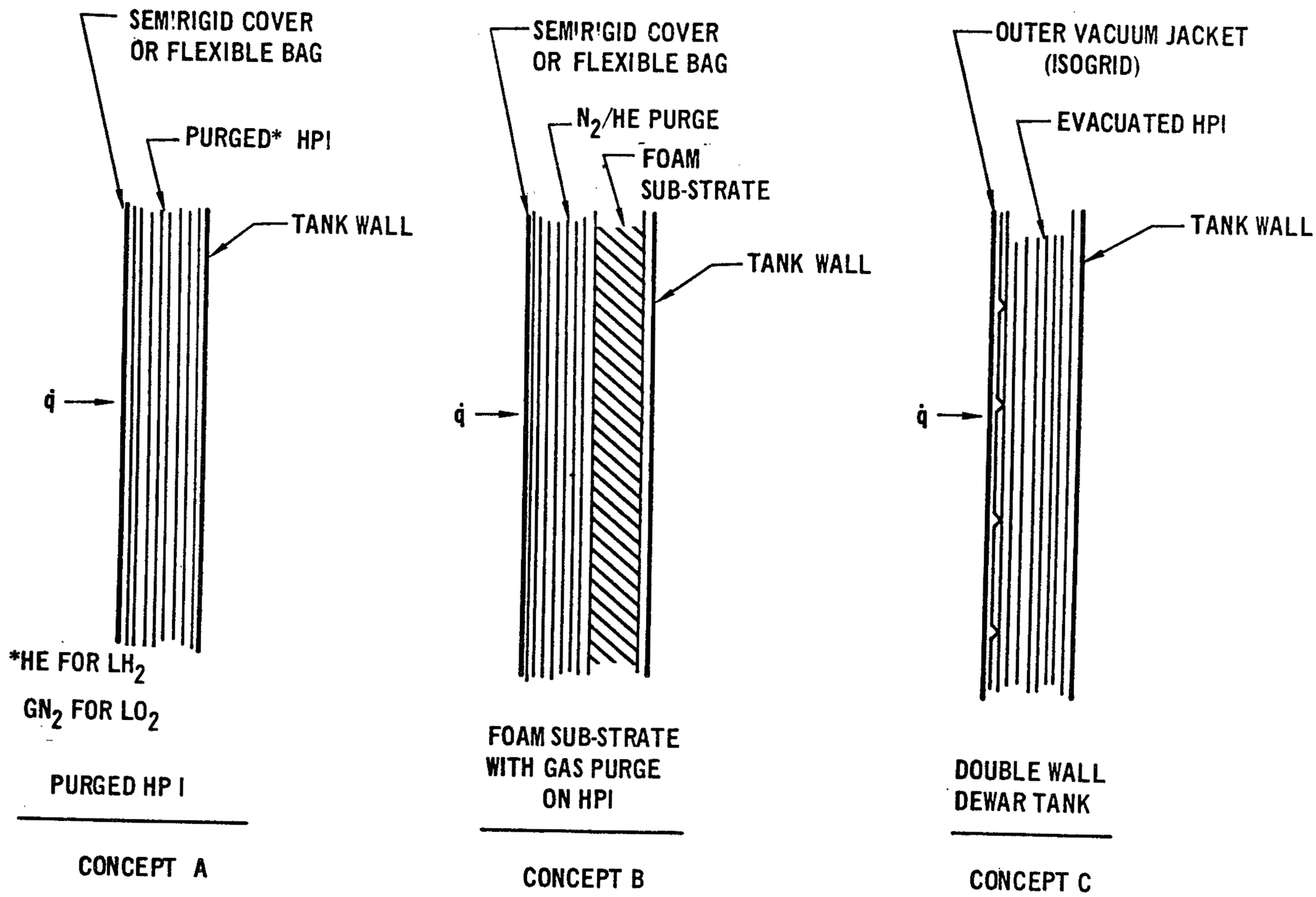

BOOST/REENTRY THERMAL PROTECTION CONCEPTS

FIGURE D-8

propellant. Thus, to avoid cryopumping on the hydrogen tank, a noncondensing gas (helium) purge (concept B-1) or helium purge followed by nitrogen purge (concept B-2) will be required during reentry.

The third protection concept employs a double-walled dewar tank and maintains the insulation in a vacuum. This obviously results in maximum thermal performance, because the insulation is always in a vacuum and boiloff losses during boost and entry are minimized; however, the outer vacuum jacket is a significant structural element, representing a high weight penalty.

Propellant losses for a typical mission were calculated for the three concepts. These are shown in Figure D-9. The simple purge approach has extremely high losses. The substrate concept reduces these by a factor of nearly five but is still greater than the dewar configuration which suffers minimum propellant loss.

Figure D-10 compares total weight penalty for several alternate approaches, including purge systems using different gases. The simple purge system and the dewar are obviously noncompetitive from a weight standpoint. Other candidates are relatively close. On this basis, the preferred configuration for hydrogen is a purged foam substrate. Although the weight penalty could be reduced by using a dual reentry purge (helium followed by nitorgen), the weight penalty is small. For these reasons a simple single purge system (nitrogen for ascent and helium for reentry) was selected. For the oxygen assembly, gaseous nitrogen can be used for purge without a substrate. Performance of candidate oxygen concepts is shown in Figure D-11. Weight penalties are smaller, and there is generally less difference between concepts than in the hydrogen systems. Either a dewar tank, or a simple nitrogen purge system, appears practical. As is true for the hydrogen systems, the dewar weights are optimistics; therefore, the nitrogen purge system was selected for oxygen.

D-1.9 <u>Tank Heat Shorts</u> - The multilayer HPI is used to reduce propellant heat transfer through the tank wall. In any cryogenic tankage design, however, it is necessary to give careful attention to the various heat shorts associated with tank mounting structure and feedlines. Previous studies have shown that point support with low conductivity trusses must be used to provide low support losses. Figure D-12 shows the influence of support materials on general thermal performance. As shown, fiber glass is one of the most attractive materials for tank support because of its high strength, low density, and low conductivity. Figure D-13

	GROUND HOLD	BOOST	EVACUATION	ORBIT	RE-ENTRY	TOTAL	REMARKS
CONCEPT A	46.4	423.0	21.0	70.0	0.8	561.2	
CONCEPT B							
-1 N_2 PURGE BOOST HE REPRESSURIZATION	4.3	34.7	5.0	70.0	0.8	114.8	0.96 IN FOAM
-2 N_2 PURGE HE AUGMENTATION	6.2	50.5	5.1	70.0	0.8	132.6	0.42 IN FOAM
CONCEPT C	0.03	0.24	0.95	70.0	0.0	71.2	

TOTAL MISSION LH_2 LOSSES
ORBITER B
(SEVENTEENTH ORBIT RENDEZVOUS)

FIGURE D-9

	CONCEPT A He PURGE	CONCEPT B-1 FOAM SUBSTRATE N_2/He PURGE	CONCEPT B-2 FOAM SUBSTRATE N_2 PURGE	CONCEPT C DEWAR TANK
LH_2 VENT LOSS - LB	561	115	133	71
HARDWARE WEIGHTS - LB				
INCREASED TANKAGE	250	47	47	18
FOAM INSULATION	-	160	70	-
HPI OUTER JACKET	180 (2)	163 (2)	166 (2)	980 (3)
PURGE GAS SUPPLY	15 (1)	15 (1)	80	-
TOTAL	445	385	363	998
TOTAL WEIGHT	1006	500	496	1069

(1) IT WAS ASSUMED THAT HELIUM COULD BE TAKEN FROM EXISTING HELIUM RESIDUALS IN THE VEHICLE AND NO PENALTY WAS CHARGED FOR THE GAS OR STORAGE BOTTLE.

(2) OUTER JACKET IS 0.02 IN FIBERGLAS.

(3) ALUMINUM VACUUM JACKET USING ISOGRID STRUCTURE CONCEPT.

LH_2 THERMAL PROTECTION COMPARISON
ORBITER B

FIGURE D-10

	N_2 PURGE	DEWAR TANK
LO_2 VENT LOSS	70 LB	34
HARDWARE WEIGHTS		
INCREASED TANKAGE	2	1
FOAM INSULATION	--	--
HPI JACKET	54	220
PURGE GAS SUPPLY	31	--
	87	221
TOTAL WEIGHT PENALTY	157 LB	255 LB

LO_2 THERMAL PROTECTION COMPARISON

ORBITER B

FIGURE D-11

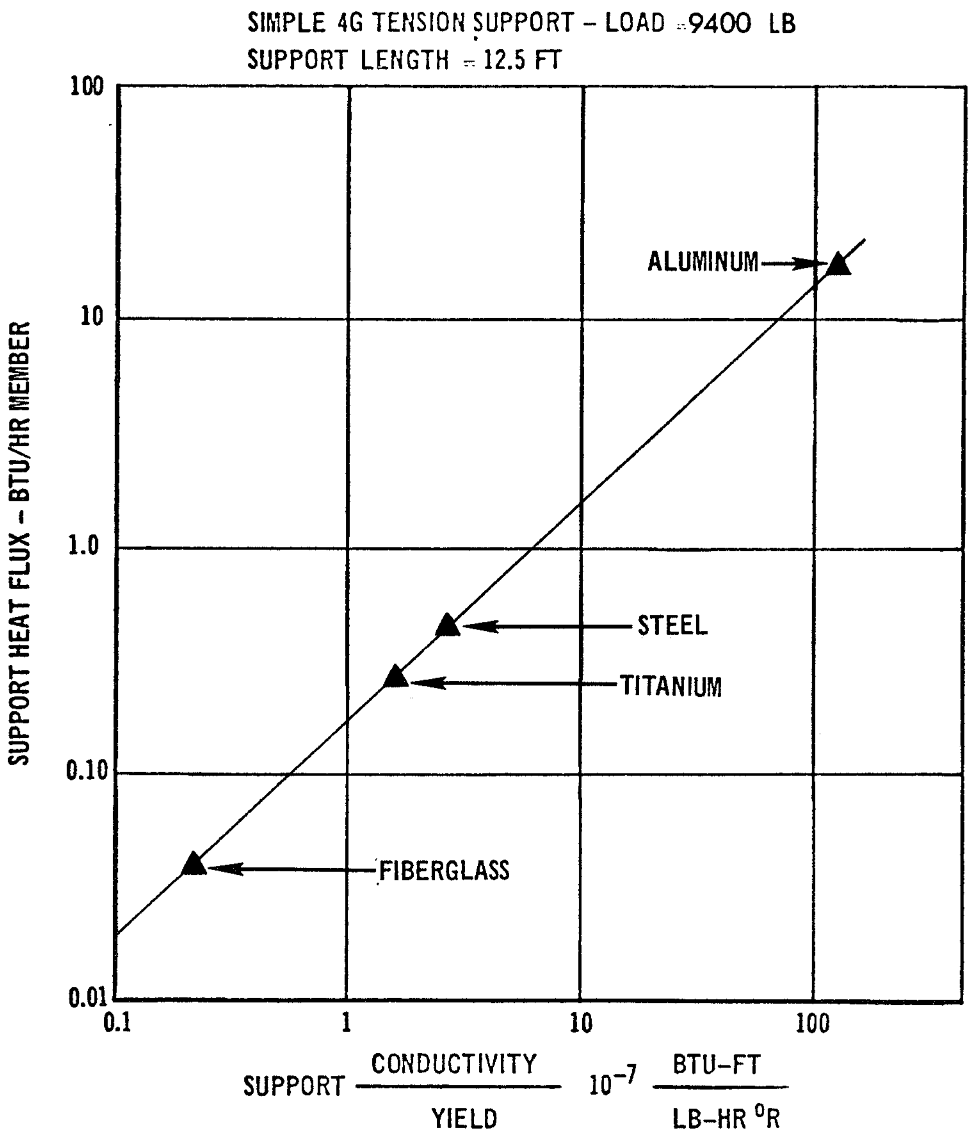

INFLUENCE OF SUPPORT MATERIAL SELECTION ON HEAT FLUX

FIGURE D-12

FIGURE D-12

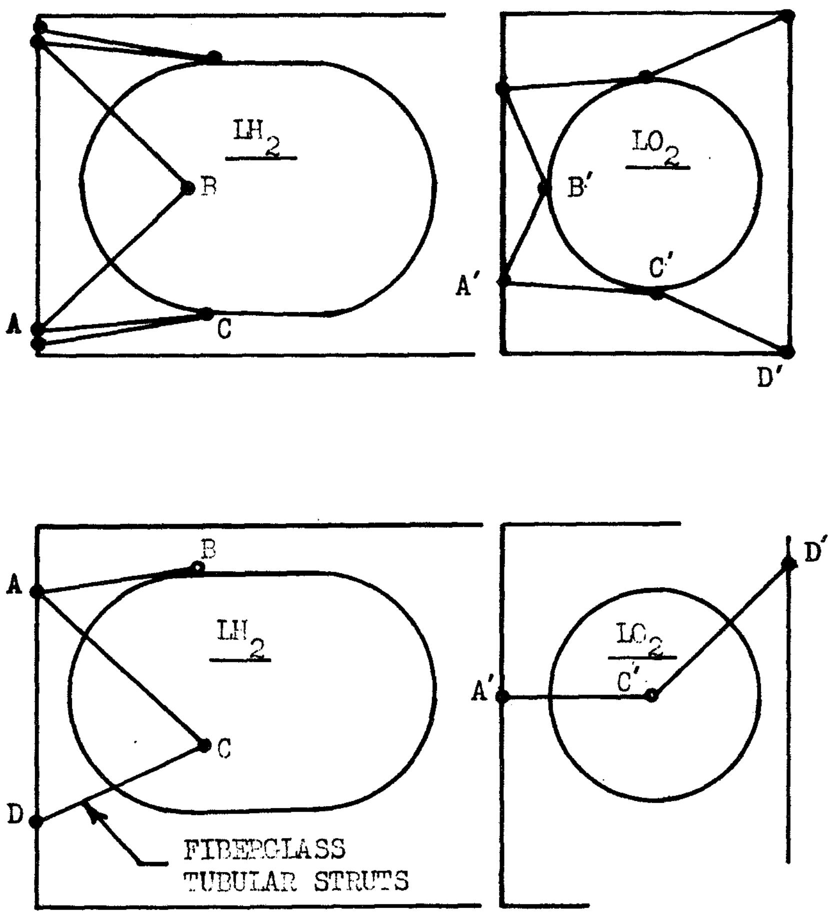

SUPPORT DIMENSIONS - IN

STRUT	LENGTH	DIA	THICKNESS
AB	159	6	0.055
AC	152	6	0.055
CD	145	6	0.100
A'B'	62	6	0.035
A'C'	102	6	0.055
C'D'	116	4.5	0.045

WEIGHT

LH_2 SUPPORT SYSTEM = 63 LB
LO_2 SUPPORT SYSTEM = 28 LB
ATTACHMENTS = 24 LB

HEAT INPUT

LH_2 SUPPORT SYSTEM = 1.1 $\frac{BTU}{HR}$
LO_2 SUPPORT SYSTEM = 0.82 $\frac{BTU}{HR}$

TANKAGE SUPPORT SYSTEM
ORBITER B

FIGURE D-13

shows a typical layout for a tubular strut tank support system. Practical strut dimensions, weight, and heat transfer characteristics are also shown. Analyses were conducted to identify the heat short through the various feed lines to the tank. These results are shown in Figure D-14.

D-1.10 Vent/Conditioning Assembly - Long term storage of cryogenics requires tank temperature control to avoid excessive losses. One technique converts vented liquid to gas in a heat exchanger and utilizes the heat of vaporization for cooling. The operation of the device is illustrated in Figure D-15. Liquid hydrogen enters the vent system at condition A, and is throttled to point B to reduce its temperature. After throttling, a two-phase mixture exists which is circulated in a heat exchanger. Heat transfer completes the vaporization until, at the heat exchanger discharge, the coolant has been completely vaporized (Point C).

D-1.11 Vent Operation - The selected vent in which liquid hydrogen is extracted from the liquid positioning device operates continuously. Figure D-16 is a schematic of the vent concept. There are four parallel circuits: one for feed line/sump cooling, one for tank support cooling, one for cooling of the storage tank insulation and pressurization lines, and one for turbopump cooling. The first two cooling circuits are essentially the same for all heat exchanger approaches. All four circuits are throttled to the same pressure, so that downstream pressure remains constant. Hydrogen is extracted from the positioning device and throttled to reduce its temperature by approximately 7°R. Defining a fixed temperature difference in this manner allows the heat exchanger design to be made independent of final tank pressure selection. Seven degrees Rankine was found to give a good balance between number of coils for feed line/sump cooling and reasonable sizes for the insulation cooling heat exchanger. Hydrogen exhausted from the hydrogen tank cooling circuit is used to provide oxygen tank cooling.

D-1.12 Heat Exchanger Concepts - The principal technical issue to be resolved in design of the vent assembly was definition of the heat exchanger concept to be used. Three basic options are feasible:

(1) a heat exchanger mounted directly to the tank structural shell
(2) a radiation shroud heat exchanger in which the cooling tubes are separated from the tank walls
(3) a compact (or internal) heat exchanger inside the propellant tank.

			HEAT TRANSFER RATE BTU/HR			
			LINE CONDUCTION	GAS CONDUCTION	RADIATION	TOTAL
LO_2 TANK:	FILL/DRAIN	(2¼ IN DIA)	1.53	0.1	0.73	2.36
	FEED LINE	(2¼ IN DIA)	1.53	0.1	0.73	2.36
	VENT/PRESSURIZATION	(1 IN DIA)	0.68	0.02	0.06	0.76
	SCREEN VENTS	(0.25 IN DIA LINES)	0.68	-	-	0.68
						6.16
LH_2 TANK:	FILL/DRAIN	(2¼ IN DIA)	1.74	0.87	0.73	3.34
	FEED LINE	(2¼ IN DIA)	1.74	0.87	0.73	3.34
	VENT/PRESSURIZATION	(1 IN DIA)	0.78	0.17	0.06	1.01
	SCREEN VENTS	(0.25 IN DIA LINES)	0.78	0.04	-	0.82
						8.51

FEED LINE HEAT TRANSFER CHARACTERISTICS

FIGURE D-14

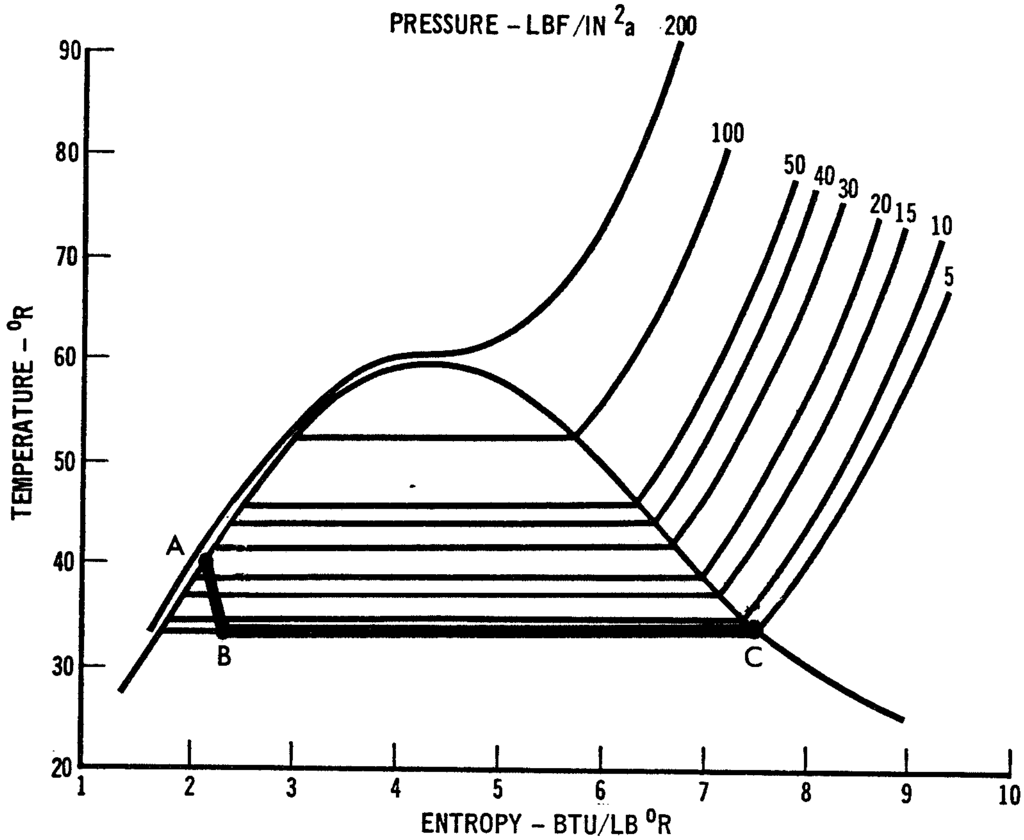

HYDROGEN THERMODYNAMIC VENT DESIGN CHARACTERISTICS

FIGURE D-15

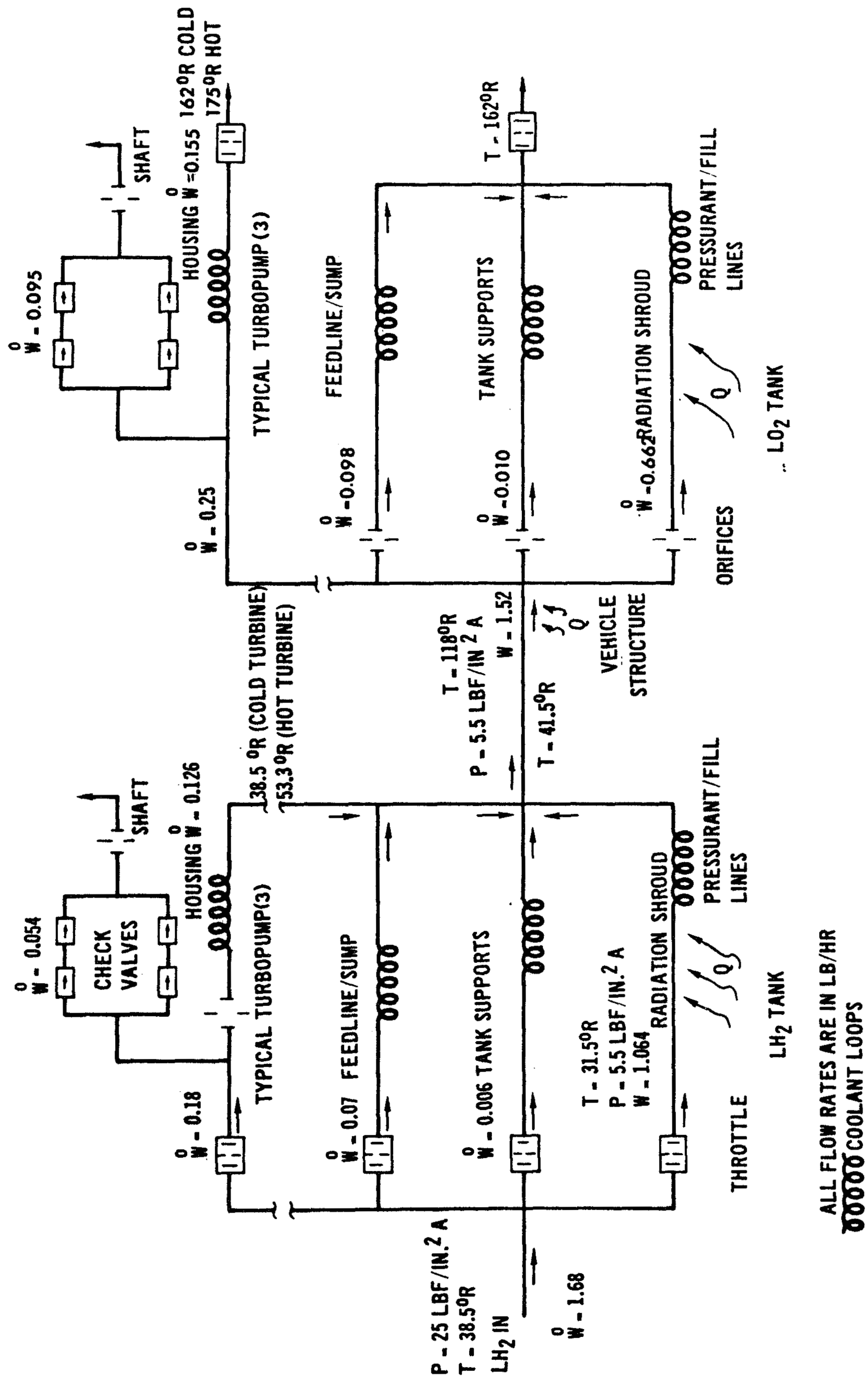

VENT SUBASSEMBLY SCHEMATIC

FIGURE D-16

The simplest heat exchanger is the wall mounted approach. This was analyzed in detail in Reference (a) which indicated that the tank wall temperature distribution could lead to a significant level of stratification which would be unacceptable to the APS, and that mixers would be required with this concept, significantly complicating design.

The use of a vent cooled radiation shroud (physically isolated from the tank so that radiation is the controlling mode of heat transfer) will essentially reduce radiation heat transfer to zero. Since shroud temperature is kept at or below tank temperature, all heat through the insulation can be effectively intercepted by the vapor and coolant. Steady state performance of a device such as this was analyzed assuming the tube-shroud arrangement shown in Figure D-17.

Use of a compact heat exchanger inside the tank has been studied and ground tested (References b and c). In this concept, tank fluid is circulated over or through the heat exchanger by a low power pump/mixer, which eliminates stratification and hot or cold spots in the tank due to unequal heat transfer. A generalized mixer sizing analysis is shown in References (d) and (e). Based on a conservative acceleration level of 10^{-5}g for the orbital gravity field, necessary fluid and mixer parameters were developed (Figure D-18) together with heat exchanger data.

D-1.13 Heat Exchanger Comparison - Advantages and disadvantages of candidate concepts are summarized in Figure D-19. The vapor-cooled radiation shroud concept is a lightweight, completely passive system, with no moving parts; therefore, it has been selected as the vent system heat exchanger concept. The internal compact heat exchanger concept has been extensively studied and has demonstrated adequate tank pressure control in 1 g testing. However, no low-g tests demonstrating destratification with very low-power mixers have been performed, and the approach is complex. The tank wall-mounted heat exchanger is also a rather complicated installation, which must be integrated with the basic propellant tank. In addition, mixers would still be required.

D-1.14 Pressurization Subassembly - Two candidate pressurization subassembly types were considered: autogenous (propellant vapor) and cold helium submerged injection. Figure D-20 presents schematics of the candidate concepts. The pressurant flow rate capability of the subassembly is sized to maintain the design

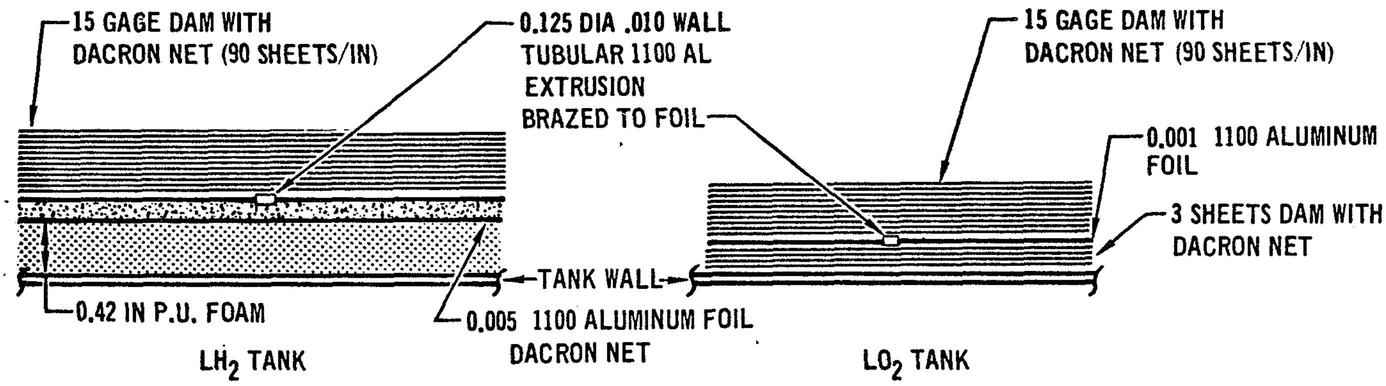

COOLED RADIATION SHROUD INSTALLATION DETAIL

	SPACING	PASSES	THICKNESS	WEIGHT
H_2 SHROUD	2.52 FT	15	0.005 IN	61.4 LB
O_2 SHROUD	2.04 FT	14	0.001 IN	5.7 LB

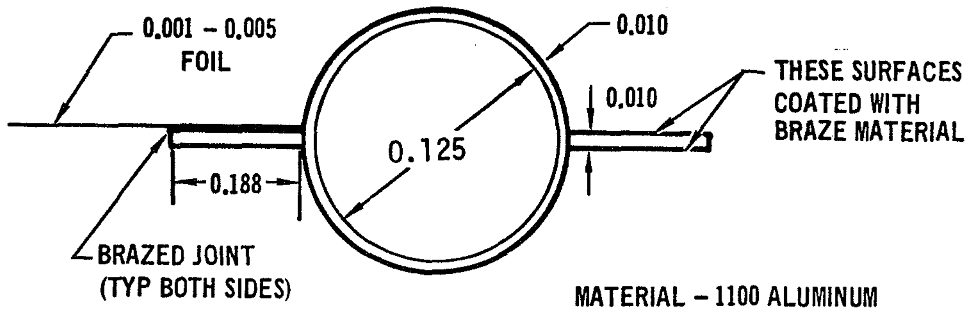

SHROUD CHARACTERISTICS

HEAT EXCHANGER CHARACTERISTICS

HEAT TRANSFER COEFFICIENT, BTU/HR-FT^2 - °R	
INSIDE	45.3
OUTSIDE	14.2
AREA, IN^2	386
TUBE DIAMETER, IN	0.25
TUBE LENGTH, IN	492
HEAT EXCHANGER WEIGHT, LB	1.16

MIXER CHARACTERISTICS

	H_2	O_2
INPUT POWER, WATTS	1.2	5.1
EFFICIENCY, PERCENT	10.0	14.0
MIXER WEIGHT, LB	0.6	0.8
OUTLET DIA, IN	1.0	1.0
BLADE DIA, IN	1.9	1.9
INTERFACE FLUID VELOCITY, FT/SEC	0.00592	0.00685
PUMPED FLOW RATE FT^3/MIN	0.127	0.081
INCREASED H_2 VENT, LB	4.0	-

INTERNAL HEAT EXCHANGER/MIXER CHARACTERISTICS

FIGURE D-18

CONCEPT	ADVANTAGES	DISADVANTAGES
√ VAPOR COOLED SHROUD	o NO MIXERS REQUIRED, NO EQUIPMENT INSIDE TANKAGE o COMPLETELY PASSIVE OPERATION o LOWEST VENT REQUIREMENTS	o HEAVIER THAN INTERNAL SYSTEM o FABRICATION AND INSTALLATION MAY BE DIFFICULT
INTERNAL HEAT EXCHANGER	o SMALLEST WEIGHT PENALTY o STATE-OF-THE-ART TECHNOLOGY o LEAKAGE WILL NOT DEGRADE INSULATION o COMPACT	o MIXER IS REQUIRED o ADDITIONAL HEAT FROM MOTORS o O_2 MIXER MUST BE PURGED
TANK MOUNTED HEAT EXCHANGER	o SMALL WEIGHT PENALTY o STATE-OF-THE-ART TECHNOLOGY	o REQUIRES DESTRATIFICATION FANS o LEAKAGE MAY DEGRADE INSULATION o ADDITIONAL HEAT FROM MOTORS o O_2 MIXER MUST BE PURGED o INTERACTS WITH PRESSURE VESSEL STRUCTURE

√ SELECTED

CANDIDATE APS THERMAL VENT SYSTEMS

FIGURE D-19

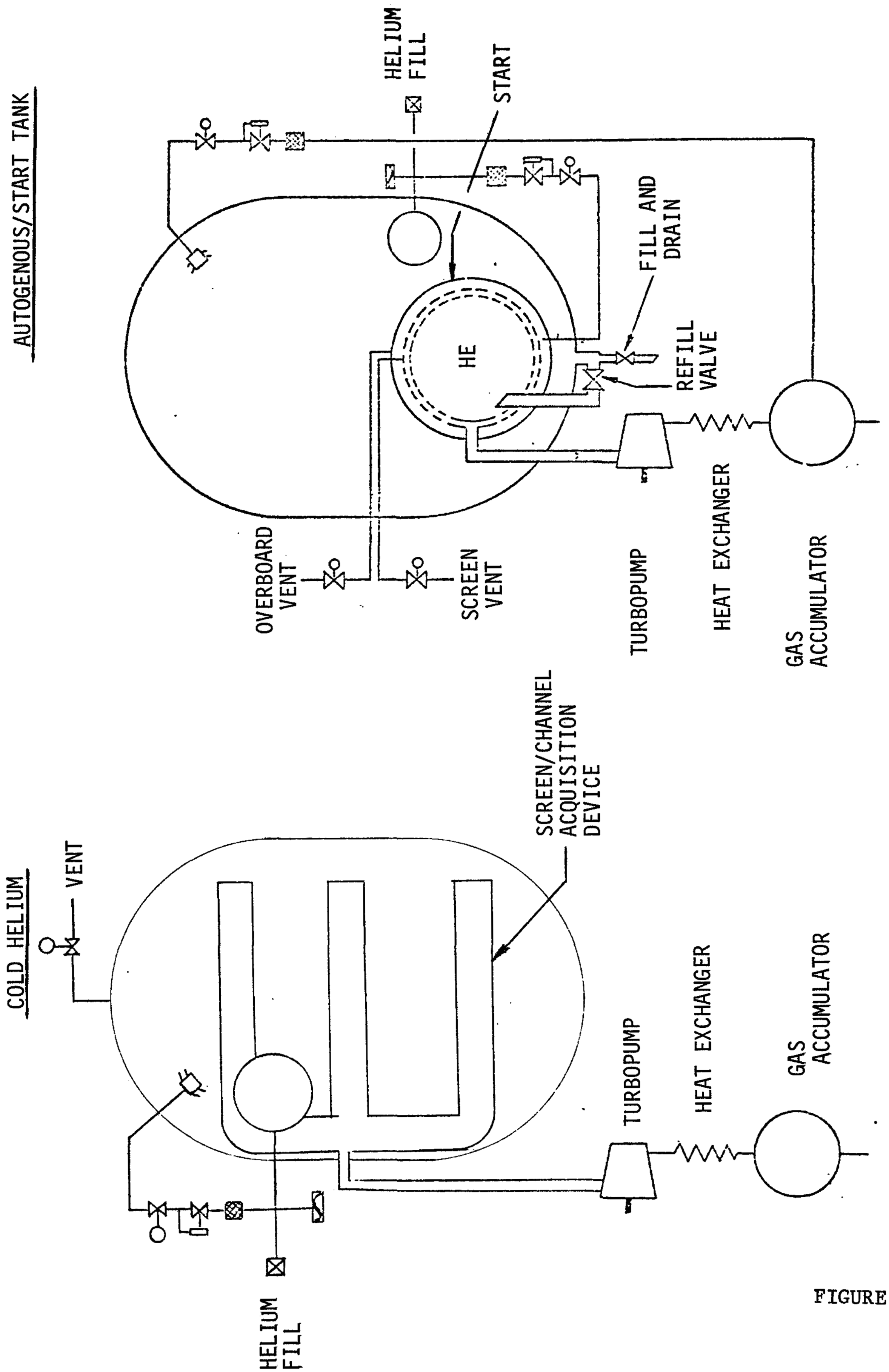

PROPELLANT TANK PRESSURIZATION CONCEPTS

FIGURE D-20

operating pressure during the maximum outflow conditions. The tank operating pressure was determined by a weight sensitivity study which showed the minimum weight subsystem resulted with a hydrogen tank pressure of 25 lbf/in^2a and an oxygen tank pressure of 30 lbf/in^2a.

D-1.15 Autogenous Pressurization Concept - With this concept, warm gaseous propellants are drawn from the accumulators and regulated to the required tank pressures. Heat transfer will initially occur primarily from the gas to the tank wall, but this heat will subsequently be transferred to the liquid. During long coast periods, thermal conduction and molecular diffusion will cause the ullage and propellant to approach thermal equilibrium. Dispersal and motion of the liquid and gas due to attitude control impulses under low-gravity conditions will cause increased surface area and convective heat transfer, thus increasing the rate at which equilibrium is reached. The effects of this process were considered in the concept evaluation.

With autogenous pressurization, warm propellant vapors present a significant heat source for the bulk liquid propellants. This heating is reduced by using intermittent pressurization whereby the tankage is only pressurized during usage. During nonusage (coast) periods, the tank pressure is allowed to decay. Both heating and pressure fluctuations effect the integrity of a passive surface tension acquisition device. Heating could vaporize a portion of the propellant under the screen, while the pressure reduction could cause vapor pockets in the liquid if the pressure dropped below the propellant vapor pressure. To ensure the performance of the acquisition device, a separate, refillable tank using cold helium pressurization has been provided. This concept yields sufficient pressure to meet NPSP requirements of the turbopumps during start-up until the APS propellant tank is fully pressurized with autogenous vapors. After the propellant has been settled and APS pressure levels achieved, the start tank refill valve is opened. Propellant simultaneously flows through the start tank to the turbopumps and refills the start tank. In this manner, the acquisition device, which is located in the start tank, can be isolated from autogenous heating.

D-1.16 Cold Helium Pressurization Concept - Helium is stored at 3000 lbf/in^2a in separate tanks submerged within the propellant tanks and regulated to the required APS tank pressures. Design of the assembly was straightforward, since the pressurization process was essentially isothermal. The tank pressure level is continuously maintained at regulated pressure (25 lbf/in^2a for hydrogen and 30 lbf/in^2a for oxygen); however, during extraction, the propellant vaporization rate will not be sufficient to maintain the equilibrium propellant partial pressure, and the helium partial pressure will increase during extraction. After extraction has ceased, the propellant will vaporize until equilibrium vapor pressure conditions are again satisfied, and tank pressure will increase above regulated pressure. An evaluation of the maximum pressure to be encountered during the mission indicates that the pressure will not rise above the pressure level associated with tankage minimum gage strength capability; thus, no tank venting would be required, and no weight penalty is involved.

D-1.17 Pressurization Subassembly Concept Comparison and Selection - The pressurization concepts were compared on a weight basis. The results of this comparison is shown in Figure D-21. The relative weights of the concepts shows that for the hydrogen tank, the autogenous pressurization concept provides a lighter weight at higher tank pressures. For the oxygen tank the cold gas helium is the obvious selection. For the hydrogen tank, the concept selection requires that the potential weight advantage of the autogenous concept be evaluated relative to increased operational and development complexity.

The cold gas helium pressurization subassembly was selected for the hydrogen tank. The small potential weight penalty associated with the selected subassembly is justified because of the inherent operational simplicity and advanced technology base for the cold gas subassemblies. A common pressurant type subassembly can be used for both propellants.

D-1.18 Tankage Design Summary - Individual subassembly design characteristics have been discussed in preceding sections. The complete assembly is summarized below and in Figure D-22.

Propellant acquisition is accomplished through screen channels, placed in such a position that some portion of the screen will always be "wetted," ensuring continuous fluid flow to the turbopump inlet.

Tanks are pressurized by a regulated supply of helium, the helium pressurant storage tanks being mounted internal to the propellant tanks, to take advantage of the volumetric efficiency gained by storing the pressurant at cryogenic temperatures.

The tankage concept consists of a 2219 Aluminum pressure vessel, layer of cryofoam (on the LH_2 tank only), cooling shroud made of 0.125 in. diameter aluminum tubing brazed to an aluminum heat barrier, HPI blanket, and fiberglass outer shell.

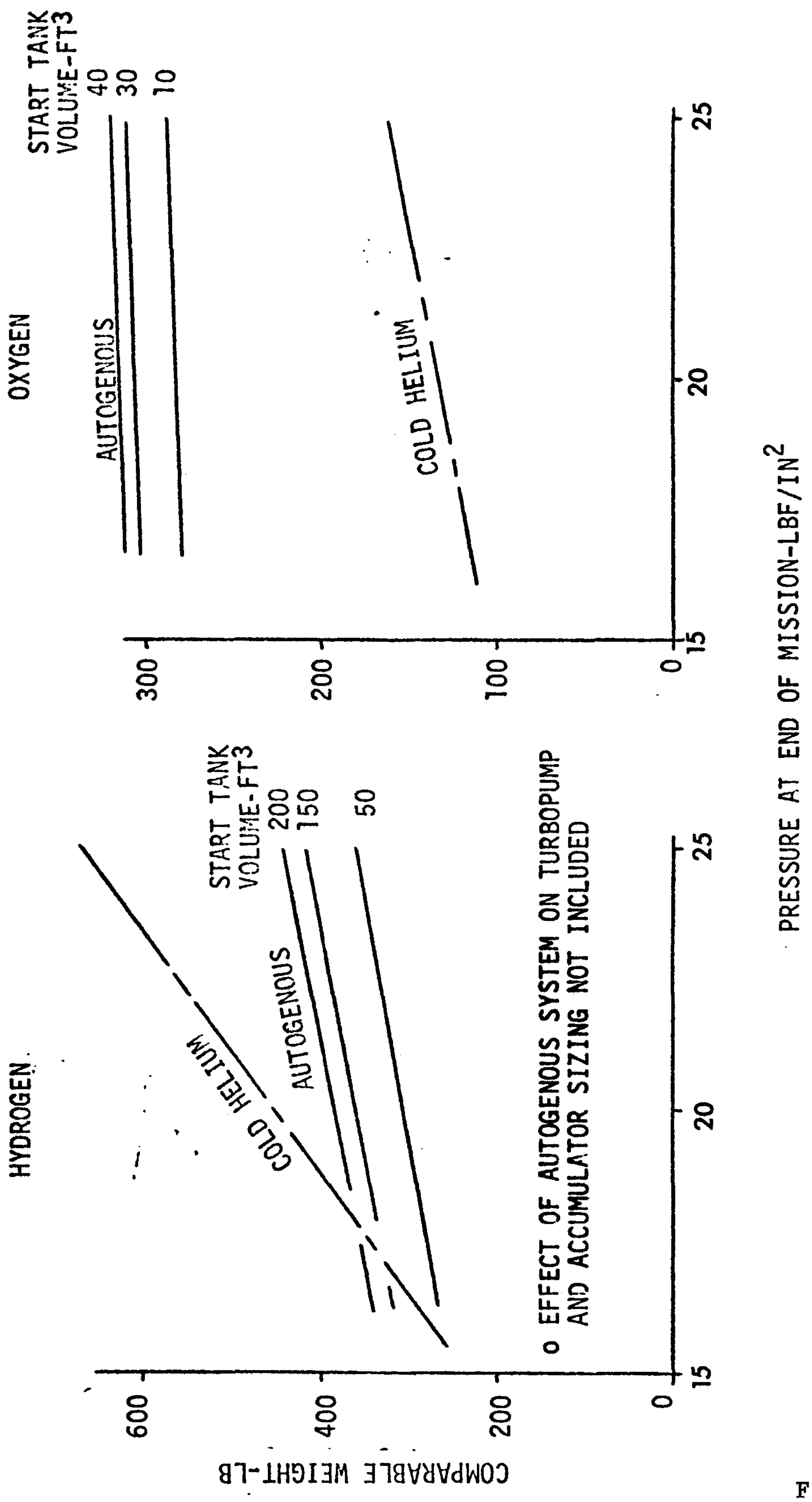

PRESSURIZATION CONCEPT COMPARISON
ORBITER B

FIGURE D-21

	ORBITER B		ORBITER C		BOOSTER	
	H_2	O_2	H_2	O_2	H_2	O_2
PRESSURIZATION	COLD HELIUM					
STORAGE PRESSURE, LBF/IN^2A	3000					
STORAGE TEMPERATURE, ^oR	37 (H_2) AND 162 (O_2)					
DELIVERY PRESSURE, LBF/IN^2A	25	30	25	30	25	30
PROPELLANT TANK VOLUME, FT^3	1449	332	1485	335	108	25
MATERIAL	2219-T87 ALUMINUM					
INSULATION	HPI/FOAM	HPI	HPI/FOAM	HPI	FOAM	NONE
THICKNESS, IN.	0.68/0.42	0.97	0.68/0.42	0.97	0.8	–
COOLING	H_2 VENT				NONE	
VENT RATE, LB/HR	1.68	–	2.01	–	N/A	N/A
SHROUD	ALUMINUM FOIL (0.005 IN. H_2, 0.001 IN. O_2)				N/A	N/A
TUBING	0.125 IN. DIAMETER, 0.010 IN. WALL				N/A	N/A
PROPELLANT ACQUISITION	SCREEN CHANNELS					
NO. CHANNELS	4	3	4	3	1	1
EXTRACTION RATE, LB/SEC	3.84	14.84	3.83	14.84	3.88	15.03
EXPULSION EFFICIENCY, PERCENT	98.3	99.4	97.5	99.4	96.5	96.5

APS PROPELLANT STORAGE DESIGN SUMMARY

FIGURE D-22

Figure D-23 illustrates the tank assembly. Temperature of the cooling shroud is maintained by a continuous hydrogen vent. LH_2 is extracted for cooling, expanded, and subcooled 7°R, then routed to the shroud, tank supports, and penetrations, where it vaporizes and absorbs tank heat leak. Thermal vent requirements are shown in Figure D-24. The fiberglass outer shell serves as an environmental shield for the tank thermal insulation system. On the ground, a constant purge of GN_2 provides an inert atmosphere surrounding the HPI protecting it against contamination and corrosion. On orbit, the fiberglass shell is vented to vacuum, enabling the HPI to function as an evacuated radiation shield. On reentry either helium (H_2) or nitrogen is purged through the cavity between the outer shell and the tank to prevent the shell from collapsing and to prevent atmospheric contamination of the HPI.

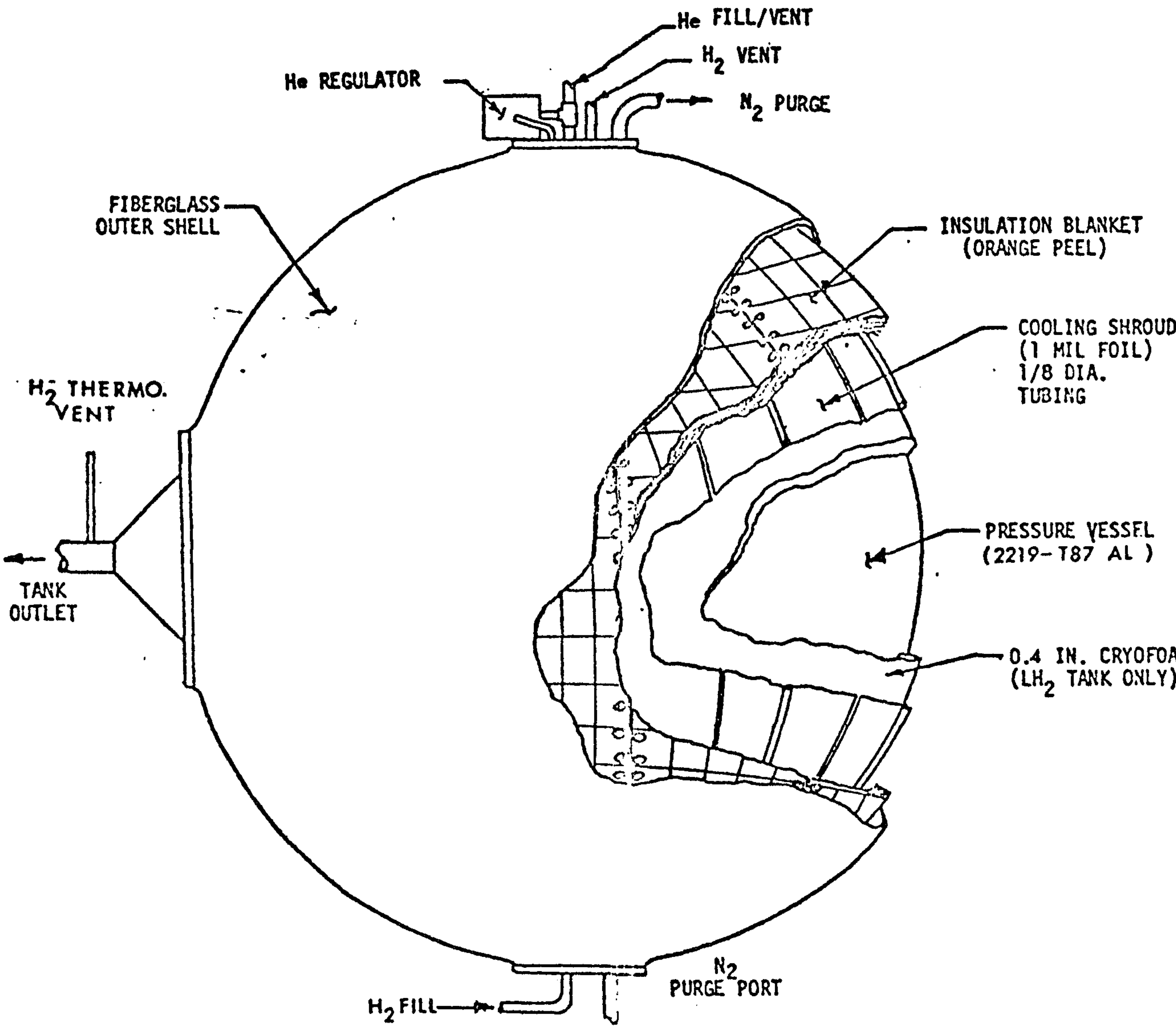

PROPELLANT TANK INSULATION/COOLING CONCEPT

FIGURE D-23

	ORBITER B		ORBITER C	
	H_2	O_2	H_2	O_2
INSULATION	196.0	83.2	267.0	113.2
TANK SUPPORTS	1.1	1.0	1.1	1.0
PRESSURIZATION/FILL LINES	5.2	3.8	5.2	3.8
SUMP/FEEDLINE	10.4	9.4	10.4	9.4
TURBOPUMP SHAFT				
HOT (1 PUMP)	45	39	45	39
COLD (2 PUMPS)	18.5	16.2	8.5	16.2
TURBOPUMP HOUSING				
HOT (1 PUMP)	30	18	30	18
COLD (2 PUMPS)	44	31	44	31
ENCLOSURE	13	12	13	13
PUMP DISCHARGE LINE	7	7	7	7
Σ HEAT INPUT	370.2 BTU/HR	220.6 BTU/HR	441.2 BTU/HR	250.6 BTU/HR
EQUIVALENT VENT FLOW RATE (MAX)*	1.68 LB_{H_2} / HR		2.01 LB_{H_2} / HR	

* INCLUDES VAPORIZATION PLUS SUPER-HEAT IN TURBINES

HEAT INPUT SUMMARY (BTU/HR)

FIGURE D-24

D-1.19 REFERENCES

(a) Cady, E. C., "A Comparison of Low-G Thermodynamic Venting Systems," DAC Report DAC-63174, April 1969.

(b) Stark, J. A., Blatt, M. H., Cryogenic Zero-Gravity Prototype Vent System, Convair/GDC Report GDC-DD367-006, October 1969.

(c) Sterbentz, W. H., Liquid Propellant Thermal Conditioning System, NASA CR 72113, April 1967.

(d) Poth, L. J., et al., A Study of Cryogenic Propellant Mixing Techniques, Final Report, GDC/Fort Worth Report FZA-439-1, November 1968.

(e) Low Gravity Propellant Control Using Capillary Devices in Large Scale Cryogenic Vehicles, Convair/GDC Report GDC-DDB70-008, August 1970.

D-2. CONDITIONER ASSEMBLY

A preliminary conditioner tradeoff study was performed in Subtask A to determine baseline configurations for each candidate APS concept so that comparisons could be performed on a consistent basis. These comparisons led to selection of a turbopump APS using 3500°R gas generators for propellant conditioning for Subtask B preliminary design. Preliminary design effort showed the selected approach to be impractical, and the concept was subsequently changed. This appendix describes the conditioner preliminary design effort leading to the selected conditioner concept shown in Figure D-25.

D-2.1 Conditioner Evaluation - During the initial part of Subtask B, a more indepth analysis of the baseline Subtask A conditioning concept (Figure D-26) was conducted to balance pump power required with the turbine power available over the complete range of operating conditions. In this analysis, updated turbine and pump component efficiencies were considered. Results of this initial analysis are presented in Figure D-27, which compares the turbine efficiency necessary for a power balance with estimated available turbine performance (reflecting reasonable turbopump design practices). Results show that, on the hydrogen side, turbine power output could not be matched to pump power requirements with realistic turbine and pump efficiencies. On the oxygen side, sufficient turbine power was available to drive the pump.

Analysis was conducted to determine modifications necessary in the Subtask A baseline assembly to provide hydrogen turbopump power balance. This analysis investigated ways both to lower pump power requirement, and/or to increase turbine power output. Pump power requirements can be reduced by lowering thruster chamber pressure or accumulator blowdown pressure ratio, since both affect pump discharge pressure requirements. Turbine power output could be increased by raising turbine pressure ratio or gas generator combustion temperature (thereby increasing assembly bypass and turbine flow rates). Figure D-28 illustrates the level to which thruster chamber pressure would need to be lowered to obtain achievable hydrogen turbopump efficiencies. As shown, a chamber pressure of approximately 300 lbf/in^2a (200 lbf/in^2 lower than the baseline) would provide turbopump power balance at reasonable turbine efficiencies and pressure ratios. Figure D-29 shows effect of lower gas generator combustion temperature (more gas flow through the turbine).

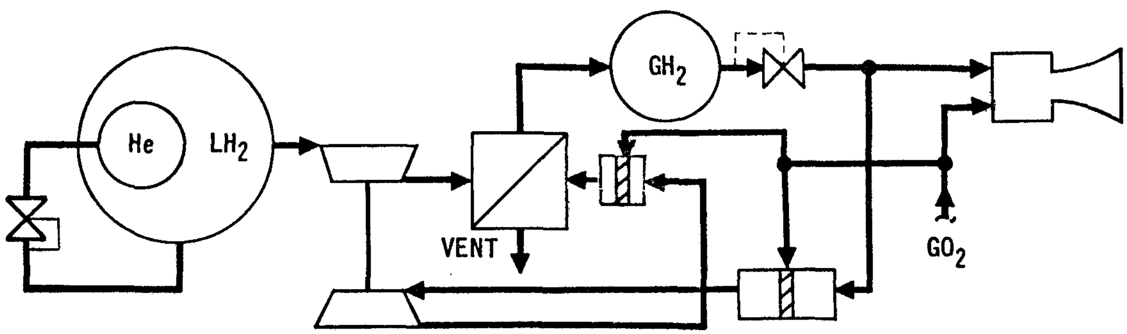

TURBOPUMP APS SCHEMATIC

FIGURE D-25

SUBTASK A SELECTED APS CONFIGURATION TURBOPUMP WITH 3500°R GAS GENERATOR/HEAT EXCHANGER

FILM COOLED THRUSTER

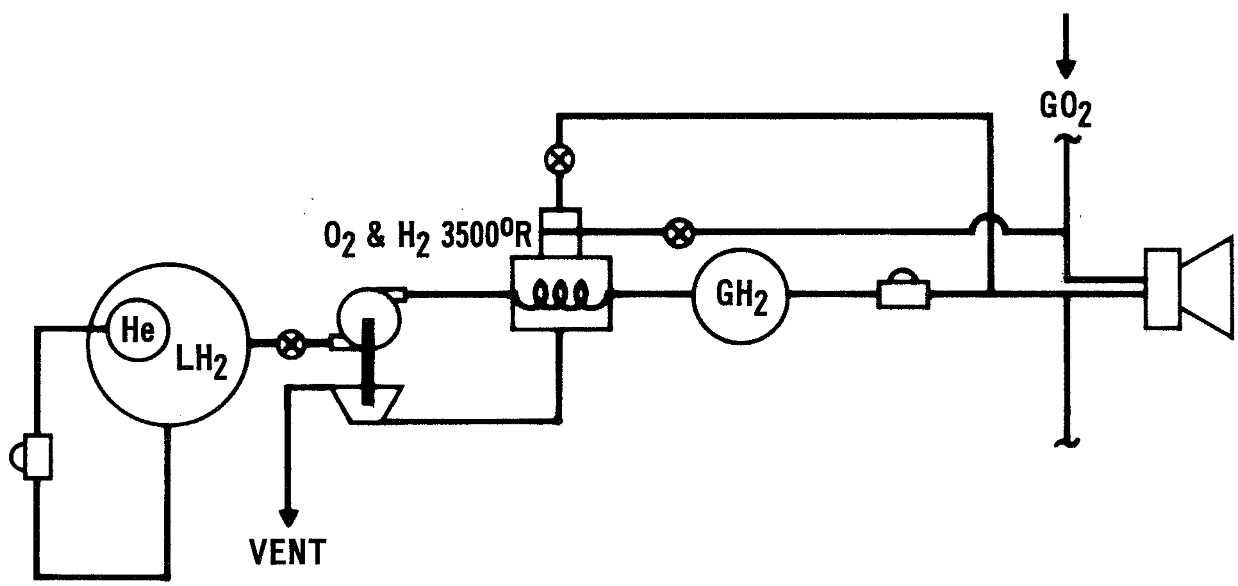

FIGURE D-26

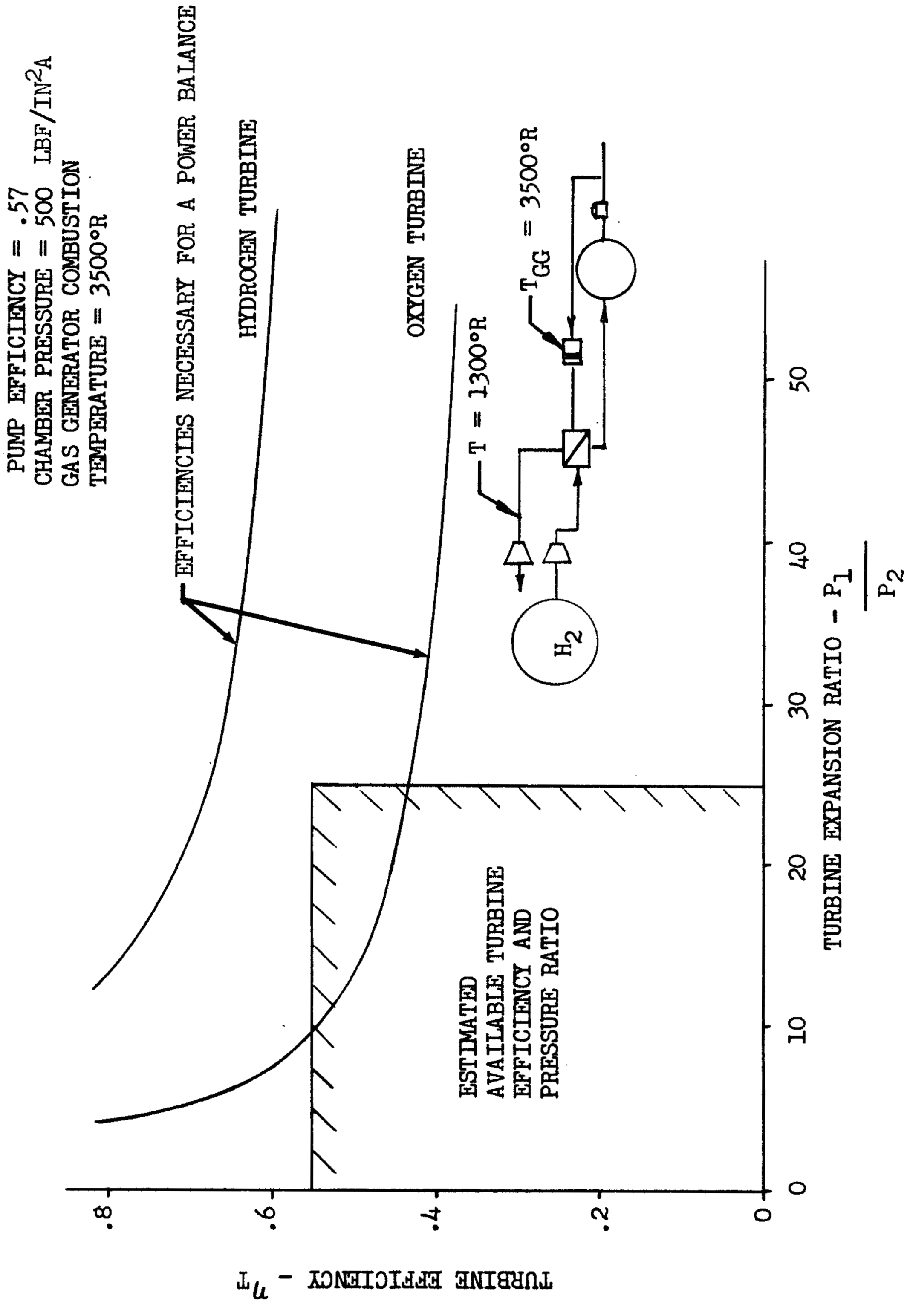

SUBTASK A BASELINE CONFIGURATION
TURBINE DESIGN REQUIREMENT

FIGURE D-27

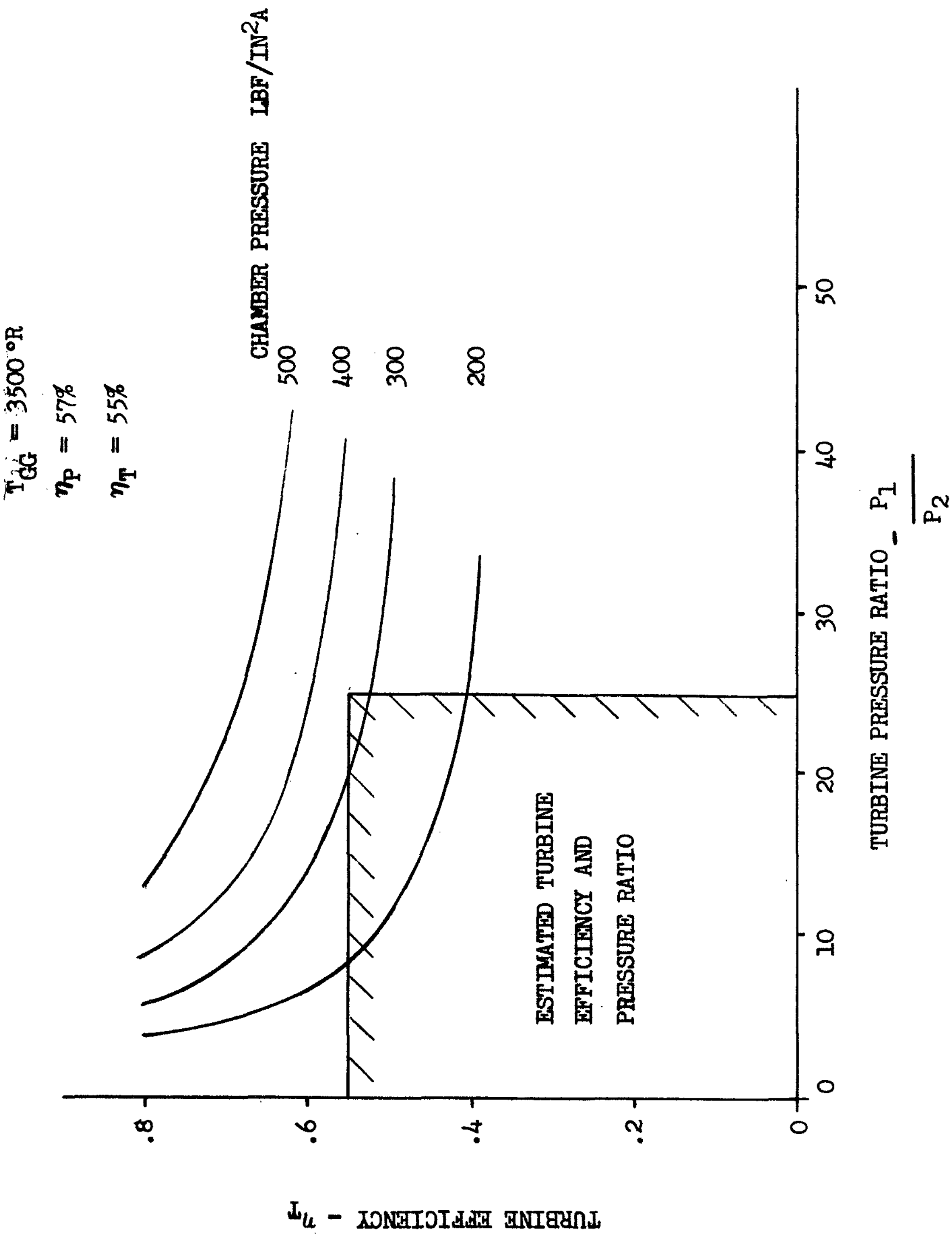

SUBTASK A BASELINE CONFIGURATION
EFFECT OF CHAMBER PRESSURE ON HYDROGEN TURBINE REQUIREMENTS

FIGURE D-28

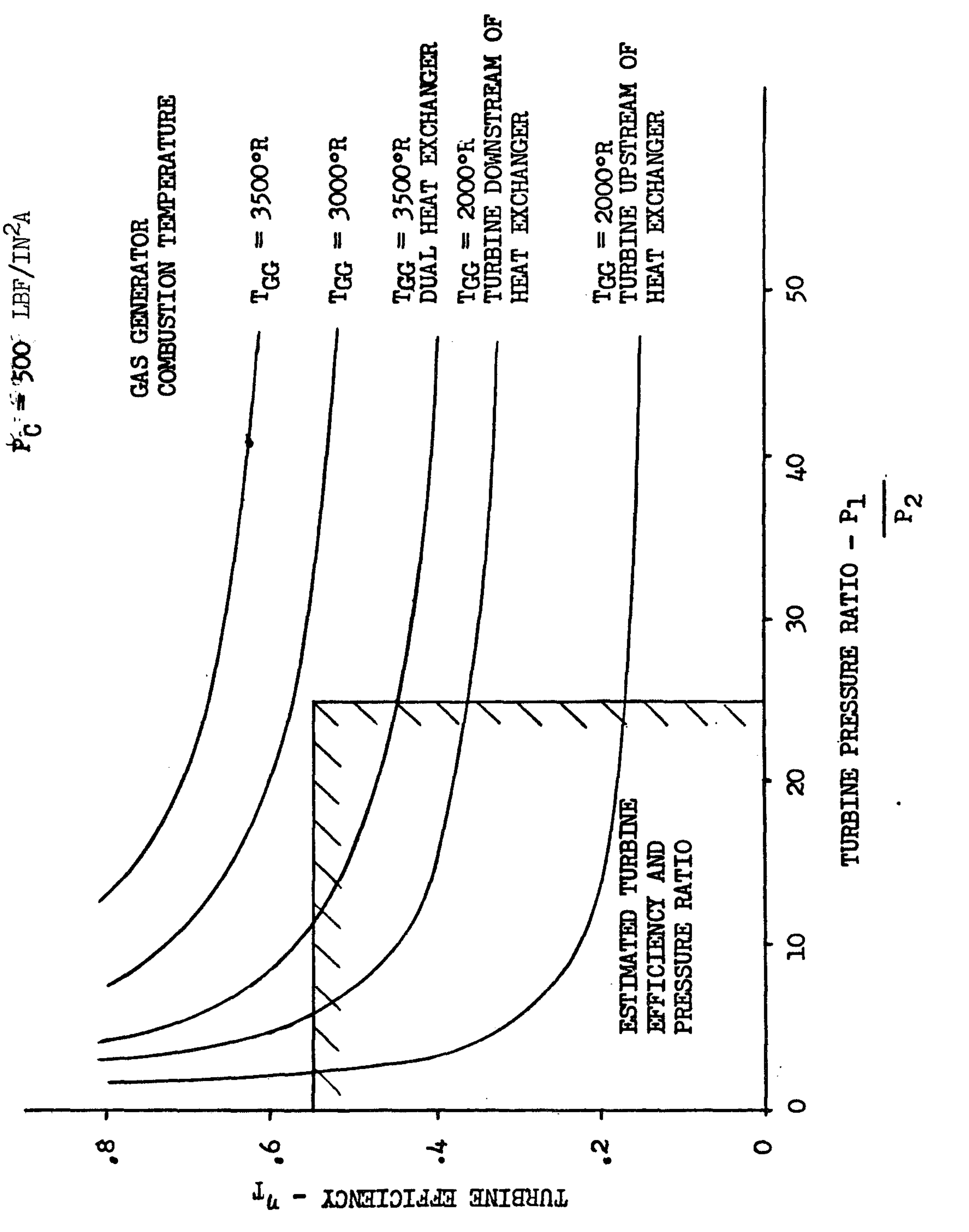

EFFECT OF CONDITIONING ASSEMBLY CONCEPT

FIGURE D-29

As illustrated, gas generator combustion temperature of 2000°R would provide turbopump power balance with low efficiencies and pressure ratios, while allowing Subtask A baseline thruster chamber pressure (500 lbf/in^2a) to be maintained.

To ensure minimum weight, it was clear that the conditioner concept selection should be reviewed in depth, considering factors not treated in Subtask A; therefore, a number of alternate conditioning assembly approaches, including the alternates considered in the Subtask A study, were evaluated. Approaches are shown schematically in Figure D-30. All alternate concepts were evaluated to define their optimum operating point over a range of chamber pressures and conditioning temperatures. Conditioning temperatures below the Subtask A baseline were considered, since, with a regenerative cooled thruster, a lower propellant conditioning temperature would be acceptable because of temperature rise through the regenerative thruster jacket.

Concept Description - Concepts A through E of Figure D-30 represent Subtask A baseline design variations. Concept A is the Subtask A baseline design used as a reference for concept weight comparison. Concept B is the Subtask A baseline design, but with chamber pressure reduced sufficiently to allow turbopump power balance. Concepts C and D are variations of a design which provide for turbopump power balance by changes in both gas generator combustion temperature and thruster chamber pressure. Lower gas generator combustion temperatures increase subsystem bypass flow, thus providing increased available turbine power. This effect is shown in Figure D-29, which illustrates turbine efficiency requirements at various gas generator temperatures. Concept E is the same as D, except that an active propulsive vent is used to provide overall increased subsystem performance. Subsystem weight is lower, due to the impulse contributed by the active vent. Analysis of vent impulse contribution was based upon one-dimensional chemical equilibrium calculations, using a vent specific impulse equal to 95 percent of theoretical.

Concept F is a modification of baseline design, using two heat exchangers. Turbine power is extracted at conditioning cycle mid-point. This provides the turbine with gas at higher operating temperature; the resulting increased turbine power available provides a significant alleviation of the turbine efficiency necessary for subsystem operation. This concept would be used with a 3500°R gas generator and still provide turbopump power balance at the Subtask A baseline

ALTERNATE CONDITIONING ASSEMBLY CONCEPTS

CONCEPT

A THRU E — SUBTASK A CONDITIONER CONFIGURATION
- GAS GENERATOR TEMPERATURES VARIED
- ACTIVE PROPULSIVE VENT INVESTIGATED

F — SUBTASK A HYBRID-CONFIGURATION
- TURBINE LOCATED IN MID-CYCLE

G — SUPPLEMENTAL O_2 CONFIGURATION
- TURBINE EXHAUST REBURNED IN HEAT EXCHANGER

H & I — COLD TURBINE CONFIGURATIONS
- HIGH AND LOW PRESSURE START ACCUMULATORS

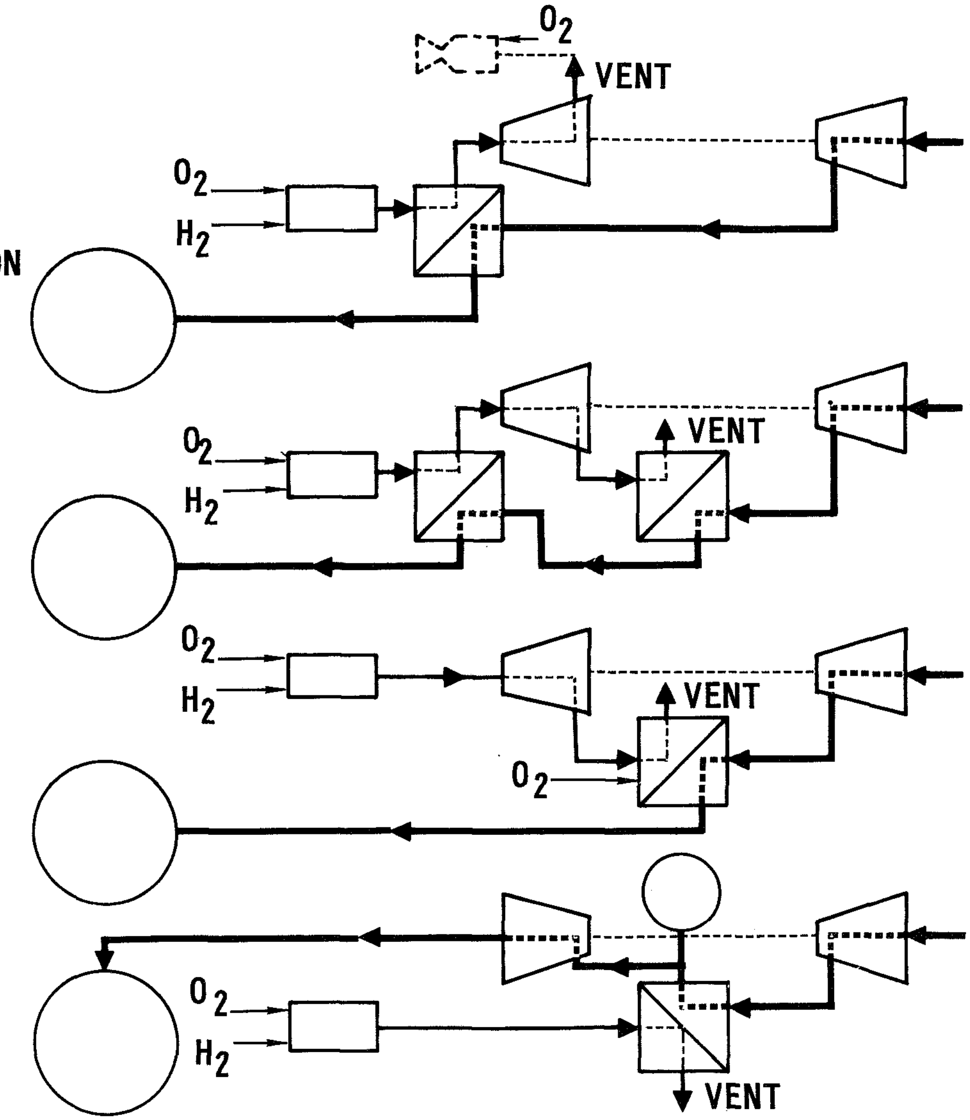

FIGURE D-30

chamber pressure of 500 lbf/in^2a. Thus, with the exception of the weight of an additional heat exchanger, this assembly provides the same overall subsystem weight as the Subtask A baseline; however, this concept is a more complicated design and is more difficult to achieve from a control (and possibly from a technology) standpoint.

Concept G is a baseline variation which uses a 2000°R gas generator in conjunction with a secondary burn heat exchanger. Sufficient flow is directed through the 2000°R gas generator to power the turbopump assembly. Turbine exhaust is directed to the secondary burn gas generator, where additional oxygen is added to produce additional heat release for propellant conditioning. Sufficient oxygen is added to the reburn heat exchanger to provide an overall mixture ratio of 2.0 for the bypass flow. This results in an equivalent conditioner combustion temperature of 3500°R, making this concept similar in total available energy to the 3500°R single Subtask A concept gas generator.

Concepts H and I use conditioned propellant from the heat exchanger instead of gas generator products to drive the turbopump assembly. Thus, turbines are cold, and resultant heat flux to the pump is reduced. In this assembly, turbine pressure ratio is equal to the difference in pump discharge pressure and accumulator pressure. Prior to pump spin-up, no propellant flow or pressure head is available for the turbine. Therefore, an additional source of power is required to start the assembly. This was provided by supplying the assembly with secondary accumulators which would "blowdown" in order to supply flow and pressure to the turbine during startup. In Concept H, the secondary accumulator is upstream of the turbine and is recharged to pump outlet pressure (turbine inlet pressure) as the turbopump comes up to operating speed. In Concept I, the secondary accumulator is valved to the upstream and downstream side of the turbine. In this manner, the start accumulator is recharged to the same pressure as the main accumulator (turbine discharge pressure). These assemblies were evaluated to determine what levels of pump discharge pressure and accumulator pressures would be required to provide sufficient turbine power for assembly matching. Figure D-31 presents results of this analysis for the hydrogen side of the assembly and shows that these assemblies could be operated at realistic pump and accumulator pressures. Further, the design point for this concept is presented in Figure D-32. This

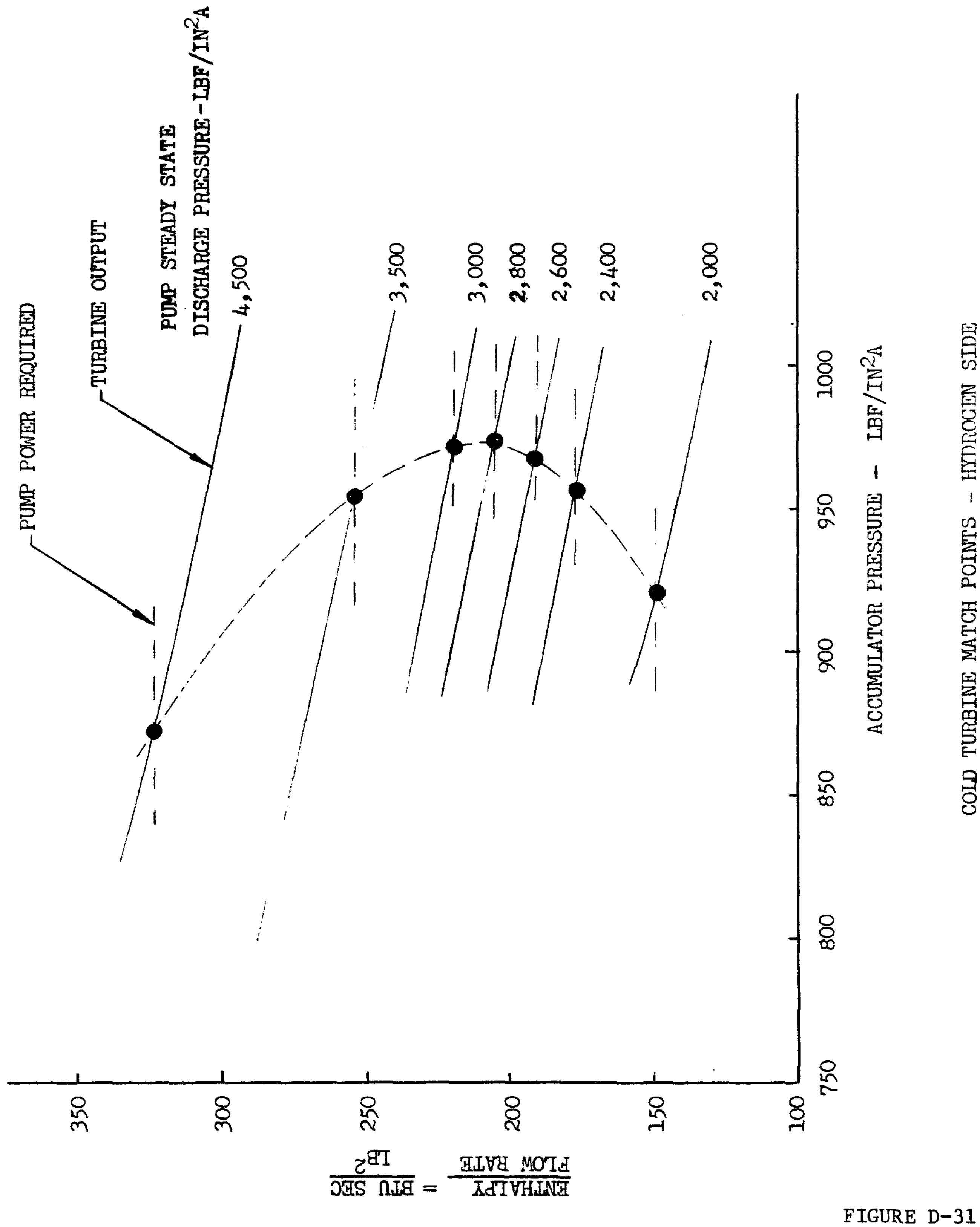
PUMP POWER REQUIRED
TURBINE OUTPUT
PUMP STEADY STATE
DISCHARGE PRESSURE-LBF/IN^{2}A
4,500
3,500
3,000
2,800
2,600
2,400
2,000
350
300
250
200
150
100
750
800
850
900
950
1000
ACCUMULATOR PRESSURE - LBF/IN^{2}A
ENTHALPY / FLOW RATE = BTU SEC / LB^2
COLD TURBINE MATCH POINTS - HYDROGEN SIDE

FIGURE D-31

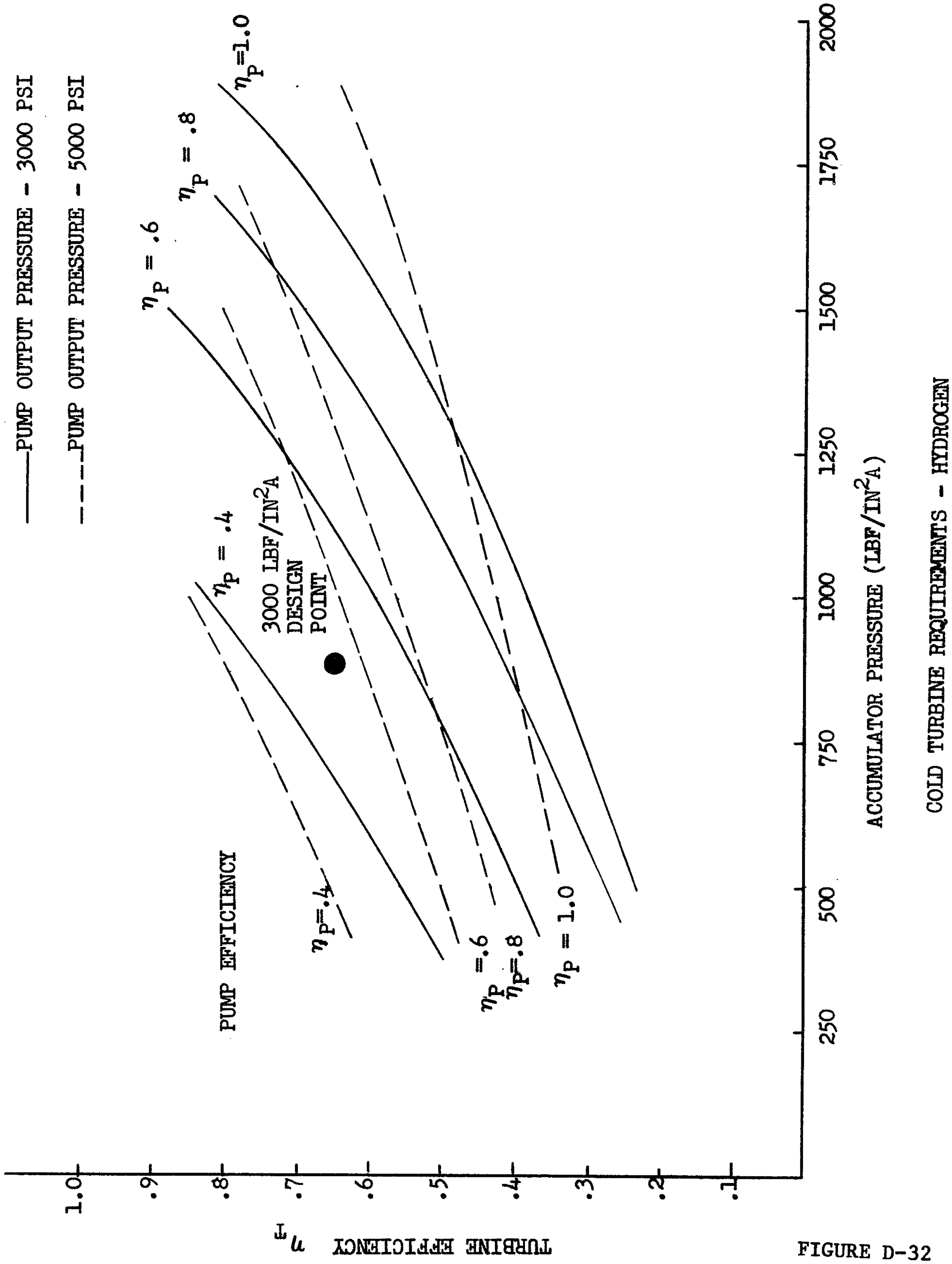
PUMP OUTPUT PRESSURE - 3000 PSI
PUMP OUTPUT PRESSURE - 5000 PSI
PUMP EFFICIENCY
η_P = .4
η_P = .6
η_P = .8
η_P = 1.0
3000 LBF/IN²A DESIGN POINT
1.0
.9
.8
.7
.6
.5
.4
.3
.2
.1
TURBINE EFFICIENCY η_T
250
500
750
1000
1250
1500
1750
2000
ACCUMULATOR PRESSURE (LBF/IN²A)
COLD TURBINE REQUIREMENTS - HYDROGEN

FIGURE D-32

assembly would require essentially the same bypass flow as the 3500°R gas generator baseline subsystem; however, additional weight would be incurred for two reasons:

(1) the subsystem chamber pressure is relatively low
(2) redundant start accumulators are required to ensure that the subsystem can be started should start accumulator pressure decay due to component failure.

Analysis of Alternate Concepts - The basic approach was to develop APS weight sensitivities as a function of chamber pressure and hydrogen conditioning temperature over a range of gas generator combustion temperatures for Concepts A through D, and G. Then, using turbine and pump efficiencies of 52 percent and 57 percent, allowable operating conditions were established. A turbine pressure ratio limit of 25:1 was imposed for these analyses, because increasing turbine pressure ratio above 25:1 does not provide any significant increase in turbine power. Examples of this analytical results are presented for Concepts A through D in Figures D-33 and D-34, which show optimum chamber pressure and conditioning temperature for a given gas generator combustion temperature. In Concept E, optimum chamber pressure and conditioning temperature of Concept D were used and the effect of providing an active propulsive vent was defined. The dual heat exchanger, Concept E, was evaluated to define the effect of providing an additional heat exchanger to the Subtask A concept. Cold turbine concepts H and I investigated the effect of using a typical engine expander cycle.

Comparison of Concepts - The above concepts were evaluated considering APS weight, flexibility to component performance, and technology requirements. Figure D-35 shows the APS weight for the various concepts compared to Subtask A, the concept design points and technical considerations. Based upon data shown in Figure D-35, a revised baseline conditioning assembly schematic (Concept G) was selected. The revised concept employs the 2000°R gas generator in conjunction with the reburn heat exchanger operating at an overall conditioner mixture of 2:1. This approach offers low overall APS weight, reasonable technology requirements, and low sensitivity to subsequent design changes; therefore, this assembly was used as a baseline for all subsequent Subtask B effort. Further baseline

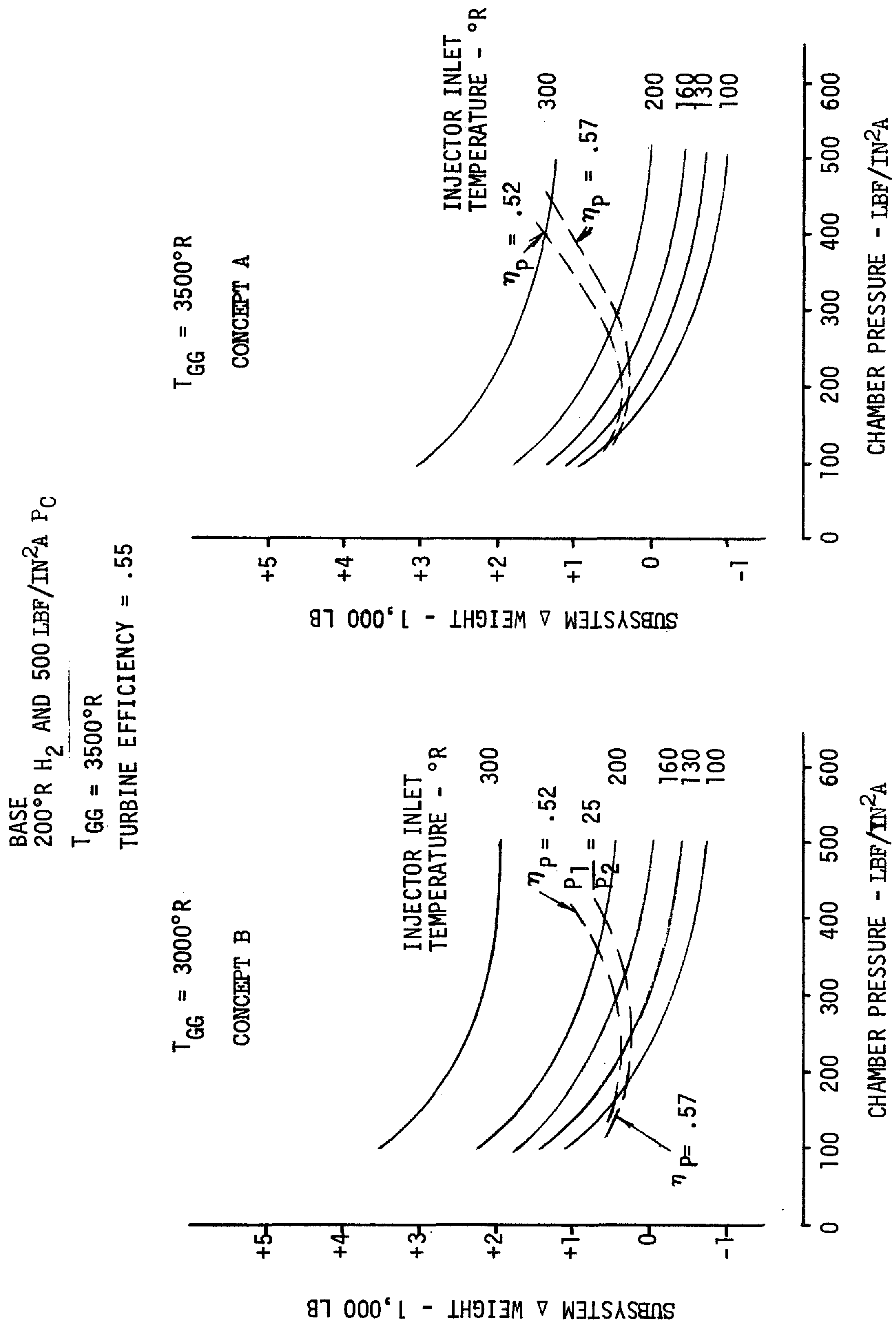

SUBTASK A CONDITIONING ASSEMBLY
OPERATING POINTS

FIGURE D-33

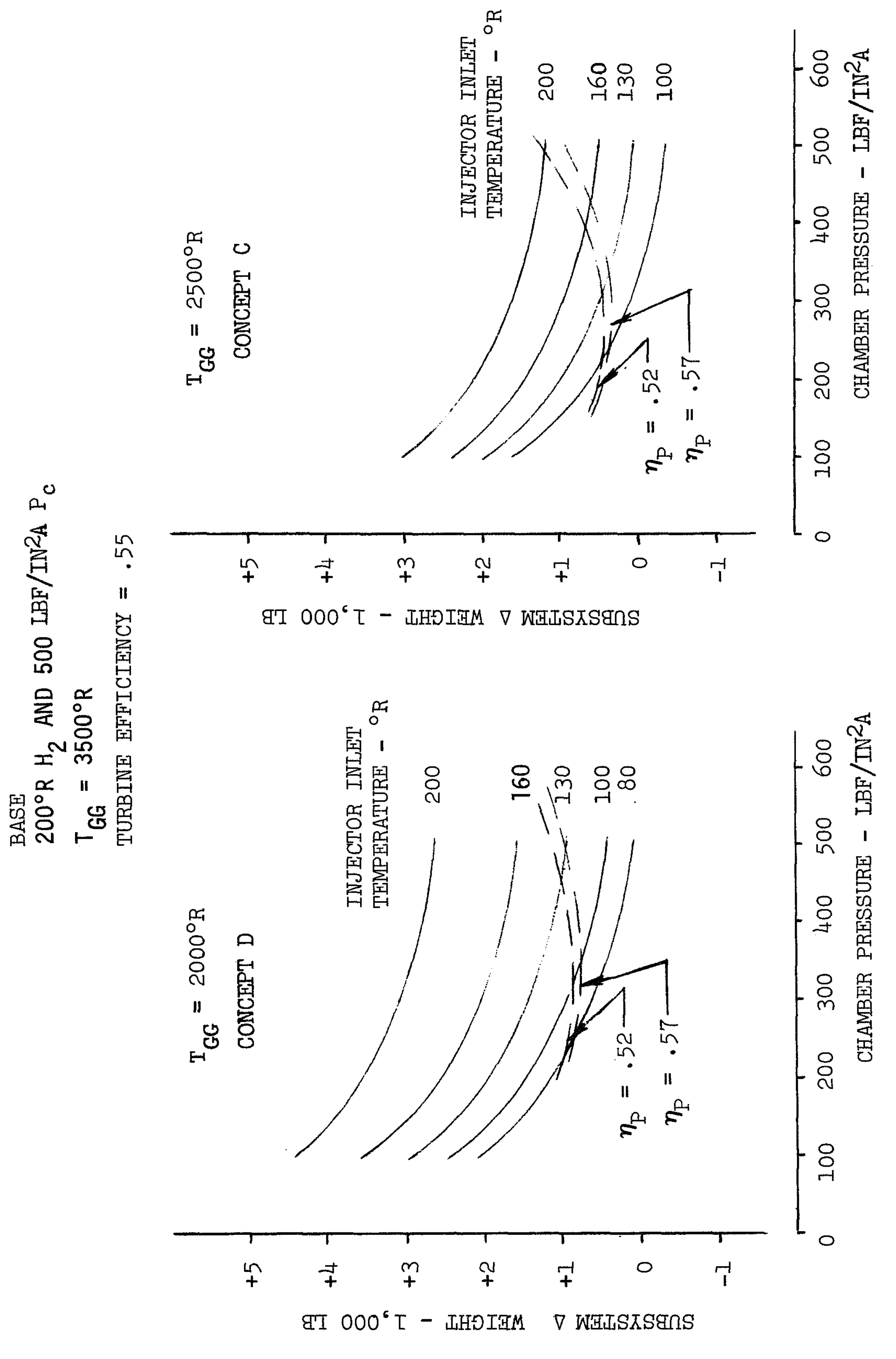

SUBTASK A CONDITIONING ASSEMBLY
OPERATING POINTS

FIGURE D-34

CONFIGURATION	OPERATING CONDITIONS: HYDROGEN TEMP °R	GAS GENERATOR TEMP °R	ACCUMULATOR PRESSURE–LBF/IN²A MAX/MIN	CHAMBER PRESSURE LBF/IN²A	WEIGHT CHANGE LB	TECHNICAL CONSIDERATIONS RELATIVE TO SELECTION
A	200	3500	2000/915	500	REFERENCE	• NOT FEASIBLE DUE TO TURBINE REQUIREMENTS.
B	145	3500	880/400	200	260	• HIGH TEMPERATURE-COOLED GG/HX REQUIRED. • MAXIMUM TURBOPUMP EFFICIENCY CRITICAL TO DESIGN.
C	120	2500	1150/520	270	320	• SAME AS B BUT COOLING PROBLEM MUCH RELAXED.
D	105	2000	1450/660	350	620	• MAXIMUM TURBOPUMP EFFICIENCY REQUIRED FOR PERFORMANCE.
E	105	2000/2000	1450/660	350	170	• TURBOPUMP EFFICIENCIES CRITICAL TO DESIGN. • REQUIRES DEVELOPMENT OF ACTIVE VENT GG
F	200	3500	2200/915	500	100	• REQUIRES DEVELOPMENT OF 2 HEAT EXCHANGERS. • SUBSYSTEM MATCHING AND CONTROL WILL BE COMPLEX. • TURBOPUMP EFFICIENCIES ARE CRITICAL TO DESIGN. • HIGH TEMPERATURE TURBINE BLADE DESIGN.
G	100	(2000/XXXX) 3500 EQ.	1570/655	350	−580	• SAME AS F EXCEPT MINIMUM CONDITIONING TEMPERATURE AND DEVELOPMENT OF SECONDARY INSTEAD OF 2 HEAT EXCHANGERS IS REQUIRED.
H	260	260	970/400 3000/800	200	1270	• REQUIRES REDUNDANT START ACCUMULATORS • O_2 TURBINE THRUST BEARING LIFE BEYOND STATE-OF-THE-ART,
I	260	260	970/200	100	2750	• SAME AS H

COMPARISON OF ALTERNATE CONDITIONER CONCEPTS

FIGURE D-35

optimization, such as increased reburn mixture ratio, and control optimization, was performed to define fully the design which would provide minimum overall subsystem weight. This optimization is provided in the following section.

D-2.2 Conditioner Assembly Control - Conditioner operation is begun and ended by accumulator pressure sensors. Accumulators operate in a blowdown mode from a maximum accumulator pressure (P_{max}) to a minimum accumulator pressure (P_{min}). During thruster operation, accumulators blowdown to a design switching pressure. At this pressure, the conditioner assembly is signaled on; it then supplies additional propellant for accumulator recharge. During lengthy steady-state firing, the conditioner assembly must supply sufficient propellant flow to the accumulator to maintain minimum accumulator pressure. When thruster flow ends, the conditioner assembly recharges the accumulator to P_{max} condition and is signaled off. Thus, APS operation requires that the conditioner assembly be sized and controlled to provide maximum steady-state thruster flow at minimum accumulator pressure. The conditioner assembly also must provide maximum pressure capability for accumulator recharge. Controls and control logic required to meet these requirements depend upon the manner in which the conditioner assembly is designed and operated.

Conditioner Assembly Control Options - The conditioner assembly consists of turbopump, heat exchanger, and gas generator. Two basic approaches to assembly control are possible. From design and control standpoints, the first of these, Concept A, (Figure D-36) is the simplest. In this concept, maximum flow and pressure are maintained within the heat exchanger during all phases of operation. This is accomplished by using a cavitating venturi at the pump outlet and a sonic diffuser at the heat exchanger outlet. Figure D-37 illustrates the operating point on the pump map. The second approach, concept B, is more difficult from both design and control standpoints, since assembly operating conditions vary during accumulator recharge. A schematic of this concept is shown in Figure D-36 and Figure D-37 shows its operation on a pump map. As illustrated, increase in pump head required during accumulator recharge for control concept B can be implemented two ways:

(1) constant pump power can be maintained as the head rises by decreasing propellant flow (operation along line HP_1)
(2) constant propellant flow can be maintained by increasing turbine power as the head rises.

For the constant pump power control approach, since propellant flow within the

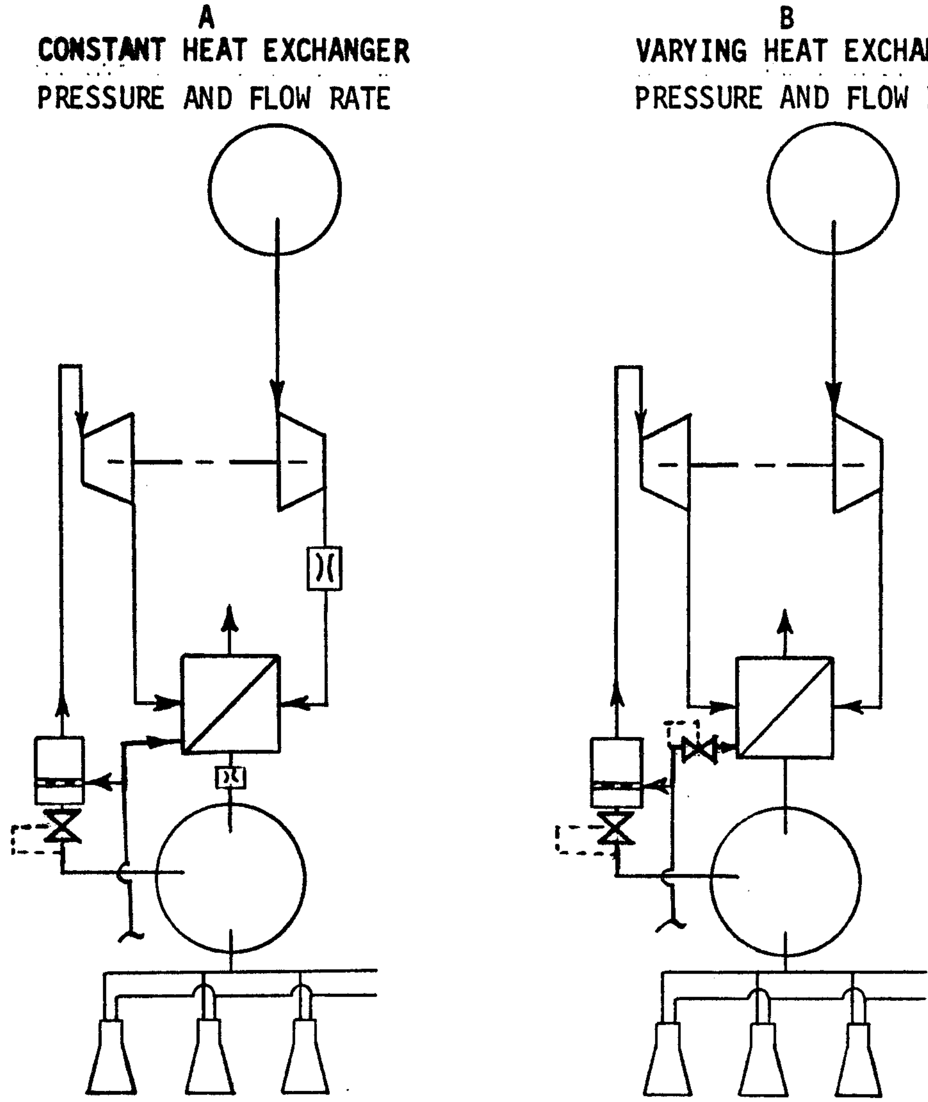

CONTROL CONCEPTS

FIGURE D-36

TURBOPUMP OPERATING CONDITIONS

CONTROL CONCEPT A

HEAT EXCHANGER FLOW
AND PUMP DISCHARGE
PRESSURE CONSTANT

CONTROL CONCEPT B_1

HEAT EXCHANGER FLOW
AND PRESSURE VARY
TURBINE POWER CONSTANT

CONTROL CONCEPT B_2

HEAT EXCHANGER
PRESSURE VARIES
TURBINE POWER THROTTLED

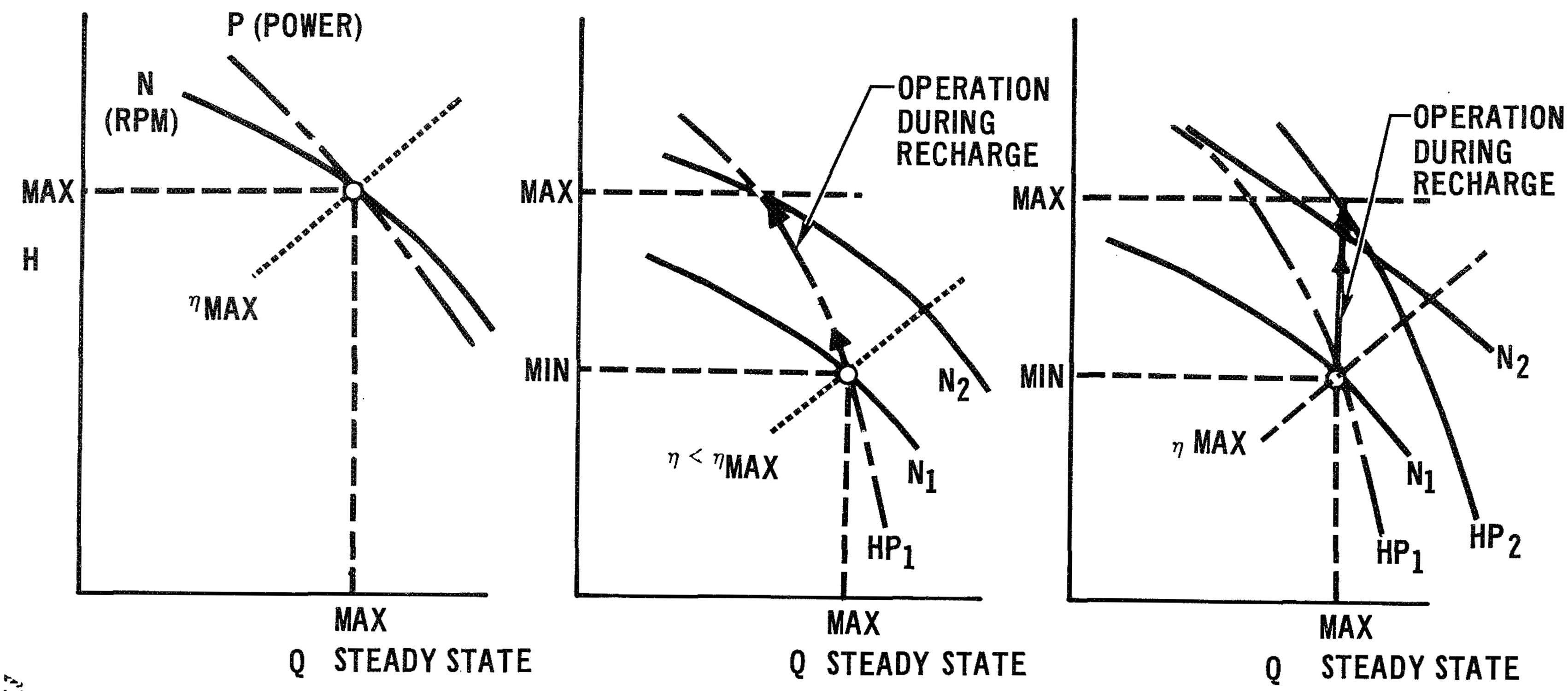

FIGURE D-37

heat exchanger is decreasing during accumulator recharge, oxygen added for reburn in the heat exchanger (and thus the heat addition) must be controlled to prevent heat exchanger overheating. For the constant pump flow control approach (since pump power requirements are increasing proportionally to accumulator pressure) the turbine must be throttled to provide additional power during recharge.

With concept A, control is possible with passive components, whereas both concept B approaches require active control components. Therefore, concept A would be the best approach from design and controls standpoints; however, concept B results in lower overall APS weight, since it can operate at a lower bypass flow during periods of continuous usage, or at a higher chamber pressure for the same bypass flow.

Conditioner Assembly Operation and Weight Analysis - Analysis of concept A operation is limited to evaluation of power balance between pump and turbine at a single design point corresponding to maximum turbopump efficiencies. As shown in Figure D-37, the two concept B approaches required consideration of a range of turbopump efficiencies in order to ensure proper accumulator recharging.

Under ideal conditions, the two concept B approaches would be designed for maximum efficiency (52 percent) at the steady-state condition to minimize steady-state bypass requirements; however, preliminary analysis showed that the constant power approach would not recharge the accumulator because the pump efficiency would begin to decrease as pump head increased above minimum. This reduction in efficiency was sufficient to cause pump power to increase above available turbine power (see Figure D-38). To remedy this operational problem, the pump was designed to operate below maximum efficiency at the steady-state condition. This allowed the pump to take advantage of increasing efficiency during recharge (see Figure D-38) and to operate at higher average efficiency, thus allowing recharge with the available turbine power. This approach results in increased bypass flow due to reduced pump efficiency during steady-state operation.

Analysis of the concept B constant pump flow approach showed that increased turbine power was needed during accumulator recharge because of increased pump head. This additional turbine power would necessitate a significant increase in turbine flow, since turbine pressure ratio, inlet temperature, and efficiencies were at maximum. Increased turbine flow could be realized by changes to either turbine nozzle flow area or to inlet pressure. Changing flow area was unattractive because it compromised turbine design and efficiency. However, increased

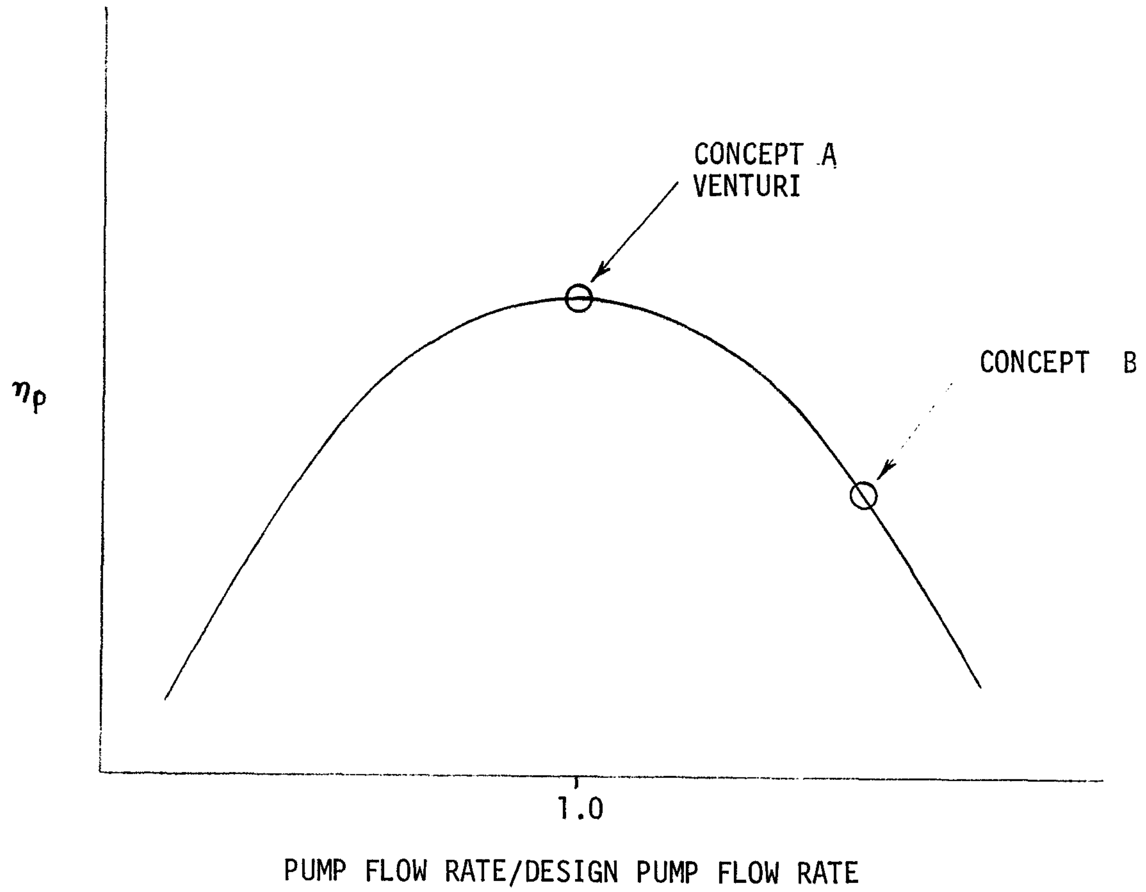

OFF-DESIGN PUMP EFFICIENCY

FIGURE D-38

inlet pressure could be obtained either by operating gas generator and turbine directly from the accumulator rather than from the regulator or by operating the gas generator in a throttled condition at the steady-state design point. With the direct accumulator feed approach, the flow to the turbine would increase as the accumulator was recharged. The method was judged impractical, since both oxygen and hydrogen accumulators would have to recharge and decay simultaneously in order to have sufficient pressure available.

The influence of the conditioner control concept upon total subsystem weight is largely measured by its effect on total bypass flow for turbopump power and heat exchanger energy balance. Pump power required is defined by accumulator pressure, which is dependent, in turn, on thruster chamber pressure. Concept A operates in a steady-state mode at maximum accumulator pressure (P_{max}), while concept B operates in a steady-state mode at minimum accumulator (P_{min}) pressure. Thus, for selected chamber pressure, concept B will result in reduced overall bypass flow, because its pump power requirement is lower at steady-state design conditions. This lower bypass flow reduces APS weight, since it reduces propellant and storage tank weight. An alternative is to use the lower pump head characteristic of concept B to reduce hardware weights, while keeping the bypass the same as that of concept A. This can be accomplished by increasing concept B chamber and accumulator pressures at steady-state design conditions until the minimum pressure is the same as the maximum accumulator pressure for concept A. At this point, the bypass flow of the two systems is the same. This results in the same APS storage weight (propellant and tankage) for both concepts, but a reduced inert weight (lower component weights) for concept B because of higher chamber pressure. Both lower bypass and lower inert weight approaches yield a concept B weight advantage.

D-2.3 Control Concept Selection - The selected baseline conditioner uses a 2000°R gas generator to power the turbopump assembly. Turbine exhaust is directed to the reburn heat exchanger where sufficient oxygen is added and reburned to provide the energy necessary for propellant conditioning. Conditioner concept comparison analysis of Section D-2.1 limited the reburn mixture ratio to provide an equivalent overall combustion temperature of 3500°R. A higher mixture ratio and the accompanying larger heat release can reduce the bypass flow required for propellant conditioning; therefore, the optimization of the baseline conditioner considered mixture ratios greater than 2:1 and different mixture ratios for oxygen and hydrogen.

The overall bypass of the hydrogen conditioner assembly is dependent upon the hydrogen turbine flow requirements, which are dictated by the propellant conditioner and turbopump requirements. The interrelationship of these is discussed in the following example. Figure D-39 presents the ratio of turbine-flow to pump-flow necessary to match the pump power requirements and provide hydrogen conditioning to 100°R. The turbine flow necessary to match the pump requirements is presented as a function of turbine pressure ratio and chamber pressure; the flow necessary to provide for propellant conditioning is shown as a function of mixture ratio and chamber pressure. The intersection of the mixture ratio and turbine pressure ratio curves represents the power match points for the subsystem and shows the turbine flow required and the chamber pressure obtainable. For example, following a constant mixture ratio curve of 2.0 shows that the turbine flow decreases with increasing chamber pressure and turbine pressure ratio. At higher chamber pressures and subsystem operating pressure, the enthalpy required for propellant conditioning is slightly reduced, requiring a lower turbine flow. Increased chamber pressure, however, requires a higher pump power. This is provided at the lower turbine flows by utilizing higher turbine expansion ratios, which provide a higher energy extraction from flow. Turbine expansion ratio was limited to 25:1 in order to have a realistic design pressure in the heat exchanger located downstream of the turbine. As shown in Figure D-39, once this limit is reached, the turbine flow is controlled by the pump power requirements such that further increases in chamber pressure results in higher flow requirements. The remaining portion of the conditioner flow, the oxidizer to the reburn gas generator, is also influenced by turbine flow. With higher flows to the propellant conditioner, the energy required from the reburn heat exchanger is reduced, thus the reburn mixture ratio is lower.

The overall conditioning bypass flow is a function of the turbine flow and reburn mixture ratio. Figure D-40 presents the conditioner bypass flow as a function of chamber pressure (turbine flow) and hydrogen conditioning temperature (reburn flow) for a mixture ratio of 2.0, and for a range of mixture ratios at the turbine expansion ratio limit of 25:1. This figure shows that the bypass flow requirement, and, thus, the subsystem propellant weight, continuously decreases with increasing conditioner mixture ratio and decreasing chamber pressure. The inert weight of the subsystem, in general, increases with decreasing chamber pressure; therefore, in order to minimize subsystem weight, the influences of

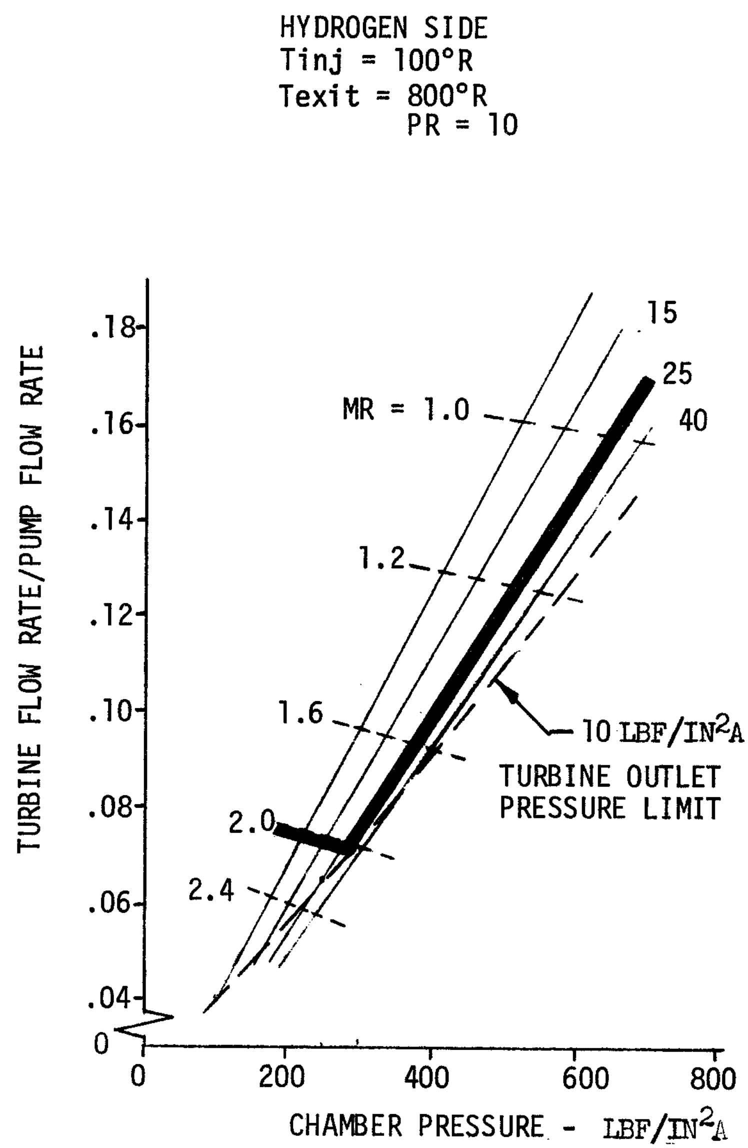

CONDITIONING CONCEPT PRELIMINARY DESIGN POINTS
SUBTASK B

FIGURE D-39

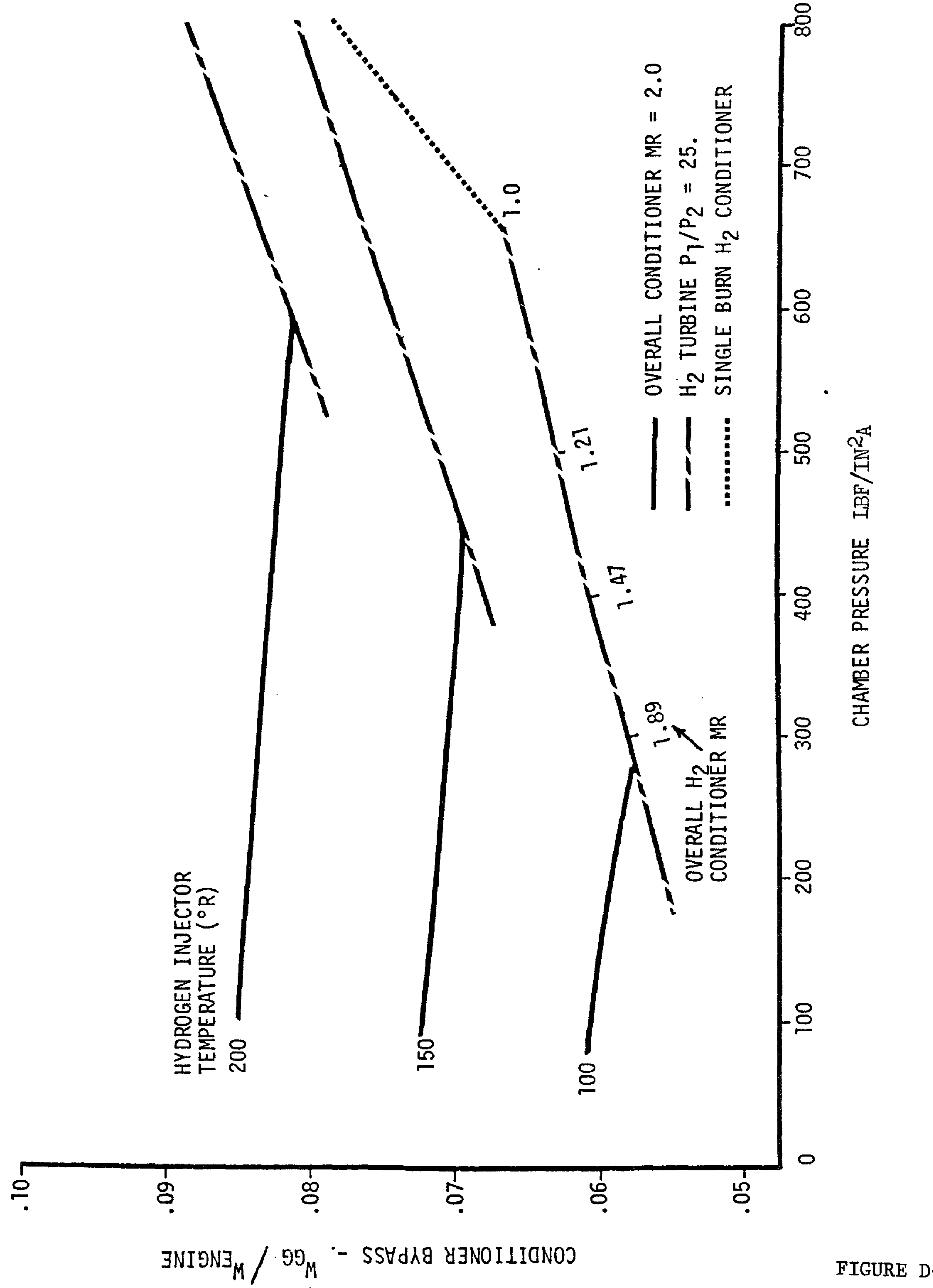

CONDITIONER BYPASS FOR REBURN CONCEPTS

FIGURE D-40

chamber pressure upon the bypass flow requirements and the inert weights were combined to allow a total subsystem weight comparison. The effect of conditioner mixture ratio and thruster chamber pressure on overall subsystem weight is presented in Figure D-41. As shown, the conditioner concept optimizes at a chamber pressure of approximately 500 lbf/in^2a. Figure D-41 also compares the baseline reburn conditioner concept with a simpler no-reburn conditioner concept. No reburn, i.e., no oxygen addition to the hydrogen heat exchanger, results in a subsystem weight not significantly greater than the minimum weight approach. The no-reburn concept is more sensitive to hydrogen conditioning temperature. This effect is presented in Figure D-42, which shows the effect of hydrogen conditioning temperature on overall subsystem weight. As shown, a temperature above 100°R results in a relatively large weight penalty for the no-reburn design. Following a review of the results discussed above (in particular the sensitivity to conditioning temperature) the judgment was made to eliminate the no-reburn concept from further consideration. In order for the concept to be weight competitive, a 100°R conditioner temperature would be required making the development of the regenerative engine mandatory to the exclusion of film cooled approaches. Similarly, a judgment was made to condition hydrogen to 200°R in the selected reburn heat exchanger approach. This induces a weight penalty into the APS, but offers less technology risk and provides the capability of using either regenerative or film cooled APS thrusters.

The above type of analytical approach was used to evaluate all subsystem control concepts described in the previous section, to determine the relative weight advantage of each. In this evaluation, hydrogen conditioning temperature was 200°R and turbine pressure ratio was limited to 25 to 1 and/or the turbine exit pressure was limited to 30 lbf/in^2a minimum, to facilitate heat exchanger ground testing. Overall conditioner mixture ratio was limited to 2.7 to 1. This mixture ratio resulted in a reasonable combustion temperature in the secondary burn gas generator and no significant weight advantage was realized at greater mixture ratios.

Figure D-43 presents the results of this analysis and shows the subsystem weight vs chamber pressure for control concept A and control concept B using two implementation approaches. At the optimum conditions, the constant power approach of concept B has a 350 lb weight advantage at chamber pressure of 500 lbf/in^2a, while the constant flow approach has a 450 lb weight advantage over concept A. Thus, the constant flow approach is the best approach on a weight basis. However,

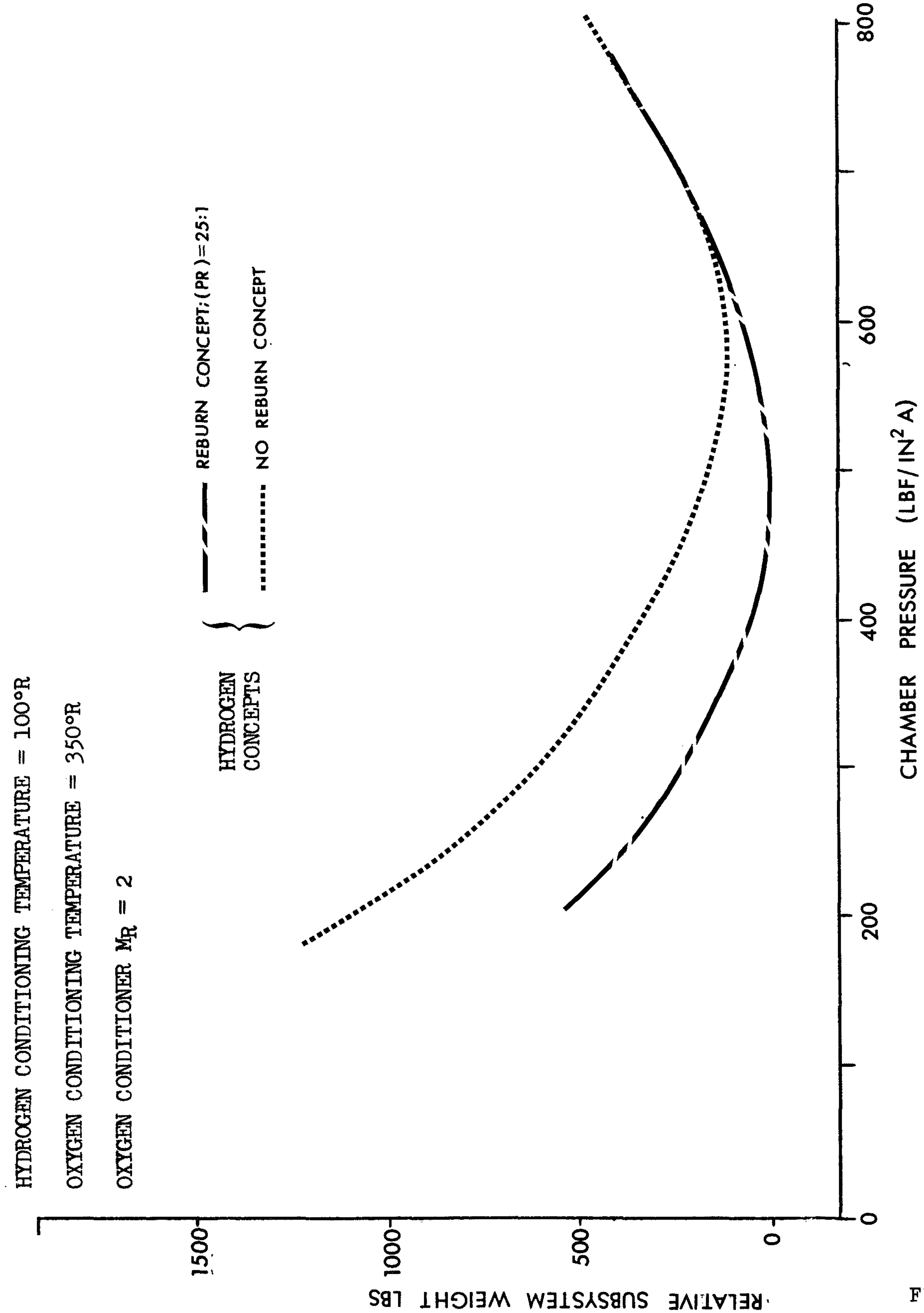

CHAMBER PRESSURE EFFECT ON SUBSYSTEM WEIGHT FOR VARIOUS GGA CONCEPTS

FIGURE D-41

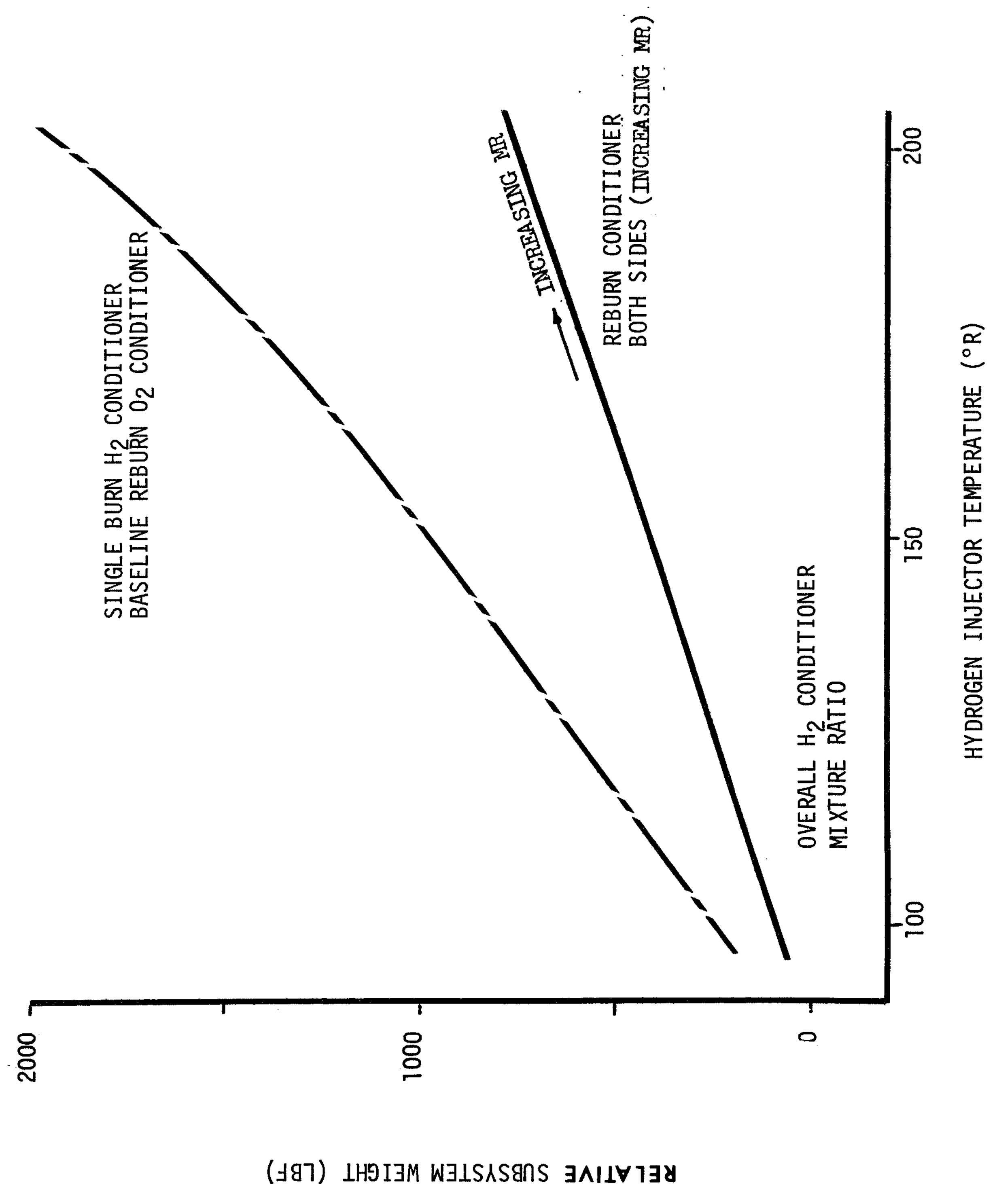

SINGLE BURN/REBURN HYDROGEN CONDITIONER CONCEPT COMPARISON

FIGURE D-42

SUBSYSTEM WEIGHT COMPARISON FOR VARIOUS CONTROL CONCEPTS

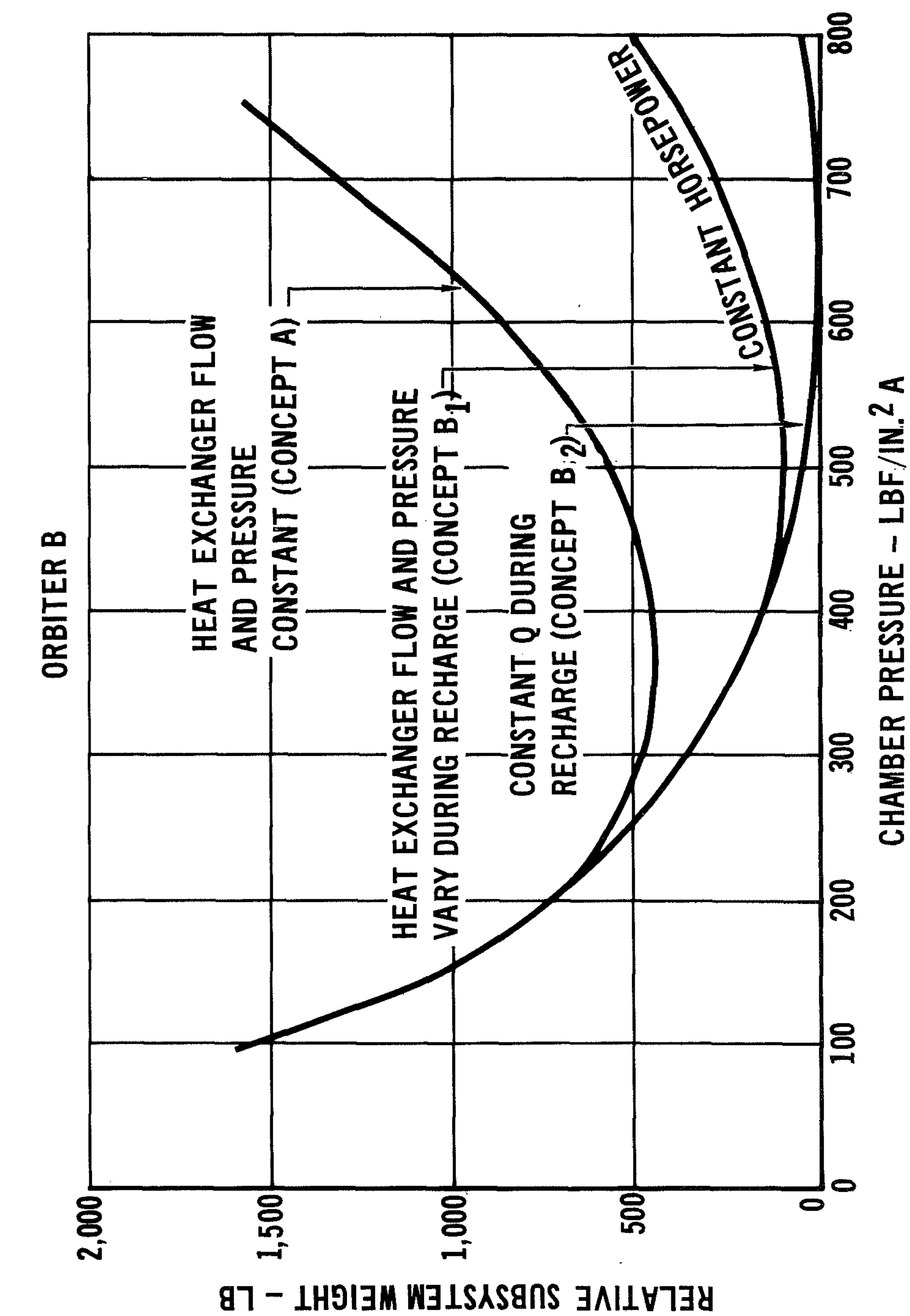

FIGURE D-43

the control technology involved is more difficult than that for the constant power approach. In addition, implementation of Concept B2 may require a lower chamber pressure than that shown because of throttling range requirements and thus lose its weight advantage. Concept B, implemented with constant power for recharge, was thus selected as the APS baseline.

This subsystem optimized at a chamber pressure of 500 lbf/in^2a and the overall mixture ratios at this condition were 2.55 and 2.69 for hydrogen and oxygen heat exchangers, respectively.

D-3. TURBOPUMP EVALUATION

The APS requires turbopumps to deliver propellant from low pressure cryogenic supply tanks to a conditioner assembly at the pressure required for subsystem operation. The pump power required to perform this function is provided from products of a 2000°R gas generator used in a staged turbine. Pump power and turbine flow requirements are significantly affected by turbopump performance. Therefore, to minimize turbine flow and ensure optimum APS design, it was necessary to evaluate turbopump performance in detail.

D-3.1 Turbopump Design - The turbopumps were designed to meet two different subsystem operation modes:

(1) provide flow and pressure required to maintain minimum accumulator pressure during steady state subsystem operation (long steady state thruster firings)

(2) provide sufficient flow and pressure to recharge subsystem accumulators to their maximum pressure. Prerequisites for these APS operational requirements are presented in Figure D-44.

As shown in Figure D-44 pump output pressure varies from approximately 1000 lbf/in^2a for steady state operation to approximately 2000 lbf/in^2a at the end of accumulator recharge. These two conditions are satisfied by permitting turbopump shaft speed to increase, and flow to decrease, as the accumulator is recharged. During recharge, gas generator flow and power from the turbine are constant, except for a slight increase in turbine power due to an efficiency increase with shaft speed. Turbopumps can be (and have been) designed to operate over this broad operating range; however, their design must incorporate provision for variations in pump imposed axial and radial thrust.

Baseline designs selected for oxygen and hydrogen units are presented in Figures D-45 and D-46 respectively. Axial thrust forces in these designs are minimized by using a modified Barsky impeller configuration. Figure D-47 presents a summary of overall turbopump design philosophy.

The LO_2 turbopump consists of a single stage pump and a 2-stage, pressure compounded, axial flow turbine. Pump impeller and turbine rotors are mounted on a common shaft, supported by LO_2 cooled/lubricated rolling element bearings. Bearing cooling/lubricating flow is tapped from the high pressure pump discharge, directed through the bearing, and reintroduced to the mainstream flow in a low

		O_2		H_2	
		MIN. ΔP	MAX. ΔP	MIN. ΔP	MAX. ΔP
PUMP	- PUMP FLOWRATE, LB/SEC	14.81	9.7	3.8	2.55
	- SUCTION PRESSURE, LBF/IN^2A	30	30	25	25
	- SUCTION TEMPERATURE, °R	162	162	37	37
	- DISCHARGE PRESSURE, LBF/IN^2A	940	2070	1043	2340
	- NUMBER OF CYCLES	50	-	50	-
TURBINE	- FLOWRATE, LB/SEC	0.274	0.274	0.442	0.442
	- INLET PRESSURE, LBF/IN^2A	500	500	500	500
	- INLET TEMPERATURE, °R	2000	2000	2000	2000
	- PRESSURE RATIO, -	4.65	4.65	16.7	16.7
	- NUMBER OF CYCLES	50	-	50	-

*TBD - TO BE DETERMINED

TURBOPUMP REQUIREMENTS

FIGURE D-44

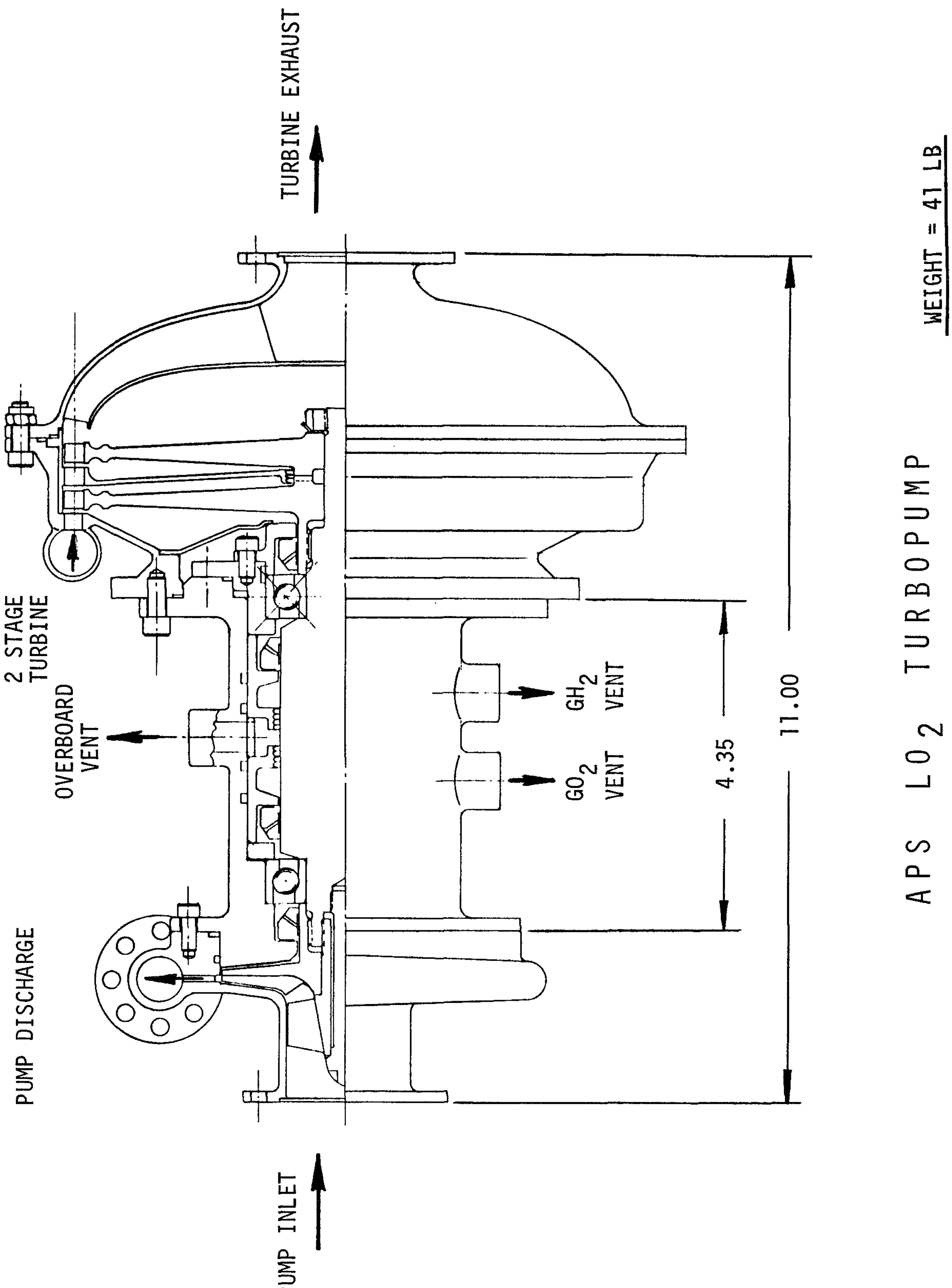
TURBINE EXHAUST
2 STAGE TURBINE
OVERBOARD VENT
PUMP DISCHARGE
PUMP INLET
GH_2 VENT
GO_2 VENT
4.35
11.00
WEIGHT = 41 LB
APS LO_2 TURBOPUMP

FIGURE D-45

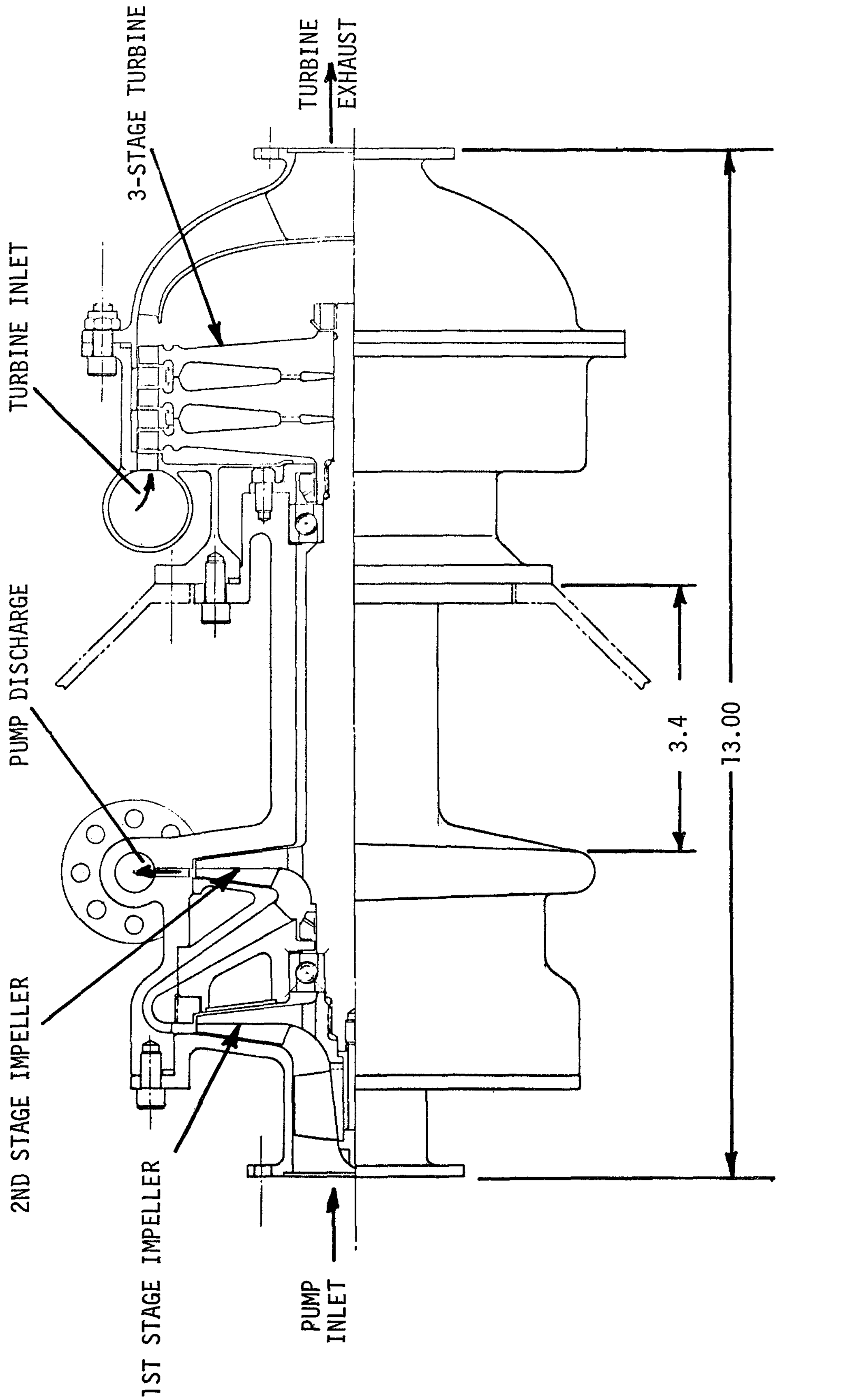

WEIGHT = 25 LB

APS LH_2 TURBOPUMP

FIGURE D-46

TURBOPUMP

- INLINE PUMP AND TURBINE
- PRELOADED BALL BEARINGS
- PROPELLANT LUBED/COOLED BEARINGS
- BEARING LUBE RECIRCULATION FLOW - 5%
- HYDROSTATIC SEAL, CONTROL PROPELLANT LEAKAGE TO TURBINE

PUMPS

- CENTRIFUGAL WITH INDUCER
- NUMBER STAGES, 1 LO_2, 2 LH_2
- MINIMUM EFFECTIVE NPSH INCLUDES THERMODYNAMIC SUPPRESSION HEAD
- SUCTION SPECIFIC SPEED = 40,000 AT BREAKDOWN
- MINIMUM CONTINUOUS NPSH = 2.0 MIN EFFECTIVE NPSH
- OPEN FACE IMPELLERS

TURBINES

- AXIAL FLOW
- NUMBER STAGES, 2 LO_2, 3 LH_2
- EQUAL ENERGY SPLIT BETWEEN STAGES
- PRESSURE COMPOUNDED
- ROTOR IMPULSE BLADED
- MEAN BLADE SPEED 650 FT/SEC LO_2, 1500 FT/SEC LH_2

DESIGN PHILOSOPHY

FIGURE D-47

pressure region at the impeller backside hub. The magnitude of the bearing coolant flow (5 percent allocated) is controlled by hydrostatic seals. The floating feature of hydrostatic seals eliminates the rub hazard normally associated with a fixed-flow control labyrinth. The interpropellant seal, which seals LO_2 from the fuel-rich hot gases of the turbine, uses a triple vent.

The fuel turbopump is similar to the LO_2 turbopump. Two pump stages are used to develop required pressure, while three pressure compounded, axial flow stages are used in the turbine. Pump impellers and turbine rotors are mounted on a common shaft, again supported by LH_2 cooled/lubricated roller element bearings. Hydrostatic shaft riding seals are used to control bearing coolant flow allocation of 5 percent. The fuel turbopump does not require an interpropellant seal to separate the propellant from hot turbine gas, since LH_2 is nonreactive with the fuel-rich turbine gases. Liquid hydrogen flow from the turbine and bearing to the turbine is minimized by the use of a hydrostatic seal.

The turbopump fuel and oxidizer pump volumes are 10.58 and 6.05 in^3, respectively from the plane of the suction flange to the plane of the discharge flange.

The turbopump has been designed for a life of 100 missions with 50 starts required per mission, or 5000 cycles. Based on the thermal shock duty requirements of the turbine rotor, cycle fatigue life is predicted to be 6000 cycles. The turbine blading for both the fuel and oxidizer turbopump turbines is the axial flow impulse type. The blade design is symmetrical, utilizing neither taper or twist, with the inlet and outlet angles equal to 21 degrees.

Both the fuel and oxidizer pump discharge volutes are designed for a proof pressure capability of 150% of maximum working pressure, and a burst pressure of 200% of proof. The hydrogen pump is designed to operate at 53,330 RPM, and the oxygen pump at 21,337 RPM. First shaft critical speeds for the hydrogen and oxygen pumps are 32,151 RPM and 33,550 RPM, respectively. This represents operation, with predicted bearing freedom, at 165% of critical for the fuel pump and 63.5% of critical for the oxidizer pump.

Both the fuel and oxidizer pump shaft support bearings operate at bearing DN values of 1.5×10^6.

D-3.2 Predicted Performance - Predicted pump head/flow, efficiency, power, and torque characteristics are shown in a normalized format in Figure D-48. Since the stage specific speeds of the LO_2 and LH_2 pump are nearly equal, their normalized characteristics will be the same. These normalized pump characteristics were used in turbopump analysis, and resulted in head/flow characteristics for values of constant shaft speed (shown in Figures D-49 and D-50 for the oxidizer and fuel turbopumps, respectively). These show pump operating characteristics during accumulator charge from steady state operating point to maximum accumulator pressure. Dotted lines shown correspond to pump power requirements matched to delivered turbine power.

The lines of Figures D-49 and D-50 show a power balance using a turbopump designed for reduced efficiency at the steady state design point. An efficiency less than the predicted maximum available was used in APS design to provide a design margin, and to reduce heat exchanger flow excursions. A summary of turbopump operating conditions is presented in Figures D-51 and D-52 for pumps which were designed for maximum efficiency at maximum output pressure.

Pump design point efficiency is primarily a function of design specific speed per stage ($N_s = N\ Q\ \ H^{3/4}$) and volume flow Q. A 2-stage, liquid hydrogen pump was used to increase pump specific speed and, in turn, to increase pump efficiency.

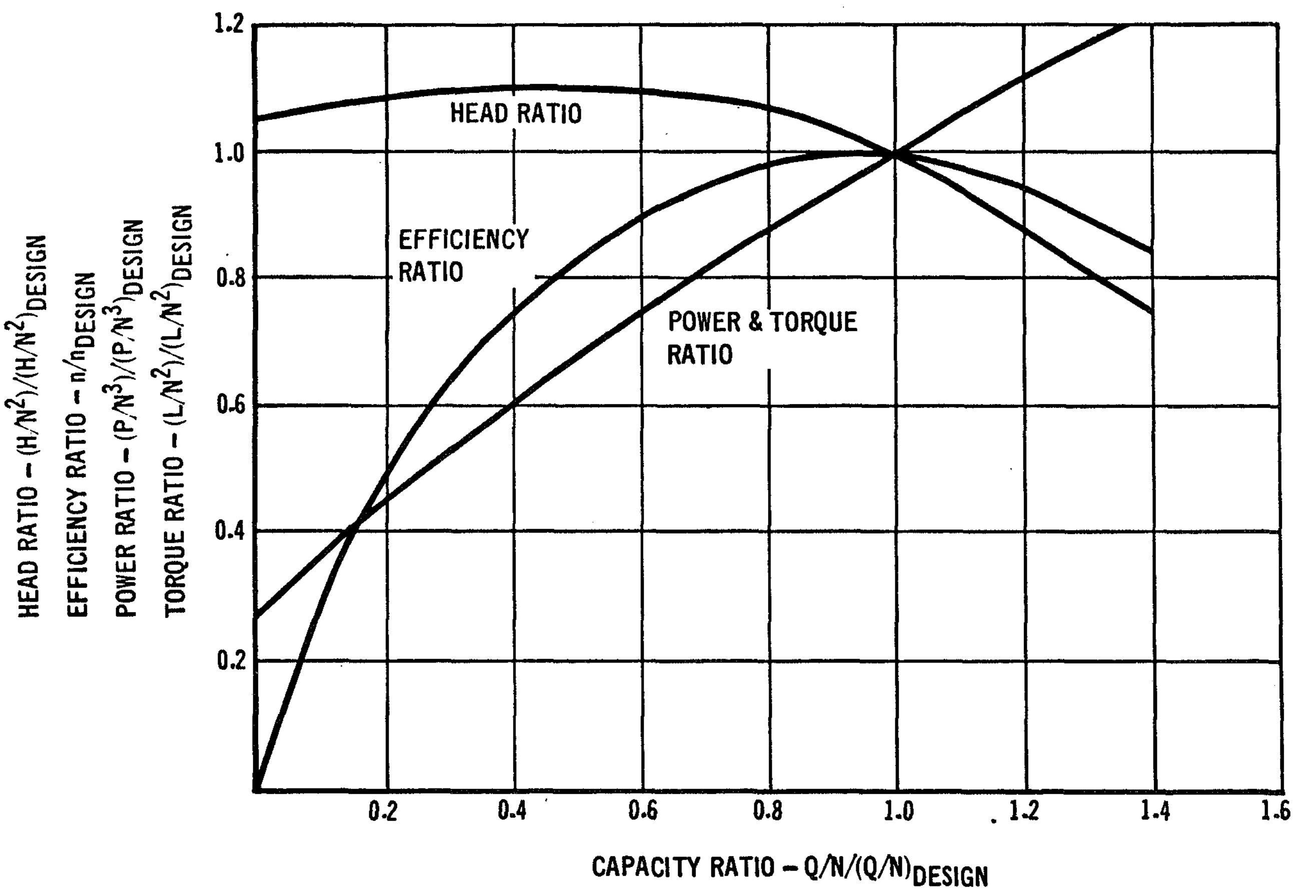

PUMP NORMALIZED PERFORMANCE PARAMETERS

FIGURE D-48

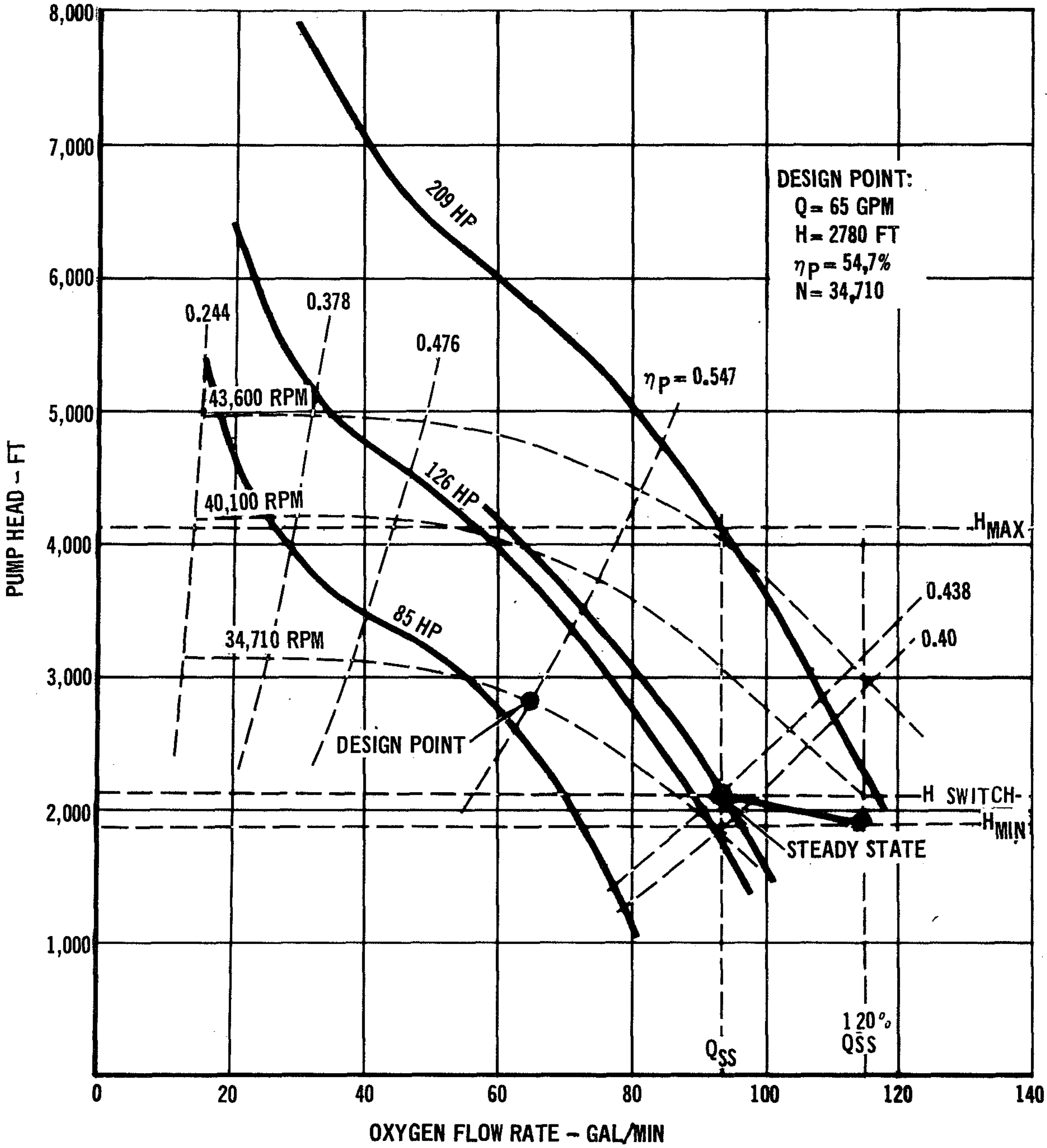

OXYGEN PUMP

FIGURE D-49

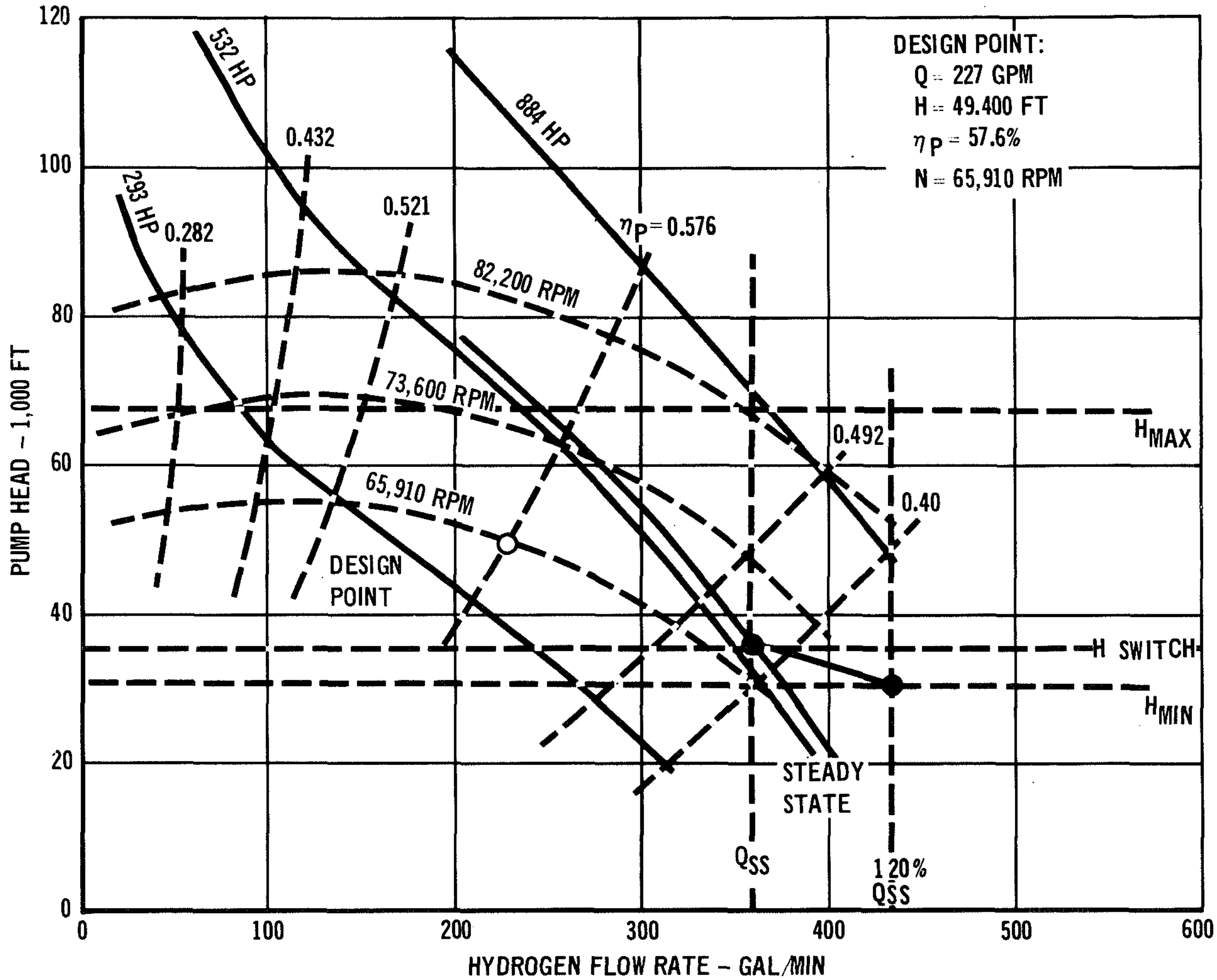

HYDROGEN PUMP

FIGURE D-50

	STEADY STATE OPERATING POINT	MAX. PRESSURE OPERATING POINT
PUMP		
WEIGHT FLOW, LB/SEC	3.84	1.37
VOLUME FLOW, GPM	367	131
(Q/N)/(Q/N) DES -	1.0	0.25
ΔP, LBF/IN^2	1030	2253
HEAD RISE, FEET	31,560	69,000
SHAFT SPEED, RPM	53,330	76,000
EFFICIENCY, %*	59	33
EFFICIENCY, EFFECTIVE, %**	56.2	31.4
SHAFT POWER, HP**	392	540
TURBINE		
INLET TEMPERATURE, °R	2000	2000
INLET PRESSURE, LBF/IN^{2}A	500	500
PRESSURE RATIO, -	16.7	16.7
MEAN BLADE SPEED, FT/SEC	1060	1510
EFFICIENCY, %	35.1	48.3
SHAFT POWER, HP	392	540
WEIGHT FLOW, LB/SEC	0.417	0.417
TURB/PUMP FLOW RATIO, -	0.108	0.304
*FRONT SIDE **INCLUDES BRG. RECIRC.	5%	5%

LH_2 TPA PERFORMANCE SUMMARY

FIGURE D-51

	STEADY STATE OPERATING POINT	MAX. PRESSURE OPERATING POINT
PUMP		
WEIGHT FLOW, LB/SEC	14.8	5.32
VOLUME FLOW, GPM	94.2	33.9
(Q/N)/(Q/N) DES -	1.0	0.25
ΔP, LBF/IN^2	905	1998
HEAD RISE, FEET	1849	4080
SHAFT SPEED, RPM	21,337	30,700
EFFICIENCY, %*	52	39.1
EFFICIENCY, EFFECTIVE, %**	49.5	37.2
SHAFT POWER, HP**	100.4	138.5
TURBINE		
INLET TEMPERATURE, °R	2000	2000
INLET PRESSURE, LBF/IN^2A	500	500
PRESSURE, RATIO, -	5.7	5.7
MEAN BLADE SPEED, FT/SEC	650	935
EFFICIENCY, %	21.4	29.5
SHAFT POWER, HP	100.4	138.5
WEIGHT FLOW, LB/SEC	0.238	0.2385
TURB/PUMP FLOW RATIO, -	0.0161	0.045
*FRONT SIDE		
**INCLUDES BRG. RECIRC.	5%	5%

LO_2 TPA PERFORMANCE SUMMARY

FIGURE D-52

Turbine predicted efficiencies are presented in Figure D-53 as a function of overall velocity ratio. Figure D-54 correlates actual and predicted turbine efficiencies as a function of stage velocity ratio. This curve shows that efficiencies predicted for the APS at the steady state operating condition are well within the range of experience. During recharge, efficiencies would be higher (as shown in the previous figure) due to increased turbopump shaft speed.

Turbine inlet temperature of 2000°R was selected for use in APS design. This is compatible with state-of-the-art turbine materials capability. Since no significant increase in power is obtained above this temperature, and efficiency is essentially unaffected, higher temperatures are not warranted. Figure D-55 presents typical weights for the hydrogen turbopump assemblies.

D-3.3 Technology Evaluation - Critical turbopump operating parameters and current demonstrated state-of-the-art pertaining to these parameters are given in Figure D-56. It can be seen that all design requirements can be achieved with existing technology except for the requirement of rapid shaft spin-up rates with rolling element bearings. This bearing design was selected to permit use of propellant-lubricated bearings and accommodate low lubricity of propellants; however, extension of current cryo-lubed bearing spin-up capability to the APS requirements appear feasible, based on current operational capability of air cooled (graphite cage pockets) bearings used in an aircraft application. These bearings provide 150K rpm/sec spin-up and a cycle life in excess of 25,000 starts. The APS requires the hydrogen turbopump to spin up in 0.25 to 0.5 sec, which results in a shaft acceleration rate on the order of 100K to 200K rpm/sec (current state-of-the-art technology is 40K rpm/sec).

D-3.4 Turbopump Cooling - It is essential to pump design and operation that the propellants at the pump inlet be in a liquid state to prevent pump cavitation and overspeed. This requirement makes it necessary for the pump to be at the temperatures of the liquid to prevent vaporization. This could be achieved by cooling the pump prior to each pump operational cycle, or by maintaining the pump in a "chilled" condition with active cooling. Cooling the pump prior to each pump cycle would require:

(1) additional controls to perform the chilldown
(2) additional propellant losses, since propellants would be used for chilldown
(3) increases in conditioner lag time with resultant increases in accumulator size.

	LO_2	LH_2
MEAN BLADE DIA. - (IN)	7.0	4.55
NOZZLE THROAT AREA - (IN^2)	0.109	0.191
POLAR INERTIA - IN-LB (SEC^2)	0.077	0.017

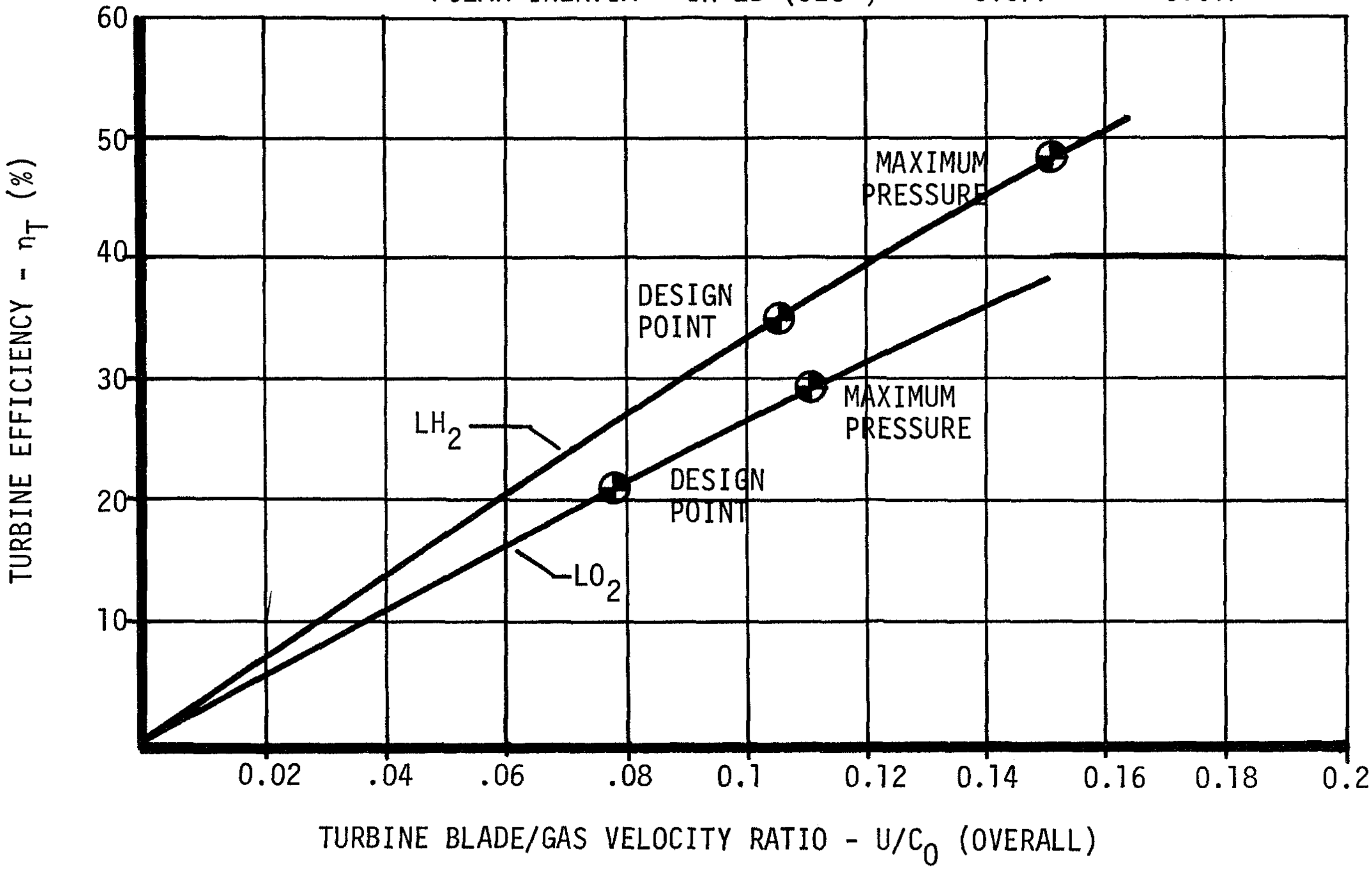

PREDICTED TURBINE EFFICIENCY

FIGURE D-53

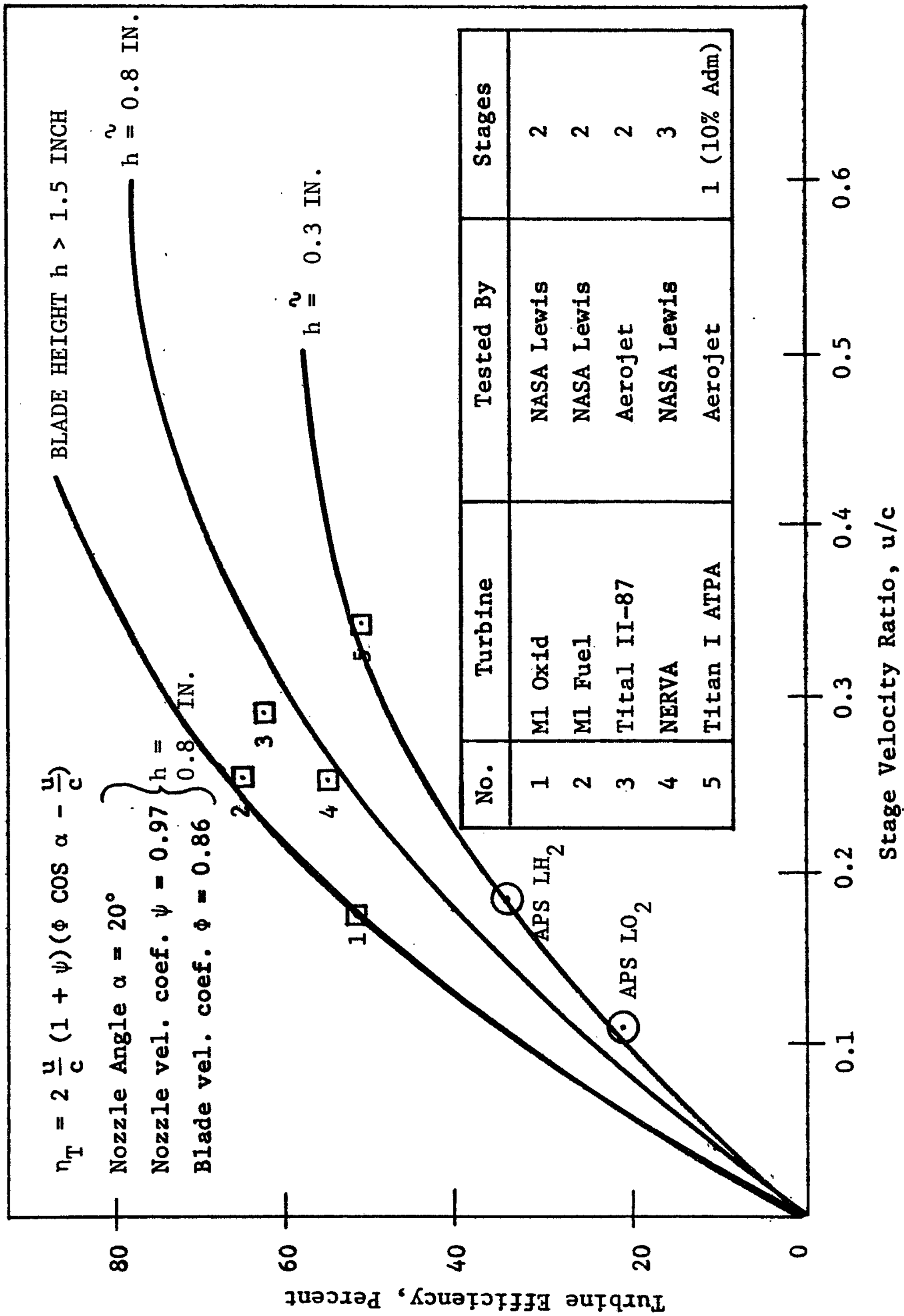

No.	Turbine	Tested By	Stages
1	M1 Oxid	NASA Lewis	2
2	M1 Fuel	NASA Lewis	2
3	Tital II-87	Aerojet	2
4	NERVA	NASA Lewis	3
5	Titan I ATPA	Aerojet	1 (10% Adm)

TYPICAL PRELIMINARY DESIGN
TURBINE DIAGRAM EFFICIENCY

FIGURE D-54

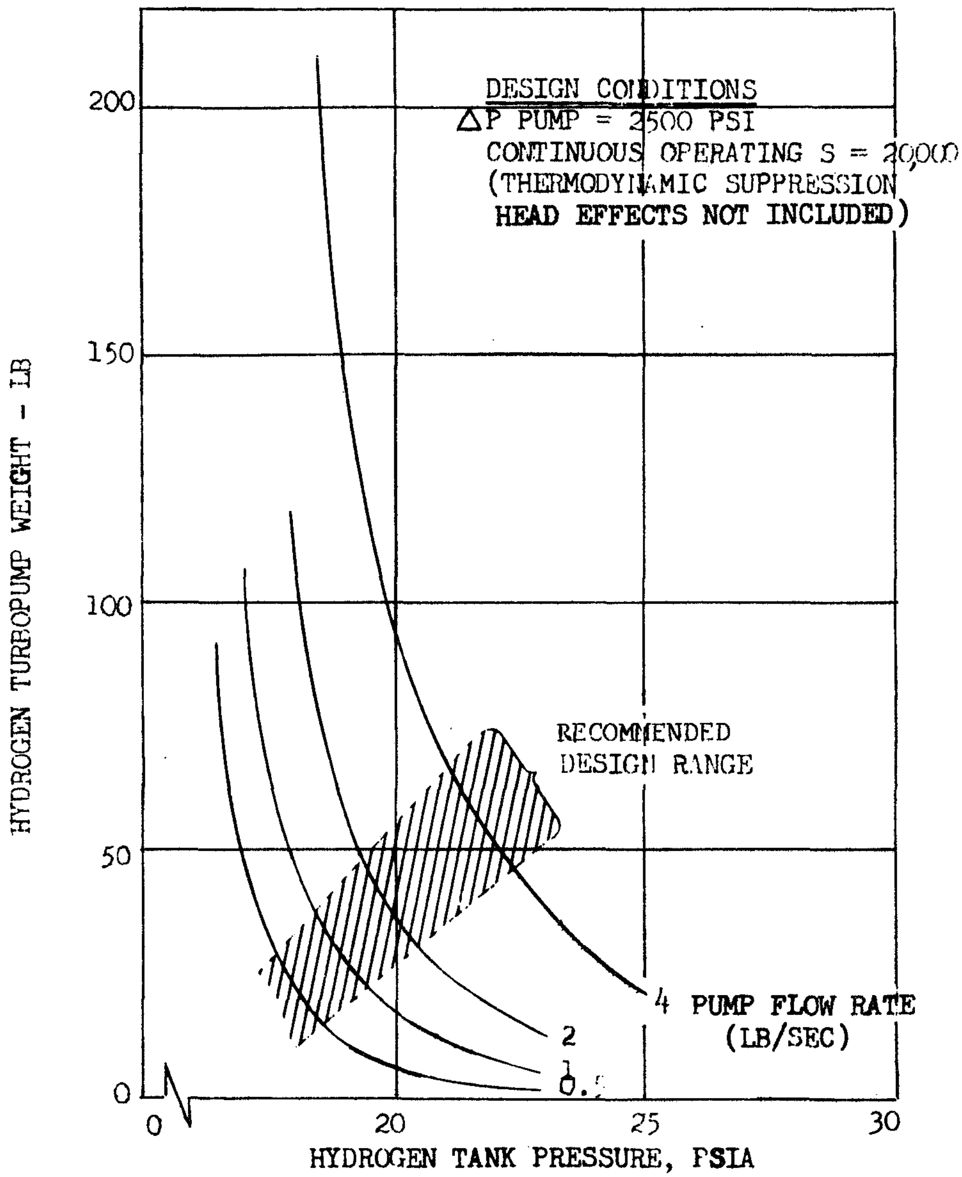

TYPICAL LH_2 TPA WEIGHTS

FIGURE D-55

TURBOPUMP		HYDROGEN APS	HYDROGEN TECHNOLOGY	OXYGEN APS	OXYGEN TECHNOLOGY
PUMP					
FLOW	LB/SEC	3.84	1 TO 100	14.8	2 TO 2800
SHAFT SPEED (MAX)	RPM	69,000	20,000 TO 70,000	30,700	3650 TO 40,000
NPSP (MIN)	LBF/IN^2	4	0.0	5	5
SUCTION SPEC. SPEED		40,000	50,000	40,000	50,000
OUTLET PRESSURE	LBF/IN^2A	2268	500 TO 5500	2018	500 TO 5500*
ΔP/STAGE	LBF/IN^2	1121	2000+	1988	500 TO 5500*
EFFICIENCY	%	42.4	TO 60	49.2	TO 65
TURBINE					
INLET PRESSURE	LBF/IN^2A	500	500*	500	520*
PRESSURE RATIO	--	16.7	10	465	20
INLET TEMPERATURE	°R	2000	2110	2000	2100
MEAN BLADE SPEED	FT/SEC	1500	1440	650	1200
EFFICIENCY	%	43.8	45*	29.8	45*
POWER TRANSMISSION					
DN OF PROPELL. LUBE BRG.	MM X RPM	1.0×10^6	1.5×10^6	1.0×10^6	1.25×10^6
SHAFT ACCEL. RATE (APS OPERATING SPEED IN 0.25 SEC)	RPM/SEC	210,000	40,000	86,000	20,000 ESTIMATE
INTERPROPELLANT SEAL		NONE REQ.	--	LOW PRES. VENTS OR PURGE	REQ. FEASIBILITY DEMONSTRATION OF LOW PRESSURE VENTS

* HIGH PRESSURE RATIO TURBINE

TURBOPUMP TECHNOLOGY EVALUATION

FIGURE D-56

Cooling the pump once and then keeping it cool would require an insulated enclosure around the pump, thermal isolation of the pump from the turbine, and continuous active cooling.

Continuous cooling was the approach selected. The weight penalty associated with the added enclosure, and coolant propellant losses, are much less than the weight penalty associated with chilldown for each cycle. This advantage occurs because the amount of liquid propellant required for continuous pump cooling is small when compared with increases in accumulator weight required by the long response time for chilldown of a hot pump prior to each cycle.

Design Description - The major areas of interest in turbopump cooling design are enclosure active cooling, and turbine/pump isolation. The heat transfer model of the turbopump enclosure used to evaluate active cooling requirements is shown in Figure D-57 with the major heat transfer mechanisms (R for radiation, C for conduction) identified for the various sections. Major heat transfer contributions are environmental radiation, heat conducted by the pump outlet lines, and heat conducted from the turbine.

The pump enclosure is an insulated aluminum shroud, employing a multilayer insulation (MLI) of about 1 in thickness to isolate thermally the pump from the environment. The active cooling scheme keeps the enclosure cool by venting liquid hydrogen through a tubular heat exchanger on the surface of the enclosure. Vented hydrogen is then passed through the turbopump shaft housing to intercept heat conducted from the turbine to ensure cooling of the pump itself during non-use periods.

Isolation of the pump from the hot turbine is accomplished by providing a heat short from the turbine to the vehicle structure, which preferentially conducts heat to the structure rather than to the pump. When combined with the active cooling of the shaft and its housing, conduction of turbine heat to the pump is minimal. To protect the pump enclosure from radiation from the structure, a 1 in layer of Micro-Quartz (a Johns Manville quartz fiber insulation) was added to the pump side of the support structure.

Analysis/Results - Active cooling requirements were evaluated for a system composed of 3 pumps/enclosures under operating conditions, with one turbopump operating and two turbines at ambient conditions. Results are presented in Figure D-58. In order to provide a conservative coolant estimate, the surrounding environment and structure were assumed to be at 600°R.

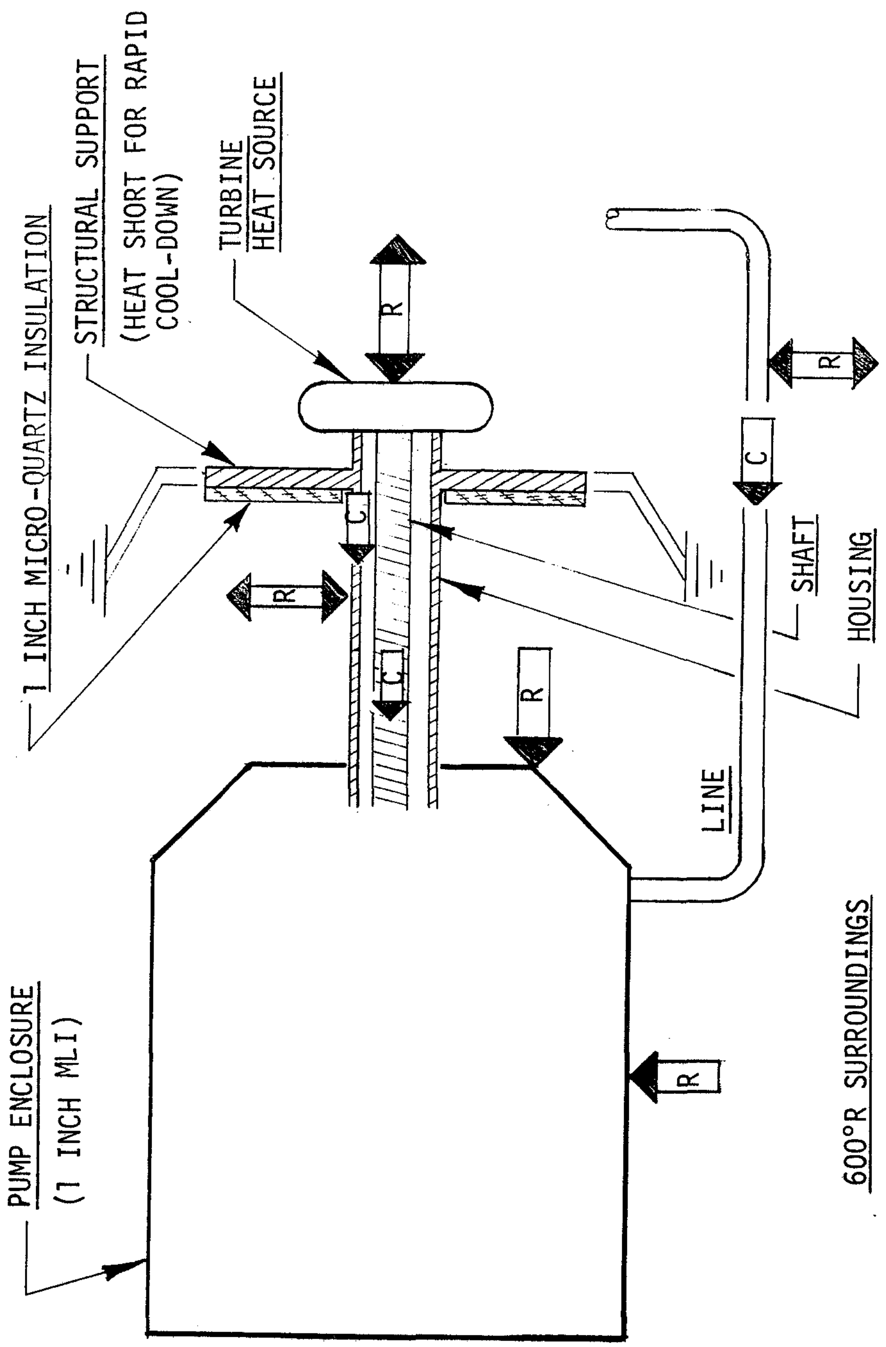

TURBOPUMP HEAT TRANSFER MODEL

FIGURE D-57

			LH_2	LO_2
1. PUMP ENCLOSURE THROUGH MULTILAYER INSULATION (MLI) @ 0.7 BTU/FT^2 HR (3 ENCL)			13	13
2. FROM HOT TURBINES				
(a) SHAFT			45	39
(b) FROM TURBINE MOUNT	LH_2 -250	LOX -227		
(c) REMOVED THROUGH THERMAL SHORT	220	209		
(d) NET DELIVERED TO PUMP THROUGH BEARING HOUSING	30	18	30	18
3. FROM COLD TURBINES (2 EACH, LOX AND LH_2)				
(a) STRUCTURE TO PUMP VIA THERMAL SHORT AND BEARING HOUSING			44	31
(b) SHAFT			18.5	16.2
4. THROUGH LINES (3 FT LONG),				
(a) RADIATION TO LINE THROUGH MLI ON LINE			2	2
(b) CONDUCTION FROM 600° SOURCE			5	4
TOTAL HEAT LEAK (BTU/HR)			157.5	123.2

TURBOPUMP ASSEMBLY HEAT LEAK (BTU/HR)

FIGURE D-58

A nominal performance of 0.7 Btu/hr/ft^2 was assumed for the MLI protecting the pump enclosure. With radiation from a 600°R environment to the 6.3 ft^2 enclosure, 13 Btu/hr was calculated for both hydrogen and oxygen systems.

Heat input to the pump from the turbine was substantially greater than from any other source. The mean turbine temperature used for evaluating the heat leak from the operating turbine was assumed to be 1500°R. The total heat leak evaluation reflects the leak for one operating and two ambient (600°R) temperature turbines. The heat leak from the hot turbine was 45 Btu/hr through the shaft and 30 Btu/hr through the housing on the hydrogen side, and 39 Btu/hr and 18 Btu/hr on the oxygen side. The total leak from the two ambient temperature turbines was 44 Btu/hr and 31 Btu/hr, for hydrogen and oxygen respectively. The total heat leak from all turbines is thus 137 Btu/hr for the hydrogen and 104.2 Btu/hr for the oxygen.

For the inactive turbopumps, one line of 1-1/2 in diameter with 0.055 in walls was assumed to be connected into each enclosure at a distance of 3 ft from a 600°R source. Conduction leaks of approximately 5 Btu/hr-line for the hydrogen line, and 4 Btu/hr-line for the oxygen line were obtained. In addition, radiative heating from the surroundings delivered to the enclosure by means of the line was estimated to be 1 Btu/hr-line.

The total heat transferred to the pump during operation is 157.5 Btu/hr for the hydrogen and 123.2 Btu/hr for the oxygen. The propellant required to cool the turbopumps is shown in Appendix D-1 and is 0.54 and 0.75 pounds per hour for the hydrogen and oxygen turbopumps respectively. The oxygen turbopumps are cooled with the efflux from the thermodynamic vent after cooling of the hydrogen part of the subsystem and does not represent a weight penality. For a three day mission the total cooling hydrogen required for the hydrogen turbopump is approximately 40 pounds. The total propellant loss for cooling the pumps over the entire mission does not represent a high penalty.

Turbine Cool-Down - Heat flux, and thus coolant requirements, after the turbine cools to ambient conditions is reduced by approximately 36 percent. To estimate the time for the hot turbine to cool to an ambient temperature, calculations have been performed for cooling by radiation and conduction. These show that the heat short designed to minimize heat flow from turbine to pump during operation will cool the turbine in about one hour.

D-4. HEAT EXCHANGER

The APS thruster assemblies require that propellant be conditioned to approximately 200°R. This requirement is provided by heat exchanger assemblies, which vaporize and superheat cryogenic liquid propellants. During Subtask A, a simple, counterflow, tube-in-shell heat exchanger design was selected. This concept used products directly from a 3500°R gas generator to provide the energy required for conditioning. In Subtask B, the propellant conditioner assembly was reevaluated, revised, and a new baseline concept established. In this revised concept, products of a 2000°R gas generator are used first to drive the turbopump, then directed to the heat exchanger where additional oxygen is added. They are reburned to provide the energy for propellant conditioning. Since design requirements of this reburn heat exchanger were significantly different from those of the Subtask A unit, an evaluation was conducted to define design and performance. The following paragraphs discuss heat exchanger requirements, alternate reburn heat exchanger concepts, the selected baseline concept, and its design.

D-4.1 Design Concept Section - On the basis of preliminary concept appraisals and overall conditioner assembly performance requirements, the following general heat exchanger characteristics were required:

(1) combustion of fuel-rich turbine exhaust gases
(2) hot side temperatures to approximately 4200°R
(3) high cycle life with hot to cold side temperature gradients in excess of 4000°R
(4) cold side propellant flow and pressure controlled on the discharge side of the heat exchanger by accumulator pressure.

A summary of heat exchanger design conditions is presented in Figure D-59.

Three primary types of heat exchangers were considered. These concepts are shown schematically in Figure D-60, and their operation is presented in Figure D-61. Concept A uses multistage injection of oxidizer into the heat exchanger. At the first oxygen injection stage, an igniter is used. The need for an igniter is eliminated at all subsequent stages by preventing the exhaust gases from cooling below autoignition level. This is accomplished by controlling the hot gas between an upper value, determined by conventional material constraints, (approximately 2000°R) and a lower limit, established by the autoignition level, (approximately 1600°R). In this concept, enthalpy for conditioning is provided with minimal stress on materials

SYSTEM		HYDROGEN		OXYGEN	
OPERATING CONDITION		MAX. FLOW	MIN. FLOW	MAX. FLOW	MIN. FLOW
COLD SIDE					
TEMPERATURE IN	(°R)	60	70	170	185
TEMPERATURE OUT	(°R)	250	250	460	460
PRESSURE IN	LBF/IN^2A	1045	2340	940	2070
ΔP ~	LBF/IN^2	25	22	25	7
FLOWRATE	(LB/SEC)	3.84	2.55	14.8	9.7
HEAT FLUX	(BTU/SEC)	2760	900	2116	660
HOT SIDE					
TEMPERATURE IN	(°R)	3750	AR < 3750	4150	AR < 4150
TEMPERATURE OUT	(°R)	~ 800	AR > 800	~ 800	AR > 800
PRESSURE IN	LBF/IN^2A	30	–	107	–
FLOWRATE	(LB/SEC)	.785	AR	.506	AR
MIXTURE RATIO	-	2.55	AR	2.7	AR

AR–AS REQUIRED

SPACE SHUTTLE APS HEAT EXCHANGERS

ORBITER B

SUMMARY OF DESIGN CRITERIA

FIGURE D-59

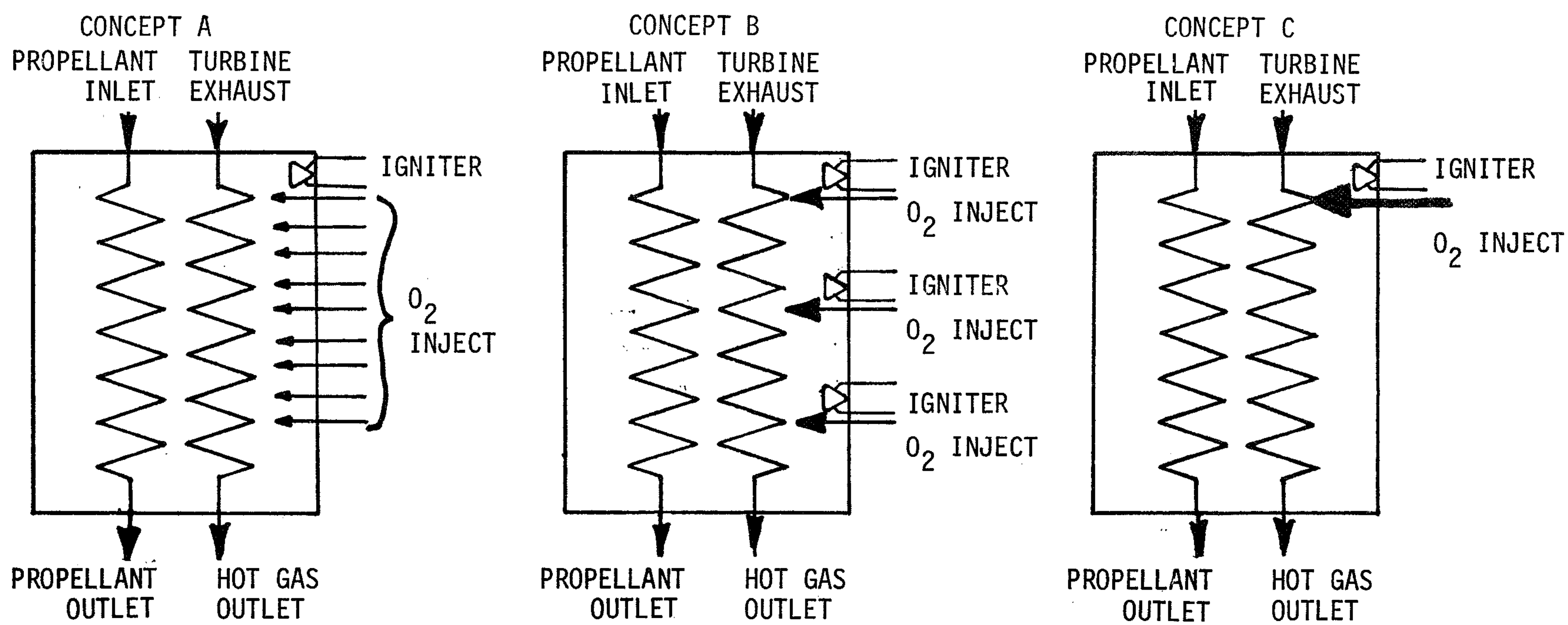

	MULTI-STAGED INJECTION SINGLE RE-IGNITER	MULTI-STAGED INJECTION MULTI-IGNITER	SINGLE STAGED INJECTION SINGLE RE-IGNITER
$T_{H_{MAX}}$ =	1800 - 2000 °R	1800 - 2000 °R	3500 - 4500 °R
$T_{H_{INJ}}$ =	1550 - 1650 °R	800 - 900 °R	1000 - 1400 °R
$T_{H_{OUT}}$ =	800 - 900 °R	800 - 900 °R	800 - 900 °R
NO. INJECTORS =	7 - 9	2 - 3	1
NO. IGNITERS =	1	2 - 3	1

FIGURE D-60

APS HEAT EXCHANGER CONCEPTS

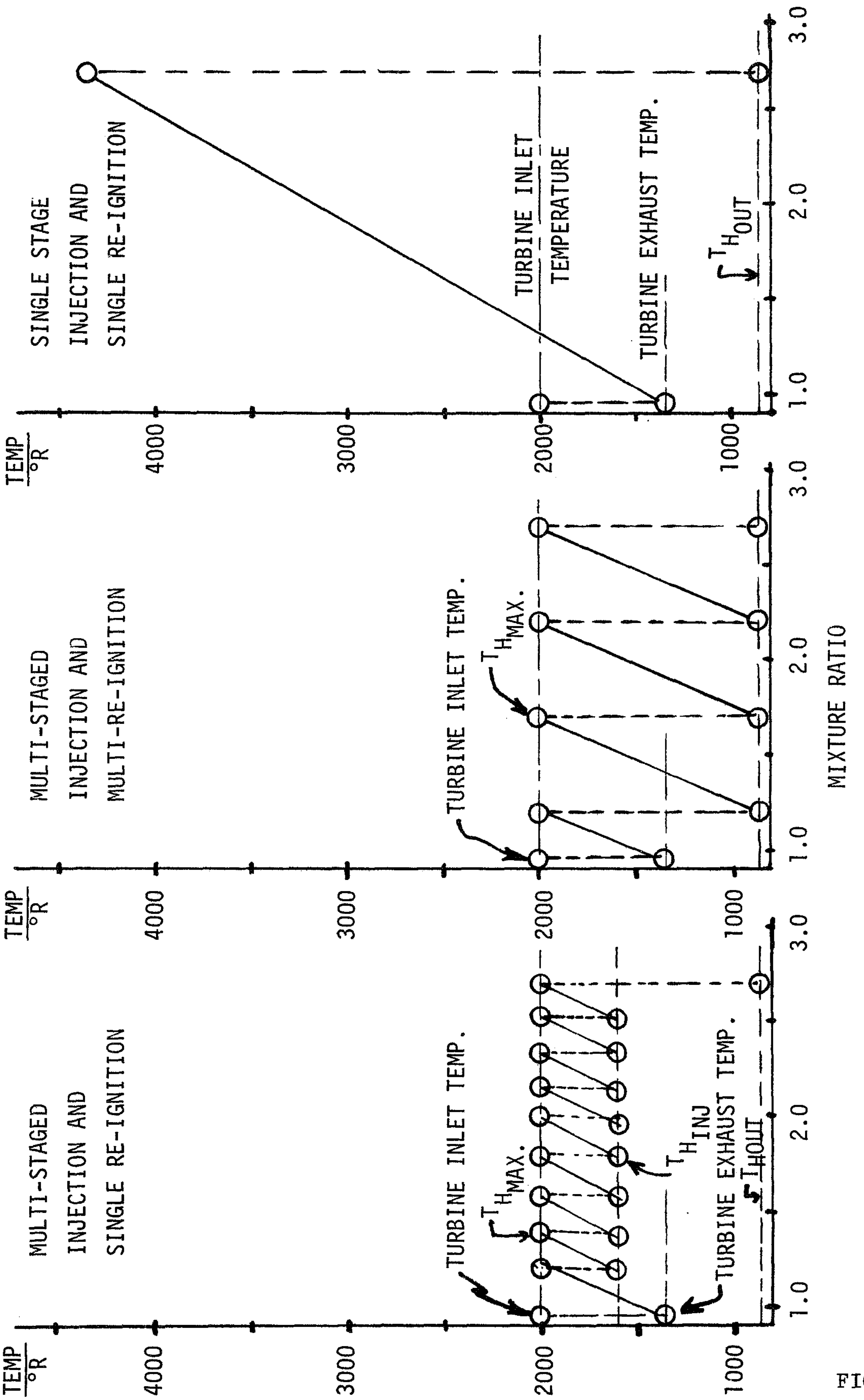

COMPARISON OF TEMPERATURES IN EQUIVALENT MR DESIGNS

APS HEAT EXCHANGERS

FIGURE D-61

technology. However, a large number of oxygen stages is required.

Concept B is similar to the previous approach. It allows gas cooling to approximately 900°R, thereby minimizing the number of oxygen stages required. As shown in Figure D-61, it does require an igniter source at each stage, since the gas falls below the autoignition level. This concept provides the benefit of minimizing thermal environment (gas temperatures less than 2000°R) at the expense of additional controls required for reignition at each oxygen stage.

Concept C features a single re-ignition cycle, accomplished in the heat exchanger. This concept introduces a more difficult design since it is required to contain and effectively utilize high temperature gases. It was considered the most desirable, however, since it minimizes the re-ignition and controls complexity associated with the reburn heat exchanger. Thus, it was selected as the baseline heat exchanger concept for the high pressure APS.

Heat exchanger design is illustrated in Figure D-62. The concept is based on application of injector plate fabrication technology developed for staged combustion engine cycles. A platelet construction technique provides controlled heat transfer coefficients for the hot gas and the cold propellant side of each plate.

All propellant to be conditioned enters the reburn heat exchanger in the base, and flows up the outside of the shell and up through the centers of the plate assemblies. The propellant is turned at the top of the shell and flows down along the inside surface. The propellant flowing up the inside of the plates is split at the top and flows down along the outside passages of the plates. The heat is transferred from the parallel flowing hot gas to the propellant in both the plates and shell. The propellant from both the shell and the plates is collected at the bottom of the heat exchanger and directed to the accumulators.

An oxygen distribution injector is provided ahead of the plates to uniformly distribute GO_2. The ignition source for the turbine exhaust gases and the GO_2 is a catalytic igniter in the GO_2 manifold as shown in Figure D-62. Igniting in the GO_2 distribution manifold provides a short duration of high mixture ratio hot gas for ignition. This approach was taken because a major developmental concern rests in providing an ignition technique to allow uniform and consistent ignition between each of the closely spaced plate assemblies. The catalytic igniter is turned off after sufficient time has elapsed to achieve uniform combustion downstream of each of the GO_2 injectors. Requiring as it does the distribution by the GO_2 injector manifold of approximately 2500 - 3000°R hot gas for short durations, this catalytic igniter concept requires special attention during investigation of the overall re-ignition cycle.

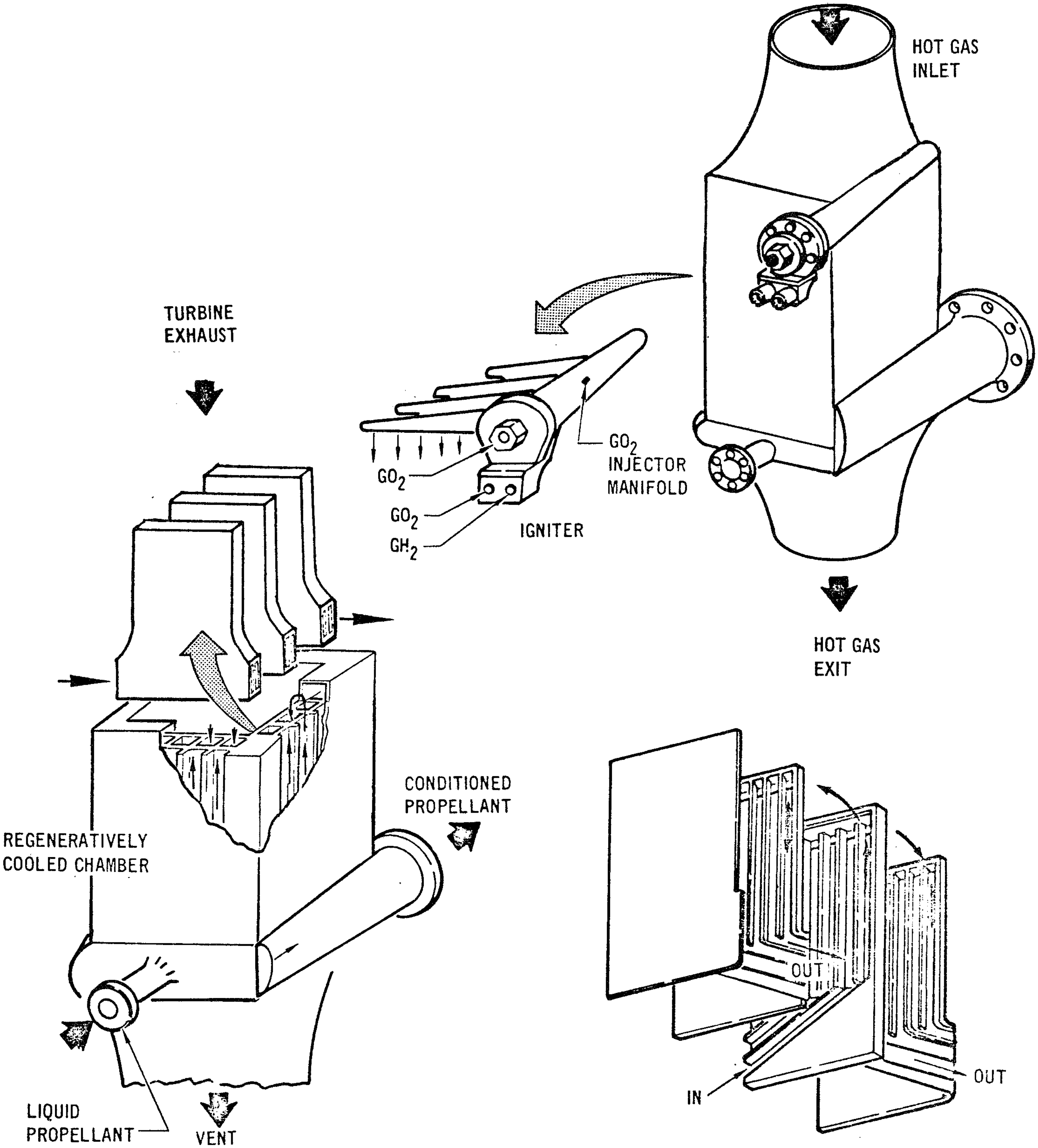

HIGH TEMPERATURE HEAT EXCHANGER

FIGURE D-62

The baseline internal platelet configuration of the heat exchangers is defined in Figure D-62a. The heat exchanger performance and weights are shown in Figure D-62b. Using the defined configuration, steady state performance operating maps were defined. The hydrogen heat exchanger operating maps are shown in Figure D-62c for a hot gas inlet (turbine discharge) pressure of 30 LBF/in^{2}A and for a hydrogen inlet pressure of 1045 LBF/in^{2}A. The operating limits are defined by limiting the wall temperature to above 500°R, and limiting the velocity at the exit to less than sonic. A 500°R minimum wall temperature is required to preclude freezing of water on the heat exchanger surfaces. The steady state heat exchanger operating point for only +X thruster usage is shown in Figure D-62c(a). At this point the conditioned hydrogen temperature is 250°R, the conditioning assembly is operating at an overall mixture ratio of 2.55 and the exhaust gas is above the condensation limit. Increasing the thruster usage by 25% to allow attitude control usage during +X thruster firing results in the operating map shown in Figure D-62c(b). During the recharge cycle the hydrogen pressure will be increasing above 1045 psia and will reach the 2000 psia shown in the performance maps defined in Figure D-62d. The corresponding operating point is shown in Figure D-62d(a).

The operating performance maps for the oxygen heat exchangers are shown in Figures D-62e and D-62f.

The application of the platelet injector technology for the heat exchanger is an extension of related technologies. A platelet heat exchanger program has been conducted, wherein plate assemblies were used to provide interpropellant heat exchange between gaseous hydrogen at room temperature and liquid oxygen. This program demonstrated the ability of the plate assemblies to effect sufficient heat exchange to convert the liquid oxygen to gas. It also identified techniques for control of the plate flow channels to achieve increased propellant side heat transfer coefficients. The basic plate fabrication techniques were also demonstrated as a part of staged combustion cycle demonstrations for several injector concepts.

D-4.2 Design Analysis - The large hot gas enthalpy change required in the heat exchanger is inherently associated with a large temperature change between hot gas inlet and outlet. At the inlet, temperatures exceed 4000°R, requiring that hot side film coefficients be as low as possible, and corresponding cold side coefficients be as high as possible to maintain wall temperatures below their upper limit. Opposite requirements are imposed at the outlet where hot gases are cooled to their lowest temperature. Here it is desirable to have high hot side coefficients and low cold side coefficients, so that the walls remain at high enough temperature to

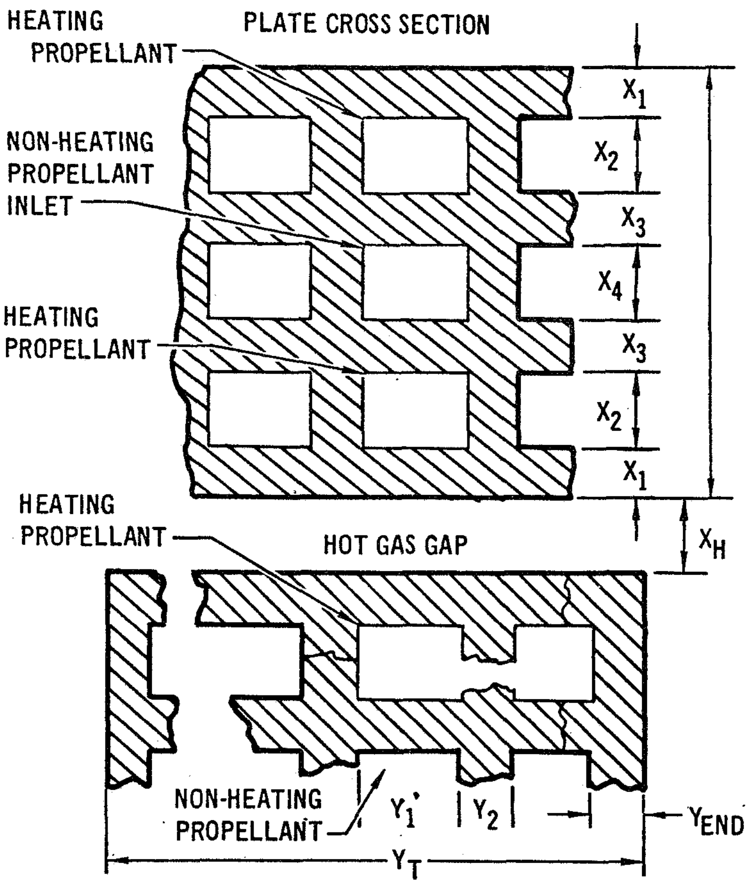

	HYDROGEN		OXYGEN	
STATION	0	19.5	0	23.5
T_{HOT} - °R	3757.2	820.6	4152.0	800.7
T_{COLD} - °R	60.0	250.4	170.0	461.3
X_1 = IN.	0.030	0.050	0.050	0.050
X_2 = IN.	0.015	0.125	0.022	0.130
X_3 = IN.	0.020	0.020	0.050	0.050
X_4 = IN.	0.220	0.015	0.176	0.060
X_T = IN.	0.350	0.405	0.420	0.520
X_H = IN.	0.115	0.070	0.130	0.030
Y_1 = IN.	0.115	0.125	0.075	0.100
Y_2 = IN.	0.030	0.020	0.075	0.050
Y_T = IN.	7.28	7.28	6.6	6.6
N_C -	800	800	420	420
N_H -	8	8	5	5
N_S -	16	16	10	10
A_{HOT} IN.^{2}	6.8998	4.3460	4.4764	1.36688
A_{COLD} IN.^{2}	1.380	12.5	0.693	5.46
HOT VELOCITY FT/SEC	3012.9	1107.4	1146.2	657.7
COLD VELOCITY FT/SEC	97.0	61.1	43.3	68.1
Y_{END} = IN.	0.030	0.025	0.1875	0.175

N_C = NO. OF COLD FLOW CHANNELS

N_H = NO. OF HOT FLOW GAPS

N_S = NO. HX SURFACES

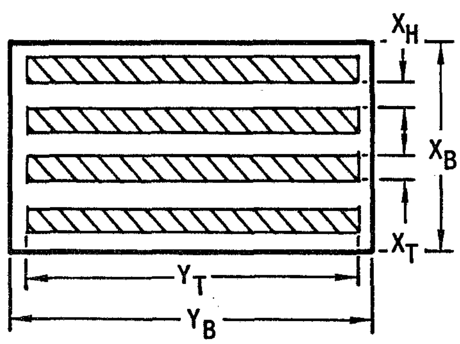

SHAPED AREAS INDICATE PLATE ELEMENTS IN CROSS SECTION OF HEAT EXCHANGER NORMAL TO HOT GAS & PROPELLANT FLOW DIRECTION.

X_T = IN.	0.350	0.405	0.420	0.530
X_H = IN.	0.115	0.070	0.130	0.030
N_H -	8	8	5	5
N_S -	16	16	10	10
X_B = IN.	3.370	3.395	2.33	2.23
Y_T = IN.	7.28	7.28		
Y_B = IN.	7.34	7.34	6.60	6.68
LENGTH OF PLATES (HEAT TRANSFER SURFACE ONLY)	19.5 IN		23.5 IN.	

HEAT EXCHANGER DESIGN DATA

FIGURE D-62a

		HYDROGEN	OXYGEN
HOT SIDE			
INLET PRESSURE (HEATING SECTION)	– PSIA	30.0	88.0
OUTLET PRESSURE (HEATING SECTION)	– PSIA	25.7	79.9
INLET TEMPERATURE (HEATING SECTION)	– °R	3757.2	4152.0
OUTLET TEMPERATURE (HEATING SECTION)	– °R	820.6	800.7
INLET VELOCITY (HEATING SECTION)	– FT/SEC	3012.9	1146.2
EXIT VELOCITY (HEATING SECTION)	– FT/SEC	1107.4	657.7
COLD SIDE			
INLET PRESSURE (HEATING SECTION)	– PSIA	1045.0	925.0
OUTLET PRESSURE (HEATING SECTION)	– PSIA	1034.8	874.3
INLET TEMPERATURE (HEATING SECTION)	– °R	60.0	170.0
OUTLET TEMPERATURE (HEATING SECTION)	– °R	250.4	461.3
INLET VELOCITY (HEATING SECTION)	– FT/SEC	97.0	43.3
OUTLET VELOCITY (HEATING SECTION)	– FT/SEC	61.1	68.1
$\dot{W}_{h_{DES}}$ (DESIGN HOT GAS FLOW RATE)	– LB/SEC	0.746	0.479
$\dot{W}_{c_{DES}}$ (DESIGN COLD SIDE FLOW RATE)	– LB/SEC	3.84	14.8
HEAT FLUX (TOTAL)	– BTU/SEC	2798.2	2139.0
HOT GAS MIXTURE RATIO	– $\dot{W}_O/\dot{W}_H$	2.55	2.7
A_h AND A_c (HEATING SURFACE)	– IN.^{2}	2271.36	1551.0
W_W (HOT/COLD METAL WEIGHT)	– LB	30.4	35.7
W_{PW} (INTERPROPELLANT METAL WEIGHT)	– LB	28.3	48.4
W_{MISC} (METAL STRUCTURE, MANIFOLD, ETC)	– LB	26.5	17.4
TOTAL HEAT EXCHANGER WEIGHT	– LB	85.2	101.5
MATERIAL	–	INCONEL 718	NICKEL 200

HEAT EXCHANGER PERFORMANCE AND WEIGHT

FIGURE D-62b

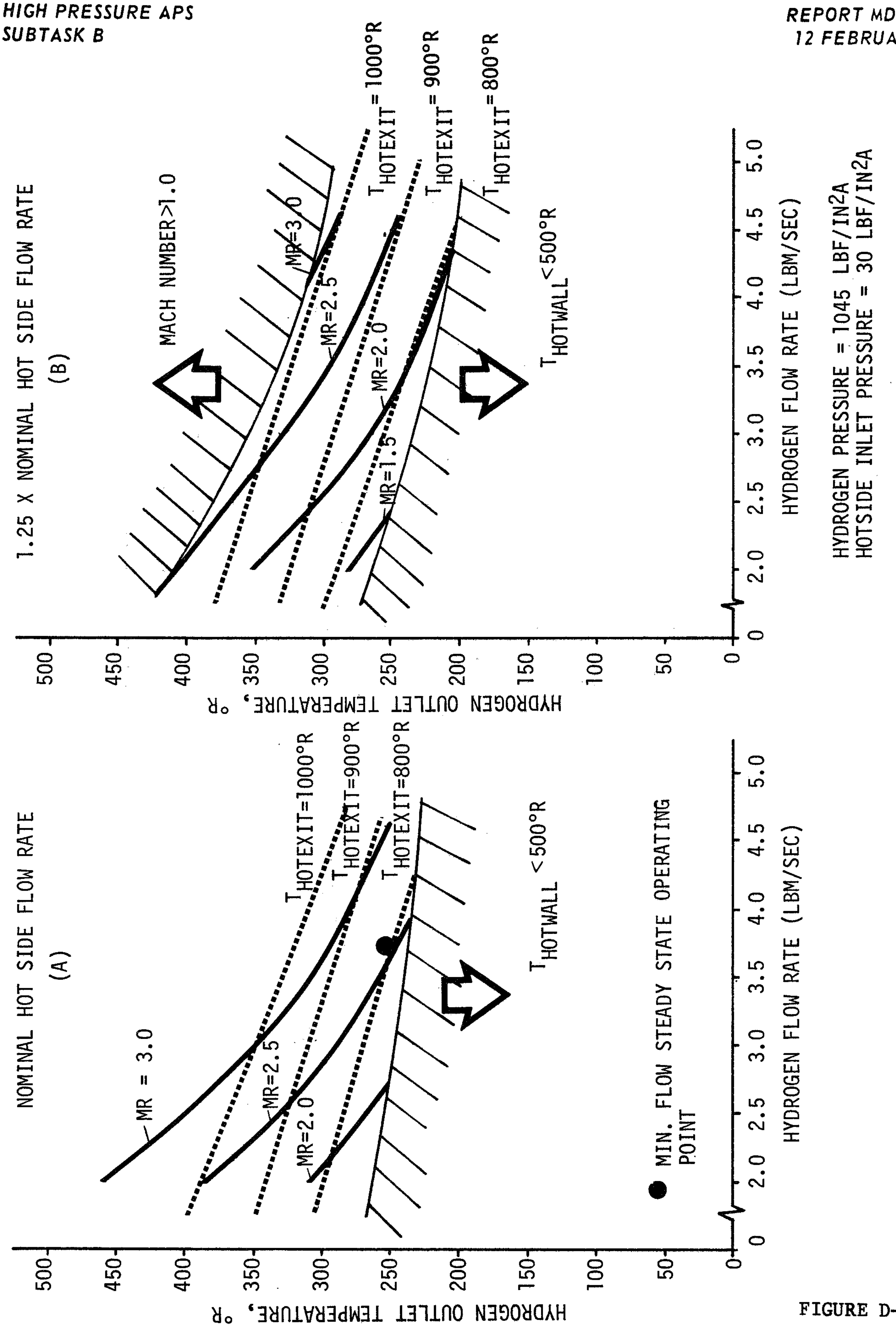

HYDROGEN HEAT EXCHANGER OPERATING MAP

FIGURE D-62c

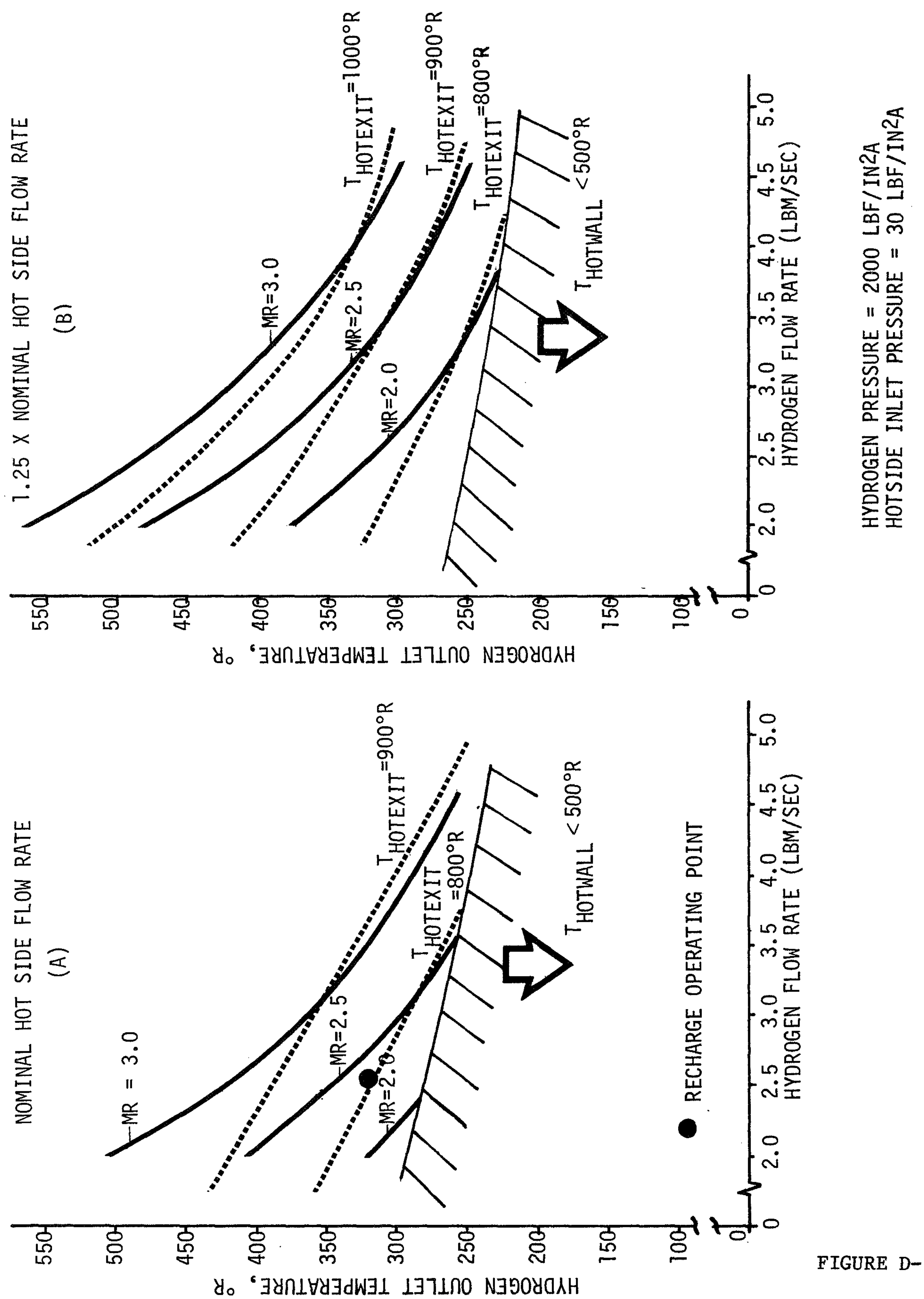

HYDROGEN HEAT EXCHANGER OPERATING MAP

FIGURE D-62d

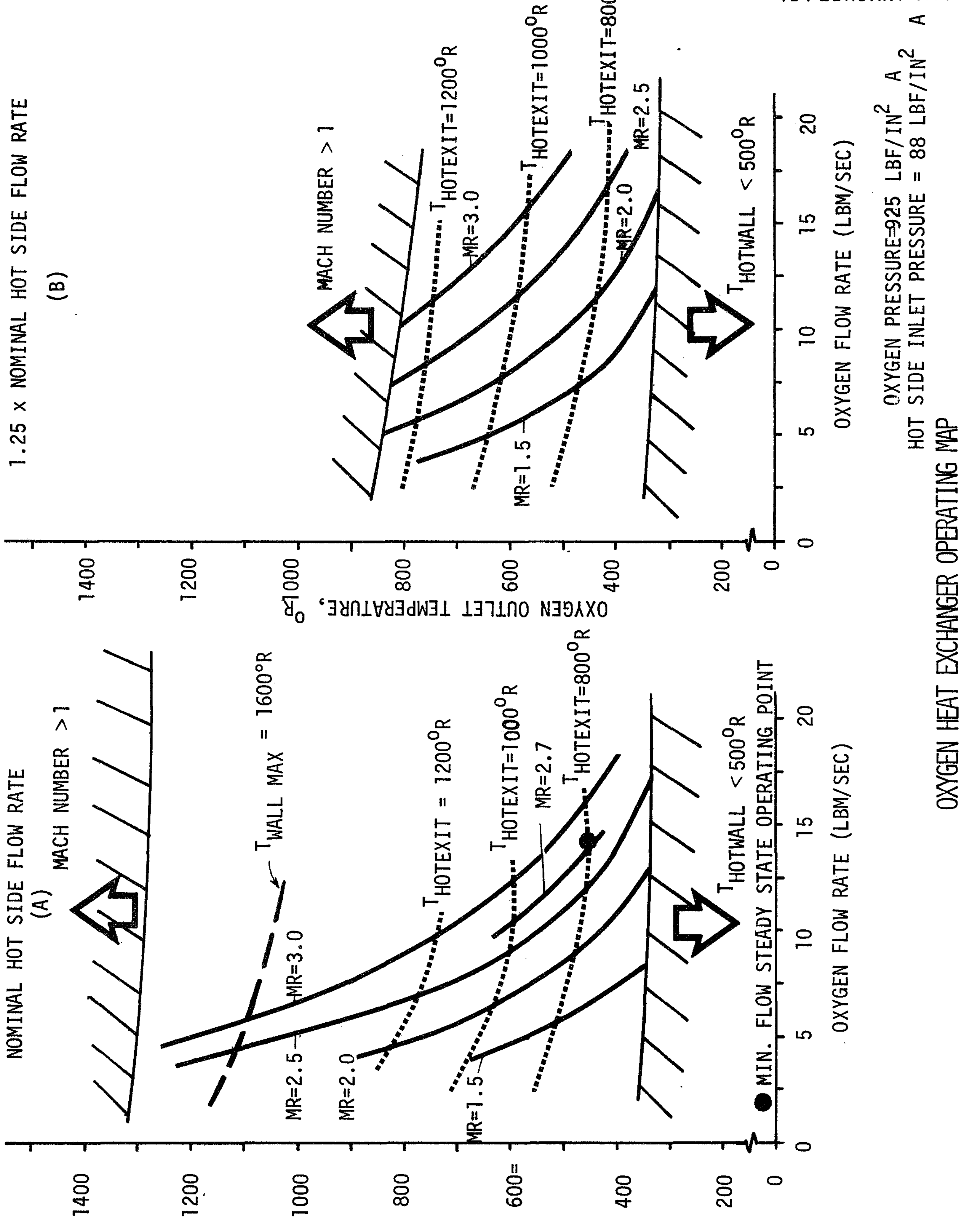

OXYGEN HEAT EXCHANGER OPERATING MAP

FIGURE D-62e

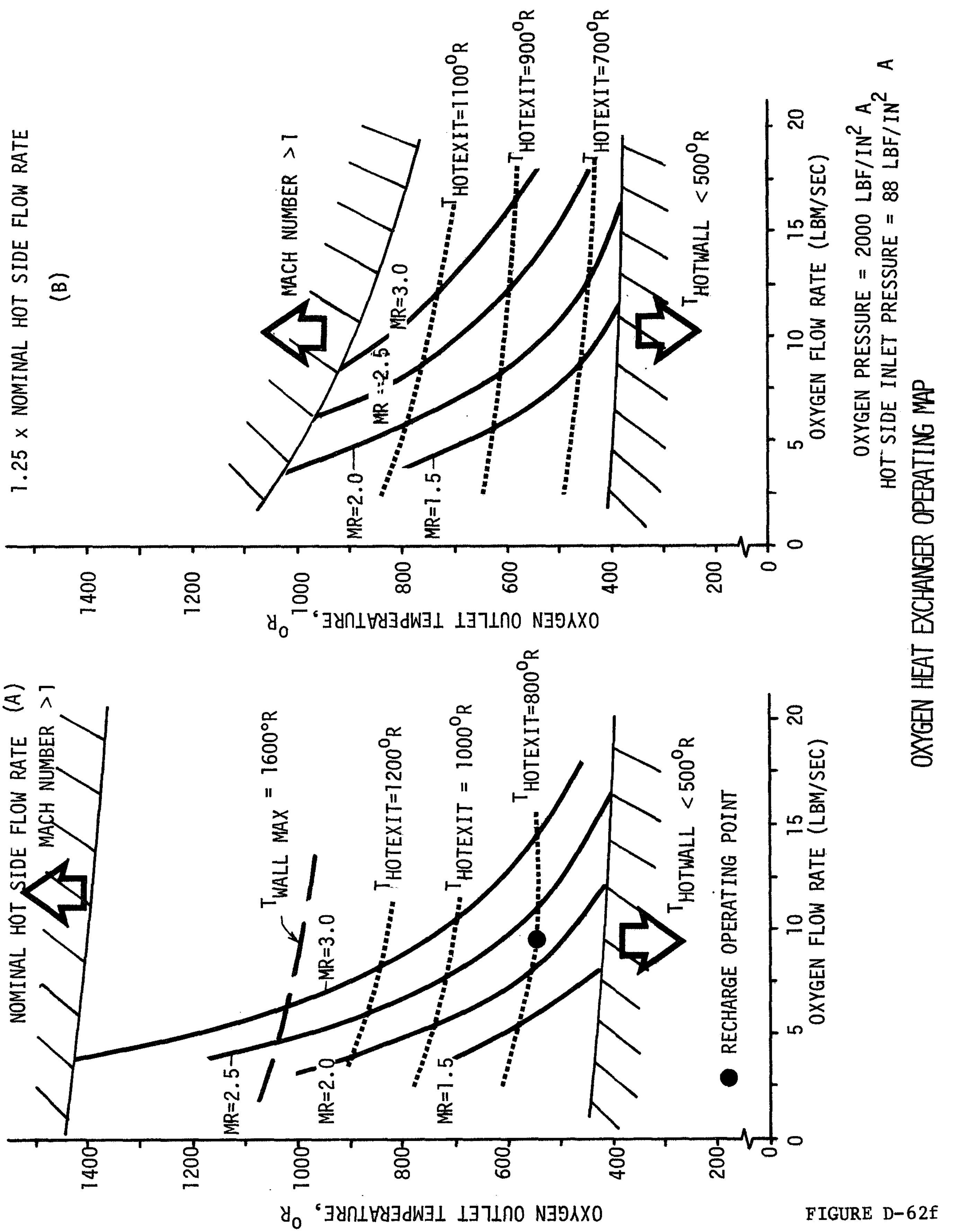
OXYGEN HEAT EXCHANGER OPERATING MAP
OXYGEN PRESSURE = 2000 LBF/IN² A
HOT SIDE INLET PRESSURE = 88 LBF/IN² A
1.25 x NOMINAL HOT SIDE FLOW RATE
(B)
MACH NUMBER >1
T HOTEXIT=1100°R
T HOTEXIT=900°R
T HOTEXIT=700°R
T HOTWALL <500°R
MR=3.0
MR=2.5
MR=2.0
MR=1.5
NOMINAL HOT SIDE FLOW RATE (A)
MACH NUMBER >1
T WALL MAX = 1600°R
T HOTEXIT=1200°R
T HOTEXIT = 1000°R
T HOTEXIT=800°R
T HOTWALL <500°R
MR=3.0
MR=2.5
MR=2.0
MR=1.5
RECHARGE OPERATING POINT
OXYGEN OUTLET TEMPERATURE, °R
OXYGEN FLOW RATE (LBM/SEC)
0
200
400
600
800
1000
1200
1400
5
10
15
20

FIGURE D-62f

preclude condensation and icing of water vapor in the hot gas products. The selected plate heat exchanger concept provides enough design flexibility to achieve the required performance within the wall temperature constraints, because the flow passage geometry of both hot and cold sides can be altered, as required, to control film heat transfer rates. Figures D-63 and D-64 show predicted outer wall temperatures and film coefficients as a function of axial position in hydrogen and oxygen heat exchanger plates, respectively.

The analytical heat exchanger design characteristics were developed by starting with an initial selection of passage geometry, plate size, number of plates, and given inlet and outlet gas conditions. An iterative procedure was followed, in which heat exchanger length and passage geometry were balanced against wall temperature. The computerized design analysis used a one-dimensional control volume approach; cold and hot flow passages were divided into finite increments for simultaneous solution of continuity, momentum, and energy equations for each section.

Plate passage geometry is presented in Figure D-65 (which shows a cross section of a typical hydrogen plate). As shown, passage width is increased as propellant flows down the plate. A flow area increase occurs as the fluid heats up and expands. The velocity and cold side film coefficient are maintained nearly constant along the plate.

The corresponding hot side flow geometry is the opposite. Near the hot side inlet, plate spacing is maximized to reduce hot side film coefficient. Plate spacing is reduced towards the outlet to increase the hot side film coefficient at the exit.

A frequent problem in cryogenic heat exchangers is the occurrence of low frequency flow and pressure oscillations. Unstable operation of supercritical, cryogenic heat exchangers has been investigated under NASA-MSFC, Contract NAS 8-21052. A simplified stability criterion was developed on the basis of theoretical analysis which allows evaluation of supercritical heat exchangers for potential instability. The criterion has been compared with experimental data and proved to be reasonably successful. It uses a steady-state analysis technique to indicate whether operation of a given design would be inherently stable or unstable. Figure D-66 shows the general classification of the effects of heat exchanger characteristics formulated by the criterion.

In applying these effects to the recharge transient, results are mixed, but the over-all influence appears to be toward greater heat exchanger stability at the higher pressures and lower flow rates as the accumulators recharge.

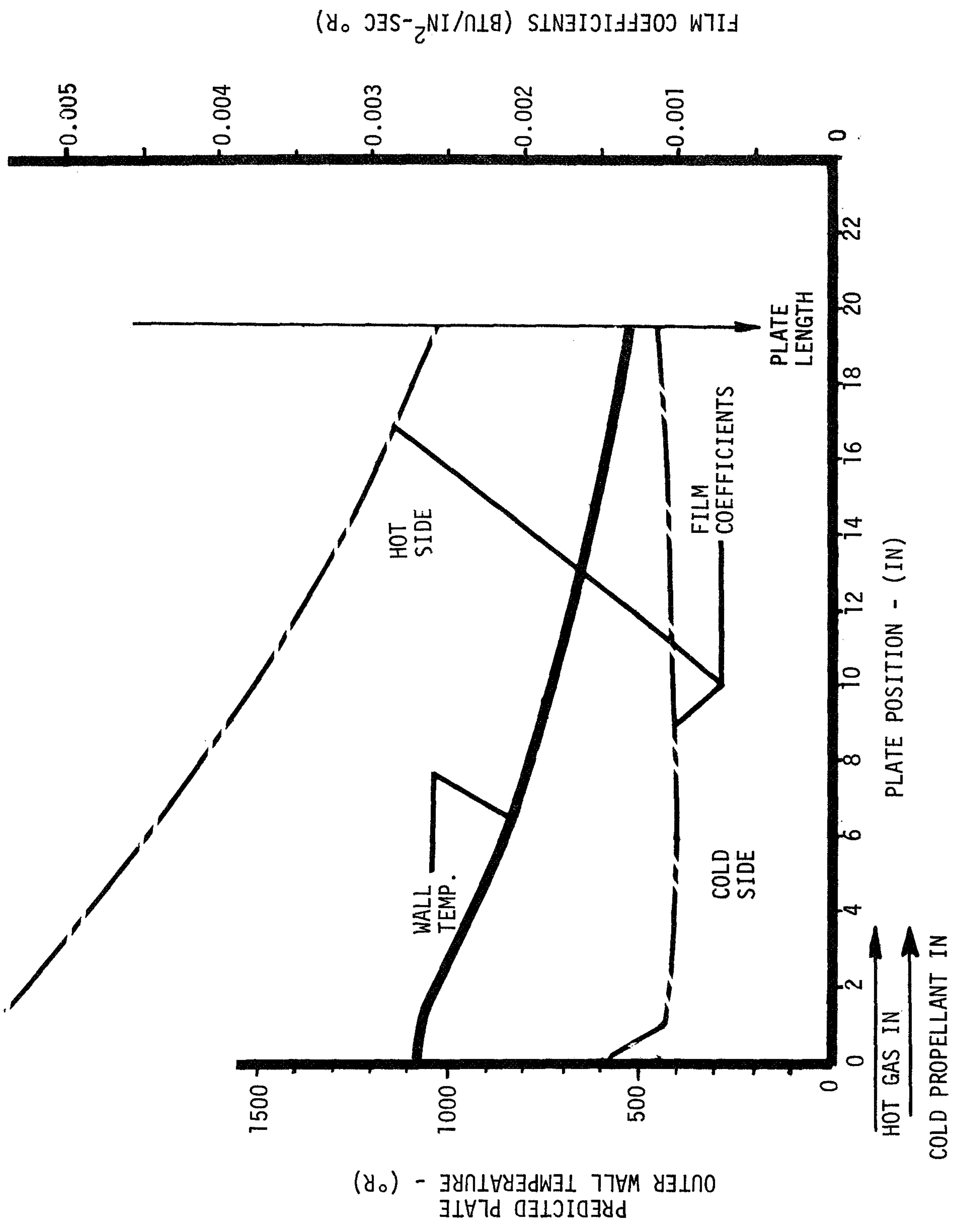

HYDROGEN HEAT EXCHANGER PLATE THERMAL CONDITIONS

FIGURE D-63

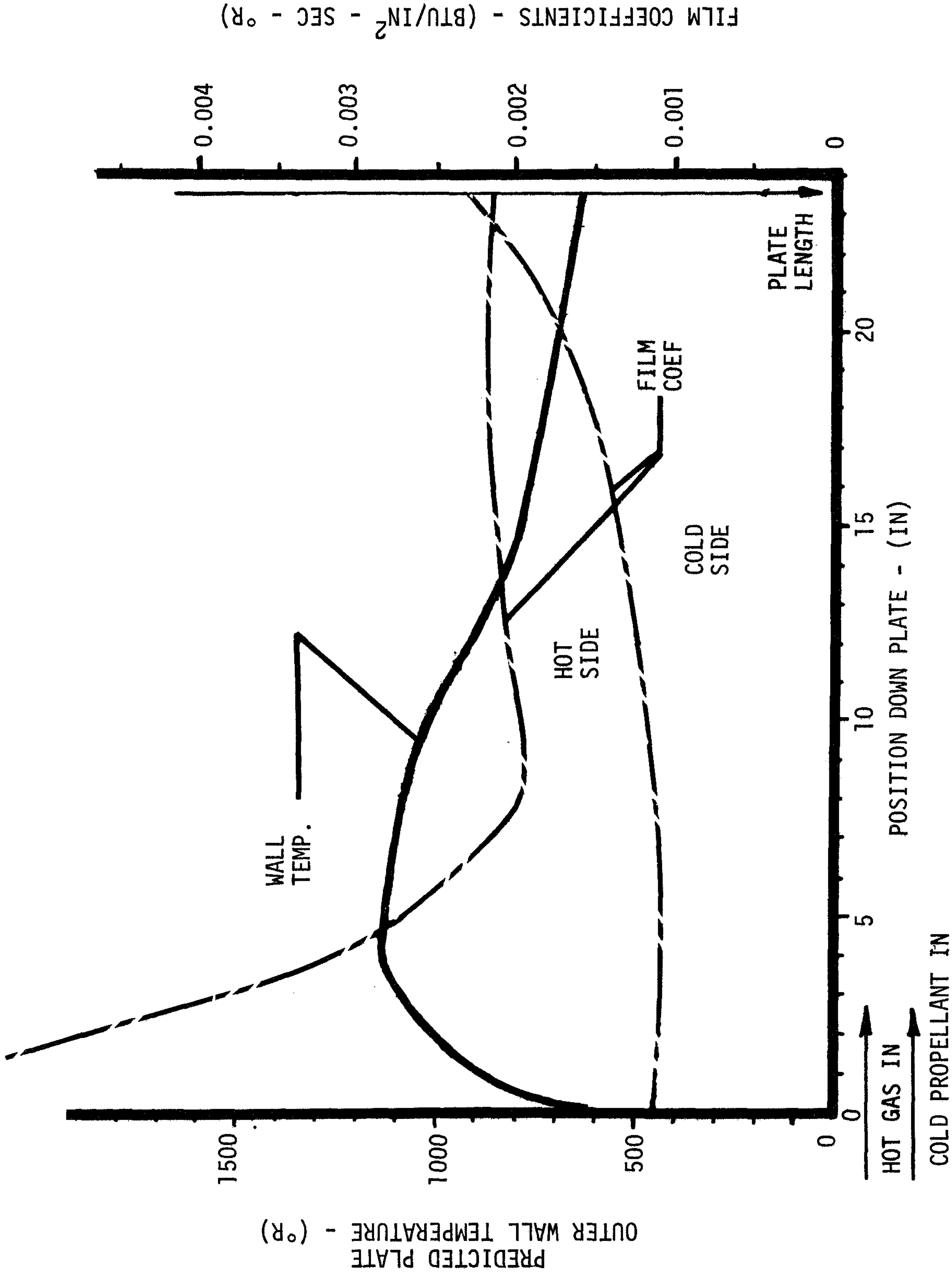

OXYGEN HEAT EXCHANGER PLATE THERMAL CONDITIONS

FIGURE D-64

APS HEAT EXCHANGER PLATE

SCHEMATIC OF FLOW PATH/GEOMETRY

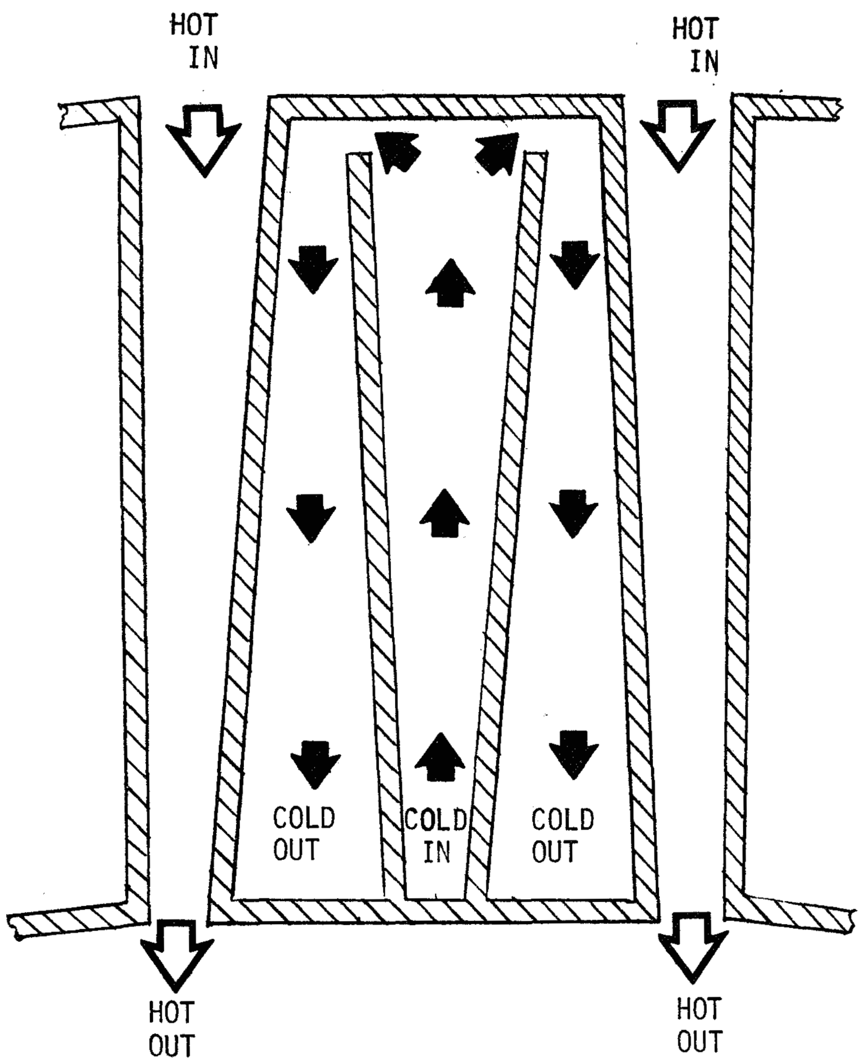

FIGURE D-65

OPERATING CHARACTERISTIC	INFLUENCE
INLET SECTION ΔP	STABILIZING
"LIQUID" SECTION ΔP	STABILIZING
"GAS" SECTION ΔP	DESTABILIZING / STABILIZING
EXIT SECTION ΔP	DESTABILIZING / STABILIZING
ACCELERATION ΔP	DESTABILIZING / STABILIZING
HIGH OUTLET VELOCITY	DESTABILIZING
LOW INLET VELOCITY	DESTABILIZING
HIGH HEAT ENERGY INPUT	DESTABILIZING
HIGH HEAT TRANSFER COEFFICIENT	STABILIZING

APS HEAT EXCHANGERS

SUMMARY OF SUPERCRITICAL STABILITY INFLUENCES

FIGURE D-66

A stress analysis was conducted using steady state wall temperatures and a maximum pressure of 2475 LBF/in^{2}A, allowing for an over shoot of the design maximum pressure. The following results were obtained.

				MARGIN OF SAFETY	
		OXYGEN	HYDROGEN	OXYGEN	HYDROGEN
FLOW CHANNEL STRESSES (KSI)	SHEAR	2.4	4.7	2.4	>10
	BENDING	4.8	18.0	2.2	HIGH
	TENSION	4.8	15.5	2.2	HIGH
HOT SURFACE THERMAL STRAIN		1.3%	1.2%		

D-4.3 Controls Requirements - Heat exchanger cold side pressures will increase, and the flow rate decrease, during accumulator recharge. This change in flow and pressure condition requires that heat exchanger oxygen flow rates be reduced to provide a corresponding reduction in the total hot gas enthalpy available. Potential control concepts are shown schematically in Figure D-68. Heat exchanger inlet and outlet temperature for each control concept are presented in Figure D-69.

For Concept A, reburn oxygen flow rate is throttled to retain a maximum hot side temperature, and liquid flow is bypassed around the heat exchanger to maintain minimum hot gas exit temperatures and requisite cold side outlet temperatures. This concept is the most complex of those evaluated and provides the most precise control of fluid temperatures and enthalpy balances.

In Concept B, heat exchanger reburn oxygen flow is throttled to retain the desired propellant outlet temperature. The throttle could be controlled on the basis of sensed pump discharge or accumulator pressure. This concept requires a continuous dynamic flow control of a small quantity of gaseous oxygen.

Concept B was selected in order to limit maximum combustion temperature, and to maintain heat exchanger outlet temperature above the condensation limit.

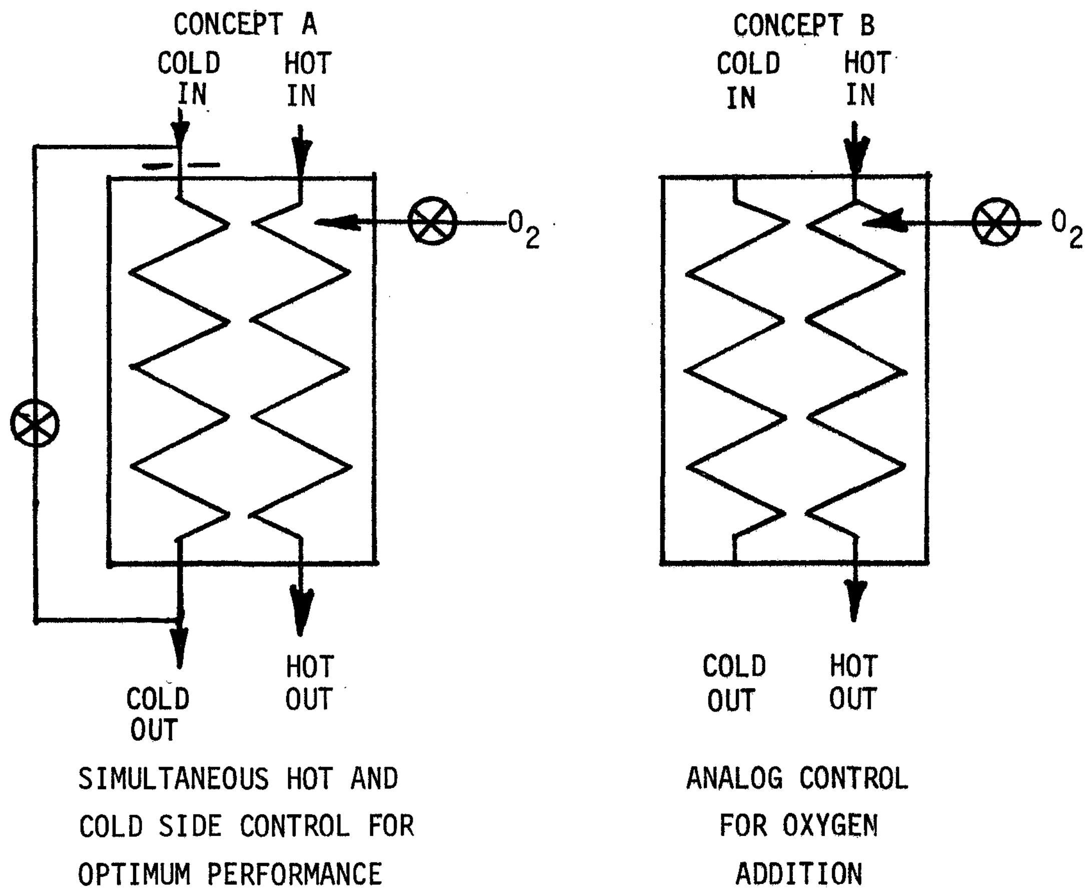

APS HEAT EXCHANGER CONTROL CONCEPTS

FIGURE D-68

APS HEAT EXCHANGER CONTROL DURING RECHARGE

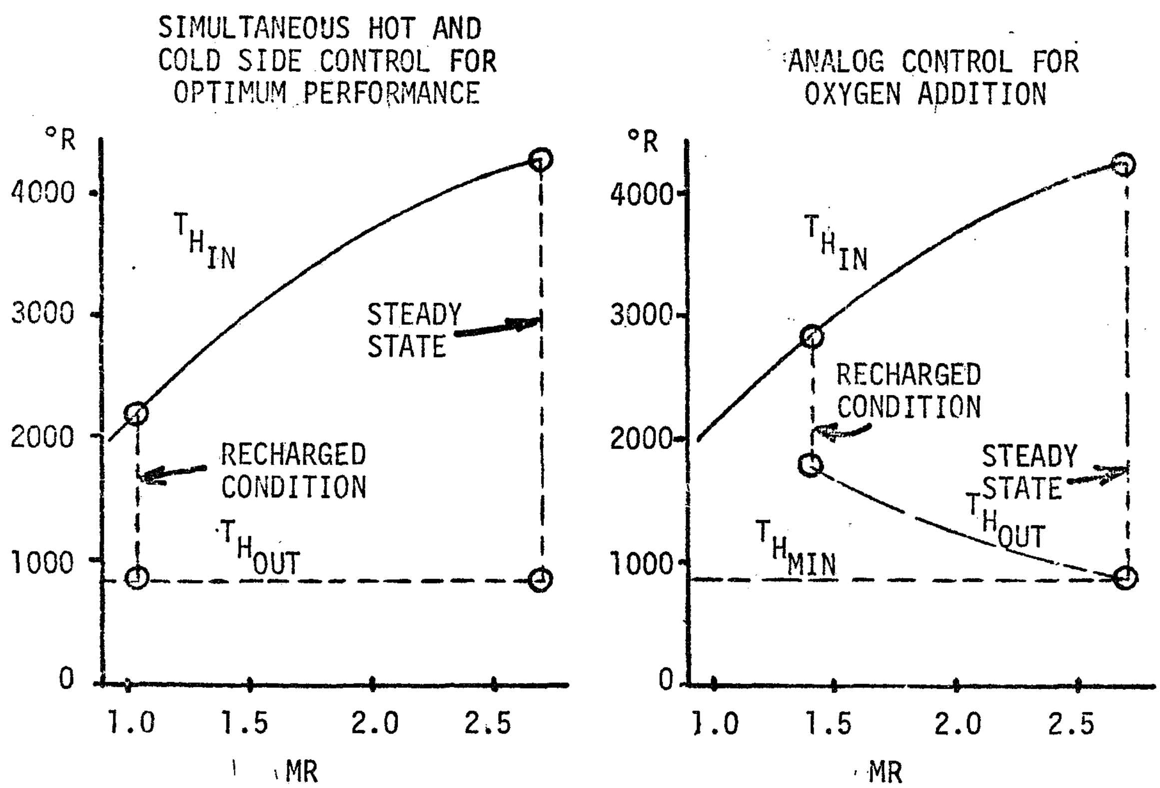

FIGURE D-69

D-5. GAS GENERATORS

The APS uses gas generator products to provide power for turbopump operation and energy to the heat exchangers. Gas generators are required to have throttling capability to maintain accumulator pressure at or near switching pressure level during steady state operation. They must also provide increased flow and power to the turbine during conditioner start-up. In addition, the gas generators must maintain exhaust temperatures within limits necessary to ensure turbine blading structural integrity.

The design conditions for these subassemblies are:

(1) a 2000°R combustion temperature

(2) flow rates of 0.44 lb/sec and 0.26 lb/sec to the hydrogen and oxygen turbines respectively

(3) a nominal operating pressure of 500 lbf/in^2a

(4) minimum propellant inlet temperature of 200°R and 350°R, respectively for hydrogen and oxygen.

This appendix discusses gas generator design, controls, performance sensitivity to propellant temperatures, and critical technology areas.

D-5.1 Design - The hydrogen gas generator design selected for the APS is shown in Figure D-70. This unit operates from gaseous hydrogen and oxygen propellants. Gaseous propellant injection has been demonstrated at chamber pressures of 100 to 800 lbf/in^2a and mixture ratios of 2 to 6; thus, it is readily adaptable to the low mixture ratio gas generator operation. The oxygen gas generator operates similar to the hydrogen unit but is slightly different physically to accommodate a lower flow rate.

The gas generator design provides linked on-off valves to control the primary propellants to the gas generator and assure proper propellant sequencing with the spark torch igniter. A parallel flow path in both propellant circuits is provided downstream of the linked valves with throttling valves in one leg of each parallel circuit to provide throttling by allowing additional flow resistance in each propellant circuit.

The propellant supply lines and injector manifolding is designed to provide propellant flow velocities of less than Mach 0.3 in the circuits up to the injector elements. The injector proposed is an impinging coaxial element concept. The element provides a uniform and homogeneous hot gas flow stream down the GG barrel and at the inlet to the turbine nozzles. The injector is fabricated of brazed 347 Stainless Steel.

An electrical spark igniter discharges and ignites a small torch flame down the center of the injector. This igniter is similar to a demonstrated engine electrical spark torch concept. Propellant to the electrical igniter is controlled by the primary gas generator on-off valves.

The flow velocities selected result in propellant feed lines of 3/8 in. internal flow diameter through the linked propellant control valves (on-off) for both the hydrogen and oxygen gas generators. The parallel bypass lines around the flow resistance orifice are 1/4 in. flow diameter through the throttling valves for the hydrogen gas generator and 1/8 in. for the oxygen gas generator. These flow circuits are sized to provide 40% greater flow capability than the flow through the primary orificed flow path. The flow orifices are sized for the primary flow of each gas generator. The manifold volumes for each propellant circuit from the linked propellant control valves to the injector face are:

$$\text{Manifold Volume} = \text{3" flow length @ 3/8" I.D.} + \text{injector volume} +$$

$$\left\{ \begin{array}{l} \text{2.5" flow length @ 1/4" I.D. (Hydrogen GG)} \\ \text{2.5" flow length @ 1/8" I.D. (Oxygen GG)} \end{array} \right\} + \text{throttling valve}$$

Injector Manifold Volumes = 2" dia - 1" dia x 1/2" thick = 1.6 cu. in.

Throttling Valve Volumes $\sim$ 0.2 cu. in.

Each Propellant Circuit for Hydrogen Gas Generator has 2.27 cu. in.

Each Propellant Circuit for Oxygen Gas Generator has 2.18 cu. in.

The injector is coupled to a subsonic chamber, having sufficient length to ensure complete propellant reaction and uniform hot gas temperatures at the turbine inlet. The insulated (adiabatic wall) chamber is fabricated of A286 alloy.

The chamber has a cylindrical barrel with a low hot gas velocity and a subsonic converging section at the exit to provide an exit Mach of 0.5.

The stress of the chamber is dependent upon the wall thickness. The wall thickness dictates the resultant hoop stress based upon the $\frac{P\,r}{t}$ relationship and the resultant thermal stress based upon the following:

$$\sigma(\text{thermal stress}) = \frac{E \cdot \alpha \cdot T_f}{(1 - \mu)\ (1.5 + \frac{3.25\ k}{h \cdot t})}$$

where; E = Young's modulus

α = Coefficient of Thermal Expansion

T_f = Suddenly applied film Temperature, °R

μ = Poisson's Ratio

k = thermal conductivity

h = heat transfer coefficient

t = material thickness

Based on a 1000°R assumed temperature at the worst gradient and a subsonic heat transfer coefficient of 7.55×10^{-4} BTU/in^2-sec-°R the resultant thermal stress for a 0.030 in. wall is 10,400 psi and for 0.050 in. wall is 16,900 psi. These levels compare to a hoop stress level of only 8,400 psi for the 0.03 in. wall thickness. The A286 has a yield strength of 20,000 psi at 1500°R. The creep stress rupture of the material is 17,000 psi sustained for 60 hours at 1500°R. These levels identify that the 0.05 in. wall thickness has sufficient design margin, however, additional thermal stress safety factor will be achieved by utilizing a 0.030 in. wall.

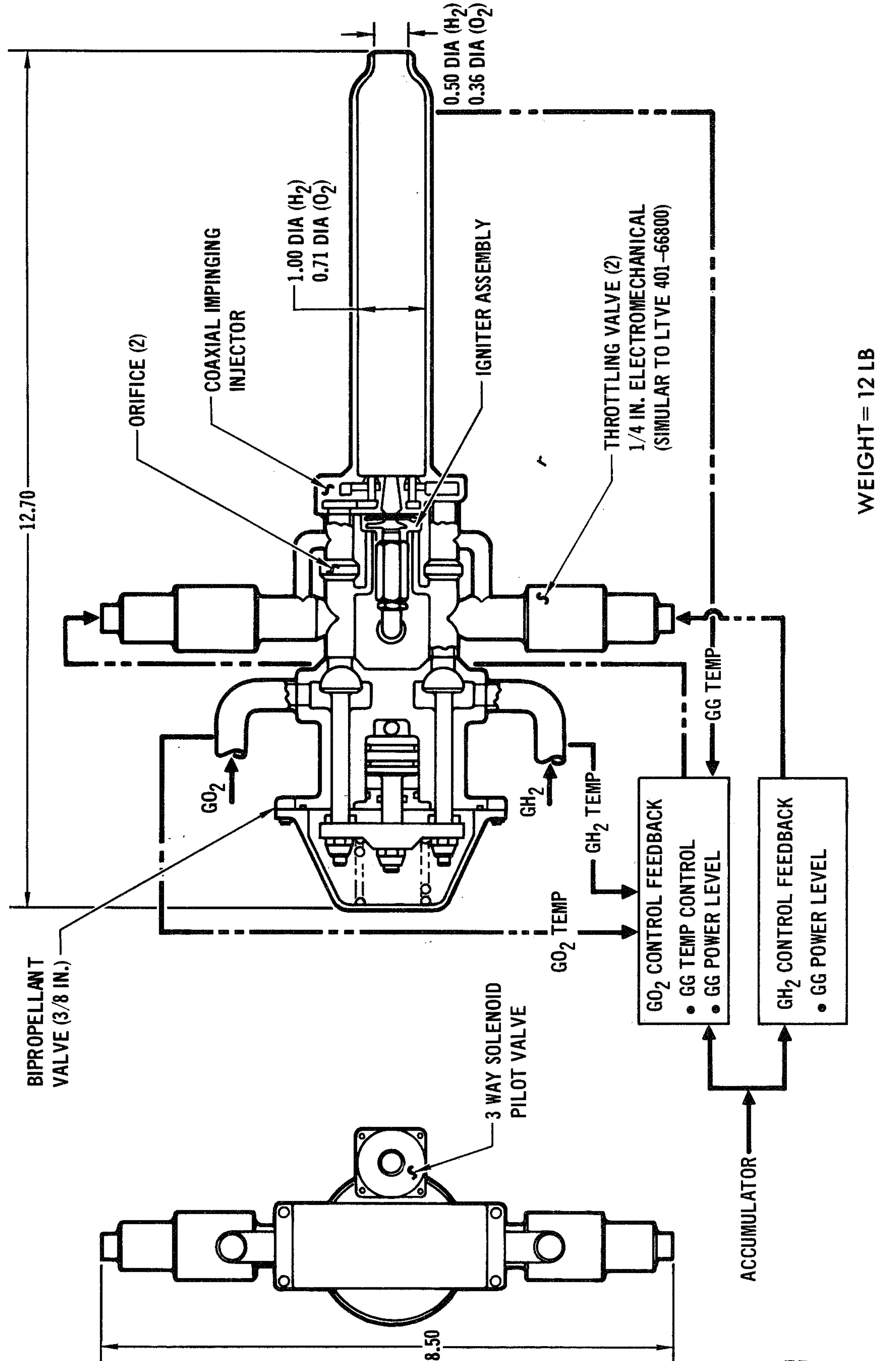

APS GAS GENERATOR

FIGURE D-70

D-5.2 Gas Generator Controls - The gas generator is sequenced on with a signal to open the linked gas generator valves and a signal to the electrical igniter. Opening the bipropellant valve sends gaseous oxygen and hydrogen through the igniter and the primary injector parallel flow circuits. The linked valve provides added assurance of proper propellant sequencing and minimizes potential mixture ratio variations due to valve inaccuracies. Calibrated orifices in each propellant flow circuit between the linked bipropellant valve seats and the gas generator injector limit gas generator operation to 80% power level. A bypass flow circuit around each orifice, with separately activated throttling valves, allows bypassing of additional hydrogen or oxygen around the calibrated orifices to adjust the power level of the gas generator on demand. The oxygen throttle valve also controls gas generator temperature and mixture ratio in response to gas generator exhaust temperatures.

Throttling of the gas generator valves for power level control would occur during major orbital maneuvers and during accumulator recharge. Before the start of a major maneuver the gas generator power level feedback controller would be activated to control to minimum accumulator pressure. The feedback controls would be sequenced to allow accumulator recharge at a reduced power level when thruster firing has terminated. The throttle valve is an electric torque motor actuated design where the pneumatically balanced poppet is actuated by a torque motor driven ball screw.

The linked bipropellant valve is shown in Figure D-70 with a piloted pneumatic actuator; however, electrical actuation with a torque motor, motor - clutch, or solenoid actuator are feasible alternatives.

D-5.3 Gas Generator Performance - Gas generator sensitivity to inlet conditions is presented in Figures D-71 through D-74a for both hydrogen and oxygen units. These figures show the sensitivity of gas generator chamber pressure and total flow rate to inlet temperature and pressure. Combustion temperature performance is presented in Figure D-75 for a range of mixture ratios and hydrogen inlet temperatures. Figure D-76 illustrates gas generator weight for various flow rates and chamber pressures.

D-5.4 Technology Areas - The development of an on/off gas generator to provide 2000°R hot gas at a pressure level of 500 lbf/in^2a is a straightforward application of APS gaseous propellant technology. The primary technology area involved requires development of throttling control capability and closed feedback loop analysis.

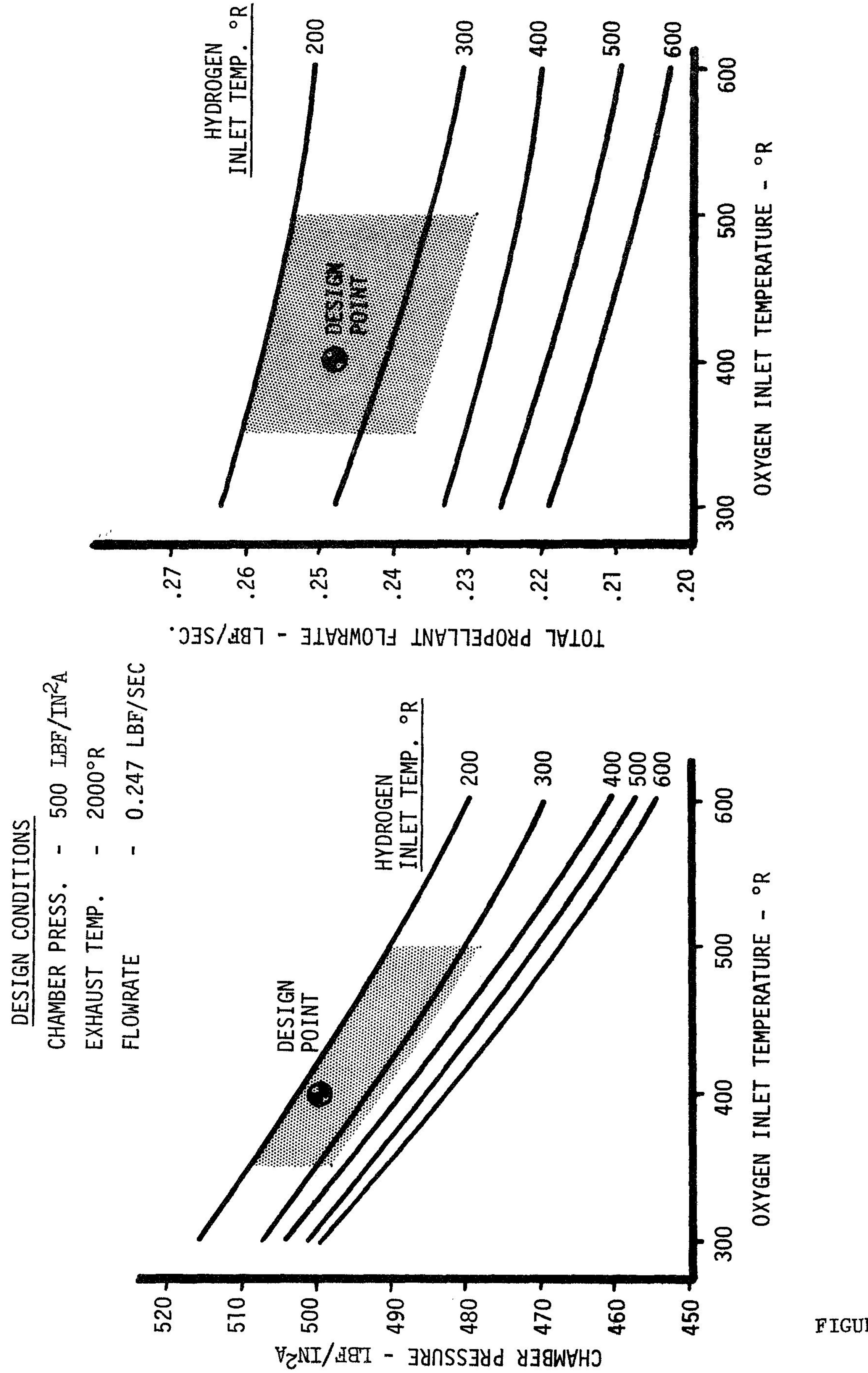

OXYGEN GAS GENERATOR SENSITIVITY

FIGURE D-71

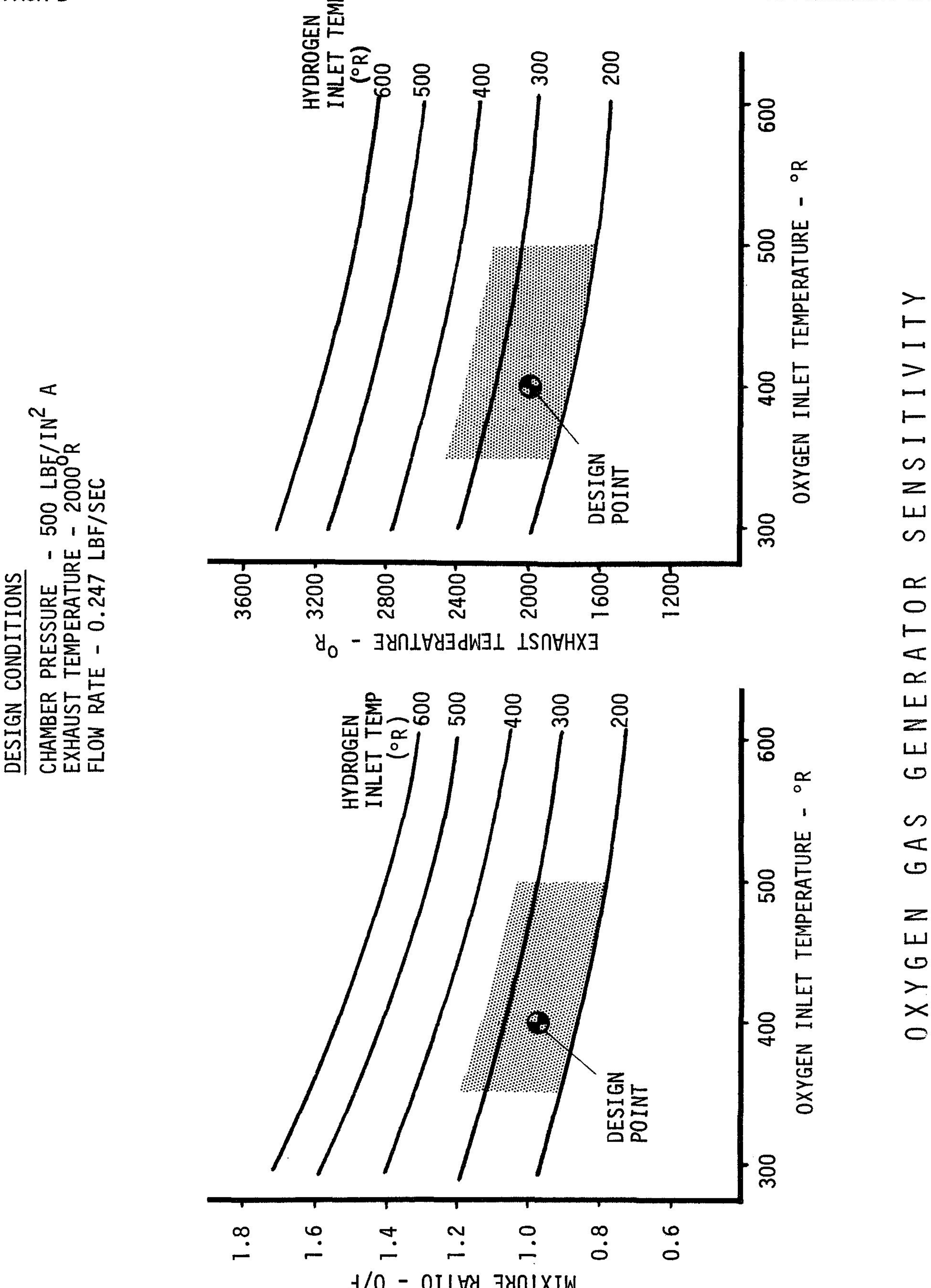
OXYGEN GAS GENERATOR SENSITIVITY
DESIGN CONDITIONS
CHAMBER PRESSURE - 500 LBF/IN^2 A
EXHAUST TEMPERATURE - 2000^{0}R
FLOW RATE - 0.247 LBF/SEC
MIXTURE RATIO - O/F
1.8
1.6
1.4
1.2
1.0
0.8
0.6
OXYGEN INLET TEMPERATURE - °R
300
400
500
600
HYDROGEN INLET TEMP (°R)
600
500
400
300
200
DESIGN POINT
EXHAUST TEMPERATURE - ^{0}R
3600
3200
2800
2400
2000
1600
1200
OXYGEN INLET TEMPERATURE - °R
300
400
500
600
HYDROGEN INLET TEMP (°R)
600
500
400
300
200
DESIGN POINT

FIGURE D-71a

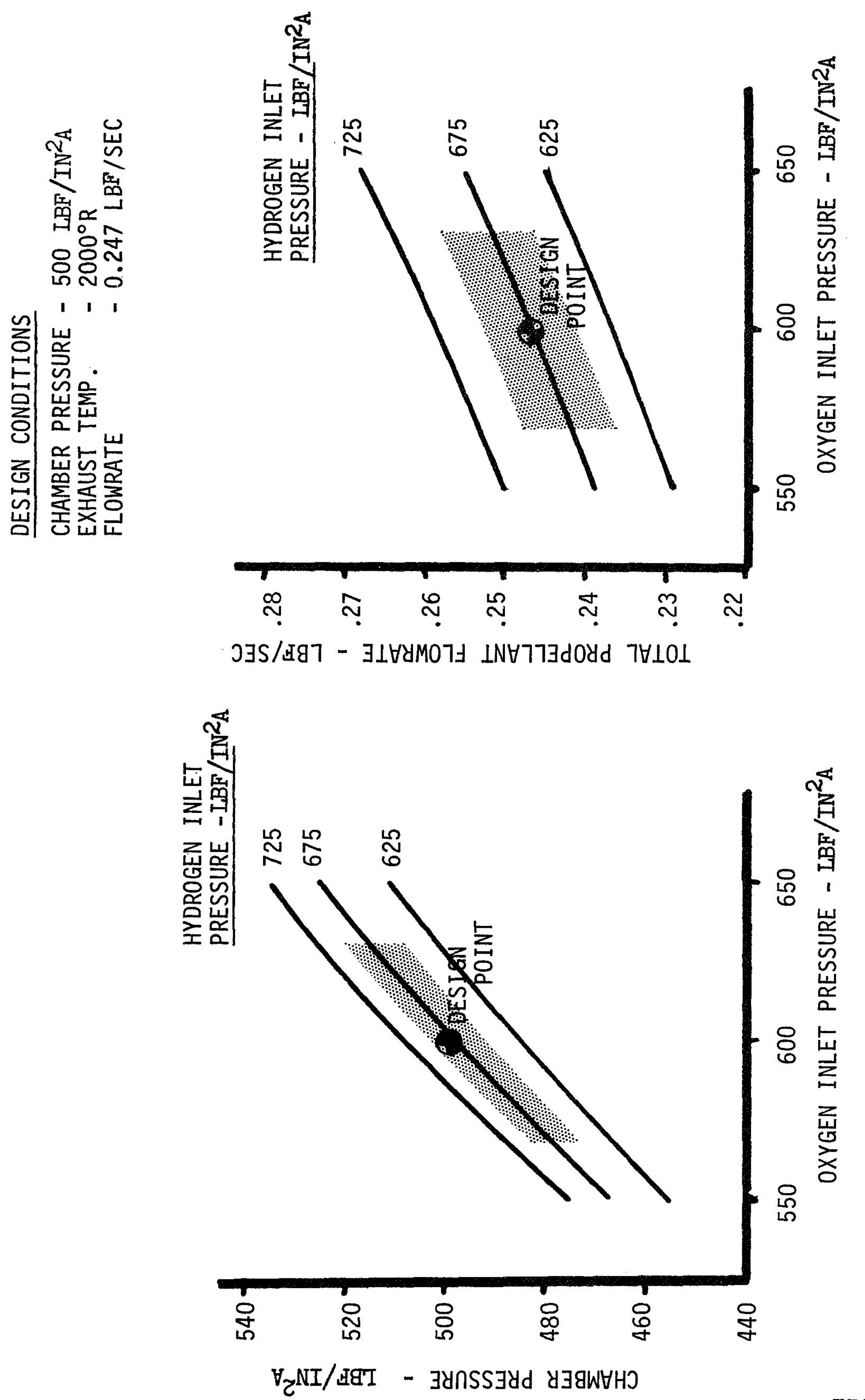

OXYGEN GAS GENERATOR SENSITIVITY

FIGURE D-72

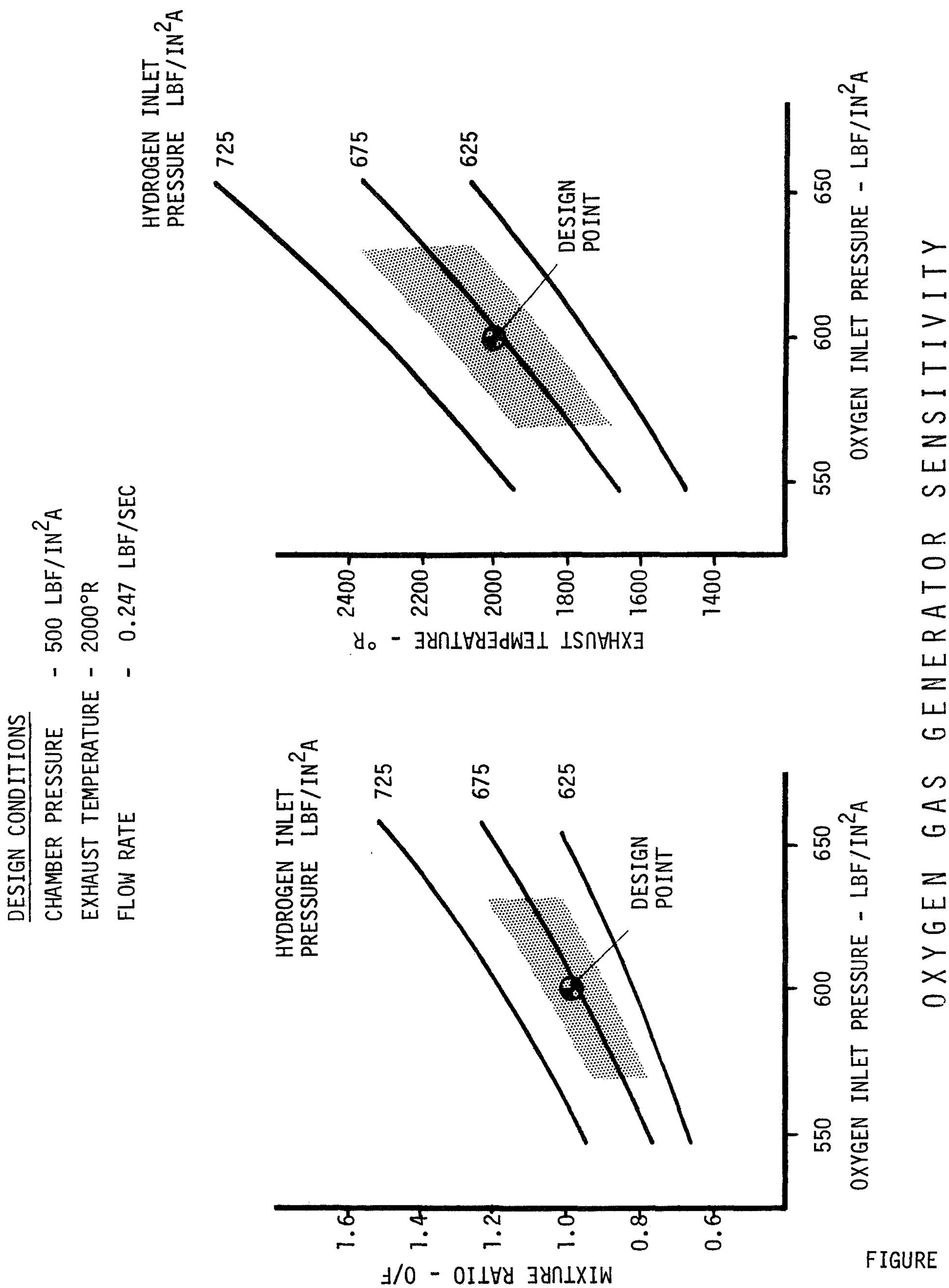
DESIGN CONDITIONS
CHAMBER PRESSURE - 500 LBF/IN²A
EXHAUST TEMPERATURE - 2000°R
FLOW RATE - 0.247 LBF/SEC
HYDROGEN INLET PRESSURE LBF/IN²A
725
675
625
DESIGN POINT
MIXTURE RATIO - O/F
1.6
1.4
1.2
1.0
0.8
0.6
550
600
650
OXYGEN INLET PRESSURE - LBF/IN²A
EXHAUST TEMPERATURE - °R
2400
2200
2000
1800
1600
1400
OXYGEN GAS GENERATOR SENSITIVITY

FIGURE D-72a

DESIGN CONDITIONS

CHAMBER PRESSURE - 500 LBF/IN^{2}A

EXHAUST TEMP. - 2000°R

FLOWRATE - 0.412 LBF/SEC

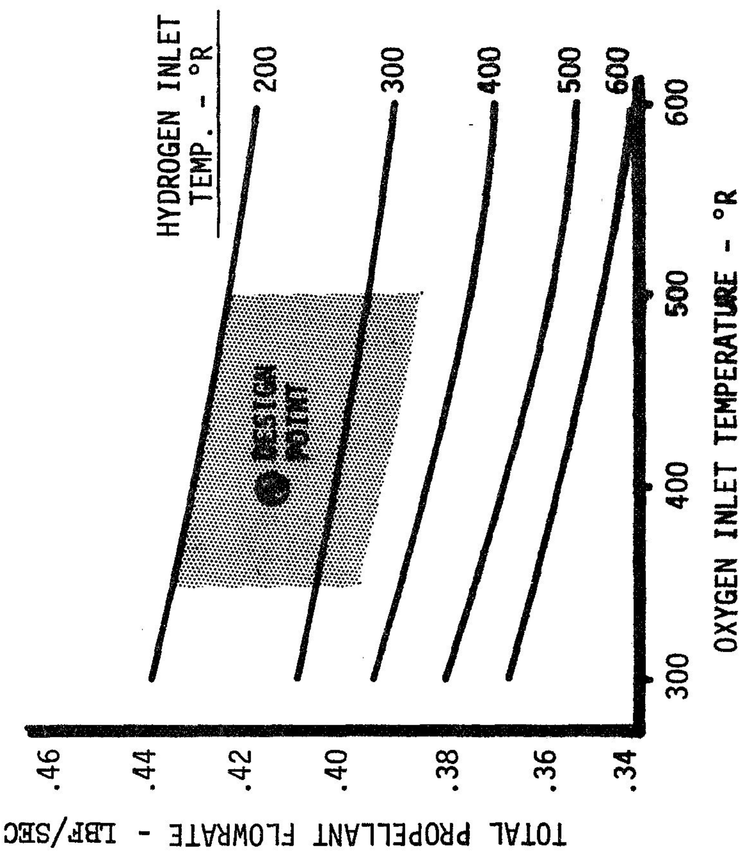

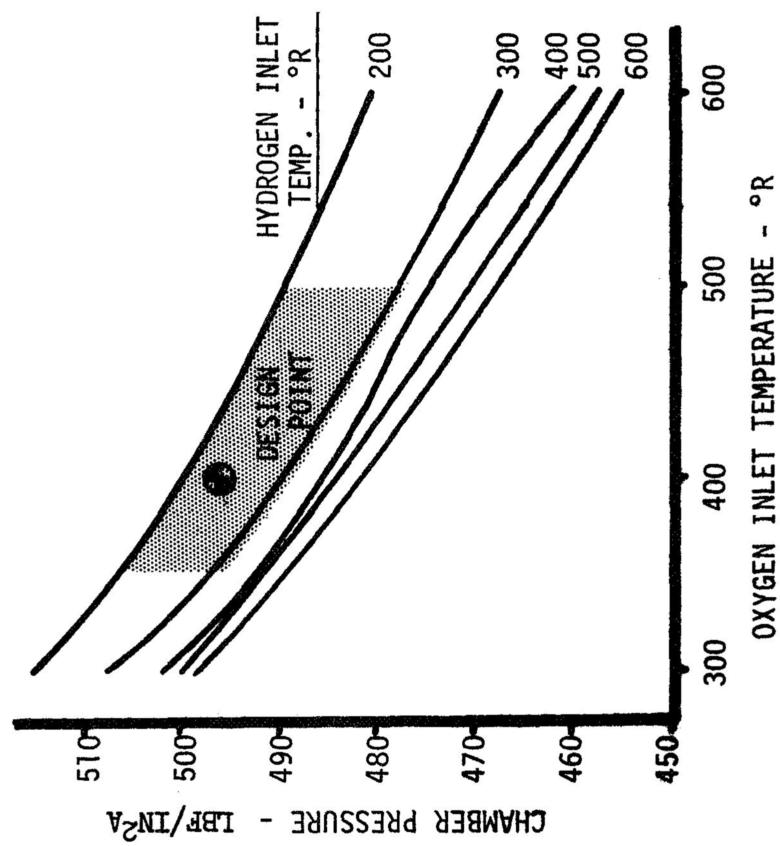

HYDROGEN GAS GENERATOR SENSITIVITY

FIGURE D-73

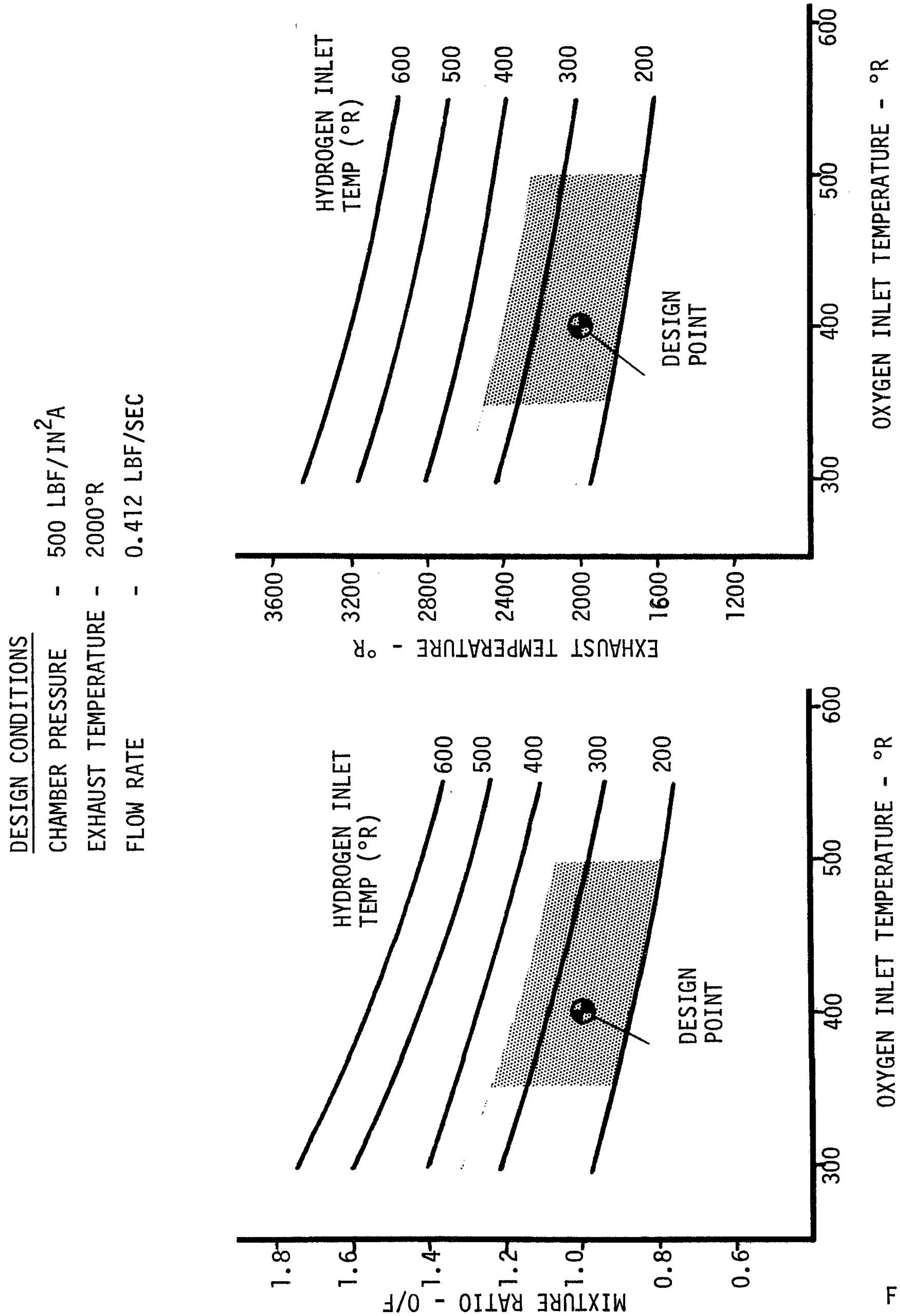

HYDROGEN GAS GENERATOR SENSITIVITY

FIGURE D-73a

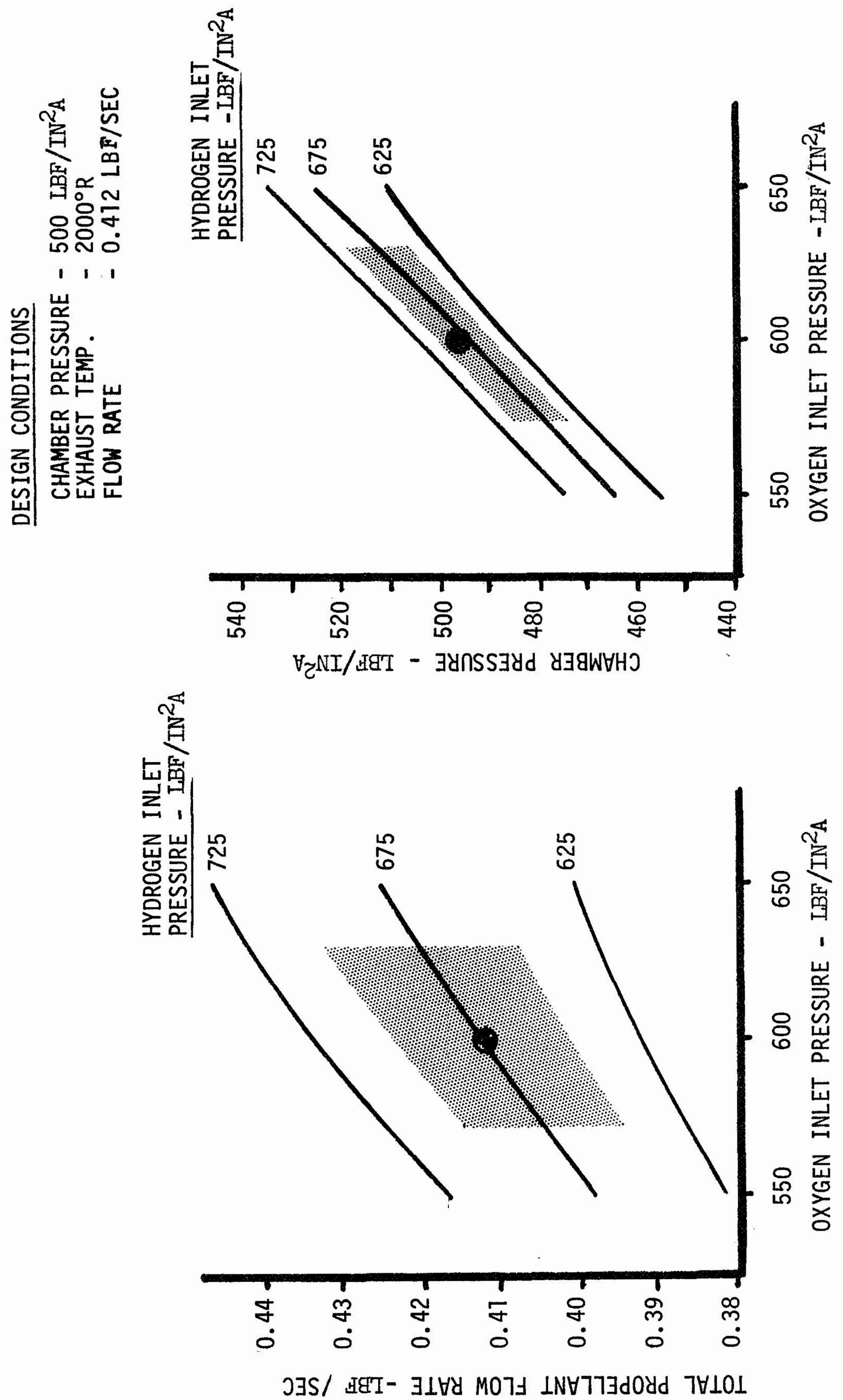

HYDROGEN GAS GENERATOR SENSITIVITY

FIGURE D-74

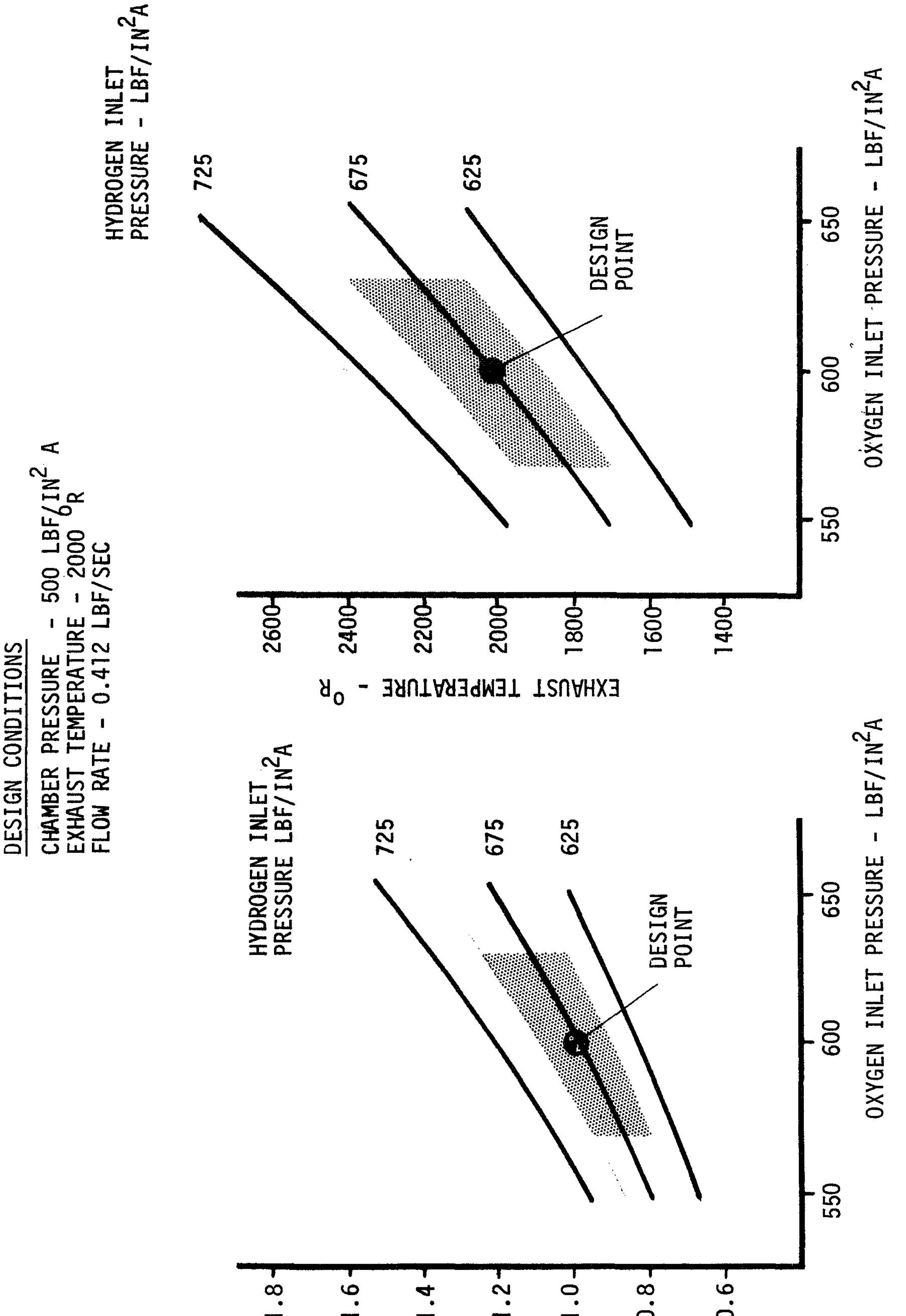

HYDROGEN GAS GENERATOR SENSITIVITY

FIGURE D-74a

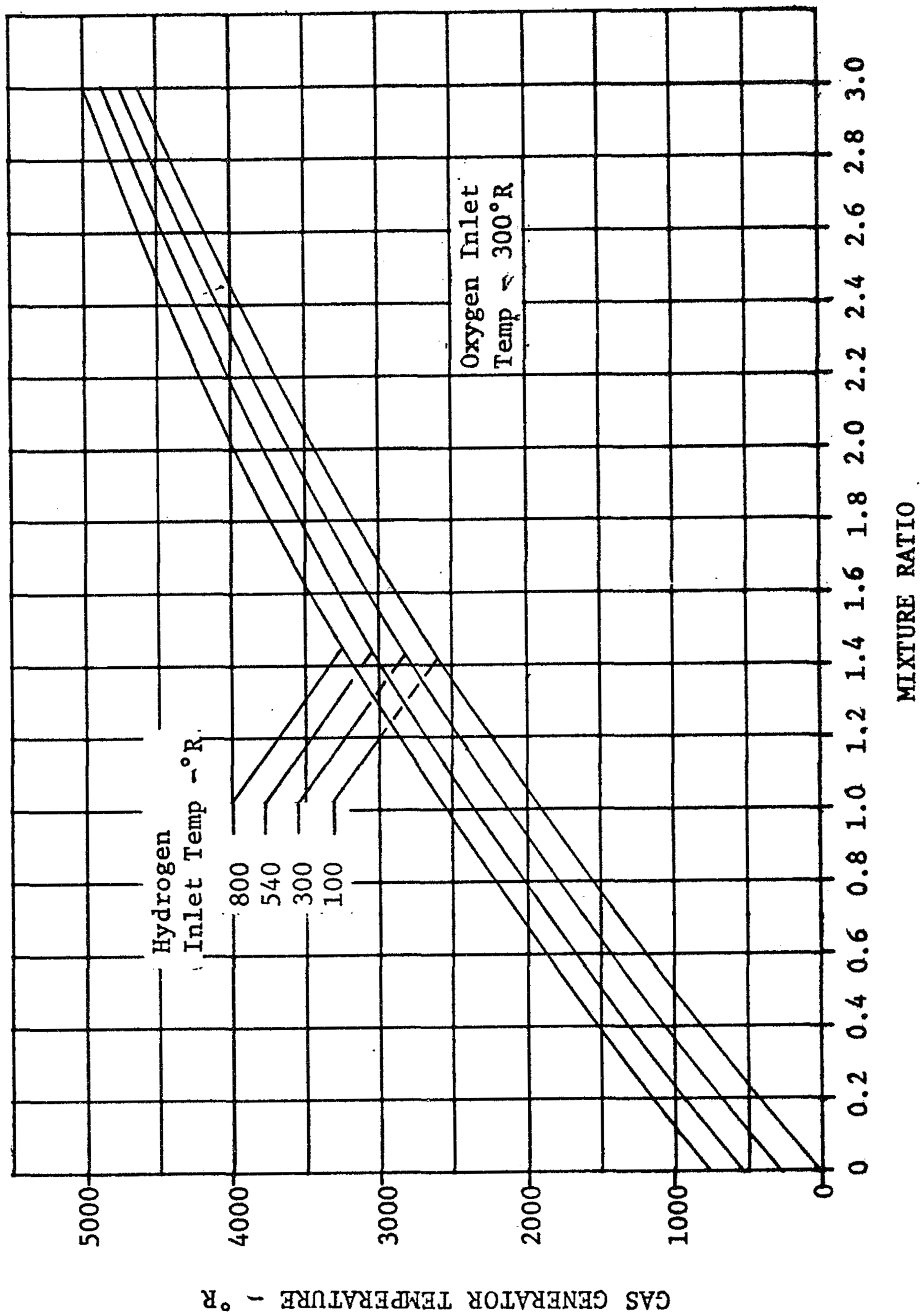

GAS GENERATOR PEFORMANCE

T_{GG} AS A FUNCTION OF MR_{GG}

FIGURE D-75

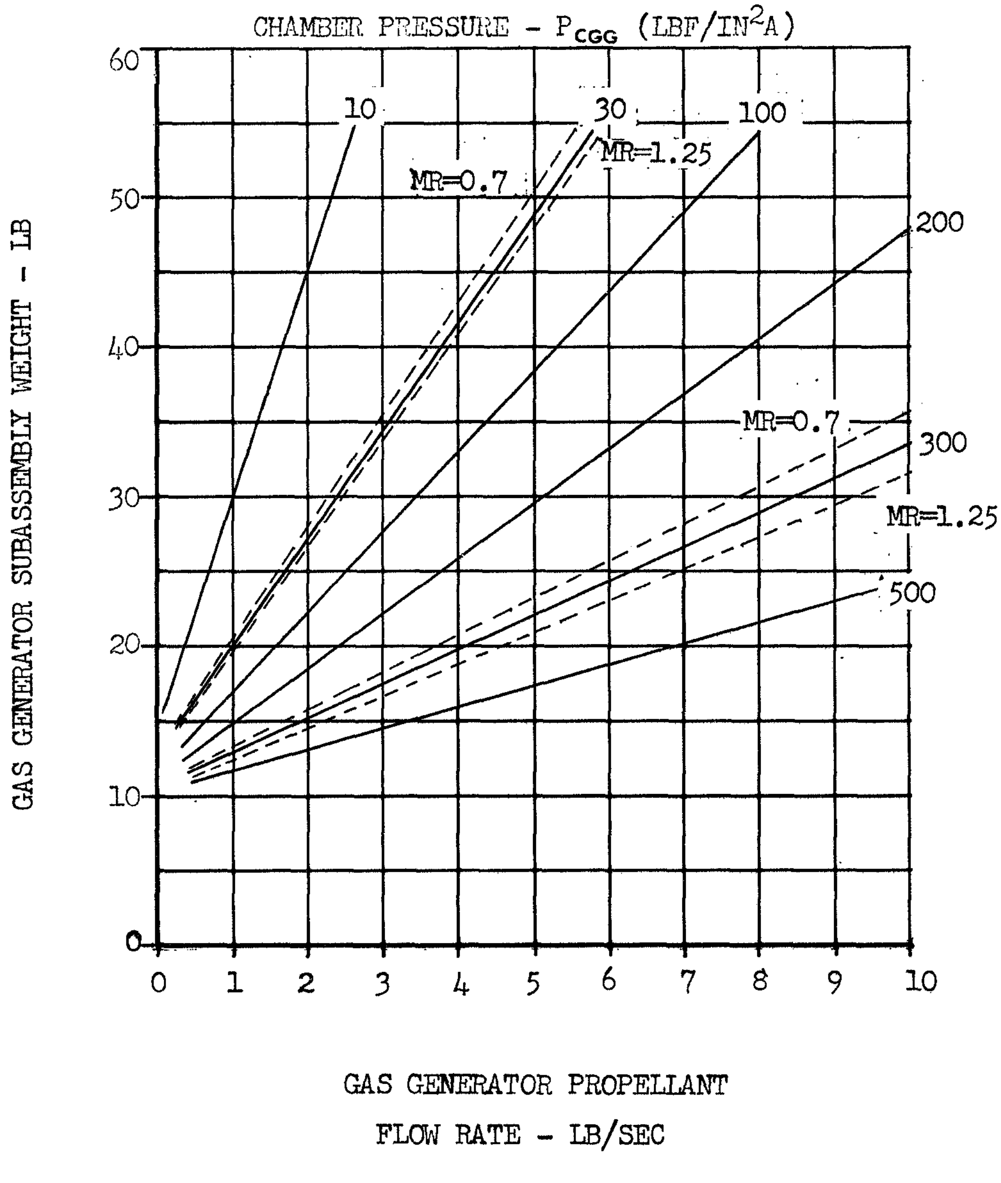

GAS GENERATOR SUBASSEMBLY WEIGHT

VERSUS

GAS GENERATOR PROPELLANT FLOW RATE

FIGURE D-76

THIS PAGE INTENTIONALLY LEFT BLANK

D-6. ACCUMULATORS

Successful vehicle control requires a reliable and responsive APS. Conditioned propellant available at all times for APS thruster operation is provided in the APS by the use of accumulators which store the gaseous propellants until they are required for use by the thruster assemblies. The accumulators operate in a blowdown mode from a maximum operating pressure to a switching pressure. At the switching pressure the conditioner assembly is actuated to re-supply conditioned propellant to the accumulator. Under conditions of maximum APS thrust, the accumulator pressure continues to decay during conditioner start-up until the conditioner is capable of supplying the accumulator outflow rate. A minimum accumulator pressure is reached and pressure then remains essentially constant until maximum thruster operation is terminated. The conditioner then recharges the accumulator to its maximum pressure.

The accumulators are sized by two criteria: 1) to limit the number of conditioner start-up cycles and 2) to limit pressure decay to a specified minimum pressure level during conditioner start-up. To limit the number of conditioner cycles, the accumulator must provide a gas storage capability, and thus total impulse, during blowdown from its maximum to its switching pressure. The number of conditioner cycles is therefore dependent upon the subsystem total impulse requirement and the total impulse storage capability during each accumulator blowdown cycle. For a selected number of conditioner start-up cycles, the blowdown gas mass and thus the blowdown pressure ratio (P_{max}/P_{sw}) required can be evaluated for a given accumulator volume. The second criteria defines accumulator volume, i.e., accumulator volume is sized such that, during the conditioner start-up transient, sufficient gas is available to keep the accumulator from decaying below a minimum pressure level. During start up, the conditioner cannot satisfy flow requirements with maximum thruster operation. Thus to keep the accumulator pressure from decaying below the minimum value required for thruster operation, it is necessary to initiate conditioner operation at a switching pressure above the minimum, providing the additional gas mass for operation during the transient. The accumulator volume necessary to provide this gas is dependent upon the APS total thrust level (outflow rate), the conditioner start-up time, and the ratio of the conditioner switching pressure to the accumulator minimum pressure (P_{sw}/P_{min}).

From the preceeding discussion it can be seen that accumulator sizing is related to several factors, total thrust level, total impulse requirement, $\frac{\text{Pmax}}{\text{Pswitch}}$ and $\frac{\text{Pswitch}}{\text{Pmin}}$, the number of cycles, and conditioner start up time. The total system thrust impulse requirements are fixed items, defined by vehicle requirements. The analyses presented in this section were conducted to determine the effect of the accumulator pressure ratios, conditioner cycle requirements, and conditioner start-up time on accumulator size and weight.

D-6.1 Conditioner Assembly Transient Analysis - To size accumulators for a minimum weight configuration and to insure a minimum pressure to the thruster assemblies, the conditioner transient startup time or equivalent conditioner lag time must be determined. For analysis convenience, an equivalent lag time is used for APS design and sizing instead of actual conditioner transient characteristics. Equivalent conditioner lag time is defined as the time with no flow into the accumulator which would produce an accumulator pressure decay equal to that exhibited by the actual assembly. Evaluation of this pressure decay and thus equivalent lag time required mathematical modeling of the dynamic behavior of the individual conditioner assembly components and their respective interfaces.

D-6.2 Conditioner Assembly Mathematical Model - The model designed for conditioner transient analysis was based upon the following assumptions:

(1) inertial effects of propellants within lines may be neglected
(2) turbine efficiency is constant
(3) all lines are frictionless
(4) all components are thermally insulated
(5) all gases are ideal with constant specific heats taken in the regions of interest
(6) valve response is equivalent to a 50 millisecond square wave delay
(7) gas generator combustion response is equivalent to a 10 millisecond square wave delay.

The valve and gas generator response were assumed to be represented by fixed square wave delays. The turbopump, heat exchanger, and accumulator transients were modeled on the basis of the above assumptions. The equations governing the dynamic behavior of these components were based upon:

(1) the turbopump equations of motion, where the rate of change of turbopump angular momentum is equal to the turbine torque minus the pump torque;

(2) the heat exchanger energy balance, where the rate of change of heat exchanger internal energy is equal to the rate of heat inflow on the hot side minus the rate of enthalpy outflow on the cold side

(3) accumulator energy balance where the rate of change of accumulator temperature and pressure was derived from simultaneous solution of the energy and mass conservation equations.

When applied to the APS conditioning assembly, these basic equations express the relationships between turbopump speed, heat-exchanger wall temperature, accumulator temperature and pressure, and their respective time derivatives. The equations were solved using a standard finite difference approach. For each time step the time derivatives were calculated, and integrated to provide new derivatives for the next time step. Figure D-77 provides a summary of design data for the baseline conditioner components. The remainder of this section presents a detailed description of the analyses of these components when integrated as a conditioner assembly.

D-6.3 Turbopump - The time rate of change of the turbopump speed is equal to the rate of change of turbopump angular momentum divided by the moment of inertia. The rate of change of angular momentum is equal to the difference between turbine and pump torque. Since turbine efficiency and power are assumed constant, the turbine torque is a linear function of speed. Pump torque was based upon the product of the pump head and mass rate of flow divided by the pump efficiency. The relationship between pump flow, efficiency, speed, and head were determined using the normalized pump performance curve of Figure D-78.

D-6.4 Heat Exchanger - The heat exchanger wall temperature time derivative is equal to the rate of change of heat exchanger internal energy divided by the product of the heat exchanger mass and specific heat. The rate of change of internal energy was the difference between the rate of heat into the exchanger on the hot-gas side and the rate of enthalpy out on the cold side. The heat rates were determined from the product of their respective steady-state heat transfer coefficients and the temperature gradient obtained using the current wall temperature. The steady-state heat transfer coefficients are chosen such that, when the wall temperature equals the log mean of the steady-state cold-side and hot-side temperatures, the rate of heat in on the hot side equals the rate out on the cold side.

PARAMETER	UNITS	VALUE	
		H_2	O_2
TURBOPUMP			
MOMENT OF INERTIA	LB/IN^2	10.386	2.664
SPEED AT MINIMUM HEAD	REV/MIN	66286.	34661.
TURBINE EFFICIENCY	%	46.0	23.1
TURBINE MEAN BLADE TIP RADIUS	INCHES	5.2	4.3
RATIO OF MEAN TIP SPEED TO SPOUTING VELOCITY	-	.29	.125
MASS RATE OF FLOW ACROSS TURBINE	LB/SEC	.4256	.254
PUMP EFFICIENCY AT MINIMUM HEAD	%	40.0	40.0
PUMP EFFICIENCY AT DESIGN CONDITIONS	%	57.6	54.7
HEAT EXCHANGER			
MASS	LB	74.1	52.7
MEAN HOT SIDE TEMPERATURE	^oR	2266.	2527
COLD SIDE EXIT TEMPERATURE	^oR	252.	458.
ACCUMULATOR			
RATE OF MASS OUTFLOW (4 ENGINES FIRING)	LB/SEC	3.66	14.15
STEADY STATE TEMPERATURE	^oR	252.	458.
MINIMUM PRESSURE	$LBF/IN^2.A$	1021.	914
VOLUME (MIN WEIGHT FOR 0.5 SEC LAG)	FT^3	29.	11.6

CONDITIONING ASSEMBLY COMPONENT DATA

FIGURE D-77

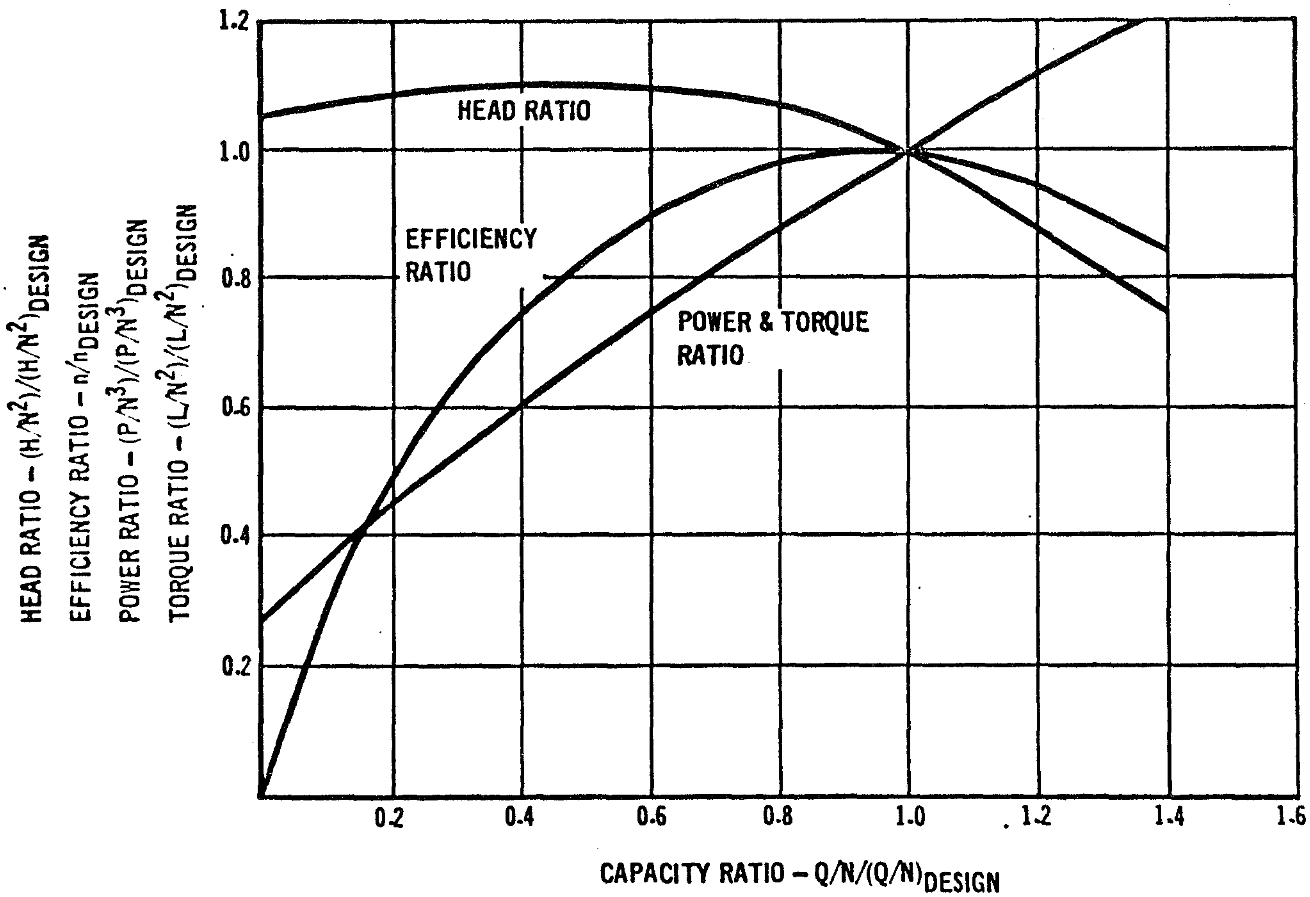

PUMP NORMALIZED PERFORMANCE PARAMETERS

FIGURE D-78

During recharge the mass flow rate through the pump decreases and the heat exchanger temperature must be reduced to avoid loading extremely high temperature propellant into the accumulator. This was accomplished by throttling the oxygen addition to the heat exchanger. This situation is simulated in the model by reducing the hot side temperature to that of the turbine outlet.

D-6.5 Conditioning Assembly Transient Analysis Results - The conditioning assembly transient model provided accumulator pressure decay histories for various accumulator volumes. Figure D-79 presents parametric data on accumulator pressures during the conditioner start transients. As shown when power is increased above that required for steady state operation the amount of accumulator pressure decay is reduced and hence the equivalent conditioner response time is improved. The reduction in pressure decay during startup is significant with only small increases in turbine power (5-10%) but further gain, by continued power increases, is limited. Based on these results it was concluded that small power increases during the conditioner start transients were a desirable feature. The power increase is achieved by the inherent sequencing characteristics of the gas generator valves which provide a high flow rate when they are initially commanded open and flow is subsequently throttled to the level commanded by accumulator pressure. For purposes of accumulator sizing an average power ratio of 1.05 was used to define equivalent conditioner start time. Analysis results simulating accumulator pressure decay for a range of accumulator volumes are shown in Figure D-79. From the volume/pressure decay data presented an equivalent conditioner response time of 0.5 sec was derived for accumulator sizing.

Analysis of the conditioning assembly performance shows that recharge require approximately 10 seconds with no thrusters firing.

D-6.6 Accumulator Sizing - Accumulator size is selected on a minimum weight basis within the constraints imposed by conditioner assembly performance, reliability criteria, and thruster design. Conditioner assembly performance defines an equivalent conditioner lag time; reliability criteria limits the number of conditioning cycles allowed per mission; and thruster design (chamber pressure) defines the minimum accumulator pressure. As previously noted within these constraints, the optimum accumulator size is a function of the total of attitude-control impulse requirements and APS total thrust capability. The optimum weight accumulator design is therefore a function of four independent parameters; equivalent conditioner lag time, attitude-control impulse requirements, number of conditioning cycles, and design chamber pressure. For a given thrust, the volume of the accumulator is

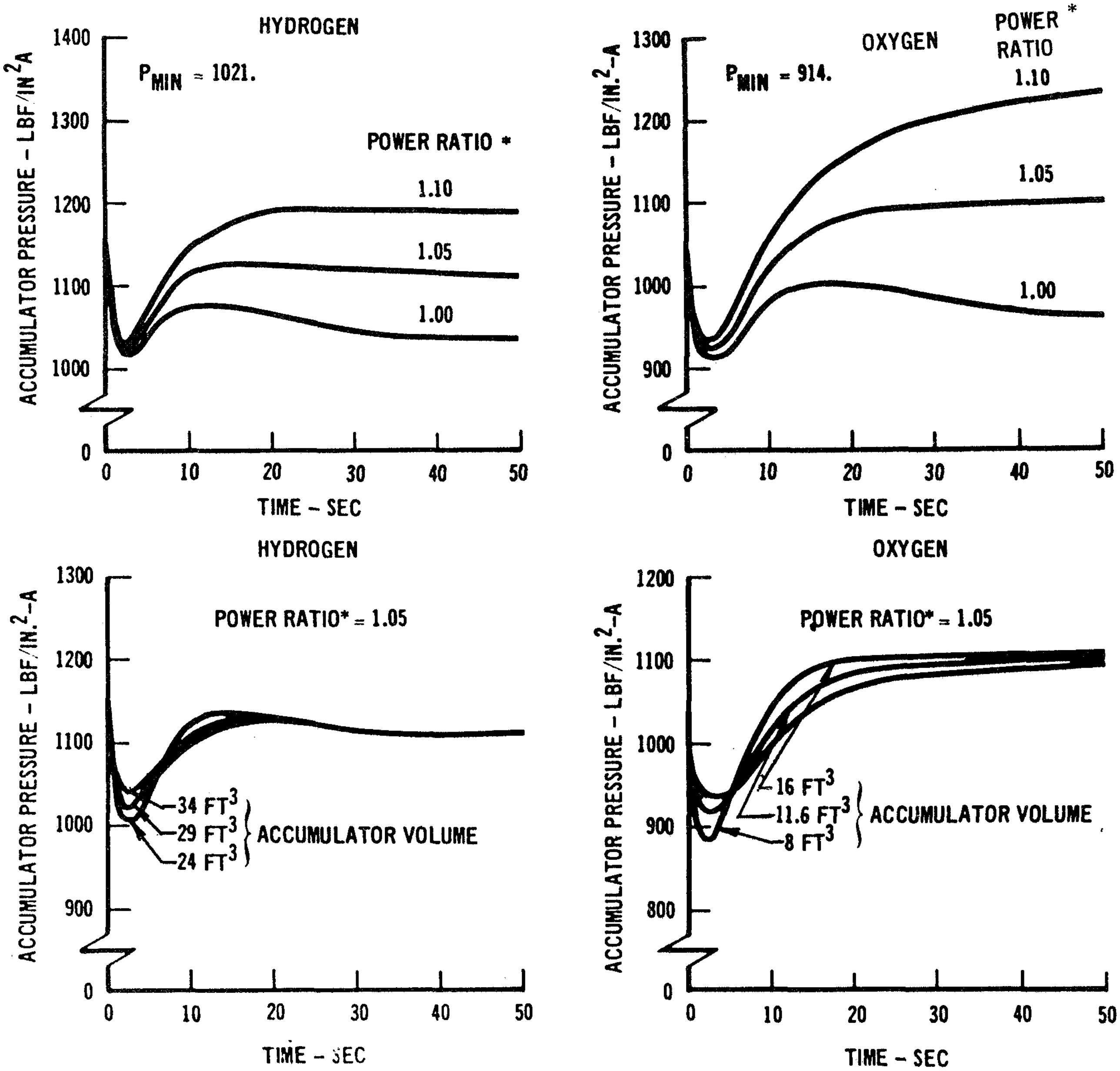

*POWER USED/POWER REQUIRED AT P_{MIN}

CONDITIONING ASSEMBLY STARTUP ACCUMULATOR PRESSURE TRANSIENTS

FIGURE D-79

sized by the conditioner lag time and ratio of the switching pressure to the minimum accumulator pressure.

The blowdown pressure ratio ($\frac{Pmax}{Pswitch}$) is determined by the allowable number of conditioning assembly cycles and the attitude control impulse requirements. The accumulator maximum pressure is selected such that the difference in accumulator propellant density, at maximum and switching pressures, multiplied by the accumulator volume, provides the mass of propellant required to perform all additional maneuvers, divided by the number of conditioner cycles. Since the wall thickness required for structural integrity increases with maximum pressure, a minimum weight tradeoff between increased volume and increased wall thickness must be performed in order to select the optimum accumulator size.

Thus, for a given lag time, minimum pressure, and number of conditioner cycles, there is a switching pressure and maximum pressure corresponding to each choice of accumulator volume, and for each combination of accumulator volume and maximum pressure, a unique accumulator weight can be assigned.

D-6.7 Accumulator Sizing Analysis Results - The conditioner assembly transient analysis showed that the hydrogen and oxygen equivalent lag times are both 0.50 sec. To provide a 500 lbf/in^{2}a chamber pressure for minimum total APS weight, the minimum accumulator pressures required are 1021 lbf/in^{2}a for the hydrogen and 914 lbf/in^{2}a for the oxygen. A conditioner assembly cycle limit of 50 per mission was selected for both hydrogen and oxygen. Nine +X translation maneuvers of appreciable magnitude are specified in the current seventeenth-orbit-rendezvous, mission duty cycle, and the conditioner assembly operates continuously during each of these maneuvers thus, nine conditioner cycles are inherently required for the conditioner. The 41 cycles remaining are for the attitude control and other axis maneuvering impulse. Figure D-80 shows the APS weight as a function of the maximum-to-switching pressure ratio for various values of switching-to-minimum pressure ratio and number of conditioning cycles, using the 0.5 second lag time and 500 lbf/in^{2}a chamber pressure. This figure shows that a switching-to-minimum pressure ratio of 1.13 in conjunction with a maximum-to-switching pressure ratio of 2.00 for both propellants yields the minimum subsystem weight. These pressure ratios correspond to switching and maximum pressures of 1153 lbf/in^{2}a and 2307 lbf/in^{2}a respectively for the hydrogen assembly and 1037 lbf/in^{2}a and 2074 lbf/in^{2}a respectively for the oxygen assembly. The corresponding accumulator volumes and weights are 29 ft^3 and 678 lb for hydrogen and 11.6 ft^3 and 320 lb for oxygen.

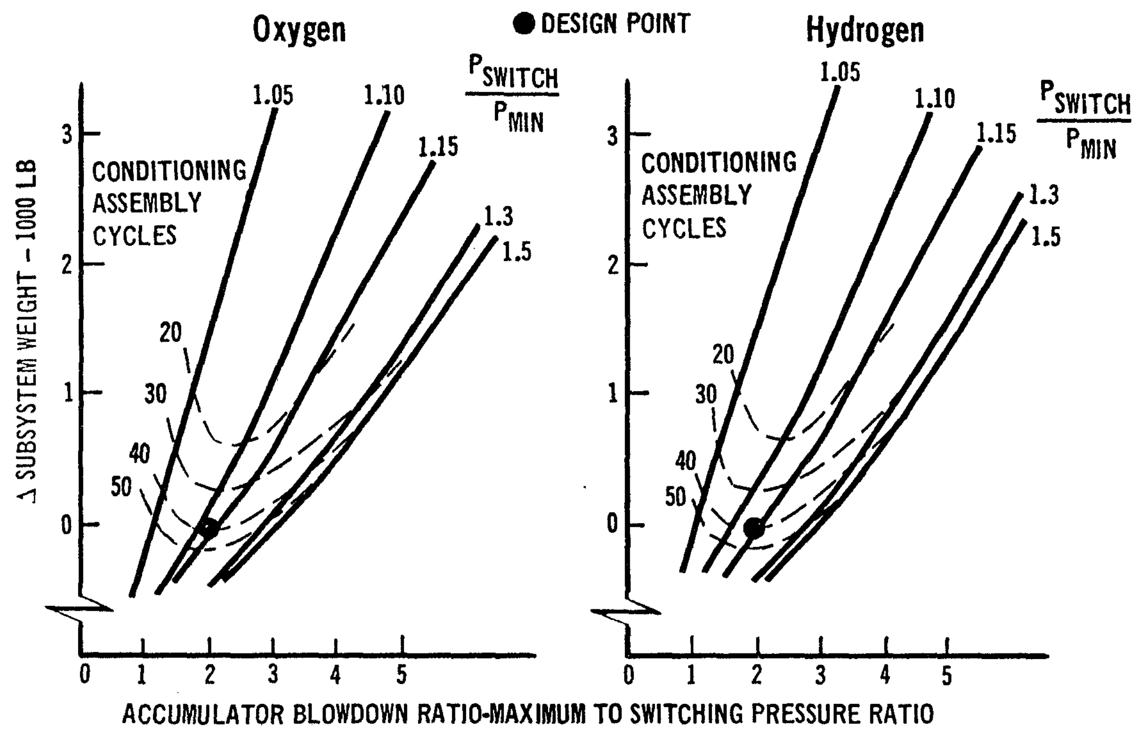

SIZING TOTAL IMPULSE $= 1.129 \times 10^6$ LB-SEC
CONDITIONING RESPONSE TIME = 0.5 SEC

ACCUMULATOR SIZING - Orbiter B

FIGURE D-80

D-7. THRUSTER ASSEMBLIES

The APS uses gaseous hydrogen oxygen thrusters to provide the impulse necessary for space shuttle vehicle attitude control and orbital maneuvers. The APS weight is very sensitive to the performance of these thrusters due to the magnitude of the APS total impulse requirements for all orbital maneuvers. To ensure a minimum weight subsystem, a detailed evaluation of thruster design and performance was conducted.

During Subtask A a film cooled thruster design (Figure D-81) was selected for the relative evaluation of the APS concepts for the three impulse levels considered. The dump/film cooled thruster represented a well-characterized design concept, with data available for a wide range of design conditions. This approach represented a compromise between thruster performance, design simplicity, and cost.

In order to verify that the relative weight comparison of the Subtask A concepts was not affected by the type of chamber cooling (thruster performance) assumed, the supercritical and the turbopump concepts of Subtask A were reevaluated for regeneratively cooled thrusters (Figure D-82). The performance level used for the regeneratively cooled concepts represented maximum performance without cycle life considerations. The turbopump APS, with regenerative cooled thrusters, was optimized for mixture ratio and chamber pressure for the three impulse classes considered. The resulting APS weights are shown in Figures D-83, D-84, and D-85. Optimum subsystem weight resulting from incorporating the regenerative cooled thruster in the supercritical subsystem is shown in Figure D-86.

The results of using the higher performance thruster is presented in Figure D-87, and shows that the weight advantage of the turbopump over the supercritical concept is amplified over the subtask A results. In those results, the turbopump APS was the lightest configuration and the supercritical APS the nearest competitor. Subsystem selection is not affected by selection of the higher performance regenerative cooled thruster, but absolute weight is strongly affected. Therefore in Subtask B, it was necessary to reevaluate thruster design and cooling methods to provide an optimum design, thus minimizing APS weight. This evaluation is presented in the following section, which discusses injector and combustion chamber concepts considered, as well as baseline design and performance.

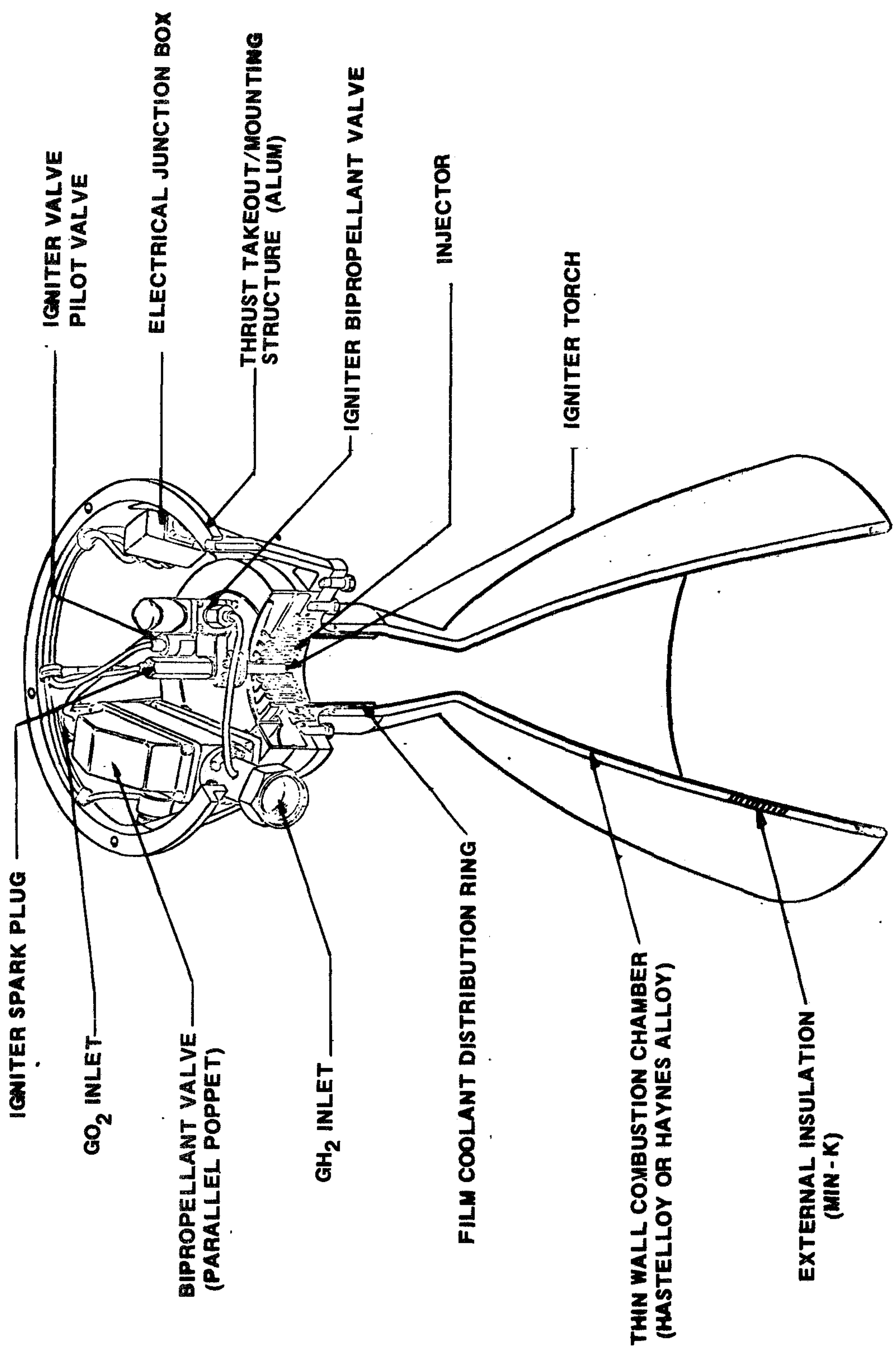

APS THRUSTER-DUCTED FILM COOLED

FIGURE D-81

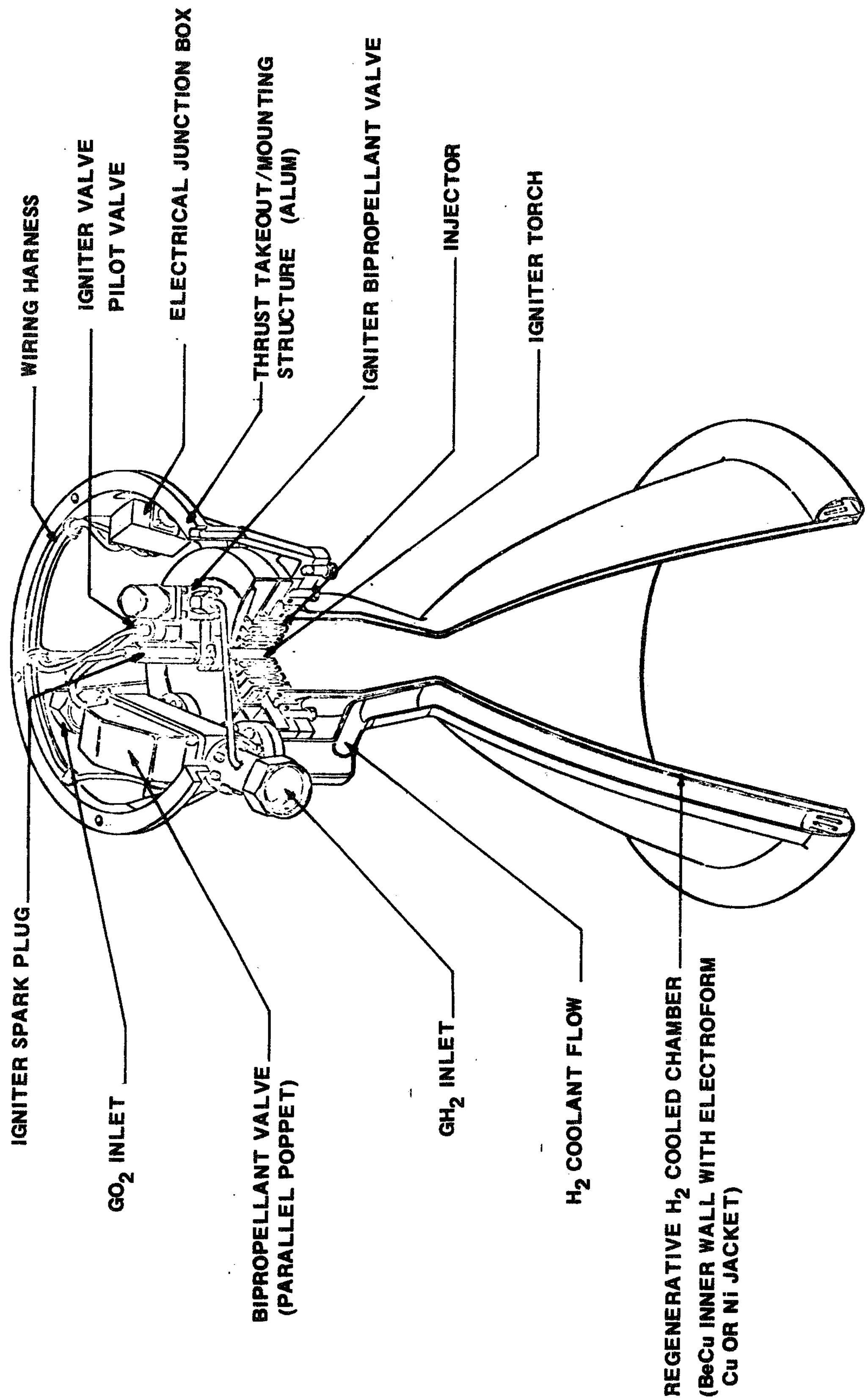

APS THRUSTER REGENERATIVELY COOLED

FIGURE D-82

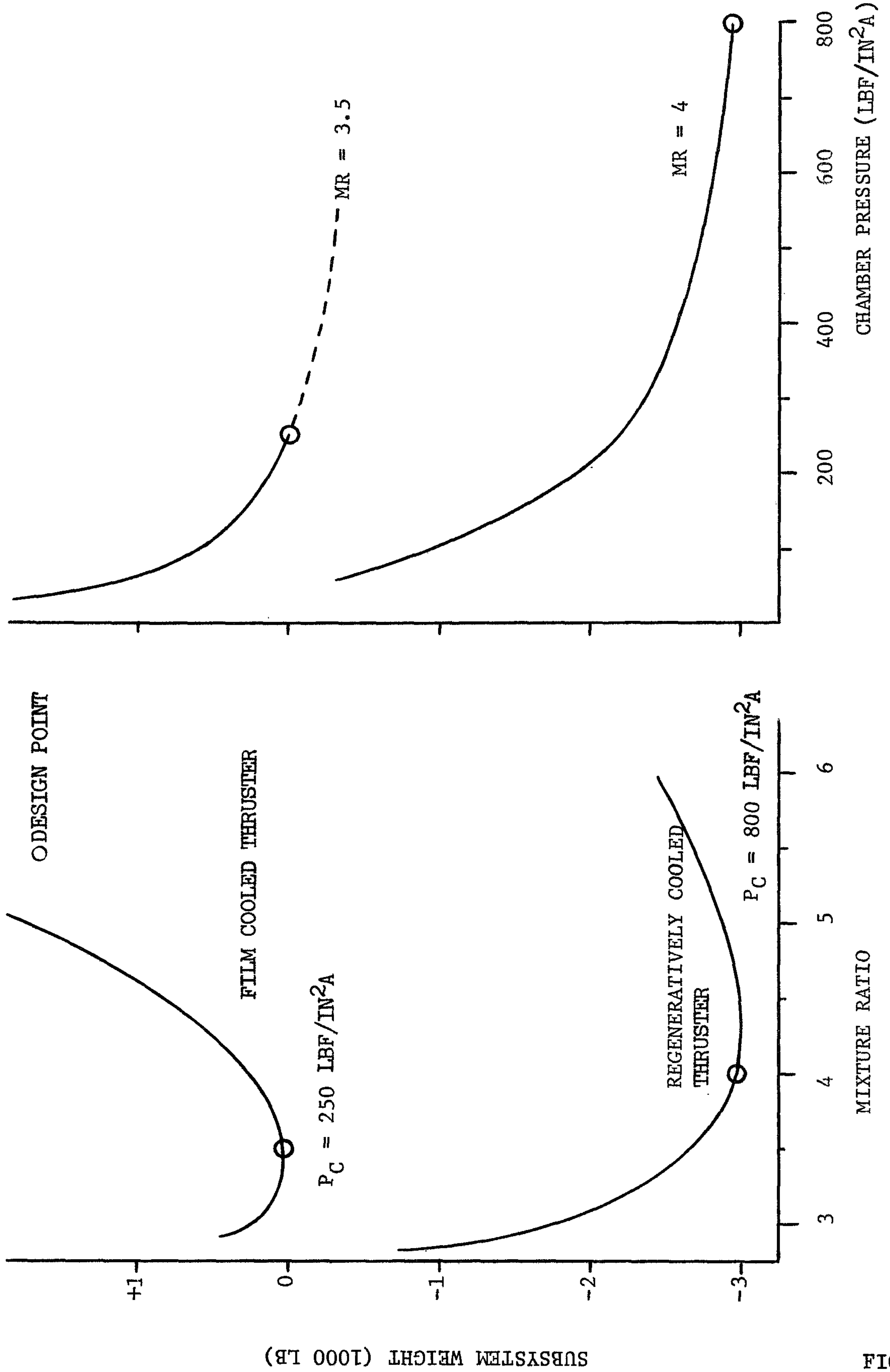

TURBOPUMP SUBSYSTEM; ORBITER A; ALL MANEUVERS

COMPARISON OF REGENERATIVE AND FILM COOLED THRUSTER CONCEPTS

FIGURE D-83

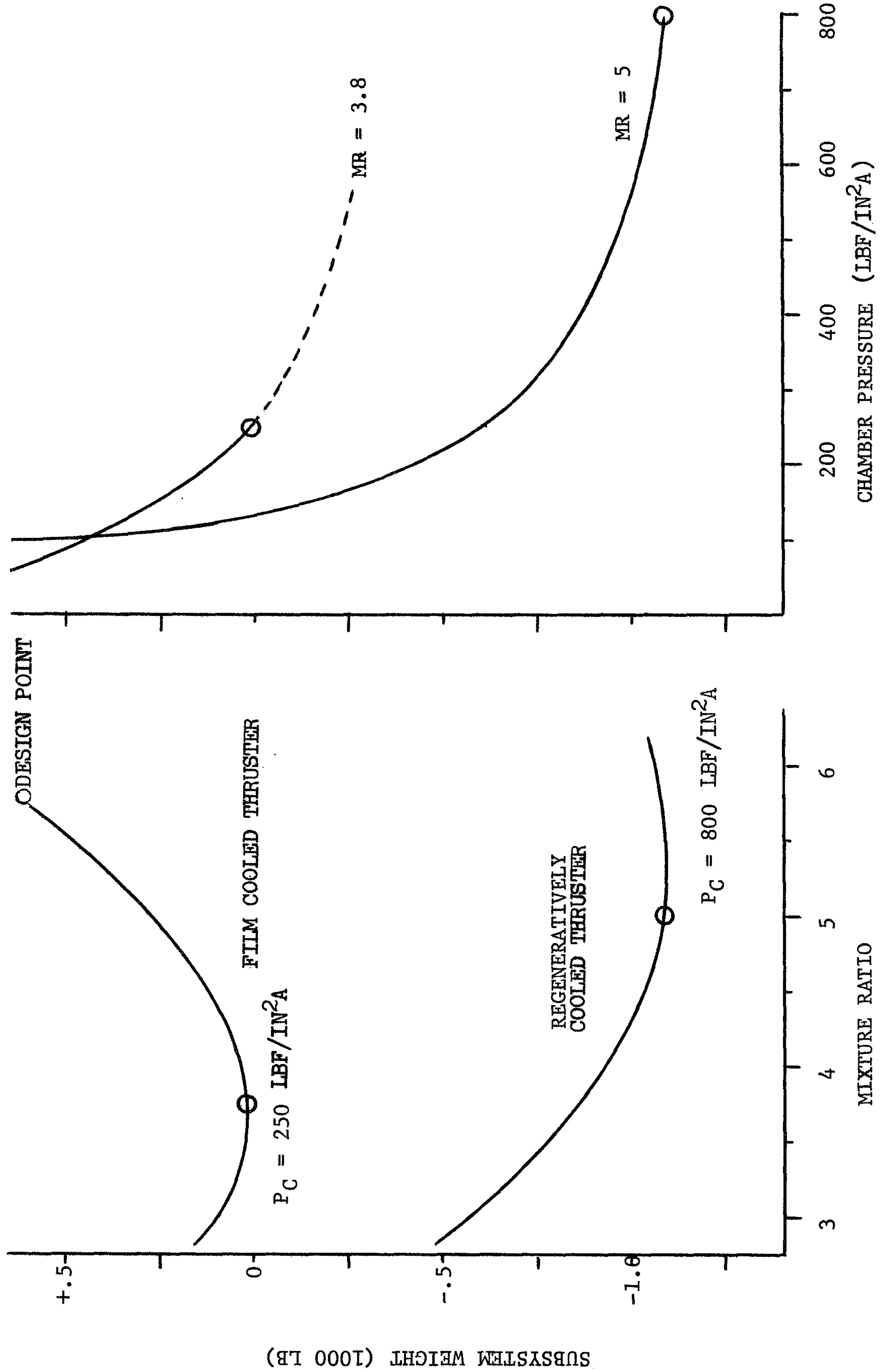

TURBOPUMP SUBSYSTEM; ORBITER A; ≤50 FPS MANEUVERS

COMPARISON OF REGENERATIVE AND FILM COOLED THRUSTER CONCEPTS

FIGURE D-84

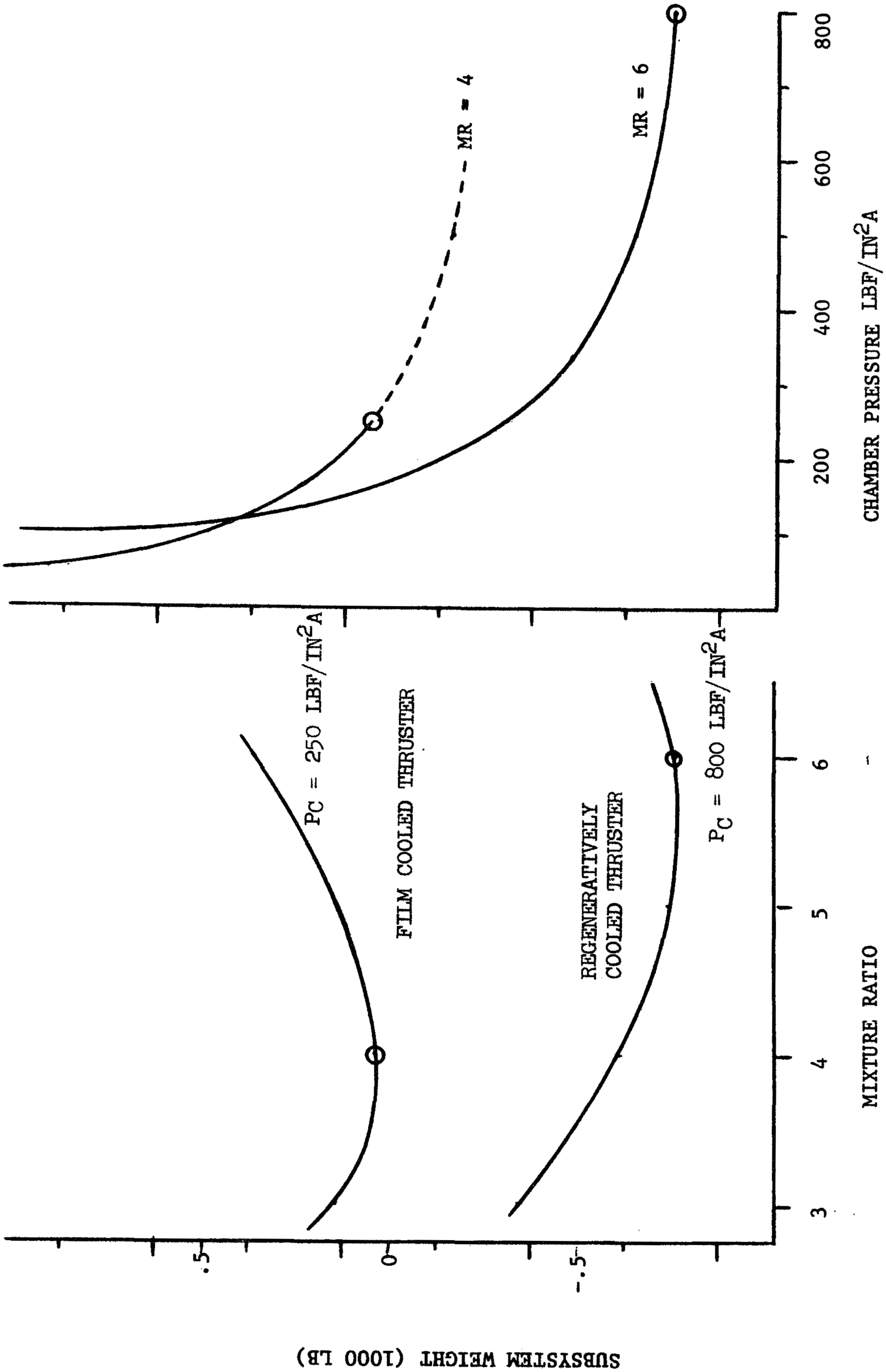

TURBOPUMP SUBSYSTEM; ORBITER A; ≤10 FPS MANEUVERS
○ DESIGN POINT

COMPARISON OF REGENERATIVE AND FILM COOLED THRUSTER CONCEPTS

FIGURE D-85

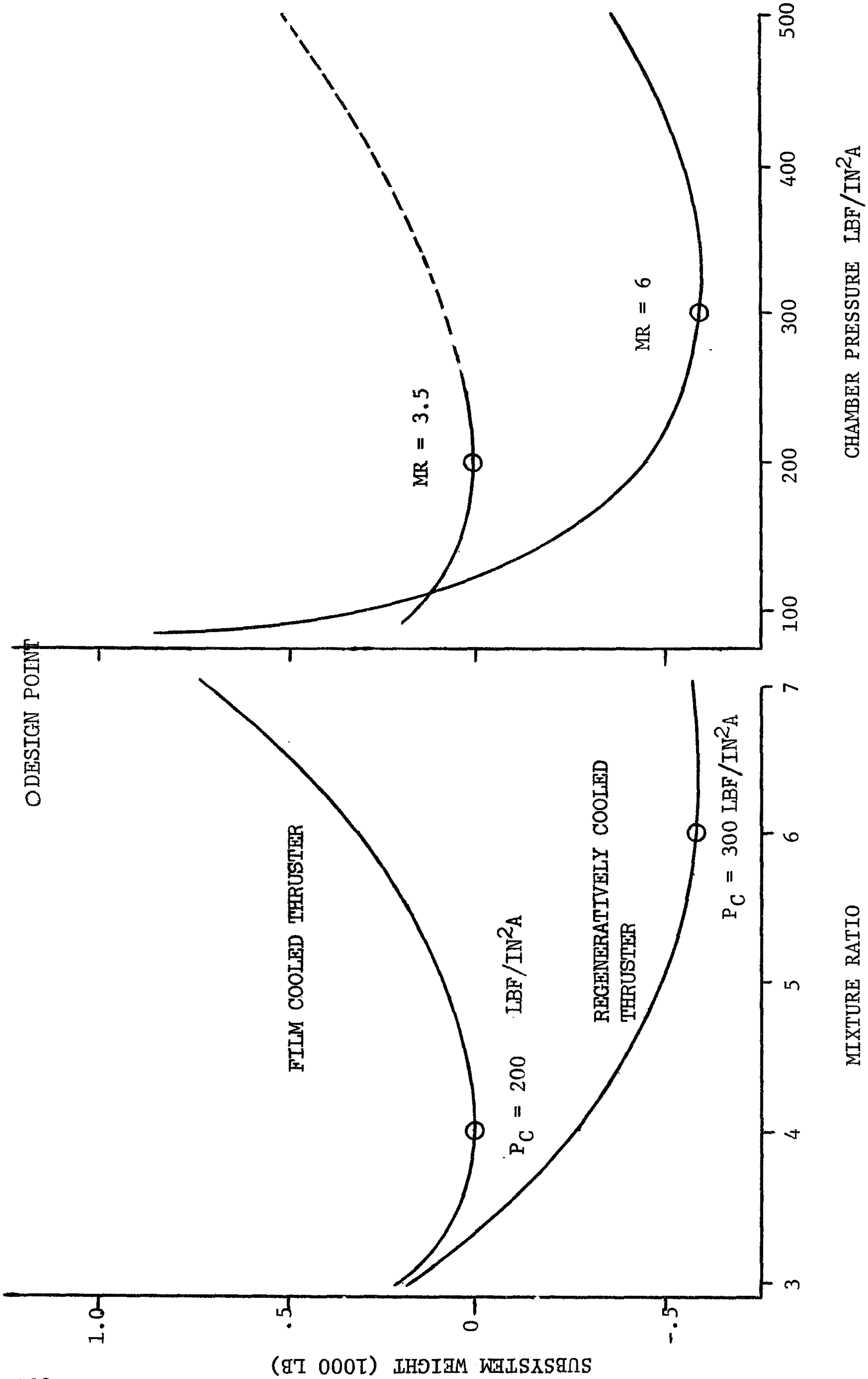

SUPERCRITICAL SUBSYSTEM; ORBITER A; ≤10 FPS

COMPARISON OF REGENERATIVE AND FILM COOLED THRUSTER CONCEPTS

FIGURE D-86

ORBITER A

- SIGNIFICANT EFFECT ON ABSOLUTE APS WEIGHT AND DESIGN POINT

- AMPLIFIES WEIGHT ADVANTAGE OF TURBOPUMP APS

	APS WT @ $\leq$10 FPS	
	FILM COOLED	REGENERATIVE
TURBOPUMP	6915	6112
SUPERCRITICAL	8164	7570

IMPACT OF BASELINE THRUSTER MODEL

FIGURE D-87

D-7.1 Thruster Concept Selection - The primary components of the APS thrusters are the propellant injector, combustion chamber, igniter, and propellant controls. Several design concepts were evaluated for each component. Injector and combustion chamber alternatives evaluated are shown in Figure D-88. In the selection of each component, consideration was given to the use of common components for attitude control and +X maneuver thrusters.

Selection of combustion chamber type and resultant coolant requirements is important, due to its influence on delivered impulse. Figure D-89 compares the performance of three basic chamber cooling concepts for a range of mixture ratios for a thruster design representative of the APS attitude control thruster. The performance of the dump/film cooled thruster characterized in Subtask A is shown by the lower curve. Performance for a fully regeneratively cooled thruster is presented to show the maximum performance capability of a thruster without consideration of cooling requirements for cycle life or adaptability of the nozzle to scarfing. The performance of a partial regeneratively cooled chamber with chamber and nozzle film cooling is the concept capable of meeting cycle life requirements and allows nozzle scarfing for attitude control installations while providing high performance. In addition, the thruster can be adapted for the major +X maneuvers without major redesign of the actively cooled portion of the thruster. The performance of the high pressure APS thrusters for attitude control and +X translation is shown in Figure D-90 for the final design point conditions.

For the Subtask B baseline design, the regeneratively/partially film cooled design was selected. This design provides a compromise between specific impulse performance and high cycle life capability.

D-7.2 Design - This thruster, shown in Figure D-91 utilizes an impinging coaxial injector, a regenerative/film cooled chamber with nozzle film cooling, electrical igniter, and parallel linked poppet propellant valves with pneumatic actuation. The propellant valves are packaged at the side of the thrust chamber to minimize overall thruster length, to shorten line connection between hydrogen valve and chamber inlet, and to provide ease of installation and maintenance. The igniter is an electrical spark type, and is sequenced to discharging hot gas down the center of the injector along the thruster axis. A separate igniter solenoid bipropellant valve provides the proper sequence for chamber ignition. The electrical circuit is redundant to increase ignition reliability.

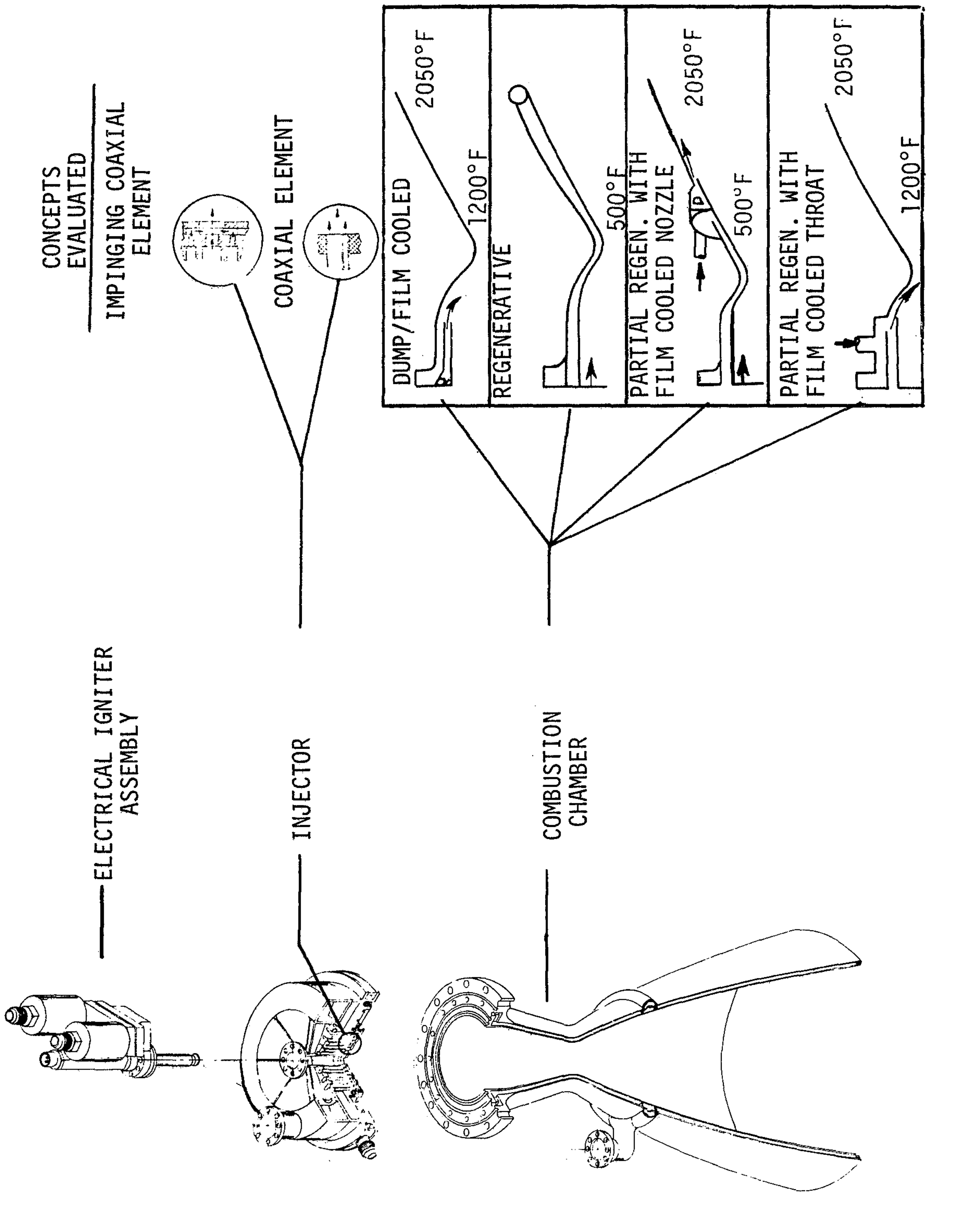

APS THRUSTER EVALUATION

FIGURE D-88

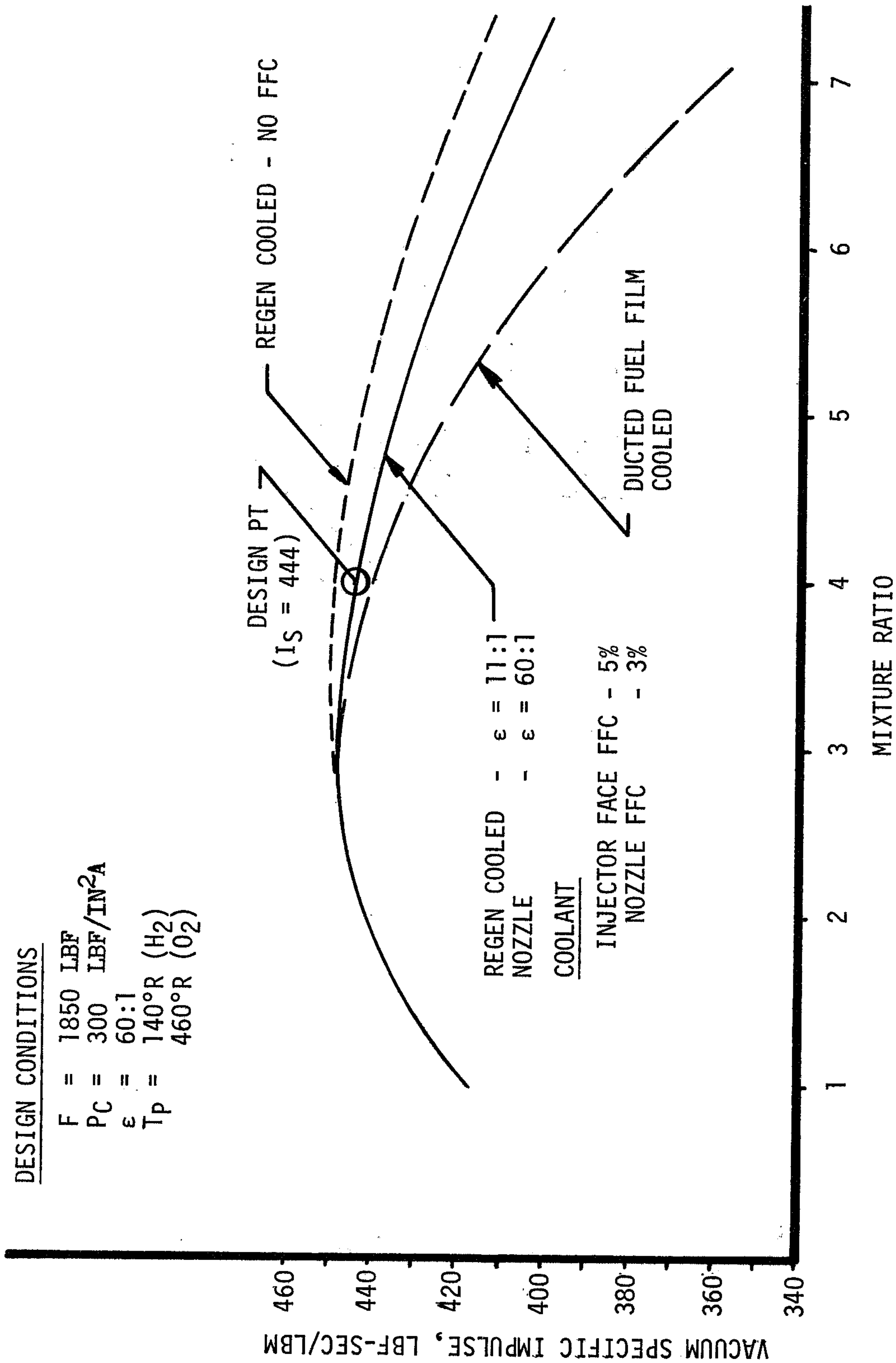

APS THRUSTER PERFORMANCE

FIGURE D-89

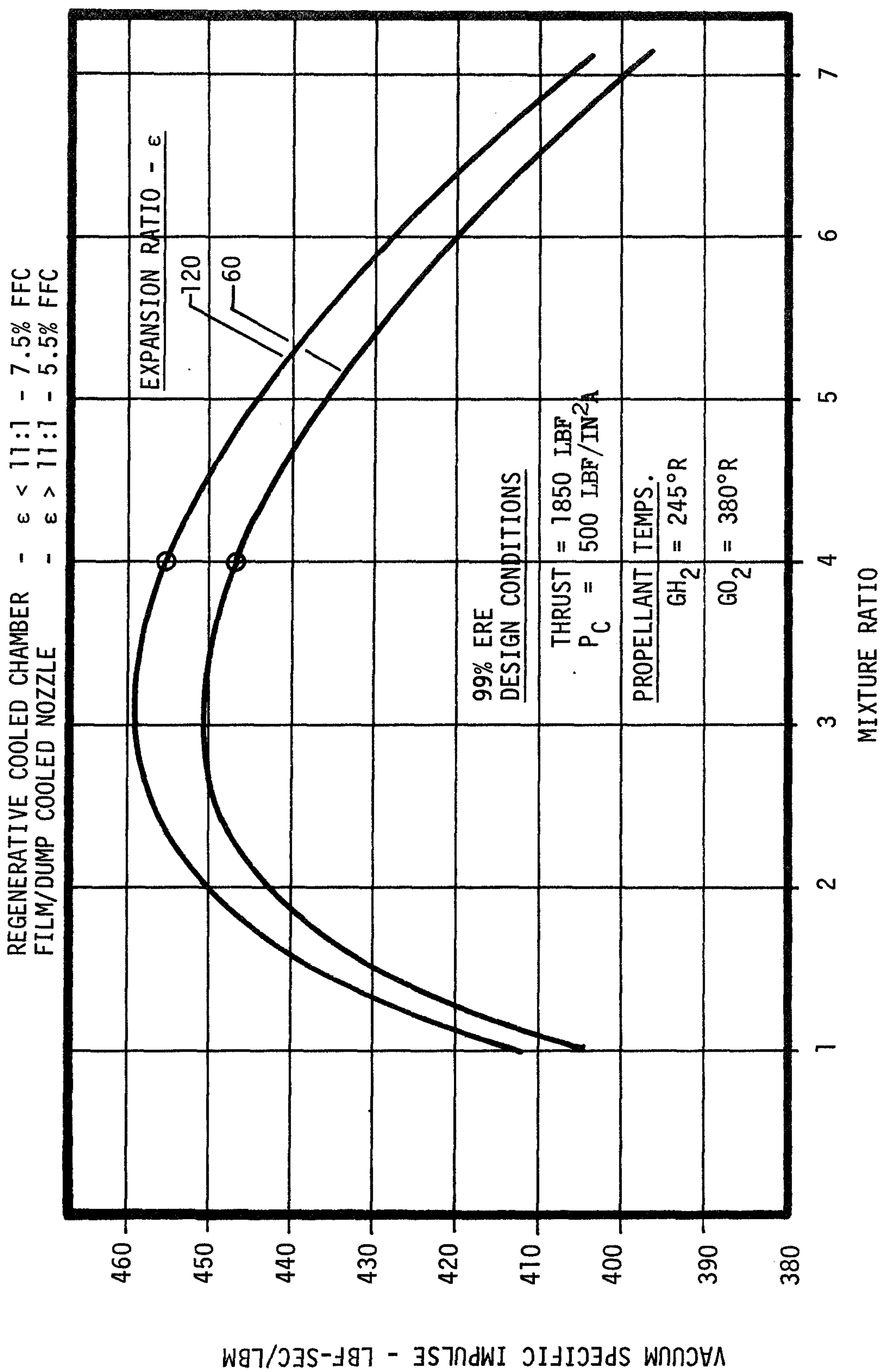

APS THRUSTER PERFORMANCE

FIGURE D-90

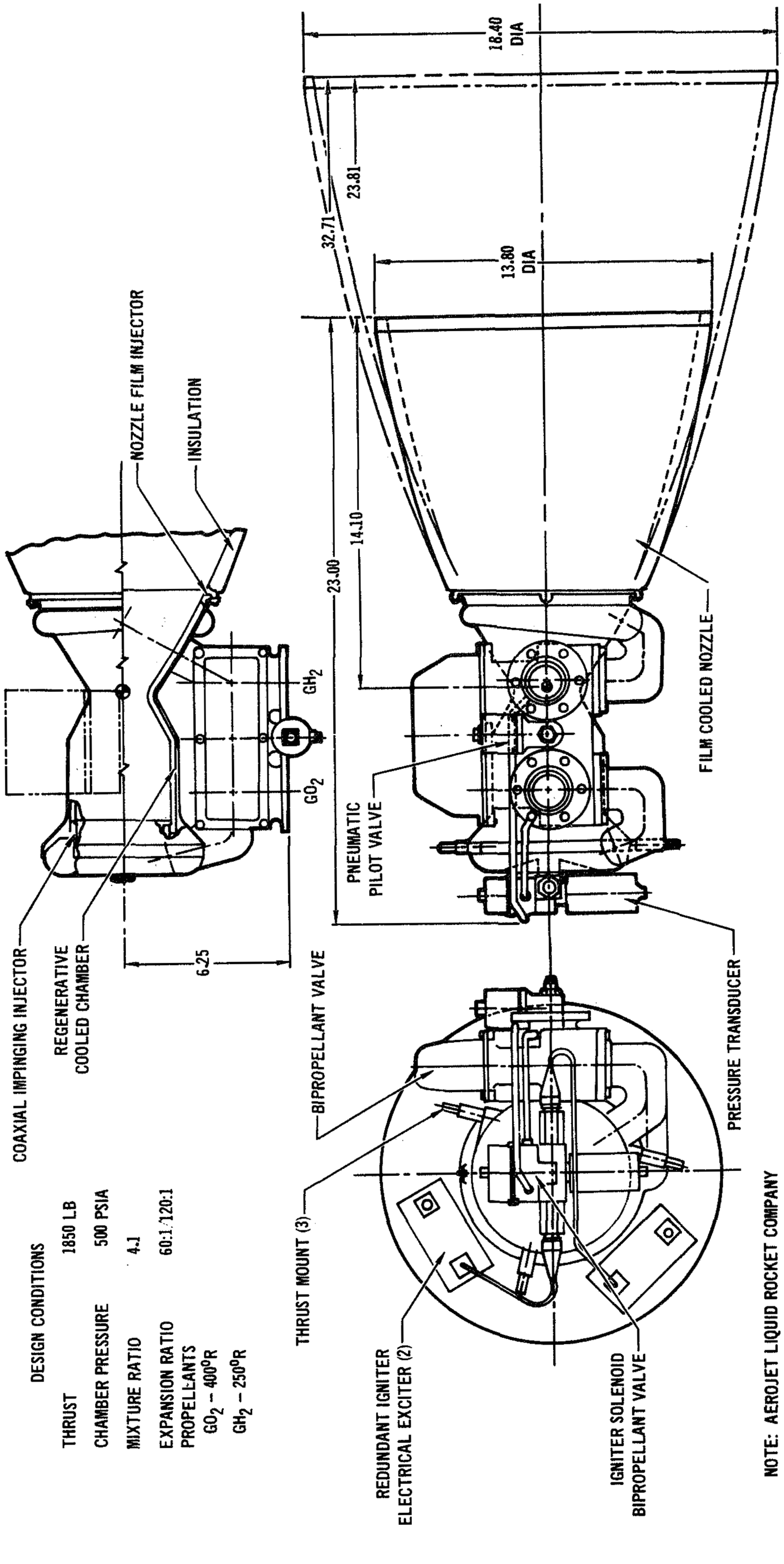

HIGH PRESSURE APS THRUSTER

FIGURE D-91

Injector - The injector concept selected for the high pressure APS thruster is an impinging coaxial design. This is a variation of the more conventional coaxial element wherein the fuel is injected paralled to and concentric with the axially directed oxidizer stream. The impinging coaxial element injects the hydrogen normal to the oxygen. The concept uses a concentric ring manifold attached to a face plate assembly containing internal fuel passages. The oxidizer channels discharge into holes which go through the face plate parallel to the chamber axis. The fuel channels feed into a labyrinth of passages in the face plate which provide regenerative and transpiration cooling of the face as well as fuel entry into each element normal to the oxidizer stream. In arriving at the coaxial type element, several concepts were considered. These include coaxial element, impinging coaxial element, impinging orifice, vane, and hyperthin.

The coaxial element design combined with a transpiration cooled face plate represents a "classical" injector design for hydrogen-oxygen propellants. This concept and the selected impinging coaxial element concept previously discussed are the two recommended approaches being evaluated by ALRC on Contract NAS 3-14354, "Hydrogen-Oxygen APS Engines", for NASA-Lewis Research Center. The conclusions reached from this injector evaluation favor the impinging coaxial design.

Combustion Chamber - The combustion chamber consists of a regeneratively cooled section, extending from the injector through a convergent/divergent nozzle. The regeneratively cooled chamber terminates at an ϵ = 11.1. The subsequent portion of the nozzle is considered as a separate component, due to its significantly different thermal and pressure environment.

The regenerative cooled chamber selected for the high pressure APS thruster employs rectangular channel geometry and a high conductivity copper alloy. The design is a single pass concept with hydrogen entering the chamber at an area ratio of 11:1 and flowing forward through 77 channels toward the injector. The flow passages discharge into a manifold which in turn feeds the injector. This manifold also supplies hydrogen to a fuel film coolant ring which distributes a small percentage of fuel down along the chamber wall. The chamber is fabricated from a Be-Mg-Cr-Cu alloy forging.

To achieve an optimum design, several heat transfer programs were used. One program defined gas side film conditions, and, in combination with another program, defined thermal conditions within the channels. Various percentages of film cooling were selected, along with variations in channel size. By means of cross plotting, a family of curves was generated defining the characteristics of the chamber for a specific set of conditions, such as propellant temperature, chamber pressure, and thrust. Based on specified thruster design conditions, a specific design was achieved which exhibits the characteristics noted in Figure D-92. This heat transfer analysis then allowed prediction of thruster cycle life. The results are shown in Figure D-93. The information on this curve is obtained by calculating the total strain range ($\Delta\varepsilon_t$).

$$\Delta\varepsilon_t = 2\alpha\Delta t$$

α = coefficient of thermal expansion

Δt = temperature gradient across wall obtained from Figure D-94.a

and entering this value in Figure D-94.b along with appropriate wall temperature from Figure D-95.

As noted in Figure D-93 for a hydrogen design flow temperature of 250°R, approximately 7 percent fuel film coolant flow is needed to ensure the desired cycle life of 10^5.

Nozzle Extension - The high pressure APS thruster has a nozzle extension attached to the regeneratively cooled chamber at an area ratio of 11:1. This attachment point was based on a balance between pressure drop, wall temperature, percentage of fuel film cooling, weight, and fabrication. Resulting wall temperature is shown in Figure D-96, and allows use of a high temperature alloy as opposed to a refractory metal. Hastelloy X is the material selected; it will extend from the attachment point to the exit diameters of 12.9 in and 18.2 in for area ratios of 60 and 120 respectively. Cooling of the extension will be achieved by introducing 4 to 5 percent fuel flow, depending on the area ratio at the point of attachment, to the regenerative cooled portion.

The film cooled nozzle extension must be capable of extended multicycle operation at high temperatures in the exhaust environment. This leads to consideration of high temperature alloys and refractory metals. Two high temperature alloys were examined, Hastelloy X and Haynes Alloy No. 188. Hastelloy X is a nickel base alloy which possesses exceptional strength and oxidation resistance. The alloy has excellent forming characteristics, and can be readily welded to itself and to stainless steel. Hydrogen compatibility with Hastelloy X will not be a problem, since the embrittling effects of hydrogen are most pronounced using

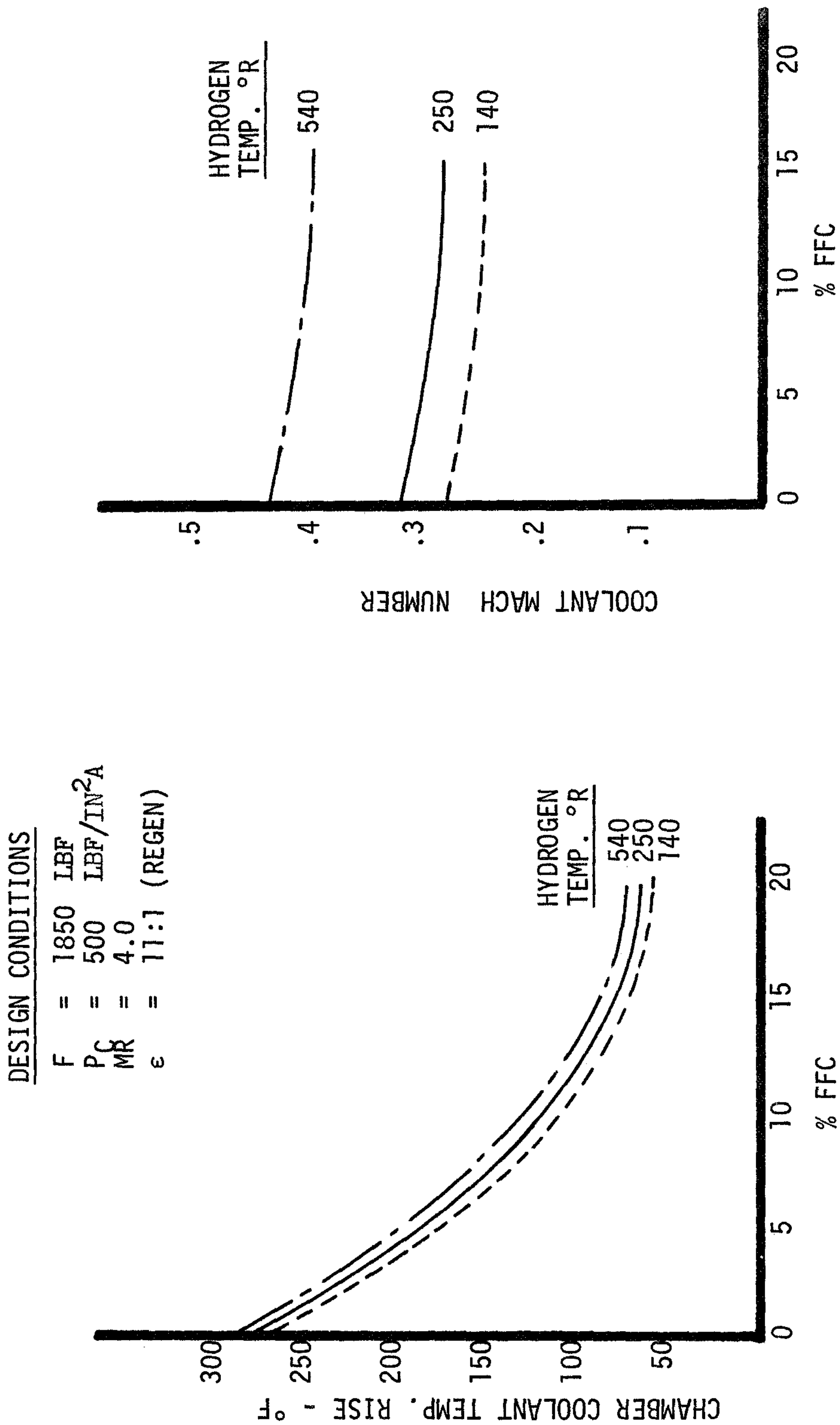

REGENERATIVE COOLED CHAMBER

FIGURE D-92

DESIGN CONDITIONS

F = 1850 LBF
P_C = 500 LBF-IN^{2}A
MR = 4.0

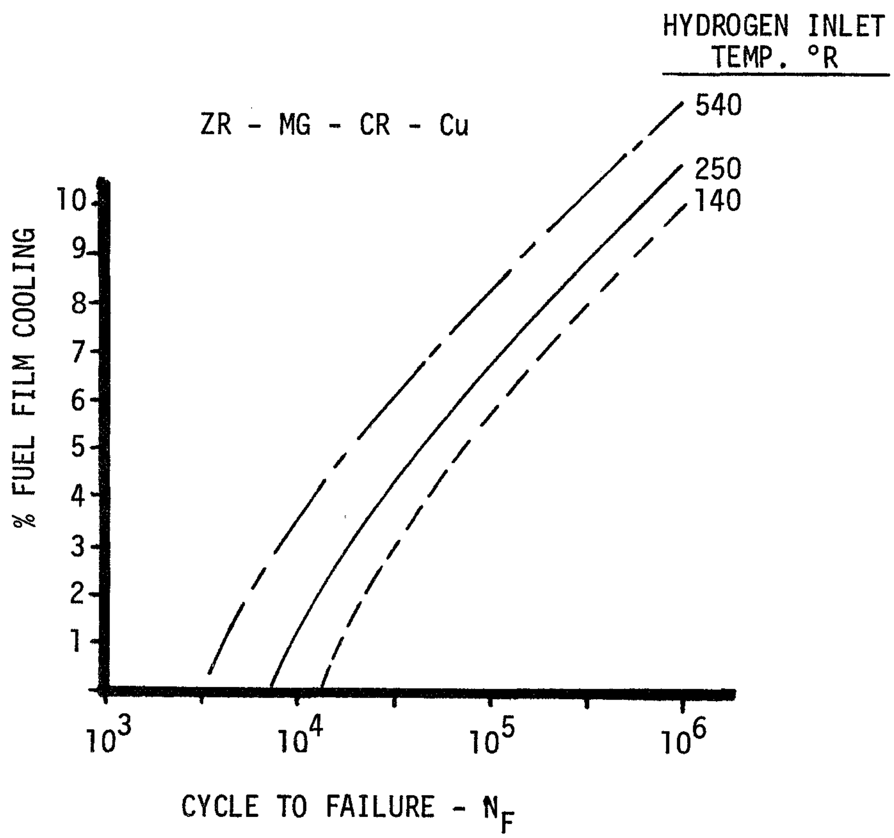

REGENERATIVE COOLED CHAMBER CYCLE LIFE

FIGURE D-93

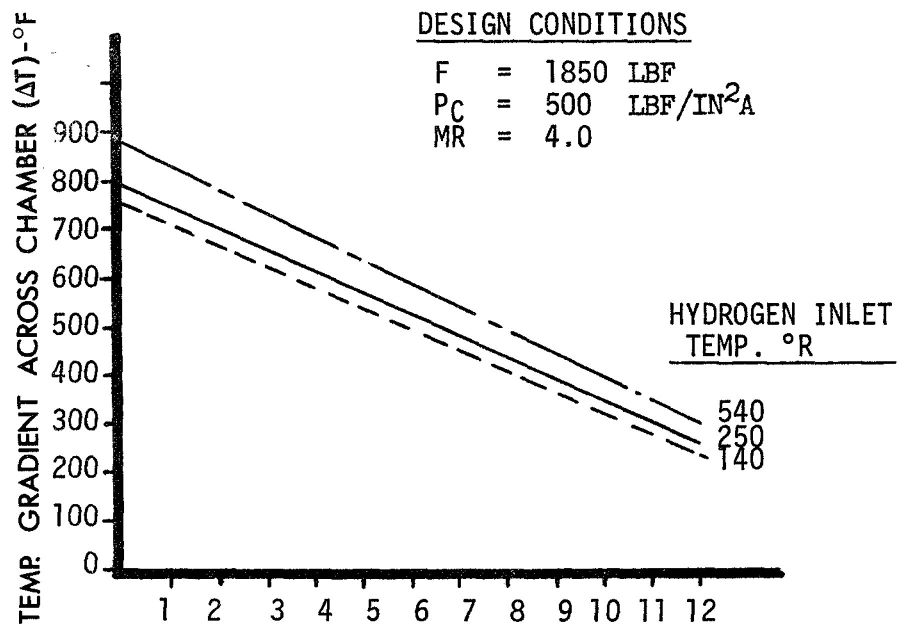

(a)

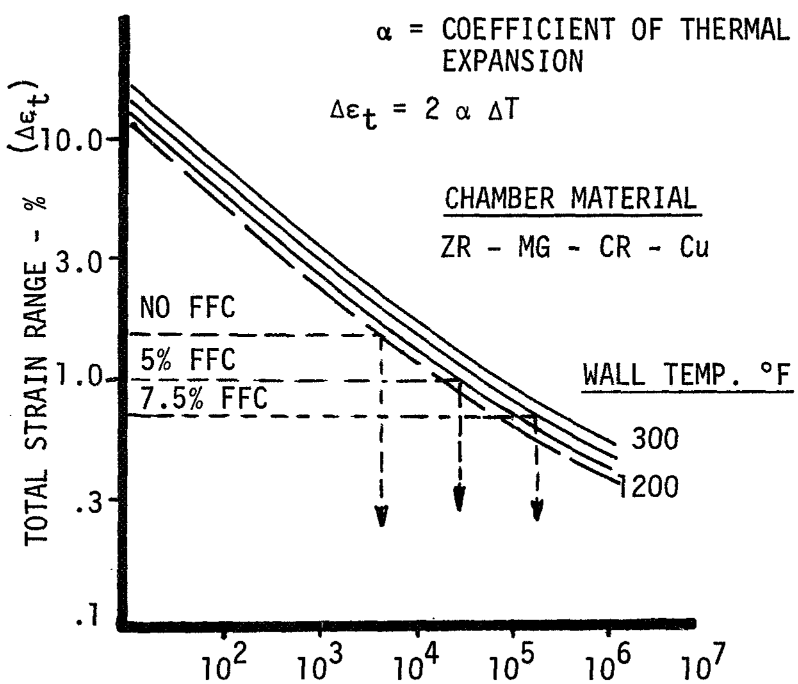

(b)

REGENERATIVE COOLED CHAMBER FIGURE D-94

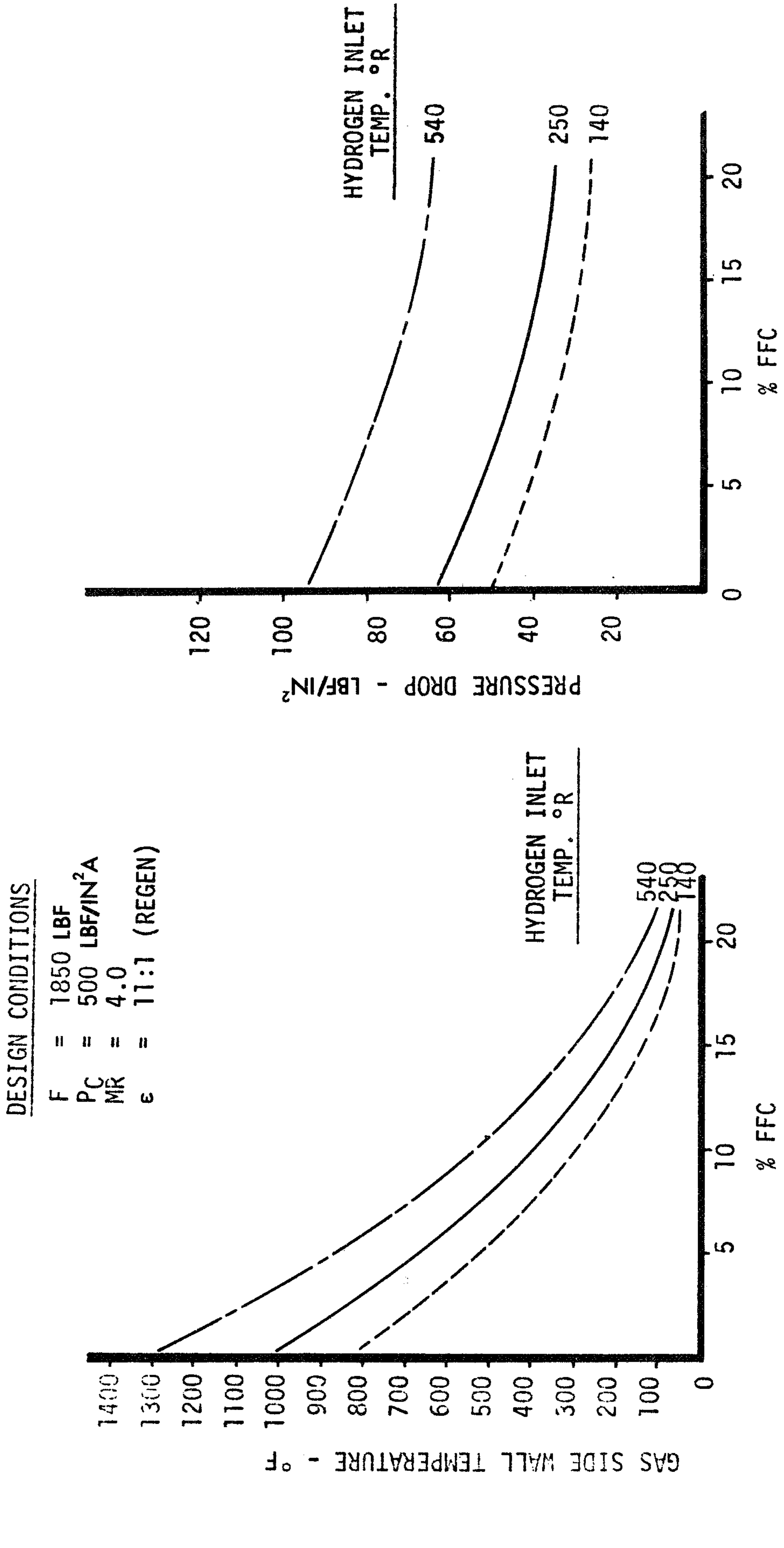

REGENERATIVE COOLED CHAMBER

FIGURE D-95

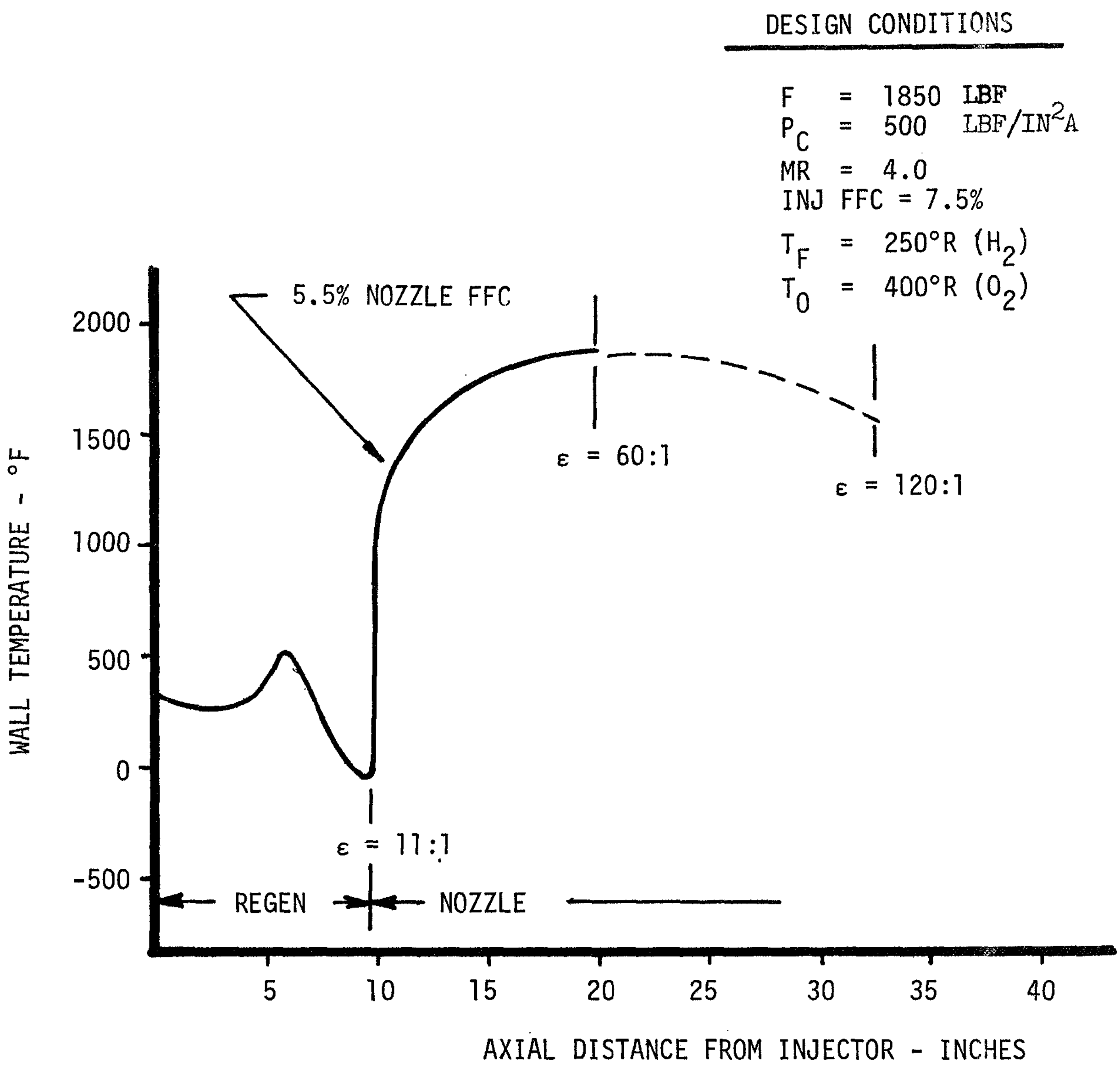

CHAMBER & NOZZLE WALL TEMPERATURE

FIGURE D-96

high pressure, high purity hydrogen at room temperature. The Hastelloy X would be exposed only to low pressure hydrogen highly contaminated with water and at an elevated temperature. The oxidation resistance of Hastelloy X is excellent; it is used in jet engine afterburner components, turbine blades, and nozzle vanes. Recent NASA tests on the resistance of nickel base materials under cyclic oxidation and thermal fatigue conditions showed Hastelloy X was among the most crack resistant of the alloys tested.

Haynes Alloy No. 188, a cobalt-base material provides strength superior to Hastelloy X at temperatures above 1800 F, but can be worked and welded similar to Hastelloy X. The Haynes 188 alloy is higher in cost, however, than Hastelloy X. The compatibility of Haynes 188 with oxidizing gases is comparable to Hastelloy X. Data on the compatibility of the Haynes 188 cobalt-base alloy in hydrogen environments is not available but is estimated to be similar to the Hastelloy X. The fatigue characteristics of this alloy are similar to Hastelloy X. Hastelloy X was selected because of slightly better fabricability and lower cost.

Columbium, molybdenum, and tantalum alloys were also considered for nozzle extensions. These refractory metals have severe oxidation limitations and coatings are not sufficiently developed to provide the design cycle life.

Igniter Description - The igniter for the APS thruster utilizes the spark discharge technique. The electrical ignition is attained by a spark discharge across the oxidizer flow stream. The addition and mixing of a small quantity of fuel immediately downstream of the spark-excited oxygen causes ignition within the igniter chamber. Figure D-97 depicts this basic design.

The igniter assembly consists of a high response bipropellant valve, a valve mounting adapter, an igniter body, an igniter combustion chamber, a spark plug, and an igniter coolant jacket.

The chamber of the pilot igniter is made from Hastelloy X. The body is made from a magnetic stainless steel to provide shielding of the electromagnetic radiation from the spark discharge. The spark igniter is a commercially available unit as is the spark igniter power supply.

The sequenced electrical igniter provides a positive and fast ignition of primary injector propellant. Figure D-98 presents experimental data during thruster pulsing and shows the typical transient characteristics for 1500 lb thrust APS engine firing a sequence of 0.100 sec duration pulses with 0.150 sec off. The initial valve signal opens the thrust chamber valve actuation pilot valve, the

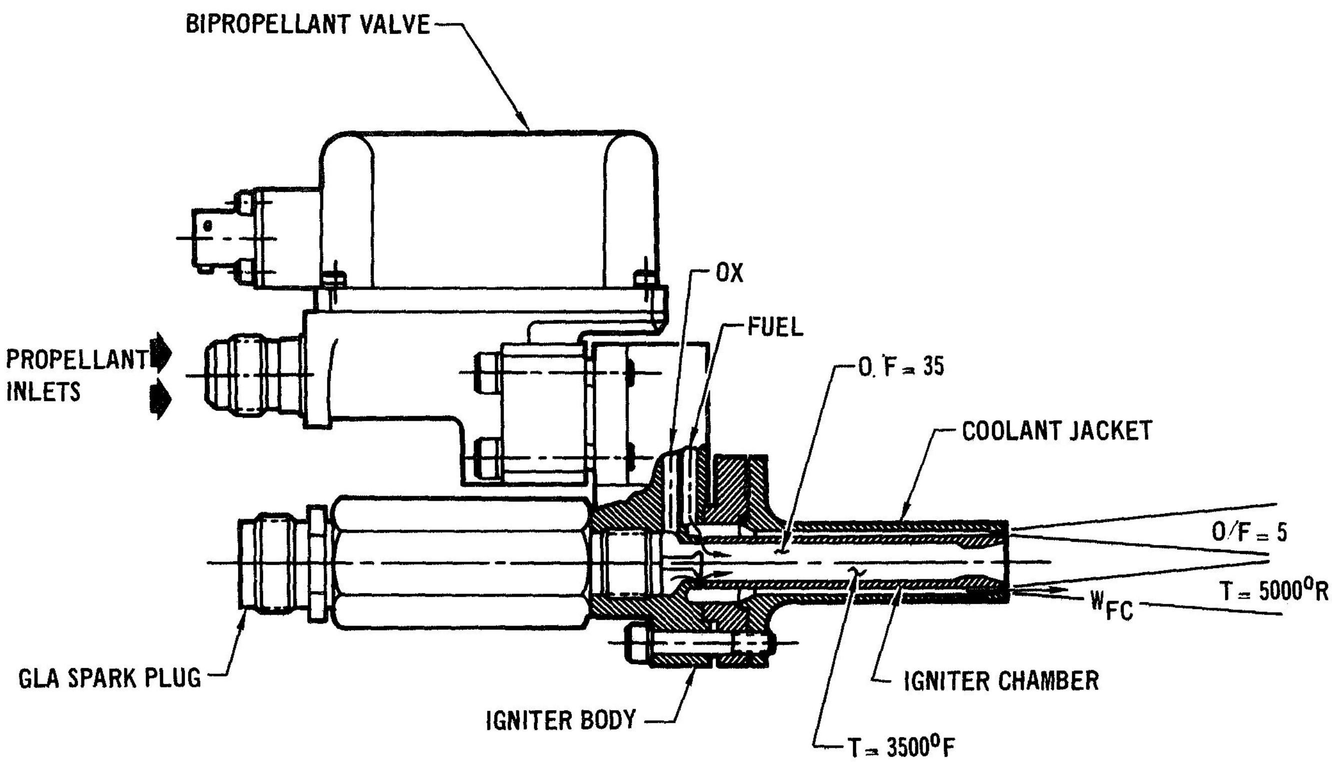

APS SPARK IGNITER

FIGURE D-97

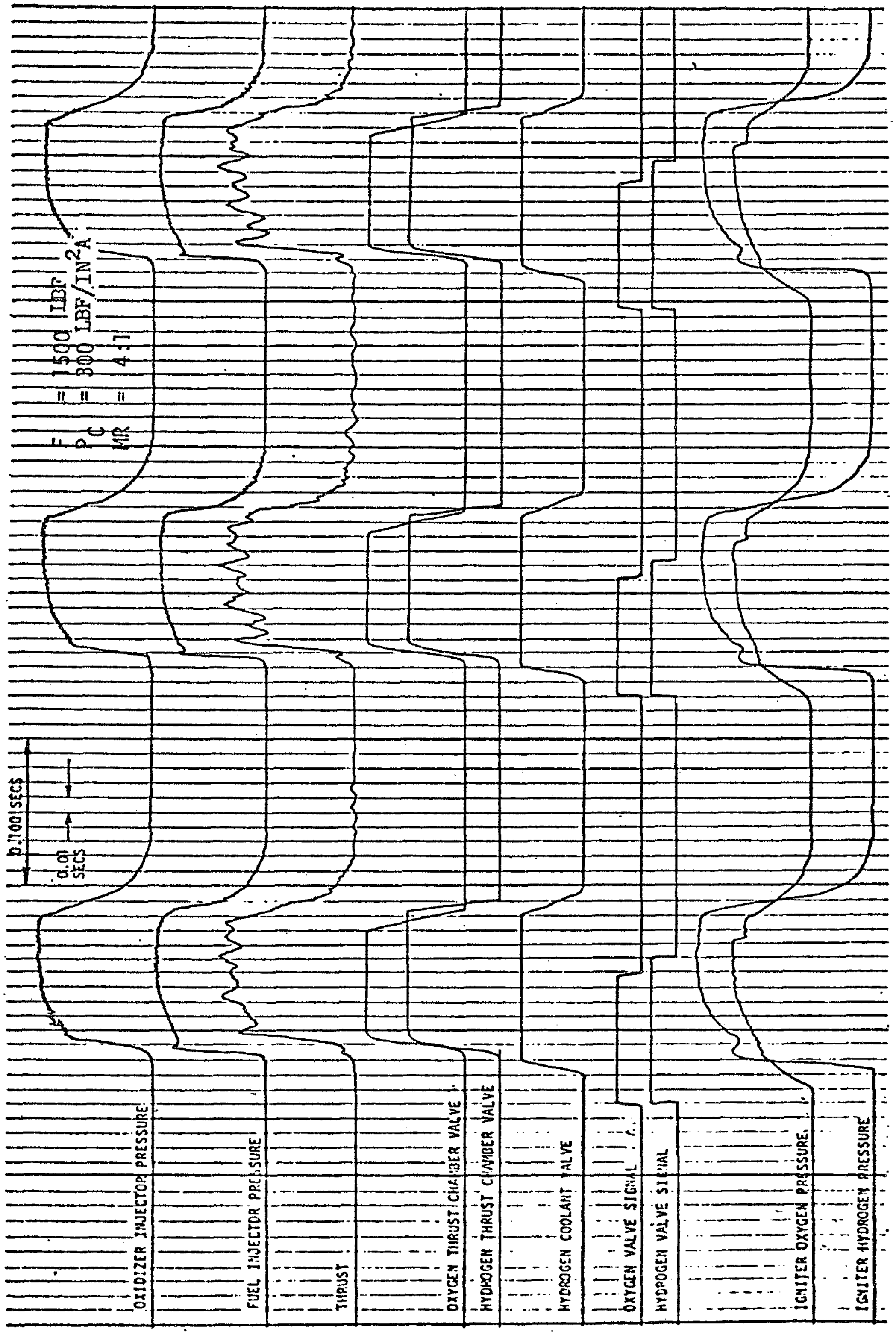

APS THRUSTER PULSING OPERATION - TEST DATA

FIGURE D-98

igniter valves, and the spark current for the electrical sequencer. The igniter torch is established in 0.025 sec as shown by the rising igniter injector pressure levels. The primary engine thrust chamber valves begin to open in 0.035 sec and are fully open 0.010 sec later. The thrust trace parallels valve opening rate and full thrust is achieved 0.045 sec after initial valve signal. The cycle is reversed for shutdown.

Valve Description - The propellant control valve for the APS thruster is a linked parallel poppet type with pneumatic actuation. The valve is shown in Figure D-99. This configuration has been tested under NASA-Lewis contract Number NAS 3-14354 and has demonstrated repeatable travel times of 0.010 sec. This type valve provides the response capability required for pulse mode operation. The poppet type valve also seals with a minimum of sealing surface wiping or surface shear which is desirable from a cycle life standpoint.

The poppet seat material is KEL-F which exhibits excellent compatibility with the propellants. Reasonable seal stress levels are achieved by control of the seat surface area and by balancing the actuator spring force. The single pneumatic actuator is coupled to both of the poppet shafts with a common link. The fast response pilot valve sequences regulated line hydrogen pressure into the pneumatic actuator to open the valve. The actuator cavity is vented when the pilot valve is sequenced closed and the actuator spring closes the valve. Venting is accomplished internally through the thruster assembly.

The igniter assembly uses separate propellant control valves to sequence the igniter during the engine start transient. The igniter torch is established prior to the initial primary propellant flow through the injector to assure smooth ignition transients. The valving for the igniter is a linked bipropellant valve actuated by a fast response solenoid to provide igniter torch ignition and operation within 0.035 sec after initial electrical signal to the engine. The linked valves provide the correct propellant entry into the igniter torch chamber.

D-7.3 Thruster Performance - Delivered specific impulse for the high pressure thruster was calculated using the JANNAF "Simplified Method" standardized performance evaluation technique. With this procedure each of the performance losses which make up the difference between delivered and theoretical vacuum specific impulse was calculated for the specific operating point. These losses are defined and are a result of: kinetic limited reactions, incomplete energy release, boundary layer heat transfer and shear drag, non-axially directed exit momentum,

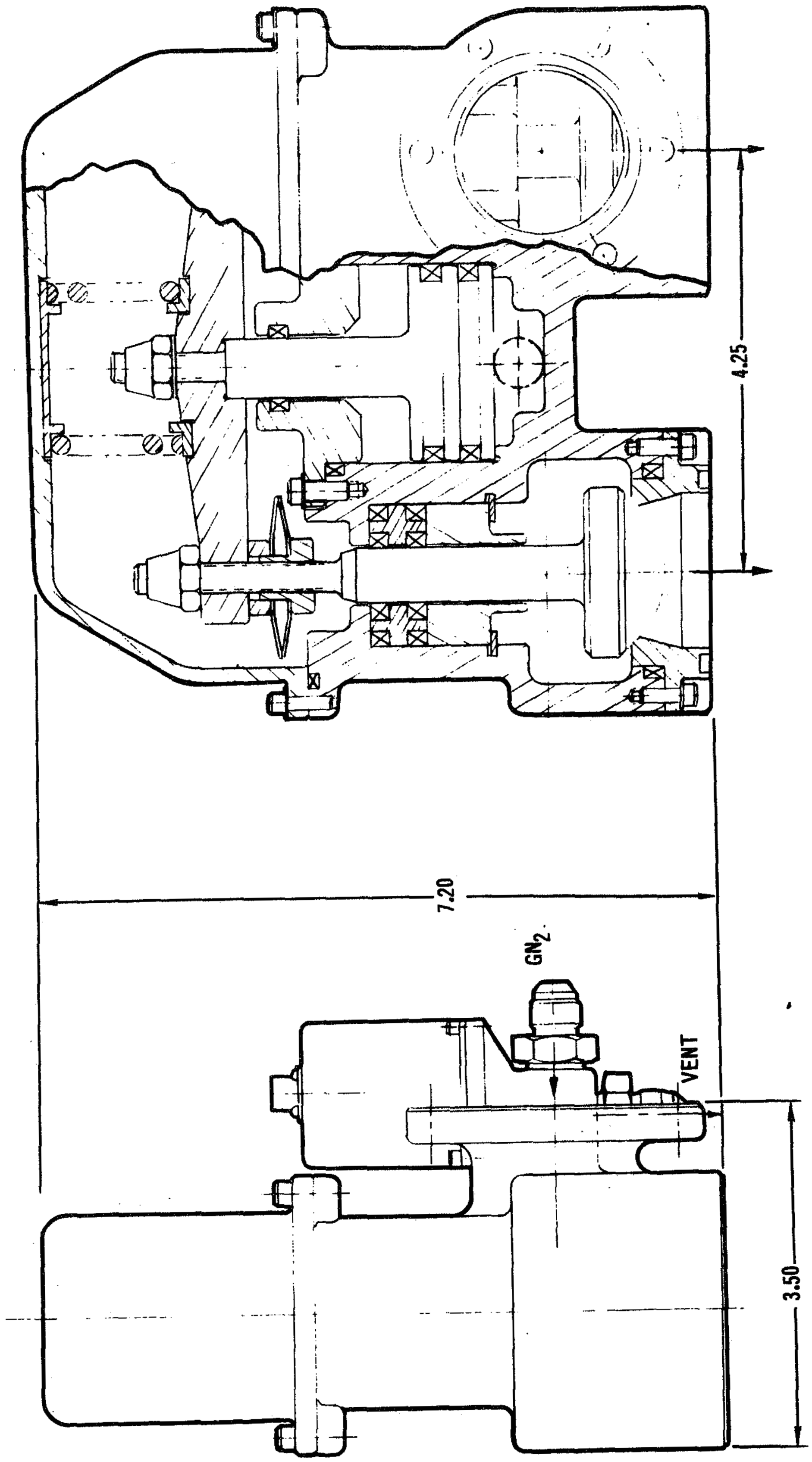

APS HIGH PRESSURE BIPROPELLANT VALVE

FIGURE D-99

mixture ratio maldistribution, propellant impurity, and supplemental cooling flow. The losses due to boundary layer heat transfer and non-axially directed exit momentum were computed via standardized loss charts. Kinetics and impurity losses were computed using the One-Dimensional Kinetics Program. Energy release losses were based on current gas/gas APS thruster technology data received from current testing under NASA-Lewis Research Center Contract NAS 3-14354. With this performance calculation procedure, the thruster performance was calculated for each operating point commensurate with the propellant inlet enthalpies, thruster size, chamber pressure, and mixture ratio.

Two of the JANNAF performance losses are based on test data. These losses are the result of incomplete energy release and supplemental film coolant flow. In order to determine these losses, computation techniques have been developed which have subsequently been verified by test data.

Energy release losses have been identified at 1 percent commensurate with a 99 percent energy release efficiency. Justification of this selection is shown in Figures D-100 and D-101 where the energy release efficiency of five injector concepts are shown for two classes of injector. The impinging coaxial injector with the "I" triplet pattern, Figure D-100, employs momentum exchange mixing to obtain a 99 percent energy release in a 5.5 in length chamber.

Figure D-101 developes a 99 percent energy release efficiency in an 8-inch chamber as a result of turbulent shear mixing between the gaseous oxidizer and fuel. Either of these two concepts have demonstrated the required 99 percent energy release efficiency which was the value used to calculate the thruster performance.

The other loss results from employment of supplemental fuel film cooling. A thermal exchange model has been developed which evaluates the cooling performance loss with a two stream tube mixture ratio maldistribution loss model. The coolant stream consists of heated hydrogen at a predicted mean bulk temperature which extracts enthalpy from the core stream assumed not to mix with the coolant and at an increased uniform mixture ratio. A mass summation of the coolant impulse and the reduced enthalpy core denotes the shifting equilibrium performance loss due to cooling. An additional loss results due to increased kinetics losses since the core mixture ratio is shifted higher due to the removal of hydrogen flow. This kinetics loss is charged to cooling in the performance loss summary. Justification of this loss computation method is shown in Figure D-102. There the

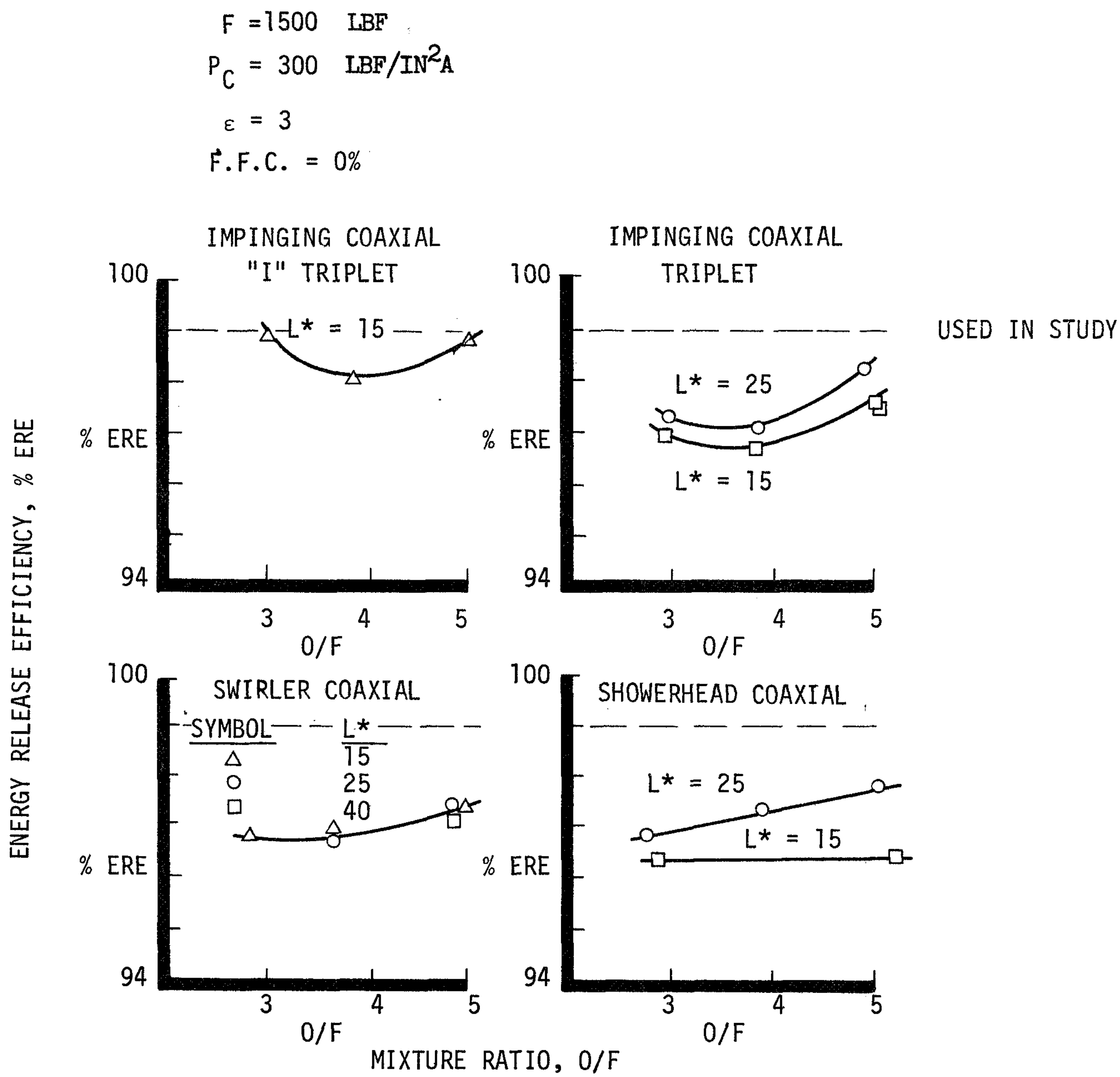

EFFECT OF MIXTURE RATIO ON ENERGY RELEASE EFFICIENCY

FIGURE D-100

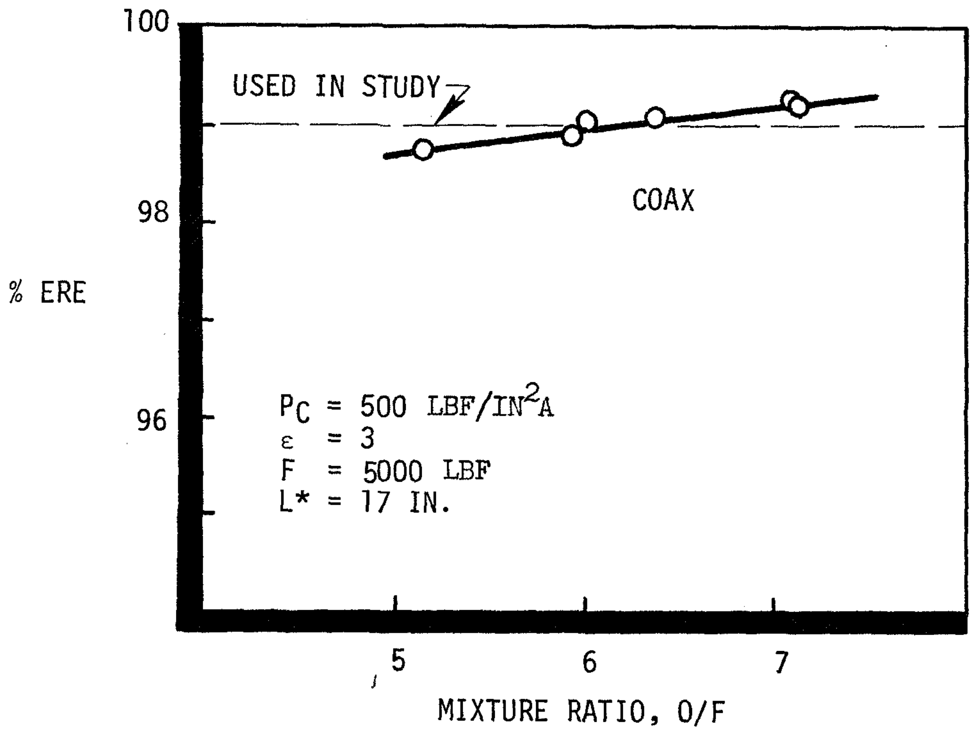

ENERGY RELEASE EFFICIENCY FOR COAX INJECTOR

FIGURE D-101

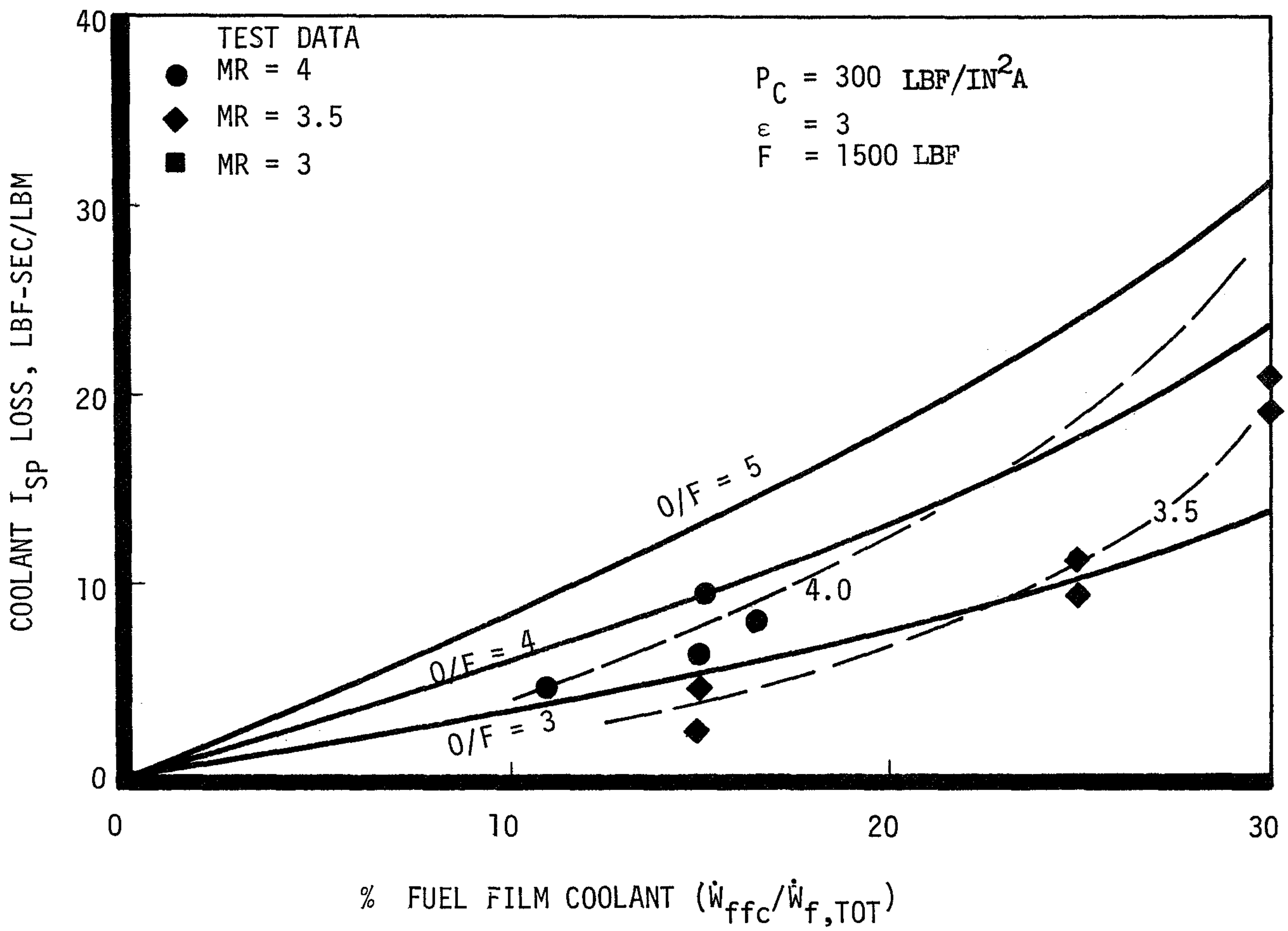

COOLANT FLOW RATE EFFECT ON COOLANT LOSS

FIGURE D-102

solid lines reflect predictions with the thermal exchange model, and the black dots and connecting dashed trends denote test data correlation. Below 10 percent coolant flow, the model appears conservative indicating slightly higher losses than the test data. From 10 to 30 percent coolant flow, a better correlation results. With this data correlation as justification of the expected cooling losses, the delivered performance was calculated for supplemental cooling percentages shown to be required from heat transfer analysis.

Performance Summary - A summary of thruster performance is presented in Figure D-103 for the thruster design conditions. This figure provides a breakdown of specific impulse losses and the resultant delivered specific impulse.

D-7.4 Thruster Weight - The thruster weight is shown in Figure D-104 as a function of chamber pressure and expansion ratio. The attitude control and +X thruster design points and weights are shown for the orbiters.

DESIGN POINT		
THRUST, LBF	1850	1850
MIXTURE RATIO	4.0	4.0
CHAMBER PRESSURE, LBF/IN^{2}A	500	500
AREA RATIO	60	120
PROPELLANT TEMP, °R		
HYDROGEN	245	245
OXYGEN	380	380
CHAMBER COOLING, % ($\epsilon <$ 11:1)	7.6	7.6
NOZZLE COOLING, % ($\epsilon >$11:1)	5.4	5.4
PERFORMANCE		
THEORETICAL I_{SP} VACUUM, LBF-SEC/LBM	472.5	481.7
COOLING LOSS, LBF-SEC/LBM	7.9	7.9
IMPURITY LOSS, LBF-SEC/LBM	1.0	1.0
CURVATURE-DIVERGENCE LOSS, LBF-SEC/LBM	3.9	2.9
KINETICS LOSS, LBF-SEC/LBM	2.7	3.0
ENERGY RELEASE LOSS, LBF-SEC/LBM	4.6	4.6
BOUNDARY LAYER LOSS, LBF-SEC/LBM	5.9	7.5
DELIVERED VACUUM SPECIFIC IMPULSE, LBF SEC/LBM	446.5	454.8

APS THRUSTER PERFORMANCE SUMMARY

FIGURE D-103

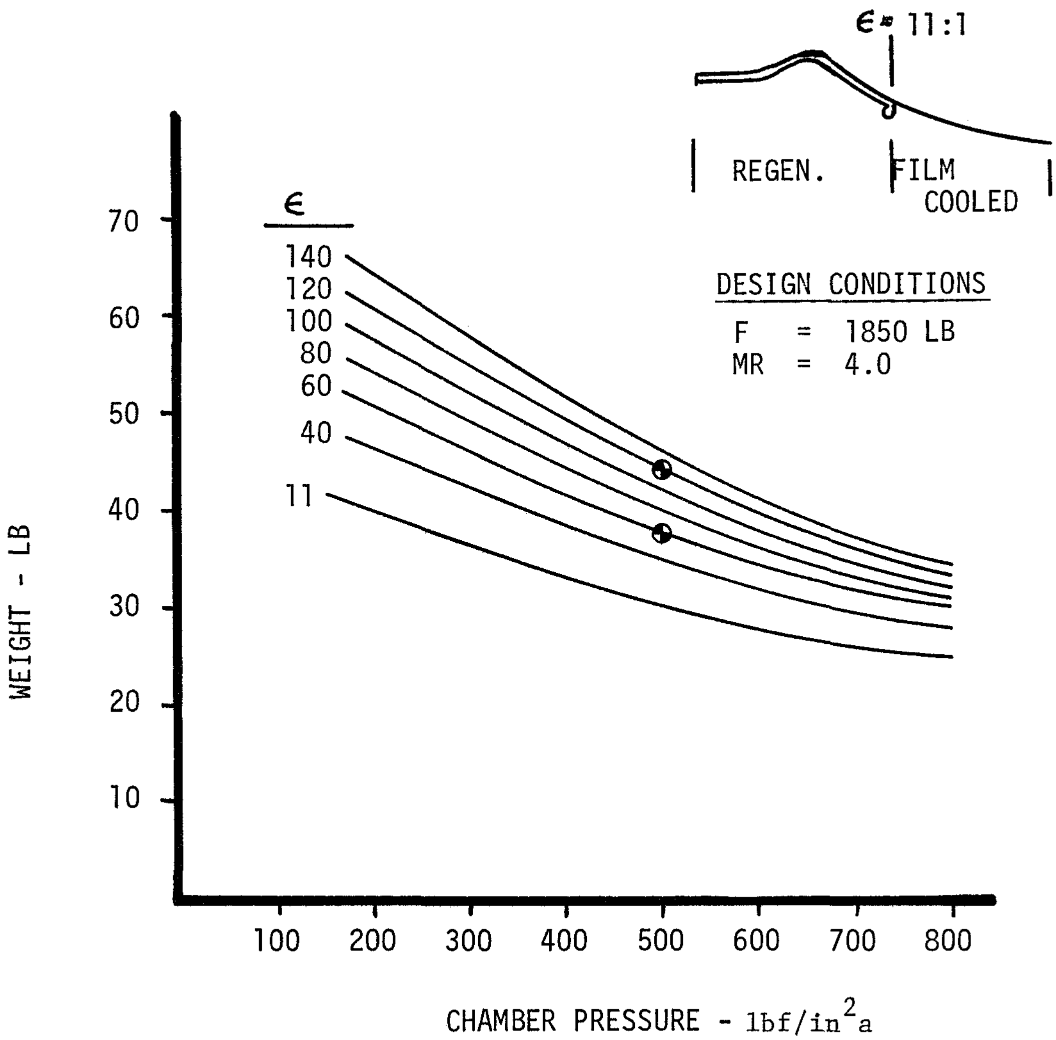

APS THRUSTER WEIGHT

FIGURE D-104

D-8. +X TRANSLATION THRUSTER INTEGRATION STUDY

Two basic functions are provided by the APS; these are 3 axis attitude control and translation capability. The baseline APS uses gaseous H_2/gaseous O_2 thrusters of the same design to perform all functions. The thrusters for attitude control and for Y and Z translation maneuvers perform a large number of small impulse burns while the thrusters for the +X translation maneuvers are required to perform a relatively small number of large steady state burns. Of the total APS impulse requirement approximately 90 percent is expended for +X translation maneuvers. Thus it was potentially advantageous to use thrusters individually designed to provide maximum specific impulse for the +X translation functions.

Integration of higher performance +X translation thrusters with the APS was investigated to evaluate the effect on overall subsystem weight.

Specifically, +X thrusters of progressively greater design deviation from the attitude control thrusters, as follows, were evaluated:

(1) thrusters using gaseous oxygen and hydrogen with increased nozzle expansion ratio

(2) thrusters with increased expansion ratio designed to operate with liquid hydrogen and gaseous oxygen

(3) thrusters with increased expansion ratio designed to operate with liquid hydrogen and liquid oxygen.

The above options represent a continuous improvement in specific impulse at the expense of increased development effort. In comparing these options, study schedule and budget considerations precluded a detailed optimization of each and it was therefore necessary to establish the ground rule that the APS turbopump assemblies would remain fixed for each thruster concept. This resulted in common mixture ratios and chamber pressures that were not necessarily optimum for the different thruster design, however, point comparisons were made to assess the effect of these on study results.

In addition this study was conducted around the design condition for a preliminary baseline APS design. Consequently a chamber pressure of 300 lbf/in^2a and hydrogen conditioning temperatures of 100°R for the regeneratively cooled APS thrusters and 200°R for the film cooled thrusters were used. The final APS design resulted in a chamber pressure of 500 lbf/in_2a and a hydrogen conditioning temperature of 200°R was selected for both thruster cooling approaches.

Figure D-105 summarizes those design conditions, used in the study which principally affect +X translation thruster performance.

The results of this study show the weight comparisons to be extremely dependent on +X thruster performance, start-childown losses, and on the design point selected for the gas/gas thrusters in terms of the conditioning temperatures of the propellants. A more in-depth +X translation subsystem analysis also considering subsystem design point optimization and minimization of start losses would be required before the lowest weight subsystem could be identified. However, this study does indicate that the incorporation of separately optimized +X translation thrusters would result in a weight savings but the amount of savings is highly dependent on the conditioning temperature of the hydrogen in the gas/gas design and on the type of gas/gas engine used, i.e., regenerative or film cooled. These results must be interpreted, not in the context of an Orbit Maneuvering Subsystem/APS comparison, but rather as an evaluation of performance improvement modifications to an existing gas/gas APS.

D-8.1 <u>+X Translation Thrusters Options</u> - Both film cooled and regeneratively cooled gas/gas thrusters were evaluated to assess the advantage of the +X translation engine alternates relative to an all maneuver APS using either film cooled or regeneratively cooled thruster concepts. Figure D-106 presents the matrix of alternates considered and shows the three concepts which were evaluated. These were:

(1) GH_2/GO_2 +X translation thrusters with either film cooled or regenerative cooled attitude control thrusters

(2) Regeneratively cooled LH_2/LO_2 +X translation thrusters with either film cooled or regeneratively cooled attitude control thrusters

(3) Regeneratively cooled LH_2/GO_2 +X translation thrusters with either film cooled or regeneratively cooled attitude control thrusters.

Concept A is the baseline APS using gas/gas thrusters for both attitude control and +X translation. Concept B uses the liquid H_2/liquid O_2 thrusters, while concept C uses the liquid H_2/gaseous O_2 for +X translation.

For the LH_2/LO_2 thrusters, bypass flow is reduced to that required to provide power for the pumps and to condition the propellants which feed the gas generators. This weight advantage is partially negated by the amount of chill down propellant lost each time the thruster is started. This propellant loss occurs

I_{SP} = FUNCTION OF

INFLUENCING FACTORS INVESTIGATED	CONDITIONS USED IN STUDY	
ENGINE TURBOPUMP DRIVE CYCLE	GAS GENERATOR	- COMMONALITY WITH APS
THRUST LEVEL	1850 LBS THRUST	- PROVIDES TURBOPUMP WITH SAME FLOW REQUIREMENT DURING APS & X-TRANSLATION OPERATION
CHAMBER PRESSURE	300 LBF/IN^{2}A	- COMPATIBLE WITH APS PUMP PRESSURE REQUIREMENTS - A HIGHER P_C COULD POSSIBLY UTILIZED DEPENDING UPON FILM COOLING REQUIREMENT
PUMP DISCHARGE PRESSURE	1600 LBF/IN^{2}A	- ALLOWS SAME PUMP & TURBINE POWER REQUIREMENT DURING APS AND X-TRANSLATION OPERATION
NOZZLE EXPANSION RATIO	120	- SAME AS APS WHICH OPTIMIZES @ APPROXIMATELY 120:1
THRUSTER MIXTURE RATIO	4:1	- OPTIMUM AT 5.5, BUT, 4:1 ALLOW PUMP TO OPERATE OVER NEARLY SAME FLOW CONDITION DURING APS & X-TRANSLATION OPERATION WITH MIN WEIGHT PENALTY
CONDITIONING TEMPERATURE (HYDROGEN)	100°R	- USED FOR REGENERATIVE COOLED GAS/GAS THRUSTERS
	200°R	- USED FOR FILM COOLED GAS/GAS THRUSTERS

INFLUENCES ON X-TRANSLATION SPECIFIC IMPULSE DETERMINATION

FIGURE D-105

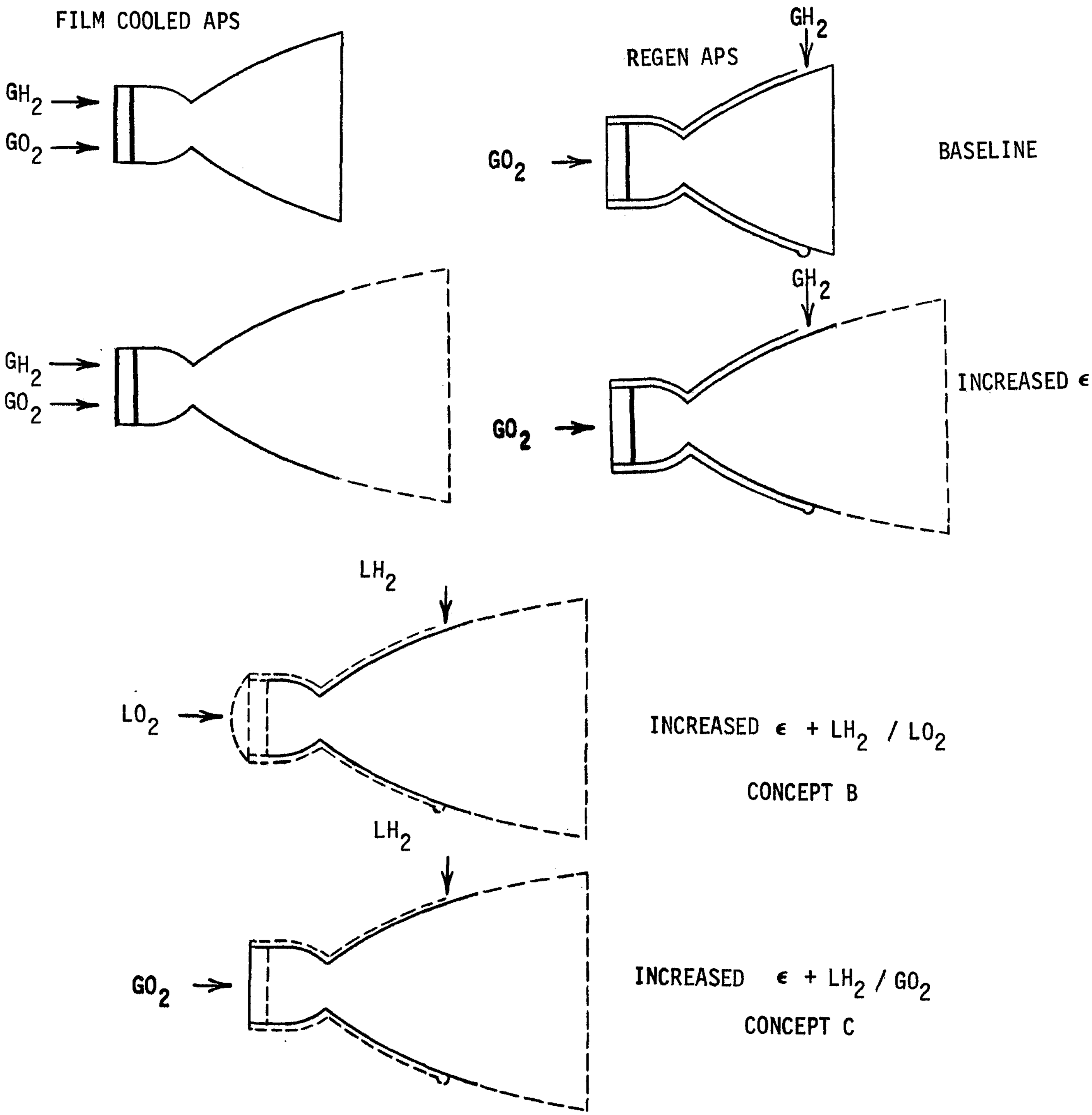

TRANSLATION THRUSTER MODIFICATION INVESTIGATION DURING APS STUDY

FIGURE D-106

for two reasons:

(1) The feed assembly must be cooled before the thruster can be started to preclude two phase hydrogen and oxygen being delivered to the thruster

(2) Any liquid hydrogen or oxygen left in the lines at the end of a burn would eventually vaporize, and therefore would not be usable in the LH_2/LO_2 thruster.

The LH_2/GO_2 +X translation thrusters have a bypass flow and specific impulse between the baseline GH_2/GO_2 subsystem and the LH_2/LO_2 subsystem as the oxygen for the thrusters is conditioned. Therefore the LH_2/GO_2 thruster bypass flow is required to provide power for the pumps and to condition the flow to the gas generators in addition to conditioning the oxygen for the +X translation thruster. Since gaseous oxygen is supplied to the thrusters, there are no start chilldown losses associated with the oxygen feed assembly.

D-8.2 Design Point Selection - As previously discussed, the +X translation thruster specific impulse level has a significant effect on overall APS weight since the majority of the total impulse requirement is expended in the +X direction. Several factors affect the specific impulse and investigation was required to define their effect. The assumption of a common turbopump assembly operating point for both APS and +X translation operation required the same flow rates and pressures for both APS and +X thrusters. The +X translation thrusters assumed:

(1) a thrust level of 1850 lb

(2) a chamber pressure of 300 psia

(3) a mixture of 4:1.

An expansion ratio of 120:1 was used throughout this study to provide for a comparison with the APS gas/gas thrusters. Figure D-107 presents the effect of expansion ratio (ε) on overall subsystem weight for these types of thruster assemblies. As shown no significant weight advantage is available with a greater than 120:1.

A study of weight sensitivity to mixture ratio and expansion ratio is shown in Figure D-108 for LH_2/GO_2. Figure D-109 shows similar data for LH_2/LO_2. The LH_2/LO_2 +X translation subsystem weight is not a minimum at a mixture ratio of 4:1; however, a mixture of 4:1 was selected to be consistent with APS operational requirements. The expansion ratio was set at 120 to make it

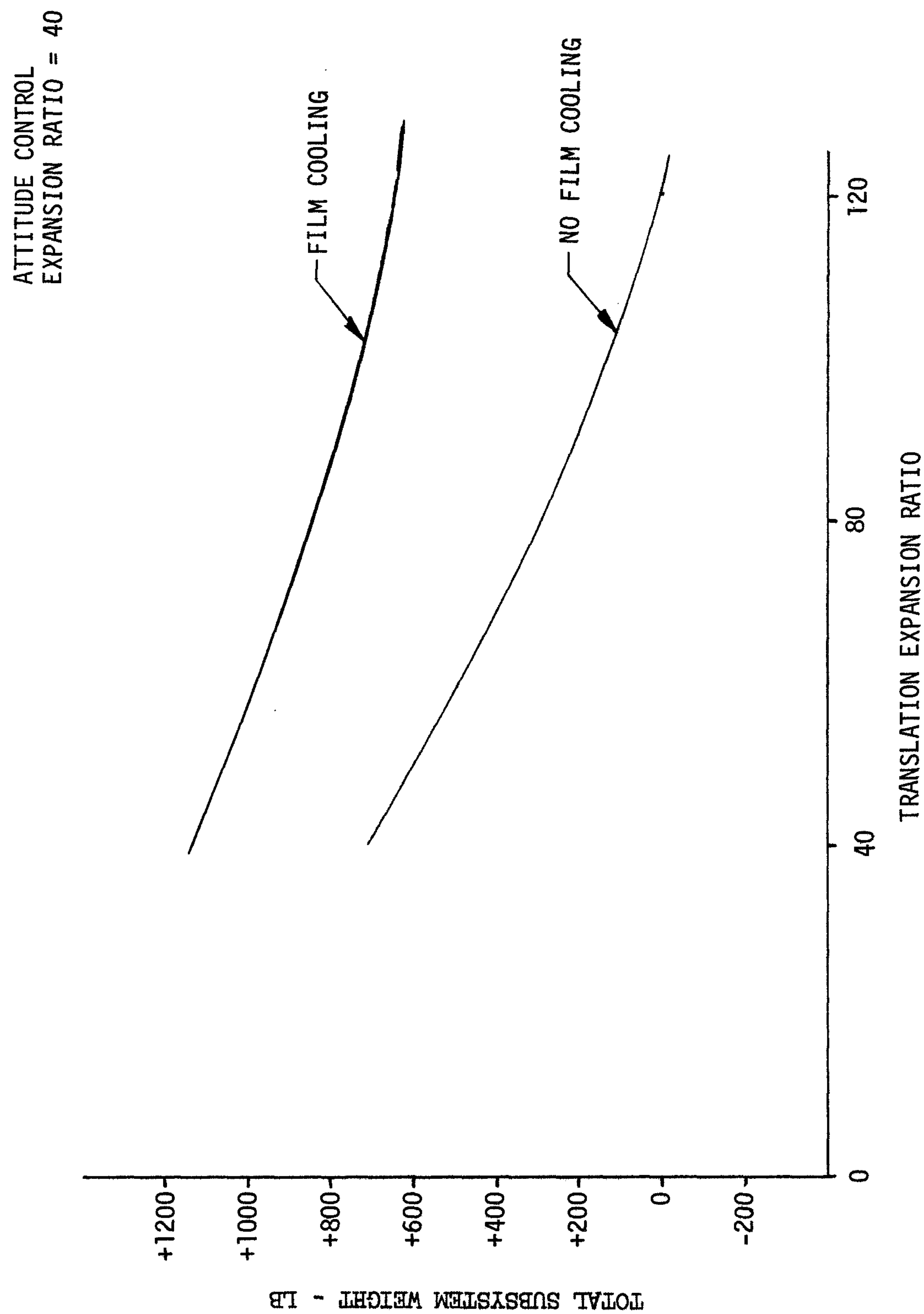

EFFECT OF EXPANSION RATIO

FIGURE D-107

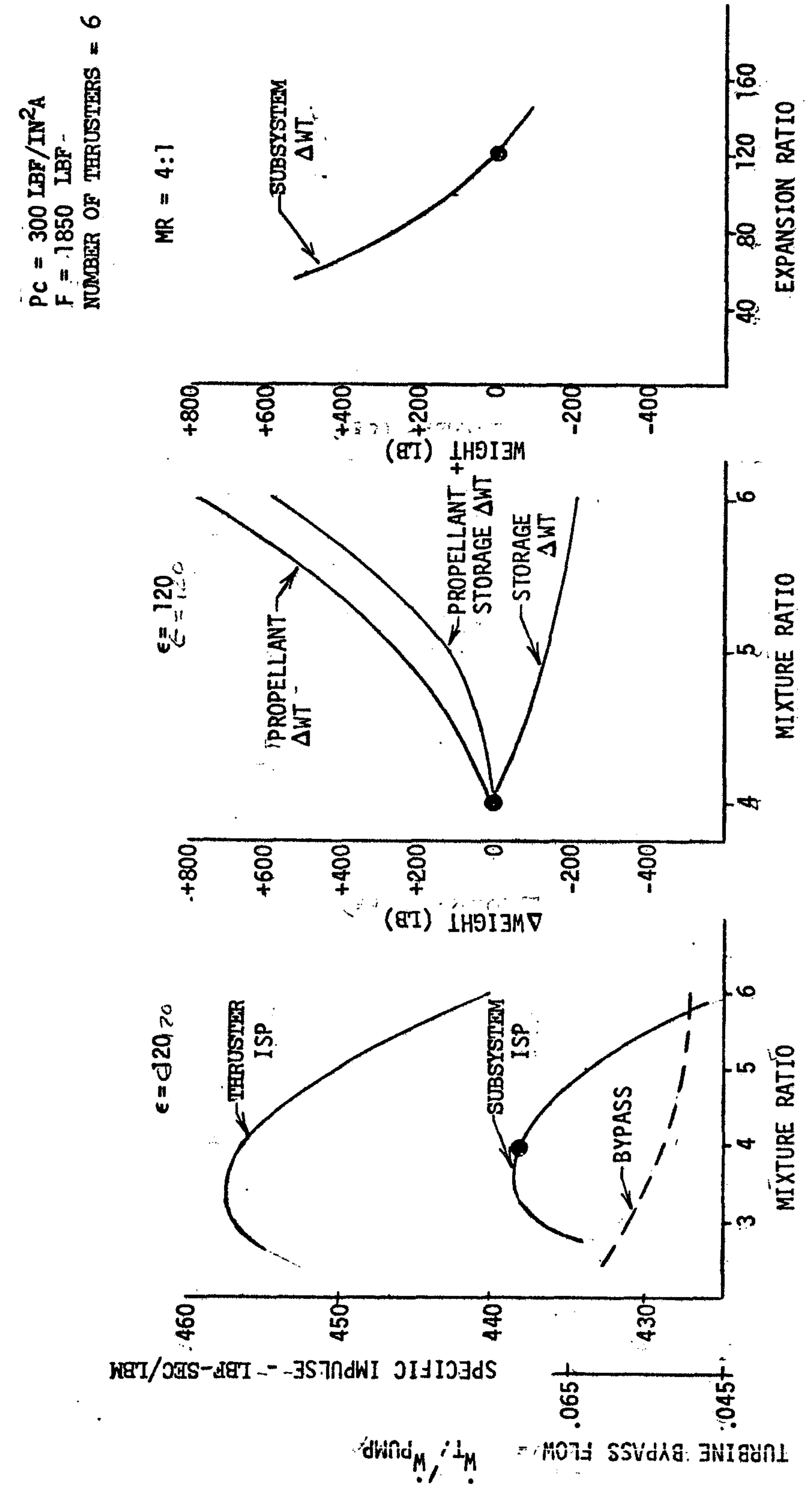

LH₂/GO₂ SENSITIVITIES

FIGURE D-108

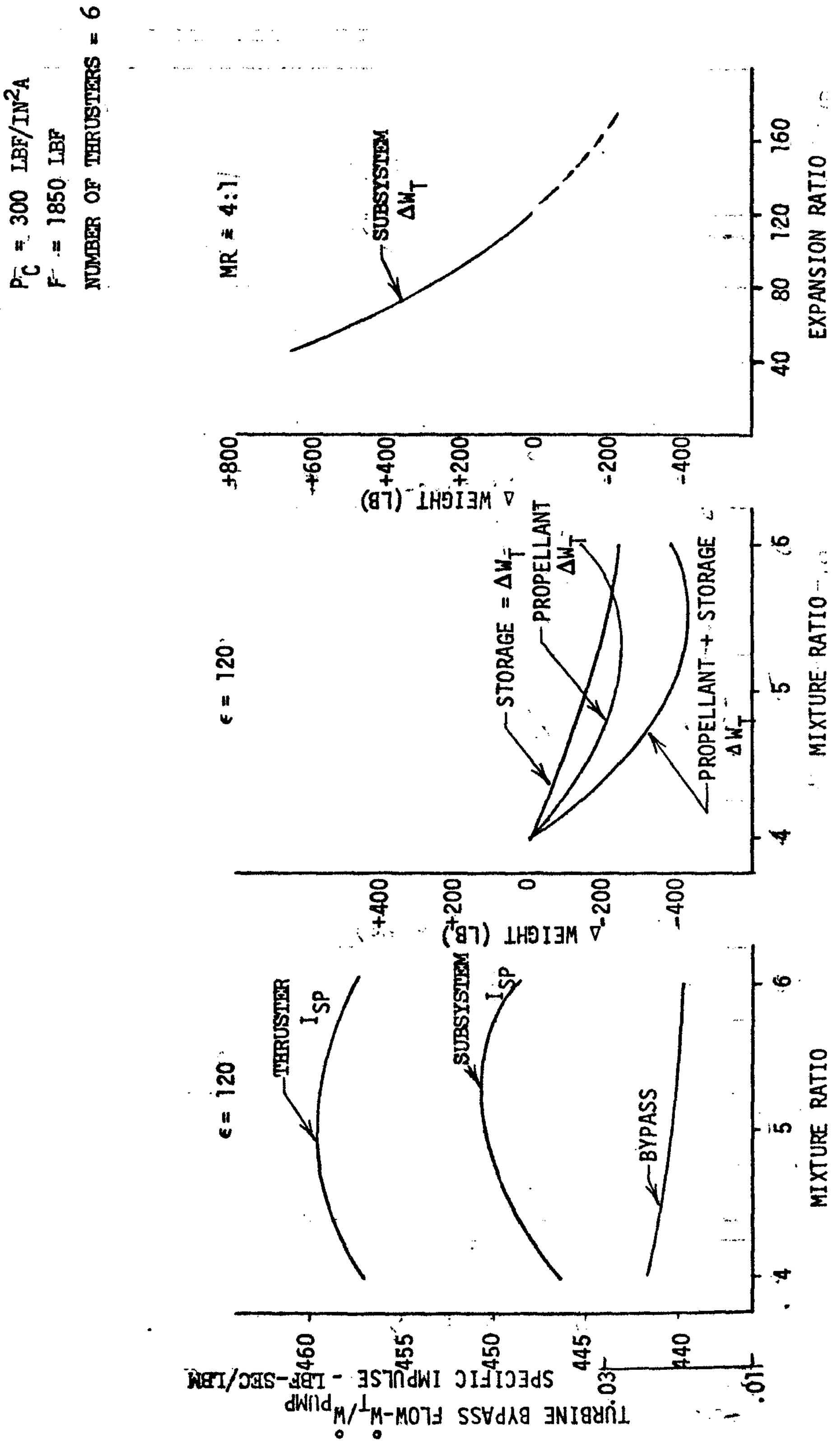

LH_2/LO_2 SENSITIVITIES

FIGURE D-109

equivalent to the GH_2/GO_2 thruster expansion ratio, thus providing a common basis for subsystem comparison.

Figure D-110 presents a summary of the design conditions used for the study. With the gas/gas option, 6 +X translation thrusters were used. For the other options two gas/gas thrusters were used with four LH_2/LO_2 or four LH_2/GO_2 thrusters. The two gas/gas thrusters are necessary in these options to satisfy very low +X maneuver impulse requirements.

These arrangements satisfy the reliability requirements by providing +X maneuver capability after a double failure (2 thrusters inoperative) by using the two aft firing gas/gas thrusters to back up the primary +X translation thrusters.

Figure D-111 presents a summary of the nine +X translation maneuvers required for a seventeenth orbit rendezvous mission. The gas/gas thrusters satisfy any additional small +X translation maneuvers such as those required during docking.

D-8.3 Maneuvering Velocity Allocation - Propellant start losses increase linearly with the number of times liquid/liquid or liquid/gas +X translation thrusters are used. Conversely average subsystem specific impulse increases as the higher performance +X thruster configurations are used for more maneuvers. These two opposing effects result in an optimum impulse allocation between liquid/liquid (or liquid/gas) thrusters and the lower performance gas/gas thrusters. For each thruster option, subsystem weight was determined as a function of the number of +X translation maneuvers performed to establish minimum weight points. At this point, the weight of the APS incorporating the new design +X translation thrusters was compared to all GH_2/GO_2 APS subsystems which utilized either film or regeneratively cooled thrusters.

Film Cooled Gas/Gas APS Thrusters

LH_2/LO_2 +X Thrusters - Figures D-112 and D-113 present relative subsystem weights as a function of velocity allocation to illustrate the effect of +X translation thruster specific impulse and start chill-down losses. As shown, neither variations in the LH_2/LO_2 specific impulse nor in the start losses have a significant effect on the optimum allocation. LH_2/LO_2 subsystem results in a maximum weight advantage at four starts over the expected range of specific impulse and propellant losses. This weight advantage is a result of the higher relative performance available with the LH_2/LO_2 thrusters. The first four maneuvers are of such an impulse magnitude that the propellant savings associated with the use of the LH_2/LO_2 thrusters more than offsets the start chill-down losses. Maneuvers five through nine are all

	APS	LH_2/LO_2 X-TRANS	LH_2/GO_2 X-TRANS
THRUST - LBF/THRUSTER	1850	1850	1850
NUMBER OF THRUSTERS	6	2/4 (1)	2/4 (1)
CHAMBER PRESSURE - LBF/IN^2A	300	300	300
PUMP DISCHARGE PRESSURE - LBF/IN^2A (MAXIMUM ACCUMULATOR PRESSURE)	1600	1600	1600
MIXTURE RATIO	3.82:1	4:1	4:1
TCA SPECIFIC IMPULSE	(ATC/TRN) 434/444.5 (2) (5)	457 (3)	456 (3)
EXPANSION RATIO	40/120	120	120
BYPASS FLOW	.059	.024	.053
VENT CONFIGURATION	NO VENT/O_2 SIDE VENT (4)	NO VENT (4)	O_2 SIDE VENT
VENT SPECIFIC IMPULSE	152	---	152
SUBSYSTEM SPECIFIC IMPULSE	407/424.5 (6)	446.3	438.1

1 2 APS (GH_2/GO_2) THRUSTERS/4 X-TRANSLATION THRUSTERS

2 INCLUDES I_{SP} LOSS FOR FILM COOLING

3 ASSUMES NO FILM COOLING

4 INSUFFICIENT PRESSURE AVAILABLE FROM SYSTEM FOR PROPULSIVE VENT DUE TO 25:1 TURBINE EXPANSION RATIO

5 TCA SPECIFIC IMPULSE (REGENERATIVELY COOLED) 443/456

6 BASED ON H_2 AND O_2 CONDITIONING TEMPERATURES OF 200°R/300°R, AND A CONDITIONER OPERATING AT T = 3500°R EFFECTIVE.

DESIGN CONDITIONS FOR COMPARISON OF
INTEGRATED APS/X-TRANSLATION THRUSTER CONCEPTS

FIGURE D-110

(+X AXIS)

MANEUVER	BURN NO	ΔV	TOTAL IMPULSE	CUMULATIVE ΔV
DEORBIT	1	496	4,184,952	496
HEIGHT ADJUSTMENT	2	282	2,379,348	778
COELLIPTIC BURN	3	239	2,016,539	1017
PHASING BURN	4	130	1,096,862	1147
DISPERSION	5	40	337,496	1187
MCC-1	6	36	303,747	1223
DISPERSION	7	25	210,935	1248
TPI	8	22	185,623	1270
MCC-2	9	19	160,311	1289
			10,875,813	

SEVENTEENTH ORBIT RENDEZVOUS MANEUVERS

FIGURE D-111

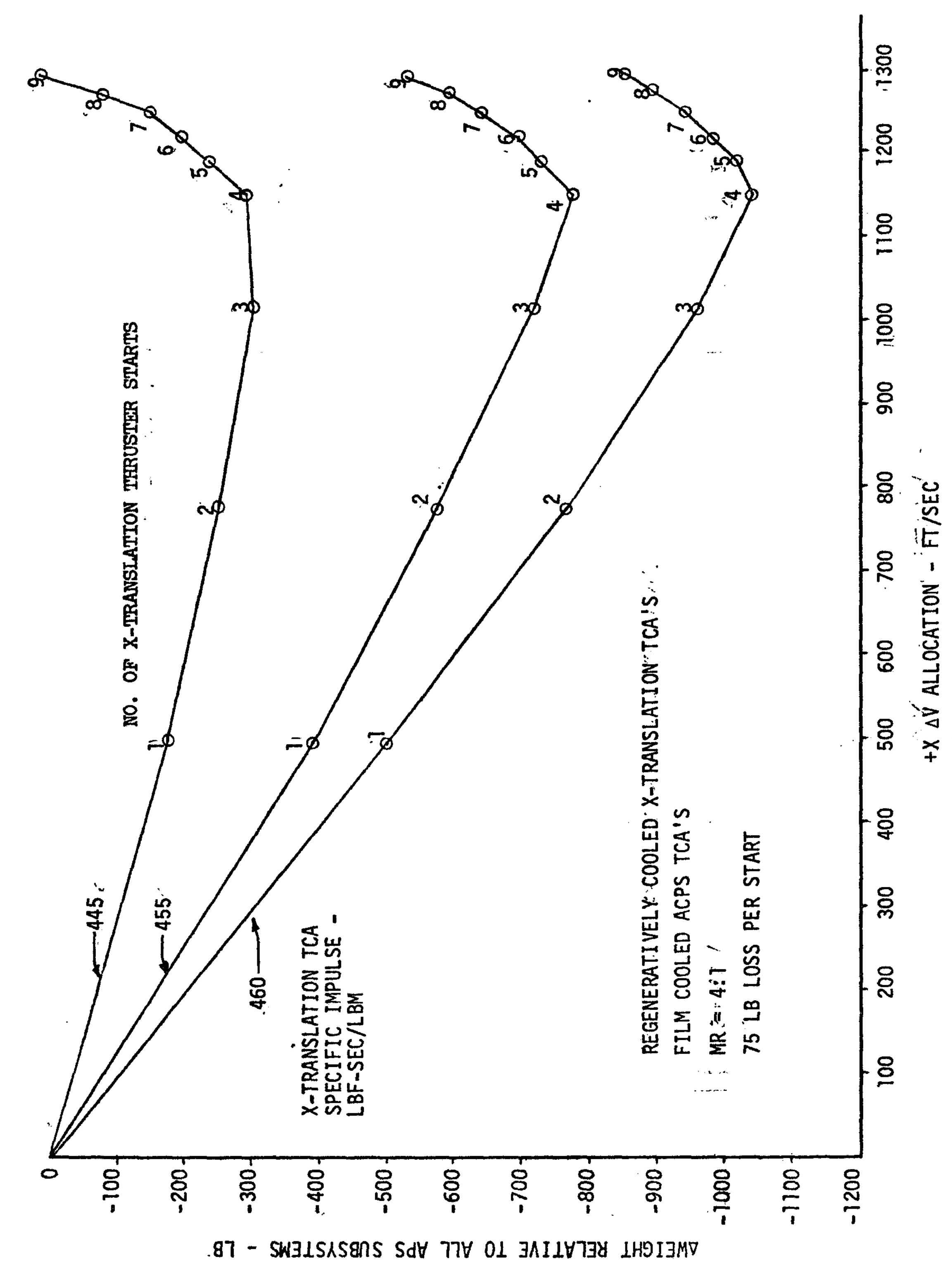

EFFECT OF TCA SPECIFIC IMPULSE ON INTEGRATED LH_2/LO_2 SUBSYSTEM WEIGHT

FIGURE D-112

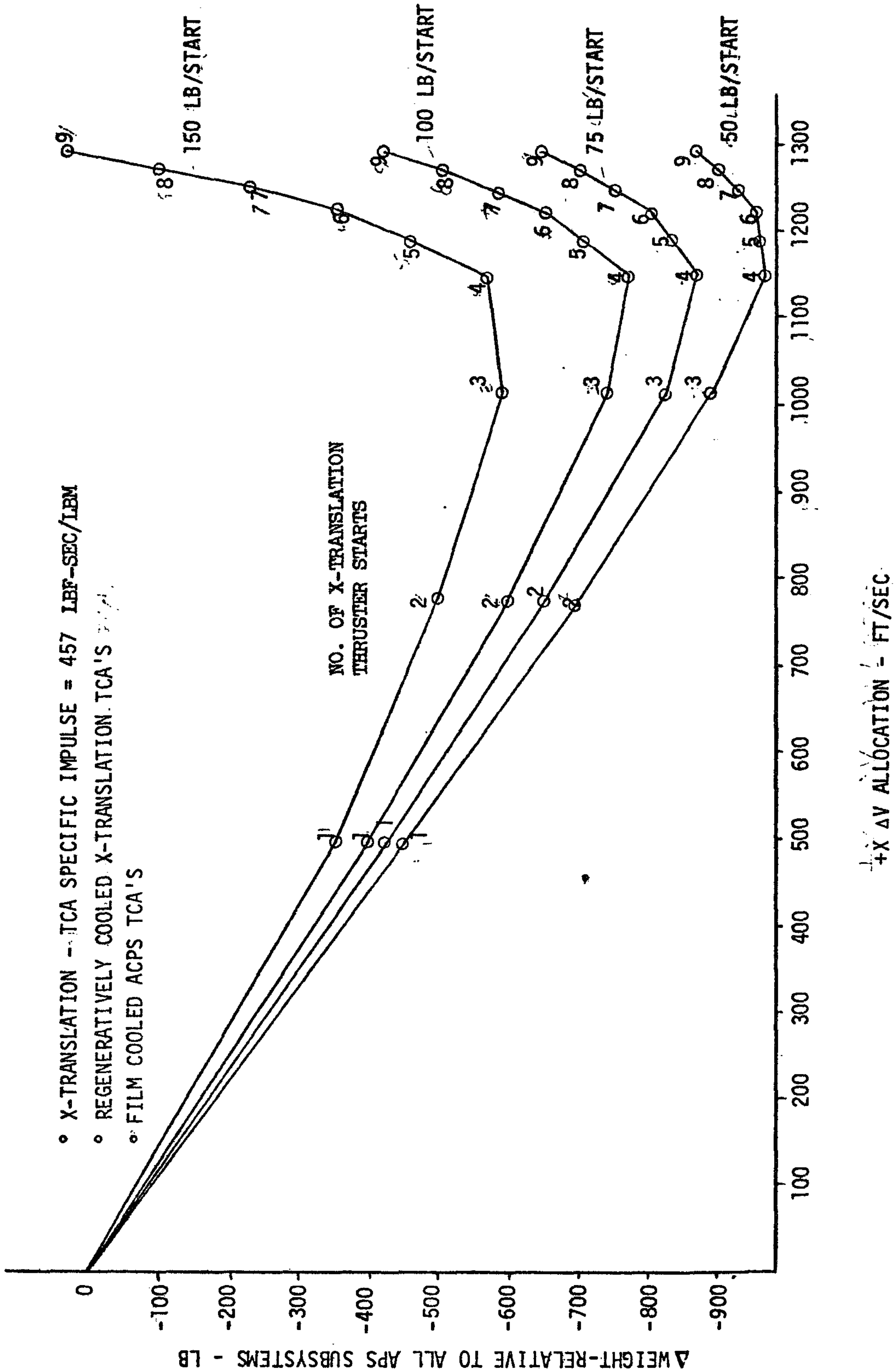

EFFECT OF START CHILLDOWN LOSSES ON INTEGRATED LH_2/LO_2 X-TRANSLATION SUBSYSTEM WEIGHT

FIGURE D-113

less than 50 ft/sec and for these maneuvers, the start chill-down losses are greater than the propellant savings. The two GH_2/GO_2 thrusters would be used for maneuvers five through nine.

LH2/GO2 +X Thrusters - Figure D-114 presents relative subsystem weight as a function of +X translation thruster starts. As shown, the LH_2/GO_2 subsystem provides a weight advantage over the all GH_2/GO_2 APS. The subsystem weight is essentially constant from five through nine starts. Thus, the LH_2/GO_2 +X translation thrusters could be used for all nine maneuvers, although two GH_2/GO_2 thrusters would still be required for docking.

Comparative Performance with Film Cooled, Gas/Gas, APS - A summary of the effect of start chill-down losses on subsystem weight for the two above mentioned alternates, compared to gas/gas translation thrusters, is presented in Figure D-115. As shown, both LH_2/LO_2 and LH_2/GO_2 offer significant weight advantages. Minimization of start-chill-down losses can amplify this weight savings, especially for the LH_2/LO_2 +X translation thrusters.

Regeneratively Cooled, Gas/Gas APS

LH_2/LO_2 +X Thrusters - Figure D-116 presents relative subsystem weight as a function of +X translation thruster starts. As with a film cooled APS, four starts provides near minimum weight, allowing the remaining five maneuvers to be performed by the two GH_2/GO_2 thrusters.

LH_2/GO_2 +X Thrusters - Figure D-117 presents relative subsystem weight as a function of +X translation thruster starts. Here the minimum is not a pronounced weight advantage and for comparative purposes nine starts were selected for the LH_2/GO_2 thrusters.

Comparative Performance for Regenerative Cooled, Gas/Gas, APS - A summary of the effect of start chilldown losses on subsystem weight for the two above mentioned alternates is presented in Figure D-118. For this case there is no advantage to the improved +X thruster performance unless start-chill-down loss is minimized.

Summary Comparison of Alternates - A summary weight comparison for all alternates is presented in Figure D-119. For these, start losses of 75 lb/start and 15 lb/starts were used for oxygen and hydrogen respectively. These include propellant losses due to line and pump chilldown and line propellant vaporization.

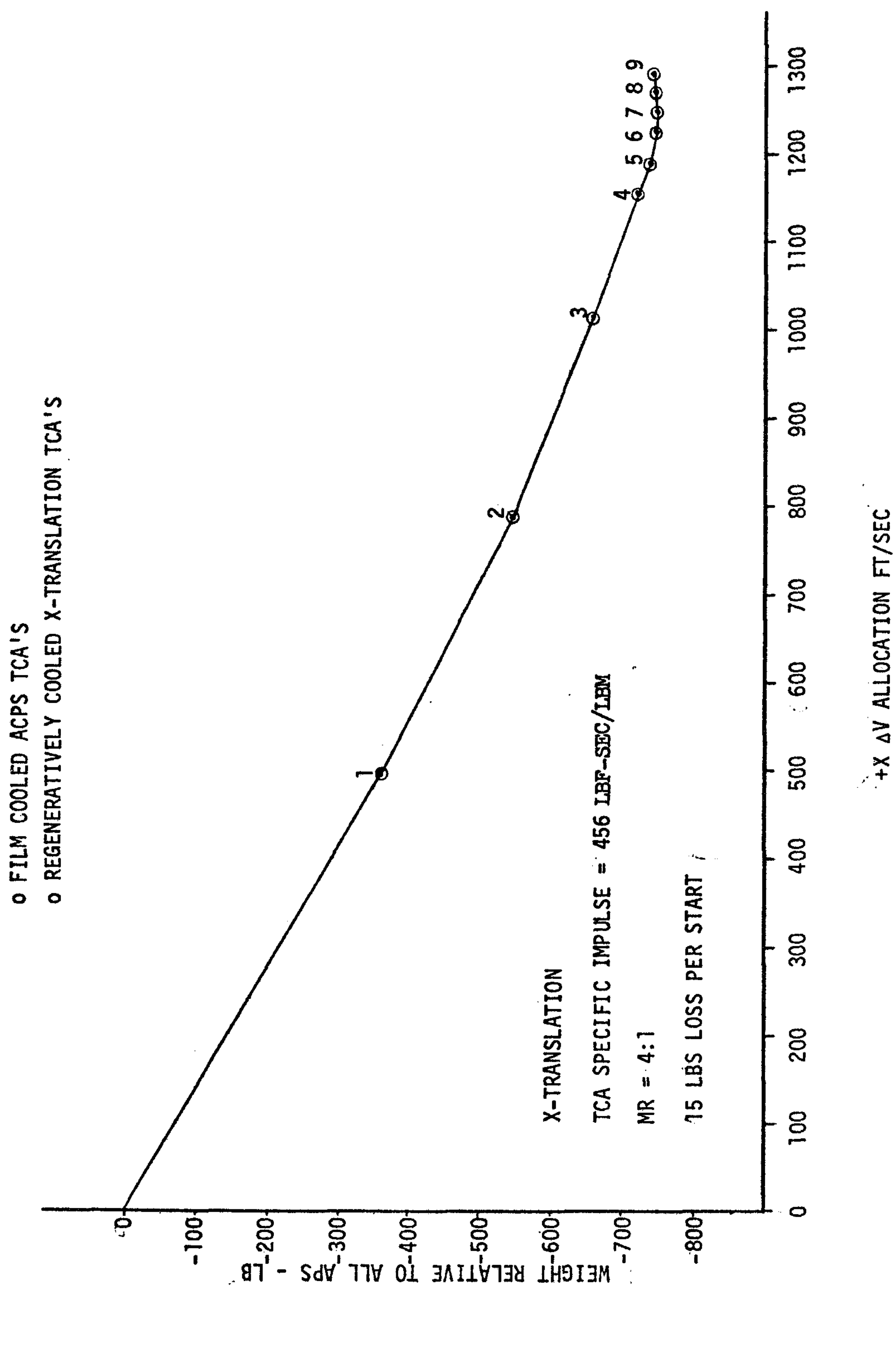

INTEGRATED LH_2/GO_2 SUBSYSTEM WEIGHT

FIGURE D-114

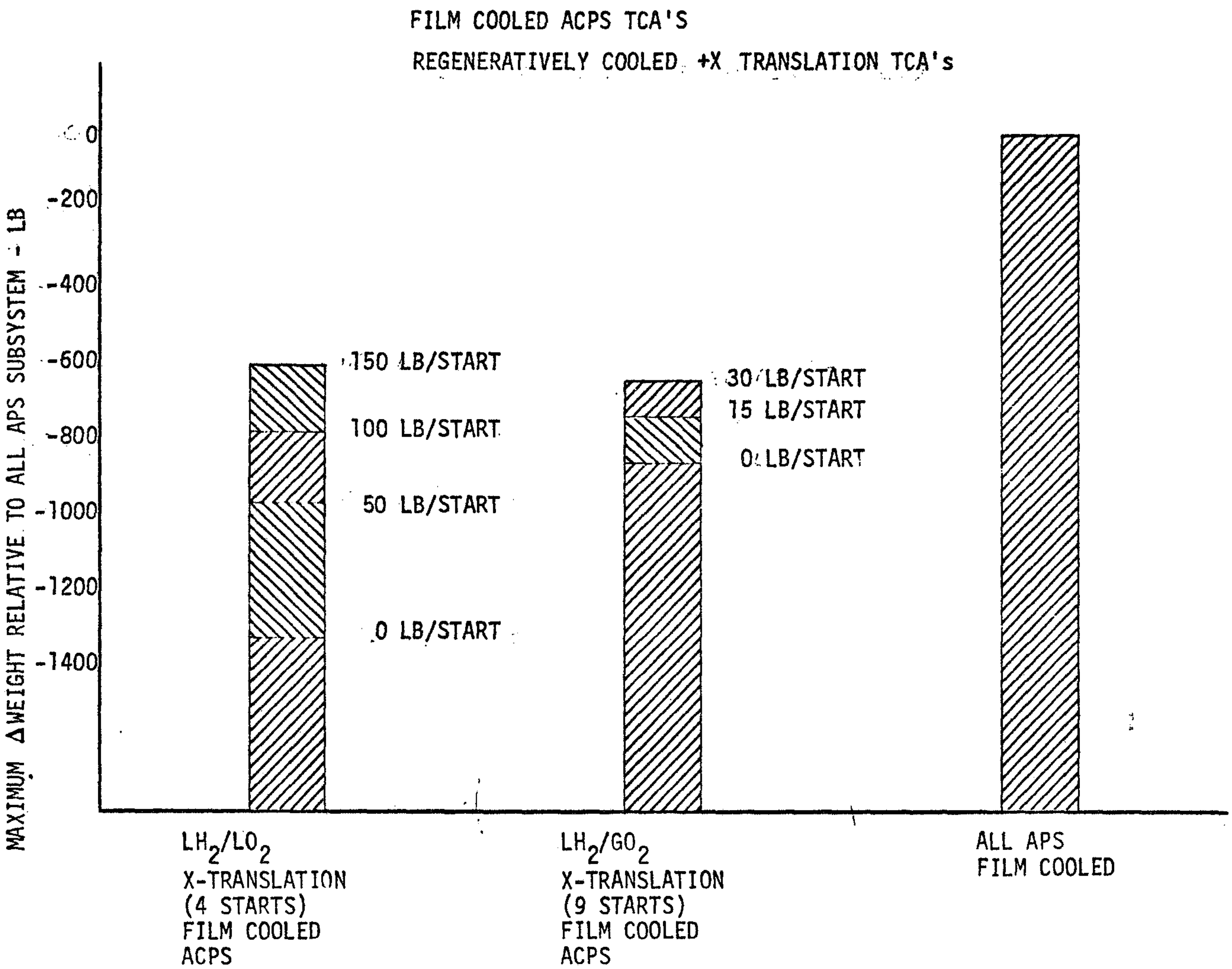

WEIGHT COMPARISON OF CANDIDATE SUBSYSTEMS

FIGURE D-115

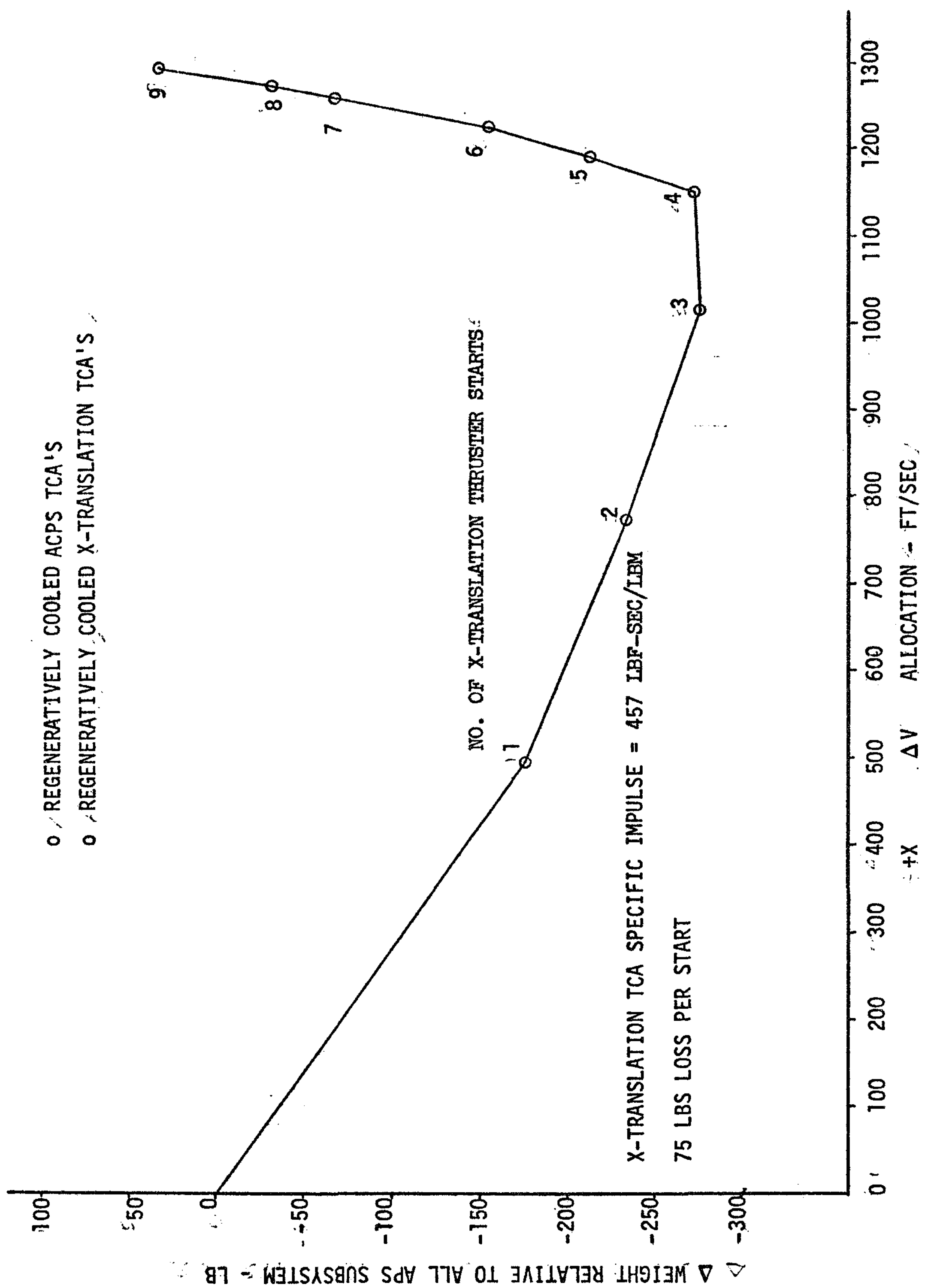

INTEGRATED LH_2/LO_2 SUBSYSTEM WEIGHT

FIGURE D-116

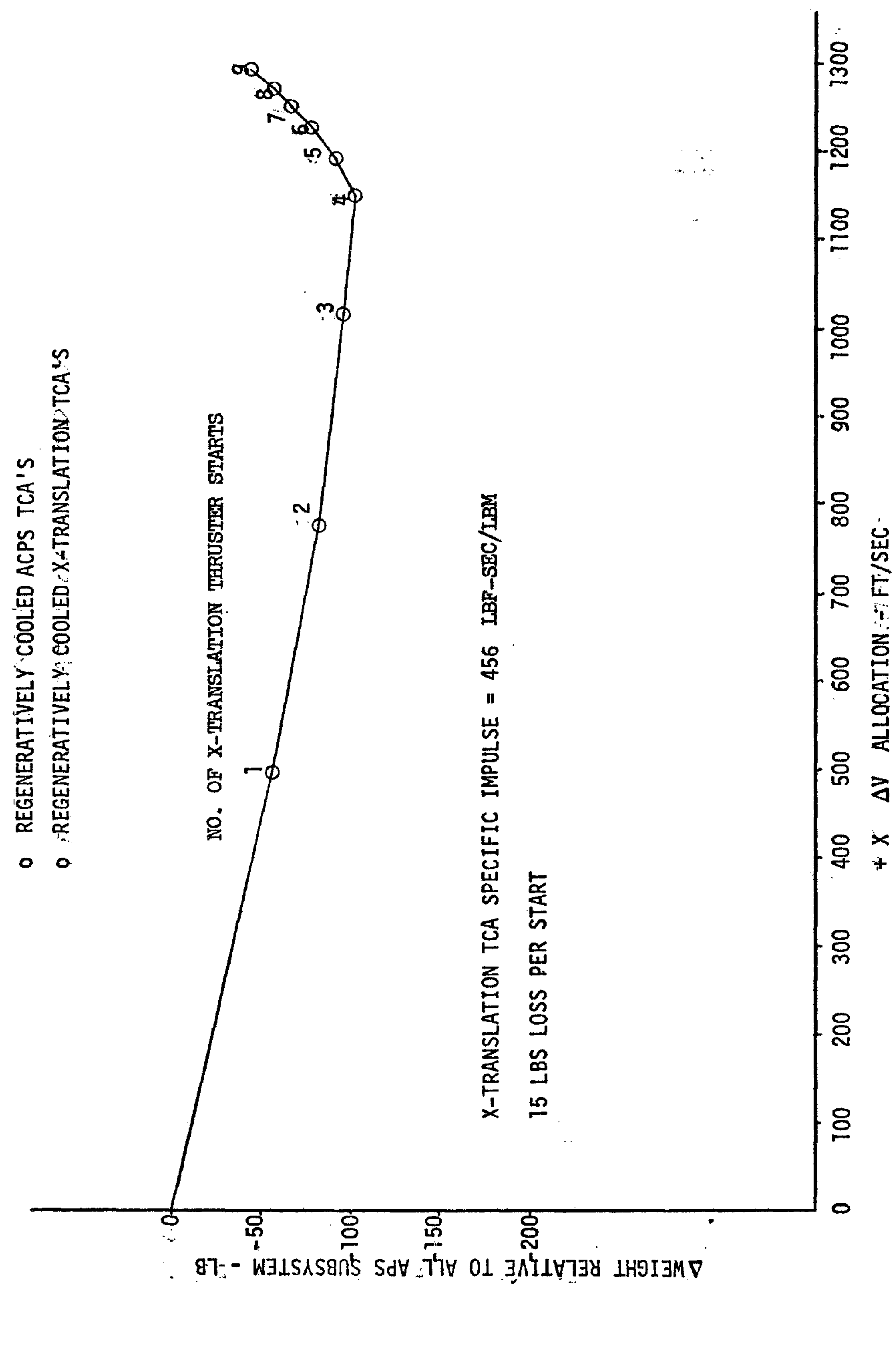

INTEGRATED LH_2/GO_2 SUBSYSTEM WEIGHT

FIGURE D-117

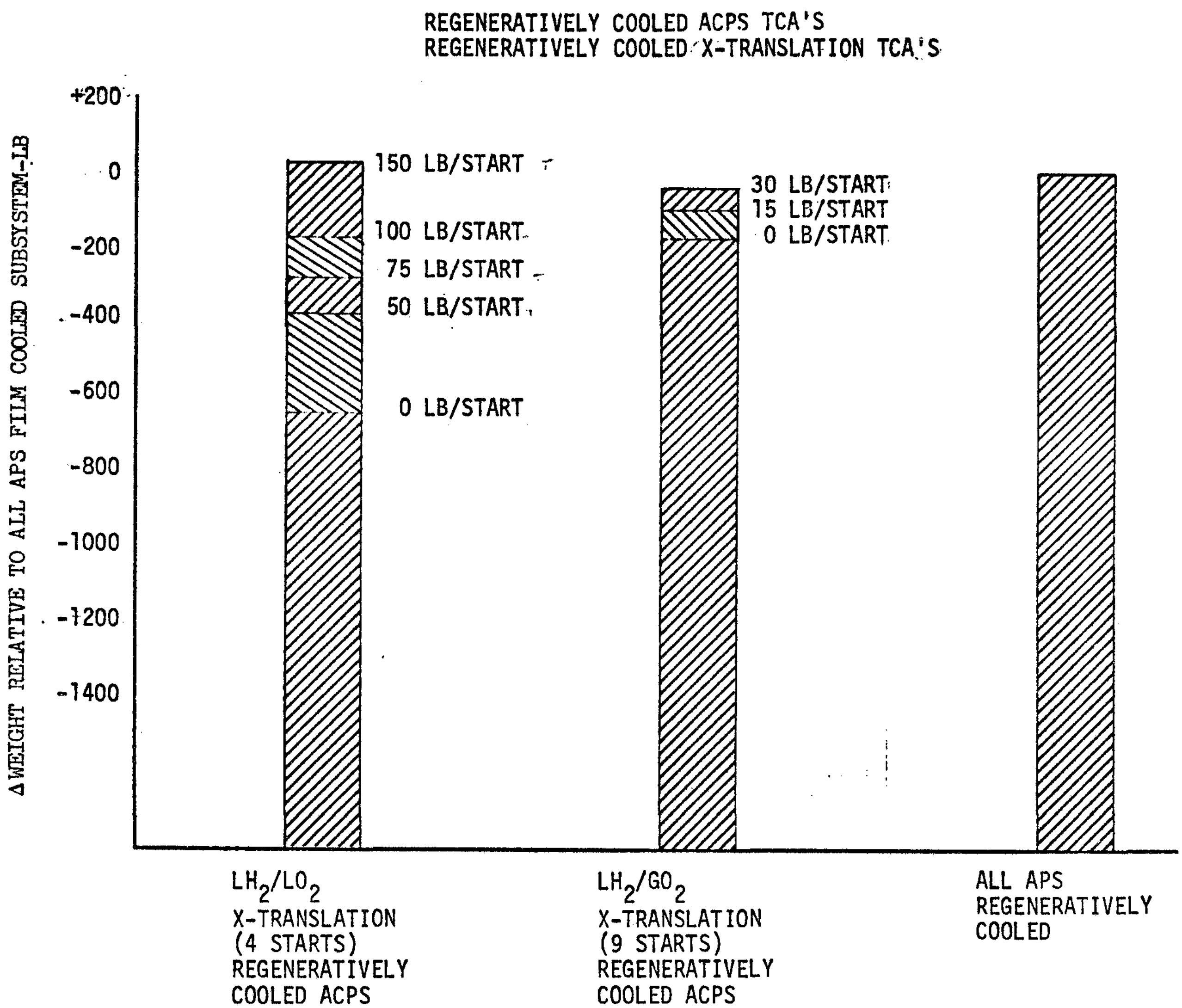

WEIGHT COMPARISON OF CANDIDATE SUBSYSTEMS

FIGURE D-118

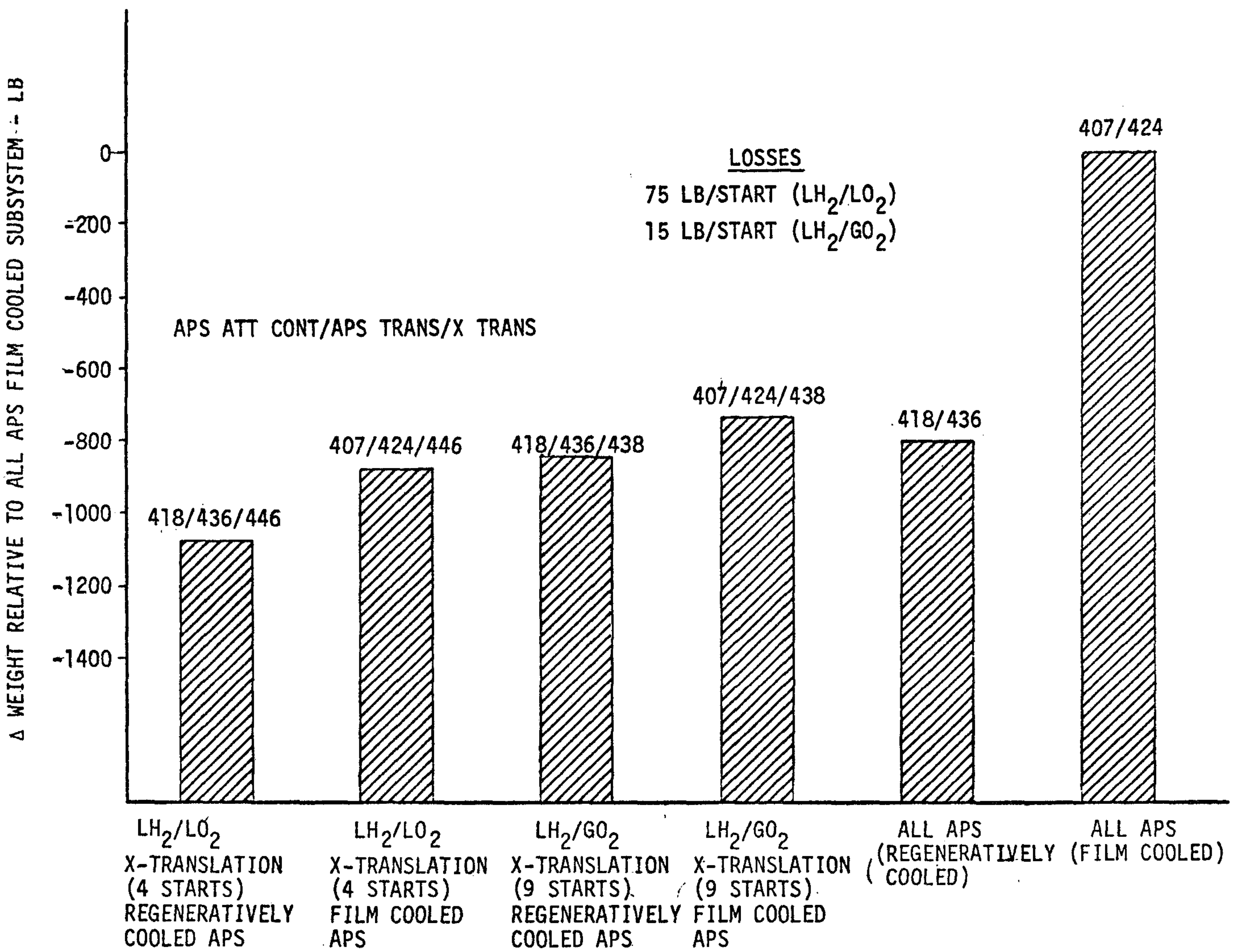

SUMMARY WEIGHT COMPARISON OF
ALTERNATE X-TRANSLATION CONCEPTS

FIGURE D-119

If regeneratively cooled GH_2/GO_2 thrusters are used, the maximum weight savings (200 lbs) is obtained by utilizing LH_2/LO_2 +X translation thrusters for four starts. If film cooled GH_2/GO_2 thrusters are used, the LH_2/LO_2 +X translation thrusters provide a weight savings of 900 lbs. The regenerative cooled gas/gas APS baseline for this study provided a hydrogen conditioning temperature of 100°R minimum at the thruster inlet. A minimum hydrogen propellant inlet temperature of 200°R was selected for the final APS design to provide the capability of using either film or regenerative cooling on the APS thrusters. This change in conditioning, combined with other changes to the final baseline APS design, result in a subsystem specific impulse approximately equal to that of the film cooled APS. It would be potentially feasible to provide an advantage of approximately 900 lbs over the final baseline by using LH_2/LO_2 thruster for +X translation maneuvers, however, this would require the development of a completely different thruster assembly with its associated development cost.

APPENDIX E

OPERATING PERFORMANCE AND TRANSIENT ANALYSIS

To fully assess APS design adequacy, analyses were conducted to evaluate operation under conditions simulating mission usage, with nominal and off-nominal component/assembly performance and transient characteristics of the thrusters when coupled to the supply lines. This appendix describes the results of both studies.

E-1. SUBSYSTEM OPERATING PERFORMANCE

The APS was sized and designed on the basis of nominal, steady state, component performance. In actual operation, heat transfer into the accumulators and supply lines will alter operating pressures and temperatures with resultant performance variations. Similarly off-nominal performance of components and/or assemblies will result in performance changes; therefore, in order to establish APS design adequacy, it was necessary to simulate APS operation during a mission. The approach taken for this study was to first simulate mission operation using nominal component performance to define the effects on performance of heat transfer into the subsystem and of normal temperature changes due to accumulator blowdown and recharge. This established nominal APS operating characteristics. Off-nominal component/assembly operation was then prescribed and missions were simulated. These results, when compared with nominal APS operation, allowed a quantative assessment of the significance of component/assembly accuracy in terms of APS performance. To accomplish these analyses, a computer program was developed which models the thrusters, supply lines, accumulators, and conditioner assembly.

E-1.1 Computer Program Description - The operating performance program was designed to provide data on the operation and performance of the feed assembly of the auxiliary propulsion subsystem for typical mission duty cycles. The program calculates thrust, total impulse, pressures, temperatures, and flow rates relating to operation of the accumulators, lines, and thrusters. The program models APS operation by assembling operating data for an increment of time, calculating the flow rates and heat transfer based on the temperatures and pressures from the previous time increment, and calculating the new temperatures and pressures. Time is then incremented, operating data assembled, and the process is repeated.

Certain ground rules were used in developing the component models and the overall program. All calculations in the program that involve propellant properties use a real gas equation of state. The environmental temperature was held constant; the thermal conductivity of the insulation material was constant with temperature; the heat capacity of the accumulator and line walls was not considered; the gas in the accumulators and lines was considered well mixed (no thermal stratification effects), and a Nusselt number of four was used for heat transfer calculations.

The propellants used in the subsystem are stored as low pressure liquids and are increased in pressure by a turbopump prior to delivery to the heat exchanger. The heat exchanger thermally conditions the propellants before they are used by the thrusters. The energy for turbopump and heat exchanger operation is provided from the combustion of a portion of the conditioned propellants. The heat exchanger used for conditioning and the turbopump used for increasing the liquid pressure do not have instantaneous response, but rather have transients that are complex functions of their detailed internal geometry. In the operating program the conditioner assembly has a time constant of zero and is actuated when the accumulator decays to its minimum pressure. This is equivalent to an actual conditioner assembly which has a finite time delay and is actuated when the accumulator decays to a switching pressure slightly above the minimum. The propellants enter the accumulator at the design conditioning temperature and the design steady-state flow rate immediately after conditioner actuation.

Approximations in the duty cycle description were required to limit calculation time. Early in the development of the program, it was shown that the pulse mode portion of the duty cycle could be accurately approximated by using an equivalent thruster flow concept; for example, a one thousand pound thrust thruster that operates in a pulse mode for one tenth of a second and is idle for nine tenths of a second can be approximated by an "equivalent thruster" of one hundred pounds thrust that operates continuously. This allows the sequence of events for the attitude control portion of a mission to be input much more easily and allows the computational time increments to be larger, making the program easier and more economical to use. The program uses an approximate conduction model to define line and accumulator gas heating. A study was conducted to determine the validity of the heat transfer analysis technique by comparing it to a more exact technique. Figure E-1 shows the result of the study. The heat transfer analysis utilized in the operational program is more conservative than the transient calculation, and, thus, shows a higher temperature rise rate.

The program has the capability to evaluate two distinct venting modes. The first is an automatic venting mode; this occurs when the accumulator and line pressures raise to more than 105 percent of their maximum pressure. The accumulator and lines are then vented to 95 percent of their maximum pressure. The second venting mode is a manual vent. In this mode the accumulators and lines blow

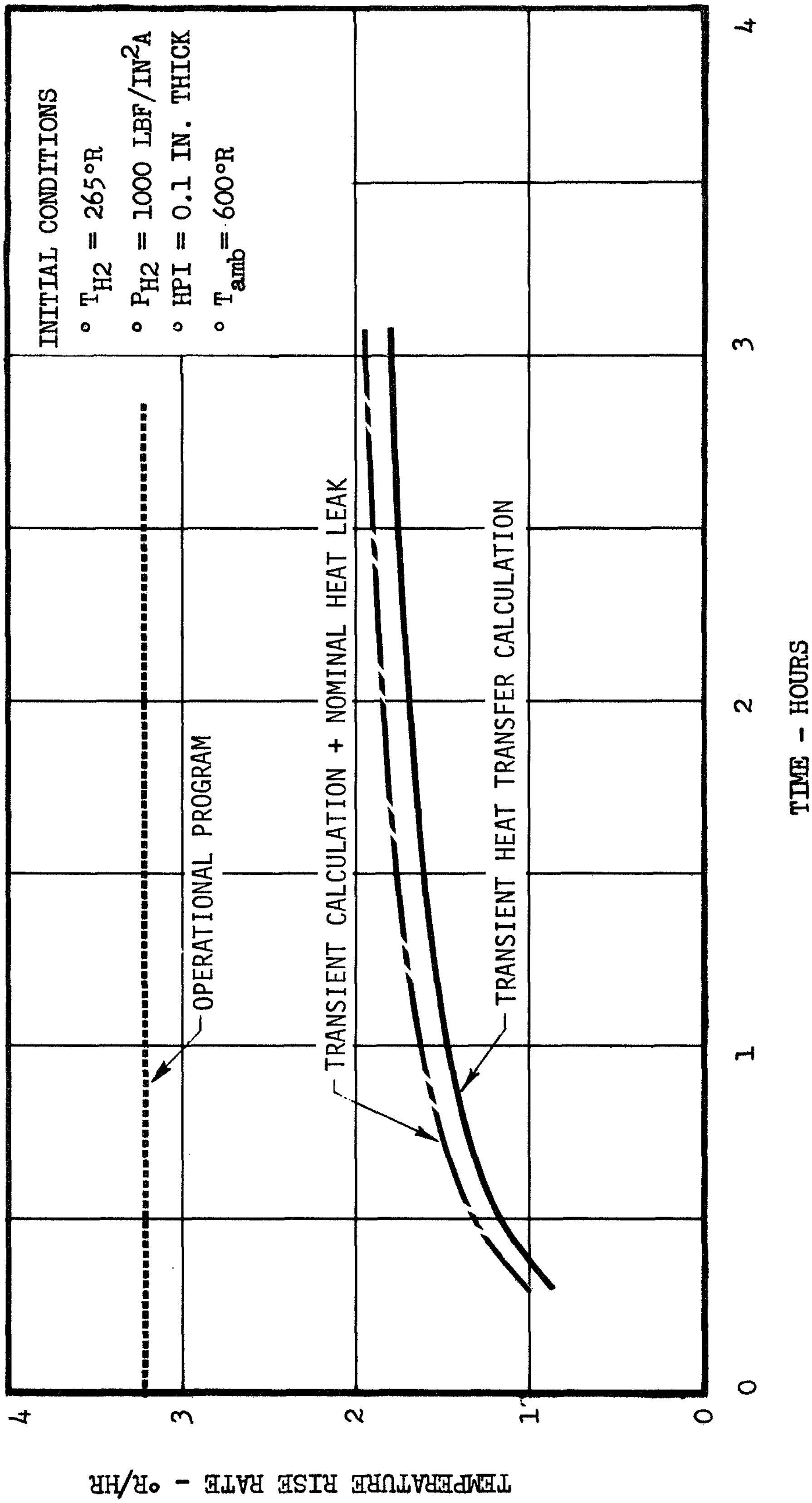

HIGH PRESSURE ACCUMULATOR

BULK H_2 VAPOR TEMPERATURE RISE RATE

FIGURE E-1

down to their minimum accumulator pressure and are then refilled to their maximum pressure with conditioned propellants. The manual vent is used to avoid the large variation in thruster mixture ratio which would result from using the higher temperature propellants that would exist after a long nonuse period.

E-1.2 APS Operating Performance - The operational program was utilized to determine the proper insulation thickness for the accumulators and lines. Figure E-2 shows the temperature rise rate for both the lines and accumulators. As shown, the rate increases slowly as the insulation thickness is decreased. At some critical value of insulation thickness the temperature rise rate rapidly increases; thus for optimum results, the temperature rise rate was kept just below the "knee" of the curve. It can be seen the temperature rise rate for the gas in the accumulators is quite small. An insulation thickness of 0.1 in was chosen for each accumulator which gives a temperature rise rate of 3°R/hour. Insulation thicknesses were chosen for the two propellant lines that give a temperature rise rate of 20°R/hour for an environmental temperature of 600°R.

The baseline missions of Reference (a), the 3rd orbit rendezvous and the 17th orbit rendezvous mission duty system, were analyzed utilizing the operational program. Four parameters were varied to determine the sensitivity of the subsystem performance to variations in operational characteristics. The parameters were hydrogen and oxygen conditioning temperature and hydrogen and oxygen regulation pressure. To establish sensitivity, the parameters were increased to an arbitrary 5 percent above their normal value on an individual basis and a mission was simulated. Figure E-3 shows the band of mixture ratio excursions for the 3rd orbit rendezvous for nominal parameter values. The maximum mixture ratio variation from the nominal value of 4.00 was ± 0.50. Figures E-4, E-5, E-6 and E-7 show the operational characteristics with the parameters varied. A change in the hydrogen parameters has a much larger effect on operational characteristics than does the same change in the oxygen parameters. The most significant parameter was the hydrogen conditioning temperature; increasing its value did not change the degree of mixture ratio variation but did shift the scale of the variation upward; i.e., the range was still ± 0.50 but the mean for the mission was 4.10 instead of 4.00. The converse was true when the oxygen conditioning temperature was raised; the range was still ± 0.5 but the mean was 3.90. Changing the regulator pressure had a similar effect on operational characteristics. The range of mixture ratio

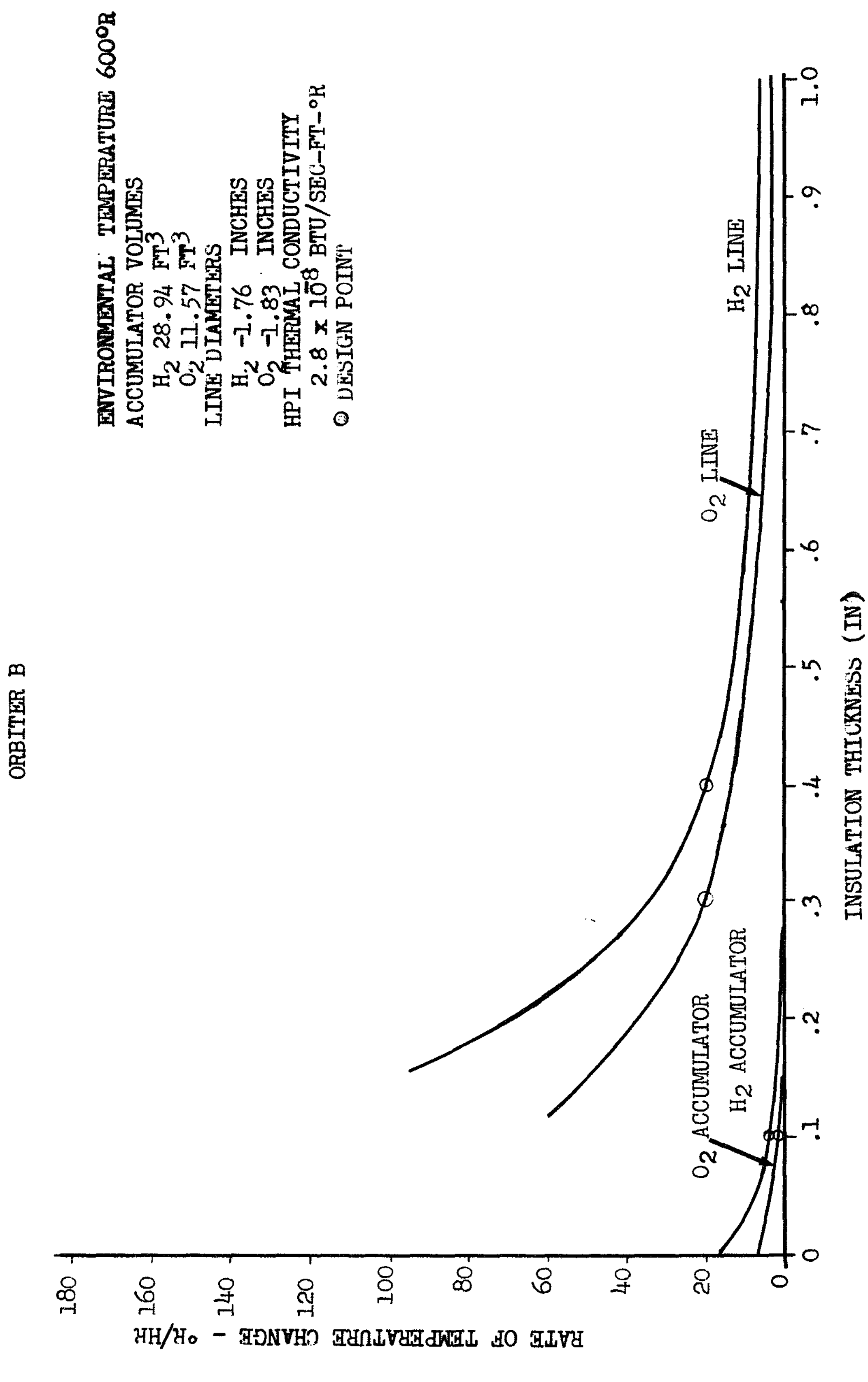

PROPELLANT TEMPERATURE CHANGE DUE TO ENVIRONMENT HEATING
(HIGH PERFORMANCE INSULATION)

FIGURE E-2

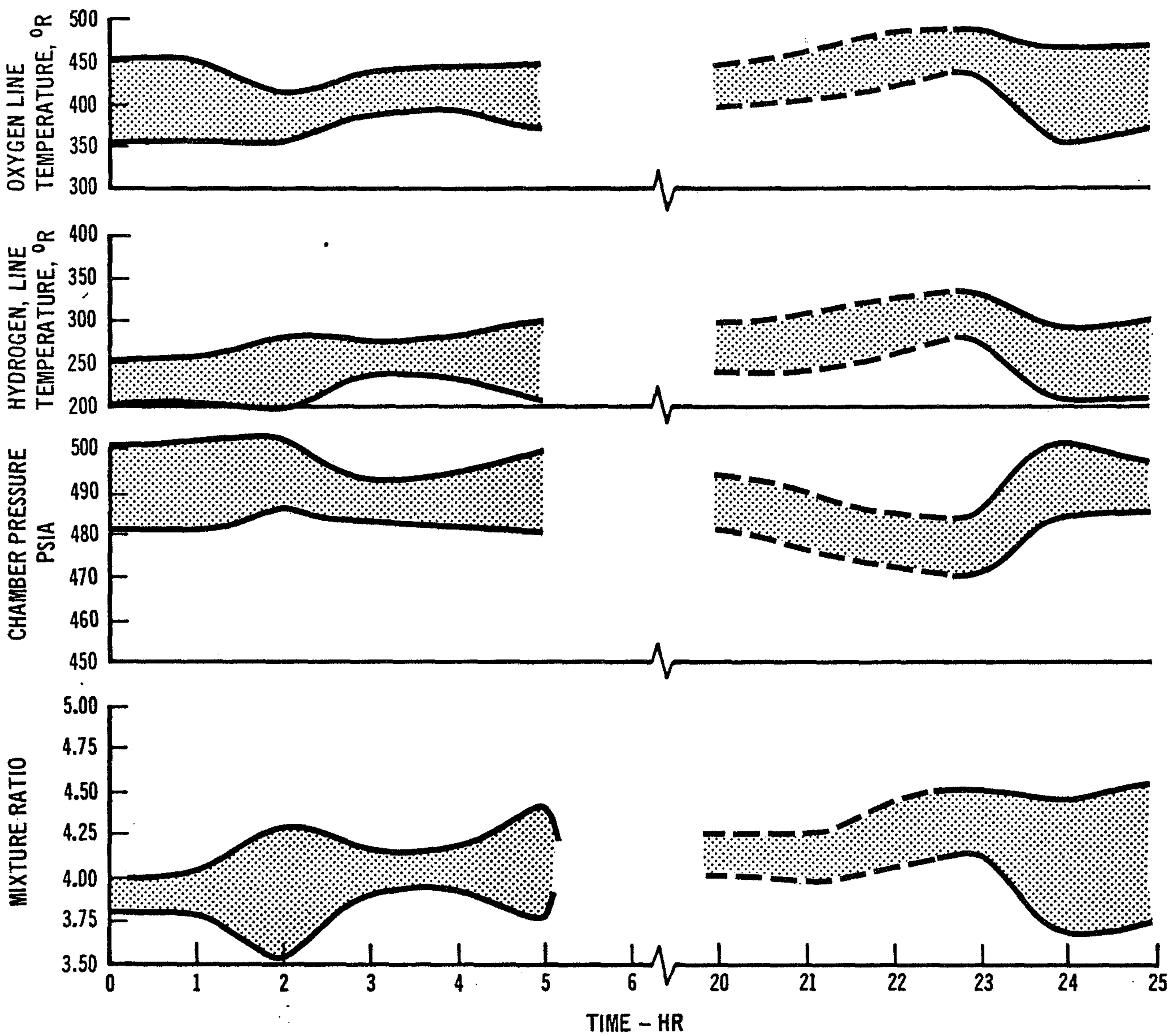

3RD ORBIT NOMINAL

LINES VENTED

FIGURE E-3

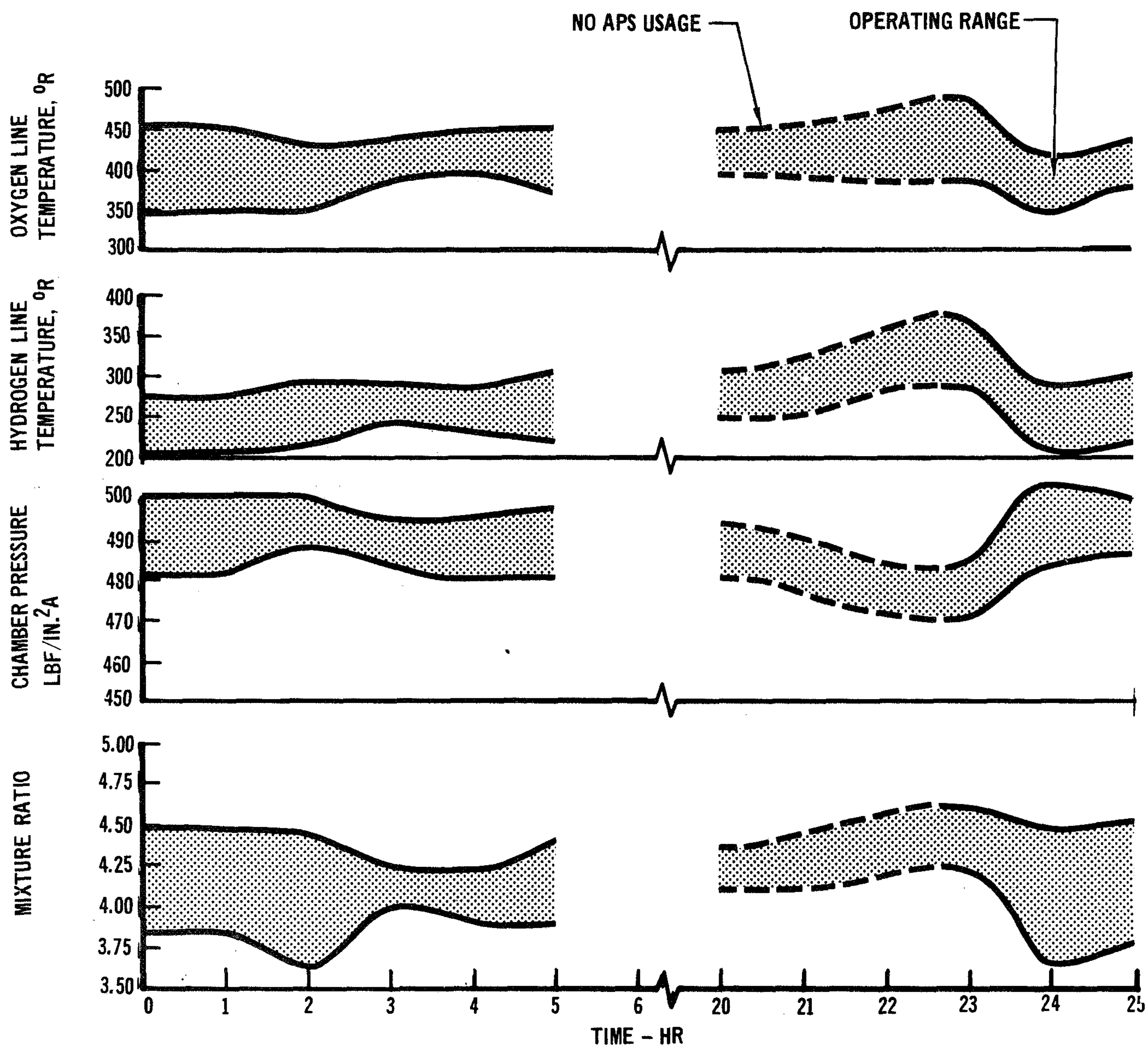

SUBSYSTEM OPERATING CHARACTERISTICS
HYDROGEN CONDITIONING TEMPERATURE INCREASED 5 PERCENT
3RD ORBIT RENDEZVOUS

LINES VENTED

FIGURE E-4

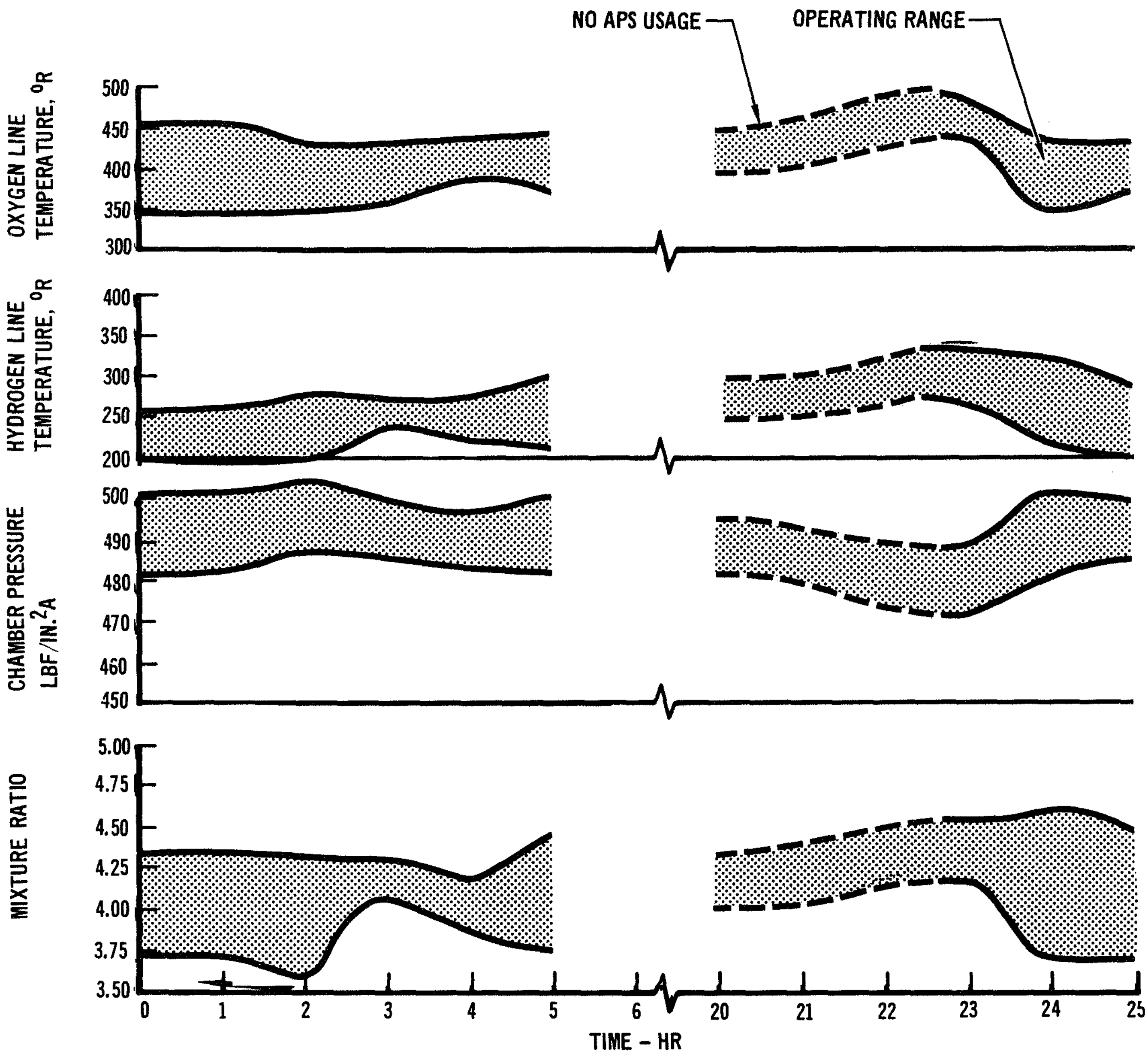

SUBSYSTEM OPERATING CHARACTERISTICS
HYDROGEN REGULATION PRESSURE INCREASED 5 PERCENT
3RD ORBIT RENDEZVOUS

LINES VENTED

FIGURE E-5

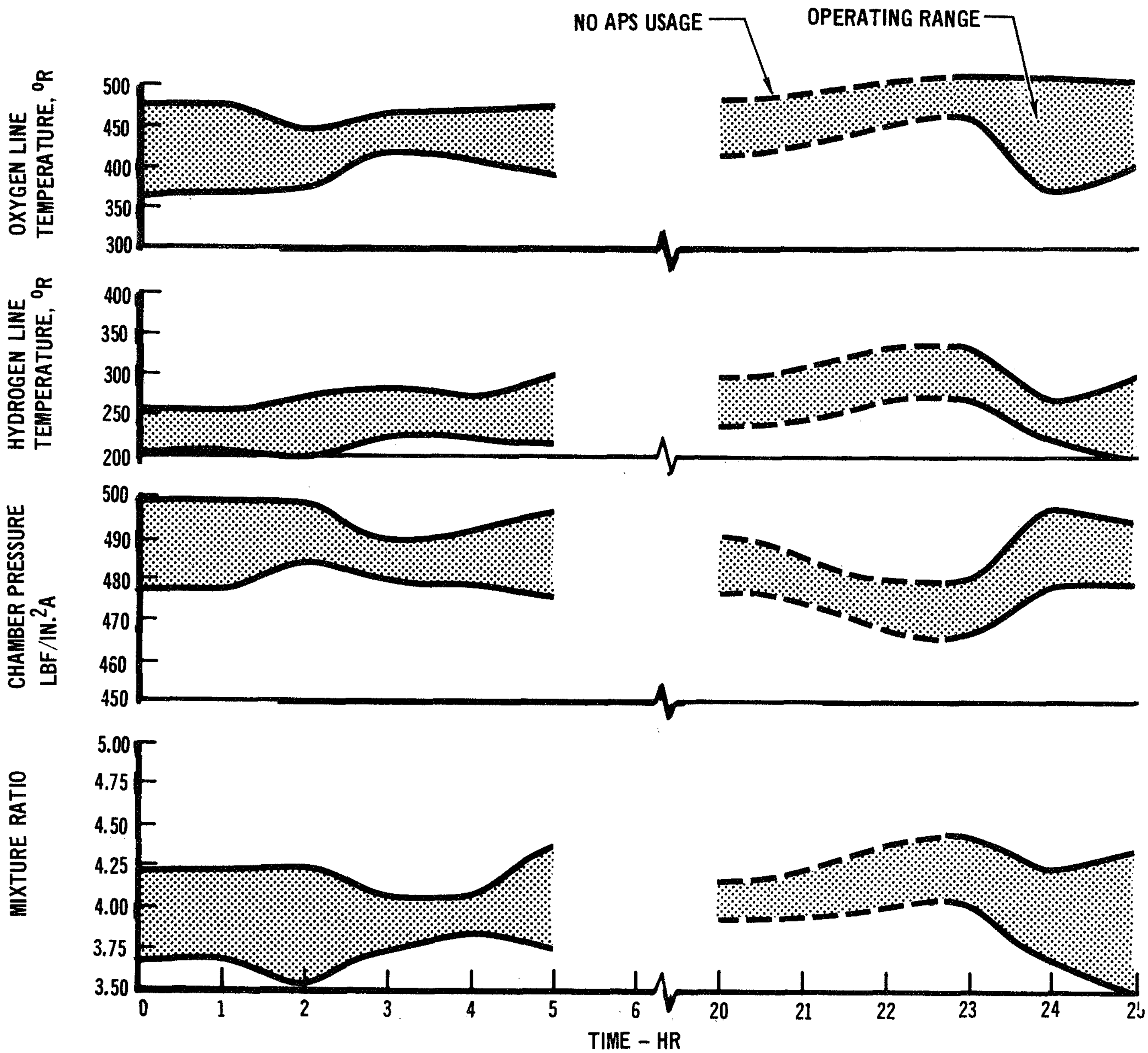

SUBSYSTEM OPERATING CHARACTERISTICS

OXYGEN CONDITIONING TEMPERATURE INCREASED 5 PERCENT
3RD ORBIT RENDEZVOUS

LINES VENTED

FIGURE E-6

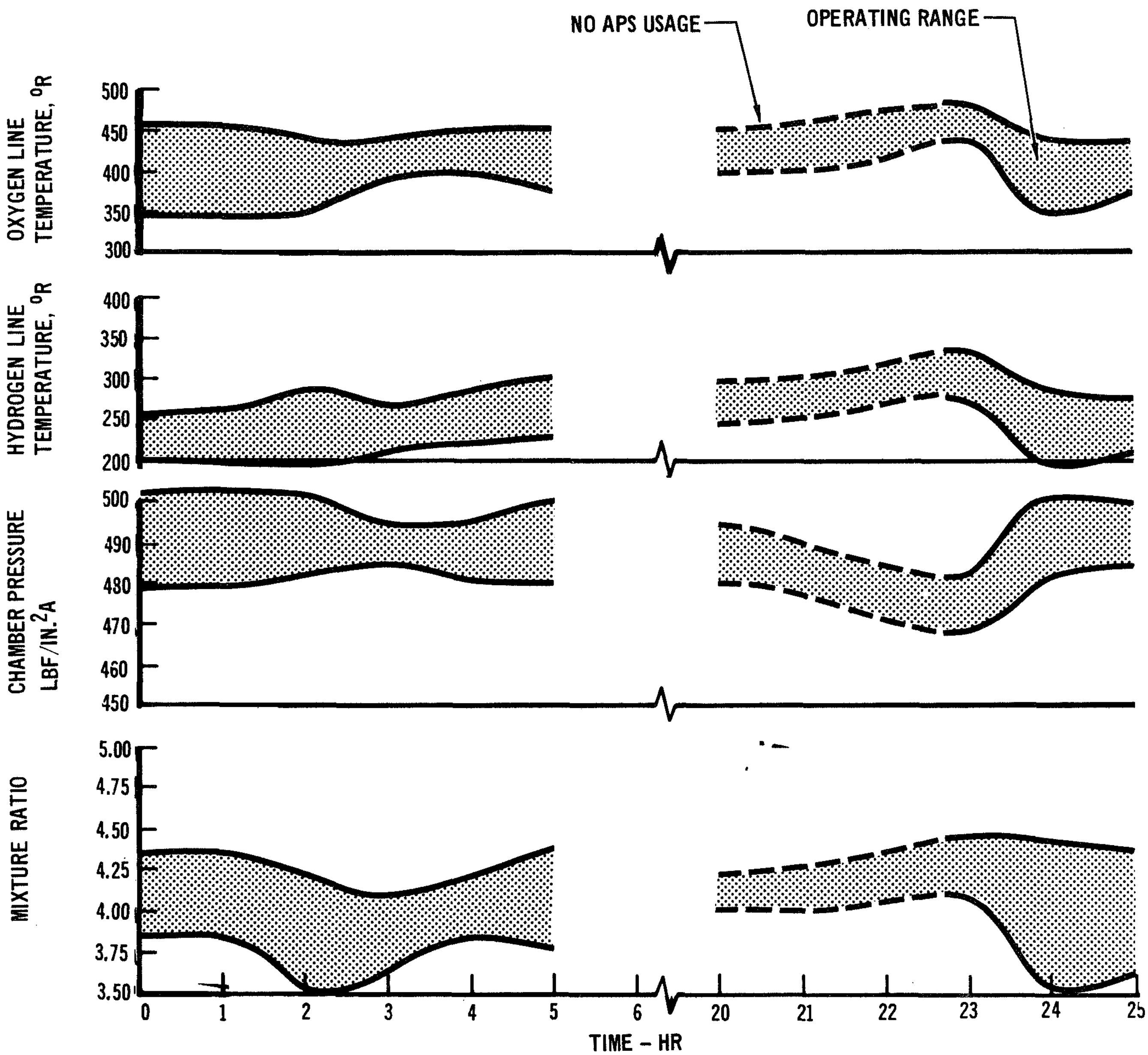

SUBSYSTEM OPERATING CHARACTERISTICS

OXYGEN REGULATION PRESSURE INCREASED 5 PERCENT

3RD ORBIT RENDEZVOUS

LINES VENTED

FIGURE E-7

variation was approximately ± 0.50 and the mean was 4.00. Figure E-8 summarizes the accumulative mixture ratio and resulting total impulse of the APS for nominal and off-nominal operation.

The 3rd orbit rendezvous mission has only two long periods where there is no activity. There is a period of 15 hours when the orbiter is on station and there is a coast period of close to 3 hours immediately after separation with no APS activity. During periods of no activity, the accumulator and line pressures and temperatures increase due to environmental heating. While automatic venting will keep the pressures within acceptable limits, the gas temperature in the accumulator and lines is not controlled. The higher than nominal temperatures cause a mixture ratio shift in the thrusters and requires the thrusters to be able to operate satisfactorily at a higher than nominal mixture ratio. Manual vent reduces this mixture ratio variation by purging the accumulators and the lines of the warm gases. Figure E-3, in conjunction with Figure E-9, shows the effect on mixture ratio of the manual vent concept. As shown in Figure E-3, the reduction in mixture ratio is quite marked. Manual vent was not required during the second period of inactivity because the variation in mixture ratio did not warrant the venting with the associated loss of propellant.

A similar analyses was performed for the 17th orbit rendezvous mission. (Figures E-10, E-11, E-12, E-13, and E-14) The same basic conclusions can be drawn about the 17th orbit rendezvous mission as were drawn about the 3rd orbit rendezvous mission; increasing the parameters for the hydrogen increase overall mixture ratio while increasing the oxygen parameters does the reverse.

The 17th orbit rendezvous mission is approximately three times as long as the 3rd orbit rendezvous mission. This mission contains three periods of APS inactivity of length eight, eleven, and forty hours. If manual vent is not utilized after each of the long inactive periods, the mixture ratios of the thrusters would be 4.76, 4.92, and 5.47. If manual vent was utilized, the mixture ratios are reduced to 4.02, 3.90, and 4.19. Thus venting significantly reduces the adverse effects associated with a large mixture ratio variation. Even though the nonvented subsystem has much larger mixture ratio variations, the overall mission mixture ratio is the same for the vented and nonvented subsystems. Figure E-15 shows the subsystem operating characteristics for the subsystem with automatic vent only.

A study was conducted to determine the effects of insulation degradation on subsystem operating characteristics. To accomplish this, the thermal

ORBITER B

DESIGN CONDITIONS	3RD ORBIT RENDEZVOUS		17TH ORBIT RENDEZVOUS	
	INTEGRATED MIXTURE RATIO	TOTAL IMPULSE LBF-SEC	INTEGRATED MIXTURE RATIO	TOTAL IMPULSE LBF-SEC
NOMINAL DESIGN CONDITIONS	4.048	12,078,498	4.027	13,336,867
NOMINAL DESIGN CONDITIONS (NO VENT)	4.048	12,077,977	4.020	13,335,566
OXYGEN CONDITIONING TEMPERATURE INCREASED 5%	3.938	11,973,966	3.931	13,204,708
HYDROGEN CONDITIONING TEMPERATURE INCREASED 5%	4.132	12,061,734	4.134	13,299,448
OXYGEN REGULATION PRESSURE INCREASED 5%	4.004	12,063,065	4.004	13,301,044
HYDROGEN REGULATION PRESSURE INCREASED 5%	4.009	12,091,579	4.039	13,334,203

APS OFF NOMINAL DESIGN SUMMARY

FIGURE E-8

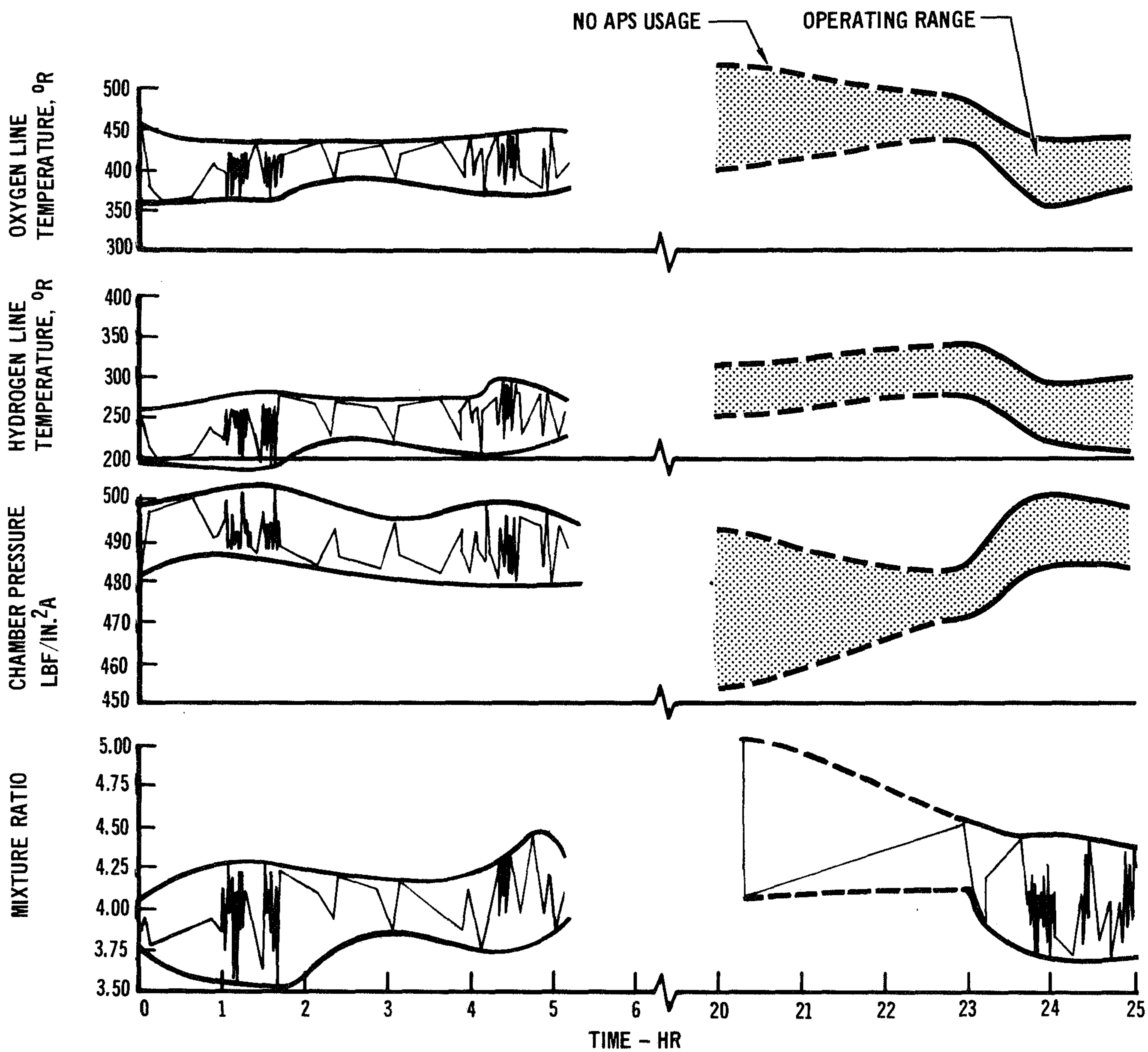

SUBSYSTEM OPERATING CHARACTERISTICS

NOMINAL DESIGN CONDITIONS (NO VENT)
3RD ORBIT RENDEZVOUS

FIGURE E-9

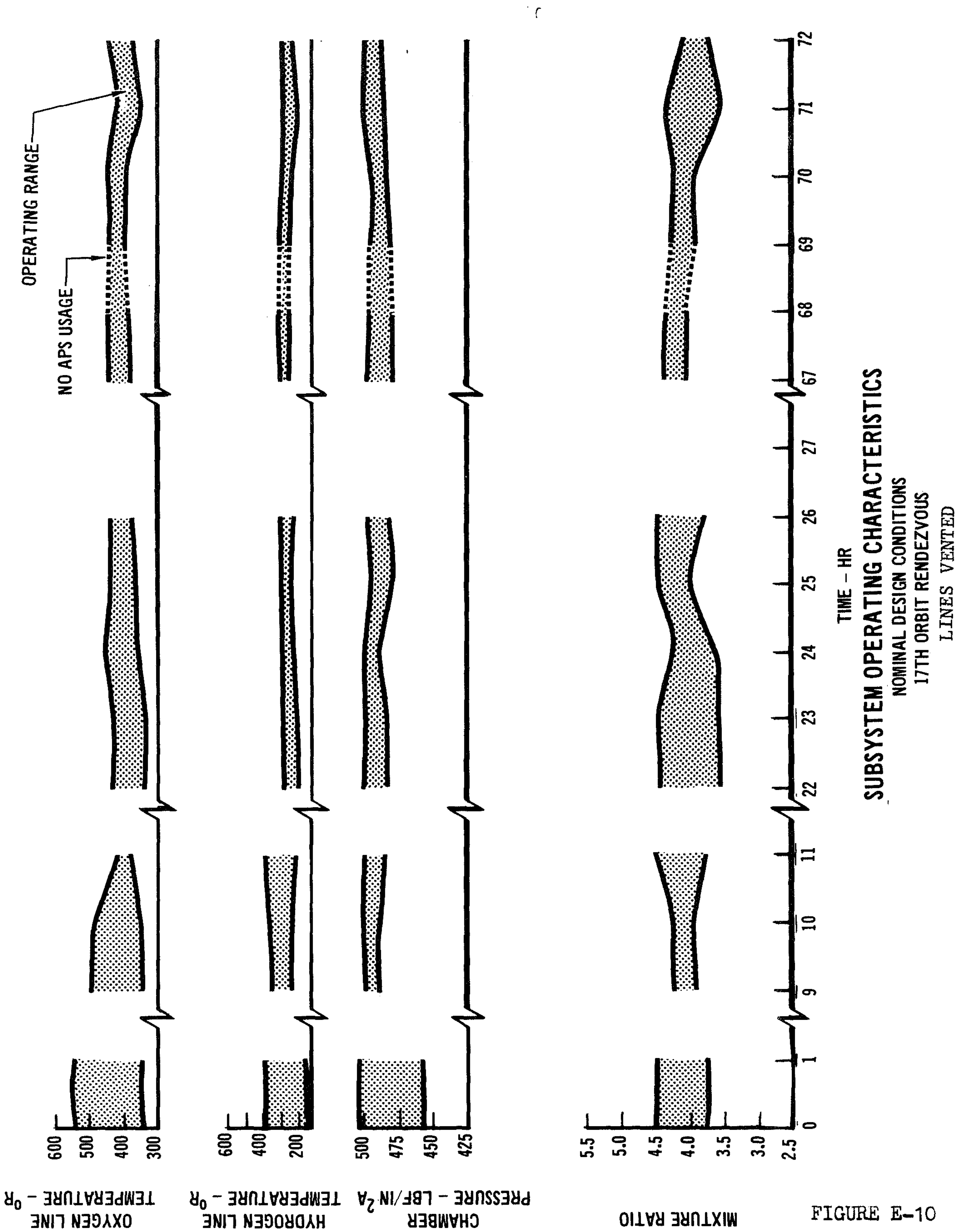
OPERATING RANGE
NO APS USAGE
OXYGEN LINE TEMPERATURE – °R
HYDROGEN LINE TEMPERATURE – °R
CHAMBER PRESSURE – LBF/IN.2A
MIXTURE RATIO
600
500
400
300
200
475
450
425
5.5
5.0
4.5
4.0
3.5
3.0
2.5
0
1
9
10
11
22
23
24
25
26
27
67
68
69
70
71
72
TIME – HR
SUBSYSTEM OPERATING CHARACTERISTICS
NOMINAL DESIGN CONDITIONS
17TH ORBIT RENDEZVOUS
LINES VENTED

FIGURE E-10

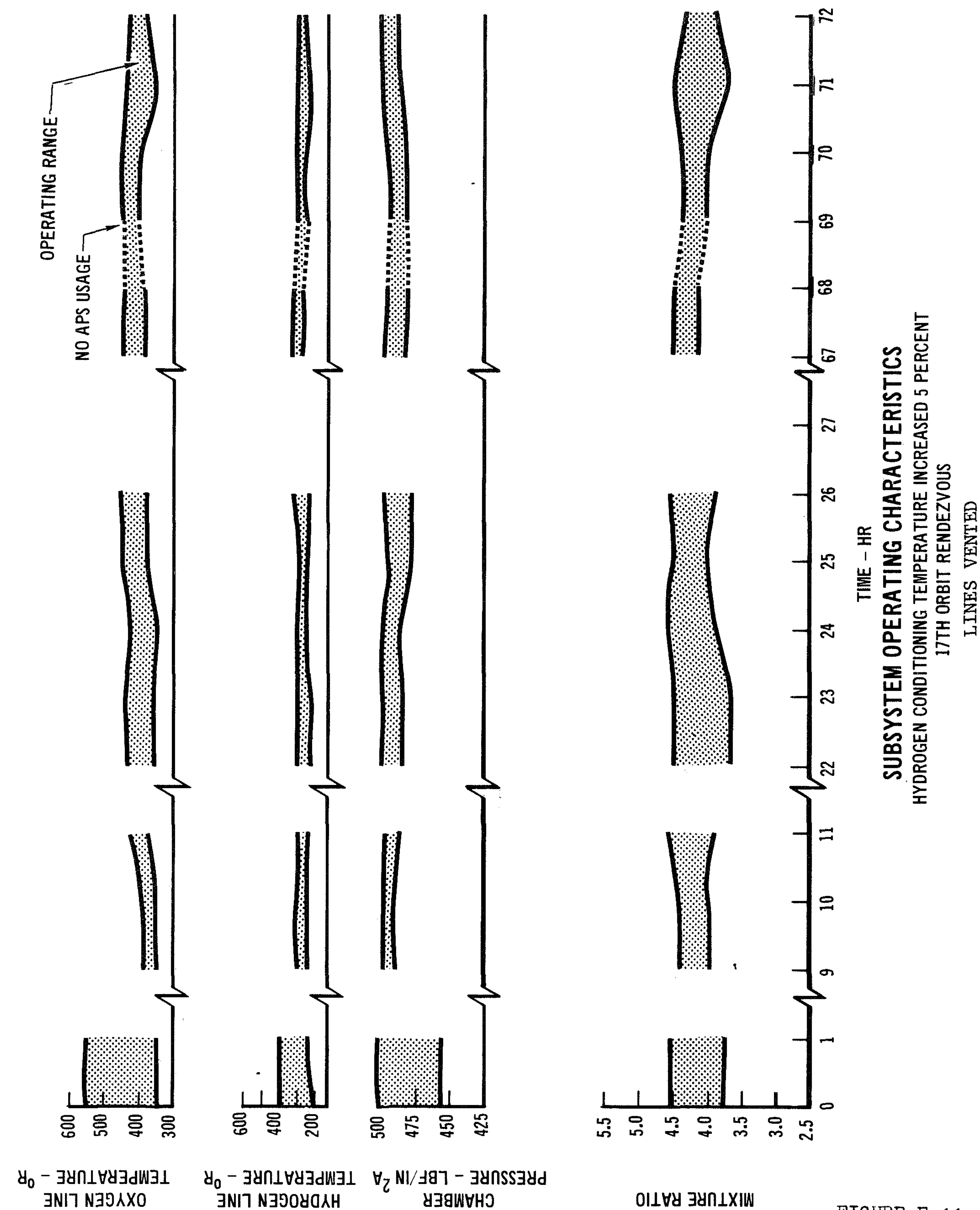

SUBSYSTEM OPERATING CHARACTERISTICS
HYDROGEN CONDITIONING TEMPERATURE INCREASED 5 PERCENT
17TH ORBIT RENDEZVOUS
LINES VENTED

FIGURE E-11

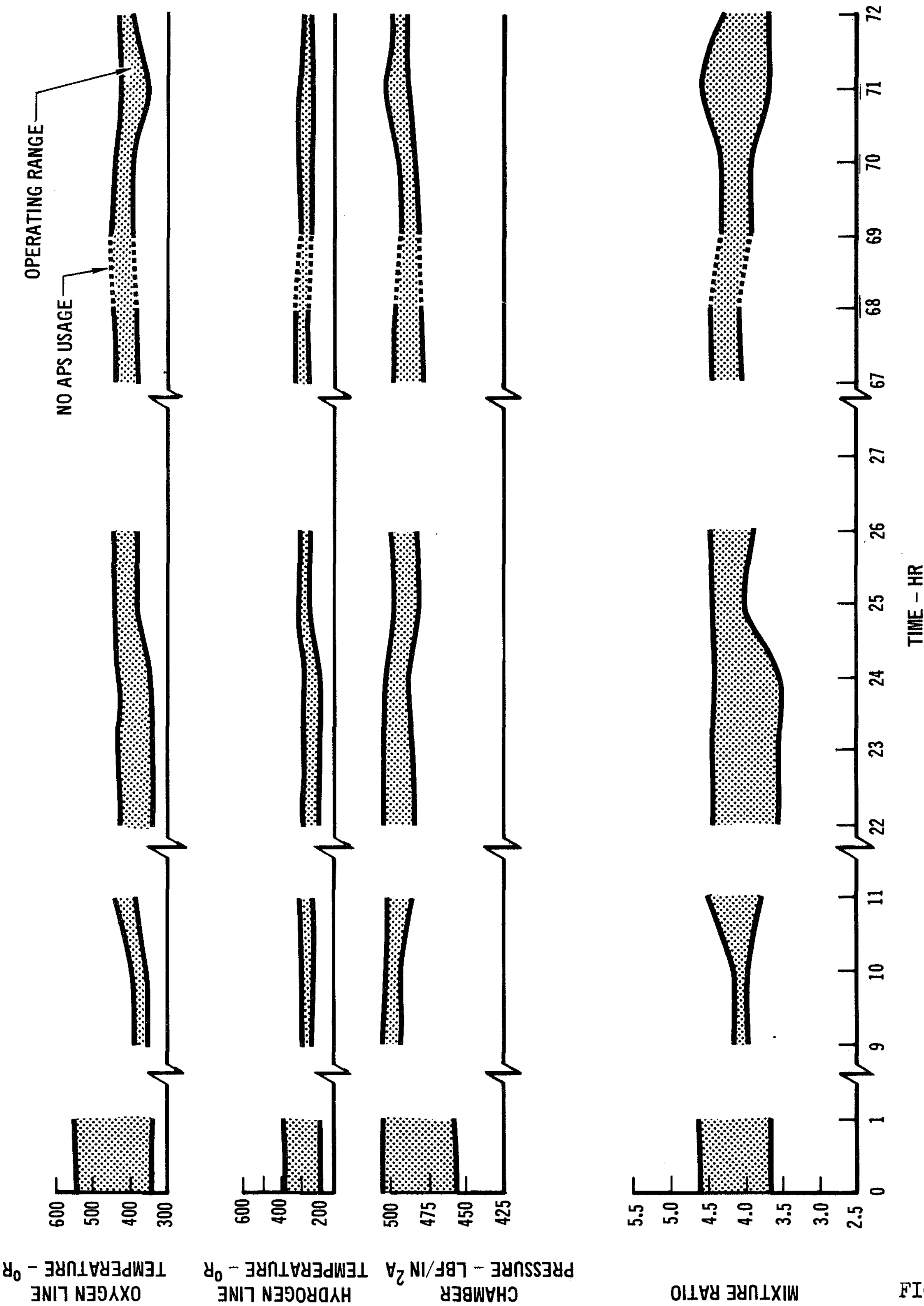

SUBSYSTEM OPERATING CHARACTERISTICS
HYDROGEN REGULATION PRESSURE INCREASED 5 PERCENT
17TH ORBIT RENDEZVOUS
LINES VENTED

FIGURE E-12

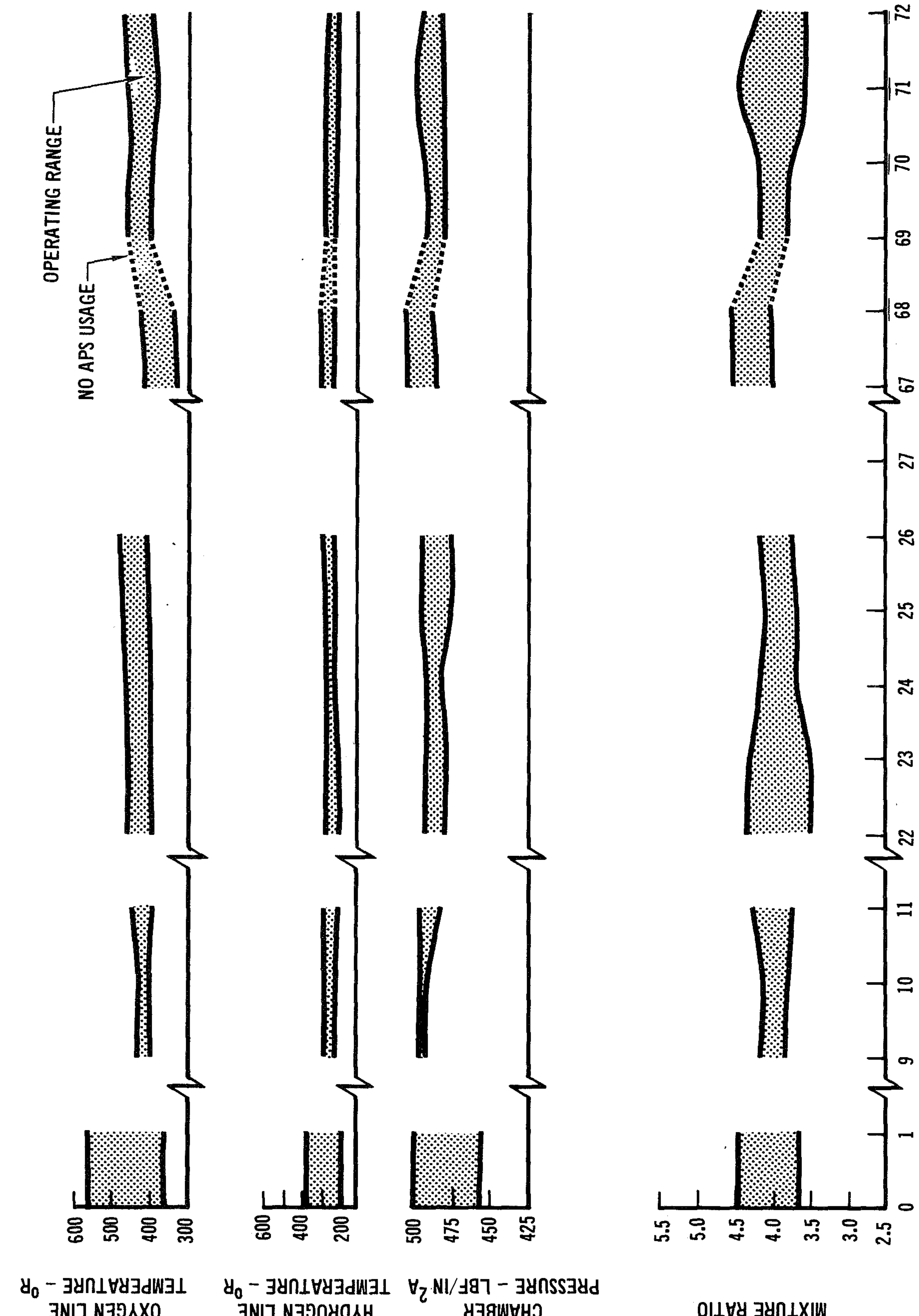

SUBSYSTEM OPERATING CHARACTERISTICS
OXYGEN CONDITIONING TEMPERATURE INCREASED 5 PERCENT
17TH ORBIT RENDEZVOUS
LINES VENTED

FIGURE E-13

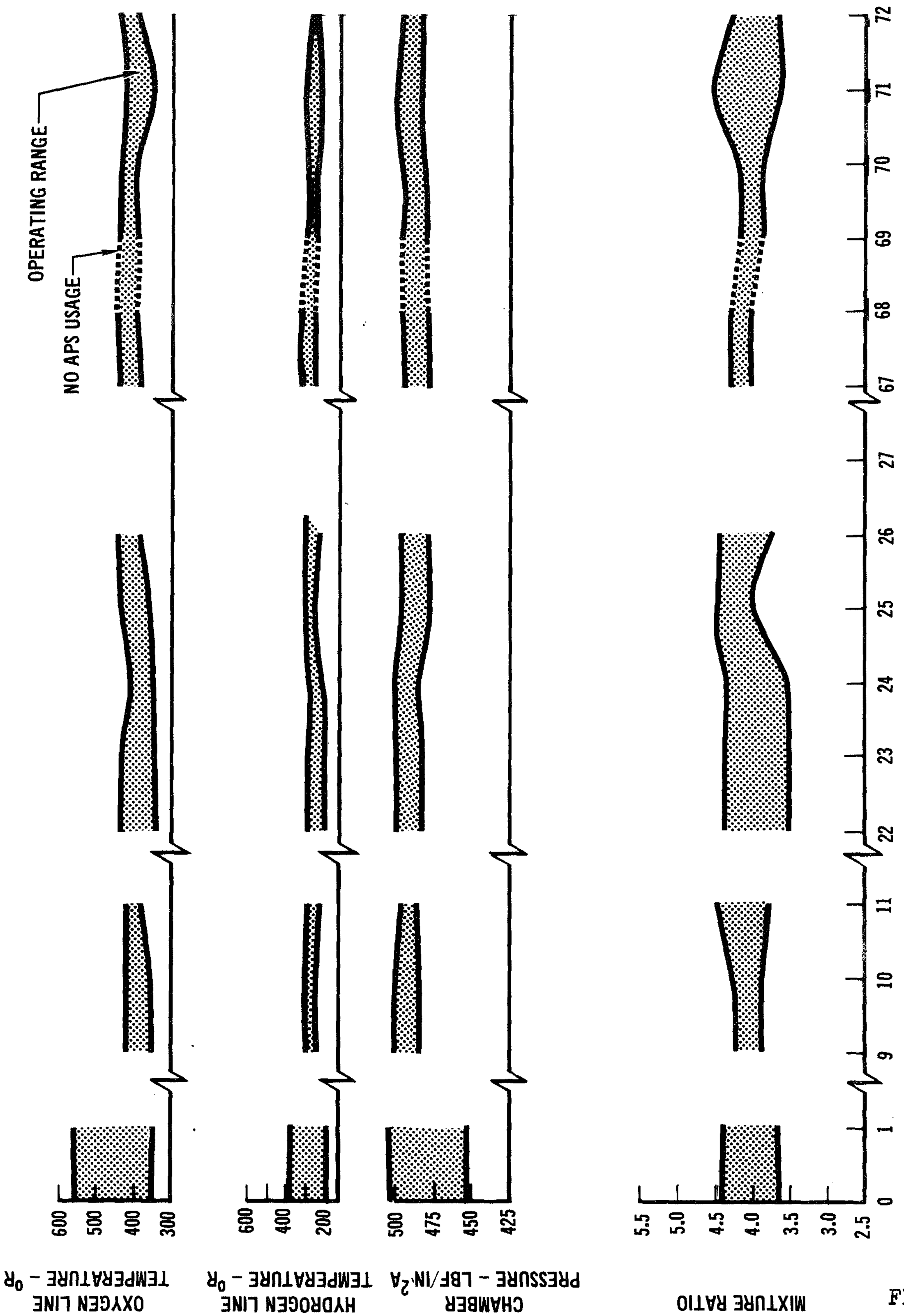

SUBSYSTEM OPERATING CHARACTERISTICS
OXYGEN REGULATION PRESSURE INCREASED 5 PERCENT
17TH ORBIT RENDEZVOUS

LINES VENTED

FIGURE E-14

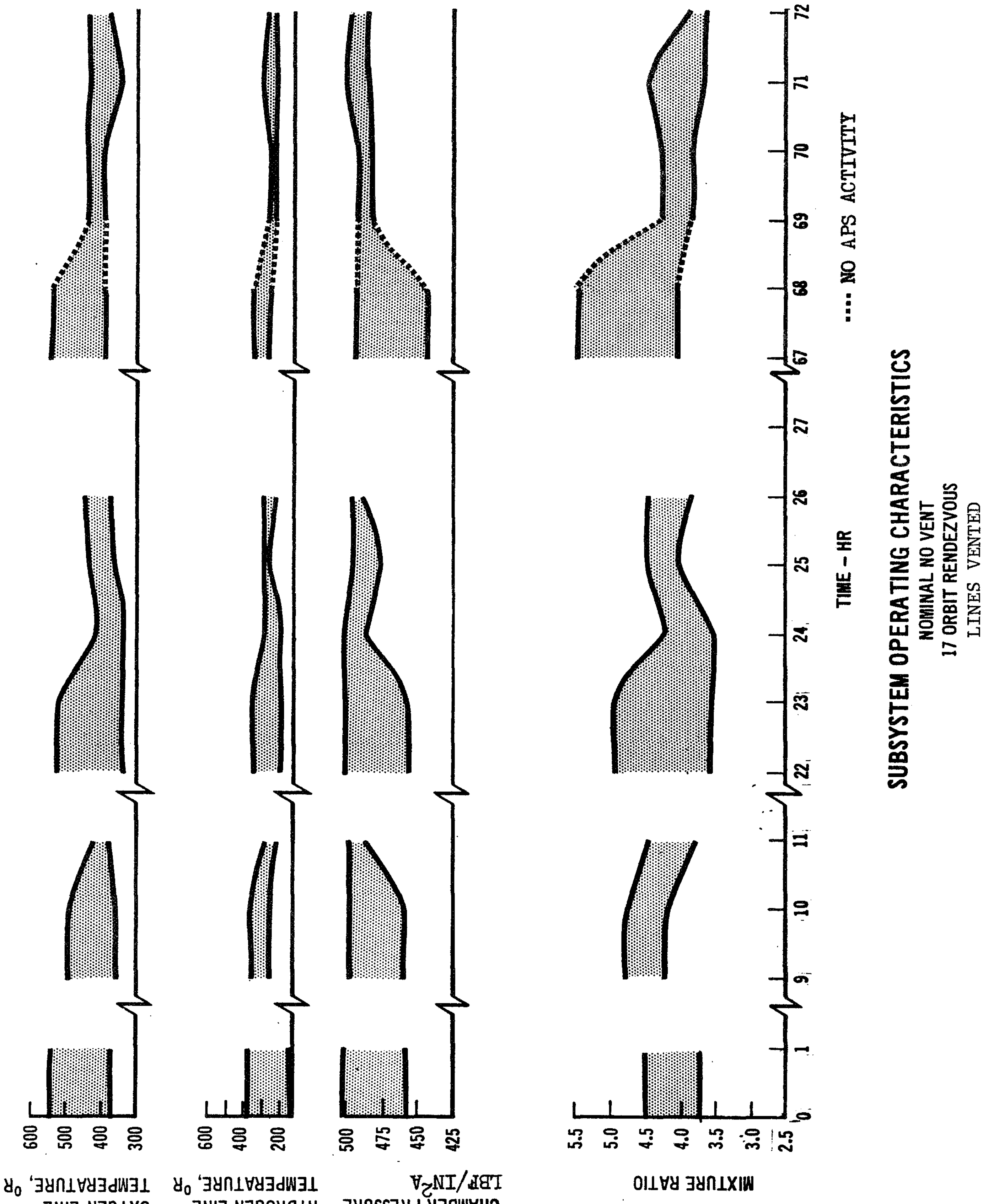
OXYGEN LINE
TEMPERATURE, °R
600
500
400
300
HYDROGEN LINE
TEMPERATURE, °R
600
400
200
CHAMBER PRESSURE
LBF/IN2A
500
475
450
425
MIXTURE RATIO
5.5
5.0
4.5
4.0
3.5
3.0
2.5
0
1
9
10
11
22
23
24
25
26
27
67
68
69
70
71
72
TIME - HR
.... NO APS ACTIVITY
SUBSYSTEM OPERATING CHARACTERISTICS
NOMINAL NO VENT
17 ORBIT RENDEZVOUS
LINES VENTED

FIGURE E-15

conductivity of the insulation on the tanks and lines was increased by a factor of two and a factor of five. Figure E-16 shows the mixture ratio variation for the above conditions compared to the reference insulation. During periods of heavy usage, the mixture ratio shift caused by insulation degradation was negligible; however, during periods of inactivity, such as the period following separation, the mixture ratio variation doubled, but is still not excessive. Figure E-17 presents the line temperatures versus time corresponding to the mixture ratio variation of the preceeding figure. As shown, during periods of inactivity the variation in line temperature is quite significant and is the predominate cause of the mixture ratio changes.

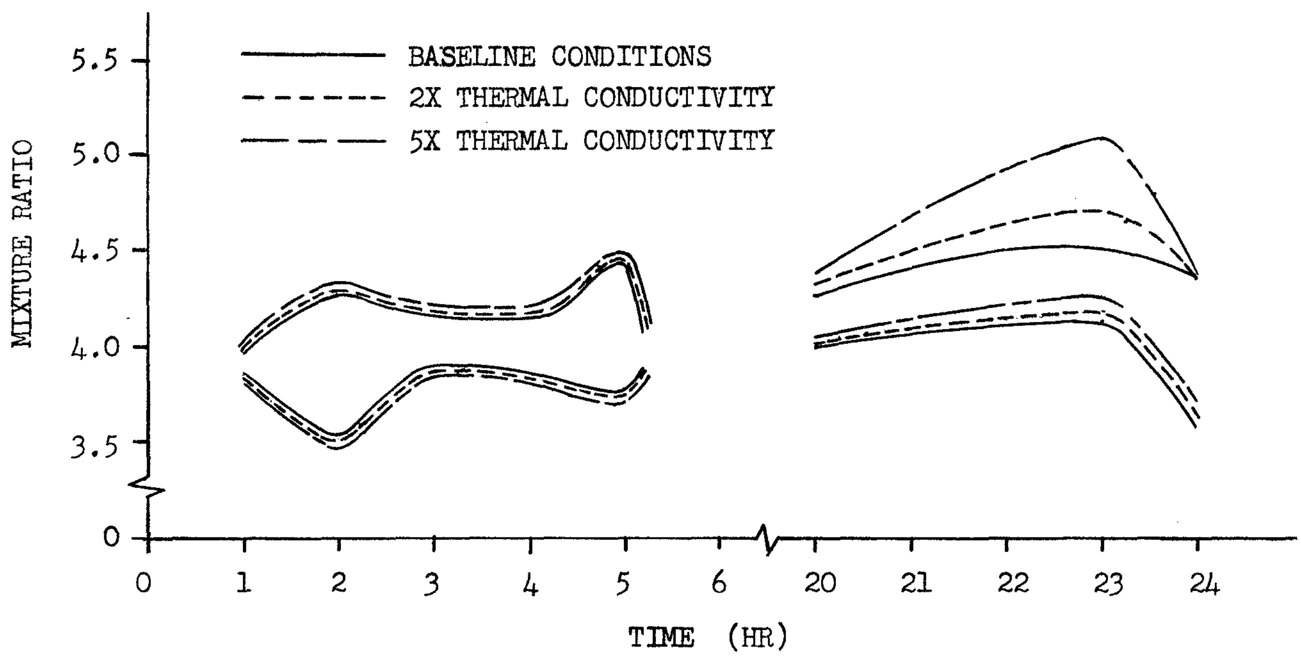

MIXTURE RATIO VERSUS TIME

3RD ORBIT RENDEZVOUS - ORBITER B

(VENTED PRIOR TO STATION SEPARATION)

FIGURE E-16

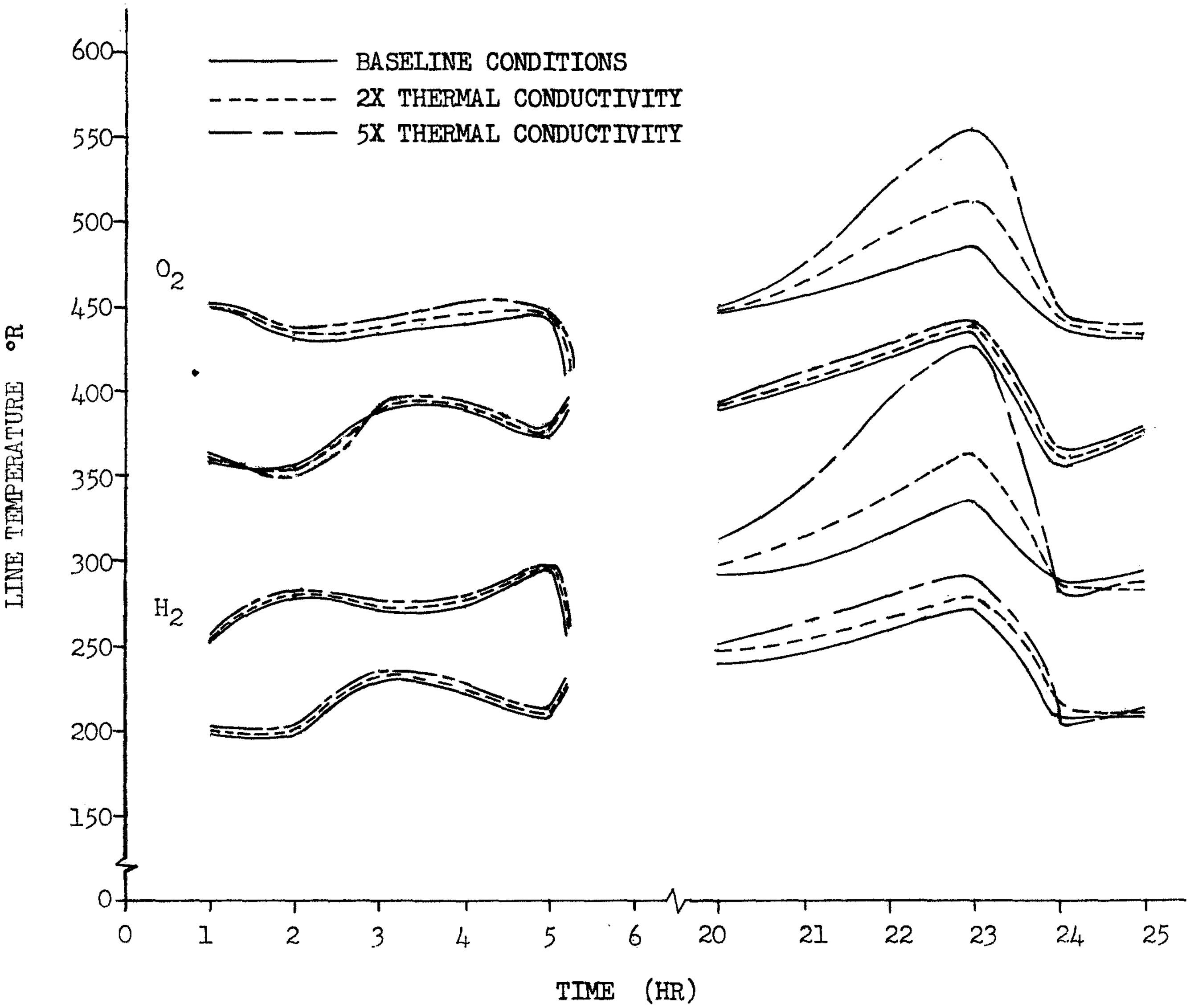

LINE TEMPERATURE VERSUS TIME

3RD ORBIT RENDEZVOUS ORBITER B

(VENTED PRIOR TO STATION SEPARATION)

FIGURE E-17

E-2. HIGH PRESSURE THRUSTER/FEED SUBASSEMBLY TRANSIENT

To determine the transient characteristics of the feed subassembly and thruster pulse mode performance, a digital computer program was developed to simulate the auxiliary propulsion subsystem thruster start and shutdown transients. Transient models were developed for lines, valves, orifices, regulators, and thrusters. These components were integrated into a transient analysis computer program to model the feed subassembly downstream of accumulators, accurately simulating line lengths, diameters, and component locations. The study was confined to the feed subassembly and thrusters because the relatively large volume of the accumulators effectively decouples this portion of the subsystem from the conditioner assembly.

E-2.1 Computer Program Description - The thruster model is used to analyze the transient flow and combustion processes in the injector and thrust chamber. Combustion and performance parameters are calculated assuming an equilibrium combustion process. That is, it is a combustor model rather than a combustion model because it calculates performance using idealized combustion data and does not analyze actual combustion processes. The set of differential equations describing the thruster are solved using the finite time increment Euler integration technique. The set of differential equations describing the mass and momentum in the lines, valves, orifices, and regulator are solved simultaneously using Hammings predictor-corrector integration technique. Program output includes a time history of temperature, pressure, and weight flow at any desired location. In addition, performance parameters such as specific impulse, total impulse, mixture ratio, and thruster chamber temperature are calculated.

E-2.2 Results - An evaluation was conducted to determine the sensitivity of thruster performance to feed line diameter. Figure E-18 shows the variation in minimum impulse bit with feed line diameter. The feed line network used simulated the Orbiter B line layout. The figure shows that the minimum impulse bit is a linear function of the line diameter in the range of a 20 percent variation.

Figure E-19 shows a typical profile of the chamber, fuel injector, and oxidizer injector pressure. The valve signature utilized for this study had a 20 ms delay, a 10 ms time to full open, 20 ms full open time, and 10 ms time to full closed. The fuel valve led the oxidizer valve by 2 ms. The chamber pressure rose slowly from the time the valves started to open until ignition

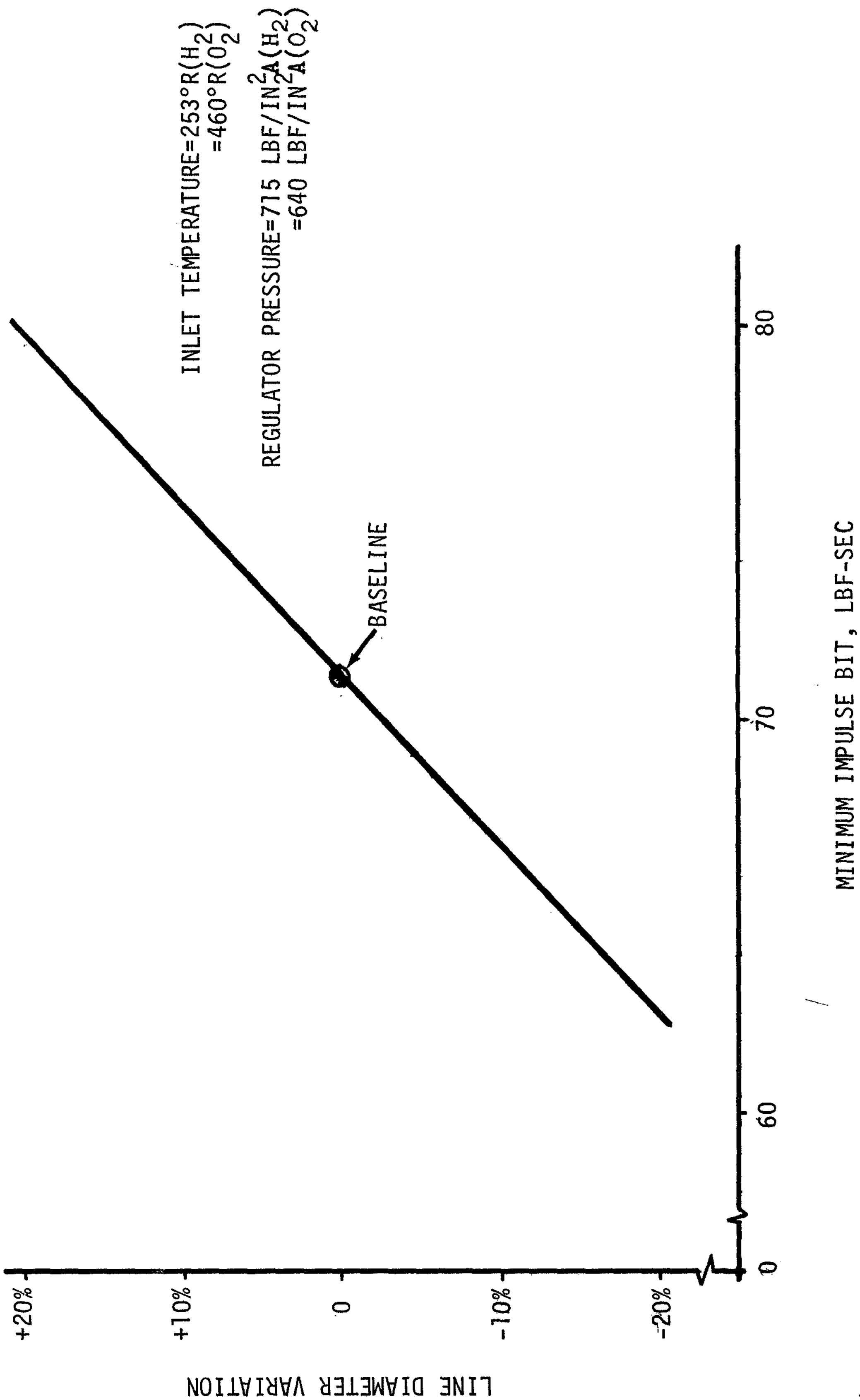

THRUSTER IMPULSE VARIATION

FIGURE E-18

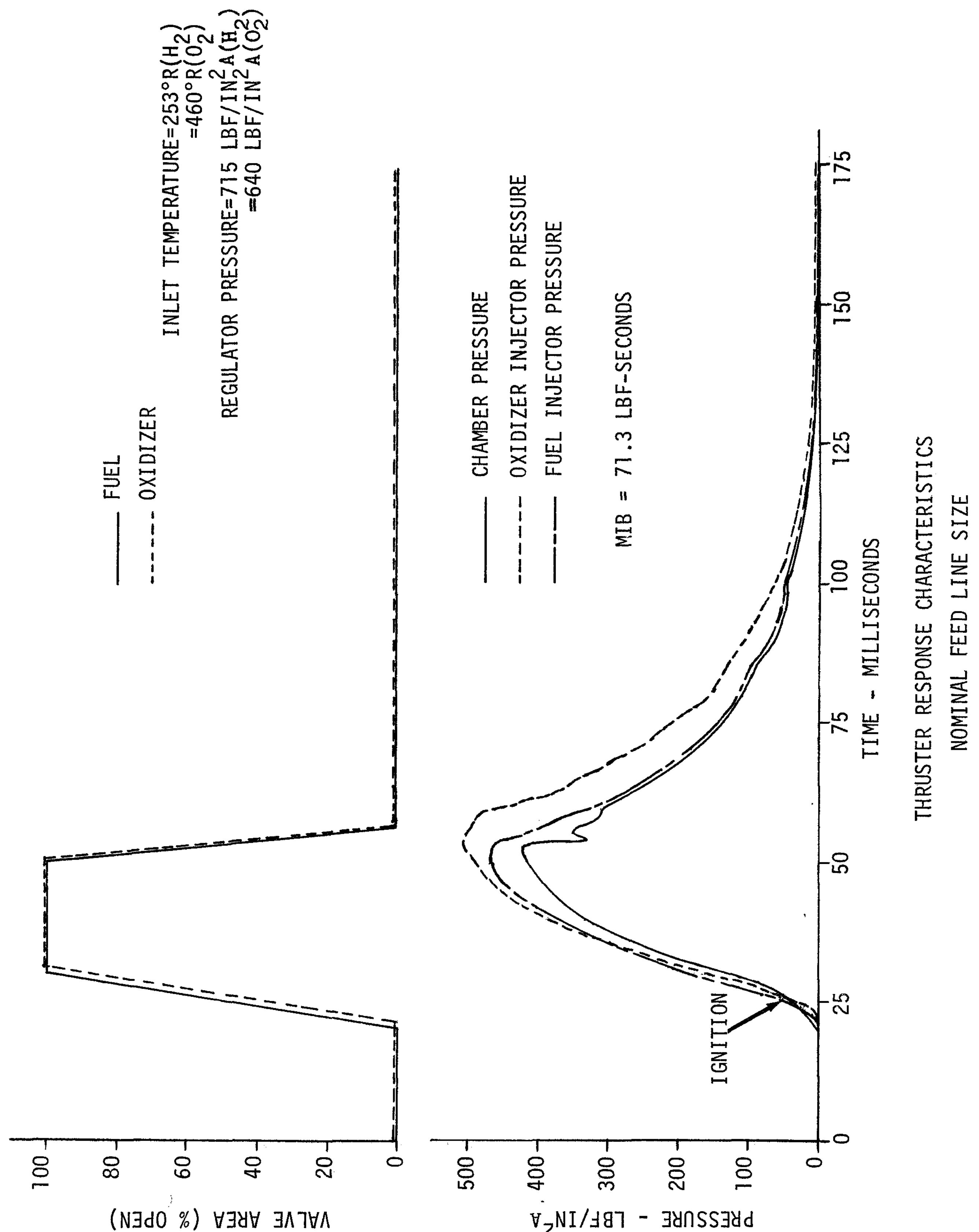
FUEL
OXIDIZER
INLET TEMPERATURE=253°R(H2)
=460°R(O2)
REGULATOR PRESSURE=715 LBF/IN2A(H2)
=640 LBF/IN2A(O2)
CHAMBER PRESSURE
OXIDIZER INJECTOR PRESSURE
FUEL INJECTOR PRESSURE
MIB = 71.3 LBF-SECONDS
IGNITION
VALVE AREA (% OPEN)
PRESSURE - LBF/IN2A
TIME - MILLISECONDS
THRUSTER RESPONSE CHARACTERISTICS
NOMINAL FEED LINE SIZE

FIGURE E-19

occurred at 25 ms; the chamber pressure then rose rapidly as the valves opened more fully, and then dropped sharply as the valves began to close. At 60 ms the valves were fully closed and the pressures decayed in 100 ms. Both injector pressures closely followed the chamber pressure trace.

A second analysis was conducted to determine transient thruster performance as a function of the full-open time of the valves. For this analysis the thruster was connected to short large-diameter fuel and oxidizer lines to eliminate line size effects. Figure E-20 shows the impulse bit sizes obtained and Figure E-21 shows the integrated vacuum specific impulse of the thruster as a function of fully-open valve time for a first pulse.

Figure E-22 shows the response characteristics for a thruster whose valves are open for 90 ms. The characteristics of such a relatively long pulse are a function not only of the thruster geometry but also of the feed assembly. The feed assembly dynamic characteristics are reflected in the cyclic oscillation of the oxidizer and fuel injector pressures which were induced by the fuel and oxidizer valves opening. The result is a decrease in chamber pressure and a variation in impulse from the expected value.

The line surge pressure experienced when the propellant valve is closed is a complex function of line diameter, the length of time the valve was open, and the closing time of the valve; however, the maximum surge pressure was less than 40 percent of the regulation pressure and thus was not considered a problem.

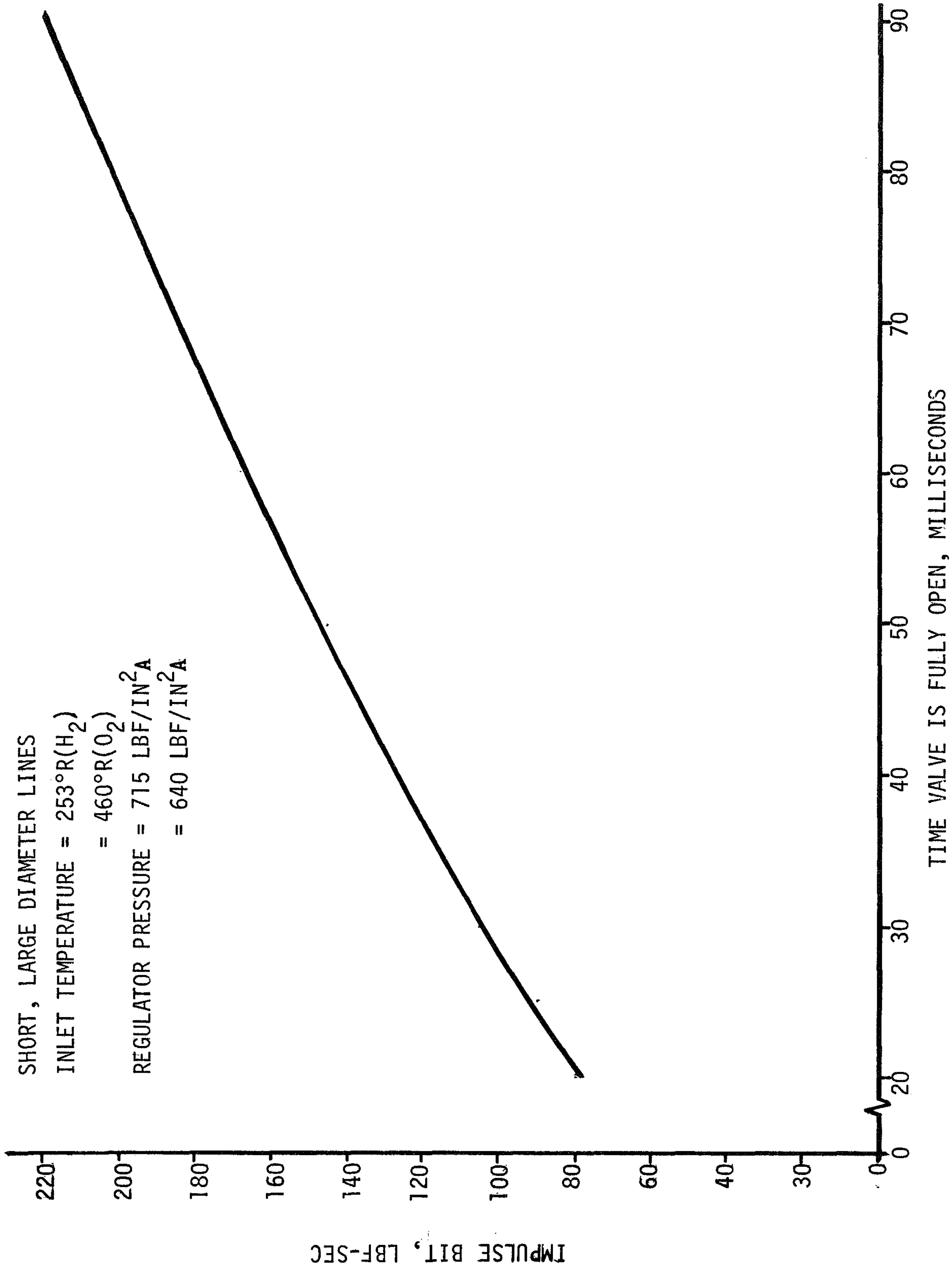

THRUSTER TRANSIENT PERFORMANCE

FIGURE E-20

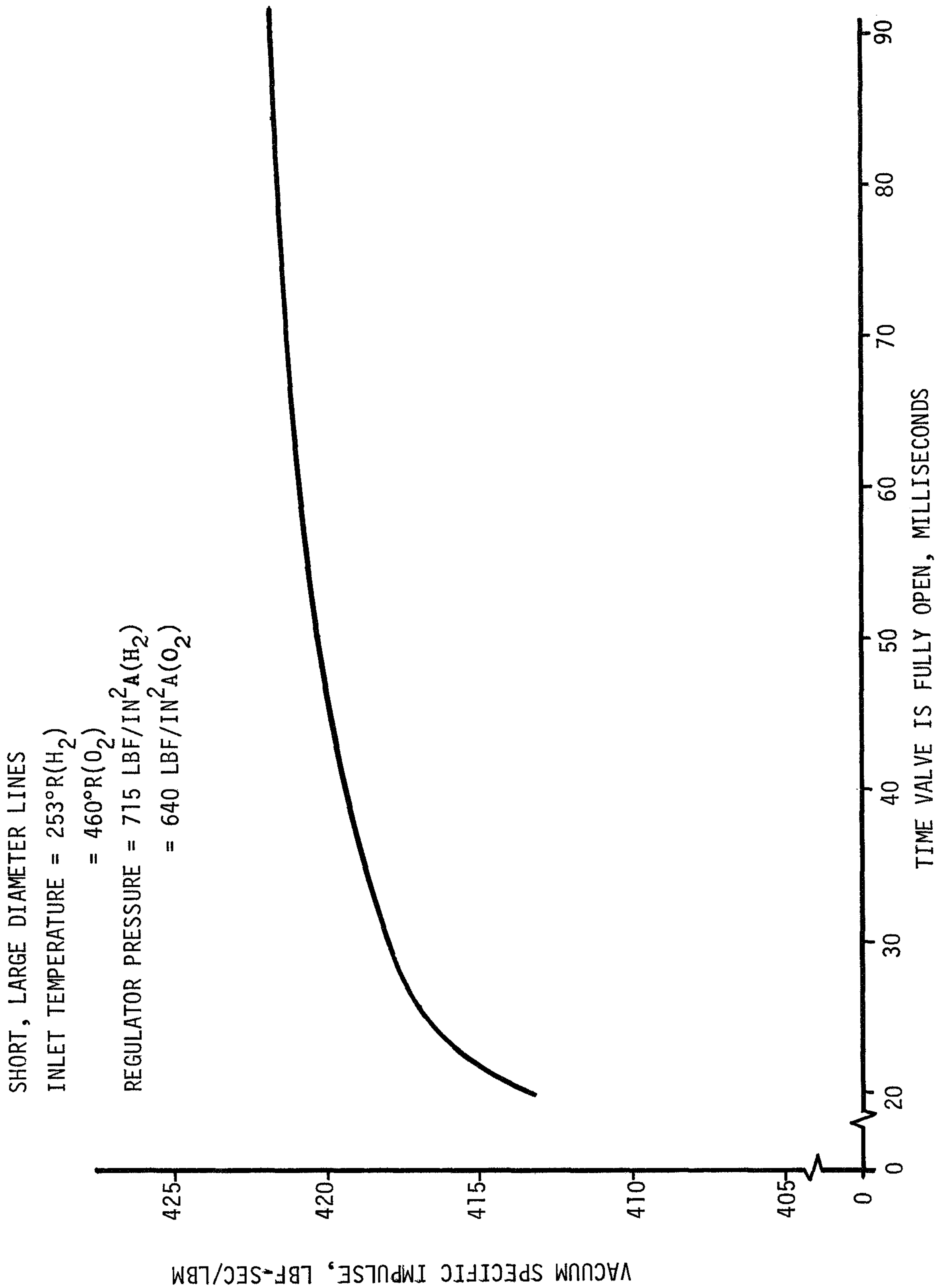

THRUSTER TRANSIENT PERFORMANCE

FIGURE E-21

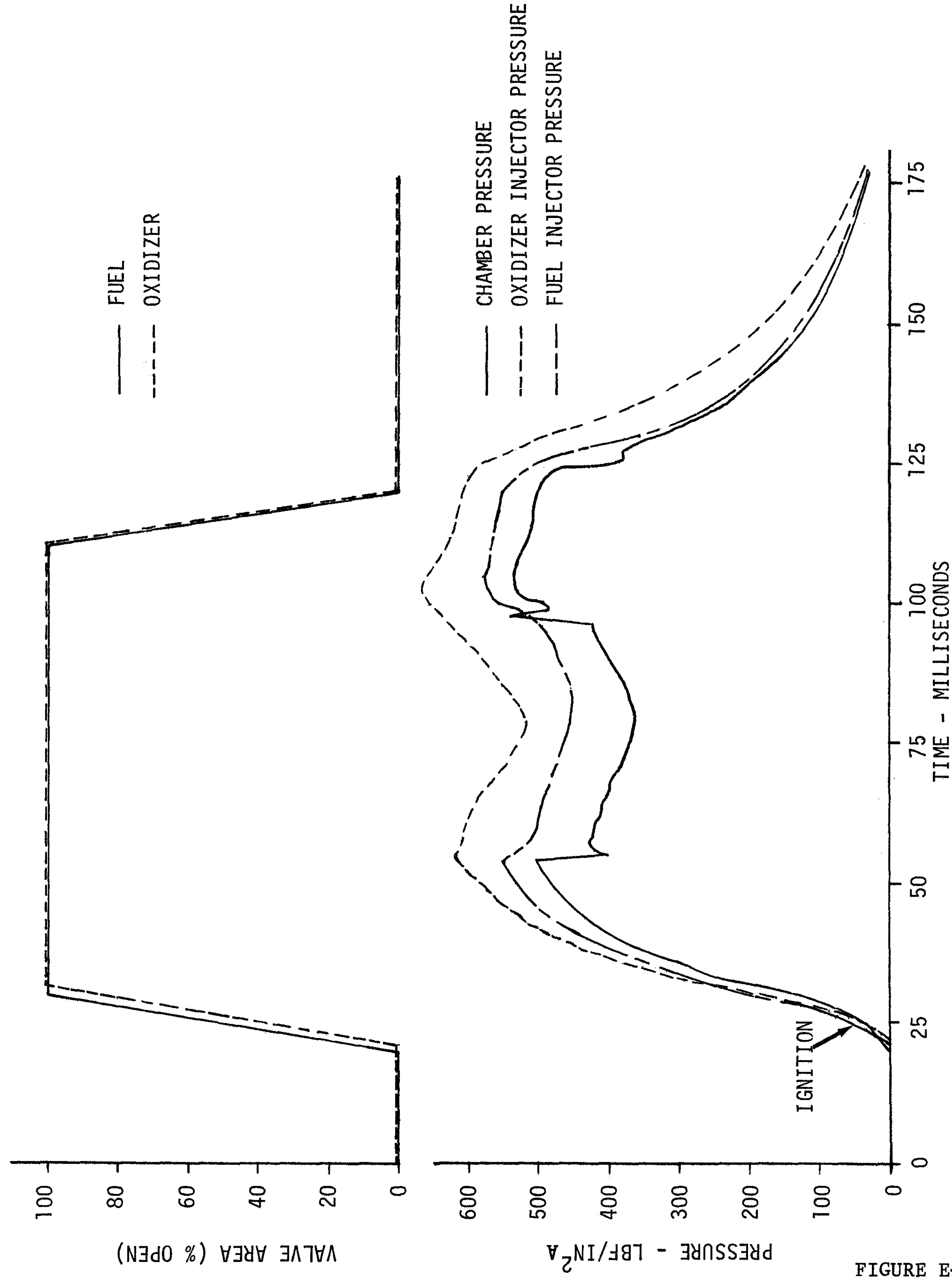

THRUSTER RESPONSE CHARACTERISTICS

FIGURE E-22

APPENDIX E

REFERENCES

(a) Space Shuttle Vehicle Description and Requirements Document: NASA-MSFC, dated 1 October 1970.

APPENDIX F
SUBSYSTEM WEIGHTS AND SENSITIVITIES

One of the major considerations involved in design evaluation of the APS is total subsystem weight. Comparison of various subsystem concepts and selection of the final baseline design required an accurate and consistent means of weight evaluation. Optimization of selected APS concepts required a rapid and accurate means of generating APS weights for different design conditions so that a minimum subsystem weight could be obtained. In order to generate accurate, representative, and consistent subsystem weights for many different design points, an automated means of weight evaluation was required. To fulfill this need an APS design and sizing computer program was developed. This program allows definition of subsystem weight and performance for any set of specified design conditions and serves as a compact library of representative component weights, volumes, and performance for a high chamber pressure turbopump APS.

Using this computer program, total subsystem weights were generated for comparison of subsystem concepts considered. After concept selection, the subsystem design point was optimized by use of linear weight sensitivities. These sensitivities show the effect on total subsystem weight of varying single design variables from their baseline values.

APS weight sensitivities to design variables for the final Subtask B baseline APS are shown in Figures F-1 to F-3 for Orbiter B, Orbiter C, and the Booster, respectively. The basis for design point selections and the reasons for the sensitivity effects are discussed in the following paragraphs.

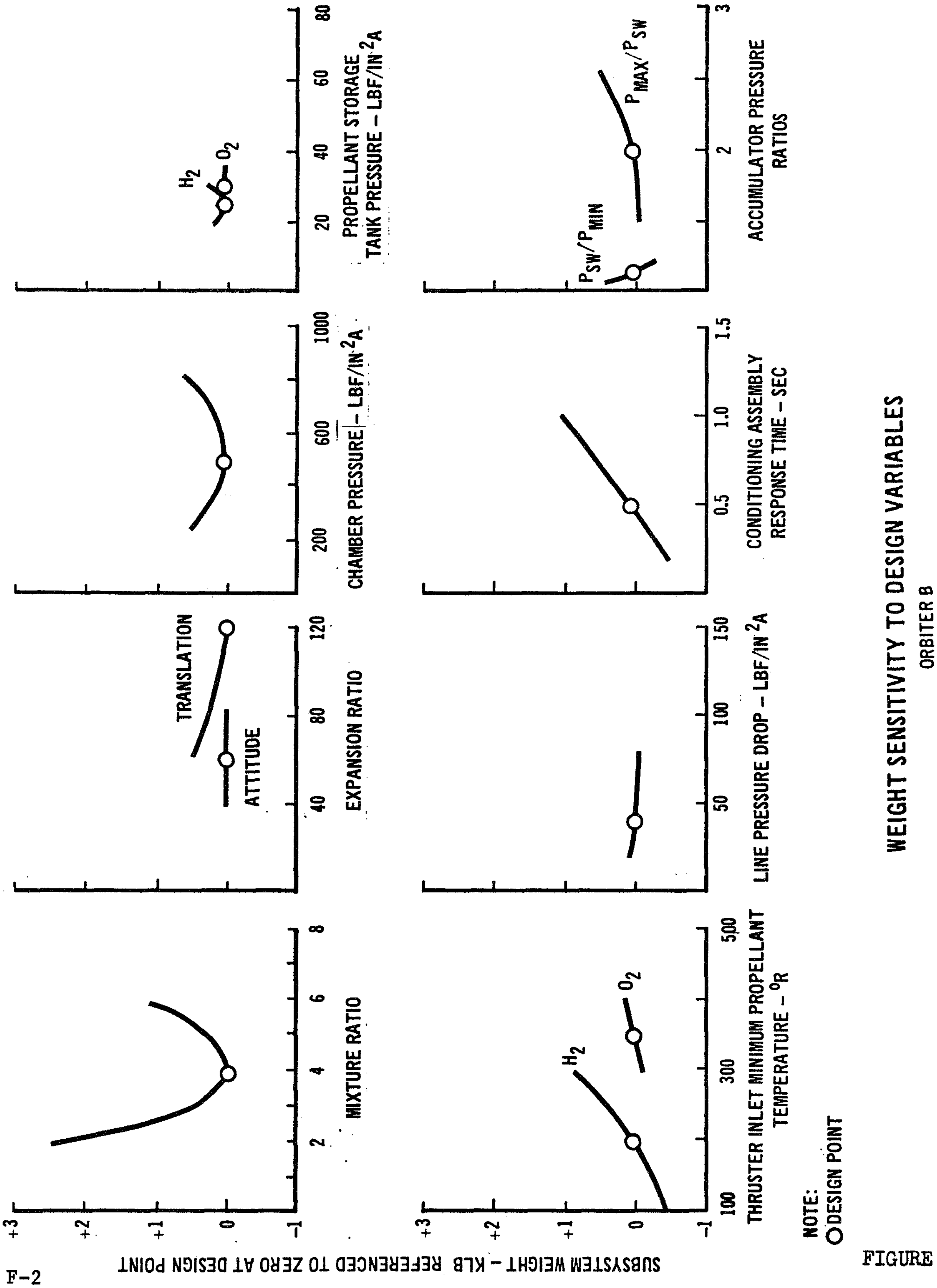
SUBSYSTEM WEIGHT – KLB REFERENCED TO ZERO AT DESIGN POINT
+3
+2
+1
0
-1
MIXTURE RATIO
2
4
6
8
EXPANSION RATIO
40
80
120
TRANSLATION
ATTITUDE
CHAMBER PRESSURE – LBF/IN²A
200
600
1000
PROPELLANT STORAGE TANK PRESSURE – LBF/IN²A
20
40
60
80
H₂
O₂
THRUSTER INLET MINIMUM PROPELLANT TEMPERATURE – °R
100
300
500
LINE PRESSURE DROP – LBF/IN²A
50
100
150
CONDITIONING ASSEMBLY RESPONSE TIME – SEC
0.5
1.0
1.5
ACCUMULATOR PRESSURE RATIOS
2
3
P_SW/P_MIN
P_MAX/P_SW
NOTE:
○ DESIGN POINT
WEIGHT SENSITIVITY TO DESIGN VARIABLES
ORBITER B

FIGURE F-1

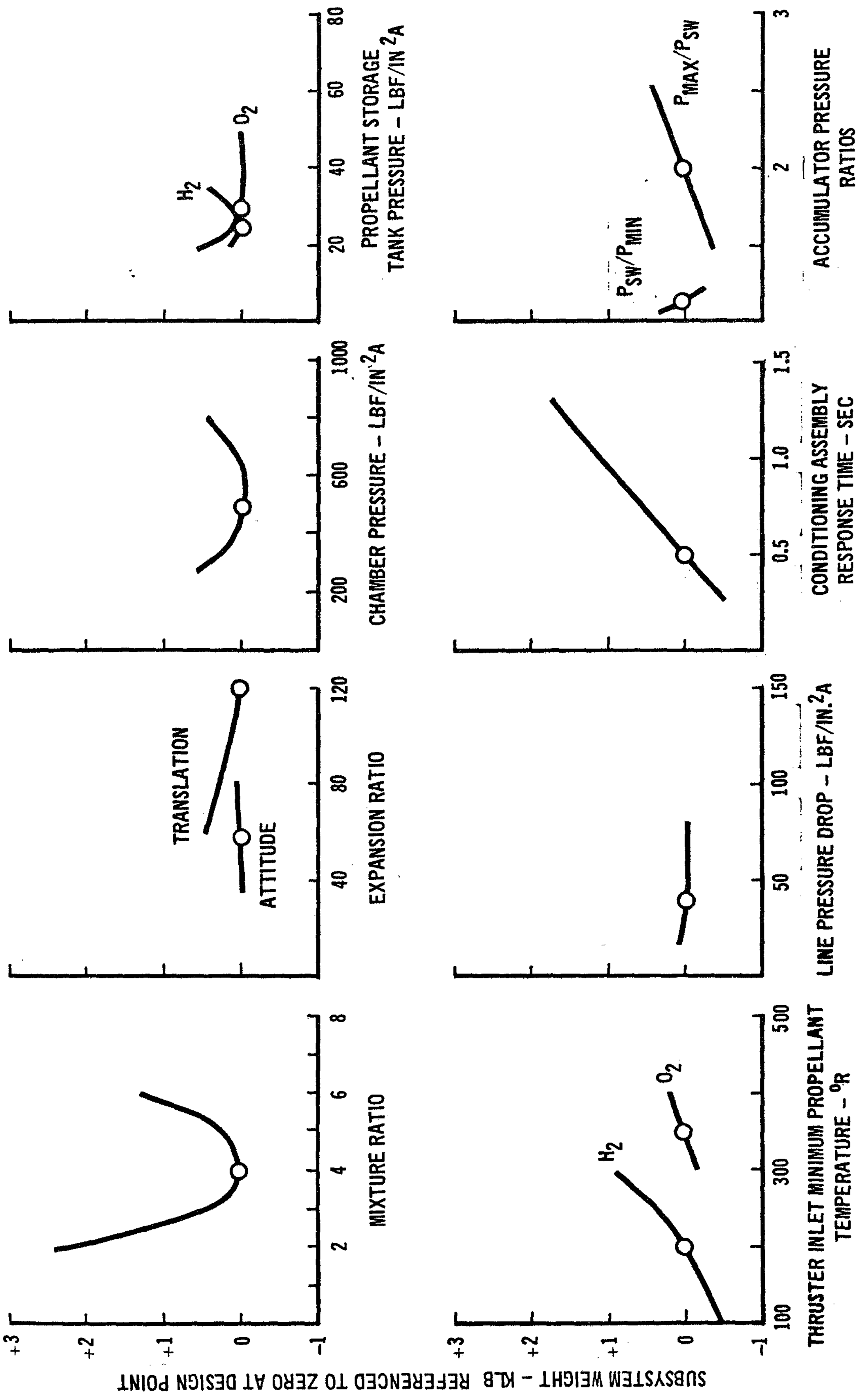

NOTE:
O DESIGN POINT

WEIGHT SENSITIVITY TO DESIGN VARIABLES
ORBITER C

FIGURE F-2

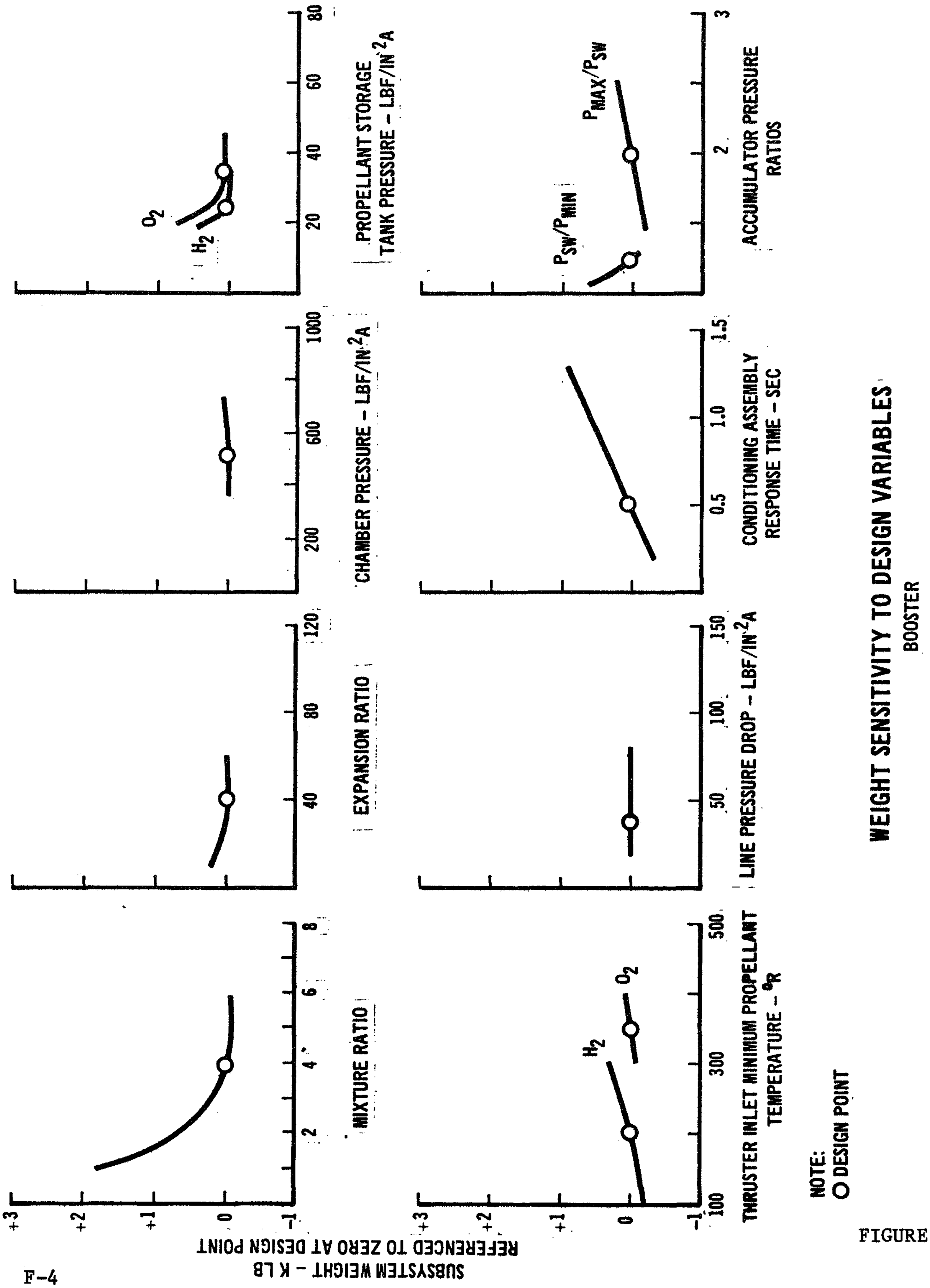
WEIGHT SENSITIVITY TO DESIGN VARIABLES
BOOSTER
SUBSYSTEM WEIGHT – K LB
REFERENCED TO ZERO AT DESIGN POINT
+3
+2
+1
0
-1
MIXTURE RATIO
2
4
6
8
EXPANSION RATIO
40
80
120
CHAMBER PRESSURE – LBF/IN^2A
200
600
1000
PROPELLANT STORAGE
TANK PRESSURE – LBF/IN^2A
20
40
60
80
O2
H2
THRUSTER INLET MINIMUM PROPELLANT
TEMPERATURE – °R
100
300
500
LINE PRESSURE DROP – LBF/IN^2A
50
100
150
CONDITIONING ASSEMBLY
RESPONSE TIME – SEC
0.5
1.0
1.5
ACCUMULATOR PRESSURE
RATIOS
2
3
PSW/PMIN
PMAX/PSW
NOTE:
O DESIGN POINT

FIGURE F-3

F-1. SENSITIVITY TO DESIGN VARIABLES

The sensitivity to thruster mixture ratio is primarily a result of thruster performance variation. Thruster specific impulse is maximum at a mixture ratio of approximately 3.5 to 1, and, at this mixture ratio, propellant weight is a minimum. The slight shift of the minimum weight to a higher mixture ratio is due to the higher storage efficiency of the liquid oxygen when compared to liquid hydrogen, i.e., lower hardware weight.

Sensitivity to thruster expansion ratio is a result of a tradeoff between thruster weight and performance. For an increased expansion ratio, the weight of the thrusters increase, but the thruster performance improves, resulting in a decreased propellant weight. The effect of changing attitude control and +X translation thruster expansion ratios are shown independently for the orbiters. The total impulse allocation between the two is approximately 90 percent for +X translation maneuvers. Only 6 orbiter thrusters are used for +X translation and the remainder are used for attitude control. These effects result in a different optimum for the two thruster types. With the attitude control thrusters, an increase in expansion ratio results in only a small propellant weight reduction because of the small impulse; conversely since there are a large number of attitude control thrusters an increase in expansion ratio results in a greater weight increase. The net effect is, as shown, almost no net weight change over a large expansion ratio change. The selected value of 60:1 was based on the fact that, at this ratio, no installation problems were foreseen and weight was low. A different effect is shown for the +X translation thrusters. Here a large total impulse is involved and small thruster performance improvements result in large propellant weight reductions. Since only a small number of thrusters are involved, the hardware weight penalty for increasing expansion ratio is minimal. The results of these two effects are that high expansion ratios are attractive for the +X translation thrusters. A value of 120:1 was selected for these, as it provided near minimum weight and acceptable volumes.

The sensitivity to chamber pressure is a result of a tradeoff between conditioner assembly bypass flow and hardware weight. Conditioner assembly bypass flow decreases with increasing chamber pressure, due to real gas effects which cause slight decrease in the enthalpy change required for conditioning. This is illustrated in the pressure-enthalpy diagram of Figure F-4, which shows that as the

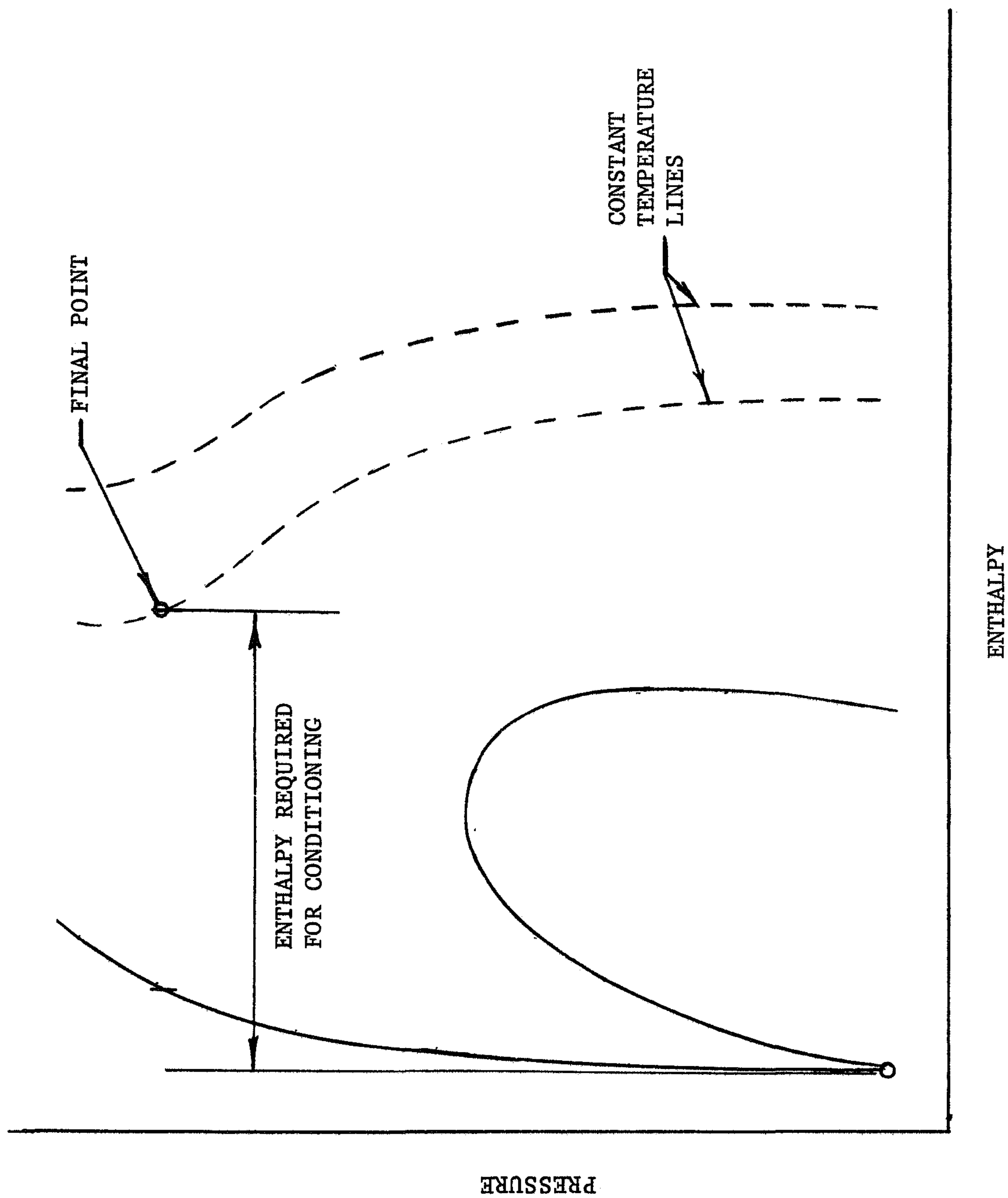

TYPICAL PRESSURE - ENTHALPY DIAGRAM

FIGURE F-4

subsystem pressure increases the enthalpy required for overall propellant conditioning decreases. Two limitations have been placed upon the conditioner:

(1) the heat exchanger hot side pressure is limited to a minimum of 30 lbf/in^2a to allow testing at sea level

(2) the turbine pressure ratio is limited to 25:1 as a practical limit on specific power.

As the chamber pressure is increased to the point where either of the above limitations is reached, the bypass flow will start to increase to balance the increased pump head requirements. This flow increase allows less oxygen addition in the heat exchanger and the overall conditioner mixture ratio goes down with a resultant decrease in conditioner performance. Hardware weight decreases as chamber pressure increases due to component size reductions, until increases in pump weights, due to head requirements, become excessive. Thus propellant weight and hardware weight tradeoff result in a minimum total subsystem weight at a chamber pressure of about 500 lbf/in^2a.

The sensitivity to propellant storage tank pressure is a result of a tradeoff between turbopump and storage/pressurization assembly weight. As the tank pressure increases, the amount of pressurant required increases, and when minimum propellant tank wall thickness is exceeded, propellant tank weight increases. Conversely the turbopump weight decreases with increased tank pressure due to the increase in pump net positive suction head. Combining these two effects results in a minimum weight subsystem at tank pressures of approximately 25 lbf/in^2a for the hydrogen tank and 30 lbf/in^2a for the oxygen tank.

The sensitivity shown for the propellant temperature is actually a sensitivity to the minimum propellant temperature allowed at the thruster inlet. The continuous increase in weight with increased propellant temperature is a result of the increase in conditioning enthalpy requirements and the corresponding increase in propellant weight for increased bypass flow. The propellant temperatures were limited to a minimum of 200°R and 350°R for the hydrogen and the oxygen respectively to allow the use of either regenerative or film cooling for the thruster assemblies.

The sensitivity to feed line pressure drop is a result of a decrease in line size as the allowed pressure drop increases. Eventually, the additional pump head incurred by increased line pressure drop will raise the turbopump weight and the conditioner bypass flow. Although a minimum does exist, the overall effect upon total weight is small compared to the effect of other design variables. The 40

lbf/in^2a line pressure drop was selected because it resulted in near minimum weight while keeping the propellant line velocity relatively low.

The sensitivity shown for conditioning assembly response time is a result of the increase in accumulator volume, and thus accumulator weight, necessary for APS operation during conditioner start up. The response time of 0.5 seconds was determined for the selected propellant conditioning assembly, as discussed in Appendix D-6.

The sensitivity to accumulator pressure ratio is primarily a result of the change in accumulator weight. An increase in the switching to minimum pressure ratio (P_{sw}/P_{min}) results in a decreased accumulator volume since more mass is obtained during the large pressure blowdown. An increase in the maximum to switching pressure ratio (P_{max}/P_{sw}) produces an increased maximum accumulator pressure resulting in an increased accumulator weight. The design point shown was selected based on the accumulator analyses presented in Appendix D-6. The pressure ratios selected result in the minimum total subsystem weight for the requirement of less than 50 conditioner assembly cycles per mission.

F-2. SENSITIVITY TO SUBSYSTEM REQUIREMENTS

In addition to the APS weight sensitivity to the various design variables, the sensitivity to the subsystem requirements were evaluated. These sensitivities for Orbiter B, Orbiter C and the Booster are presented in Figures F-5 to F-7. An explanation of the subsystem sensitivity to each of the design requirements is given below.

The sensitivity to thrust/thruster is a result of a combination of the increase in thruster weight as thrust level increases and the decrease in propellant weight due to an improvement in thruster specific impulse. This sensitivity was generated for a constant total thrust level for the APS (i.e., fixed conditioner capacity).

The sensitivity to subsystem total thrust is a result of an increase in hardware weight (i.e., accumulators, feed lines, valves, conditioner assembly) for an increase in total thrust capabilities. This sensitivity uses a constant thrust level per thruster.

The sensitivity to total impulse is a result of an increase in propellant, storage tank, and pressurization system weights for an increase in total impulse requirements.

The sensitivity to the number of thrusters is simply a result of the change in the total number of thrusters on the vehicle.

F-3 Summary of Results - After the design requirements were established for the selected subsystem concept, a component weight breakdown summary was defined for reference during the component evaluation phase. The component weight breakdowns for the different vehicles are presented in Figures F-8 to F-10. In addition to the weight of each component, the design requirements of each component are shown in Figures F-11 to F-13 for the selected subsystem designs.

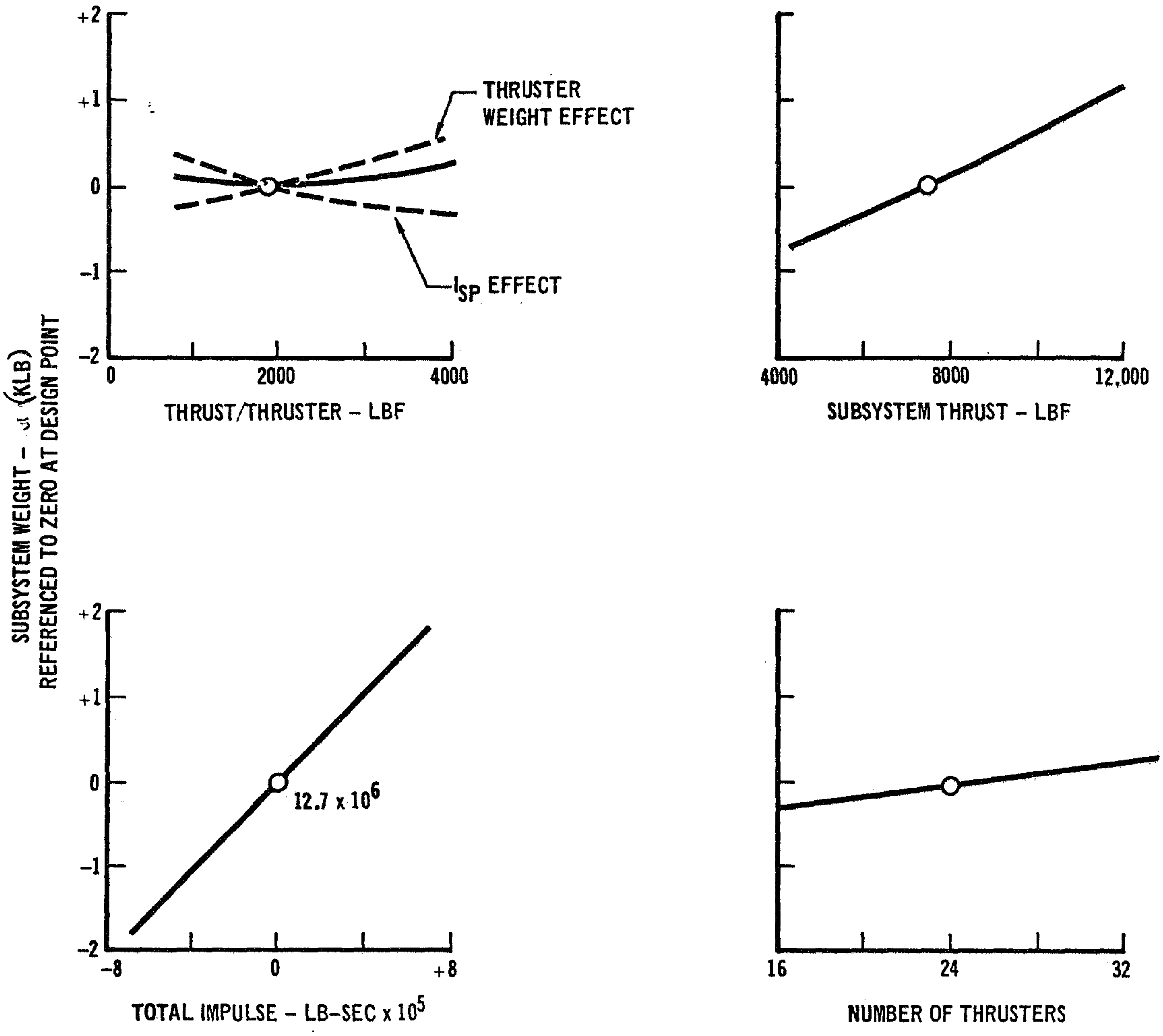

WEIGHT SENSITIVITY TO DESIGN REQUIREMENTS
Orbiter B

FIGURE F-5

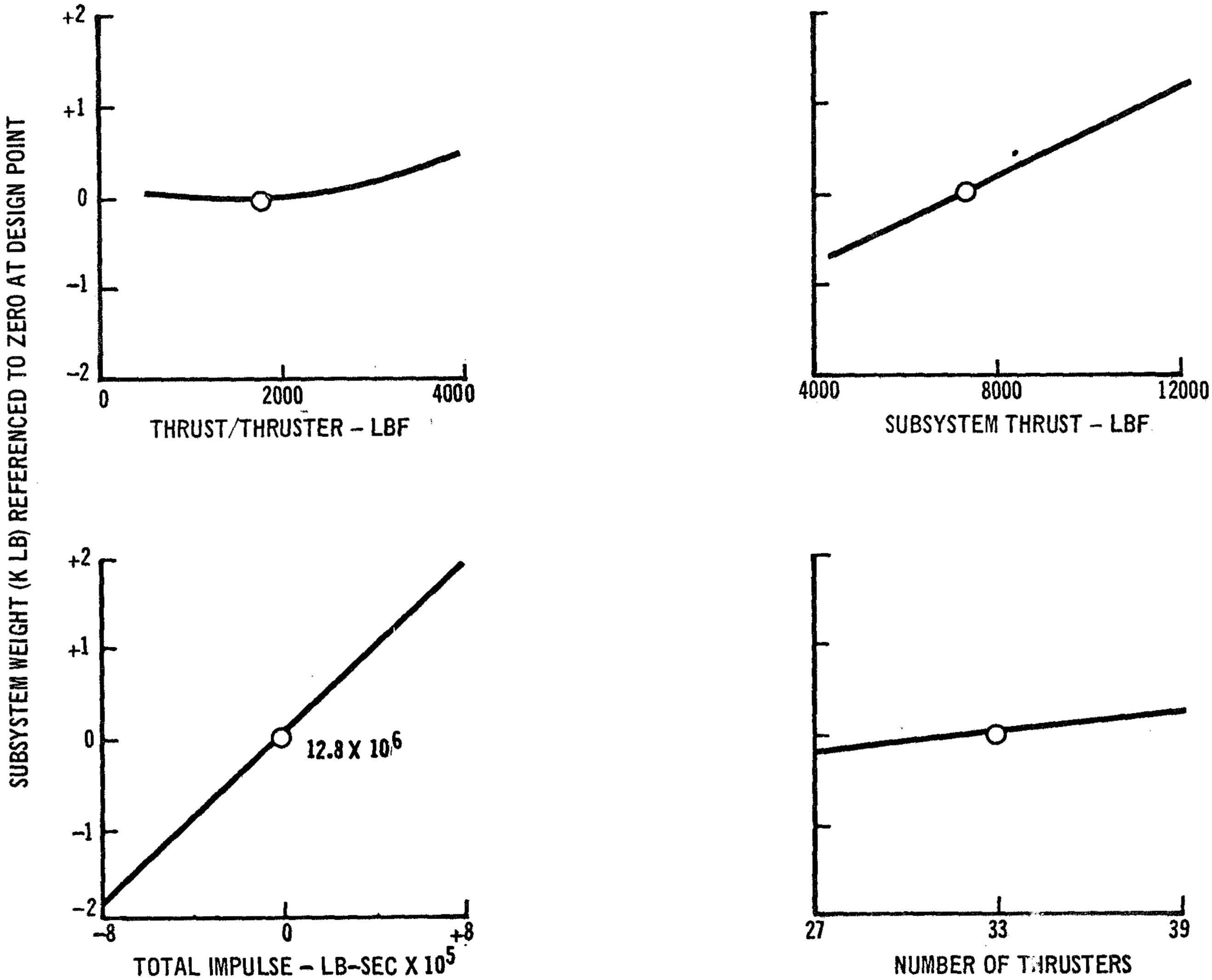

WEIGHT SENSITIVITY TO DESIGN REQUIREMENTS

Orbiter C

FIGURE F-6

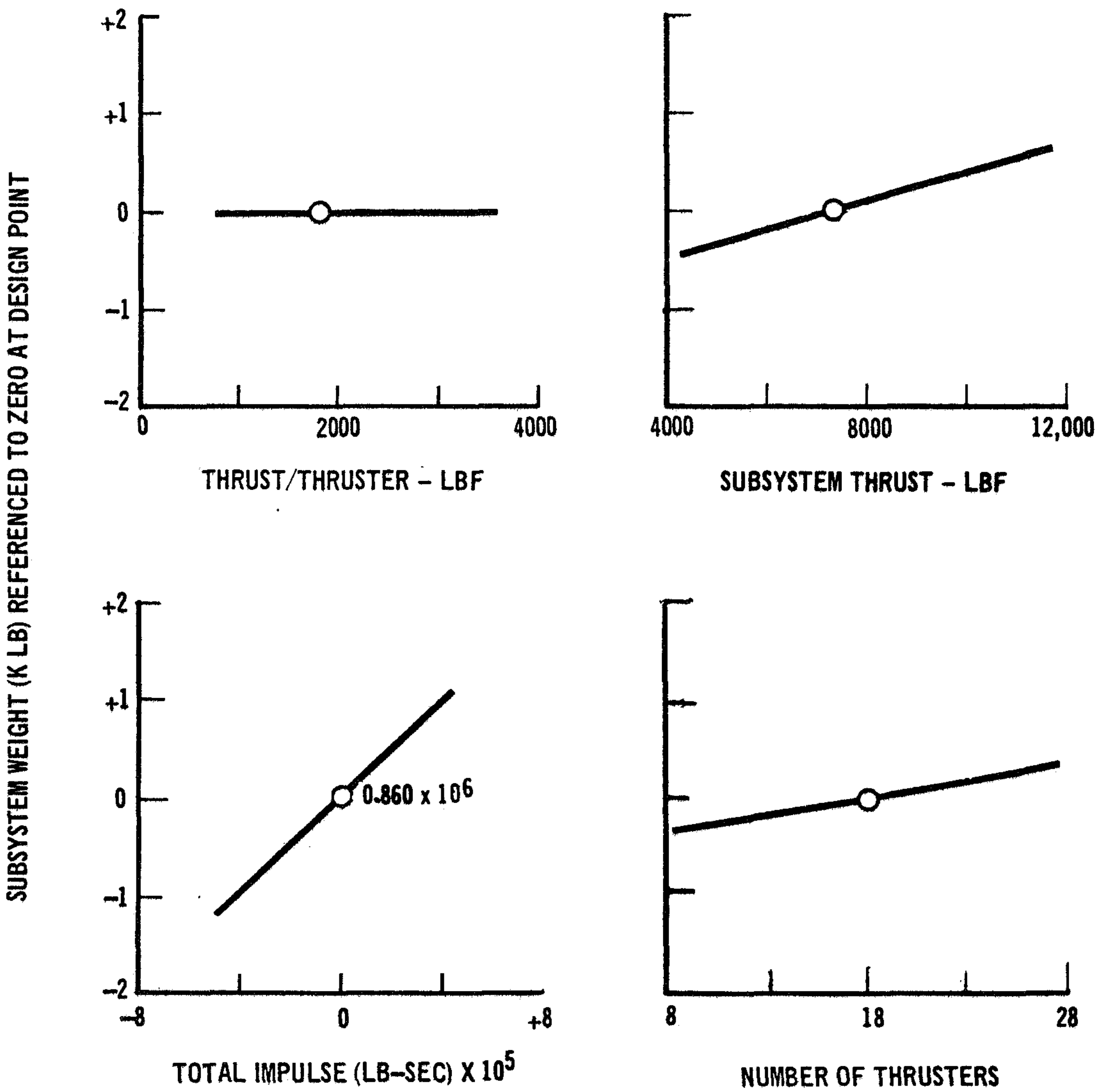

WEIGHT SENSITIVITY TO DESIGN REQUIREMENTS
BOOSTER

FIGURE F-7

SUBSYSTEM ELEMENTS	WEIGHT – LB		VOLUME – FT^3	
	H_2	O_2	H_2	O_2
PROPELLANT AND COMPONENTS				
TOTAL PROPELLANT	469	1737		
PROPELLANT TANKAGE	225	138	108	25
PRESSURANT AND TANKAGE	34	8		
INSULATION	30	4		
CONDITIONING ASSEMBLY				
HEAT EXCHANGERS (3)	259	297		
TURBOPUMPS (3)	86	98		
GAS GENERATORS (3)	37			
FEED ASSEMBLY				
ACCUMULATORS (1)	437	200	17	7
LINES	141	146		
REGULATORS (6)	28	29		
VALVES (THRUSTER ISOLATION (2) AND MANIFOLD)	134	122		
THRUSTER (18)	609			
VENT AND LINES	11	7		
TOTAL SUBSYSTEM	5310		1157	

* ATTITUDE/TRANSLATION

APS COMPONENT WEIGHT BREAKDOWN
Booster

FIGURE F-8

SUBSYSTEM ELEMENTS	WEIGHT – LB		VOLUME – FT^3	
	H_2	O_2	H_2	O_2
PROPELLANT AND COMPONENTS				
TOTAL PROPELLANT	6334	23,552		
PROPELLANT TANKAGE	1036	417	1449	332
PRESSURANT AND TANKAGE	450	79		
INSULATION	248	50		
CONDITIONING ASSEMBLY				
HEAT EXCHANGERS (3)	255	297		
TURBOPUMPS (3)	76	124		
GAS GENERATORS (3)	37			
FEED ASSEMBLY				
ACCUMULATORS (1)	679	321	29	12
LINES	146	152		
REGULATORS (6)	26	29		
VALVES (THRUSTER ISOLATION (2) AND MANIFOLD)	105	90		
THRUSTER (18/6) *	917			
PROPULSIVE VENT AND LINES	275	184		
TOTAL SUBSYSTEM	35,879		1822	

* ATTITUDE/TRANSLATION

APS COMPONENT WEIGHT BREAKDOWN
Orbiter B

FIGURE F-9

SUBSYSTEM ELEMENTS	WEIGHT – LB		VOLUME – FT^3	
	H_2	O_2	H_2	O_2
PROPELLANT AND COMPONENTS				
TOTAL PROPELLANT	6487	23,748		
PROPELLANT TANKAGE	1338	477	1485	335
PRESSURANT AND TANKAGE	454	80		
INSULATION	317	63		
CONDITIONING ASSEMBLY				
HEAT EXCHANGERS (3)	255	297		
TURBOPUMPS (3)	75	124		
GAS GENERATORS (3)	37			
FEED ASSEMBLY				
ACCUMULATORS (1)	700	332	30	12
LINES	162	169		
REGULATORS (6)	26	29		
VALVES (THRUSTER ISOLATION (2) AND MANIFOLD)	111	96		
THRUSTER (27/6) *	1,244			
PROPULSIVE VENT AND LINES	269	180		
TOTAL SUBSYSTEM	37,070		1862	

* ATTITUDE/TRANSLATION

APS COMPONENT WEIGHT BREAKDOWN
Orbiter C

FIGURE F-10

THRUSTER	ATTITUDE CONTROL		TRANSLATION (+ X)	
CHAMBER PRESSURE, LBF/IN.^{2}A	500		500	
EXPANSION RATIO	60		120	
THRUST LEVEL, LB	1850		1850	
NUMBER OF CYCLES	600		–	
BURN TIME, SEC	–		<1560	
INLET TEMP, H_2, MAX/MIN/NOM, °R	600/200/252		600/200/252	
INLET TEMP, O_2, MAX/MIN/NOM, °R	600/350/406		600/350/406	
INLET PRESSURE, LBF/IN.^{2}A	675 H_2 – 600 O_2		675 H_2 – 600 O_2	
MIXTURE RATIO MAX/MIN/NOM	4.7:1/3.5:1/ 4:1		4.7:1/3.5:1/4:1	
GAS GENERATORS/HEAT EXCHANGERS	H_2 (GG)	O_2 (GG)	H_2 (HX)	O_2 (HX)
COMBUSTION PRESSURE, LBF/IN.^{2}A	500	500	30	107
COMBUSTION TEMP, °R	2000	2000	3750	4151
MIXTURE RATIO	1	1	0.78	0.85
NUMBER OF CYCLES	50	50	50	50
BURN TIME, SEC	<1560	<1560	<1560	<1560
INLET TEMP, H_2, MAX/MIN/NOM, °R	600/200/252	600/200/252	1410	1830
INLET TEMP, O_2, MAX/MIN/NOM. °R	600/350/406	600/350/406	600/350/406	600/350/406
INLET PRESSURE	675 H_2/600 O_2	675 H_2/600 O_2	30	107
FLOW RATE	0.443	0.274	0.785	0.506
REGULATORS	H_2	O_2		
INLET PRESSURE, MAX, LBF/IN.^{2}A	2318	2066		
INLET PRESSURE, MIN. LBF/IN.^{2}A	1021	914		
INLET TEMP, MAX/MIN/NOM, °R	600/253/253	600/420/440		
REGULATED PRESSURE, LBF/IN.^{2}A	715	640		
FLOW RATE, LB/SEC	3.67	14.18		
NUMBER OF CYCLES	15,600	15,600		

HEAT EXCHANGER	H_2	O_2
PRESSURE, COLD SIDE–IN, LBF/IN.^{2}A	1043	921
PRESSURE, COLD SIDE–OUT, LBF/IN.^{2}A	1021	914
PRESSURE, HOT SIDE–IN, LBF/IN.^{2}A	30	107
PRESSURE, HOT SIDE–OUT, LBF/IN.^{2}A	26	80
TEMP, COLD SIDE–IN, °R	37	162
TEMP, COLD SIDE–OUT, °R	253	425
TEMP, HOT SIDE–IN, °R	1410	1830
TEMP, HOT SIDE–OUT, °R	800	800
FLOW RATE LB/SEC	0.785	0.506
NUMBER OF CYCLES	50	50
TURBOPUMP		
PUMP		
PUMP FLOW RATE, LB/SEC	3.84	14.84
INLET PRESSURE, LBF/IN.^{2}A	25	30
INLET TEMP, °R	37	162
OUTLET PRESSURE, MAX/MIN, LBF/IN.^{2} A	2340/1043	2073/921
NUMBER OF CYCLES	50	50
TURBINE		
FLOW RATE, LB/SEC	0.443	0.274
INLET PRESSURE, LBF/IN.^{2}A	500	500
INLET TEMP, °R	2000	2000
PRESSURE RATIO	16.7:1	4.65:1
NUMBER OF CYCLES	50	50

(1) NUMBER OF CYCLES IS CYCLES/MISSION

TURBOPUMP COMPONENT REQUIREMENTS
Orbiter B

FIGURE F-1

THRUSTER	ATTITUDE CONTROL	TRANSLATION (+X)
CHAMBER PRESSURE, LBF/IN.^{2}A	500	500
EXPANSION RATIO	60	120
THRUST LEVEL, LB	1850	1850
NUMBER OF CYCLES	600	-
BURN TIME, SEC	-	<1560
INLET TEMP, H_2, MAX/MIN/NOM, ^oR	600/200/252	600/200/252
INLET TEMP, O_2, MAX/MIN/NOM, ^oR	600/350/406	600/350/406
INLET PRESSURE, LBF/IN.^{2}A	675 H_2 – 600 O_2	675 H_2 – 600 O_2
MIXTURE RATIO MAX/MIN/NOM	4.7:1/3.5:1/ 4:1	4.7:1/3.5:1/4:1

GAS GENERATORS/HEAT EXCHANGERS	H_2 (GG)	O_2 (GG)	H_2 (HX)	O_2 (HX)
COMBUSTION PRESSURE, LBF/IN.^{2}A	500	500	30	107
COMBUSTION TEMP, ^oR	2000	2000	3750	4151
MIXTURE RATIO	1	1	0.77	0.85
NUMBER OF CYCLES	50	50	50	50
BURN TIME, SEC	<1560	<1560	<1560	<1560
INLET TEMP, H_2, MAX/MIN/NOM, ^oR	600/200/252	600/200/252	1410	1830
INLET TEMP, O_2, MAX/MIN/NOM. ^oR	600/350/406	600/350/406	600/350/406	600/350/406
INLET PRESSURE	675 H_2/600 O_2	675 H_2/600 O_2	30	107
FLOW RATE	0.443	0.274	0.784	0.506

REGULATORS	H_2	O_2
INLET PRESSURE, MAX, LBF/IN.^{2}A	2307	2056
INLET PRESSURE, MIN. LBF/IN.^{2}A	1021	914
INLET TEMP, MAX/MIN/NOM, ^oR	600/253/253	600/421/441
REGULATED PRESSURE, LBF/IN.^{2}A	715	640
FLOW RATE, LB/SEC	3.67	14.18
NUMBER OF CYCLES	19,800	19,800

HEAT EXCHANGER	H_2	O_2
PRESSURE, COLD SIDE-IN, LBF/IN.^{2}A	1043	921
PRESSURE, COLD SIDE-OUT, LBF/IN.^{2}A	1021	914
PRESSURE, HOT SIDE-IN, LBF/IN.^{2}A	30	107
PRESSURE, HOT SIDE-OUT, LBF/IN.^{2}A	26	[illegible]
TEMP, COLD SIDE-IN, ^oR	37	162
TEMP, COLD SIDE-OUT, ^oR	253	425
TEMP, HOT SIDE-IN, ^oR	1410	1830
TEMP, HOT SIDE-OUT, ^oR	800	800
FLOW RATE LB/SEC	0.784	0.506
NUMBER OF CYCLES	50	50

TURBOPUMP	H_2	O_2
PUMP		
PUMP FLOW RATE, LB/SEC	3.83	14.84
INLET PRESSURE, LBF/IN.^{2}A	25	30
INLET TEMP, ^oR	37	162
OUTLET PRESSURE, MAX/MIN, LBF/IN.^{2}A	1043/2329	921/2063
NUMBER OF CYCLES	50	50
TURBINE		
FLOW RATE, LB/SEC	0.443	0.274
INLET PRESSURE, LBF/IN.^{2}A	500	500
INLET TEMP, ^oR	2000	2000
PRESSURE RATIO	16.7:1	4.67:1
NUMBER OF CYCLES	50	50

(1) NUMBER OF CYCLES IS CYCLES/MISSION

TURBOPUMP COMPONENT REQUIREMENTS
Orbiter C

FIGURE F-12

THRUSTER	ATTITUDE CONTROL
CHAMBER PRESSURE, LBF/IN.^{2}A	500
EXPANSION RATIO	40
THRUST LEVEL, LB	1850
NUMBER OF CYCLES	100
BURN TIME, SEC	< 360
INLET TEMP, H_2, MAX/MIN/NOM, ^oR	600/200/259
INLET TEMP, O_2, MAX/MIN/NOM, ^oR	600/350/414
INLET PRESSURE, LBF/IN.^{2}A	675 H_2 – 600 O_2
MIXTURE RATIO NOM	4:1

GAS GENERATOR/HEAT EXCHANGER	H_2(GG)	O_2 (GG)	H_2(HX)	O_2(HX)
COMBUSTION PRESSURE, LBF/IN.^{2}A	500	500	30	119
COMBUSTION TEMP, ^oR	2000	2000	3843	4160
MIXTURE RATIO	1	1	0.81	0.85
NUMBER OF CYCLES	16	16	16	16
BURN TIME, SEC	<360	<360	<360	<360
INLET TEMP, H_2, MAX/MIN/NOM, ^oR	600/200/259	600/200/259	600/200/259	600/200/259
INLET TEMP, O_2, MAX/MIN/NOM, ^oR	600/350/414	600/350/414	600/350/414	600/350/414
INLET PRESSURE, LBF/IN.^{2}A	675 H_2/600 O_2	675 H_2/600 O_2	30	119
FLOW RATE, LB/SEC	0.448	0.282	0.809	0.520

REGULATORS		
INLET PRESSURE, MAX, LBF/IN.^{2}A	2532	2258
INLET PRESSURE, MIN, LBF/IN.^{2}A	1021	914
INLET TEMP, MAX/MIN/NOM, ^oR	600/260/260	600/429/450
REGULATED PRESSURE, LBF/IN.^{2}A	715	640
FLOW RATE, LB/SEC	3.71	14.36
NUMBER OF CYCLES	1800	1800

HEAT EXCHANGERS	H_2	O_2
PRESSURE, COLD SIDE–IN, LBF/IN.^{2}A	1043	921
PRESSURE, COLD SIDE–OUT, LBF/IN.^{2}A	1021	914
PRESSURE, HOT SIDE–IN, LBF/IN.^{2}A	30	119
PRESSURE, HOT SIDE–OUT, LBF/IN.^{2}A	26	80
TEMP, COLD SIDE–IN, ^oR	37	162
TEMP, COLD SIDE–OUT, ^oR	260	433
TEMP, HOT SIDE–IN, ^oR	1410	1820
TEMP, HOT SIDE–OUT, ^oR	800	800
FLOW RATE, LB/SEC	0.809	0.520
NUMBER OF CYCLES	16	16
TURBOPUMP		
PUMP		
PUMP FLOW RATE, LB/SEC	3.83	15.03
INLET PRESSURE, LBF/IN.^{2}A	25	35
INLET TEMPERATURE, ^oR	37	162
OUTLET PRESSURE, MAX/MIN, LBF/IN.^{2} A	2554/1043	2280/921
NUMBER OF CYCLES	16	16
TURBINE		
FLOW RATE, LB/SEC	0.448	0.282
INLET PRESSURE, LBF/IN.^{2} A	500	500
INLET TEMPERATURE, ^oR	2000	2000
PRESSURE RATIO	16.7:1	4.21:1
NUMBER OF CYCLES	16	16

(1) NUMBER OF CYCLES IS CYCLES/MISSION

TURBOPUMP COMPONENT REQUIREMENTS
Booster

FIGURE F-

APPENDIX G
TECHNOLOGY CRITIQUE

Space shuttle control requirements and APS installation considerations dictate APS thrust levels of approximately 1850 lb per thruster. This thrust level, combined with space shuttle reuse requirements of 100 missions without major refurbishment are far beyond the requirements of any current auxiliary propulsion subsystem, and no components for an APS with these requirements are in existence. The APS design resulting from the NASA conceptual subsystem definition studies is considered to be capable of satisfying all requirements; however, to make the APS design as realistic as possible it must be based on a balance between APS performance and component technology extensions. This results in a design that neither requires any technology developments that are considered to be unrealistic nor is based completely on available component technology. The design requires technology advances in areas where they appear reasonable and the performance gains resulting from the advances warrant the extension. The following paragraphs discuss the specific areas of technology concerns that exist with the High Pressure APS component and assembly designs.

G-1. PROPELLANT STORAGE ASSEMBLY TECHNOLOGY

The propellant storage assembly is made up of an aluminum pressure vessel with high performance insulation, an active vent/thermal barrier and an outer protective shell; a propellant positioning subassembly; and a pressurization subassembly. During APS studies, this tank design was established as the best compromise between overall APS performance and technology concern. Specifically, there are: venting of the outer tank jacket, design of the propellant positioning subassembly, and the cooling approach with its associated controls.

The concern with jacket venting is primarily that a small pressure gradient, developed between the inner and outer shells during venting, could cause crushing and thereby significantly alter the heat transfer characteristics of the multilayer insulation. The tank insulation subassembly design requires pressurization of the outer shell during boost and entry to prevent collapse pressure loads on the fiberglass outer shell. This outer shell is provided because it is known that condensation of air or water vapor within the multilayer insulation severly degrades insulation performance. Without the shell, the condensation would most certainly occur during entry as ambient air was admitted to the vehicle and came in contact with the cold insulation. The alternative to a fiberglass shell is to provide the tank with a vacuum jacket capable of withstanding collapse pressure loads. With this approach the weight penalties are high. Data are available which indicate that multilayer insulation of this type will freely vent without significant pressure gradients when no protective covering is used; however, data are not available to show that repeated pressurization and vent cycles will not alter the heat transfer characteristics of high performance insulation or to show that venting can be readily accomplished when a protective covering is used.

The principal concern with the design of the propellant storage assembly is the propellant positioning device. Data are available which clearly demonstrate the validity of the surface tension approach for propellant acquisition. Surface tension screens fabricated to date have, however, been limited to approximately 1 ft in diameter. Basic fabrication limitations indicate the screen liner configuration should be limited to tank diameters of 5 ft or less. The APS capacity requirements dictate a hydrogen tank size equivalent to a sphere 15 ft in diameter. Use of multiple tankage does not reduce this requirement appreciably. A second and significant requirement for the surface tension screen design is that it must be designed for cryogenic liquid; the design used must prohibit vaporization within the contained propellant as this could result not only in a loss of pressurant, if the screen liquid/vapor interface were broken down, but also vapor ingestion by the oxygen turbopump which could be catastrophic. The passive surface tension screen approach for propellant positioning is the only reasonable method for the shuttle application. Other devices such as bladders, diaphragms, or bellows are not practical. The current positioning subassembly design consisting of ring channels offers a high probability of satisfying all requirements; however, the design is unique and there is not sufficient background on cryogenics to conclusively prove that it will satisfy requirements. The ring channel design has only point contact with the tank walls and thus heat transfer to the propellant in the containment cavities should be near zero. The design allows checkout of the containment device prior to launch and is installed so that boost vibration accelerations will not affect the interface stability. With this approach, screen size requirements are quite reasonable and there should be little difficulty in obtaining effective pore sizes that will give adequate containment capability; however, significantly more effort will be required to establish the ring channel screen design and to demonstrate achievement of a satisfactory design.

One of the requirements of the storage assembly is to provide a storage tank heat barrier and cooling to the turbopumps which will be mounted in the vicinity of the tanks. The significant area in the vent cooling subassembly is turbopump cooling. These pumps must be kept at liquid temperatures during all times when the APS is active, and this must be done in the presence of two standby, ambient temperature, turbines and one hot operating turbine. The conventional approach to pump chill-down is to circulate propellant through the pump for a short period of time prior to start. However, this is not acceptable for this application because of the number of starts and associated large propellant loss. The conditioner response time must be of an order of less than a second or excessive accumulator weight penalties will result. The accumulator is sized to provide operation during the start transients but the size and weight are quite sensitive to conditioner response time. The current design provides an isolated compartment for all of the turbopumps. All heat into this compartment is intercepted by a cooling loop. This design has been based on only preliminary installation layouts and on preliminary analysis of the turbopump assembly heat transfer rates. The current installation arrangement requires a heat short to the vehicle structure to provide a conduction path from the turbine to the structure and limit conduction down the shaft and housing to the pump end of the turbopump assembly.

G-2. CONDITIONER ASSEMBLY TECHNOLOGY

The conditioner assembly provides all pressure and thermal conditioning of the propellants required by the thrusters. The assembly is made up of the turbopumps, the propellant heat exchangers, the gas generator, and their associated controls. As with the storage tank assembly, APS studies have shown that the turbopump design offers the best balance between overall subsystem performance and the technology risk involved with subsystem development. There are, for each component, specific technology areas that are of concern. Many of these are interrelated because of the strong interdependence of component interfaces but, for clarity, they are discussed under the individual component headings below.

The basic complexity of the component interfaces in this assembly makes the performance of the overall integrated assembly a technology concern. The focal point for this concern is control of the assembly. As identified previously, control of pressure and temperature is a mandatory requirement. APS studies to date have not fully explored potential tolerances within the assembly, the accuracy of sensors and controls nor have they defined the three sigma performance boundaries. For this reason, more detailed analysis of the integrated assembly, in parallel with exploratory programs on the specific components, is a vital technology requirement.

G-3. TURBOPUMP TECHNOLOGY

The turbopump assembly design is considered to be realistic; however, there are several areas which push or exceed current technology limits and there are not sufficient data to fully validate the current component design and performance predictions. Without question, the turbopump is one of the most critical components in this assembly.

There are three primary areas of concern in the turbopump assembly. These are:

(1) life capability
(2) response
(3) operating temperature of the turbine blades.

Life requirements for the turbopump are several orders of magnitude above those of current rocket engine turbopumps. Reductions in the required number of turbopump operating cycles would result in a large increase in subsystem weight, since in order to limit operating cycles, the accumulator would have to be enlarged. The design life requirements for the assembly are currently 5000 operating cycles over a 100 mission vehicle life. Service life of this order has been achieved in other industries with other types of turbo-machinery. In general, these applications have been far less stringent in terms of the ability to cool and/or lubricate the components. To verify that life predictions are reasonable, significantly more effort is required in this area.

Almost all previous turbopump applications have provided a relatively slow pump spinup during which propellant was bled through the unit to provide cooling and lubrication. In this application fast pump start times (less than one second) are mandatory and bearing loads or wear induced by these fast start transients will have a significant impact on the life capability of the unit. Reduction in response requirements would result in a large increase in subsystem weight since, when reduced, the accumulators must be sized to store additional propellant to supply the thrusters during the start transient. The acceleration levels for pump spinup that are available with a high pressure, high torque turbine are entirely adequate to provide the response required. The principal concern is the ability of the cryo-lubed bearings to respond to the high shaft acceleration rates and the resultant effect on bearing life.

The turbines are supplied with hot gas directly from the gas generator; thus the turbine blade temperature is approximately 2000° Rankine. This is near the point where almost all materials exhibit extreme strength degradation with small changes in temperature. Provision for blade cooling is quite complex and very undesirable for the assembly. Reduction in gas generator temperature to alleviate this problem is feasible, within limits, but would result in a somewhat higher subsystem bypass flow and increased subsystem weight. The true significance cannot be fully assessed without an in-depth analysis of the overall assembly to define turbine inlet temperature tolerances and to define the accuracy of gas generator control in maintaining turbine inlet temperature. Significantly more data is also required to define the true effect of temperature variations on turbine blade life and to define the nominal life capability at the design temperatures.

G-4. HEAT EXCHANGER TECHNOLOGY

This component is the most critical area in the subsystem from a technology standpoint. Technology developed for a similar application may be applicable, but extensive modifications and extensions are required. Actively cooled fins have been utilized previously on rocket engine injectors to maintain combustion stability. An extension of this technology is applicable to the heat exchanger as is previously developed regeneratively cooled engine chamber technology. Areas of technological concern are primarily the ability to

(1) actively cool the structure and heat transfer surfaces to maintain structural margins

(2) provide satisfactory ignition and uniformity of combustion.

G-4.1 <u>Heat Transfer and Structural Margins</u> - Heat transfer in the heat exchanger is a critical technology from several standpoints. First, the ability to calculate and provide required film coefficients is not a well-established science and tests will be required to provide design data. Second, the large ΔT's in the heat exchanger can provide extremely high thermal stress loads and the cycle life will be adversely affected. Third, thermal shock loading in the heat exchanger is severe because of the very rapid response required for the conditioner assembly. This thermal shock loading in conjunction with the required number of operating cycles provides an area of technological concern.

G-4.2 <u>Reignition and Uniform Combustion</u> - The requirement for low pressure, low flow rate injection and recombustion in the turbine exhaust gas stream is unique and represents a technology area that reqiires development and a feasibility demonstration. Control and heat transfer rates and metal wall temperatures will be sensitive to the mixing efficiency that can be obtained in the staged combustion region. Hot streaks and uneven mixture ratio distribution will degrade the control capability and thereby reduce performance and cycle life potential.

Reignition of the turbine exhaust gas after mixing with supplemental oxygen is accomplished by pre-ignition of the oxygen mixed with a small amount of hydrogen prior to injection and mixing with the turbine exhaust. The pre-ignition concept is fairly well established technology. One form of this ignition technology has previously been demonstrated in an Aerojet Liquid Rocket Company sponsored program to evaluate an advanced combustion cycle for oxygen/hydrogen engines. During the course of this program an oxygen rich gas generator was operated successfully at a mixture ratio of approximately 100:1.

G-5. GAS GENERATOR TECHNOLOGY

At the design operating temperature of 2000°R, the gas generator can be considered a simple uncooled unit. No problems are anticipated in the development of this unit from a thermal standpoint. Performance and ignition requirements appear reasonable and, if required, cooling can be provided with minimal complexity. Thermal fatigue in this assembly is not considered a significant technology problem. The principal concern is with the gas generator combustion temperature fluctuations which will have a significant impact on the life of the turbine and the required control valves. Active vernier control valves are required to maintain turbine flow and horsepower with variations in inlet propellant temperatures and pressures. This linked bipropellant valve must be both quick opening and provide throttling capability around the open position. Combustion temperature sensing and feedback modulation control to the oxygen valve is required in addition to the other throttling requirements. This results in a complex valve which may be difficult to develop.

G-6. ACCUMULATOR/REGULATOR TECHNOLOGY

This subassembly consists of the gas storage accumulators, pressure regulators, propellant supply lines, and the thruster assemblies. The accumulator is a simple high pressure, aluminum pressure vessel. The concerns with this component are:

(1) the number of pressure cycles (5000) that the unit shall be subjected to over a 100 mission life

(2) the reusability of the high performance insulation on the accumulators and supply lines.

Regarding the first of these, more information is required on the pressure cycle fatigue characteristics of aluminum at low temperature to confidently define the safety factors to be used for the design and hence the weight of the accumulators. With regard to insulation, the lines and accumulators are insulated with a multilayer Mylar insulation similar to that used on the propellant tanks. Condensation effects during entry will have the same impact, however, this insulation is not as critical to APS performance as that on the tank and some degradation of insulation effectiveness could be allowed. Current expectations are that a flexible evacuated cover could be used around the insulation to avoid internal condensation. This arrangement would result in crushing cycles on the insulation within the atmosphere. In the extreme case, where insulation effectiveness becomes a more significant factor in APS performance and the multilayer type could not be made to operate satisfactorily, vacuum jacketing of the lines and accumulators, with the attendant weight increase, would be required. More data on the crushing/condensation characteristics of HPI type insulation application is required technology for APS development.

One of the concerns with this subassembly is the pressure regulators. The pressure regulators required must be capable of positive shutoff, high accuracy, high flow rate capability, and high cycle life. Mechanical regulators with the capacity, accuracy, and life required have not been developed previously for this type application with cryogenic propellants. Investigation of the capability of conventional mechanical regulators indicates the requirements are difficult to satisfy but probably can be achieved. The current APS design postulates a mechanical type regulator; however, a motor driven throttle valve for pressure regulation must also be considered. Preliminary analyses indicate that requirements could also be satisfied with this approach and that response would be adequate. No such unit has been designed and data are not available to confirm this approach. Since this is the case, a parallel technology effort should be initiated. One path should concentrate on mechanical regulators and the second on an electronically controlled, motor/valve approach. Based on the result of these efforts, a final selection of the type of pressure control could be made.

G-7. THRUSTER ASSEMBLIES

The thruster assemblies were an obvious concern when emphasis was first given to gaseous oxygen/hydrogen APS, and exploratory research programs were initiated by NASA on thruster development, ignition, cooling, and valves. To date these programs and the work of several propulsion companies have shown that ignition and performance goals can be relatively easily accomplished. Thruster cooling programs will aid in identification of design criteria and the type of cooling to be used for a prescribed cycle life. Valve development programs are not far along, but, based on design effort to date, APS requirements can be achieved without extreme difficulty. Further effort applicable to the thruster assemblies should stress certain aspects that have been identified by the APS studies to be significant. Specifically these are:

(a) Thruster cooling/life. The current APS thrusters use a combination of regenerative and film cooling. The chambers are regeneratively cooled with hydrogen to a nozzle expansion ratio of 11:1. The remainder of the nozzle is filmed cooled with hydrogen. Additional film cooling is also required in the chamber to supplement the regenerative cooling. This approach was used to take advantage of the high performance of a regenerative thruster while maintaining the ease of nozzle scarfing possible with a film cooled design. Two concerns exist with this approach. These are:

(1) current thermal cycle forecasts for the thruster are approximately 50,000 cycles for 100 shuttle missions. These predicted values are subject to change as shuttle design progresses and alternate mission timelines are investigated. Inherent in regenerative thruster design is a high thermal gradient in the cooled wall. Thermal predictions show that gradients are compatible with the required fatigue life, but this has not been demonstrated.

(2) since the thrusters are completely buried within the vehicle (low radiation cooling), nozzle film cooling must be effective since nozzle temperatures would approach the combustion temperature during a steady burn.

Calculation of film cooling effectiveness is approximate and boundary layer mixing could cause appreciable analysis errors. Significant errors in the amount of film cooling required and life limitations could reduce performance to the point that the selection of a partial regenerative cooling approach may not be the best selection. Further research effort in the thruster cooling area must resolve these concerns.

(b) Minimum Impulse Bit. In the present shuttle concept, the orbiter will remain docked to the space station during all extended stays in orbit. Under this mode of operation APS design is not highly sensitive to minimum impulse bit. If the method of operations is to maintain both spacecraft independently in a station keeping mode, then under these conditions, a very low minimum impulse bit delivery would be highly desirable. The most attractive means of reducing impulse are:

(1) to use the thruster igniter only

(2) to use hydrogen or oxygen as a monopropellant.

The current approach to thruster design precludes the latter of these since the primary propellant valves are linked to a common actuator. Use of the igniter as an independent thruster, however, is a distinct possibility and should be investigated further in anticipation of the need for extended limit cycle operation.

APPENDIX H
SUBSYSTEM RELIABILITY

The ability to withstand one component failure but retain full mission capabilities, and the ability to withstand two component failures but retain sufficient control to ensure crew survival, are prime APS requirements. To achieve these capabilities, an analysis of subsystem reliability was required. This analysis consisted of:

(1) incorporating component redundancy into the baseline subsystem design to ensure reliability

(2) analyzing failure modes of the subsystem

(3) evaluating baseline design reliability on the basis of failure mode analysis results.

The following paragraphs discuss these analyses and delineate the malfunction detection methods required.

H-1. GUIDELINES AND CONSTRAINTS

To provide a basis for reliability analyses, the following criteria were established:

(1) structure, such as lines, tanks fittings, and static seals were assumed to have a reliability of 1.0

(2) thrusters will not fail in a catastrophic mode as long as propellants are supplied at an acceptable pressure and mixture ratio

(3) a shutoff valve will not fail open prior to first flight operational cycle, and internal leakage will be of a magnitude which will not degrade subsystem operation

(4) a "NORMALLY OPEN" shutoff valve will not fail closed prior to first flight operational cycle

(5) liquid propellant storage tanks will not normally require venting, other than that necessary to satisfy the thermodynamic venting requirement

(6) the subsystem will be considered operational up to the point at which one additional failure jeopardizes safe mission completion

(7) component external leakage can be virtually eliminated by special attention to component design details. Redundancy for this failure mode will not be considered in this study except for turbopump and heat exchanger leakage.

H-2. APS SCHEMATIC

Figure H-1 presents the high pressure subsystem schematic with complete component redundancy for Orbiter B. Subsystem schematics for Orbiter C and the Booster are similar. Structural components such as tanks, accumulators, and lines are not duplicated, on the assumption that structural reliability is equal to 1.0. The conditioner assembly incorporates two completely redundant assemblies for the two-failure fail-safe requirement. The remaining components are either doubly redundant, or are designed in such a manner that the function of a failed component can be met by another component, thus meeting APS requirements.

In general, the philosophy in implementing fail-operational/fail-safe redundancy is to provide triple redundancy where feasible. Three parallel redundant regulators are provided for each pressure regulating function. Three completely independent conditioning assemblies are provided for each propellant loop. When the primary conditioning assembly fails, it is isolated and a new conditioning assembly is activated. Each thruster has isolation valves in series with the thruster propellant valves, allowing individual isolation of a failed-open thruster. A second set of valves isolates each propellant manifold to provide isolation of a double thruster valve failure and its individual isolation valve. Tanks, accumulators, lines and fittings were considered structure, and redundancy was not provided. Figure H-1 depicts the depth of redundancy provided for each function, and shows the relationship of each component's operation and failure to a successful and/or safe mission.

The analysis of the failure modes of this subsystem design schematic and the resultant reliability is discussed below.

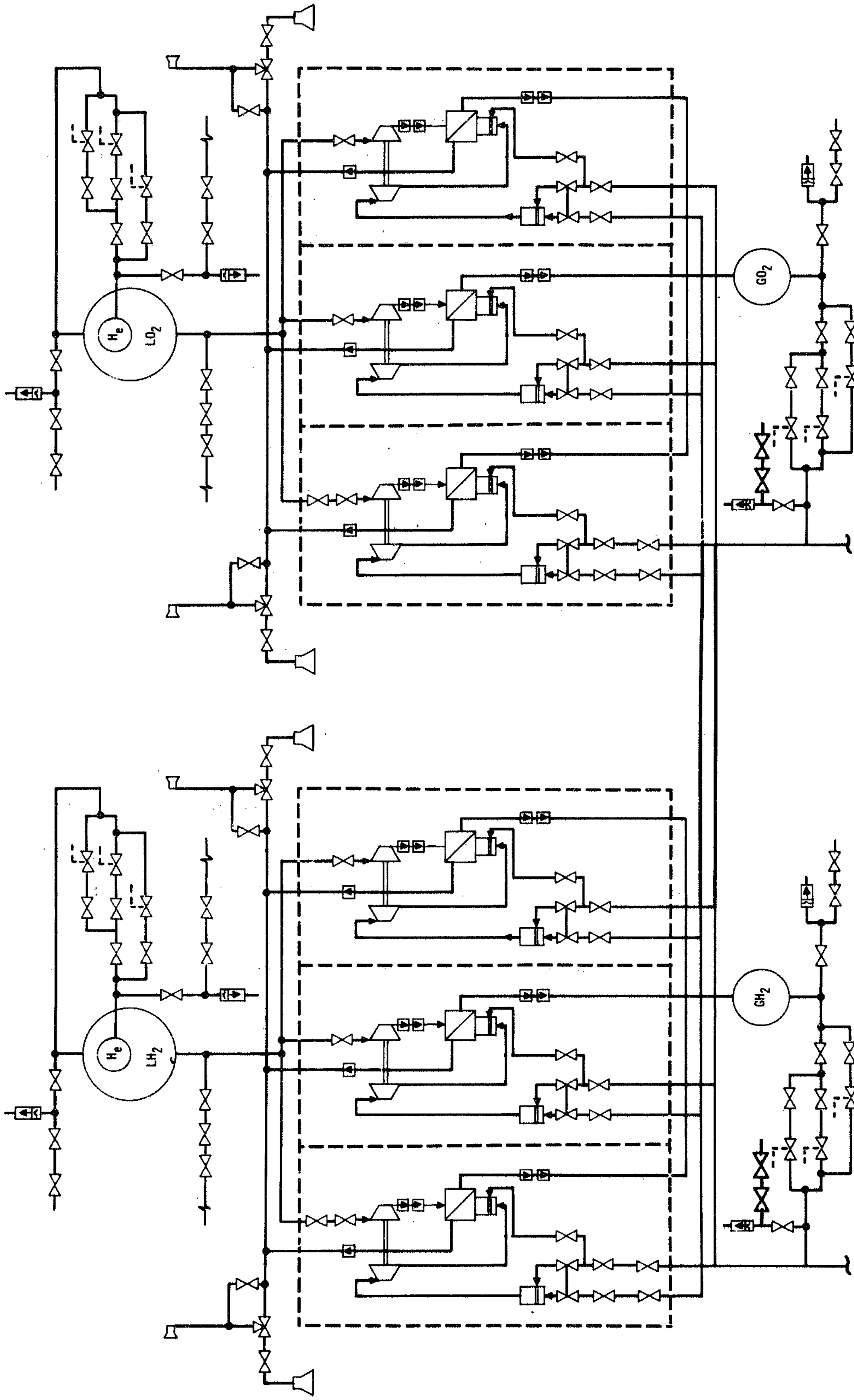

APS ORBITER SCHEMATIC

FIGURE H-1

H-3. FAILURE MODE ANALYSIS

The effect upon subsystem operation of component failure was analyzed using two basic reliability tools; the functional flow diagram and the failure mode and effect analysis. APS functional flow diagrams are presented in Figure H-2. These diagrams display, in a logical manner, the relationship of each component function and failure with the completion of a successful mission and/or a safe return from earth orbit. These diagrams also exhibit the depth of redundancy and the fail-operational/ fail-safe features for each component failure mode.

The orbiter APS was divided into the following functional groups:

(1) liquid propellant storage and pressurization

(2) propellant conditioning

(3) propellant accumulation and pressure regulation

(4) propellant distribution and thrusters.

The flow diagrams for all functional groups except propellant distribution and thrusters can be applied to all vehicles. The functional groups are schematically identical for the fuel and the oxidizer, so that the functional flow diagram presented is applicable to both. The functional flow diagrams for propellant distribution and thrusters were simplified by considering the success and failures of functional groups of valves and thrusters rather than individual components. The booster APS is schematically the same as the orbiter APS except that the booster APS does not incorporate propulsive venting of hot gas from the conditioning assemblies and since propulsive venting is not required for successful operation of the orbiter it was excluded from the flow diagrams.

Component failure modes shown in the diagrams are generally "GO, NO-GO" type failure modes. No attempt was made to include degrees of failure in the flow diagrams. For example, the "FAIL OPEN" failure mode for valves included all valve positions from failure in the full open position down to the lowest leakage rate affecting subsystem operation.

A functional group schematic is presented with each flow diagram to facilitate interpretation. The component identification numbers shown on the schematic were arbitrarily assigned for this study to quickly identify the component being discussed without a lengthy component description.

The failure mode and effect analysis (FMEA) presented in Figure H-3 examines the depth of redundancy provided for each component failure mode critical to a

FUNCTIONAL FLOW DIAGRAM

SHUTTLE HIGH PRESSURE APS - LIQUID PROPELLANT STORAGE AND PRESSURIZATION

ORBITER AND BOOSTER

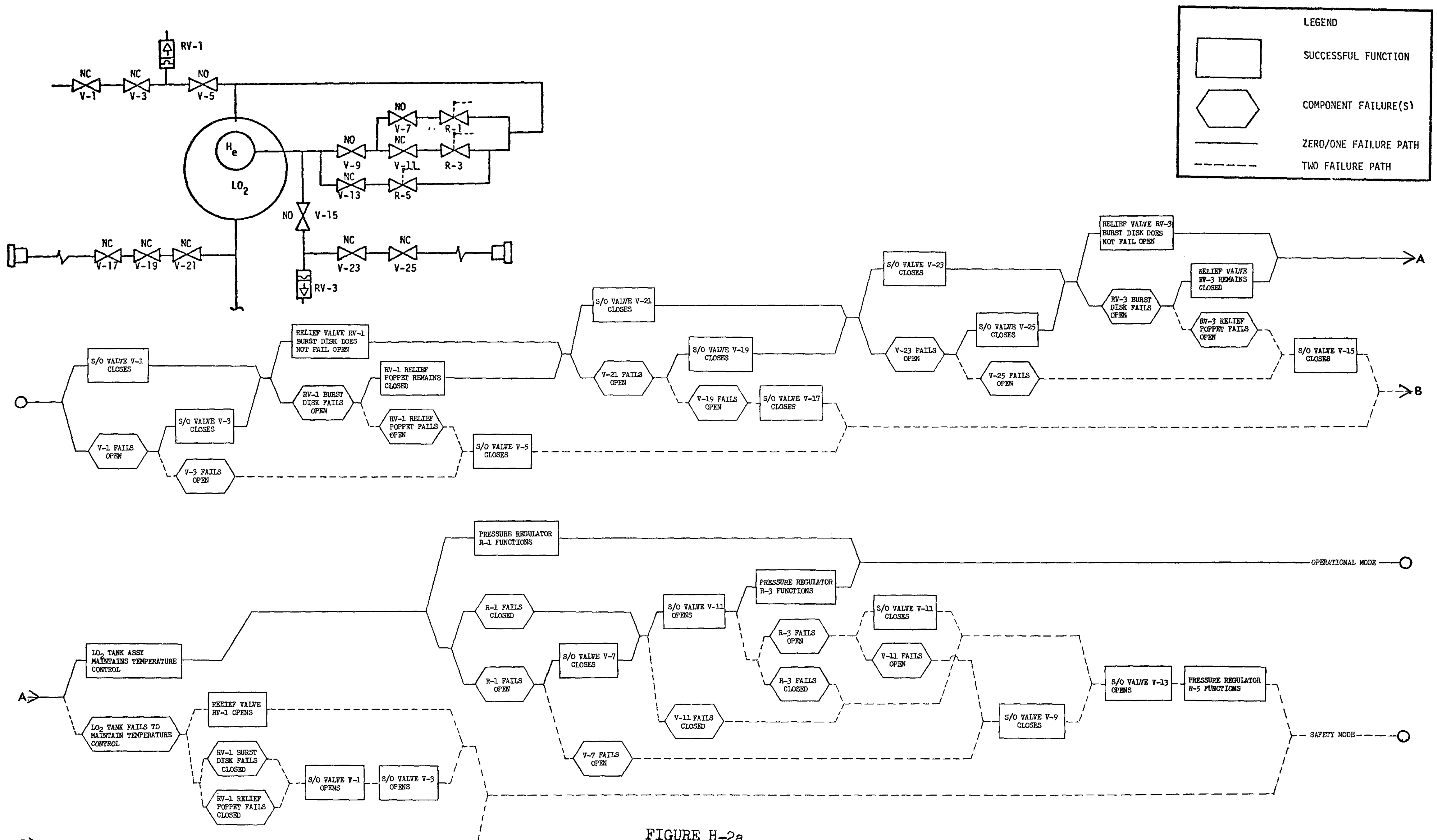

FIGURE H-2a

LIQUID PROPELLANT CONDITIONING
SHUTTLE HIGH PRESSURE APS
ORBITER AND BOOSTER

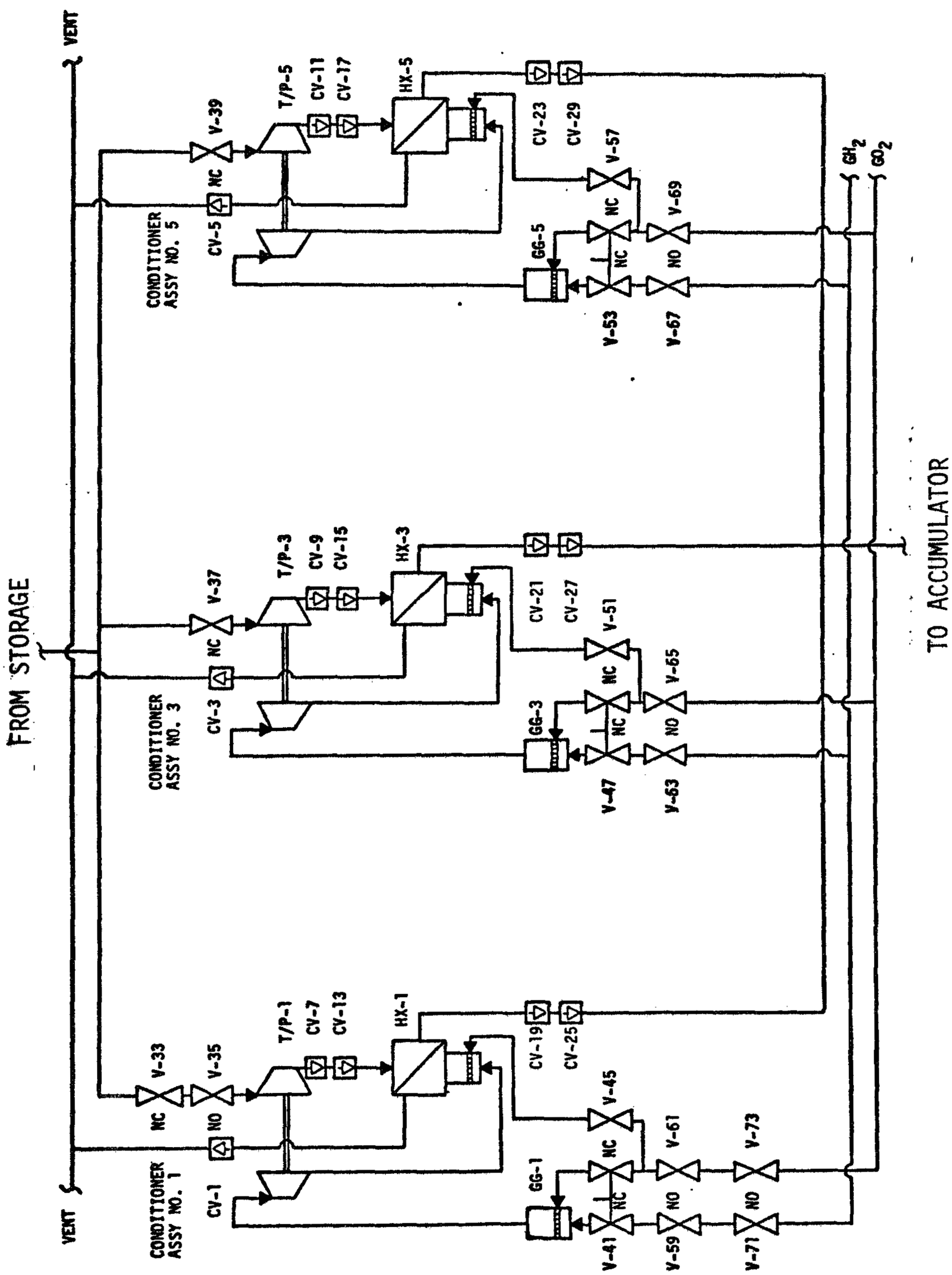

FIGURE H-2b

FUNCTIONAL FLOW DIAGRAM
SHUTTLE HIGH PRESSURE APS-LIQUID PROPELLANT CONDITIONING
ORBITERS AND BOOSTER

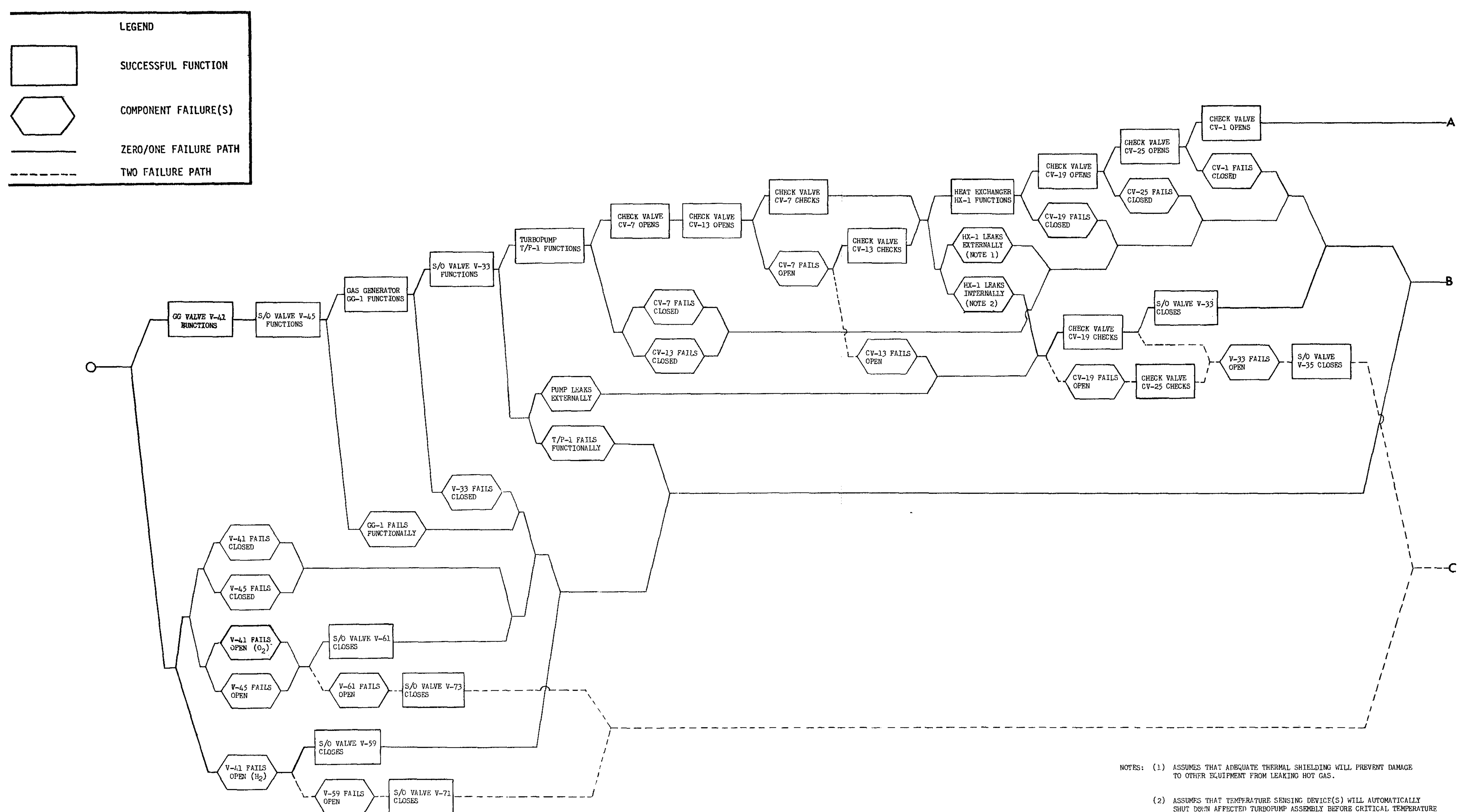

NOTES: (1) ASSUMES THAT ADEQUATE THERMAL SHIELDING WILL PREVENT DAMAGE TO OTHER EQUIPMENT FROM LEAKING HOT GAS.

(2) ASSUMES THAT TEMPERATURE SENSING DEVICE(S) WILL AUTOMATICALLY SHUT DOWN AFFECTED TURBOPUMP ASSEMBLY BEFORE CRITICAL TEMPERATURE IS REACHED IN THE O_2 HEAT EXCHANGER.

FIGURE H-2b (Cont.)

FUNCTIONAL FLOW DIAGRAM
SHUTTLE HIGH PRESSURE APS-LIQUID PROPELLANT CONDITIONING
ORBITERS AND BOOSTER

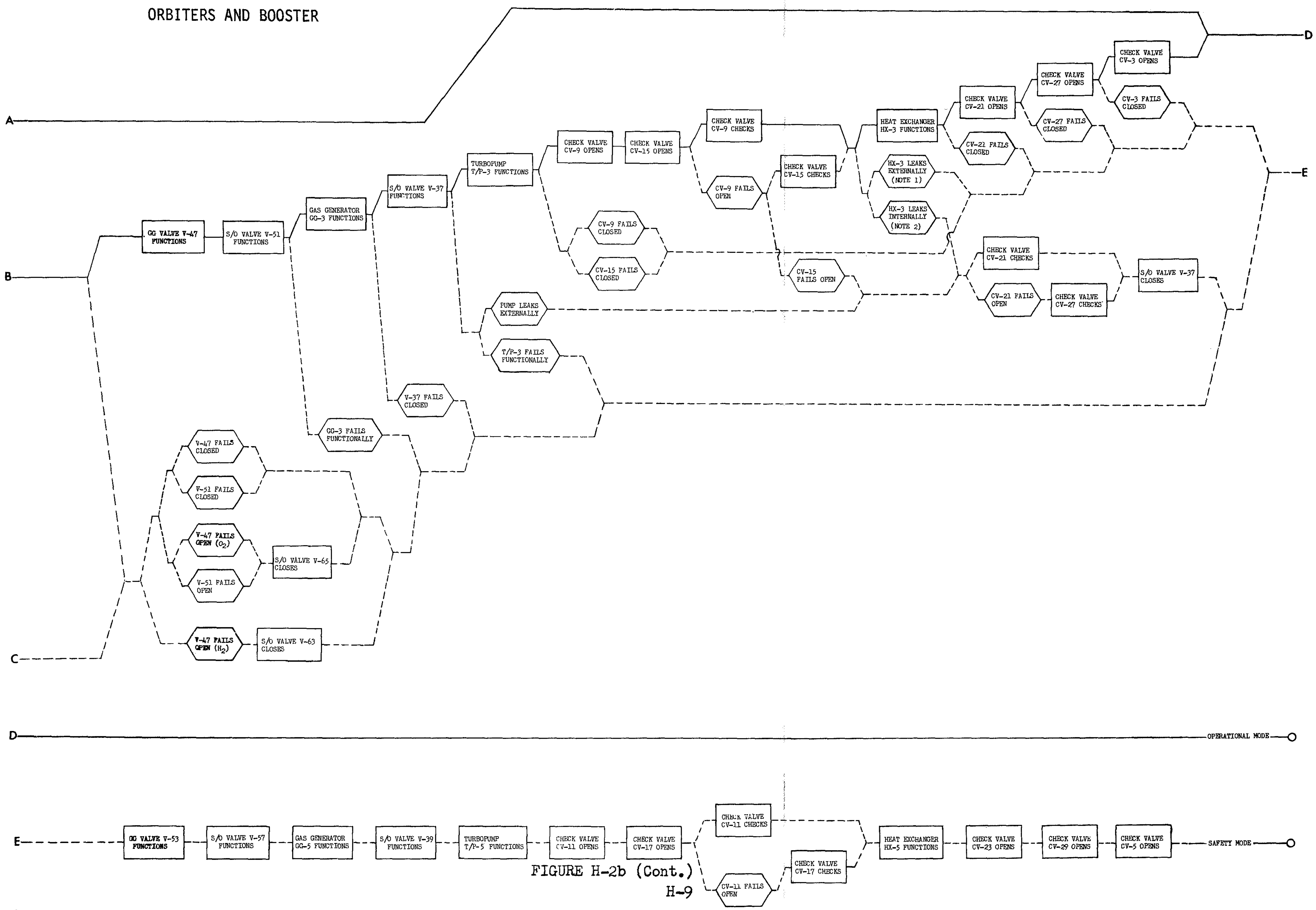

FIGURE H-2b (Cont.)

SHUTTLE HIGH PRESSURE APS-PROPELLANT ACCUMULATION AND PRESSURE REGULATION

ORBITER AND BOOSTER

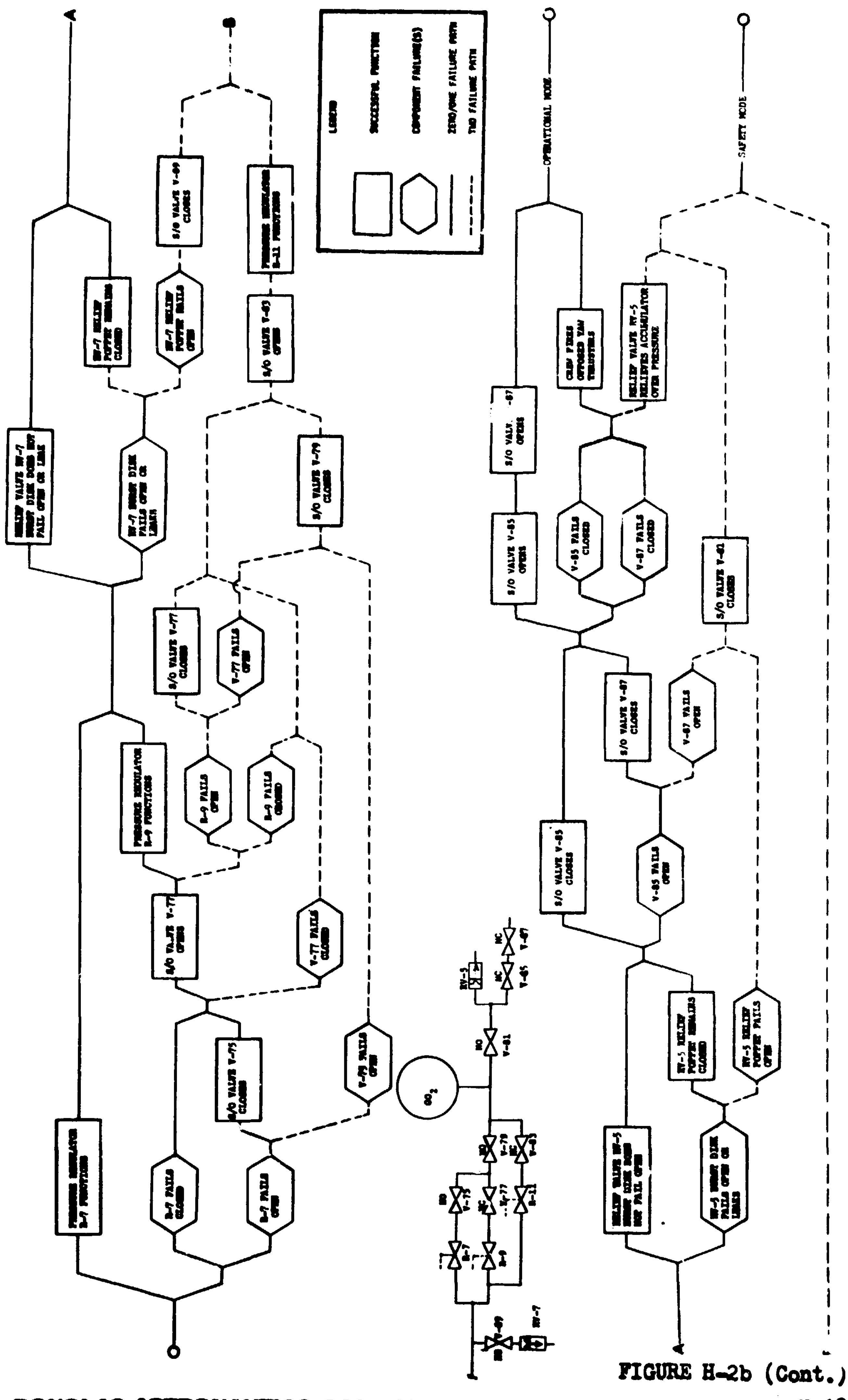

FIGURE H-2b (Cont.)

ORBITER B PROPELLANT DISTRIBUTION

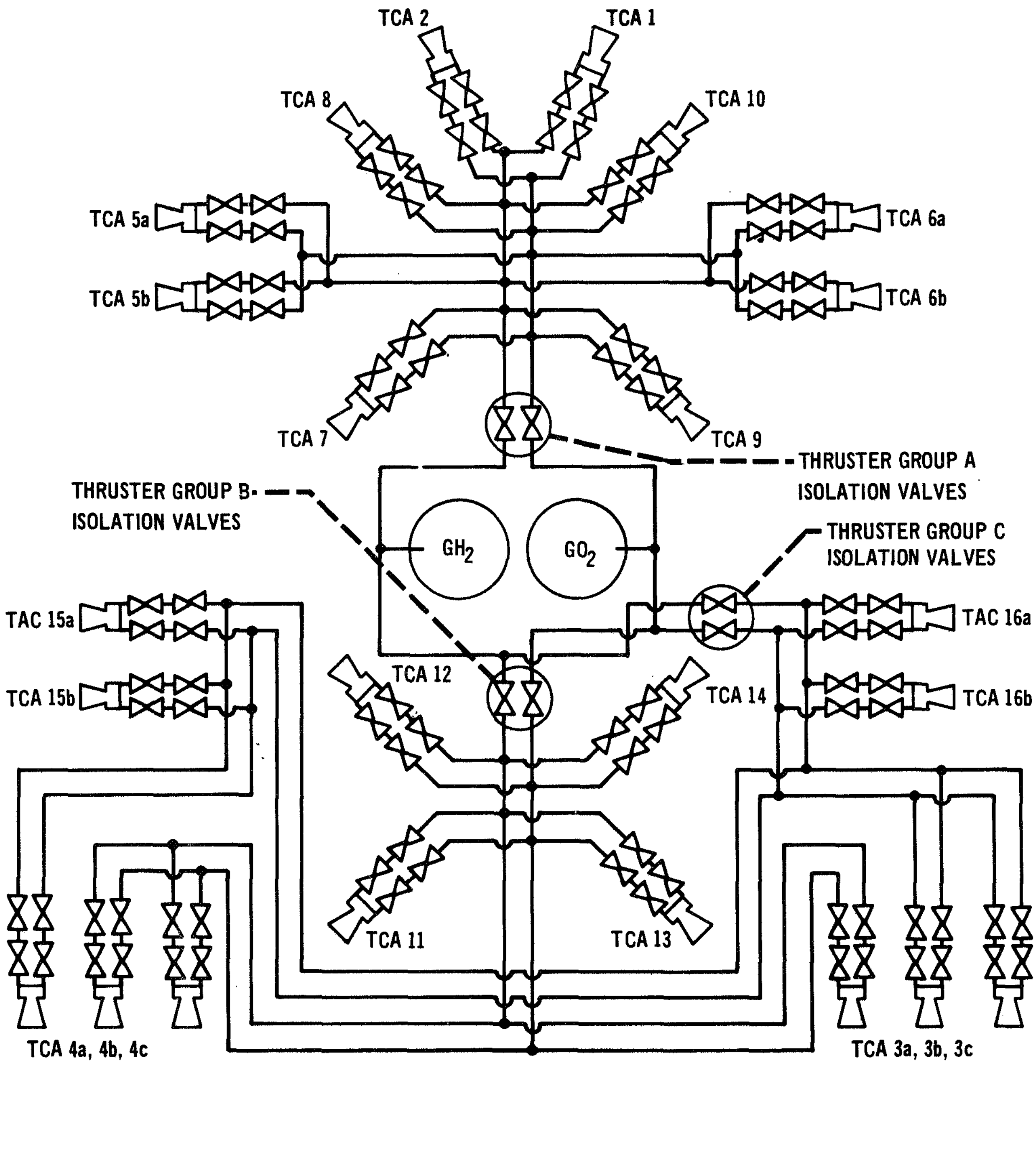

FIGURE H-2b (Cont.)

FUNCTIONAL FLOW DIAGRAM (SIMPLIFIED)
SHUTTLE HIGH PRESSURE APS-ORBITER B PROPELLANT DISTRIBUTION AND THRUSTERS

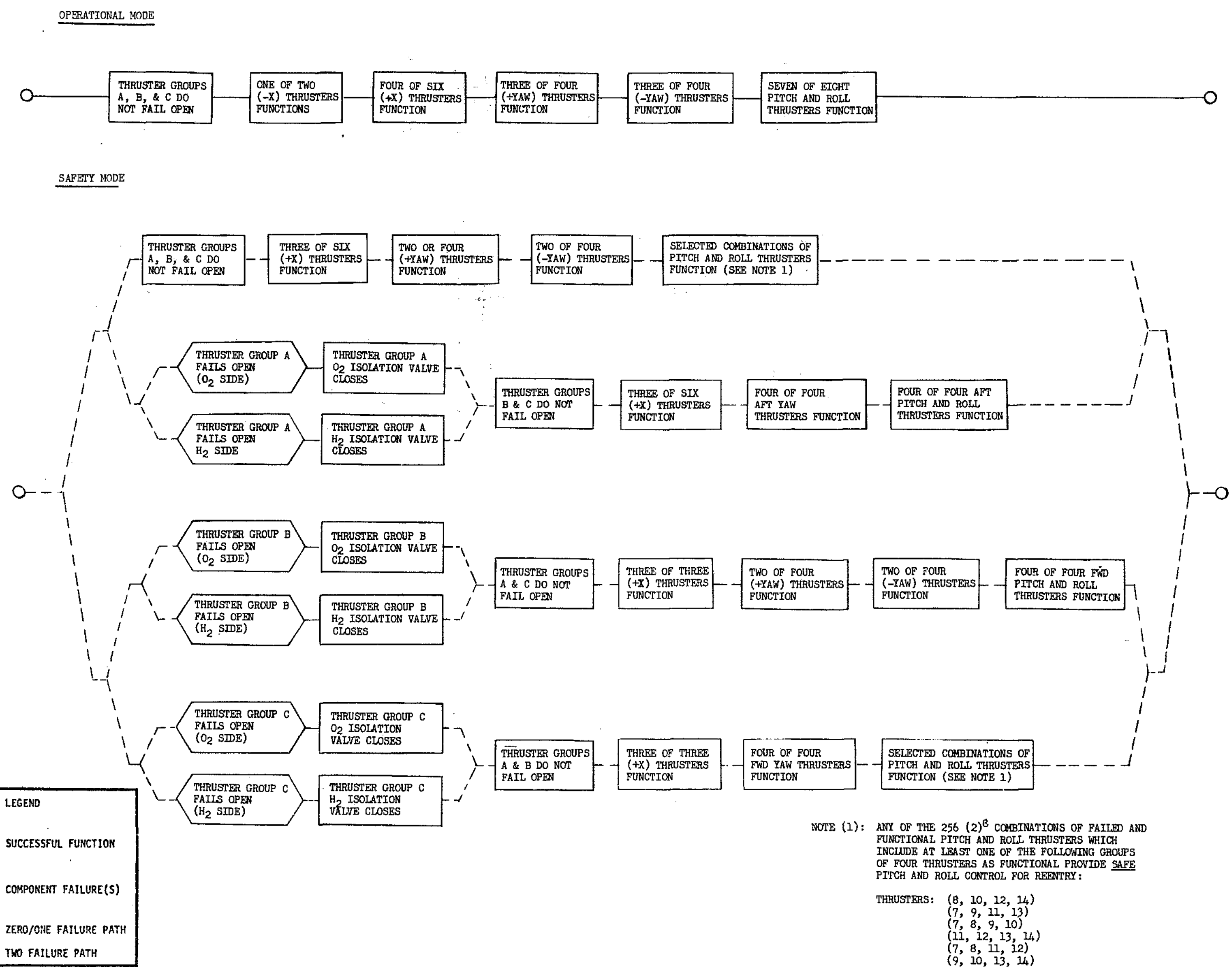

NOTE (1): ANY OF THE 256 $(2)^8$ COMBINATIONS OF FAILED AND FUNCTIONAL PITCH AND ROLL THRUSTERS WHICH INCLUDE AT LEAST ONE OF THE FOLLOWING GROUPS OF FOUR THRUSTERS AS FUNCTIONAL PROVIDE SAFE PITCH AND ROLL CONTROL FOR REENTRY:

THRUSTERS: (8, 10, 12, 14)
(7, 9, 11, 13)
(7, 8, 9, 10)
(11, 12, 13, 14)
(7, 8, 11, 12)
(9, 10, 13, 14)

FIGURE H-2b (Cont.)

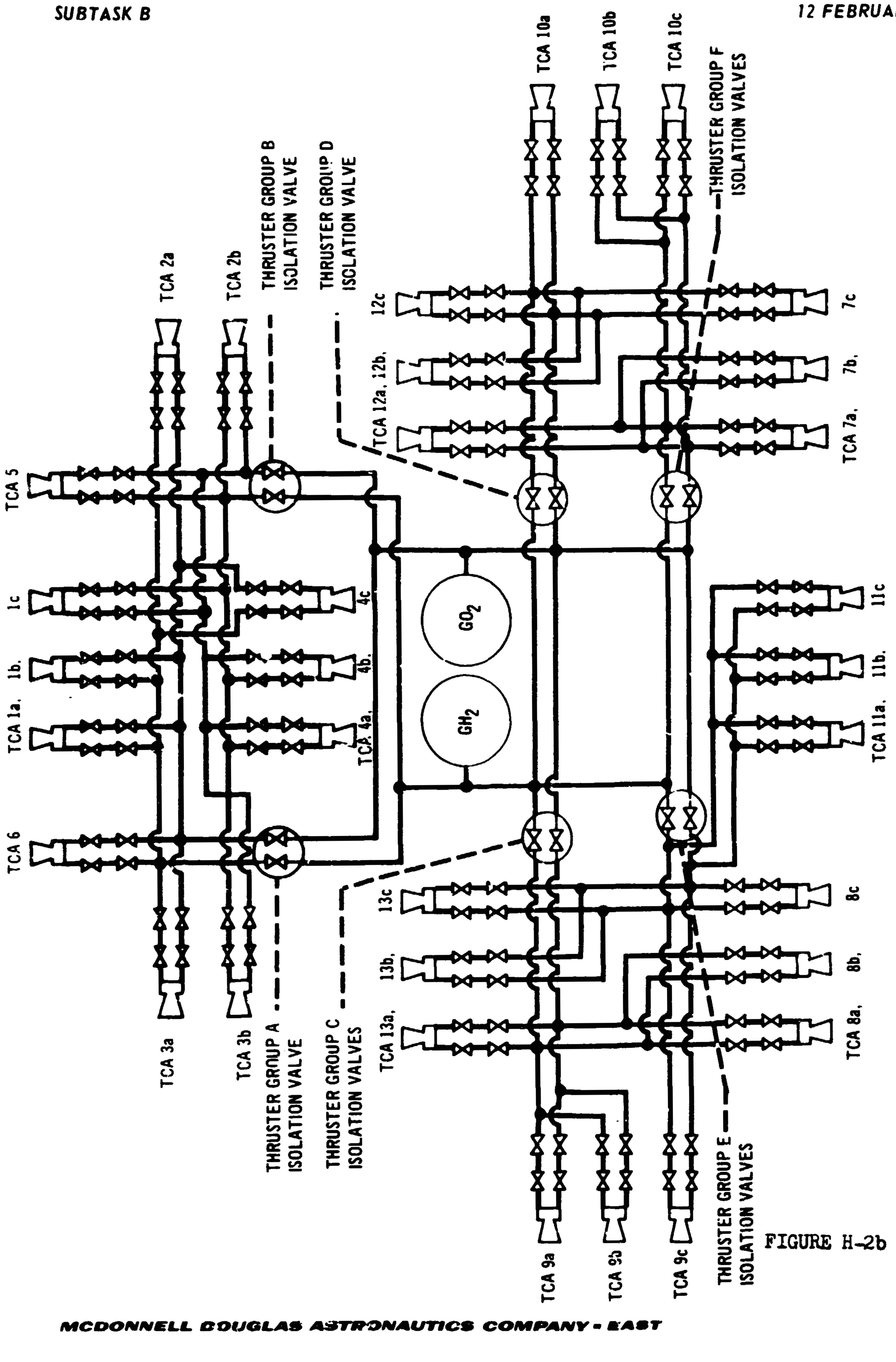

ORBITER C PROPELLANT DISTRIBUTION

FIGURE H-2b (Cont.)

FUNCTIONAL FLOW DIAGRAM (SIMPLIFIED)
SHUTTLE HIGH PRESSURE APS-ORBITER C PROPELLANT DISTRIBUTION AND THRUSTERS

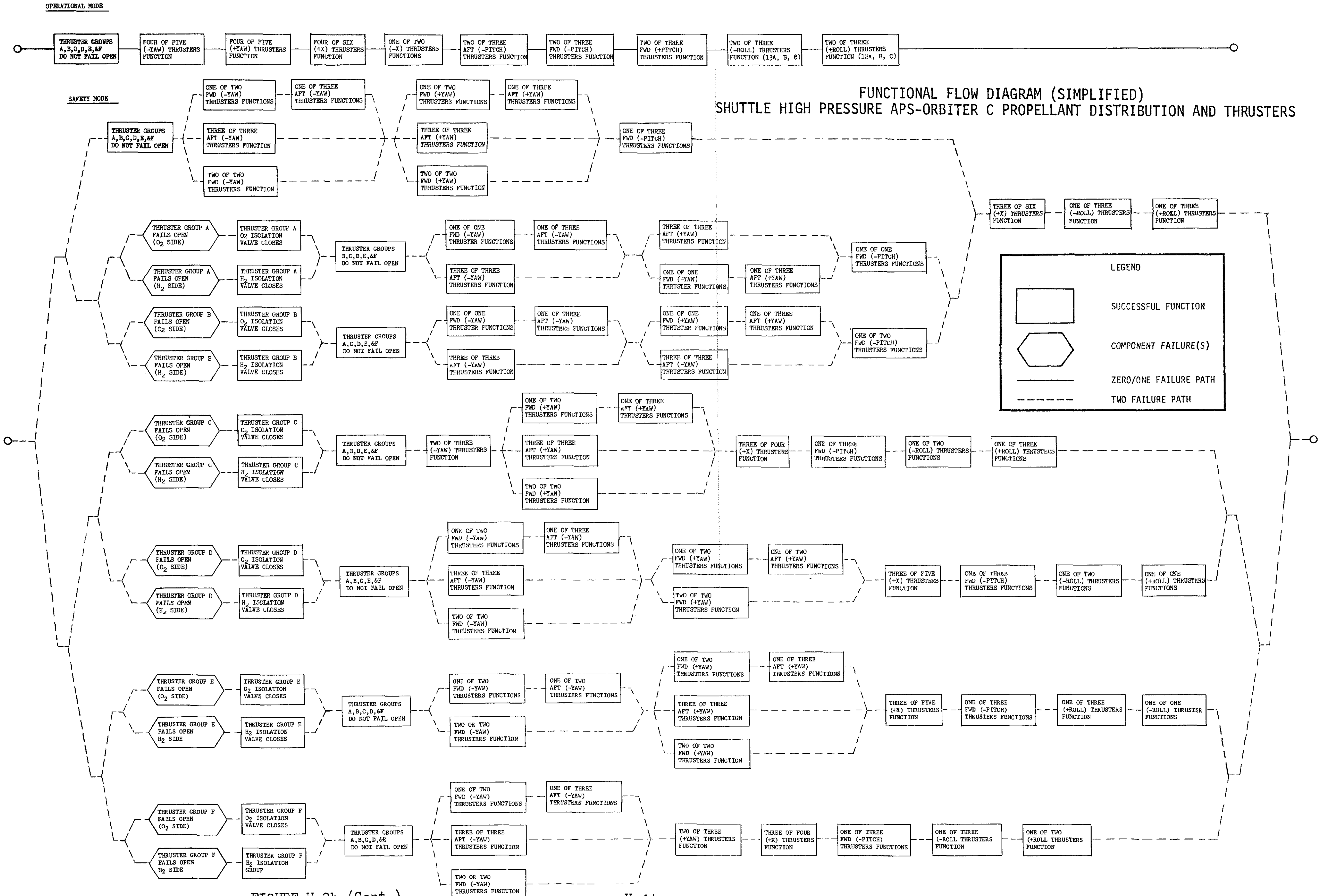

FIGURE H-2b (Cont.)

BOOSTER PROPELLANT DISTRIBUTION

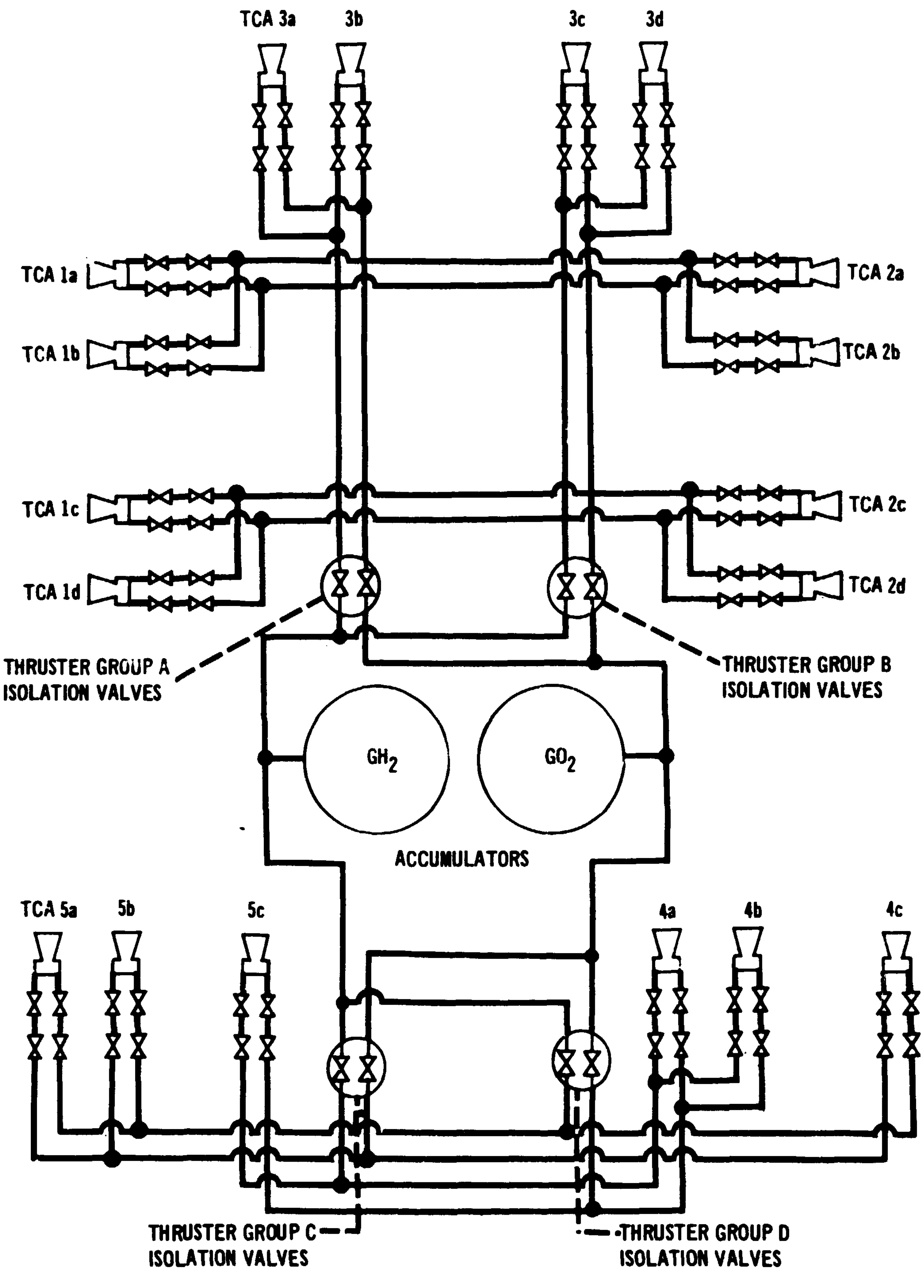

FIGURE H-2b (Cont.)

FUNCTIONAL FLOW DIAGRAM
(SIMPLIFIED)
SHUTTLE HIGH PRESSURE APS-PROPELLANT DISTRIBUTION AND THRUSTERS
BOOSTER

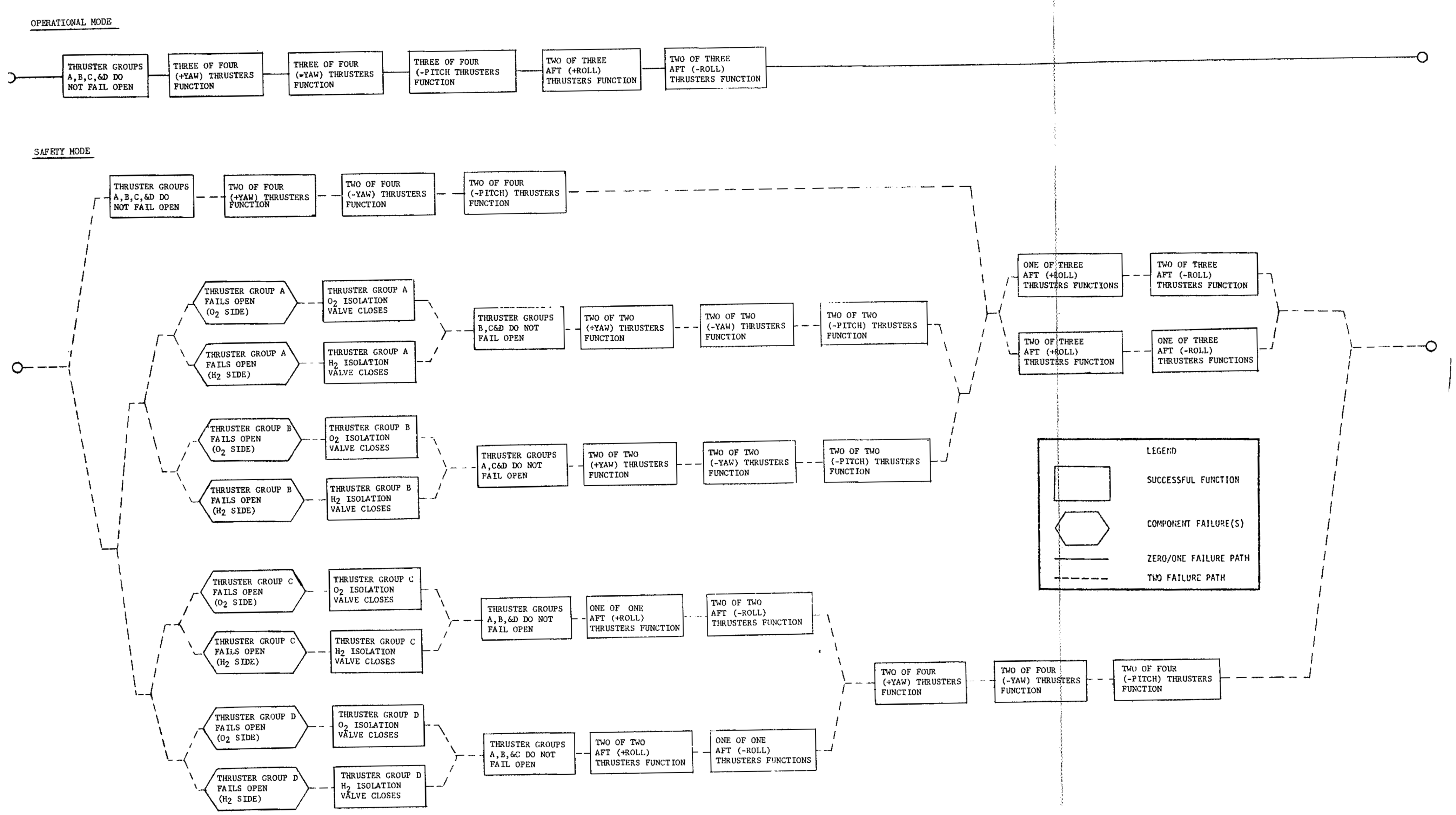

FIGURE H-2b (Cont.)

FAILURE MODE AND EFFECTS ANALYSIS
PRIMARY COMPONENTS

FUNCTION: LO_2 STORAGE AND PRESSURIZATION (LH_2 STORAGE AND PRESSURIZATION IDENTICAL)

COMPONENT	FUNCTION	DUTY CYCLE	FAILURE MODE	FAILURE EFFECT/DETECTION	FAIL-OP FAIL SAFE REDUNDANCY EVALUATION
V-1 VALVE, SHUTOFF, PNEUMATIC ACTUATION, NORMALLY CLOSED	OPENED DURING GROUND FILL OPERATION TO VENT BOIL-OFF.	1 CYCLE	FAILS OPEN	NO EFFECT UNLESS V-3 ALSO FAILS OPEN. DOUBLE FAILURE CAN BE DETECTED BY MONITORING HE TANK PRESSURE DECAY TREND.	N/C VALVE V-3 IS SERIES REDUNDANT FOR THIS FAILURE MODE AND N/O VALVE V-5 CAN BE CLOSED IN THE EVENT OF DOUBLE FAILURE OF V-1 AND V-3 IN THIS MODE.
RV-1 VALVE, PRESSURE RELIEF	RELIEVES LO_2 TANK OVERPRESSURE IF THE TEMPERATURE CONTROL MALFUNCTIONS OR REGULATOR FAILS OPEN.	1 CYCLE	BURST DISK FAILS OPEN	NO EFFECT UNLESS RELIEF POPPET ALSO FAILS OPEN. DOUBLE FAILURE CAN BE DETECTED BY MONITORING HE TANK PRESSURE DECAY TREND.	VALVE IS INTERNALLY REDUNDANT FOR THIS FAILURE MODE AND N/O VALVE V-5 CAN BE CLOSED IN THE EVENT OF DOUBLE FAILURE.
V-21 VALVE, SHUTOFF, PNEUMATIC ACTUATION, NORMALLY CLOSED	OPENED DURING GROUND FILL OPERATION FOR FILLING LO_2 TANK.	1 CYCLE	FAILS OPEN	NO EFFECT.	N/C VALVES V-17 AND V-19 PROVIDE "FAIL-OP, FAIL-SAFE" REDUNDANCY.
V-23 VALVE, SHUTOFF, SOLENOID ACTUATED NORMALLY CLOSED	OPENED DURING GROUND FILL OPERATION FOR SERVICING HE TANK.	1 CYCLE	FAILS OPEN	NO EFFECT UNLESS V-25 ALSO FAILS OPEN. DOUBLE FAILURE CAN BE DETECTED BY MONITORING HE TANK PRESSURE DECAY TREND.	N/C VALVE V-25 IS SERIES REDUNDANT AND N/O VALVE V-15 CAN BE CLOSED IN EVENT OF DOUBLE FAILURE OF V-23 AND V-25 IN THIS MODE.
RV-3 VALVE, PRESSURE RELIEF	PROVIDES EMERGENCY PRESSURE RELIEF IN THE EVENT OF ACCIDENTAL OVER-PRESSURE OF HE TANK DURING GROUND FILL OPERATION.	1 CYCLE	BURST DISK FAILS OPEN	NO EFFECT UNLESS RELIEF POPPET ALSO FAILS OPEN. DOUBLE FAILURE CAN BE DETECTED BY MONITORING HE TANK PRESSURE DECAY TREND.	VALVE IS INTERNALLY REDUNDANT FOR THIS FAILURE MODE AND N/O VALVE V-15 CAN BE CLOSED IN EVENT OF DOUBLE FAILURE.
LO_2 TANK ASS'Y	PROVIDES CRYOGENIC STORAGE FOR LO_2.	ORBITERS - 72 HOURS BOOSTER - 0.1 HOURS	FAILS TO MAINTAIN TEMPERATURE CONTROL	LO_2 TANK PRESSURE RISE MAY RESULT IN LOSS OF OXIDIZER BY OVERBOARD VENTING. FAILURE CAN BE DETECTED BY MONITORING LO_2 TANK TEMPERATURE AND PRESSURE.	DEPENDING UPON THE LOSS RATE, THIS FAILURE MAY REQUIRE PREMATURE REENTRY. RELIEF VALVE RV-1 WILL PROVIDE PRESSURE RELIEF. IF RV-1 FAILS CLOSED, N/C VALVES V-1 AND V-3 CAN BE OPENED TO RELIEVE PRESSURE.
R-1 REGULATOR, LO_2 TANK PRESSURE	MAINTAINS REGULATED PRESSURE IN LO_2 TANK BY ADDING HIGH PRESSURE HELIUM AS REQUIRED.	ORBITERS - 72 HOURS BOOSTER - 0.1 HOURS	FAILS CLOSED (REGULATES LOW)	LO_2 TANK PRESSURE WILL DECAY RESULTING IN DEGRADED POSITIVE EXPULSION CAPABILITY. DETECTED BY MONITORING LO_2 TANK PRESSURE.	PRESSURE REGULATORS R-3 AND R-5 PROVIDE "FAIL-OP, FAIL-SAFE" REDUNDANCY.
			FAILS OPEN (REGULATES HIGH)	EXCESSIVE LO_2 TANK PRESSURE. FAILURE DETECTED BY MONITORING LO_2 TANK PRESSURE AND TEMPERATURE.	N/O VALVES V-7 AND V-9 PROVIDE "FAIL-OP, FAIL-SAFE" REDUNDANCY FOR THIS FAILURE MODE. REDUNDANT PRESSURE SWITCHES WILL BE USED TO ISOLATE R-1 PRIOR TO CRITICAL OVERPRESSURE. RELIEF VALVE RV-1 PROVIDES EMERGENCY RELIEF.

FIGURE H-3

FAILURE MODE AND EFFECTS ANALYSIS
PRIMARY COMPONENTS

FUNCTION: PROPELLANT ACCUMULATION AND PRESSURE REGULATION (O_2 & H_2 IDENTICAL)

COMPONENT	FUNCTION	DUTY CYCLE	FAILURE MODE	FAILURE EFFECT/DETECTION	FAIL-OP FAIL SAFE REDUNDANCY EVALUATION
R-7 REGULATOR, PRESSURE, GASEOUS PROPELLANT	REGULATES PRESSURE OF PROPELLANT SUPPLIED TO THE APS THRUSTERS	ORBITERS - 72 HOURS BOOSTER - 0.1 HOURS	FAILS CLOSED (REGULATES LOW)	THE FLOW OF PROPELLANT TO THE THRUSTERS IS DEGRADED OR PREVENTED WITH RESULTING LOSS OR DEGRADATION OF APS FUNCTION. DETECTED BY SENSING LINE PRESSURE DOWNSTREAM OF THE REGULATOR.	REGULATORS R-9 AND R-11 PROVIDES "FAIL-OP, FAIL-SAFE" REDUNDANCY.
			FAILS OPEN (REGULATOR HIGH)	PROPELLANT PRESSURE TO THE THRUSTERS IS EXCESSIVE. DETECTED BY MONITORING LINE PRESSURE DOWNSTREAM OF REGULATOR.	S/O VALVES V-57 AND V-59 PROVIDE "FAIL-OP, FAIL SAFE" REDUNDANCY. PRESSURE SWITCHES OR SENSORS CAN BE USED TO CLOSE THE VALVES. RELIEF VALVE RV-7 PROVIDES EMERGENCY RELIEF FOR RAPID OVERPRESSURE.
RV-5 VALVE, PRESSURE RELIEF	PROVIDES EMERGENCY RELIEF FOR CRITICAL ACCUMULATOR OVERPRESSURE.	1 CYCLE	BURST DISK FAILS OPEN	NO EFFECT UNLESS RELIEF POPPET ALSO FAILS OPEN. DOUBLE FAILURE CAN BE DETECTED BY MONITORING ACCUMULATOR PRESSURE DECAY TRENDS.	VALVE IS INTERNALLY REDUNDANT FOR THIS FAILURE MODE AND VALVE V-81 CAN BE CLOSED IN EVENT OF A DOUBLE FAILURE.
V-85 OR V-87 VALVE, SHUTOFF, SOLENOID ACTUATED, NORMALLY CLOSED	OPENED TO VENT ACCUMULATOR OVERPRESSURE	3 CYCLES MAX. ORBITER ONLY	FAILS CLOSED	NORMAL VENTING OF ACCUMULATOR OVERPRESSURE IS PREVENTED. CAN BE DETECTED BY MONITORING ACCUMULATOR PRESSURE AND/OR BY SENSING VALVE POSITION.	"FAIL-OP" CAPABILITY CAN BE PROVIDED BY CREW RELIEVING OVERPRESSURE BY FIRING OPPOSED YAW THRUSTERS. "FAIL-SAFE" REDUNDANCY IS PROVIDED BY RELIEF VALVE RV-5.
			FAILS OPEN	NO EFFECT UNLESS BOTH VALVES FAIL OPEN. FAILURE CAN BE DETECTED BY MONITORING ACCUMULATOR PRESSURE AFTER VENT CYCLE AND/OR BY SENSING VALVE POSITION.	THESE VALVES ARE REDUNDANT FOR THIS FAILURE MODE. "FAIL-SAFE" REDUNDANCY IS PROVIDED BY N/O VALVE V-81.
RV-7 VALVE, PRESSURE RELIEF	PROVIDES EMERGENCY RELIEF OF THRUSTER PROPELLANT PRESSURE IN THE EVENT A PRESSURE REGULATOR FAILS OPEN AND IS NOT ISOLATED RAPIDLY.	1 CYCLE	BURST DISK FAILS OPEN	NO EFFECT UNLESS RELIEF POPPET ALSO FAILS OPEN. DOUBLE FAILURE CAN BE DETECTED BY MONITORING ACCUMULATOR AND/OR PROPELLANT LINE PRESSURE DECAY TRENDS.	VALVE IS INTERNALLY REDUNDANT FOR THIS FAILURE MODE. N/O VALVE V-89 COMPLETES "FAIL SAFE" REDUNDANCE.

FIGURE H-3 (Cont.)

FAILURE MODE AND EFFECTS ANALYSIS
PRIMARY COMPONENTS

FUNCTION: LIQUID PROPELLANT CONDITIONING (O_2 AND H_2 ARE IDENTICAL IN FUNCTION)

COMPONENT	FUNCTION	DUTY CYCLE	FAILURE MODE	FAILURE EFFECT/DETECTION	FAIL-OP FAIL SAFE REDUNDANCY EVALUATION
V-41 VALVE, BIPROPELLANT, MOTOR DRIVEN FLOW MODULATING	CONTROLS ON-OFF FLOW OF GASEOUS PROPELLANTS TO GAS GENERATOR GG-1. ALSO MODULATES FLOW OVER A RANGE OF APPROXIMATELY 10% OF MAXIMUM FLOW TO PROVIDE CONSTANT TURBINE POWER - ALSO HAS OVERRIDE ON THE OXYGEN CONTROL TO LIMIT TEMPERATURE.	ORBITERS - 0.66 HOURS, 50 CYCLES	FAILS TO MODULATE FLOW	TEMPERATURE IN HEAT EXCHANGER WILL BE TOO LOW OR TOO HIGH. AN EXCESSIVE HIGH TEMPERATURE WILL CAUSE SHUTDOWN OF CONDITIONING ASSEMBLY #1. IF THE TEMPERATURE IS TOO LOW THE TURBINE SPEED WILL DROP. OVERTEMPERATURE WILL BE DETECTED BY MONITORING HEAT EXCHANGER TEMPERATURE. OTHER FAILURES DETECTED BY MONITORING TURBINE SPEED.	THE TWO ADDITIONAL CONDITIONING ASSEMBLIES IN EACH PROPELLANT LOOP PROVIDE "FAIL-OP, FAIL-SAFE" REDUNDANCY FOR THIS FAILURE MODE.
			FAILS CLOSED	GAS GENERATOR GG-1 IS INOPERATIVE. DETECTED BY MONITORING GAS GENERATOR TEMPERATURE AND PRESSURE.	SAME AS ABOVE.
			FAILS OPEN OR LEAKS	LEAKAGE OF BOTH PROPELLANTS RESULTS IN CONTINUED COMBUSTION IN GAS GENERATOR. LEAKAGE OF FUEL ONLY RESULTS IN EXCESSIVE FUEL CONSUMPTION. LEAKAGE OF OXIDIZER ONLY DURING IDLE PERIODS NOT ONLY RESULTS IN EXCESSIVE OXIDIZER CONSUMPTION BUT MAY RESULT IN AN IMMEDIATE OVERTEMPERATURE CONDITION IN THE GAS GENERATOR AND HEAT EXCHANGER WHEN THE CONDITIONING ASSEMBLY IS ACTIVATED. THIS WILL RESULT FROM THE OXIDIZER RICH MIXTURE CAUSED BY THE LEAKING O_2. THIS OVERHEATING MAY CAUSE STRUCTURAL FAILURE OF THE HEAT EXCHANGER, DAMAGE TO SURROUNDING EQUIPMENT OR FIRE. LOSS OF PROPELLANTS MAY BE DETECTED BY MONITORING ACCUMULATOR PRESSURE DECAY DURING IDLE PERIODS. THE OVERTEMPERAUTRE CONDITION CAN BE DETECTED BY MONITORING GAS GENERATOR AND HEAT EXCHANGER TEMPERATURES.	"FAIL-OP, FAIL-SAFE" REDUNDANCY AGAINST LOSS OF PROPELLANTS IS PROVIDED BY S/O VALVES V-59 AND V-71 OR V-61 AND V-73 WHEN CONDITIONING ASSEMBLY #1 IS ISOLATED. TEMPERATURE SENSING DEVICES MUST BE INSTALLED IN THE CONDITIONING ASSEMBLY TO ACCOMPLISH IMMEDIATE SHUTDOWN AND ISOLATION IF OVERHEATING OF THE HEAT EXCHANGER OR DUCTS OCCURS DURING OPERATION. THE POTENTIAL SAFETY HAZARD INVOLVED SHOULD BE SUBJECTED TO FURTHER EVALUATION.
V-45 VALVE, SHUTOFF, SOLENOID ACTUATED, NORMALLY CLOSED	CONTROLS FLOW OF GASEOUS O_2 WHICH WHICH IS INJECTED INTO HEAT EXCHANGER HX-1 TO MIX WITH HOT TURBINE EXHAUST TO RAISE HEAT EXCHANGER GAS TEMPERATURE TO THE DESIRED LEVEL.	ORBITERS - 50 CYCLES BOOSTER - 16 CYCLES	FAILS OPEN OR LEAKS	THIS FAILURE WILL HAVE ESSENTIALLY THE SAME EFFECT AS LEAKING O_2 THROUGH V-41 DESCRIBED ABOVE.	SAME AS ABOVE FOR O_2 LEAK THROUGH V-41
			FAIL CLOSED	HEAT EXCHANGER GAS TEMPERATURE WILL BE TOO LOW RESULTING IN DEGRADED PERFORMANCE. DETECTED BY MONITORING HEAT EXCHANGER TEMPERATURE AND PROPELLANT TEMPERATURE AS IT LEAVES THE HEAT EXCHANGER.	THE TWO ADDITIONAL CONDITIONING ASSEMBLIES IN EACH PROPELLANT LOOP PROVIDE "FAIL-OP, FAIL-SAFE" REDUNDANCY FOR THIS FAILURE MODE.

FIGURE H-3 (Cont.)

FAILURE MODE AND EFFECTS ANALYSIS
PRIMARY COMPONENTS

FUNCTION: LIQUID PROPELLANT CONDITIONING (O_2 AND H_2 ARE IDENTICAL IN FUNCTION) (CONTINUED)

COMPONENT	FUNCTION	DUTY CYCLE	FAILURE MODE	FAILURE EFFECT/DETECTION	FAIL-OP FAIL SAFE REDUNDANCY EVALUATION
GG-1 GAS GENERATOR	PROVIDES HOT GAS TO OPERATE TURBOPUMP T/P-1 AND TO PROVIDE HEAT SOURCE FOR HEAT EXCHANGER HX-1.	ORBITERS - 0.66 HOURS, 50 CYCLES BOOSTER - 0.1 HOURS 16 CYCLES	IGNITION FAILURE OR DEGRADED OPERATION	THE OPERATION OF TURBOPUMP T/P-1 AND HEAT EXCHANGER HX-1 WILL BE LOST OR DEGRADED. CAN BE DETECTED BY MONITORING GG-1 COMBUSTION CHAMBER TEMPERATURE AND/OR TURBINE SPEED DURING OPERATION AND BY MONITORING GENERAL CONDITIONING ASSEMBLY PERFORMANCE.	SAME AS ABOVE
V-33 VALVE, SHUTOFF, SOLENOID ACTUATED NORMALLY CLOSED.	CONTROLS ON-OFF FLOW OF LIQUID PROPELLANT TO TURBOPUMP T/P-1.	OBRITERS- 50 CYCLES BOOSTER - 16 CYCLES	FAILS CLOSED	LOSS OF TURBOPUMP T/P-1. DETECTED BY MONITORING FLOW RATE OF LIQUID PROPELLANT TO THE PUMP AND/OR BY MONITORING VALVE POSITION.	SAME AS ABOVE
			FAILS OPEN	NO SIGNIFICANT EFFECT UNLESS TURBOPUMP T/P-1 OR HEAT EXCHANGER HX-1 ARE ALSO LEAKING. FAILURE MAY BE DETECTED BY MONITORING VALVE POSITION. DOUBLE FAILURE MAY BE DETECTED BY MONITORING CONTINUING FLOW OF LIQUID PROPELLANT AFTER SHUTDOWN.	N/O VALVE V-35 COMPLETES THE "FAIL-OP, FAIL-SAFE" REDUNDANCY FOR THIS FAILURE MODE.
T/P-1 TURBOPUMP, CRYOGENIC	PRODUCES ΔP REQUIRED TO TRANSFER LIQUID PROPELLANT FROM THE STORAGE TANK, THROUGH THE HEAT EXCHANGER TO THE ACCUMULATOR AND MAINTAIN ACCUMULATOR PRESSURE.	ORBITERS - 0.66 HRS, 50 CYCLES BOOSTER - 0.10 HRS 16 CYCLES	INOPERATIVE OR DEGRADED OPERATION	ACCUMULATOR PRESSURE WILL NOT BE MAINTAINED. CAN BE DETECTED BY MONITORING TURBINE SPEED AND PRESSURE AT PUMP OUTLET.	TWO PARALLEL REDUNDANT CONDITIONING ASSEMBLIES PROVIDE "FAIL-OP, FAIL-SAFE" REDUNDANCY.
			LEAKS PROPELLANT EXTERNALLY	EXCESSIVE PROPELLANT CONSUMPTION. SIGNIFICANT LEAKAGE WILL RESULT IN DEGRADED CONDITIONING ASSEMBLY PERFORMANCE	SHUTOFF VALVES V-33 AND V-35 PROVIDE "FAIL-OP, FAIL-SAFE" REDUNDANCY FOR LEAKAGE AND THE REDUNDANT CONDITIONING ASSEMBLIES PROVIDE "FAIL-OP, FAIL-SAFE" OPERATIONAL REDUNDANCY.
CV-7 OR CV-13 VALVE CHECK	PROVIDES BACK-PRESSURE PROTECTION FOR THE TURBOPUMP FOLLOWING SHUT-DOWN.	ORBITERS - 0.66 HRS. 50 CYCLES BOOSTER - 0.10 HRS 16 CYCLES	FAILS CLOSED OR RESTRICTS FLOW	PREVENTS FLOW OF PROPELLANT FROM THE PUMP. CAN BE DETECTED BY MONITORING PROPELLANT FLOW RATE TO THE PUMP FROM THE STORAGE TANK.	TWO PARALLEL REDUNDANT CONDITIONING ASSEMBLIES PROVIDE "FAIL-OP, FAIL-SAFE" REDUNDANCY
			FAILS OPEN	NO EFFECT UNLESS BOTH CHECK VALVES FAIL OPEN. DOUBLE FAILURE MAY RESULT IN PUMP DAMAGE DUE TO BACK-PRESSURE. CAN BE DETECTED BY MONITORING PRESSURE AT TURBOPUMP INLET.	THESE VALVES ARE REDUNDANT FOR THIS FAILURE MODE. THE TWO PARALLEL REDUNDANT CONDITIONING ASSEMBLIES PROVIDE "FAIL-OP, FAIL-SAFE" REDUNDANCY FOR A DAMAGED PUMP.

FIGURE H-3 (Cont.)

FAILURE MODE AND EFFECTS ANALYSIS
PRIMARY COMPONENTS

FUNCTION: LIQUID PROPELLANT CONDITIONING (O_2 AND H_2 ARE IDENTICAL IN FUNCTION) (CONTINUED)

COMPONENT	FUNCTION	DUTY CYCLE	FAILURE MODE	FAILURE EFFECT/DETECTION	FAIL-OP FAIL SAFE REDUNDANCY EVALUATION
HX-1 HEAT EXCHANGER	APPLIES HEAT TO LIQUID PROPELLANT TO CHANGE IT TO GASEOUS STATE	ORBITERS - 0.66 HRS, 50 CYCLES BOOSTER - 0.10 HRS 50 CYCLES	LEAKS HOT GAS EXTERNALLY	POSSIBLE DAMAGE TO SURROUNDING EQUIPMENT FROM THE HOT GAS. THIS IS A STRUCTURAL FAILURE AND WAS INCLUDED TO CALL ATTENTION TO POSSIBLE DAMAGE TO OTHER EQUIPMENT. SHOULD BE EVALUATED WHEN PLANNING INSTALLATION.	ADEQUATE THERMAL PROTECTION MUST BE PROVIDED TO SURROUNDING EQUIPMENT AND BY ADEQUATE STRUCTURAL DESIGN OF HEAT EXCHANGER. TWO PARALLEL REDUNDANT CONDITIONING ASSEMBLIES PROVIDE REQUIRED OPERATIONAL REDUNDANCY.
			LEAKS PROPELLANT INTERNALLY	EXCESSIVE PROPELLANT USAGE RATE DURING CHARGE CYCLES. IN THE H_2 HEAT EXCHANGER, THE LEAKAGE OF COLD FUEL INTO THE HOT GAS WOULD REDUCE THE TEMPERATURE AND EFFICIENCY OF THE HEAT EXCHANGER. IN THE O_2 HEAT EXCHANGER, THE LEAKAGE OF ADDITIONAL O_2 INTO THE HOT GAS WOULD CREATE EXCESSIVELY HIGH TEMPERATURES. THIS COULD BE ESPECIALLY CRITICAL, IF O_2 IS LEAKED INTO THE HOT GAS CAVITY DURING IDLE PERIODS. WITH O_2 PRESENT, THE INTRODUCTION OF HOT GAS FROM THE TURBINE EXHAUST WOULD RESULT IN AN IMMEDIATE CRITICAL TEMPERATURE RISE. THIS COULD CAUSE STRUCTURAL FAILURE OF THE HEAT EXCHANGER, DAMAGE TO SURROUNDING EQUIPMENT, AND POSSIBLY FIRE. EITHER FAILURE CAN BE DETECTED BY SENSING HEAT EXCHANGER TEMPERATURES.	SHUTOFF VALVES V-33 AND V-35, AND CHECK VALVES CV-19 AND CV-25 PROVIDE "FAIL-OP, FAIL-SAFE" REDUNDANCY AGAINST EXCESSIVE LOSS OF PROPELLANT AFTER SHUTDOWN OF THE CONDITIONING ASSEMBLY. TEMPERATURE SENSING DEVICES MUST BE INSTALLED IN THE HEAT EXCHANGER CAVITY TO ACCOMPLISH IMMEDIATE SHUTDOWN AND ISOLATION OF THE CONDITIONING ASSEMBLY IF OVERHEATING OF HEAT EXCHANGER OCCURS DURING OPERATION. THE EFFECT OF LEAKING O_2 INTO THE HEAT EXCHANGER CAVITY DURING IDLE PERIODS SHOULD BE THE SUBJECT OF FURTHER EVALUATION DUE TO THE POTENTIAL SAFETY HAZARD INVOLVED. THIS MAY ALSO BE CONSIDERED A STRUCTURAL FAILURE.
CV-19 OR CV-25 VALVE, CHECK	PREVENTS BACKFLOW OF PROPELLANT FROM ACCUMULATOR TO HEAT EXCHANGER	ORBITERS - 50 CYCLES BOOSTER - 16 CYCLES	FAILS CLOSED OR RESTRICTS FLOW	PREVENTS TRANSFER OF PROPELLANT THROUGH CONDITIONER ASSEMBLY #1. CAN BE DETECTED BY MONITORING PRESSURE UPSTREAM AND DOWNSTREAM OF VALVE.	TWO PARALLEL REDUNDANT CONDITIONING ASSEMBLIES PROVIDE "FAIL-OP, FAIL-SAFE" REDUNDANCY.
			FAILS OPEN	NO EFFECT UNLESS BOTH VALVES FAIL OPEN AND HEAT EXCHANGER LEAKS.	THESE VALVES PROVIDE "FAIL-OP, FAIL-SAFE" REDUNDANCY FOR PROPELLANT LEAKAGE FROM THE HEAT EXCHANGER.
CV-1 VALVE CHECK	PREVENTS HOT GAS FROM ANOTHER CONDITIONING ASSEMBLY FROM BEING FORCED INTO CONDITIONING ASSEMBLY #1 AFTER SHUTDOWN.	ORBITER - 50 CYCLES BOOSTER - 16 CYCLES	FAILS CLOSED OR RESTRICTS FLOW	RESULTS IN LOSS OF OPERATION OF CONDITIONER ASSEMBLY #1 OR DEGRADED OPERATION. CAN BE DETECTED BY MONITORING PRESSURE IN HEAT EXCHANGER EXHAUST LINE.	THE TWO PARALLEL REDUNDANT CONDITIONING ASSEMBLIES PROVIDE "FAIL-OP, FAIL-SAFE" OPERATIONAL REDUNDANCY. PRESSURE SENSING DEVICES WILL BE INCORPORATED TO SHUTDOWN CONDITIONING ASSEMBLY IN EVENT OF HEAT EXCHANGER OVER PRESSURE.
			FAILS OPEN	NO SIGNIFICANT EFFECT EXCEPT FOR HEATING EFFECTS.	NONE REQUIRED.

FIGURE H-3 (Cont.)

FAILURE MODE AND EFFECTS ANALYSIS
PRIMARY COMPONENTS

FUNCTION: PROPELLANT DISTRIBUTION AND THRUSTERS (ORBITERS AND BOOSTER)

COMPONENT	FUNCTION	DUTY CYCLE	FAILURE MODE	FAILURE EFFECT/DETECTION	FAIL-OP FAIL SAFE REDUNDANCY EVALUATION
THRUST CHAMBER	PROVIDES REQUIRED IMPULSE ON DEMAND	9 TO 906 CYCLES	FAILURE TO IGNITE OR DEGRADED PERFORMANCE	LOSS OR DEGRADATION OF THRUST WILL RESULT IN ABNORMAL COUPLING AND/OR DEGRADED V. FAILURE CAN BE DETECTED BY MONITORING CHAMBER PRESSURE AND BY DETECTING ABNORMAL COUPLING MOMENTS DURING OPERATION.	THRUSTERS ARE INCORPORATED AND ARRANGED TO ALLOW FOR COMPLETE LOSS OF THRUST FROM ANY ONE THRUSTER WITHOUT SIGNIFICANTLY AFFECTING APS PERFORMANCE. LOSS OF ANY TWO THRUSTERS (MORE IN SOME CASES) MAY DEGRADE OR PREVENT COMPLETION OF THE MISSION BUT WILL NOT PREVENT SAFE REENTRY. THERE IS ONE QUESTIONABLE AREA OF FULL "FAIL-OP, FAIL SAFE" REDUNDANCY FOR ORBITER B. PRELIMINARY ANALYSIS INDICATES FAILURE OF SELECTED PAIRS OF PITCH AND ROLL THRUSTERS MAY CREATE CONTROL PROBLEMS DURING REENTRY DUE TO COUPLING. THESE SELECTED PAIRS ARE: THRUSTERS 7 AND 14, 8 AND 13, 9 AND 12, AND 10 AND 11. SOME RELIEF FOR THE CONTROL PROBLEM CAN BE GAINED BY USING THE ROLL MOMENT OBTAINED WHEN +Y THRUSTERS ARE FIRED, HOWEVER, THIS PROBLEM SHOULD BE INVESTIGATED IN DETAIL.
VALVE, THRUST CHAMBER, BIPROPELLANT, PNEUMATIC ACTUATION	CONTROLS ON-OFF FLOW OF PROPELLANT TO THE THRUST CHAMBER.	SAME AS THRUST CHAMBER	FAILS CLOSED OR RESTRICTS FLOW	LOSS OR DEGRADATION OF IMPULSE FROM ONE THRUST CHAMBER WILL RESULT IN ABNORMAL COUPLING AND/OR DEGRADED ΔV. CAN BE DETECTED BY MONITORING VALVE POSITION AND/OR CHAMBER PRESSURE.	SAME AS ABOVE.
			FAILS OPEN OR LEAKS	LEAKAGE OF BOTH FUEL AND OXIDIZER WILL RESULT IN CONTINUED COMBUSTION AT A LOWER THAN NORMAL RATE. FAILURE IN FULL OPEN POSITION WILL RESULT IN CONTINUOUS FIRING AT NORMAL THRUST LEVEL. LEAKAGE OF ONE PROPELLANT WILL RESULT IN EXCESSIVE USAGE, AND IN THE EVENT OXIDIZER IS LEAKED INTO THE THRUST CHAMBER, MAY RESULT IN AN ABNORMAL TEMPERATURE RISE OR HARD START AT THE NEXT FIRING CYCLE. THIS POTENTIALITY SHOULD BE EVALUATED FULLY DURING ENGINE DEVELOPMENT TO DETERMINE ANY SAFETY HAZARD. FAIL OPEN OR LEAKAGE OF BOTH PROPELLANTS CAN BE DETECTED BY MONITORING CHAMBER PRESSURE. LOW LEAKAGE RATES OF ONE PROPELLANT WILL BE DIFFICULT TO DETECT. HIGH LEAKAGE RATES CAN BE DETECTED BY MONITORING ACCUMULATOR PRESSURE DECAY AND/OR BY MONITORING PROPELLANT FLOW RATE TO THE DIFFERENT GROUPS OF THRUSTERS DURING IDLE PERIODS.	N/O ISOLATION VALVES IN SERIES WITH THE THRUST CHAMBER VALVES PROVIDE "FAIL-OP" REDUNDANCY. LOSS OF ONE THRUSTER WILL NOT PREVENT COMPLETION OF THE MISSION. A SECOND PAIR OF ISOLATION VALVES CAN BE USED TO ISOLATE A GROUP OF THRUSTERS. THIS MAY DEGRADE THE MISSION BUT WILL NOT PREVENT SAFE REENTRY THUS PROVIDING "FAIL-SAFE" REDUNDANCY FOR THIS FAILURE MODE.

FIGURE H-3 (Cont.)

successful mission and/or vehicle and crew safety. It also provides a preliminary review of the instrumentation required to detect inflight malfunctions by indicating those parameters which must be monitored to aid in failure detection and isolation. No attempt is made to design and instrument the subsystem or to define the depth of redundancy required for parameter sensing devices.

The FMEA is limited to the same component failure modes shown in the functional flow diagrams. In order to simplify the FMEA for a triple-redundant system, the analysis was further limited to those failure modes of primary components which affect normal subsystem operation. Primary components are defined as those appearing in the primary (top) path of the functional flow diagrams. The remaining components are discussed in the redundancy evaluation.

H-4. RELIABILITY EVALUATION

To provide some measure of the potential numerical reliability of the high pressure APS, estimates of operational and fail-safe probabilities of success have been derived. The results of these estimates are presented in Figures H-4 and H-4a. Figure H-4a shows the probability of a zero failure mission and indicates that on an average, the necessity for component replacement (maintenance action) can be expected every five orbiter missions and every thirty booster missions due to inflight component operational malfunctions. The reliability estimates were basically derived by applying the component failure rates and duty cycles listed in Figures H-5 and H-6 to the subsystem functional flow diagrams. In some instances, approximation techniques were used to compute the estimates for redundant and complex component groups. In view of the preliminary nature of component and subassembly design, the accuracy of these approximations is well within the accuracy of the failure rates used in the analysis. Standby redundancy was considered only for the conditioner assemblies. It is probable that some thrusters will be held in standby; however, for this analysis, the thrust cycle requirements for each thruster location point were assumed to be equally divided between all thrusters at that location.

The failure rates used in the analyses were selected after a review of available failure rate lists. They are representative of the failure rates that can be expected of these types of components. The percentage of the failure rate assigned to each component failure mode was a judgement figure based on a review of available failure data. Duty cycles shown for each component are for a 72 hour mission timeline. Environmental and operational factors were not applied to these duty cycles because components are in general designed for much more severe environments than those encountered in actual usage.

SHUTTLE HIGH PRESSURE AUXILIARY PROPULSION SUBSYSTEM

RELIABILITY ESTIMATE (ROM)

	ORBITER B		ORBITER C		BOOSTER	
FUNCTIONAL GROUP	OPERATIONAL	FAIL SAFE	OPERATIONAL	FAIL SAFE	OPERATIONAL	FAIL SAFE
LO_2 STORAGE AND PRESSURIZATION	0.999990	0.99999997	0.999990	0.99999997	0.999998	0.99999999
LH_2 STORAGE AND PRESSURIZATION	0.999990	0.99999997	0.999990	0.99999997	0.999998	0.99999999
PROPELLANT CONDITIONING - O_2	0.999876	0.99999929	0.999876	0.99999929	0.999992	0.99999999
PROPELLANT CONDITIONING - H_2	0.999876	0.99999929	0.999876	0.99999929	0.999992	0.99999999
PROPELLANT ACCUMULATION AND PRESSURE REGULATION - O_2	0.999991	0.99999997	0.999991	0.99999997	0.999999	0.99999999
PROPELLANT ACCUMULATION AND PRESSURE REGULATION - H_2	0.999991	0.99999997	0.999991	0.99999997	0.999999	0.99999999
PROPELLANT DISTRIBUTION AND THRUSTERS	0.998150	0.99983946	0.999346	0.99999930	0.999978	0.99999998
SUBSYSTEM	.997864	.99983792	.999060	.99999776	.999956	.99999992

ASSUMPTIONS INCLUDED IN THIS ESTIMATE

(1) COMPONENT EXTERNAL LEAKAGE WILL NOT DEGRADE SYSTEM OPERATION EXCEPT TURBOPUMP AND HEAT EXCHANGER LEAKAGE.

(2) THE NON-OPERATING FAILURE RATE FOR APS COMPONENTS WILL NOT BE SIGNIFICANT.

(3) STRUCTURAL RELIABILITY IS EQUAL TO 1.0.

(4) SENSING AND SWITCHING RELIABILITY IS EQUAL TO 1.0, i.e. COMPONENT FAILURE MODES WHICH COULD CAUSE A DESTRUCTIVE FAILURE DUE TO OVERSTRESS OR OVER TEMPERATURE WILL BE DETECTED PRIOR TO REACHING CRITICAL LEVEL.

FIGURE H-4

FUNCTIONAL GROUP	PROBABILITY OF ZERO FAILURE MISSION		
	ORBITER B	ORBITER C	BOOSTER
LO_2 STORAGE AND PRESSURIZATION	.98802	.98802	.99669
LH_2 STORAGE AND PRESSURIZATION	.98802	.98802	.99669
PROPELLANT CONDITIONING - O_2	.98168	.98168	.99537
PROPELLANT CONDITIONING - H_2	.98168	.98168	.99537
PROPELLANT ACCUMULATION AND PRESSURE REGULATION - O_2	.99103	.99103	.99971
PROPELLANT ACCUMULATION AND PRESSURE REGULATION - H_2	.99103	.99103	.99971
PROPELLANT DISTRIBUTION AND THRUSTERS	.88947	.89281	.98363
SUBSYSTEM	.82181	.82490	.96754

INDICATES THAT ON AN AVERAGE, THE NECESSITY FOR COMPONENT REPLACEMENT (MAINTENANCE ACTION) CAN BE EXPECTED EVERY FIVE (5) ORBITER MISSIONS AND EVERY THIRTY (30) BOOSTER MISSIONS DUE TO INFLIGHT COMPONENT OPERATIONAL MALFUNCTION.

SHUTTLE HIGH PRESSURE AUXILIARY PROPULSION SUBSYSTEM

RELIABILITY ESTIMATE

FIGURE H-4a

SHUTTLE HIGH PRESSURE AUXILIARY PROPULSION SUBSYSTEM

COMPONENT DUTY CYCLES, FAILURE MODES, AND FAILURE RATES

ORBITERS AND BOOSTER

COMPONENT TYPE	IDENTIFICATION NUMBERS (SCHEMATIC)	MISSION DUTY CYCLE	FAILURE MODE	FAILURE RATE x 10^6	SOURCE OF BASIC FAILURE RATE
GAS GENERATOR	GG-1, GG-3	ORBITERS-0.66 HOUR BOOSTER-0.10 HOUR	FAILS TO FUNCTION	1000/HOUR	AEROJET GENERAL CORP. ESTIMATE
	GG-5	ORBITERS-0.20 HOUR (REENTRY) BOOSTER-0.10 HOUR			
HEAT EXCHANGER, REBURN	HX-1, HX-3	ORBITERS-0.66 HOUR BOOSTER-0.10 HOUR	PROPELLANT LEAKAGE	765/HOUR	AEROJET GENERAL CORP. ESTIMATE
	HX-5	ORBITERS-0.20 HOUR BOOSTER-0.10 HOUR	HOT GAS LEAKAGE	765/HOUR	
PUMP, CRYOGENIC, TURBINE DRIVE	T/P-1, T/P-3	ORBITERS-50 CYCLES, 0.66 HOURS BOOSTER-16 CYCLES 0.10 HOUR	FAILS TO FUNCTION LEAKS EXTERNALLY	60.0/CYCLE + 5400/HOUR 40.0/CYCLE + 3600/HOUR	CYCLIC - MDAC ESTIMATE HOURLY - AEROJET GENERAL CORP. ESTIMATE
	T/P-5	ORBITERS-15 CYCLES 0.20 HOUR REENTRY BOOSTER-16 CYCLES 0.10 HOUR			
REGULATOR, PRESSURE	R-1, R-3, R-5, R-7, R-9, R-11	ORBITERS-72.0 HOURS BOOSTER-0.1 HOUR	FAILS OPEN FAILS CLOSED	30/HOUR 11/HOUR	MDAC GEMINI EXPERIENCE
TANK ASSEMBLY, LIQUID PROPELLANT	LO_2 TANK, LH_2 TANK	72 HOURS	FAILS TO MAINTAIN TEMPERATURE CONTROL	NEGIGIBLE	
THRUST CHAMBER, REGENERATIVE COOLED (INCLUDING VALVES)	ALL THRUSTERS	SEE TABLE H-1	FAILS TO FUNCTION FAILS OPEN OR LEAKS	5.0/CYCLE 7.5/CYCLE	MDAC ESTIMATE - AFTER DISCUSSION WITH ENGINE MANUFACTURERS (AEROJET, BELL, MARQUARDT, AND ROCKETDYNE
VALVE, CHECK HEAT EXCHANGER EXHAUST	CV-1, CV-3	ORBITERS-50 CYCLES BOOSTER-16 CYCLES	FAILS OPEN FAILS CLOSED	2.2/CYCLE 0.1/CYCLE	AVCO RELIABILITY ENGINEERING DATA SERIES, FAILURE RATES, APRIL 1962 (AVERAGE)
	CV-5	ORBITERS-15 CYCLES (REENTRY) BOOSTER-16 CYCLES			
VALVE, CHECK, GAS, PROPELLANT, HIGH PRESSURE	CV-19, CV-21, CV-25, CV-27	ORBITERS-50 CYCLES BOOSTER-16 CYCLES	FAILS OPEN FAILS CLOSED	4.4 /CYCLE 0.3 /CYCLE	(MAXIMUM) STANFORD RESEARCH INSTITUTE REPORT - CONTRACT NAS 7-751 GIVES RATIO FOR GAS VS LIQUID CHECK VALVES
	CV-23, CV-29	ORBITERS-15 CYCLES REENTRY BOOSTER-16 CYCLES			
VALVE, CHECK, LIQUID PROPELLANT, HIGH PRESSURE	CV-7, CV-9, CV-13, CV-15	ORBITERS-50 CYCLES BOOSTER-16 CYCLES	FAILS OPEN FAILS CLOSED	13.2/CYCLE 1.2/CYCLE	(MAXIMUM x 3)
	CV-11, CV-17	ORBITERS-15 CYCLES (REENTRY) BOOSTER-16 CYCLES			
VALVE, THROTTLING, BI-PROPELLANT WITH VERNIER THROTTLING OF OXIDIZER, MOTOR DRIVEN	V-41, V-47	ORBITERS-50 CYCLES 0.66 HOUR BOOSTER-16 CYCLES, 0.10 HOUR	FAILS OPEN FAILS CLOSED	40/CYCLE + 80/HOUR 10/CYCLE + 20/HOUR	HOURLY-LTV ELECTROSYSTEMS DATA CYCLIC - STANFORD RESEARCH INSTITUTE REPORT - CONTRACT NAS 7-751 (ELECTROMECHANICAL ACTUATOR)
	V-53	ORBITERS-15 CYCLES, 0.20 HOUR BOOSTER-16 CYCLES, 0.10 HOUR			
VALVE S/O, MOTOR DRIVEN OR PNEUMATIC ACTUATION ISOLATION	V-33, V-37	ORBITERS-50 CYCLES, BOOSTER-16 CYCLES	FAILS OPEN FAILS CLOSED	16/CYCLE 3.3/CYCLE	NASA DATA - SATURN (SHUTOFF VALVES)
	V-39	ORBITERS-15 CYCLES (REENTRY) BOOSTER-16 CYCLES			
	V-5, V-35, AND ALL THRUSTER GROUP ISOLATION VALVES	1 CYCLE (AS REQUIRED)			
VALVE, S/O, PNEUMATIC ACTUATION, FILL AND VENT	V-1, V-3, V-17, V-19, V-21	1 CYCLE EACH	FAILS OPEN FAILS CLOSED	510/CYCLE 100/CYCLE	FARADA - SATURN
VALVE, SOLENOID ACTUATED, HELIUM CONTROL	V-7, V-9, V-11, V-13, V-15 V-23. V-25	1 CYCLE (AS REQUIRED)	FAILS OPEN FAILS CLOSED	8/CYCLE 0.77/CYCLE	THIOKOL CHEMICAL CORP. (SURVEYOR)
VALVE, SOLENOID ACTUATED PROPELLANT CONTROL	V-45, V-51	ORBITERS-50 CYCLES BOOSTER-16 CYCLES	FAILS OPEN FAILS CLOSED	5.8/CYCLE .56/CYCLE	NASA DATA - SATURN
	V-57	ORBITERS-15 CYCLES (REENTRY) BOOSTER-16 CYCLES			
	V-59, V-61, V-63, V-65, V-67 V-69, V-75, V-77, V-79, V-81, V-83, V-89, AND THRUSTER ISOLATION VALVES	1 CYCLE (AS REQUIRED)			
	V-85, V-87	ORBITER-3 CYCLES BOOSTER-1 CYCLE (AS REQUIRED)			
VALVE, RELIEF PRESSURE	RV-1, RV-3, RV-5, RV-7	1 CYCLE (AS REQUIRED)	FAILS OPEN FAILS CLOSED	5.3/CYCLE 1.5/CYCLE	NASA DATA - SATURN
(BURST DISK)	RV-1, RV-3, RV-5, RV-7		FAILS OPEN FAILS CLOSED	60/UNIT 40/UNIT	STANFORD RESEARCH INSTITUTE CONTRACT NAS 7-751

FIGURE H-5

VEHICLE	THRUSTER	DUTY CYCLE EACH THRUSTER
ORBITER B	PITCH AND ROLL	500 CYCLES
	YAW	650 CYCLES
	-X	10 CYCLES
	+X	25 CYCLES
ORBITER C	FWD - PITCH	295 CYCLES
	FWD + PITCH	285 CYCLES
	AFT - PITCH, ± ROLL	600 CYCLES
	AFT + PITCH, ± ROLL	450 CYCLES
	FWD ± YAW	335 CYCLES
	AFT ± YAW	220 CYCLES
	+X	25 CYCLES
	-X	10 CYCLES
BOOSTER	PITCH AND ROLL	100 CYCLES
	YAW	40 CYCLES

HIGH PRESSURE APS

AVERAGE THRUSTER DUTY CYCLE/MISSION

FIGURE H-6

H-5. RESULTS

The ability of the APS to meet the one failure operational, failure safe requirements are presented below. Included is the APS operation description after component failure, the numerical reliability of the APS, and the malfunction detection methods.

The following assumptions were used in the evaluation and must be considered when comparing the estimated reliability of this subsystem baseline to the estimated reliability of another subsystem.

(1) component external leakage will not degrade subsystem operation or safety and, therefore, is not included in this estimate

(2) failure sensing and switching reliability is equal to 1.0

(3) structural reliability of tanks, lines, static seals, etc., is equal to 1.0

(4) the non-operating failure rate for APS components will not be significant.

H-6. "FAIL-OP, FAIL-SAFE" REDUNDANCY

The foregoing analyses indicate that the baseline APS design presented in this report will meet the redundancy requirements with component external leakage and structural failure excluded. This is dependent, however, upon integration with an instrumentation subsystem and guidance and control subsystem capable of using the component redundancy incorporated in the baseline.

One area of concern is the Orbiter B pitch and yaw thrusters. A preliminary analysis indicates that failure of selected pairs of pitch and roll thrusters could create undesirable control moments during reentry. These probably can be tolerated; however, an in-depth subsystem control analysis is required to ensure that the present configuration will perform adequately. A simplified solution to this potential problem is to add an additional four thrusters at the pitch-roll location either in the forward or aft vehicle positions.

H-7. SUBSYSTEM RELIABILITY

The reliability estimates presented in Figure H-4 indicate that the baseline design offers high potential reliability for both orbiter and booster application. Attaining these high reliabilities is dependent upon sensing and switching capability which can detect and isolate failures, especially those failures which could cause overstress and/or over-temperature conditions leading to structural failure of components. These critical areas are discussed below.

The relatively low fail-safe reliability of Orbiter B is due to the potential control problem associated with the pitch-roll thrusters which was charged against the fail-safe reliability.

H-8. MALFUNCTION DETECTION

The critical malfunction monitoring locations in the APS are in the areas where a malfunction could cause a structural failure due to overstress and/or over-temperature. The gas generators, turbopumps, reburn heat exchangers, and thrusters are critical areas.

H-8.1 Gas Generators - The critical conditions in the gas generators are over-temperature during combustion due to improper mixture ratio caused by variations in inlet pressure and/or temperature or by oxygen leakage into the chamber prior to ignition. The throttling capability of the vernier gas generator propellant valves provides a degree of control against improper mixture ratio. A feedback control which monitors temperature and provides a vernier control to the oxygen valve will further protect against normal variations in propellant pressures. Oxygen leakage into the gas generator prior to commanded initiation could result in an excessively hot start. Backup shut-off valves can be provided to prevent oxygen leakage since it may be more advantageous to assure that leakage will not occur than to require a detection method.

This backup oxygen isolation valve can also be used to prevent flow to the reburn heat exchanger and provide a backup shut-off capability for this component.

H-8.2 Turbopumps - Turbopump overspeed is the critical condition for this component. The speed and speed rise rate will be monitored and used to control the gas generator and pump suction valves. Other turbopump malfunctions will be evidenced by subsystem performance loss (primarily lower pump discharge pressure and/or flow) and are not critical malfunctions.

H-8.3 Reburn Heat Exchangers - The critical condition for the heat exchanger is over-temperature due to an oxygen-rich mixture ratio. This can be caused by oxygen being present in the heat exchanger at ignition due to valve leakage during non-use periods, or, in the case of oxygen, heat exchanger internal leakage from the propellant coils anytime. Over-temperature sensors and feedback control to the oxygen inlet valve will be provided for the reburn heat exchangers. This will prevent over-temperature during operation. Oxygen leakage during non-use periods can be prevented with the same valves used to isolate the gas generator oxygen supply during non-use periods. Minor amounts of O_2 leakage may be tolerated since it will diffuse out the vent, and valve sequencing will delay addition to the turbine exhaust gases until the flow is partially established. Temperature sensors in the heat exchanger will be used to shutdown and isolate the entire conditioner assembly before the temperature reaches a critical level.

H-8.4 Thrust Chambers - Linked propellant thruster valves provide mixture ratio and sequencing control for the thrusters. Possible fuel leakage during non-use periods generates the only critical malfunction detection monitoring requirement. Minor leakage presents no problems because of diffusion out of the chamber in orbit. Major amounts of leakage can be detected by monitoring pressure decay in the APS propellant distribution subassembly during non-use periods.

H-9. STRUCTURAL REDUNDANCY

All reliability analyses assumed that all structural components were failure free. Structure does not have a reliability of 1.0 as assumed; therefore, one task of this study was to investigate ways of increasing subsystem reliability by adding structural redundancy. Various methods and degrees of incorporating structural redundancy were investigated for the APS.

Structural redundancy already exists in the following areas as a result of providing functional redundancy.

(1) conditioner assemblies - three completely independent conditioner assemblies are incorporated in each propellant loop. A structural failure (nondestructive to surrounding equipment) within a conditioning assembly can be isolated completely.

(2) propellant distribution - because provision has been incorporated to provide isolation for each thruster individually, and also to further isolate by groups, the subsystem is protected against structural failure in many lines and fittings as a result of protection against thruster leakage.

If the accumulators were implemented as two pressure vessels instead of one with equal volumes then redundancy could be achieved with little or no weight penalty. However, both accumulators would be used continuously and failure sensing and switching would be required. In order to alleviate this requirement and hold one accumulator in reserve (as a spare), the weight penalty would be 679 and 321 pounds for Orbiter B hydrogen and oxygen, respectively. Another method of implementing redundant accumulators would be to utilize small accumulators capable of supplying only enough propellant to allow the conditioner assembly to start.

The implementation of additional lines to the thruster manifolds from the pressure regulators downstream of the accumulators provides a significant degree of redundancy. Also, redundant manifolds and valves which allow isolation and switching requires approximately an additional 200 pounds of lines and valves.

If the retrograde propellant were separated from the main propellant supply and stored in a separate tank along with independent pressurization, the weight penalty would be in the order of 100 lbs, as shown in Figure H-7. The separate propellant storage does not incur weight penalties in the tank, however, additional pressurization lines and regulators, tank supports, and nonusable propellant account for the indicated weight penalty.

Providing redundant retrograde propellant does, however, incur a significant weight penalty since additional propellant and associated tankage and pressurization is required to provide this capability. The incurred penalty is above 10,000 pounds.

One single point structure is the line from the propellant tank to the conditioner assembly. This line then splits to the 3 turbopump inlets. Adding redundant line and valves for both hydrogen and oxygen incurs a weight penalty of approximately 30 pounds.

One of the methods investigated to implement structural redundancy was to utilize separated retrograde propellant, a small second accumulator, and connect one of the triple redundant conditioner assemblies with these components. This configuration is shown in Figure H-8. The operation of this configuration has not been investigated in detail.

EFFECTS OF STRUCTURAL REDUNDANCY*

COMPONENTS REQUIRING REDUNDANCY	OPTIONS	Δ WEIGHT OVER BASELINE, LBS
PROPELLANT TANKS	SEPARATE RETROGRADE PROPELLANT (PROVIDES REDUNDANCY UNTIL MAIN TANK PROPELLANT EQUALS RETROGRADE PROPELLANT)	100
	ADDITIONAL RETROGRADE PROPELLANT & TANK	10,610
CONDITIONER ASSEMBLY TO ACCUMULATOR LINE	ADDITIONAL LINE	30**
ACCUMULATORS	2-1/2 SIZE ACCUMULATORS	0
	REDUNDANT ACCUMULATORS	1000
	SMALL SECOND ACCUMULATOR	100
ACCUMULATORS TO THRUSTER MANIFOLDS LINES	ADDITIONAL LINE	200**
THRUSTER MANIFOLDS AND ISOLATION VALVES	ADDITIONAL MANIFOLDS AND VALVES	

* DESIGNED FOR FAIL SAFE ONLY
** HPI INSULATION ONLY

FUNCTIONAL REDUNDANCY ALSO PROVIDES SIGNIFICANT STRUCTURAL REDUNDANCY, ONLY COMPONENTS CONSIDERED WERE THOSE NOT OTHERWISE REDUNDIZED

FIGURE H-7

STRUCTURAL REDUNDANCY CONSIDERATIONS

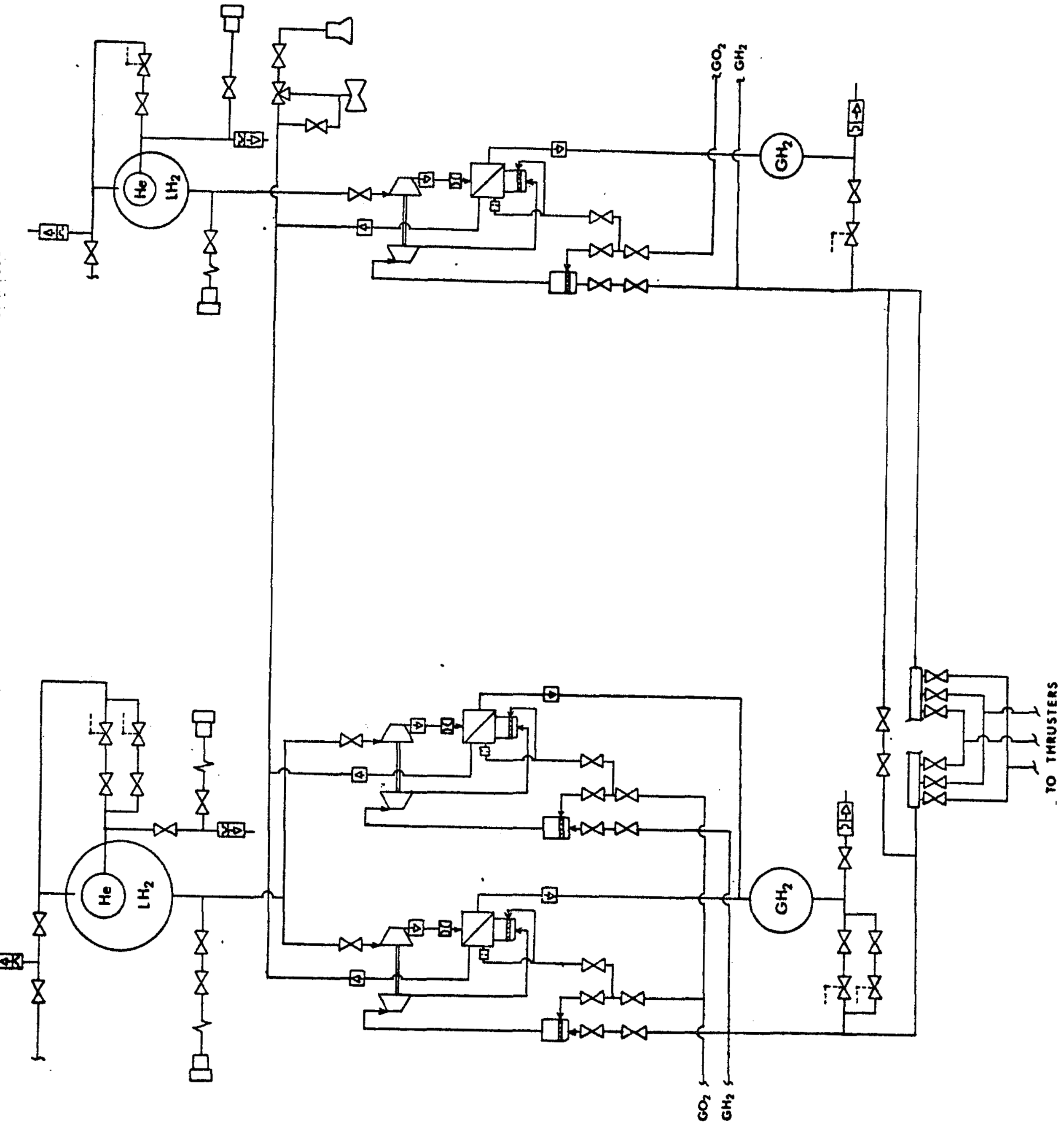

FIGURE H-8

APPENDIX I

DISTRIBUTION LIST FOR FINAL REPORT
CONTRACT NAS 8-26248

INSTRUCTIONS

Report is to be sent directly to the "Recipient" marked with an "X" under the column headed "Designee" on pages I-1 and I-2 only. On pages I-2 thru I-8, the report should be sent to the Technical Librarian of the "Recipient" with a carbon copy of the letter of transmittal to the attention of the person named under the column "Designee." The letter of transmittal should contain the contract number and complete title of the final report. The distribution list should be included in the final report as an appendix.

COPIES	RECIPIENT	DESIGNEE
	NASA-Marshall Space Flight Center Marshall Space Flight Center, Alabama 35812	
2	Office of Technical Information, A&TS-MS-IP	(X)
1	Technical Library, A&TS-MS-IPL	(X)
1	Purchasing Office, A&TS-PR-M	(X)
1	Patent Office, A&TS-PAT	(X)
1	Technology Utilization Office, A&TS-TU-T	(X)
1	Dale Burrows, S&E-ASTN-PJ	(X)
15	J. McCarty, (COR), S&E-ASTN-PP	(X)
2	Keith D. Coates, S&E-ASTN-EPA	(X)
1	C. Johnson, PD-RV	(X)
1	E. Jacobs, PD-RV	(X)
1	James S. Strong, S&E-ASTN-RRI	(X)
	NASA/Asst. Director for Propulsion, OART, Code RP Washington, D.C. 20546	
1	Attn: Mr. A. O. Tisehler	(X)
1	Attn: Mr. Don Hart	(X)
1	Mr. Philip E. Culbertson, Code MT Director, Advanced Manned Missions Office of Manned Space Flight NASA Headquarters, Washington, D.C. 20546	(X)
3	Mr. Jerome Malament, Code MTG Advanced Development Office of Manned Space Flight NASA Headquarters, Washington, D.C. 25046	(X)
2	Mr. Charles W. Matthews, Code MF Director, Space Station Task Force Office of Manned Space Flight NASA Headquarters, Washington, D.C. 20546	(X)

COPIES	RECIPIENT	DESIGNEE
3	Mr. William H. Woodward, Code RP Director, Space Propulsion and Power Division Office of Advanced Research and Technology NASA Headquarters, Washington, D.C. 20546	(X)
1	Mr. Joseph E. McGolrick Chief, Advanced Programs and Technology Programs, SV Office of Space Science and Applications NASA Headquarters, Washington, D.C. 20546	(X)
2	NASA Scientific and Technical Information P.O. Box 33 College Park, Maryland 20740	(X)
1	Dr. Leonard Roberts Mission Analysis Division NASA-Ames Research Center Moffett Field, California 24035	(X)
2	Ames Research Center Moffett Field, California 90435	H. J. Allen
2	Goddard Space Flight Center Greenbelt, Maryland 20771	Merland L. Moseson Code 620
2	Jet Propulsion Laboratory California Institute of Technology 4800 Oak Grove Drive Pasadena, California 91103	Henry Burlage, Jr. Propulsion Div. 38
2	Langley Research Center Langley Station Hampton, Virginia 23365	Dr. Edgar M. Cortwright Director
2	Lewis Research Center 21000 Brookpark Road Cleveland, Ohio 44135	Dr. Bruce T. Lundin Director Mr. Ed Otto Spacecraft Technology Division Code 9700
1	Marshall Space Flight Center Marshall Space Flight Center, Ala. 35812	Mr. Hans G. Paul S&E-ASTN-P
5	Manned Spacecraft Center Houston, Texas 77001	Dr. Robert Gilruth Director Mr. J. G. Thibodaux Code EP-

COPIES	RECIPIENT	DESIGNEE
	Manned Spacecraft Center (Continued) Houston, Texas 77001	Mr. H. Pohl Code EP-4 Mr. C. Vaughn Code EP-4 Mr. N. Chaffee Code EP-4
3	John F. Kennedy Space Center, NASA Kennedy Space Center, Florida 32899	Dr. K. H. Debus Director Mr. Bill Malloney LV-MEC-24 LCC Room 2R12
GOVERNMENT INSTALLATIONS		
1	Aeronautical Systems Division Air Force Systems Command Wright-Patterson Air Force Base Dayton, Ohio 45433	D. L. Schmidt Code ASRCNC-2
1	Air Force Missile Development Center Holloman Air Force Base, New Mexico	Maj. R. E. Bracken Code MDGRT
1	Air Force Missile Test Center Patrick Air Force Base, Florida	L. J. Ullian
1	Space & Missile Systems Organization Los Angeles, California 90045	Colonel Clark Technical Data Center
1	Arnold Engineering Development Center Arnold Air Force Station Tullahoma, Tennessee 37389	Dr. H. K. Doetsch
1	Bureau of Naval Weapons Department of the Navy Washington, D.C.	J. Kay RTMS-41
1	Defense Documentation Center Headquarters Cameron Station, Building 5 5010 Duke Street Alexandria, Virginia 22314 Attn: TISIA	
1	Headquarters, U.S. Air Force Washington, D.C. 20025	Col. C. K. Stambaugh AFRST

COPIES	RECIPIENT	DESIGNEE
1	Picatinny Arsenal Dover, New Jersey 07801	I. Forsten, Chief Liquid Propulsion Laboratory, SMUPA-DL
1	Air Force Rocket Propulsion Laboratory Research and Technology Division Air Force Systems Command Edwards, California 93523	RPRR/Mr. H. Main
1	U. S. Army Missile Command Redstone Arsenal Alabama 35809	Dr. Walter Wharton
1	U. S. Naval Ordnance Test Station China Lake California 93557	Code 4562 Chief, Missile Propulsion Div.
CPIA		
1	Chemical Propulsion Information Agency Applied Physics Laboratory 8621 Georgia Avenue Silver Spring, Maryland 20910	Tom Reedy
INDUSTRY CONTRACTORS		
2	Aerojet Liquid Rocket Company P.O. Box 1947 Technical Library, Bldg. 2015, Dept. 2410 Sacramento, California 95809	R. Stiff C. Williams
1	Aeronutronic Philco Corporation Ford Road Newport Beach, California 92663	D. A. Garrison
1	Aerospace Corporation 2400 East El Segundo Boulevard P.O. Box 95085 Los Angeles, California 90045	John G. Wilder MS-2293 Propulsion Dept.
1	Arthur D. Little, Inc. 20 Acorn Park Cambridge, Massachusetts 02140	Library
1	Astropower Laboratory Douglas Aircraft Company 2121 Paularino Newport Beach, California 92663	Dr. George Moc Director

COPIES	RECIPIENT	DESIGNEE
1	Astrosystems International, Inc. 1275 Bloomfield Avenue Fairfield, New Jersey 07007	A. Mendenhall
1	Atlantic Research Corporation Edsall Road and Shirley Highway Alexandria, Virginia 22314	Dr. Ray Friedman
1	Beech Aircraft Corporation P.O. Box 1 Buffalo, New York 14240	J. H. Rodgers
1	Bellcom 1100 17th Street Washington, D.C.	Library
1	Bendix Systems Division Bendix Corporation 3300 Plymouth Road Ann Arbor, Michigan	John M. Brueger
1	Boeing Company 1625 K. Street N. W. Washington, D.C. 20006	Library
1	Boeing Company P.O. Box 3707 Seattle, Washington 98124	Library
1	Boeing Company P.O. Box 3999 Seattle, Washington 98124	A. M. Momenthy MS 8K-93
1	Boeing Company P.O. Box 1680 Huntsville, Alabama 35801	Ted Snow
1	Boeing Company P.O. Box 1470 Huntsville, Alabama 35807	Max T. Braun (Space Shuttle)
1	Missile Division Chrysler Corporation P.O. Box 2628 Detroit, Michigan 48231	John Gates
1	CCSD Michoud Operation P.O. Box 29200 New Orleans, Louisiana 70129	C. E. Tharrott Dept. 2760

COPIES	RECIPIENT	DESIGNEE
1	Wright Aeronautical Division Curtiss-Wright Corporation Wood-Ridge, New Jersey 07075	G. Kelly
1	Missile and Space Systems Division McDonnell Douglas Aircraft Corp. 5301 Bolsa Avenue Huntington Beach, California 92647	R. W. Hallet Chief Engineer Advanced Space Tech.
1	Aircraft Missiles Division Fairchild Hiller Corporation Hagerstown, Maryland 10	J. S. Kerr
1	General Dynamics/Convair Library & Information Services (128-00) San Diego, California 92112	Frank Dore
1	Re-Entry Systems Department General Electric Company 3198 Chestnut Street Philadelphia, Pennsylvania 19101	F. E. Schultz
1	Advanced Engine & Technology Dept. General Electric Company Cincinnati, Ohio 45215	D. Suichu
2	Grumman Aircraft Engineering Corp. Bethpage, Long Island New York 11714	Joseph Gavin Fred Raymer (Plant 25 - Space Shuttle)
1	Ling-Temco-Bought Corporation Astronautics P.O. Box 5907 Dallas, Texas 75222	Warren C. Trent
2	Lockheed Missiles and Space Co. Attn: Technical Information Center P.O. Box 504 Sunnyvale, California 94088	Y. C. Lee John Lloyd, Manager, Alternate Space Shuttle Concept Study Dept. G1-51, Building 538
1	The Marquardt Corporation 16555 Saticoy Street Van Nuys, California 91409	Leo Bell

COPIES	RECIPIENT	DESIGNEE
2	Denver Division Martin Marietta Corporation P.O. Box 179 Denver, Colorado 80201	Dr. J. M. Murphy Richard Vandekoppel, 0431
4	McDonnell Douglas Corporation P.O. Box 516 Municipal Airport St. Louis, Missouri 63166	R. A. Herzmark L. F. Kohrs P. J. Kelly Sherman L. Hislop Director of Booster/ Orbiter Integration
3	Space Division North American Rockwell, Inc. 12214 Lakewood Boulevard Downey, California 90241	Lou Duncan Joe Monroe B. Hello Vice President, Corporate Wide General Manager Space Shuttle Program
2	Rocketdyne (Library 586-306) 6633 Canoga Avenue Canoga Park, California 91304	Dr. R. I. Thompson S. J. Domokus
1	Northrop Space Laboratories 3401 West Broadway Hawthorne, California	Dr. William Howard
1	Astro-Electronics Division Radio Corporation of America Princeton, New Jersey 08540	S. Fairweather
1	Reaction Motors Division Thiokol Chemical Corporation Denville, New Jersey 07832	Dwight S. Smith
1	Space General Corporation 9200 East Flair Avenue El Monte, California 91734	C. E. Roth
1	Stanford Research Institute 333 Ravenswood Avenue Menlo Park, California 94025	Dr. Gerald Marksman

COPIES	RECIPIENT	DESIGNEE
2	TRW Systems Group TRW Incorporated One Space Park Redondo Beach, California 90278	G. W. Elverum Dr. H. Burge
1	TAPCO Division TRW Incorporated 23555 Euclid Avenue Cleveland, Ohio 44117	P. T. Angell
1	Thiokol Chemical Corporation Huntsville Division Huntsville, Alabama	John Goodloe
1	Research Laboratories United Aircraft Corporation 400 Main Street East Hartford, Connecticut 06108	Erle Martin
1	United Technology Center 587 Methilda Avenue P.O. Box 358 Sunnyvale, California 94088	Mr. Robert Taylor
1	Aerospace Operations Walter Kidde and Company, Inc. 567 Main Street Belleville, New Jersey 07109	R. J. Hanville Director of Research Engineering
1	Florida Research and Development Pratt and Whitney Aircraft United Aircraft Corporation P.O. Box 2691 West Palm Beach, Florida 33402	R. J. Coar
1	Rocket Research Corporation 520 South Portland Street Seattle, Washington 98108	Foy McCullough, Jr.

MCDONNELL DOUGLAS ASTRONAUTICS COMPANY • EAST

Saint Louis, Missouri 63166   314·232·0232